The Western Palaearctic evolution of the water vole *Arvicola*

Mark Ruddy

Submitted to Royal Holloway College, University of London, for the Degree of Doctor of Philosophy.

June, 2011

Declaration of Authorship

I, Mark Ruddy, hereby declare that this thesis and the work presented in it is entirely my own. Where I have consulted the work of others, this is always clearly stated.

Signed:

Date:
16th of June, 2011

After Darwin (1837)

I think

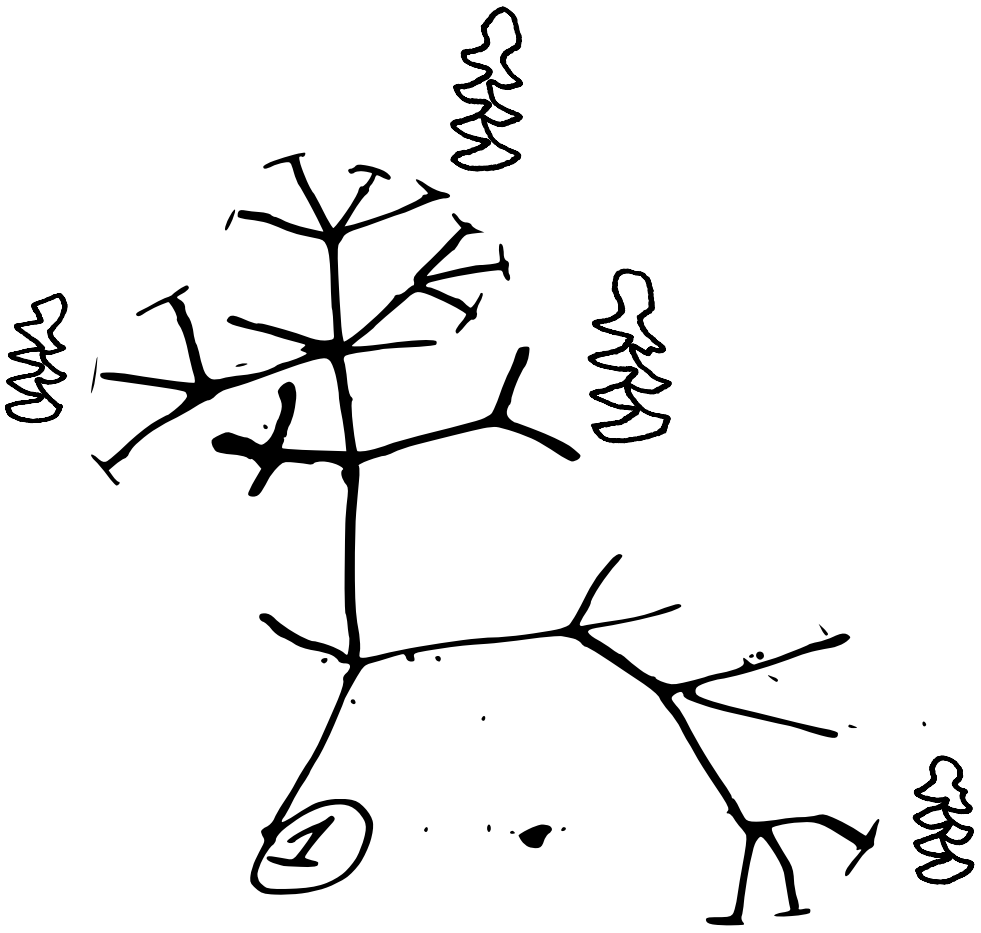

Abstract

The water vole is common in Middle and Late Pleistocene temperate Palaearctic faunas. It is widely used in biostratigraphy because of temporal trends in the size, shape and structure of the first lower molar (M_1). However, geographic variation in the evolutionary development of the M_1 has restricted the precision and accuracy of age-estimations. This thesis explores morphological variation in the M_1 of fossil and extant populations of the lineage *Mimomys savini–Arvicola*, and uses the phenotype and the genotype to develop evolutionary hypotheses. Geometric and traditional morphometric methods are used to quantify tooth shape and enamel thickness from over 4000 digital photographs of M_1s taken from specimens originating from 146 modern and fossil groups across the western Palaearctic. M_1s are photographed to obtain a true cross-section, giving a more accurate description of molar shape. Morphological variation is explored in terms of sample-size, taphonomy, and ontogeny. Sample sizes of less than 10 are likely to provide inaccurate summary statistics of morphometric variables but depositional type appears to have no systematic effect on within-group variation. Change in the morphology of M_1s through ontogeny is an important source of morphological variation, explaining up to 29% of molar shape within-specimens and up to 95% of enamel thickness within enamel layers of specimens. Removal of ontogenetic variation from molar shape improves congruence between morphological and molecular data, indicating age-corrected variables should be used when assessing evolutionary patterns. Temporal and spatial patterns in the enamel thickness quotient (SDQ), based on age-corrected enamel thicknesses, mirror those from published data but differ in some details. Methodological differences mean absolute SDQ values cannot be compared. Qualitative patterns include a large decrease in SDQ across MIS 12 and a steep east–west morphocline during the late Middle Pleistocene.

Contents

List of Figures

List of Tables

Acknowledgments

This research was made possible by funding from the Leverhulme Trust as part of the *Ancient Human Occupation of Britain Project II–Ancient Britain and its European context*. My gratitude is extended AHOB II and the Leverhulme Trust for their generous support (from the original award and with additional grants for radiocarbon dating), and for offering me the unique opportunity to carry out this research. I would also like to specifically thank Prof. Chris Stringer for an additional funding contribution.

This research also received support for a visit to the Royal Belgian Institute of Natural Sciences, Brussels, Belgium from the SYNTHESYS Project (http://www.synthesys.info/; award number BE-TAF-4725), which is financed by the European Commumity Research Infrastructure Action under FP6 "Structuring the European Research Area".

My deep gratitude goes to Prof. Danielle Schreve for her supervision, expert knowledge, good humour, patience, encouragement, meticulous proof-reading skills, and support in many other forms. I would not have started and could not have completed this thesis without her belief in me.

Thanks go to Dr. David Polly who, despite fleeing Great Britain for the United States as I began my research, has been constantly available to provide inspiration, expert knowledge, encouragement, country and western tunes, and a null model for a natural historian.

Mr. Andrew Currant has been a constant source of support at the Natural History Museum, London. He has always been available to impart his deep knowledge of fossil mammals, as well his unique perspective on the subject. The lengthy, interesting discussions we shared, and his irrepressible wit and encouragement during sometimes difficult times, will always be cherished.

Thanks are extended to Dr. Ian Barnes and Dr. Selina Brace of the School of Biological Sciences, Royal Holloway College, University of London. The friendship

and welcoming atmosphere they afforded to this palaeontologist I feel went beyond the call of duty for molecular biologists.

During data collection I visited many museums and universities across Europe. In every instance I received a warm reception, an interest in my work, and a helpful environment. Many of those who helped me during my visits are mentioned in Table A.1. However, there are some individuals who I would like to thank specifically for their kindness and the contribution they made to my research and to my positive experience of the research community. In alphabetical order: Prof. Alexander Agandjanian, Mr. Thomas Engel, Dr. Mihai Gasparic, Dr. Thomas Keller, Dr. Lázló Kordos, Mr. Stéphane Madelaine, Dr. Jadranka Mauch-Lenardić, Dr. Lutz Maul, Prof. Adam Nadachowski, Dr. Doris Nagel, Mr. Alexandru Petculescu, Dr. Gernot Rabeder, Prof. Leonid Rekovets, Prof. Benedetto Sala, Mr. Pawel Socha, Dr. Alexey Tesakov, Dr. Borut Toškan, and Prof. Thijs van Kolfschoten.

The members of staff at the Natural History Museum, London, have provided a friendly, open, enquiring, and encouraging environment during my research. Some of the many I would like to mention include, in alphabetical order, Mr. Mark Lewis, Mr. Simon Parfitt, Dr. John Stewart, and Prof. Chris Stringer. Special thanks also go to Mr. Harry Taylor of the photography unit at the NHM for his advice and time.

The staff and students of Royal Holloway College, University of London, Department of Geography have always been available with friendship and advice. Some of the many I would like to mention include, in alphabetical order, Dr. Ian Candy, Dr. Caroline Juby, Dr. Alison Macleod, Dr. Ian Matthews, Dr. Dora Moutsiou, and Prof. Jim Rose

I am grateful to the following individuals for the loan of fossil material from their private collections: Mr. John Clayden, Ms. Maud Gransard, Prof. Wolf-Dieter Heinrich, Prof. Danielle Schreve, and Dr. John Stewart.

Lastly, but most importantly, I could not have carried out or completed this thesis without the support of my wife Mary, who has endured many privations in the course of my research, yet she has remained my steadiest companion and most vocal supporter throughout. I dedicate this thesis to Mary and to our daughter Irma, who arrived in this world during Chapter 4.

Chapter 1

Introduction

Water voles are a group of rodents that straddle the palaeontological and neontological study of species. They have an indistinct origin in the Early Pleistocene but from the Middle Pleistocene to the Holocene a rich fossil record chronicles the evolution of a single lineage, from the extinct species *Mimomys savini* to the younger fossil and extant genus *Arvicola*. Modern species are ecological generalists, being fossorial and semi-aquatic inhabitants of a wide range of environments in much of Eurasia (e.g., Reichstein, 1982d; Gromov and Polyakov, 1992). Despite conservatism in their gross morphology, water voles exhibit a degree of intraspecific variation that has led to the recognition of numerous subspecies, both in Recent and fossil representatives (e.g., Hinton, 1926).

Morphological variation is present geographically and temporally and the latter has given fossil water voles prominent status in Pleistocene studies because of the difficulties in dating sedimentary deposits during this geological period. The evolution of the dentition of the water vole is sufficiently rapid to allow morphological change in the lower first molar (M_1) to be used as a practical biostratigraphic tool (e.g., Heinrich, 1978), however, there is empirical spatial and temporal patterning in the evolution of this character that can disrupts long-distance correlations based on the water vole M_1 (e.g., Paunescu *et al.*, 2004; Maul and Markova, 2007). This appears to reflect the presence of intraspecific lineages (Kolfschoten, 1992; Maul *et al.*, 1998a) and correlations between environmental factors and morphology (Röttger, 1987). There are also difficulties independently dating fossil water vole assemblages to calibrate the 'vole clock'. Furthermore, differences in research methodology between workers may limit comparability between studies (Parfitt pers. comm., 2008).

This thesis gathers together a spatially broad and temporally deep dataset that aims to explore morphological variation at the level of the species, lineage, population, and individual. The study takes an initial sample of over 4 000 digital photographs of M_1 teeth and concludes with a dataset of 2 269 molar shapes and 1 275 individual SDQ measurements that are used to assess the variation associated

with ontogeny, geography, and geological time.[1] The study includes samples from across the western Palaearctic—from Azerbaijan to Scotland, and from Spain to the White Sea in northwest Russia—and stretches from the Recent to the Brunhes-Matuyama palaeomagnetic boundary (around 780 k yr BP). Using these data, an attempt is made to improve the understanding of the evolution of the water vole. This is done by testing the methodology used to describe the morphology of the M_1 tooth in terms of the prevalent metric of evolutionary change, the enamel thickness quotient or SDQ, and occlusal shape. The availability of molecular phylogenies for the group is significant (Taberlet *et al.*, 1998; Piertney *et al.*, 2005; Brace, 2010) and allows hypotheses of relationships based on morphology to be compared and tested against robust models of phylogeny. The morphological perspective of the palaeontologist can therefore be linked with the genetic perspective of the molecular biologist. Many studies using ancient DNA are now showing levels of intraspecific diversity in contemporary and extinct populations to be far greater than previously understood (Shapiro *et al.*, 2004; Barnes *et al.*, 2007). Yet to small-mammal palaeontologists such subspecific structuring is familiar, albeit difficult to define precisely. The combined issues of identifying and delimiting boundaries between intraspecific groups and the rate of morphological change across groups lie at the heart of the study of the water vole.

[1] The images and morphometric data used in the thesis can be found in Appendix C.

Chapter 2

Taxonomy and systematics

Water voles are a group of large Palaearctic voles (Class Mammalia, Order Rodentia) comprising extant and fossil members of the genus *Arvicola*, and the fossil species *Mimomys savini*. This chapter evaluates the history and methodology of the taxonomic and systematic study of the group, the aim being to highlighting issues and uncertainties surrounding the evolution of the group that provide structure to the thesis. This study is not a systematic one, and so will not attend in detail to nomenclatural issues, rather the focus is on pattern and process in the evolution of the water vole, and the data used investigate and document evolution. Attention is paid to characteristics of the dentition, in particular the lower first molar (the M_1), because these elements are well preserved in the fossil record and can be recognised in both extant and fossil specimens. Nevertheless, it is important to give recognition to other attributes such as the cranial and post-cranial skeleton, pelage colour, ecological preferences, and genetic structure, that are employed in the classification of extant *Arvicola* in order to understand biology, ecology, phylogeny, and biogeography as fully as possible.

2.1 History

2.1.1 Research

2.1.1.1 Extant water voles

All extant voles, along with many other rodents, were first grouped within the genus *Mus* by early natural philosophers (Kretzoi, 1990). The first recorded description of the water vole was by Linnæus (1758) under the name *Mus amphibius* (Miller, 1912; Hinton, 1926; Kretzoi, 1990). This record was based upon the writings of John Ray, which, according to Miller, was '. . . nothing more than a figment of the imagination based on Ray's misconception that there is a large aquatic vole with webbed feet' (Ray, 1693, cited in Miller, 1896, p. 11). R. F. Hensel (1855,

1856, cited in Kretzoi, 1990) recognised the taxonomic potential of molar tooth morphology, and by the end of the 18th century workers were revising the classification of Linnæus and recognising voles as a distinct group (Kretzoi, 1990). The genus name *Arvicola* was first used for the water vole by the French naturalist and politician Comte de Lacepède (Comte de Lacepède, 1799, *Tableau des divisions, sous divisions, ordres et genres des mammifères, amphibius*, p. 10). Gray (1821) formed the distinct group Arvicolidae on morphology of molar teeth, noting '...grinders prismatic, with a flat top, entirely composed of vertical lamina, soldered by a vertical substance' (Gray, 1821, p. 303). Gray's ideas were eventually accepted and the voles and lemmings were grouped and elevated, either as a distinct family or a subfamily, within the murids or cricetids. Debate arose, however, around synonymy of *Arvicola* with *Microtus* and as a result the use of Microtidae, Microtinae or Microtini gained prevalence in the literature as the collective name of the voles and lemmings for many decades (e.g., Miller, 1896; Hinton, 1926; Ellerman, 1940; Simpson, 1945; Corbet, 1978).

The full generic status of *Arvicola* as a natural group distinct from *Microtus* was rapidly established following the work of Miller (1912) and Hinton (1926). Hinton (1926) noted that in '... [sweeping] away the more or less artificial systems of his predecessors', Miller initiated a general process of condensing a confusing arvicolid taxonomy; one that had inflated to more than a hundred genera and subgenera and over a thousand species and subspecies by the turn of the 20th century (Kretzoi, 1990). This process was driven by a move away from a typological taxonomy to one based on biological theory. In the taxonomy of Miller (1912) fourteen species and subspecies were listed within the genus *Arvicola*. This was derived in part from the recognition of synonymy between *Arvicola* and four other previously recognised extant western European genera of voles. The number of species and subspecies of water vole recognised in many 20th century taxonomies remained substantial, however: Hinton (1926) cited nineteen species, Ellerman (1940) listed four species and twenty-nine subspecies, and Corbet (1978), in a review of earlier literature, listed no fewer than sixty-two species and subspecies. Not until the detailed morphological work of Reichstein (1963) and Corbet *et al.* (1970), and the cytological data provided by Matthey (1957, 1958), did it become clear that only two extant groups could be securely defined as biological species (*sensu* Mayr, 1963): namely *Arvicola terrestris* Linnæus 1758 and *Arvicola sapidus* Miller 1908.

2.1.1.2 Fossil water voles

Fossil arvicolids have appeared in the literature since the early part of the 19th century (e.g., Buckland, 1823; Cuvier, 1824). Croizet and Jobert (1828), Münster

(1833), and Owen (1846) described and allied fossil voles with the neontological genus *Arvicola* as was understood at that time. Giebel (1845, 1847, and 1851, cited in Heinrich, 1990a) was apparently the first to record fossil water vole as '*Hypudaeus amphibius*' (= *A. terrestris*) from the Quaternary deposits at Seveckenberg in Saxony, Germany (Heinrich, 1990a). E. T. Newton was the first worker to formally resolve a difference between fossil and Recent *Arvicola* by erecting the new species *intermedius* for water voles from the 'preglacial' (i.e., early Middle Pleistocene) deposits of East Anglia (Newton, 1881, cited in Hinton, 1910). Miller (1896) considered the use of rooted and unrooted molars as taxonomically significant (Kretzoi, 1990) and proposed the creation of separate genera for 'early *Arvicola*' species. This stimulated Forsyth-Major to erect the genus *Mimomys* to contain 'all those voles with rooted molars which are clearly different from *Evotomys*, *Phenacomys* and *Dolomys*' (Hinton, 1926, p. 350).

A similar trend for taxonomic profusion occurred in the naming of fossil taxa as happened with extant forms. Kretzoi (1965), however, instigated a new period in the study of the evolutionary history of the water vole by synonymising many species of the genus *Mimomys* together in the single species *Mimomys savini*. The basal species of *Arvicola* quickly followed suit under the name *Arvicola cantiana* (Sutcliffe and Kowalski, 1976). Later work has focussed on quantification of evolutionary trends within water voles (e.g., Heinrich, 1978), with consequent biostratigraphic applications (e.g., Maul *et al.*, 1998a), and on palaeoecological and palaeoenvironmental research (e.g., Chaline *et al.*, 1993)

2.1.2 Origins

2.1.2.1 The voles and lemmings

Molecular and morphological evidence shows the voles and the lemmings to be a monophyletic group of rodents—the family Arvicolidae *sensu* Reichstein (1982c)—descendant from Late Miocene or Early Pliocene cricetid-like ancestors in Europe and North America (Repenning, 1968; Chaline, 1987; Chaline *et al.*, 1999). Resolving historical relationships within the group has proven difficult because polytomies are persistant features of phylogenies derived from extant taxa (Chaline and Graf, 1988; Conroy and Cook, 1999; Martin *et al.*, 2000), but many authors suggest these patterns reflect abrupt, discrete pulses of cladogenesis driven by large-scale shifts in the climate system around 5–3 M yr BP for arvicolids in general and 2 M yr BP for *Microtus* (Repenning *et al.*, 1990; Vrba, 1993; Conroy and Cook, 1999; Maul *et al.*, 2007). Certainly the arvicolids rapidly spread across the Holarctic in a series of expansions that constitute some of the most explosive mammalian diversifications known (Chaline *et al.*, 1999). The success of the group has been linked to the development of a series of profound modifications

to the teeth and skull that enable arvicolids to exploit a diet of coarse vegetation (Hinton, 1926; Repenning, 1968; Chaline *et al.*, 1999). The appearance of these features is coincident in the fossil record with the expansion of grasslands, which suggests that arvicolids, along with other mammalian groups such as horses (Hulbert, 1993), evolved in response to the rise of grasses to form a major component of the grazing fauna.

2.1.2.2 The water vole

The extant water vole—genus *Arvicola*—is generally considered to descend from the large, early Middle Pleistocene vole species *Mimomys savini* (e.g., Hinton, 1926; Heim de Balsac and Guislain, 1955; Chaline, 1972; Koenigswald, 1973; Kolfschoten, 1993b; Neraudeau *et al.*, 1995; Koenigswald and Kolfschoten, 1996; Maul and Markova, 2007; Maul and Parfitt, 2010). Evidence for this relationship comes from the shared gross morphology of the molars (Figure 2.3) and the co-occurrence of molars with characteristics found in *Mimomys* (such as roots) alongside molars with characteristics found in *Arvicola* (such as lack of roots) in a number of late Middle Pleistocene European fossil faunas (e.g., Fejfar, 1961; Sala, 1983). These assemblages are considered to be evolutionary 'snapshots' that show populations in transition between rooted and unrooted conditions.

A number of other models for the origins of *Arvicola* exist including a polyphyletic *Arvicola* with *A. sapidus* and *A. terrestris* derived from *M. savini* and *M. milleri* respectively, and a Siberian origin for *A. terrestris* from the species *Cromeromys intermedius* (Kolfschoten, 1993b).

2.2 The lower first molar: a model system for evolutionary studies

This study will use the morphology of the lower first molar (M_1) to investigate evolution in the water vole. Although the upper third molar (M^3) has received some attention, the M_1 has been the main structure of choice used in palaeontological research of the water vole for many years (e.g., Schmidtgen, 1911; Hinton, 1926; Kretzoi, 1965; Heinrich, 1978; Agadjanian, 1983; Röttger, 1987; Masini *et al.*, 2003; Escudé *et al.*, 2008a) because it is easily identifiable to genus level, is plentiful in the fossil record, presents a fairly complex but easily accessible morphology for analysis, and shows a range of morphological trends and variation. A long history of research has left a rich legacy of fossil and modern water vole M_1s in museum and university collections, offering a large dataset of readily accessible material that no other part of the skeleton can match. This is significant because morphological change is often small over Quaternary timescales (Lister, 1992) and water vole M_1 morphology can be extremely variable (e.g., Nadachowski, 1982), meaning that large sample sizes are highly desirable in order to adequately characterise variation within a population (Caumul and Polly, 2005).

The use of the M_1 is not only practically attractive and allows continuity with the existing literature, it also provides a theoretically strong model system for phylogenetic studies. The morphology of a tooth is determined early in development (Hillson, 1986; Jernvall *et al.*, 2000) and does not change shape after eruption, save through wear (see Section 2.2.3). This suggests that the morphology of the M_1 should contain a high proportion of genetically determined, phylogenetically significant information compared with other parts of the skeleton such as the mandible, which may be subject to remodelling through ecophenotypic effects (Lister, 1992; Polly, 2001; Caumul and Polly, 2005). Empirically there is a good deal of evidence to suggest that this is the case, and molar morphology has been used previously to investigate evolution both at the inter- and intra-specific level: Zejda *et al.* (1994) used a large dataset of M_1 (6865 mandibles) and M^3 (6600 maxillae) of *Clethrionomys glareolus* from Austria and the Czech Republic to investigate population-level molar morphology to detect morphological differences between populations; Polly (2001, 2003) used the M_1 to investigate palaeophylogeography in races of extant and fossil European *Sorex araneus* and concluded that there were strong, but temporally limited, correlations between morphological and molecular divergence; and Caumul and Polly (2005), in a study of morphology and phylogeny in extant species of Palaearctic marmot, found that M_3 shape was able to recover the main phylogenetic groupings indicated by *cytb* mtDNA.

2.2.1 The morphology of the M_1

Figure 2.1: Occlusal-lingual view of a right M_1 of *Arvicola*. Scale bar = 2 mm.

The M_1 is positioned at the front of the molar row, behind a diastema. It is a high-crowned tooth formed from opposing triangles (also referred to as prisms or fields) of dentine bounded by a layer of enamel (Figures 2.1, 2.2). This gives the tooth a distinctive 'christmas tree'-like occlusal outline consisting of a trefoil shaped anteroconid complex (ACC), five alternating triangles or prisms (T1–T5), and a posterior loop (PL; Figure 2.2a). The occlusal surface is created by continuous wear on the crown (Section 2.2.3) caused partly through abrasion by hard material present in food (e.g., phytoliths), but mainly by tooth-on-tooth attrition (Rensberger, 1973; Koenigswald, 1982a; Massey *et al.*, 2007). Projecting prisms may also be referred to as salient angles, anticlines or folds; spaces inbetween are described as re-entrant angles, valleys, infolds or troughs. The faces of prisms in lower molars are concave mesially and convex distally while in upper molars the reverse is true. Dentine fields within triangles may be fully or partially closed by the re-entrant angles of opposing enamel prisms (e.g., T3 in Figure 2.2a). Deposits of cementum can be found in the re-entrant angles.

The nature of the contact between opposing upper and lower sets of molars is determined by the morphology of the mandible and its propalinal motion against the maxillary teeth. The ACC is highly variable in size and shape relative to the rest of the M_1 (e.g., Nadachowski, 1982), with many fossil and some extant forms displaying a small additional triangle—the *Mimomys*-fold—in BRA3 (Figure 2.2c). Many specimens of *Mimomys* also exhibit a small isolated pit of enamel, the 'enamel island', within the ACC, close to BRA3 (Figure 2.2c). This pit is the surficial expression of a closed fold that may penetrate deep into the lower part of the molar.

In extant water voles the M_1 is rootless and ever-growing but early Middle Pleistocene forms possess roots of varying degrees of development. A *linea sinuosa* marks the junction between the dentine of the tooth and the enamel of the crown (Figure 2.3).

2.2.2 Study approach

The occlusal surface is realistically the only feature of the M_1 that can be recruited for use in evolutionary studies. This is because it is the only morphologically

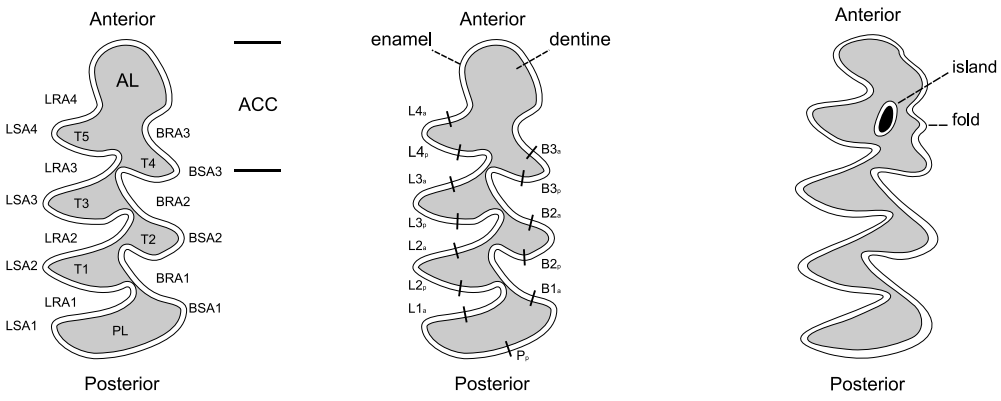

(a) (b) (c)

Figure 2.2: Graphical representation of the occlusal surface of the water vole M_1 showing dentine fields (grey) and enamel layers (white). (a) Terminology applied to the M_1 based on and modified from Heinrich (1978) and Van der Meulen (1973): ACC, anteroconid complex; AL, anterior lobe; PL, posterior lobe; BRA1–3, buccal reentrant angles; LRA1–4, lingual reentrant angles; BSA1–3 buccal salient angles; LSA1–4, lingual salient angles; T1–5, crown triangles. (b) Locations of enamel thickness measurements following Heinrich (1982) but with only one PL trailing edge measurement used (see Section 4.2.4). Terminology for enamel layers devised for this study: buccal (B), lingual (L), and posterior (P) edges; anterior (or leading) edges, subscript a; posterior (or trailing) edges, subscript p. (c) Generalised morphology of the M_1 of *Mimomys savini*, showing an 'enamel island' and *Mimomys*-fold. Right M_1 tooth shown, not to shared scale.

complex part of the M_1 shared by both *Mimomys* and *Arvicola*. Studies of the occlusal surface fall into one of two camps: i) occlusal shape and features of the occlusal surface, and ii) studies of enamel thickness.

2.2.2.1 Occlusal shape

Qualitative descriptions In studies of *Mimomys* and early populations of *Arvicola* the *Mimomys*-fold and 'enamel island' are often used as presence-absence characters or their degree of development is scored (e.g., Maul *et al.*, 2000), and such measures are useful indicators of plesiomorphy and ontogenetic age.

In terms of the gross shape of the occlusal outline reference can be made to the extent of development of the reentrant angles or the degree of confluence between dentine fields (e.g., Ventura, 1991). Nadachowski (1985) used this approach to characterise three morphotypes—'*milleri*', '*majori*', and '*savini*'—based on the level of development of BRA3 and LRA4 in the analysis of the *Mimomys* and *Arvicola* faunas of Kozi Grzbiet, Poland.

Quantitative measurements Quantitative analysis of the occlusal surface has in the main been through traditional morphometrics, although Marcolini (2006) and Escudé *et al.* (2008b) adopted a novel approach in using Fourier analysis to investigate the whole of the M_1 outline. Size has been quantified in terms of the length and width of the tooth. Shape has been described either by the use of ratios such as A/L (the ratio of ACC to tooth length; Van der Meulen, 1973), which expresses the relative size of the front part of the M_1 (e.g., Heinrich, 1990b; Ventura, 1991; Maul *et al.*, 1998b), or by the angles subtended between enamel prisms (e.g., Rekovets, 1990).

2.2.2.2 Enamel thickness

Differences in the thickness of enamel bounding distal and mesial faces of enamel prisms (Figure 2.2b) has been the most widely used metric in palaeontological studies of the water vole. *Mimomys* and early forms of *Arvicola* from the Middle Pleistocene posses thicker trailing enamel edges of lower molars than their complementary leading edges (*Mimomys*- or negative-differentiation), a state that is reversed in extant populations of *A. terrestris* from Western Europe (*Microtus*- or positive-differentiation; e.g., Hinton, 1926; Martin, 1987; Röttger, 1987). The terms trailing and leading edge are often used for the distal and mesial edges of enamel prisms respectively as they relate the face of the salient angle to the propalinal movement of the jaw during mastication (Koenigswald, 1982a). Koenigswald (1973) noted a gradual temporal change from the *Mimomys*- to *Microtus*-differentiation, a transition that was quantified in a number of papers by

Heinrich as the *Schmelzbanddifferenzierungsquotient* (enamel differentiation ratio) or SDQ, the ratio of the thickness of the trailing to leading enamel bands multiplied by 100 (Equation 2.1; Heinrich, 1978, 1982, 1987, 1990b).

$$\text{SDQ} = 100.\frac{\text{trailing edge thickness}}{\text{leading edge thickness}} \tag{2.1}$$

The SDQ can be calculated for each individual specimen (SDQ_i) or for a population (SDQ_p) but methodological differences exist in the measurement of the SDQ between workers. Markova (1982) used a metric she termed 'k', the inverse of Heinrich's SDQ (i.e., leading/trailing enamel multiplied by 100). Some authors measure enamel in the manner of Heinrich (1978), from all seven triangles of the M_1 (e.g., Maul *et al.*, 1998a; Maul and Parfitt, 2010). Others still have used the ratio between enamel from three (e.g., Rekovets, 1990; Markova, 1998) or just one (LRA4, Röttger, 1987) enamel prism. Measurement technique of individual researchers also appears to play some part in the enamel thicknesses obtained (Parfitt, pers. comm., 2008).

2.2.3 Ontogenetic changes

2.2.3.1 Tooth shape

The morphological changes that take place in the M_1 during the life of an individual have been recognised since the beginnings of serious study of the group (Miller, 1912; Hinton, 1926; Chapter 5). On eruption the M_1 is bunodont but as the crown grows, molars from the opposing jaw come into contact and the flat occlusal surface characteristic of the vole molar forms through erosion (Miller, 1912; Hinton, 1926; Figures 2.3 and 2.4). Because the uppermost parts of the crown differ in cross-sectional shape and internal structure with respect to the lower parts, as erosion and growth of the tooth continues novel occlusal morphologies are constantly being exposed. These trends include:

- Progressive expansion of dentine fields—in particular of the anterior lobe—with respect to the total size of the tooth (Figure 2.4)
- Curvature of the edges of enamel triangles (Miller, 1912; Figure 2.4 b–c)
- Thickening of anterior relative to posterior enamel walls (Kratochvíl, 1980)

These changes can be found in both *Arvicola* and *Mimomys* but in *Mimomys*, because the morphology of the ACC may be highly convoluted, attritional wear may additionally generate an enamel fold (the *Mimomys*-fold) or an 'enamel island' in the anterior part of the M_1 (Figure 2.2c). Folds can be found in geologically

older specimens of *Arvicola* (e.g., Maul *et al.*, 2000) but these features become progressively reduced or may disappear with increasing ontogenetic age of the tooth (e.g., Koenigswald, 1982b). Further ontogenetic changes in the molars of *Mimomys* relate to differential development of the root and *linea sinuosa*, and the height of the crown. Roots either do not appear until later in ontogeny or become increasingly well-developed with age, and the maturation of the root signals an end to crown growth, meaning that tooth wear may eventually cause the crown to shorten after its early increase in height. This is in contrast to the ever-growing molars of *Arvicola*, which remain high-crowned throughout life.

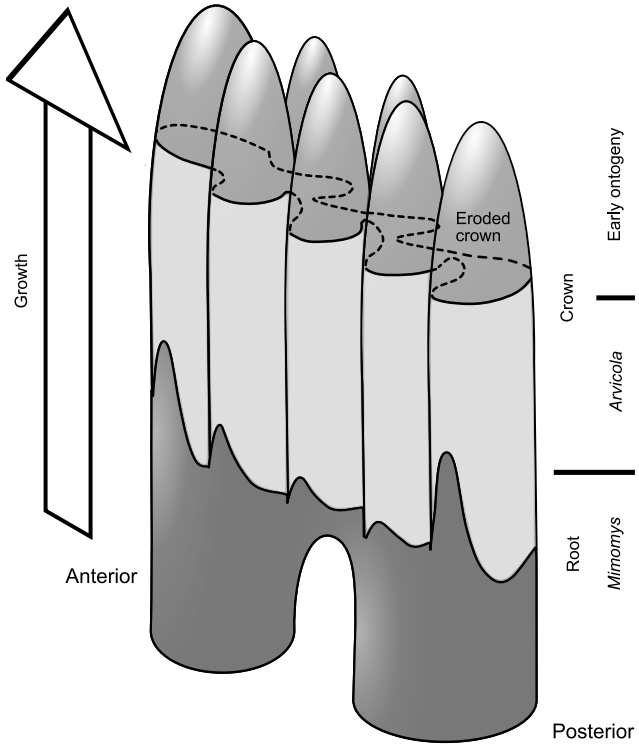

Figure 2.3: Schematic representation of a right M_1 tooth of the water vole in postero-labial view. At the base of the tooth, roots are only present in *Mimomys* and early populations of *Arvicola*, while the loss of roots and continual growth of the tooth crown characterises *Arvicola*. The *linea sinuosa* marks the boundary between tooth dentine and the enamel-covered crown. On eruption the tooth is bunodont but because the crown is continually eroded by attritional wear a flat occlusal surface is produced.

2.2.3.2 Enamel thickness

Kratochvíl (1980), in a study of Recent *Arvicola terrestris* from central Europe, observed that all enamel layers become thicker during development. Furthermore, young individuals in the first few weeks of life away from the nest (>3 weeks old

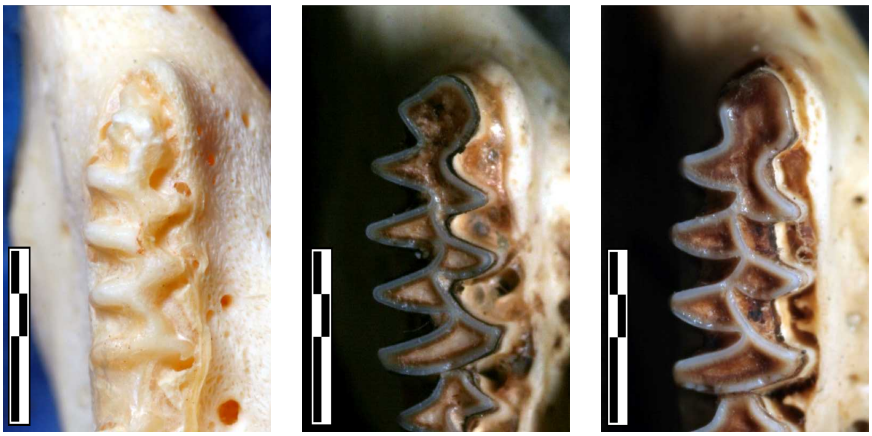

(a) (b) (c)

Figure 2.4: Examples of M_1 shape change through ontogeny. a) an M_1 very early in ontogeny, probably from an individual just a few days old, the occlusal surface is yet to be worn (Specimen 1085, Museum ref - HAZM 27.6388); b) age-class 2, a few weeks or months old (Specimen 454, Museum ref - NHML 66.4376); c) an adult (Specimen 457, Museum ref - NHML 66.4378). All specimens are modern *Arvicola* from southern England. Scale bar = 2 mm.

Corbet and Harris, 1991) show SDQ >100, i.e., thicker posterior than anterior enamel. These enamel thickness patterns reverse with age, such that older individuals possess SDQ values that stabilise at <100. These changes have important implications for the application of metrics such as the SDQ in studies of evolution and biostratigraphy (Heinrich, 1982) and is explored in greater depth in Section 5.4.

2.3 Systematics

A feature of the systematic study of the water vole has been the large numbers of species, subspecies, and chronospecies attributed to the group. This is, in the main, an artificial phenomenon caused by historical taxonomic hangovers, or investigators from different taxonomic traditions or contrasting research interests—perhaps working in geographic isolation—perceiving higher levels of species diversity than actually exists. Kretzoi (1990) asserted that this taxonomic inflation hindered research and understanding of the evolution of the water vole. This certainly seems the case but it is partly understandable—and intriguing—because water voles do display high levels of morphological variation in time and space, and extant populations possess varied and plastic ecologies.

This systematic review provides an historical background to the study of evolution of the water vole and places the systematics of the group within a framework of evolutionary theory. The intention is to give an appreciation of the systematic approaches taken in the study of the water vole, and to illustrate the diversity—both real and artificial—present in the group. Although water voles are widely distributed across the Palaearctic, the review is restricted to the area of interest of the study, the western Palaearctic, and is limited to extinct and extant members of the genus *Arvicola* and its supposed immediate ancestor *Mimomys savini*. The describing author and year of description of a species is given where known, as well as the type locality and published geological age for fossil forms. If unknown at the time of writing, these details are marked by a '?'.

2.3.1 Extant forms

Class Mammalia LINNÆUS 1758
Order Rodentia BOWDICH 1821
Family Arvicolidae GRAY 1821
Genus *Arvicola* LACÉPÈDE 1799

Synonyms *Alviceola* BLAINVILLE 1817, *Hemiotomys* DE SÉLYS-LONGCHAMPS 1836–1862, *Ochetomys* FITZINGER 1867, *Paludicola* BLASIUS 1857, *Praticola* FATIO 1867

Type Species *Mus amphibius* LINNÆUS 1758

Diagnosis

Size Relatively large voles, head and body length 120–220 mm, condylobasal length 32–44 mm, hind-foot length 22–35 mm (Ellerman, 1940; Boyce, 1991; Reichstein, 1982a,b). Sexual dimorphism in *Arvicola* is limited to body size, with females 80–100% the size of males (Reichstein, 1982b).

Skull and mandible The skull is robustly built and continues to grow into adulthood, becoming angular and ridged. There is a strong jaw musculature and the associated muscle attachment areas are correspondingly well-developed. Alveolar capsules deeply penetrate the floor of the orbits and braincase as well as the mandible. In the lower jaw, capsules are displaced either side of the lower incisors to produce swellings on the lateral surfaces of mandibles, which in adults give mandibles a sturdy appearance. A long diastema is present from the incisors to the molars, and is highest immediately behind the incisors. The mandible is thick, deep and robust (Hinton, 1926; Reichstein, 1982d).

Incisors Incisors are persistently growing and typical for rodents in general, being formed of a thin buccal layer of enamel covering a core of dentine. Upper incisors can be orthodont or pro-odont—characteristics that have been related to semi-aquatic and fossorial ecologies respectively (Hinton, 1926; Montgomery, 1975)—but always more strongly recurved than lower incisors. Orthodont incisors may be flattened meso-distally, in contrast to rounder cross-sections in pro-odont teeth (Hinton, 1926).

Molars Molars are high-crowned (hypsodont) and rootless (arhizodont), and persistently grow throughout life (hypselodont). Wear to the occlusal surfaces of molars reveal a cross-section of alternating or opposing lateral triangles of dentine encircled by a thin sheet of enamel (e.g., Figures 2.1, 2.2, 2.3 for the M_1).

The M^1, M^2, M_2 and M_3 are morphologically conservative in occlusal shape between species (Hinton, 1926; Thaler, 1962; Chaline, 1972). The M_1 and M^3 are morphologically variable (Section 2.2) but have not been employed in classification of extant forms. A detailed description of the morpohology of the M_1 can be found in Section 2.2.1.

Karyotype and genotype In contrast to the polymorphisms and polytypisms present in the chromosomes of *Microtus* (Zima, 2004), *Arvicola* is notable in only possessing two different karyotypes: 2n=40 in *Arvicola sapidus* and 2n=36 in *Arvicola terrestris*. mtDNA studies of the genus show *A. sapidus* to be ancestral with respect to *A. terrestris*, with a most recent common ancestor around 3 M yr BP (Taberlet *et al.*, 1998). At least three lineages of *A. terrestris* exist in Europe: an Italian lineage (Taberlet *et al.*, 1998), and 'western' and 'eastern' European

lineages (Taberlet *et al.*, 1998, Piertney *et al.*, 2005; Brace, unpublished).

Remarks *Arvicola* is morphologically and ecologically close to the genus *Microtus* SCHRANK 1798 (Musser and Carleton, 1993), a cause of much systematic debate during the 19th century and early 20th century centuries (Kretzoi, 1990). Two extant species are now strongly supported by genetic data: *A. terrestris* (LINNÆUS 1758) and *A. sapidus* MILLER 1908. A third species, '*richardsoni*', from northwestern North America, has been included by some authors (e.g., Miller, 1896; Nowak and Paradiso, 1983), however, molecular, morphological, and distributional data show this taxon to be a member of *Microtus* (Reichstein, 1982d; Musser and Carleton, 1993, p. 528 and references therein). *Arvicola* is, therefore, an entirely Old World genus.

The genus displays a high degree of morphological and ecological variability but Heim de Balsac and Guislain (1955), Reichstein (1963), and Corbet *et al.* (1970) showed that many of the forms of *Arvicola*, referred to by Miller (1912) and Hinton (1926) either as species or subspecies, cannot be quantitatively separated from one another in a range of cranial characteristics, and therefore it was argued that they do not constitute distinct species. Most workers continue to employ a small number of named forms or subspecies within *A. terrestris* and *A. sapidus*, either pragmatically as means of communication or more formally to imply some biologically significant point.

Arvicola sapidus MILLER 1908. Ann. Mag. Nat. Hist. 8, p. 195 (Santo Domingo de Silos, Burgos, Spain).

Named forms From Ellerman, 1940; Corbet, 1978; Reichstein, 1982a; Musser and Carleton, 1993

musiniani LATASTE; ?; ?
tenebricus MILLER 1908; Biarritz, Basses-Pyrenees, France

Distribution Most of Iberia and western France and can be found from sea-level to over 2000 m altitude in the Pyrenees and the Sierra Nevada (Reichstein, 1982a).

Diagnosis

Size Large size. In adults, body length over 46 mm and weight over 100 g, hind-foot length 30 mm. Skull angular, condylobasal length always over 36 mm.

Inter-orbital area always over 21 mm (Reichstein, 1963, 1982a; Corbet, 1978).

Skull and mandible Nasals almost as broad as rostrum anteriorly, always over 4.6 mm long and narrowing rapidly posteriorly. *Foramen mandibulare* situated above the swelling of the I_1 canal (Reichstein, 1982a).

Dentition Uppper incisors orthodont. Molars very high-crowned. Lower molars form a pronounced wedge in lingual view. M_1 triangles superficially more rounded than in *A. terrestris*. M^3 predominantly with two closed triangles (>96%, n = 127: Reichstein, 1982a). Maxillary tooth row >10 mm, (Reichstein, 1963; Corbet, 1978). Enamel thickness SDQ $\approx$ 120 (Röttger, 1987)[1]. M_1 with strongly developed enamel, no erosion present at front of ACC as in some *A. terrestris*.

Karyotype 2n = 40 (Matthey, 1955)[2].

Remarks *A. sapidus* is a large vole, less variable in size and morphology than *A. terrestris*, and exclusively semi-aquatic; found from brackish water, rivers, canals, and lakes (Reichstein, 1982a). In the Pyrenees *A. sapidus* overlaps with populations of fossorial *A. terrestris* but the two species are ecologically segregated (Miller, 1912) and *A. terrestris* is much smaller in size in these areas (Röttger cited in Kolfschoten, 1990). Two subspecies, *sapidus* and *tenebricus*, have been proposed, *tenebricus* being a dark coloured form recognised by Miller in the Pyrenees and the coast of southwest France (Miller, 1912). However, this division cannot otherwise be morphologically supported and Centeno-Cuadros *et al.* (2009) found no molecular evidence for such intraspecific groups.

[1]Note that Röttger (1987) derived this SDQ value from a single M_1 triangle, LRA4. See Section 2.2.2.2

[2]Not 2n = 60 as stated in Gromov and Polyakov (1992, p. 348)

Arvicola amphibius (LINNÆUS 1758), Syst. Nat. 10, p. 61 (Uppsala, Sweden)

Named forms From Hinton, 1926; Ellerman, 1940; Corbet, 1978; Reichstein, 1982b; Gromov and Polyakov, 1992; Musser and Carleton, 1993

abrukensis REINWALDT 1927; West Isles, Estonia
albus BECHSTEIN 1801; Strasburg, Germany
americana GRAY 1842; ?
amphibia ?; ?
amphibius LINNÆUS 1758; England
aquaticus CUVIER 1817; ?
argentoratensis DESMAREST 1822; ?
argyropus CABRERA 1901; Persia
armenius THOMAS 1907; ?
arvalis ?; ?
ater BILLBERG 1827; ?
barabensis ?; ?
brigantium THOMAS 1928; Huddersfield, England
buffonii FISCHER 1829; ?
cantabriae VENTURA & GOSÁLBEZ 1989; Cantabrian Mountains, Spain
canus BECHSTEIN 1801; ?
castaneus DE SÉLYS-LONGCHAMPS 1845; ?
caucasicus OGNEV 1933; Vladikawkas, Caucasus
cernjavskii PETROV 1949; Ponot, Stara Planina Mountains, Former Yugoslavia
destructor SAVI 1839; ?
djukovi OGNEV & FORMOZOV 1927; Daghestan
exitus MILLER 1910; St. Gallen, Switzerland
fuliginosus DE SÉLYS-LONGCHAMPS 1845; ?
ferrugineus OGNEV 1950; Northern Russian coast
hintoni AHARONI 1932; Northern Syria
hyperryphaeus ?; ?
illyricus BARRETT-HAMILTON 1899; Bosnia
italicus SAVI 1839; Pisa, Italy
karatshaicus; ?; ?
korabensis MARTINO 1937; Korab Mountains, Former Yugoslavia
kuruschi HEPTNER & FORMOZOV 1928; Aul Kurusch, Daghestan
littoralis BILLBERG 1827; ?
martinoi PETROV 1949; Belgrade, Former Yugoslavia

meridionalis OGNEV 1923; Tscherepinski Kanal, Ural Region, Russia
minor DE SÉLYS-LONGCHAMPS 1845; ?
monticola DE SÉLYS-LONGCHAMPS 1838; St. Bertrand de Comminge, Hautes-Pyrénées, France
musignani DE SÉLYS-LONGCHAMPS 1839; Rome, Italy
niger LINNÆUS:1788 1788; ?
nigricans DE SÉLYS-LONGCHAMPS 1845; ?
obensis ?; ?
ognevi TUROV 1926; Kalakai Village, North Ossetien, Caucasus
pallasii OGNEV 1913; Northern Urals
paludosus LINNÆUS 1788; ?
persicus DE FILIPPI 1865; Sultanieh, South Elburz, Iran
pertinax SAVI 1839; ?
reta MILLER 1910; Aberdeen, Scotland
rufescens SATUNIN 1908; Podkumok, Karacai Territory, N. Caucasus
scherman SHAW 1801; Strasburg, Germany
scythicus THOMAS 1914; Southern Kazakhstan
stankovici PETROV 1949; Suvo Rudiste, Kapaonik Mountains, Former Yugoslavia
tanaiticus KALABUCHOW & RAJEWSKIL 1930; Donez Region, Russia
terrestris LINNÆUS 1788; Uppsala, Sweden
uralensis ?; ?
volgensis OGNEV 1933; Volga Delta, Russia

Distribution Northern Iberia and Europe - excluding southern and western France, far northern Finland, southern Greece, and Ireland; Eurasia; Asia Minor; Palestine; Zagros mountains (and beyond the western Palaearctic across northern Tien Shan; Siberia almost to the Pacific coast). Recorded up to 2400 m in the Alps.

Diagnosis

Size Highly variable in size. Condylobasal length 30–45 mm, body length (without tail) up to 234 mm, weight 120–320 g. British forms are the largest extant examples of the species.

Skull and mandible Nasals always narrower than rostrum. *Foramen mandibulare* situated laterally to the the mandibular swelling caused by the I_1 canal . The skull of older individuals becomes angular and developed with ridges at places of jaw muscle attachment, such as the interorbitals (Hinton, 1926).

Dentition Upper incisors orthodont or pro-odont. Molars: maxillary tooth row <10 mm, (Reichstein, 1963; Corbet, 1978). Enamel SDQ usually <100 (Röttger, 1987). As a rule M_1 with one buccal and two lingual closed enamel triangles. M^3 shows two variants, one with closed triangles buccally and lingually and another with two closed triangles buccally with one lingually. These M^3 variants exist in varying proportions but always with the former being dominant (Reichstein, 1982b, p. 220).

Karyotype 2n = 36 from samples of specimens identified as *amphibius*, *scherman*, and *terrestris* (Matthey, 1955).

Remarks *A. terrestris* is a widely distributed species that displays a number of intriguing clines and partitions in morphological variation and ecology across its range. In describing the subspecific variability of *A. terrestris* Hinton (1926) noted the intergrading nature of morphology between populations and observed that 'All the forms are very closely related to each other and the essential characters of the species as a whole shade off through such forms...' (Hinton, 1926, p. 403). Hinton further speculated on the continuous nature of *A. terrestris* across its whole Palaearctic range, save for Iberia and Central Europe, an idea supported by Ellerman, 1940, p. 629 who reports Vinogradov as noting that the subspecies *amphibius, terrestris* and *scherman* are separable in western European but cannot be distinguished in the material from the Eurasia and the eastern Palaearctic.

A. terrestris is well-supported genetically as a group, but at least three lineages of unknown temporal depth exist within the species: an Italian lineage (Taberlet *et al.*, 1998), and 'western' and 'eastern' European lineages (Taberlet *et al.*, 1998, Piertney *et al.*, 2005; Brace, unpublished). More, informal, morphological forms are recognised by many mammalogists. The form *terrestris* itself is described as a moderately-sized, semi-aquatic group from northern Europe (Reichstein, 1982b) that has been recognised as different from the central European *scherman*, a small, pro-odont, fossorial form thought to have close affinities with *exitus* of the Alps, *monticola* of the Pyrenees, and *cantabriae* or northern Spain (Hinton, 1926; Reichstein, 1963; Ventura and Gosalbez, 1989; Kolfschoten, 1990). The name *italicus* has been attributed to a fossorial form restricted to Italy Hinton (1926); Reichstein (1982b). In Great Britain, *amphibius* was for many years regarded as a separate, large, semi-aquatic species, however, Corbet *et al.* (1970) found no morphological basis for this, and no molecular support can be found either (Piertney *et al.*, 2005). The Russian and Asian forms *meridionalis* and *scythicus* show lesser and greater degrees of fossorial specialisation respectively (Hinton, 1926). They encompass large geographical expanses and the literature is moot as to whether either of these types are or are not distinct from *terrestris*.

2.3.2 Extinct forms

Genus †*Mimomys* FORSYTH MAJOR 1902
†***Mimomys savini*** HINTON 1911

Synonyms †*intermedius* NEWTON 1881 (but preoccupied by BONAPARTE 1845; Kretzoi, 1965), †*majori* HINTON 1910, †*milleri* KRETZOI 1958

Diagnosis Diagnosis based upon morphology of the M_1 (Figure 2.2c) and M^3. Molars hypsodont but with roots forming at some point during ontogeny. Molar enamel always thicker on trailing rather than leading edges of lower molar triangles (*Mimomys*-differentiation). A *Mimomys*-fold and 'enamel island' often present in the M_1 (Figure 2.2c). Root and occlusal morphology of the M_1 is intimately related to ontogeny. Root formation occurs in the adult and the *Mimomys*-fold and 'enamel island' (Figure 2.2c) are in the main features of ontogenetically young individuals.

Genus *Arvicola* LACÉPÈDE 1799

Named forms From Hinton, 1926; Sutcliffe and Kowalski, 1976; Rekovets, 1990; Gromov and Polyakov, 1992; Kowalski, 2001; Cuenca-Bescós *et al.*, In press

†*abbotti* HINTON 1910; Late Pleistocene-Early Holocene; Ightham Fissures, Kent, England
†*antiquus* POMEL 1853; Late Pleistocene; Breche de Coudes, Puy-de-Dome, France
†*bactonensis* HINTON 1926; 'Cromerian'; Ostend near Bacton, Norfolk, England
†*cantiana* KOENIGSWALD 1970; Middle Pleistocene; Ingress Vale, England
†*cantiana dapycis* RĂDULESCU & SAMSON 1976; Late Middle Pleistocene; Dobrogea, Romania
†*cantiana istri* RĂDULESCU & SAMSON 1977; Late Middle Pleistocene; Dobrogea, Romania
†*cantiana-terrestris* KOENIGSWALD 1973; Pleistocene; Great Britain
†*cantianus* HINTON 1910; Middle Pleistocene; Ingress Vale, England
†*chosaricus* ALEXANDROVA 1976; Middle Pleistocene Hazari faunas of the Chernoyarsy Sands; Lower reaches of the Volga
†*gracilis* HELLER 1955; Late Pleistocene 'Würm'; Weinberg Mountains, Elbe, Germany
†*greenii* HINTON 1926; 'Cromerian'; Ostend near Bacton, Norfolk, England
†*hensenlii* ?; ?; ?

†*hunanensis* CARLS 1986; Saalian; Hunas, southern Germany
†*intermedius* NEWTON 1881; 'Cromerian'; East Anglia, England
†*jacobaeus* CUENCA-BESCOS 2010; 'Early Pleistocene Red Lower Unit'; Sima del Elefante site, Sierra de Atapuerca karst complex, Burgos, Spain
†*jordanica* HAAS 1966; ?; Ubeidiya, Israel
†*kalmankensis* ZAZHIGIN ?; ?; ?
†*moenana* HELLER 1969; 'Cromer Interglacial III or IV'; Mosbach, Germany
†*mosbachensis* SCHMIDTGEN 1911; 'Cromer Interglacial III or IV'; Mosbach, Germany
†*praeceptor* HINTON 1926; MIS 9; Grays Thurrock, Essex
†*sapidus aupsensis* RADULESCU 1989; Grotte des Cèdres, France
†*weinheimensis* HELLER 1962; 'Late Cromerian'–'Early Hoxnian'; Pilgerhaus near Weinheim, Germany

Diagnosis Upper incisors orthodont or pro-odont. Molars robust, high-crowned and without roots. Cement usually present in reentrant angles. Gross structure the same as for extant forms (Sections 2.2.1, 2.3.1). In geologically older specimens, enamel is thicker on the trailing rather than leading edges of lower molar triangles (*Mimomys*-differentiation). Additionally, the M_1 may rarely exhibit a *Mimomys*-fold (e.g., Maul *et al.*, 2000), and even more rarely an 'enamel island' (Hinton, 1926). In geologically younger, and ontogenetically older, specimens there is a tendency to display the reverse enamel configuration of thinner trailing edges with respect to leading edges (*Microtus*-differentiation; Heinrich, 1978; Kratochvíl, 1983b; Section 5.4) and a simple occlusal outline. Historical changes in enamel thickness have been used as a means to subdivide the evolutionary lineage of water voles.

The SDQ value of 100 has been used as a boundary to distinguish between 'primitive', rootless water voles such as *Arvicola cantianus* (SDQ $>$ 100) and the more derived condition found in the extant species *A. terrestris* (SDQ $<$ 100; Heinrich, 1978).

2.3.3 The use of names

Extant forms Only two extant biological species of water vole, *sensu* Mayr (1963), are currently recognised, which may appear to make much of the nomenclatural diversity reported above redundant. However, many neontologists continue to use a variety of named forms in informal ways or more formally as subspecies. These are employed to convey ideas about ecological preference, geographic extent or isolation, or general morphology. For instance, Kolfschoten (1990) restricted his description of extant European *A. terrestris* to five sub-

species[1] in order to summarise the geographical ranges of various forms, and Cubo *et al.* (2006) investigated the evolution of digging adaptations in *A. terrestris* and compared *monticola* and *scherman* with *italicus* as a way to indicate the use of regionally distinct ecological types.

Extinct forms In the palaeontological literature names are used to communicate aspects of morphological variation in the same manner as for extant forms. For fossil taxa the use of names reflect temporal as well as spatial variation and in some instances convey ideas of common ancestry. Generally, the trio of species, *M. savini*, *A. cantianus*, and *A. terrestris*, commonly describe the evolutionary transition from early Middle Pleistocene water voles with molar roots, to Middle Pleistocene water voles without molar roots and with *Mimomys*-differentiation of enamel, to water voles without molar roots and with *Microtus*-differentiation of enamel.

Mimomys Hinton (1926) lists three species of *Mimomys*, from the Freshwater Bed at West Runton, England, but Kretzoi (1965) showed these to be synonymous and that *M. savini* has priority. Although *M. savini* is most prevalent in the literature, some authors in eastern Europe and the former Soviet Union regard there to be a greater diversity of Middle Pleistocene large voles than indicated by Kretzoi (1965). Rekovets and Nadachowski (1995) recognised a form of *Mimomys* distinct from *M. savini* characteristic of southeastern Europe and the Ukraine, which they referred to as *Mimomys milleri*. Rekovets and Nadachowski saw *M. savini* as closer to *Arvicola* than *M. milleri* and concluded that *M. savini* was a likely ancestor to *Arvicola* while *M. milleri* became extinct. These ideas were echoed by some authors who allied *M. savini* with the genus *Cromeromys* Zazhigin 1980 as *Cromeromys intermedius* or *Mimomys* (*Cromeromys*) *intermedius* (Kretzoi, 1969; Zazhigin, 1980; Kolfschoten, 1993b; Neraudeau *et al.*, 1995; Rekovets and Nadachowski, 1995). Debate surrounding these ideas is confused by perceived nomenclatural inconsistencies such as the continued use of *Mimomys intermedius* major 1902 by some eastern European authors as a synonym for *M. savini* (e.g., Rekovets, 1990; Gromov and Polyakov, 1992; Rădulescu and Samson, 1993), despite the priority of *M. savini* (Kretzoi, 1965). This thesis will use *M. savini* to refer to the immediate rooted water vole ancestor of *Arvicola* but the possibility of multiple 'species' within *M. savini* cannot strictly be ruled out.

Arvicola Re-examination of fossil material initially described by Hinton and White (1902) as the type specimen of *Mimomys cantianus* by O. Fejfar revealed

[1] *amphibius*, *exitus*, *persicus*, *scherman*, *terrestris*

no evidence of a root (Koenigswald, 1970, pp. 418–420). *M. cantianus* was therefore reclassified to the genus *Arvicola*, and Koenigswald (1970) proposed *Arvicola cantiana* as the oldest valid species name available. *A. cantiana* is the name used by most workers to describe Middle Pleistocene water voles without roots and with *Mimomys*-differentiation of enamel, but this name is, in fact, invalid. An examination of the International Code of Zoological Nomenclature (hereafter 'the Code') shows why this should be the case. Article 34.2 of the Code (International Commission on Zoological Nomenclature, 1999) demands that a species-group name be the same gender as its genus name, irrespective of previously accepted usage. The gender of the genus name *Arvicola*, being a compound word, is not immediately obvious, but article 30.1.1 of the Code states that the gender of a compound genus-group name derives from its ending, and article 30.1.4.2 of the Code specifically instructs that genus names ending *—cola* should be treated as either masculine or common gender, unless they were initially treated as feminine by the author of the name. In the case of *Arvicola*, Comte de Lacepède used the species name *amphibius*, which is masculine (Comte de Lacepède, 1799, *Tableau des divisions, sous divisions, ordres et genres des mammifères*, p. 10). *Arvicola* should therefore be treated as masculine and, as *cantianus* is masculine, the name *Arvicola cantianus* is the valid form (Rădulescu and Samson, 1977; Maul *et al.*, 1998b; Rekovets and Nadachowski, 1995).

Maul *et al.* (2000) proposed that *A. cantianus* be abandoned as the type species for the earliest *Arvicola* for *Arvicola mosbachensis* SCHMIDTGEN 1911 because the type material of *A. cantianus* is fragmentary. *A. mosbachensis* is plentiful and well-preserved, with a rich accompanying fauna (Section 3.5.1.2) and Maul *et al.* (2000) argued that this therefore presents a more useful reference taxon. In addition, many eastern European and Russian authors have been notable in using *A. mosbachensis* to describe the earliest members of *Arvicola* for some time (e.g., Agadjanian, 1983). Although *A. cantianus* should strictly be retained as the correct name to describe the earliest unrooted water voles, this thesis will instead use *A. mosbachensis* throughout. This is because the approach of this thesis is based upon the analysis of morphological variation in assemblages and the fossil assemblage of Mosbach 2 (Section 3.5.1.2) forms one of, if not the, earliest representatives of *Arvicola* in the dataset presented here. The use of *A. mosbachensis* is an explicit statement of the approach and perspective.

Chapter 3

Sites

This chapter provides a review of the sites from which fossil material used in this study originate. Some of the assemblages examined are well-known localities with important, well-studied water vole assemblages (e.g., West Runton, Great Britain, Section 3.6.1.2), others may be familiar to researchers but the water vole assemblage has not yet been reviewed (e.g., Merlin's Cave, Great Britain, Section 3.6.3.4), while a number are less well known and, to the knowledge of this author, some may not have previously received accounts in English (e.g., Poeymaü, France, Section 3.4.1.3). The information contained in this chapter is intended as a reference, not only for this study, but for future work.

Sites are listed first by country in alphabetical order and then grouped within countries by approximate age: early Middle Pleistocene, late Middle Pleistocene, and Late Pleistocene and Holocene. The location of each site is described and its latitude and longitude given in decimal coordinates. A brief historical account is provided, together with palaeoenvironmental and lithological information, a review of the water vole material found—including the archive holding fossil material—and a stratigraphic interpretation. Site location data can be found summarised in Table 3.1 and in the map in Figure 3.1. Dating and archive summaries for individual assemblages can be found in Table 3.3.

The numbers of specimens examined referred to within each site description in this chapter may not correspond to the numbers of specimens used in later analyses. This is because poor preservation of specimens may preclude morphometric description. For the same reason, as data exploration unfolds throughout the thesis, some of the assemblages described in this chapter are discarded from later analyses, mainly for taphonomic reasons. However, the whole data set is a useful reference tool nontheless. Assemblages or groups of specimens are sometimes referred to as Operational Taxonomic Units (OTUs). This terms describes samples of specimens that are regarded as representing discrete biological units to be used in later phylogenetic analysis.

Chronology All radiocarbon dates are uncalibrated unless otherwise stated and where possible are accompanied with a $\pm 1\sigma$ error. Radiocarbon lab codes are as listed at `http://www.radiocarbon.org/Info/labcodes.html`. Unless otherwise stated all calibrations of radiocarbon dates have been carried out using the IntCal04 calibration curve (Reimer *et al.*, 2004) using the radiocarbon calibration program CalPal (Weninger *et al.*, 2009).

For assemblages that lie beyond the limits of radiocarbon dating, the age of each assemblage is estimated by reference to stages of the Marine Isotope Stratigraphy (MIS). Specifically, dates are taken from the stacked record of Lisiecki and Raymo (2005) with sub-stage terminology derived from Martinson *et al.* (1987). Absolute ages for mid-points and termini of stages and sub-stages were estimated by this author from the Lisiecki and Raymo (2005) curve. For assemblages that date to the later part of the Last Cold Stage, and where stratigraphy of the site appears appropriate, reference is made to the Greenland Ice Core Chronology (Andersen *et al.*, 2006; Rasmussen *et al.*, 2006). The date for the base of the Holocene is taken as 11 700 yr b2 k (before AD 2000; Walker *et al.*, 2009). Regional stratgraphic terms are, wherever possible, avoided, except in the context of historical discussion or where there is local difficulty applying the MIS record (e.g., in some parts of Russia).

Recent material The provenance of Recent water vole specimens used in this study are not discussed but Table 3.2 and Figure 3.2 give summaries of geographical and archival information from each Recent assemblage examined. Two Recent assemblages, Central Scotland and Welsh Borders, represent groupings of individual specimens from nearby localities that are considered together as they are thought to represent examples of the same haplotypes based on the phylogeographic analysis of Piertney *et al.* (2005).

Table 3.1: Location information for the 54 fossil localities examined by this study. MapID refers to labels on location map Figure 3.1.

MapID	Locality	Country	Latitude	Longitude
Abz	Abzac	France	44.94	1.01
Bal	Balla	Hungary	48.05	20.53
Bdn	Biedensteg	Germany	51.11	9.14
Bsk	Biśnik	Poland	50.42	19.67
BTg	Bolshoi Tigany	Russia	55.14	50.15
Box	Boxgrove	England	50.86	-0.69
BPt	Bridged Pot	England	51.21	-2.67
Brl	Brillenhöhle	Germany	48.41	9.78
BgS	Burgtonna	Germany	51.06	10.72
Chg	Chigirin	Ukraine	49.08	32.67
CCIV	Clacton	England	51.79	1.16
Crb	Courbet	France	44.05	1.66
CGr	Cudmore Grove	England	51.79	0.99
DvB	Divje babe I	Slovenia	46.11	13.91
DNg	Donskaya Negatchevka	Russia	52.06	39.00
DSC	Dzeravá skala Cave	Slovak Republic	48.50	17.32
FUt	Fortuna utca	Hungary	47.49	19.04
FiK	Fuchsloch im Krockstein	Germany	51.75	10.87
GBr	Grotta del Broion, Sala Grande	Italy	45.46	11.59
Gun	Gunki	Ukraine	49.27	33.60
Hvl	Horváti-lik	Hungary	48.21	20.44
Hvg	Hórvölgy	Hungary	48.08	20.50
Hun	Hundsheim	Austria	48.14	16.93
IFs	Ightham Fissures	England	51.29	0.30
IKo	Ilovayski Kordon	Russia	53.06	40.32
KLb	Kálmán Lambrecht	Hungary	48.12	20.60
Kar	Kartstein	Germany	50.54	6.66
Kom	Komarowa	Poland	50.80	19.12
Kor	Korotoyak-4	Russia	50.95	39.09
KGr	Kozi Grzbiet	Poland	50.85	20.35
Kuz	Kuznetsovka	Russia	51.87	42.20
MJn	Marie-Jeanne Cave	Belgium	50.21	4.83
Mdz	Medzhybozh-2	Ukraine	49.43	27.42
Mer	Merlin's Cave	England	51.84	-2.65
Mhm	Miesenheim I	Germany	50.40	7.41
Msb	Mosbach	Germany	50.07	8.27
Nvk	Novonekrasovka	Moldova	45.38	28.70
OEy	Ossom's Eyrie Cave	England	53.09	-1.85
Psk	Peskö	Hungary	48.05	20.43
Pil	Pilisszántó	Hungary	47.65	19.16
Psd	Pisede	Germany	53.74	12.76
Poe	Poeymaü	France	43.10	-0.45
Reg	Régourdou	France	45.06	1.17
RDT	Rotbav-Dealul Ţiganilor	Romania	45.83	25.51
RSb	Rybnaya Sloboda	Russia	55.60	49.40
Sch	Schöningen	Germany	52.14	10.97
Ton	Tönchesberg	Germany	50.37	7.38
Tor	Tornewton Cave	England	50.49	-3.68
TdF	Trou du Frontal	Belgium	50.22	4.96
Vnd	Vindija	Croatia	46.30	16.34
Vld	Vladimirovka	Russia	51.93	42.58
WRF	West Runton	England	52.94	1.24
WsM	Westbury	England	51.25	-2.70

Continued on next page

Table 3.1 continued from previous page

MapID	Locality	Country	Latitude	Longitude
WLw	Wigber Low	England	53.06	-1.70

Table 3.2: Location, archive, and sample size information for Recent samples. MapID refers to labels on location map Figure 3.2. Archive abbreviations refer institution names listed in Appendix Table A.1.

MapID	Sample name	Country	Latitude	Longitude	Archives	n
Agl	Aggeel	Azerbaijan	40.02	47.66	ZMMS	16
Cas	Casian	Romania	44.72	28.38	ISER	6
CSc	Central Scotland	Scotland	56.13	-3.15	NHML & NAZM	14
ChG	Cheshskaya Guba	Russia	65.00	46.00	ZMMS	21
CSE	Court St Etienne	Belgium	50.64	4.56	RBINS	16
DDt	Don Delta	Russia	47.20	39.70	ZMMS	14
Fam	Frankfurt am Main	Germany	50.11	8.68	SFIF	15
Ghe	Ghent	Belgium	51.03	3.43	RBINS	21
Hue	Huesca	Spain	42.13	0.22	NAZM	8
KBa	Kabardino-Balkariya	Russia	43.00	44.00	ZMMS	23
KVg	Kama-Volga	Russia	55.49	49.26	ZMMS	17
Len	Leninsky	Russia	48.75	45.20	ZMMS	30
LdR	Linares de Riofrio	Spain	40.58	-5.92	SFIF	15
Mcw	Moscow	Russia	54.85	38.13	ZMMS	25
Nvm	Novomirgorod	Ukraine	48.78	31.65	KIEV	13
Orm	Ormozu	Slovenia	46.44	16.18	NHML	15
Prk	Prokhladny	Russia	43.80	43.00	ZMMS	20
SBC	St. Bertrand de Comminge	France	43.02	0.57	RBINS	12
Tsm	Tsimlyansk	Russia	47.65	42.10	ZMMS	21
WBd	Welsh Borders	England	52.50	-2.48	NHML	21

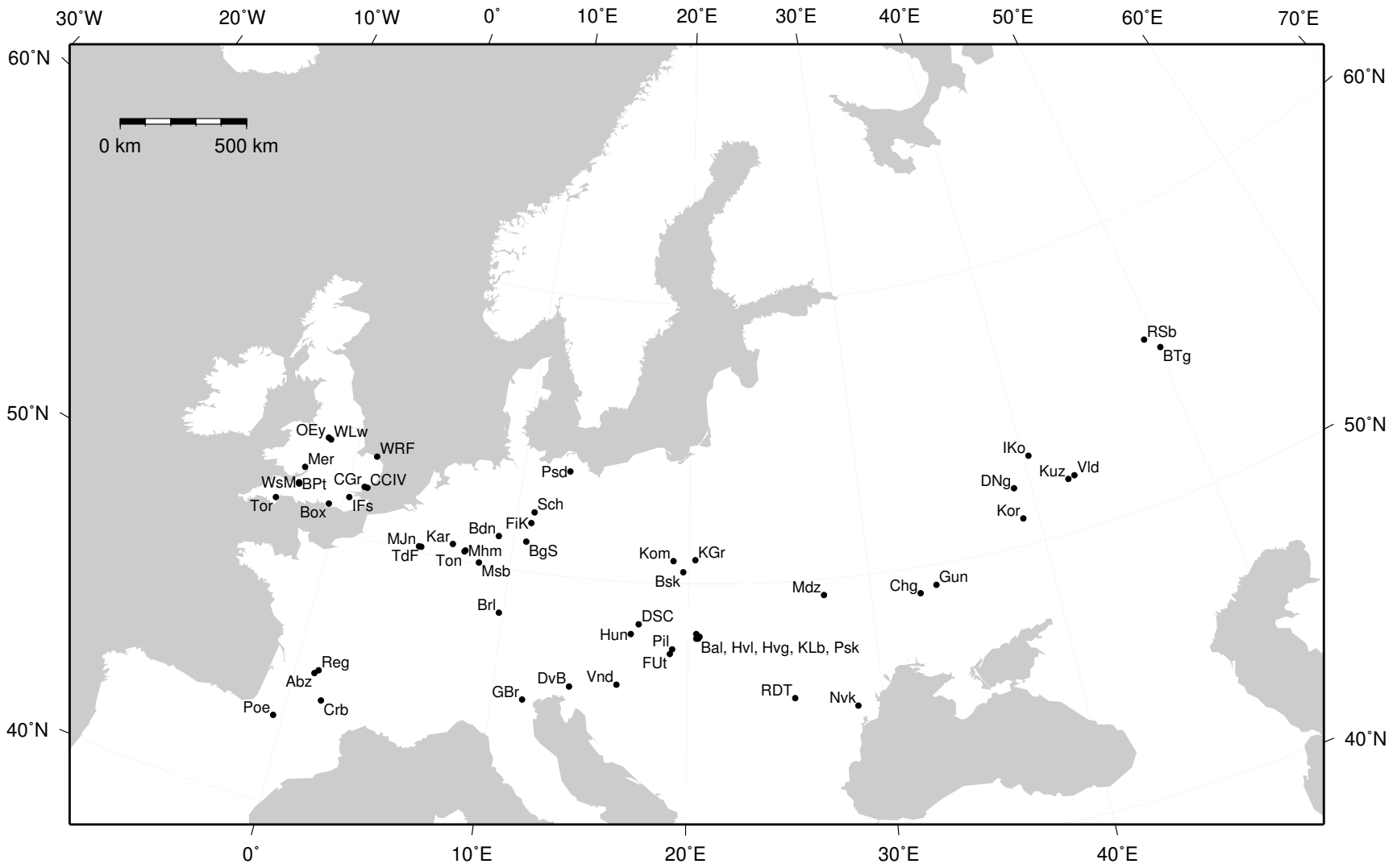

Figure 3.1: Location map of fossil localities. Labels correspond to MapID in Table 3.1.

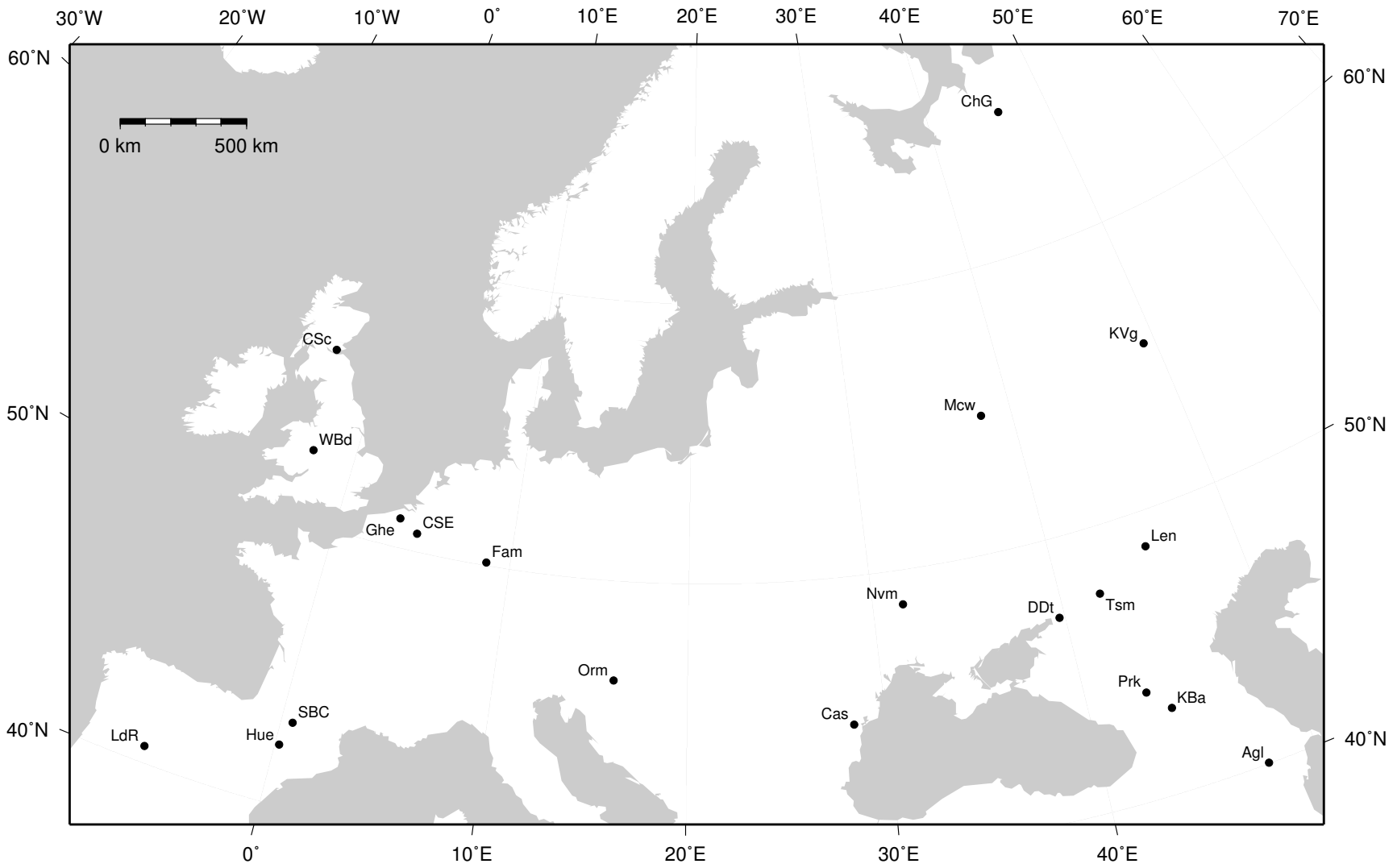

Figure 3.2: Location map of Recent localities. Labels correspond to MapID in Table 3.2.

Table 3.3: Dating summary, archive, and sample size information for fossil assemblages examined by this study. Minimum and maximum ages are in calendar years and refer to age estimates in the assemblage descriptions in this chapter. Archive abbreviations refer institution names listed in Appendix Table A.1.

Assemblage	Country	Min age	Max age	Archives	n
Abzac	France	12900	14700	LEMP	24
Balla	Hungary	14700	15180	HIGB	12
Biedensteg	Germany	29000	57000	SFIF	12
Biśnik 12-13	Poland	106000	132000	UNW	15
Bolshoi Tiganye	Russia	9200	10300	MIPA	31
Boxgrove 4b	England	478000	621000	NHML	27
Boxgrove 4c	England	478000	621000	NHML	33
Bridged Pot inner slope	England	0	11650	NHML	16
Brillenhöhle IV	Germany	12900	14700	SFIF	19
Burgtonna South Black-earth	Germany	71000	116000	SFIW	36
Chigirin	Ukraine	374000	424000	MIGG	44
Clacton Channel IV	England	116000	132000	DBC	22
Courbet	France	14100	14700	NHML	53
Cudmore Grove	England	279000	337000	NHML	51
Divje babe I A	Slovenia	29000	57000	SLOV	7
Donskaya Negatchevka	Russia	374000	424000	MIPA	19
Dzeravá skala Cave	Slovak Republic	26480	27880	HIGB	34
Fortuna utca 16-18/2	Hungary	374000	621000	HIGB	23
Fuchsloch im Krockstein	Germany	11270	13120	MFNB	26
Grotta del Broion, Sala Grande N	Italy	45000	116000	UNIFE	36
Grotta del Broion, Sala Grande Q4	Italy	45000	116000	UNIFE	27
Grotta del Broion, Sala Grande Q5	Italy	45000	116000	UNIFE	34
Grotta del Broion, Sala Grande R1	Italy	45000	116000	UNIFE	42
Gunki II	Ukraine	374000	424000	KIEV & MIGG	23
Horváti-lik 8	Hungary	71000	116000	HIGB	29
Horváti-lik 9a	Hungary	71000	116000	HIGB	35
Horváti-lik 13	Hungary	71000	116000	HIGB	22
Hórvölgy	Hungary	191000	337000	NHMH	13
Hundsheim	Austria	478000	621000	IPUW	47
Ightham Fissures	England	9510	28230	NHML	17
Ilovayski Kordon	Russia	478000	621000	MIPA	28
Kálmán Lambrecht IV	Hungary	57000	116000	NHMH	12
Kartstein	Germany	6000	12900	SFIF	16
Komarowa D	Poland	29000	44000	ISEK	18
Korotoyak-4	Russia	478000	621000	MIPA	27
Kozi Grzbiet 2	Poland	478000	712000	ISEK	49
Kuznetsovka	Russia	478000	621000	MIPA	101
Marie-Jeanne Cave 2	Belgium	1500	11700	RBINS	19
Marie-Jeanne Cave 4	Belgium	29000	71000	RBINS	11
Marie-Jeanne Cave 6	Belgium	29000	71000	RBINS	19
Medzhybozh-2	Ukraine	374000	424000	KIEV	22
Merlin's Cave	England	2820	12370	NHML	110
Miesenheim I	Germany	478000	621000	LEID	24
Mosbach 2	Germany	478000	621000	SFIF & MAIN	121
Novonekrasovka upper	Moldova	116000	132000	MIGG	17
Ossom's Eyrie Cave	England	1000	1700	MUM	49
Peskö brick red strata	Hungary	20000	25000	HIGB	47
Pilisszántó	Hungary	16580	16900	HIGB	44
Pisede III	Germany	3200	3360	MFNB	31
Pisede IV&V	Germany	2500	3200	MFNB	36

Continued on next page

Table 3.3 continued from previous page

Assemblage	Country	Min age	Max age	Archives	n
Poeymaü BS	France	11320	11880	LEMP	19
Régourdou 3	France	29000	57000	LEMP	13
Régourdou 5	France	57000	106000	LEMP	21
Régourdou 7	France	57000	106000	LEMP	26
Rotbav-Dealul Ţiganilor Clay-A	Romania	478000	621000	ISER	32
Rybnaya Sloboda	Russia	374000	424000	MIGG	23
Schöningen 13-II-4	Germany	279000	424000	LEID	33
Tönchesberg II 11-13	Germany	116000	132000	LEID	23
Tornewton Cave Red Cave Earth	England	25114	132000	NHML	19
Trou du Frontal	Belgium	10490	11010	RBINS	13
Vindija E-F	Croatia	18500	27000	CRIQ	26
Vindija G	Croatia	27000	42000	CRIQ	45
Vladimirovka 2	Russia	374000	424000	MIPA	33
West Runton Freshwater Bed	England	563000	780000	NHML	47
Westbury 11	England	478000	621000	NHML	16
Westbury 14	England	478000	621000	NHML	38
Wigber Low 26	England	2500	4000	SCM	56

3.1 Austria

3.1.1 Early Middle Pleistocene

3.1.1.1 Hundsheim

Location Southern slopes of the Hainburger Hills, north-west of the town of Hundsheim, Lower Austria, Austria

Co-ordinates 48.14°N, 16.93°E

Age MIS 15 or MIS 13

Archive Institut für Paläontologie der Universität Wien, Vienna, Austria

Description Hundsheim is a fissure-filling developed in the karstified Triassic limestone of the Hainburger Hills in eastern Austria. Mining activities exposed the fossil-rich fissure, which was first excavated in 1902 by F. Toula and later worked on by numerous researchers until Thenius in 1951 (Rabeder pers. comm.). Early reports indicate the fissure to have been completely filled with a diverse fossil assemblage of molluscs, crustaceans, amphibians, reptiles, birds, and large and small mammals, found in both loess and breccia deposits (Frank and Rabeder, 1997). No botanical or archaeological remains were found.

Hundsheim lies at the western edge of the Carpathians, at an intermediate position between European phylogeographic regions. This is highlighted by Pleistocene overlap of currently separated intraspecific lineages, (e.g., *Ursus arctos*, Hofreiter *et al.*, 2004), overlap in the modern distributions of northern and southern species (e.g., various birds, Mlíkovský, 2009), and the source of populations implicated in post-glacial recolonisation of northern Europe (e.g., *Microtus agrestis*, Jaarola and Searle, 2002).

Material examined Forty-seven M_1s were photographed. Two molars were unable to provide a full complement of landmarks, but this aside, specimens were in an excellent state of preservation. Very little staining was evident, enamel triangles were well-defined, and enamel layers were clearly visible and well-defined. Approximately half the M_1s were within mandibles.

Kormos (1937) referred the water vole remains to *Arvicola bactonensis* and *Arvicola greenii* based on the molar size and shape criteria of Hinton (1926). More recent interpretations have recognised the specimens as *Arvicola cantiana* (Heinrich, 1987; Frank and Rabeder, 1997) and *Arvicola cantianus* (Koenigswald and Heinrich, 1999): both synonyms of *Arvicola mosbachensis* (Rekovets and Nadachowski, 1995; Maul *et al.*, 2000). M_1s are rootless and enamel thickness measure-

ments show the assemblage to have a *Mimomys*-differentiation (Heinrich, 1987; Table 3.4).

The taphonomy of the fauna found in the fissure is potentially complex. The cave evidently acted as a trap for large carnivores, lured by dead or dying animals within. It was also a roost for numerous bat species, as well as birds of prey, which are the likely agent of accumulation for small mammals such as *Arvicola*. The similarity in preservational state of all the specimens does perhaps suggest that the assemblage is temporally discrete, but this cannot be assumed. Numerous bat species were found, and in the bird assemblage the remains of eagles, falcons, and owls further reflect the use of the cave as a roost. To the knowledge of this author no detailed stratigraphy exists for the site, which to some degree limits discussion on other aspects of the taphonomy of the *Arvicola* assemblage.

Table 3.4: Published SDQ values from Hundsheim.

Author	SDQ			
	n	min	mean	max
Heinrich (1987)	17	102[a]	135.15	152[a]

[a] Estimated from Heinrich (1987, Figure 1)

Palaeoenvironments The faunal assemblage from Hundsheim—described in Frank and Rabeder (1997)—is diverse, and contains a range of temperate species showing the existence of warm, mesic, temperate conditions with a mosaic of woodland and grassland. Moderately-sized herpetofaunal and avian assemblages are complemented by a rich molluscan fauna containing terrestrial and freshwater species characteristic of a warm, humid environment. In the small mammals, woodland taxa such as birch mouse *Sicista* sp., the dormice *Muscardinus* sp. and *Glis* sp., and several woodland bat species are present alongside open-landscape indicators such as *Microtus gregaloides* and hamster *Citellus* sp. The presence of the moles *Talpa europaea* and *Talpa minor* and shrews *Sorex* spp. indicate a temperate climate with well-developed soils. The occurrence of desman *Desmana* spp. shows that riparian habitats existed in the area.

Stratigraphy and correlation Kormos (1937), Rabeder (1972, 1981), and Mlíkovský (2009) gave an early Middle Pleistocene age for Hundsheim; the last author correlating the site with the Hungarian Tarkőian faunal stage of Jánossy (1986). Kowalski (2001) listed the site as dating from the Holsteinian, while the Paleoclimate Database of the Quaternary (2001) gives the age as anywhere between MIS 13 and MIS 5e.

Rabeder (pers. comm., 2010) asserts that the fossil assemblage represents a single biozone, and the taxonomic list provided by Frank and Rabeder (1997) shows a number of biostratigraphically significant species that suggest Hundsheim is an early Middle Pleistocene deposit. The principal taxa are the vole chronospecies *Microtus gregaloides* (which may be the last appearance of this taxon: Maul and Markova, 2007), and three extinct species: *Drepanosorex* sp., *Pliomys episcopalis*, and *Talpa minor* (Koenigswald and Heinrich, 1999; Maul and Markova, 2007), but also cited as highly significant is the presence of *Arvicola mosbachensis*—rather than *Mimomys savini*—bearing SDQ values consistent with other water vole assemblages from the latest part of the early Middle Pleistocene (Heinrich, 1987; Koenigswald and Heinrich, 1999). The occurrence of *Arvicola* at Kärlich G in the central Rhine region of Germany has been dated to MIS 15 or MIS 16, and may provide a minimum age for the appearance of *Arvicola* in central Europe in general (Koenigswald and Kolfschoten, 1996; Koenigswald and Heinrich, 1999). Given these data, and the temperate nature of the Hundsheim fauna, it is possible that the site dates from MIS 15 or MIS 13. Although SDQ values point to the later part of the early Middle Pleistocene, to avoid dating circularity a possible age range of MIS 15 or MIS 13 will be attributed to the *Arvicola* assemblage.

3.2 Belgium

3.2.1 Late Pleistocene and Holocene

3.2.1.1 Marie-Jeanne Cave

Location Hastière-Lavaux, Namur, Belgium

Co-ordinates 50.21°N, 4.83°E

Age MIS 4 to MIS 1

Archive Royal Belgian Institute of Natural Sciences, Brussels, Belgium

Description Marie-Jeanne Cave is situated in the middle of the valley of the river Féron, a tributary of the Meuse, near the village of Hastière-Lavaux in the Namur region of Belgium. The cave was found at the start of the 19th century but was not excavated until the summer of 1943 by the Royal Belgian Institute of Natural Sciences, Brussels. A detailed description of the stratigraphy and palaeontology of the cave can be found in Gautier and de Heinzelin (1980). The cave comprises a corridor within Carboniferous limestone containing clays, silts and sands divided into ten lithologically distinct layers (Figure 3.3) with layers 1 to 6 containing fossil mammals (Gautier and de Heinzelin, 1980). Prior to layer 6 the cave was not externally accessible.

Material examined *Arvicola* were found in Layers 2 to 6 but photographs were only taken of material from Layers 2, 4, and 6 due to limited access time to the collections at the Royal Belgian Institute of Natural Sciences, Brussels, Belgium, giving 19, 11, and 19 specimens respectively. Molars were generally darkly coloured, although a small number were apparently unstained. Generally, preservation was very good, specimens were covered with fine-grained, light-yellow or red sediment that was brushed aside to clearly reveal occlusal surfaces. According to Gautier and de Heinzelin (1980) the small mammals were derived from the pellets of birds of prey.

Palaeoenvironments The fauna from layers 4 and 6 indicate a cold continental climate with greater biodiversity than that of Belgium today (Gautier and de Heinzelin, 1980). Layer 6 is reported to have yielded the cool-climate voles and lemmings *Microtus gregalis*, *Lemmus lemmus*, and *Dicrostonyx torquatus*, along with the cold-climate lagomorphs *Ochotona pusilla* and *Lepus timidus*. Occassional finds of red squirrel *Sciurus vulgaris* also occur, indicating the presence of

some woodland (Gautier and de Heinzelin, 1980). Layer 4 contains an impoverished cool-temperate assemblage but from layer 3 more humid conditions apparently appear, still without appreciable woodland (Gautier and de Heinzelin, 1980). In layer 2 temperate conditions are indicated and woodland became prevalent.

Stratigraphy and correlation Gautier and de Heinzelin (1980) attributed layers 6 and 4 to the 'Last Cold Stage' based on palaeoclimatic evidence of cool, but not cold, climates and the presence of a 'Mousterian' point in layer 3. If the age of the Middle/Upper Palaeolithic transition is considered to be *c.* 40 k yr BP (Mellars, 2004), this provides the minimum age for layers 6 and 4. However, Gautier and de Heinzelin (1980) urge caution with the chronological use of 'Mousterian' points from Belgium. Layer 2 is made up of sediments laid upon the irregular surface of a stalagmite floor and the origins of the fauna found within it may be complicated by taphonomic mixing (Gautier and de Heinzelin, 1980). Layer 1 contains a mixed fauna of Late Pleistocene, Early to Middle Holocene, and historical origins; it also contains Roman and Bronze Age archaeology (Gautier and de Heinzelin, 1980). An attempt by this study to radiocarbon date an *Arvicola* mandible from layer 2 failed due to low yield of organic matter from the sample. Stalagmite floors are general features—although not indicative—of early Holocene cave sequences and therefore Layer 2 can be tentatively considered to post-date the beginning of the Holocene but pre-date Layer 1, which appears to be at least Bronze Age/Roman in age.

Based on the lack of secure dating evidence available, layers 4 and 6 will be given the same potential age-ranges of MIS 4 to MIS 3. Layer 2 may possibly date from the beginning of the Holocene to the end of the Roman period.

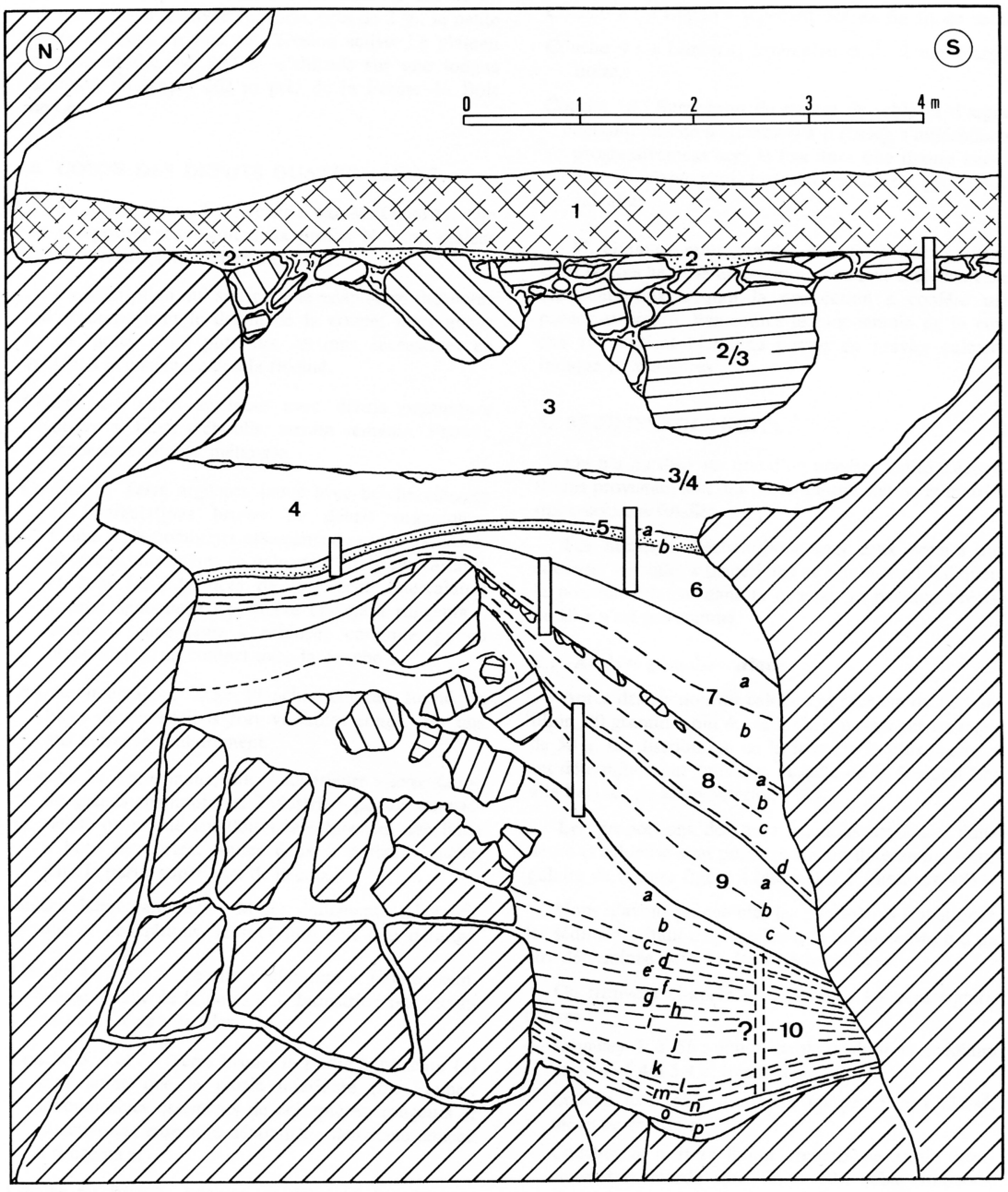

Figure 3.3: The sequence at Marie-Jeanne Cave. *Arvicola* were sampled from Layers 2, 4, and 6. From Gautier and de Heinzelin (1980).

3.2.1.2 Trou du Frontal

Location Furfooz, Ardennes, Belgium

Co-ordinates 50.22°N, 4.96°E

Age *c.* 11–10 k yr BP

Archive Royal Belgian Institute of Natural Sciences, Brussels, Belgium

Description Located near the town of Furfooz in the Belgian Ardennes, Trou du Frontal was first excavated in 1864 by Édouard Dupont and most recently in the 1980s by the Service de Préhistoire, University of Liège. The site is an open, shallow, limestone cave above the river Lesse containing alluvial clays and angular limestone conglomerates (Charles, 1998). Dupont reported a *1^er^ niveau ossifère* in the uppermost part of the stratigraphy, which produced human remains from a Neolithic burial at the rear of the cave, Magdalenian artefacts such as flints and worked bone, and the remains of large and small mammals.

Material examined Thirteen *Arvicola* M_1s were photographed. All molars were *in situ* in mandibles and had a clean appearance, enabling landmarking and enamel thickness measurements to be easily taken. No assessment of the small mammal fauna from Trou du Frontal has been published; in her review of the site Charles (1998) only deals with the human and large mammal finds. The water vole specimens were assigned to *Arvicola terrestris* at the Royal Belgian Institute of Natural Sciences, Brussels, Belgium.

The specimens originated from the *1^er^ niveau ossifère*. This layer appears to be stratigraphically mixed, probably during or post-excavation (Charles, 1998), and therefore the *Arvicola* assemblage may be temporally mixed.

Palaeoenvironments The majority of the fauna appears to be domesticated large mammals (Charles, 1998). There is little information available on the large mammal fauna dating to the Lateglacial–Holocene transition and no taxonomic list for the small mammals. This scarcity of information and apparent lack of stratigraphic control on fossil and archaeological finds means that no detailed statements can be made about palaeoenvironments. The geography of the surrounding area is highly variable, with steep limestone gorges, slow and fast-flowing water courses, and flat upland areas, and this is likely to have allowed a number of differing habitats to develop locally through the Lateglacial–Holocene transition. Woodland or marginal woodland is indicated by the presence of red deer *Cervus elaphus* and beaver *Castor fiber*; the latter species shows the importance of wetland, riparian landscapes, which may inform on the ecology of *A. terrestris*.

The presence of horse *Equus ferus* shows that open grasslands were also present, although the relative abundance of horse in the fossil assemblage is the result of butchery by humans.

Stratigraphy and correlation The majority of the fauna found is of late prehistoric or historic age (e.g., ovi-caprids, wild boar *Sus scrofa*, and cow *Bos* sp.) and the human remains from the burial have been radiocarbon dated to the Neolithic (Charles, 1998). The flints and worked bone, however, are late Magdalenian, and a small proportion of the fauna, according to Charles (1998), consists of Lateglacial and early Holocene elements such as brown bear *Ursus arctos* and *C. fiber*, although both these taxa coexisted in Belgium until much later (Schreve pers. comm., 2010). Radiocarbon dating of human modified bone and other bones show that these elements originate from GS-2 to GS-1, and a single *Arvicola* mandible submitted for radiocarbon dating by this study gave an early Holocene date (Table 3.5). Charles (1998) suggested that the *1er niveau ossifère* is a composite layer made from strata that were originally separate but were either excavated together or not recorded as distinct. The dating evidence supports this conclusion and further suggests that two distinct accumulations exist: one at least from late GS-2 to the earliest Holocene; and another in the Middle to Late Holocene, which is possibly human mediated.

The evidence of stratigraphic mixing means it cannot be certain that all specimens in the *Arvicola* assemblage date from only one of these phases of accumulation, but the radiocarbon date obtained from *Arvicola* does suggest its origins are in the earlier of the two accumulations, and so it may be assumed that no *Arvicola* originate from the Neolithic or later. Of the radiocarbon dates shown in Table 3.5, the determinations from large mammal bone may not aid in constraining an age for a small mammal such as *Arvicola*, and therefore only the radiocarbon date obtained for the *Arvicola* specimen will be used as an age for the *Arvicola* OTU.

Table 3.5: Radiocarbon determinations from the *1er niveau ossifère*, Trou du Frontal.

Lab no.	Material	^{14}C BP	cal BP
OxA-21078[a]	*Arvicola* mandible	9 455 ± 55	10 750 ± 130
Lv-1135[b,c]	Indet. bone fragments	10 350 ± 150	12 178 ± 314
OxA-4197[b]	*Equus ferus* cut metacarpal	12 800 ± 130	15 285 ± 359
Lv-1749[b,c]	Not specified	12 950 ± 170	15 762 ± 508
Lv-1750[b,c]	Not specified	13 130 ± 170	16 050 ± 390

[a] This study [b] Charles (1998) [c] Conventional date

3.3 Croatia

3.3.1 Late Pleistocene

3.3.1.1 Vindija

Location Near the town of Ivanec, Mount Ravna gora, Varaždin County, Croatia

Co-ordinates 46.3°N, 16.34°E

Age Layer G, *c.* 42–27 k yr BP; Layers E–F, *c.* 27–18.5 k yr BP

Archive Institute for Quaternary Paleontology and Geology, Zagreb, Croatia

Description Vindija Cave in northern Croatia is a large cavern (50 m long, 28 m wide, 10 m high) containing a sedimentary sequence spanning MIS 6 to the Holocene. It is most notable for the remains of *Homo neanderthalensis* and early modern humans found within, which have provided significant insights on the changing distribution of these two hominin species at the Middle to Upper Palaeolithic transition (e.g., Higham *et al.*, 2006). The site has also yielded an abundant cave bear assemblage as well as other large mammals, small mammals, birds, herpetofauna, fish, and molluscs (Paunović *et al.*, 1999; Mauch Lenardić, 2007).

Vindija was first excavated from 1928 to 1955 by S. Vuković and in the 1970s and 1980s by M. Malez but always received research attention, most recently through aDNA studies of *H. neanderthalensis* (e.g., Green *et al.*, 2006). A 12 m thick sequence of breccias, sands, silts, and clays has been documented (Figure 3.4) but unfortunately the excavation protocols of Malez led to the mixing of finds from some parts of the stratigraphy. The water vole fossils examined originated from layers G–F, a part of the stratigraphy that offers the best contextual certainty for fossils in the sequence (Mauch Lenardić pers. comm., 2008) and one that has received much attention due to the presence of hominin fossils in Layer G. Layers E–F consist of a yellow sand with some limestone rubble and overlie the reddish, green, and grey clays of Layer G (Paunović *et al.*, 1999).

Material examined The *Arvicola* M_1s examined derived from the following groupings of stratigraphic layers: E–F ($n = 26$), G upper ($n = 9$), G_2 ($n = 15$), G lower ($n = 19$). Groups G upper and lower constitute an amalgamation of sub-layers G_1–G_3 and, although these strata are lithologically different, they are indistinguishable in terms of dating (see below). It was felt that, given the inability to separate sub-layers within G from the dating evidence, the *Arvicola* groups from

G upper, G lower, and G_2 should be combined to form a single OTU from Layer G with $n = 43$. This has the advantage of increasing the number of individuals within the OTU, which is important in accurately defining morphometric variables (Cardini and Elton, 2007).

The majority of the twenty-six M_1s from Group E–F were partially damaged mandibles with only two isolated molars present. Fine, reddish sediment was found adhered to some mandibles and specimens showed a range of colouration, from dark-brown/black to seemingly unstained bone. This diversity of preservation states raises some concerns over stratigraphic mixing. One posterior lobe was fractured but in general occlusal surfaces were in good condition.

The forty-three M_1s from Group G contained a much greater proportion of isolated molars than Group E–F. Generally occlusal surfaces were in good condition. Specimens showing a range of dark and light colourations were present and reddish or yellowish sediment could be found on some teeth and mandibles. This reflects the lithological differences between sub-layers within Layer G.

Mauch Lenardić (2005) identified the water vole as *Arvicola terrestris*, observed that molar teeth were smaller than those from contemporaneous *Arvicola* assemblages, and speculated that the these water voles may have been fossorial. She also noted that morphotype A—an inflated anterior lobe with LSA3 anterior to BSA2, and LSA4 and BSA3 moderately developed (Nadachowski, 1982)—made up nearly half the M_1s in the sequence. The dominance of this morphotype mirrored patterns in other *Arvicola* assemblages of similar age, however, the M^3 increases in length from Layers G to F which is the opposite pattern to that seen in other European sites of this age (Mauch Lenardić, 2005).

Palaeoenvironments Not all of the palaeontological remains were attributable to individual layers, which poses problems for palaeoenvironmental reconstruction. Pollen was exclusively found in Layers G and F and analysis found that low levels of pine was the only arboreal pollen present in Layer F, indicating an open landscape with minimal or distant tree cover (Paunović *et al.*, 1999). In the assemblage from Layer G, woodland molluscs were attributable to sub-layer G_1 but the bank vole *Clethrionomys glareolus*—a woodland indicator—was rare here, instead *A. terrestris* and *Microtus* spp.—suggesting more open habitats—were prevalent in the small mammals. The large mammals suggest that some woodland was present alongside open terrain. Large mammal remains were dominated throughout by cave bear *Ursus spelaeus*. Red deer *Cervus elaphus* was absent from sub-layers G_1 and G_2 but present elsewhere, and giant deer *Megaloceros giganteus* was absent from sub-layer G_1 (Paunović *et al.*, 1999). Overall the evidence suggests that woodland cover was limited or non-existent at times and open grassland prevailed.

Considering the site in its regional context, Vindija was only around 100 km from the maximum extent of Alpine glaciation during the Last Glacial Maximum (Ehlers and Gibbard, 2004) and so the colonisation of the locale, even by a generalist species such as *Arvicola*, may have been sporadic and restricted to the most temperate periods. Given that *A. terrestris* dominates the small mammal fauna the palaeoenvironmental information adds some support to the possibility that the water vole found at Vindija was fossorial.

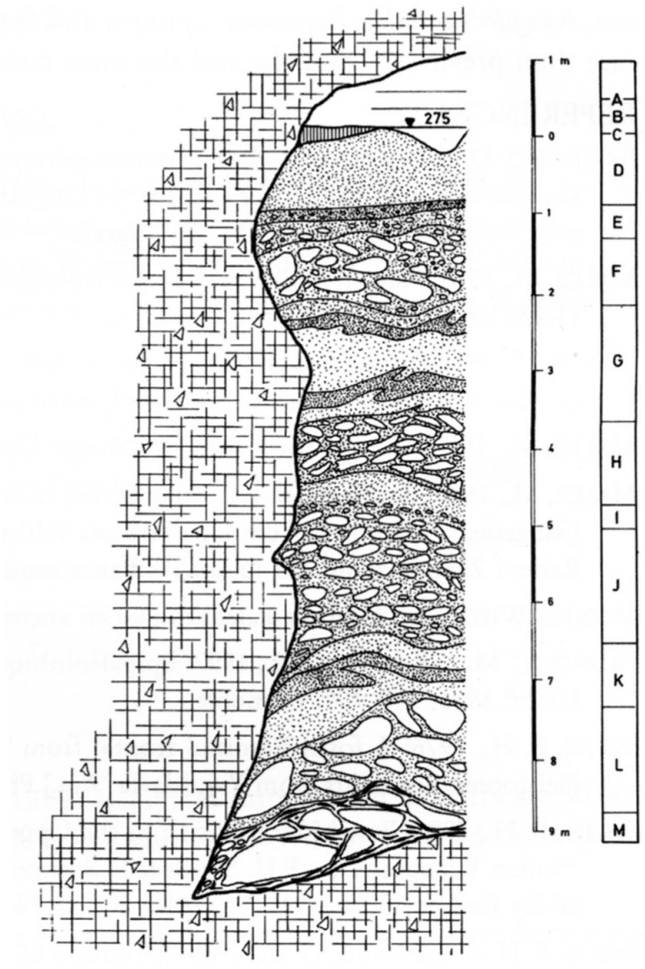

Figure 3.4: Generalised stratigraphy of Vindija Cave. Taken from Paunović *et al.* (1999).

Stratigraphy and correlation A significant number of ^{14}C and U-Th dates are available for the sequence at Vindija (Paunović *et al.*, 1999; Vermeersch and Boon, 2010). Broadly, age estimations from these different methodologies agree on dating Layers E–F to *c.* 27–18.5 k yr BP and Layer G to *c.* 42–27 k yr BP. Revised ^{14}C dating of two *H. neanderthalensis* bones using the ultrafiltration pretreatment technique (Bronk Ramsey *et al.*, 2004) has recently given an older age estimate for level G_1 of between 34—32 k yr BP (Higham *et al.*, 2006). This determination

shows that some previous ^{14}C dates may be inaccurate.

Absolute dating of these layers have employed *U. spelaeus* bones and teeth, *H. neanderthalensis* bone, and charcoal. These materials may not have the same age-distribution as the *Arvicola* assemblage. The proximity of Vindija to the Alpine ice-sheet means that the colonisation of the area by *Arvicola* may have been sporadic and perhaps restricted to the most temperate parts of MIS 3, but the potential for stratigraphic mixing of the *Arvicola* assemblage through bioturbation, cryoturbation, and excavation approach means that correlation of *Arvicola* assemblages from different parts of the stratigraphy with individual warm periods, such as Greenland Interstadials, is not possible. A conservative series of age estimates based upon the radiometric evidence will therefore be used for the *Arvicola* groups, namely: Layers E–F *c.* 27–18.5 k yr BP and Layer G *c.* 42–27 k yr BP.

3.4 France

3.4.1 Late Pleistocene

3.4.1.1 Abzac

Location Village of Les Eyzies-de-Tayac-Sireuil, Dordogne, France

Co-ordinates 44.94°N, 1.01°E

Age GI-1

Archive Museé National de Préhistoire, Les Eyzies-de-Tayac-Sireuil, France

Description Abzac is a limestone cave situated in the 'Gorge d'Enfer' of the river Vézère. It was briefly excavated at the end of the 19$^{\text{th}}$ century before being more thoroughly investigated in 1934 by D. Peyrony (Vialou, 2004, p. 182). Two sedimentary layers containing Magdalenian archaeology and large mammal remains were recorded, separated by a *couche d'interoccupation*: a period of apparent human absence, rich in small mammals. The main focus of research interest has been the art and artefacts found within the cave.

Material examined *Arvicola* were abundant, and a subsample of twenty-four M_1s were selected for photography. Specimens were generally in very good condition, although three M_1s had partially damaged salient angles. Most molars were *in situ* within mandibles and enamel bands were clearly visible.

The *Arvicola* assemblage originated from the *couche d'interoccupation*, an accumulation attributed to predation by owls (Peyrony, 1947). The *Arvicola* were

identified as *Arvicola arvalis amphibius* (= *Arvicola terrestris*) by M. Stehlin (Peyrony, 1947). No descriptions of the material were given but the assignment to *amphibius* suggests that Stehlin found commonalities with British water voles. No studies of the water vole or other small mammals from Abzac have been published.

Palaeoenvironments In the lower parts of the lower Magdalenian layer, large quantities of reindeer were found; in the upper Magdalenian layer, smaller numbers of horse, deer, and bovids occurred. This suggests that a cold tundra environment was present during accumulation of the lower Magdalenian layer, and a more temperate environment existed at the time that the upper Magdalenian layer accumulated. In the *couche d'interoccupation* the small mammal fauna includes *A. terrestris*, northern vole *Microtus ratticeps* (= *Microtus oeconomus*), common vole *Microtus arvalis*, pika *Lagomys* (= *Ochotona*) *pusillus*, wood mouse *Mus* (= *Apodemus*) *sylvaticus*, garden dormouse *Elyomis* (= *Eliomys*) *quercinus*, and stoat *Mustela erminea*. These species indicate the presence of woodland as well as open grassland within mesic climate.

Stratigraphy and correlation D. de Sonneville-Bordes regarded the archaeology found at Abzac as Upper Magdalenian (Vialou, 2004; cf. Peyrony, 1947), and as occurring within a temperate, mesic period sandwiched between two cold episodes (see above). This interpretation suggests that the *couche d'interoccupation* dates to a warm phase during the Lateglacial, either GI-1e or GI-1abc of the Lateglacial Interstadial. *Arvicola*, however, do not occur alongside the archaeology and could have potentially accumulated during the whole of the Lateglacial Interstadial. In the absence of other information, for the purposes of this study, the *Arvicola* assemblage will be generally assigned to this Lateglacial Interstadial period.

3.4.1.2 Courbet

Location Opposite the village of Bruniquel, Tarn-et-Garonne, France

Co-ordinates 44.05°N, 1.66°E

Age GI-1e

Archive Natural History Museum, London, Great Britain

Description Roc du Courbet is a cave developed in a Jurassic limestone cliff, approximately 12 m above the river Aveyron in the Tarn region of southwest France. It is one of many such caves and rock-shelters around the village of Bruniquel that contain Upper Palaeolithic artefacts. The cave has also been known as Trou des Forges and Caverne de Bruniquel, but is now more commonly referred to as Courbet (Kaagan, 2000). It was first discovered by the Vicomte de Lastic Saint-Jal in 1863 and was brought to the attention of Prof. Richard Owen, of the British Museum (Natural History). Owen regarded the site to be of great enough importance to warrant the purchase of a large proportion of the fossil and archaeological remains for the museum (Cook and Welté, 1995; Kaagan, 2000).

Courbet consists of a cavern approximately 20 m deep, 6 m wide, and 3 m high. The sediments within were not described in great detail by the Vicomte de Lastic or Owen. The majority of the animal and archaeological remains derive from a *couche noire* (black layer) that occurred beneath a stalagmite floor (Kaagan, 2000).

Material examined A large quantity of *Arvicola* material is curated in the collections at the Natural History Museum, London. This presented an opportunity to describe morphological variation in a fossil assemblage of large size. A subsample fifty-three M_1s were photographed. Around half of M_1s were isolated molars and all specimens were stained light-brown and were dusted with light-brown, medium to fine-grained sediment. Occlusal shape was in general well-preserved but eight molars were unable to give full landmark configurations. The posterior enamel layers of enamel triangles were in many cases eroded, sometimes to the point of being breached. This limited the number of full SDQ measurements that could be made and may also affect the precision and accuracy of enamel thickness measurements.

The *Arvicola* remains were likely found in the black layer but this stratigraphic context may not be wholly correct (Kaagan, 2000). No study has been been published on the *Arvicola* assemblage but specimens were identified as *Arvicola terrestris* in the museum collections. Molars were rootless and qualitatively dis-

played enamel with a *Microtus*-differentiation. Interestingly, two molars displayed a *Mimomys*-fold.

Palaeoenvironments No detailed palaeoenvironmental analysis of Courbet has been published. The dating of the *Arvicola* assemblage to the Lateglacial Interstadial (see below), however, gives an indication that the environment at the time would have been mesic and temperate, with the development of patches of mixed woodland as well as open grassland, especially on the areas above the valley.

Stratigraphy and correlation The majority of the archaeological finds, thought to derive from the black layer, have been dated to the Upper Magdalenian (Magdalenian V or VI, Kaagan, 2000). Three radiocarbon dates, taken on human bone and a horse premolar (Table 3.6), indicate that these remains date to GI-1e (Bølling interstadial). Assuming the fossil material all or mainly derive from the black layer, the *Arvicola* assemblage can be cautiously attributed to the early part of the Lateglacial Interstadial age: i.e., GI-1e.

Table 3.6: Radiocarbon dates from Courbet, France.

Lab no.	Material	^{14}C BP	cal BP
OxA-6667[a]	Horse P_3	13 230 ± 90	14 211 ± 413
GifA-90169[b]	Human bone	13 400 ± 260	14 328 ± 516
GifA-90170[b]	Human bone	13 490 ± 260	14 409 ± 520

[a] Kaagan (2000), [b] Vermeersch and Boon (2010).

3.4.1.3 Poeymaü

Location Approximately 1 km southwest of the village of Arudy, Pyrénées–Atlantiques, France

Co-ordinates 43.10°N, 0.45°W

Age *c.* 12–11 k yr BP

Archive Museé National de Préhistoire, Les Eyzies-de-Tayac-Sireuil, France

Description This site is a cave developed in Early Cretaceous limestone in the foothills of the French Pyrenees, near the village of Arudy and the town of Lourdes. Poeymaü was discovered in 1922 by R. Couste, and was the subject of extensive study by G. Laplace from 1948 to 1979 (Vialou, 2004, p. 1090). The cave was found to contain a 7 m thick succession of breccias and fossil-rich sediments thought to span the Lateglacial to the Middle Holocene. A travertine, present in the middle of the stratigraphy, helps to constrain dating of the site. The deposits have yielded end-Magdalenian archaeology, Mesolithic burials and artefacts, and a fossil assemblage of mammals and molluscs, making the site an important record of Lateglacial and Postglacial faunal change in this part of southwest Europe.

Material examined Nineteen *Arvicola* M_1s were photographed, all in good condition with full occlusal surfaces available for landmarking. Enamel edges were clean and easily discernible. Almost all specimens were complete mandibles covered in a light coating of buff coloured, fine-grained sediment. The specimens were derived from a single layer, the *Blocaille Supérieure* (Upper Breccia, see 'Stratigraphy and correlation' below), and only identified to the generic level. No prior assessment has been published of this material and no details of associated fauna in this part of the stratigraphy were available, the main focus of prior research having been the archaeology.

Palaeoenvironments No additional information on the fauna from the Upper Breccia of Poeymaü was available and so other lines of evidence must be relied upon to infer palaeoenvironments. The site lies near the limit of ice extent in the Pyrenees during the Last Glacial Maximum, and during the Lateglacial Stadial, mountain glaciers would likely have been only a few kilometres distant (Hérail *et al.*, 1986; Calvet, 2004). Pollen analysis in the nearby Lourdes basin shows that a steppe landscape existed in the Lateglacial until a birch, juniper, and pine expansion at around 15 k yr BP to 12.5 k yr BP. The Lateglacial Stadial saw an increase in grasses and *Artemisia* into the early Holocene when sudden increases

in pine and oak pollen are recorded (Reille and Andrieu, 1995; Gonzalez-Samperiz *et al.*, 2005). In modern times *Arvicola* has been found in the pine forests of the Pyrenees (D. Harrison pers. comm., 2007), which demonstrates the ability of water vole to colonise these habitats. It must also be noted that the area around Poeymaü is topographically complex, presenting opportunities for arboreal or mesophyllic vegetation to persist or develop in areas sheltered from climatic deterioration (Jalut *et al.*, 1992; Gonzalez-Samperiz *et al.*, 2005).

Stratigraphy and correlation The *Arvicola* material examined originated from the *Blocaille Supérieure* (Upper Breccia) located below a stalagmite floor and immediately above a *Couche á petits éléments*, which itself occured above a *Blocaille inférieure* (Lower Breccia). The stalagmite floor has been dated to between 10420 ± 200 BP and 11540 ± 230 BP[1], and end Magdalenian archaeology from the Upper Breccia has been dated to $12\,000 \pm 250$ cal BP (Ly-1384). The Upper Breccia was therefore attributed to the later part of the Lateglacial Stadial (Stéphane Madelaine pers. comm., 2008[2]).

A single *Arvicola* mandible was submitted for radiocarbon dating for this study and gave a calibrated date of $11\,600 \pm 140$ cal BP (Table 3.7). This is instructive in that it supports existing information on the age of the Upper Breccia and, although one radiocarbon date cannot be used to constrain the range of the entire *Arvicola* assemblage, alongside the date provided by the archaeology and the minimum age imposed by the stalagmite floor, it appears that the *Arvicola* assemblage originates from a discrete period at the Lateglacial/Holocene transition. For the purposes of this study the radiocarbon date from *Arvicola* will be used as an age for the OTU.

Table 3.7: Radiocarbon determination made for this study of an *Arvicola* mandible from Poeymaü.

Lab no.	Material	^{14}C BP	cal BP
OxA-21079	*Arvicola* mandible	$10\,065 \pm 45$	$11\,600 \pm 140$

[1]Dating references Ly-1386 and Ly-1385 respectively
[2]Museé National de Préhistoire, Les Eyzies-de-Tayac-Sireuil.

3.4.1.4 Régourdou

Location Near the village of Montignac, Dordogne, France

Co-ordinates 45.06°N, 1.17°E

Age MIS 5c–MIS 3

Archive Museé National de Préhistoire, Les Eyzies-de-Tayac-Sireuil, France

Description A cave formed in Cretaceous limestone situated a few hundred metres from the famous Grotte de Lascaux. Régourdou is best known for a Neanderthal burial associated with the bones of numerous brown bears. A 7 m thick series of fossiliferous sands and breccias (Figure 3.5) was excavated in 1960 by E. Bonifay. This followed the discovery of the cave and hominin remains in the late 1950s by a local inhabitant.

Material examined Samples of *Arvicola* were taken from three levels within the stratigraphy: layers 7 ($n = 26$), 5 ($n = 21$), and 3 ($n = 13$). *Arvicola* were abundant layers 7 and 5 and so the M_1s photographed constituted a subsample of well-preserved specimens (see below). Specimens were lightly covered in reddish, fine-grained sediment; some mandibles were dark-brown in colour and some were broken or had other M_2s or M_3s missing.

No study of the water vole from Régourdou has been published but the specimens were assigned as *Arvicola terrestris* in the Museé National de Préhistoire, Les Eyzies-de-Tayac-Sireuil.

Palaeoenvironments Simard (1966) documented changes in small mammal fauna through the Régourdou sequence. A discernible decrease in woodland species such as wood mouse *Apodemus sylvaticus*, squirrel *Sciurus vulgaris*, and bank vole *Clethrionomys glareolus* occurred from Layers 7–3. This change in woodland taxa is mirrored by a relative growth in numbers of short-tailed field vole *Microtus agrestis* and *Arvicola* over the same period: the former species today inhabits meadow and marginal woodland zones. In Layers 4 and 3 the open grassland steppe lemming *Lagurus lagurus* appears, and a cold-climate assemblage with reindeer can be found in Layer 2 (Bonifay *et al.*, 2007).

These patterns of faunal change indicate a decrease in woodland and an increase in open grassland, reflecting a progressive cooling of climate which appears, for the most part, mesic until the onset of cold-climate in Layer 2.

Stratigraphy and correlation Dating of the Régourdou sequence has employed both climatostratigraphy and dating of archaeological industries. The chronology of Bonifay *et al.* (2007) suggested Layers 8–4, which contained Middle Palaeolithic artefacts, date from the beginning of the *Würm ancien* (90–60 k yr BP), and Layer 3 was deposited during *le premier interstade Würm* (60–55 k yr BP).

A single conventional radiocarbon date on charcoal associated with Neanderthal remains in Layer 4 gave an age of $45\,500 \pm 1\,800$ ^{14}C BP (GrN-4308). This suggests the age of the estimation by Bonifay *et al.* (2007) may be too old. However, being only a single determination made on material susceptible to contamination, the significance of this date can be questioned. The following possible age ranges will be given to the *Arvicola* assemblages, restricted by the dates given by Bonifay *et al.* (2007): Layer 7 MIS 5c–4, Layer 5 MIS 5c–4, and Layer 3 MIS 3. The expectation is that layers assigned the same age will resolve themselves into stratigraphic succession during analysis.

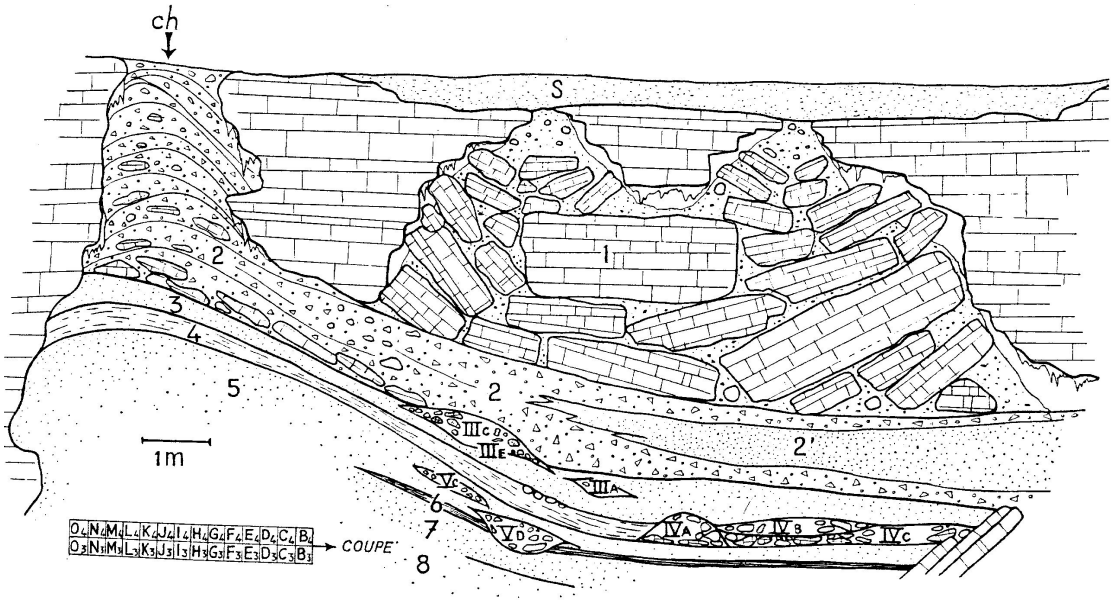

Figure 3.5: Longitudinal cross-section of the stratigraphy at Régourdou. See text for discussion. Taken from Bonifay (1964).

3.5 Germany

3.5.1 Early Middle Pleistocene

3.5.1.1 Miesenheim I

Location On the river Nette near the village of Miesenheim, Rheinland-Pfalz, Germany

Co-ordinates 50.40°N, 7.41°E

Age MIS 15 or MIS 13

Archive Universiteit Leiden, Leiden, the Netherlands

Description Miesenheim I is an open site situated on a small spur of land on the eastern bank of the river Nette, a small tributary of the Rhine. The site was excavated between 1982 and 1990 after fossil bones were discovered following quarrying for pumice and basalt. The sedimentary sequence had a maximum thickness of 2.8 m, and consisted of clays, sands, and gravels associated with the nearby river, colluvium deposits, and loess (Table 3.8). Originally this entire sequence was covered by a thin layer of pumice and a thick basalt ash, this has since been removed through quarrying. Fossils were found from the transition between Units H–G, the top of Unit G, Unit F, and Unit C (Kolfschoten, 1988).

Table 3.8: Simplified stratigraphy at Miesenheim I. From Kolfschoten (1988).

Unit	Lithology	Depositional environment
Not named	Loess	Cold climate aeolian
Gleeser Basalt	Tephra	Volcanic
Wehrer Pumice	Pumice	Volcanic
A	Loess	Cold climate aeolian
B	Gravel	Cold climate fluvial
C	Loamy colluvium	
F*	Clays and loams	Marsh
G	Calcareous colluvium and loam	
H	Calcareous loam	
I	Fine sand and loam lenses	

* Units D and E subsumed within Unit F.

Material examined A rich assemblage of small mammals was recovered from Units C–G, including over 2 000 *Arvicola* molar teeth (Kolfschoten and Turner, 1996). None of these molars showed signs of root formation and were assigned to *Arvicola terrestris cantiana* because they possess enamel with *Mimomys*-differentiation (Kolfschoten, 1988).

A subsample of twenty-four M_1 molars were used for this study. The molars were stained a rich brown colour and were in excellent condition with enamel bands and salient angles clearly defined. Enamel thickness data available in the literature (Table 3.9) show high SDQ values for the fossil assemblage, although with slightly differing means, which may possibly be ascribed to different sample sizes.

Palaeoenvironments The fossiliferous deposit is clearly interglacial, as shown by the presence of woodland species such as garden dormouse *Eliomys quercinus* and hazel dormouse *Muscardinus avellanarius*. Open habitats are also indicated nearby through the occurrence of *Microtus* sp. There is also a mesic character to the assemblage; although this may be a local signal given the sedimentological evidence for nearby fluvial influence. Norway lemming *Lemmus lemmus* is a notable member of the fauna because this species is only found in cold, arctic, climates later in the Pleistocene (Kolfschoten and Turner, 1996). Its occurrence in interglacial conditions here supports other studies (Koenigswald, 1973; Koenigswald and Tobien, 1987) that have suggested that the ecological requirements and tolerances of this species were different earlier in the Pleistocene to the Late Pleistocene and the present day.

Stratigraphy and correlation It is evident that the fossiliferous deposits of Miesenheim I accumulated during a warm period, and palaeobotanical evidence further suggests that deposition occurred toward the end of an interglacial (Kolfschoten, 1988). The large mammal fauna contains some characteristic early Middle Pleistocene taxa such as the extinct wolf *Canis lupus mosbachensis* and Deninger's cave bear *Ursus* cf. *deningeri* (Kolfschoten and Turner, 1996; Koenigswald and Heinrich, 1999).

In the small mammal fauna, the co-occurrence of *Arvicola* with *Microtus* places the site within the Middle Pleistocene and Late Pleistocene Toringian biozone of Fejfar and Heinrich (1981). Analysis of *Arvicola* enamel thickness ratios (Table 3.9) and M_1 lengths led Maul *et al.* (2000) to suggest Miesenheim I dates from MIS 13 or MIS 11, although to prevent circularity, the use of an *Arvicola*-based dating approach is inadmissible for pre-analysis dating of sites in the present study. An MIS 11 age is at odds with biostratigraphic evidence from the large mammal fauna (see above) and furthermore, different SDQ values for the site have appeared

in the literature (Kolfschoten, 1988; Table 3.9).

At Miesenheim I, *Arvicola mosbachensis* occurs within sediments rich in augite. Augite is also found at the nearby site of Kärlich in Unit H but not in the underlying Kärlich Gb, which is normally magnetised and contains hornblende as well as *A. mosbachensis*. The heavy minerals present in the strata at Kärlich are the product of volcanism in the Eifel region, and their imprint can be detected in the fluvial and shallow-marine sediments of the Rhine that form the Dutch 'Cromerian Complex'. Kärlich Gb has been correlated with the Cromer III 'Interglacial', and Kärlich H—and by analogy Miesenheim I—may be attributed to a post-Cromer III warm period (Koenigswald and Kolfschoten, 1996; Kolfschoten and Turner, 1996; Preece and Parfitt, 2000). Radiometric dating of the Eifel volcanics has proved problematic, but Cromer III is often correlated with MIS 15 (e.g., Maul and Markova, 2007). Miesenheim I therefore may be correlated with MIS 13, however, there is nothing to indicate that Miesenheim I is a distinct interglacial—merely that is it stratigraphically later than Kärlich Gb (Kolfschoten and Turner, 1996)—and it is possible that substage variability within MIS 15 could accommodate Miesenheim I (e.g., Lisiecki and Raymo, 2005). Therefore, the Miesenheim I *Arvicola* assemblage can strictly only be said to date from the later part of the early Middle Pleistocene: i.e., a warm period within MIS 15 or MIS 13. This age-range will be applied to the *Arvicola* assemblage from Miesenheim I.

Table 3.9: Published SDQ values of *Arvicola* from Miesenheim I.

Author	SDQ			
	n	min	mean	max
Maul *et al.* (2000)	9	123.32	140.62	155.26
Kolfschoten (1988)	29	126	152.03	180

3.5.1.2 Mosbach 2

Location Wiesbaden, Hesse, Germany

Co-ordinates 50.06°N, 8.26°E

Age MIS 15 or MIS 13

Archive Senckenberg Forschungsinstitut und Naturmuseum, Frankfurt, and Rheinland-Pfalz Natural History Museum, Mainz, Germany

Description Thick deposits of fluvial sands of the Rhine and Main rivers are found at Wiesbaden and are extracted on an industrial scale. Deposition in the area is fault-controlled and has allowed over 13 m of early Middle Pleistocene sands to be accommodated in three units—Mosbach 1, 2, and 3—which lie unconformably on Late Miocene limestone (Koenigswald and Tobien, 1987; Maul *et al.*, 2000; Keller pers. comm., 2008). The palaeontology of the Mosbach sands has been studied since the late 19th century investigations of F. Sandberger, and fossils continue to be actively collected[1]. Many thousands of large and small mammal finds have been made from Mosbach 2, also known as the *Graues Mosbach*, and these include large quantities of *Arvicola* remains.

Material examined The numerous *Arvicola* fossils found in the Mosbach 2 sands provide an excellent opportunity to amass a large sample of individuals for morphological analysis. One hundred and twenty-one M_1s were photographed. Specimens were lightly stained a red-brown colour, and generally occlusal outlines and enamel layers were in good condition, although in most specimens the dentine fields of enamel triangles had partially disintegrated. In some instances this appears to have structurally weakened the molar, causing sections of the tooth to break apart, and allowing only one hundred and nine M_1s to provide full configurations of landmarks.

Mosbach 2 is a thick deposit of fine-grained sand. The time-span represented by this deposit is not well constrained and the taphonomy of the *Arvicola* assemblage has not been considered. Given the depositional environment, the potential for temporal mixing in the assemblage appears considerable (see Popova, 2004).

Schmidtgen (1911) first described fossil water voles from Mosbach 2 as *Microtus mosbachensis*. Although some early authors also assigned material to *Arvicola greenii* and *Arvicola moenana*, most taxonomists have referred all the water vole from Mosbach 2 to *Arvicola mosbachensis* (Heller, 1933, 1969; Bahlo and Malec,

[1]Collection and sedimentological studies by T. Keller and the Rheinland-Pfalz Natural History Museum, Mainz

1969; Andres, 1971; Koenigswald and Tobien, 1987; Maul *et al.*, 2000). The characters supporting this identification are the absence of roots in most individuals, relatively small size, enamel with *Mimomys*-differentiation (Table 3.10), and persistence of a *Mimomys*-fold in a large proportion (27%) of adult M_1s (Maul *et al.*, 2000). The presence of incipient roots in a small percentage of specimens led Maul *et al.* (2000) to conclude that the water vole from Mosbach 2 was a very early *Arvicola* population. These authors further proposed that *Arvicola* from Mosbach 2 be used as the reference for early populations of rootless water vole instead of the type *Arvicola cantianus* from Great Britain (Section 2.3.3).

Table 3.10: Published SDQ values of *Arvicola* from Mosbach 2.

Author	SDQ			
	n	min	mean	max
Maul *et al.* (2000)	45	117.6	133.34	159.27

Palaeoenvironments The fossil fauna clearly indicates a temperate, mesic, interglacial environment, which Maul *et al.* (2000) compared to that of the present day in the central Rhine. The presence of beaver *Castor fiber* and desman *Desmana moschata* suggests that freshwater pond and riparian habitats were important parts of the landscape. Given these habitat indicators and the abundance of *Arvicola* a semi-aquatic ecology for the fossil water vole population seems likely. Obligate woodland taxa such as wood mouse *Apodemus sylvaticus* are not present, which suggests that dense woodland habitats did not exist, although *C. fiber* indicates that trees were present. Lemming *Lemmus* sp. is a seemingly contradictory member of the fossil assemblage, but its Middle Pleistocene distribution is apparently not restricted to the cold environments that characterise the distribution of *Lemmus lemmus* in the Late Pleistocene and Holocene (Koenigswald, 1973; Koenigswald and Tobien, 1987; Maul *et al.*, 2000).

Stratigraphy and correlation The presence of the mole *Talpa minor*, shrew *Sorex* (*Drepanosorex*) *savini*, and archaic vole *Pliomys episcopalis* suggests that Mosbach 2 dates to the later part of the early Middle Pleistocene (Koenigswald and Heinrich, 1999; Maul *et al.*, 2000). These taxa also co-occur at Miesenheim I, which is thought to date to MIS 15 or MIS 13 (Section 3.5.1.1).

The role played by fossil water voles has become important in attempts to date the Mosbach 2 sands. The first appearance of *Arvicola* in central Europe has been dated to the Cromer III Interglacial (Koenigswald and Kolfschoten, 1996), which

has been correlated with MIS 15 (e.g., Maul and Markova, 2007). This agrees with other biostratigraphic evidence in suggesting an age for Mosbach 2 in the later part of the early Middle Pleistocene, but also provides a possible maximum age. The evidence from morphometric analysis of *Arvicola* also supports a late early Middle Pleistocene age (Maul *et al.*, 2000), however, SDQ and M_1 length are unable to resolve the relative relationships between Mosbach 2 and Miesenheim I. Morphometric evidence from other arvicolids sugegst that Mosbach 2 is older than the nearby German site of Miesenheim I (Section 3.5.1.1) and the British site of Boxgrove (Section 3.6.1.1), and perhaps contemporary with Westbury-sub-Mendip (Section 3.6.1.3) in Great Britain (Maul and Parfitt, 2010)

The published morphometric evidence from *Arvicola* is not admissible in this study. Other biostratigraphic evidence from the mammal assemblage and the weight of evidence supporting an absence of roots in the molars of water vole in this part of Europe by MIS 15 does suggest a possible MIS 15 or MIS 13 age for Mosbach 2.

3.5.2 Late Middle Pleistocene

3.5.2.1 Schöningen II

Location Opencast lignite mine, east of the town of Schöningen, Lower Saxony, Germany

Co-ordinates 52.14°N, 10.97°E

Age MIS 11 or MIS 9

Archive Universiteit Leiden, Leiden, The Netherlands

Description At the site of Schöningen, a series of overlapping fluvial channels, cut by a now absent river, occurs within a subsiding graben basin. Six channel sequences containing fossiliferous, interglacial, lacustrine silts and peats have been found, three of which—Schöningen I, II, and III—are of late Middle Pleistocene age (Thieme, 2007). The deposits were exposed through open-cast mining for brown-coal and research excavations continue alongside ongoing mining activity.

The *Arvicola* remains used in the present study come from the Schöningen II channel. This channel is most famous for finds of wooden spears and other archaeology, but a considerable vertebrate and molluscan fauna, and a detailed pollen and plant macrofossil record, were also recovered from five horizons within the sequence (Kolfschoten, 1993a; Urban, 2007). The deposits of Schöningen II have been identified as a late Middle Pleistocene interglacial, regionally named the Reinsdorf interglacial, but correlation with the global marine oxygen isotope stratigraphy

remains contentious (Kolfschoten, 1993a; Thieme, 1997; Schreve and Bridgland, 2002; Thieme, 2007).

Material examined A representative subsample of thirty-three M_1s was photographed from the large quantity of *Arvicola* fossils recovered from Schöningen II. All molars were stained very dark-brown or black, and were in a good state of preservation. In most cases occlusal outlines and enamel layers were well-defined, although four M_1s could not provide full compliments of landmarks due to breakage.

The *Arvicola* specimens examined derived from horizon 4 in the Schöningen II channel (specifically, excavation area 13 in horizon 4: Schöningen 13 II-4). This stratum is a dark, organic-rich, peat and silt layer, containing evidence of climatic warming from a cool steppe to a boreal forest environment (see below). The depositional setting appears to have been a low energy fluvio-lacustrine system, which would suggest that the the fossil assemblage may not suffer from the same degree of taphonomic mixing as would a higher energy channel-lag deposit (see Behrensmeyer, 1993).

The water vole was referred to *Arvicola terrestris cantiana* (= *Arvicola mosbachensis*) by Kolfschoten (1993a). Enamel thickness measurements by the same author gave SDQ values of 120–130.

Palaeoenvironments Schöningen lies in a subsiding valley set between low hills, and the presence of a fluvial system running through this area led to the development of persistent and extensive wetland environments. This is indicated by sedimentary evidence and in Schöningen II by the abundance of semi-aquatic taxa such as desman *Desmana moschata*, beaver *Castor fiber*, and in all likelihood *A. mosbachensis*. Evidence for the the mesic nature of the local environment is reinforced by the occurrence of northern vole *Microtus oeconomus* (Kolfschoten, 1993a). The presence of a mosaic landscape of wood and grassland can be inferred from finds of bank vole *Clethrionomys glareolus* and roe deer *Capreolus capreolus*, alongside common vole *Microtus arvalis*, short-tailed field vole *Microtus agrestis*, and horse *Equus* sp.—the latter an important prey species of hominins (Kolfschoten, 1993a; Thieme, 2007).

Within the Schöningen II sequence three warm–cool oscillations have been discerned (Thieme, 2007). In the basal horizon, Schöningen II-1, a mosaic of open, temperate, mixed-woodland and grassland is indicated. A travertine was deposited at this time and the presence of the terrapin *Emys orbicularis* indicates that climate was warmer than that of the region at present (Thieme, 2007). Subsequent horizons document general climatic cooling and palaeoenvironmental variation. In Schöningen II-4—the context of the *Arvicola* assemblage considered here—there

is evidence of a cool to cool-temperate trend (Thieme, 2007).

Stratigraphy and correlation The three lower channels—Schöningen I, II, and III—all lie above glacial deposits attributed to the Elsterian (= MIS 12), and below glacial deposits attributed to the Saalian (Thieme, 2007). The channel deposits are temperate accumulations and palaeonenvironmental evidence from Schöningen II-4 suggests that this horizon was deposited toward the end of this interglacial, in the Reinsdorf B stadial and interstadial (Thieme, 2007, and see Palaeoenvironments above). U-Th dating of the travertine at the base of Schöningen II has given an age of *c.* 320 k yr BP (Thieme, 2007, p. 72), which suggests a correlation of the Reinsdorf interglacial with MIS 9. Schreve and Bridgland (2002) drew comparisons between Schöningen II and the sites of Bilzingsleben II in Germany and Swanscombe in the Lower Thames of southern England. These sites are believed to be MIS 11 in age. Also worthy of note, although inadmissible as dating evidence for this study, is the *Arvicola* SDQ values (see above), which are similar to those from Holsteinian (= MIS 11) sites in central Europe such as Bilzingsleben (Kolfschoten, 1993a).

For the purposes of this study the *Arvicola* assemblage will be assumed to be either MIS 11 or MIS 9 in age.

3.5.3 Late Pleistocene

3.5.3.1 Biedensteg

Location	Near the town of Bad Wildungen, Hesse, Germany
Co-ordinates	51.11°N, 9.14°E
Age	MIS 3
Archive	Senckenberg Forschungsinstitut und Naturmuseum, Frankfurt, Germany

Description A former loess pit located in a topographic depression to the south-east of the town of Bad Wildungen, Biedensteg was first excavated in 1932 by amateur palaeontologist F. Pusch who recovered a variety of vertebrate remains dating from the later part of the Last Cold Stage. Pusch investigated the fauna until his death in 1948, after which his younger collaborator, Eduard Jacobshagen, continued the work. A monograph on the site was published in 1963, which also contained a stratigraphic analysis based on sections and boreholes made in other parts of the pit in 1962 (Jacobshagen, 1963).

The main excavations were carried out on exposures in the northern part of the pit from the 1930s to the 1950s; a summary profile of the sediment sequence found is shown in Figure 3.6. A loess sequence was observed laying directly upon both Triassic *Bundsandstein* sandstones and a fluvial gravel ridge. The top 1.7 m of the sequence is a *Fließerde* (geliflucted soil) overlain by a Holocene humic soil. The lower 2 m of the loess sequence is waterlogged and decalcified. Numerous vertebrate fossils were found from the uppermost parts of Horizon I and throughout the brown and yellow loess of Horizons II, III, and IV. Concentrations of small mammal remains were found in two discrete *Gewölle-Schichten* (Pellet-Layers) which bound Horizon II. These layers consisted of sediments concentrated in the pellets of birds of prey, which in some instances were still intact and attributable to owls (Jacobshagen, 1963). The Pellet-Layers were laterally discontinuous and, for the most-part, localised concentrations.

Material examined The *Arvicola* used in this study were derived from the Pellet-Layers of Horizon II and were identified, although no taxonomic discussion was made, as *Arvicola amphibius* (= *Arvicola terrestris*) by Jacobshagen (1963). *Arvicola* were found in such horizons in many parts of the loess pit, which presumably represent the same period of accumulation. The material seen by this study was part of Pusch's original collections from the north of the site.

Twelve M_1s were photographed. All molars were similar in appearance, suggesting a shared taphonomic history: pitted and darkly-stained dentine, and brown, transparent enamel. The enamel layers were easily visible but slightly eroded, and this may contribute to error in enamel thickness measurements. Evidence of erosion presumably represents corrosion from stomach acids during digestion, but may also be the result of erosion during residence time within soils (Ruddy, 2005).

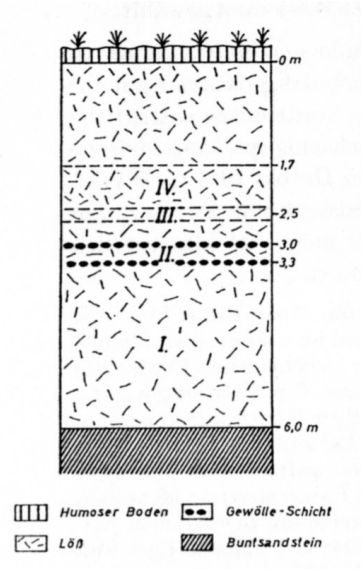

Figure 3.6: Summary stratigraphy of the loess deposits at Biedensteg. See text for explanation. Taken from Jacobshagen (1963).

Palaeoenvironments The thick loess deposits of Horizon I would have accumulated during periods of cold climate, and the upper parts of this layer contain cold-climate taxa such as the lemmings *Dicrostonyx* sp. and *Lemmus lemmus*, and arctic fox *Alopex lagopus*. The occurrence of the Pellet-Layers of Horizon II suggests that a break in deposition occurred. *Dicrostonyx* sp. and *L. lemmus* are still present from the fauna found in Horizon II, but occur alongside bank vole *Clethrionomys glareolus*, northern vole *Microtus oeconomus*, and *A. terrestris*, which in-

dicate the development of more temperate, mesic conditions (Storch, 1969). Above Horizon II the renewed deposition of loess shows that climate became colder and drier; *Dicrostonyx* sp. and narrow-skulled vole *Microtus gregalis* have been found here and the sediments have been effected by cryoturbation. A Holocene soil tops the sequence.

Stratigraphy and correlation The faunal remains from Horizon II are not biostratigraphically diagnostic, but ecologically mixed assemblages such as the one found have been considered typical of MIS 3 faunas of north and west Europe (e.g., Stewart, 2008). The geliflucted and cryoturbated sediments immediately below the Holocene soil were probably the result of the intense cold of the Last Glacial Maximum. A conventional radiocarbon date of 29 200 ^{14}C BP (Koenigswald, 1985, no laboratory reference given) was determined on a small mammal bone from the '*Rotbraunen Gewölleschicht*'. It is difficult to determine from where in the loess pit this refers, but pellet layers throughout the pit are likely to reflect the same climatically controlled depositional event and be stratigraphically equivalent.

The climatostratigraphic and faunal dating evidence available seem to agree in attributing the pellet layers of Horizon II to MIS 3. The radiocarbon date suggests a late MIS 3 age for this horizon, but without radiocarbon dating of the *Arvicola* specimens a late MIS 3 age cannot be assumed for the whole water vole assemblage. A conservative age-estimate of MIS 3 will therefore be applied to the *Arvicola* specimens.

3.5.3.2 Brillenhöhle

Location	Near the village of Blaubeuren, Baden-Württemberg, Germany
Co-ordinates	48.41°N, 9.78°E
Age	GI-1
Archive	Senckenberg Forschungsinstitut und Naturmuseum, Frankfurt, Germany

Description Brillenhöhle is a cave excavated between 1955 and 1963 by G. Riek and is one of a number of caves containing Late Pleistocene deposits in the steep-sided Blaubeuren valley. The valley was originally formed in the Early Pleistocene by the river Danube, which later bypassed the area in favour of a more southerly course. Excavations recovered Aurignacian, Gravettian, and Magdalenian archaeology, as well as a relatively rich fossil fauna (Riek, 1973; Conard and Moreau, 2004). Eight sedimentary units were identified in an approximately 2.5 m long se-

quence, predominantly made up of angular, clast- or matrix-supported limestone breccia (Riek, 1958, 1973; Figure 3.7).

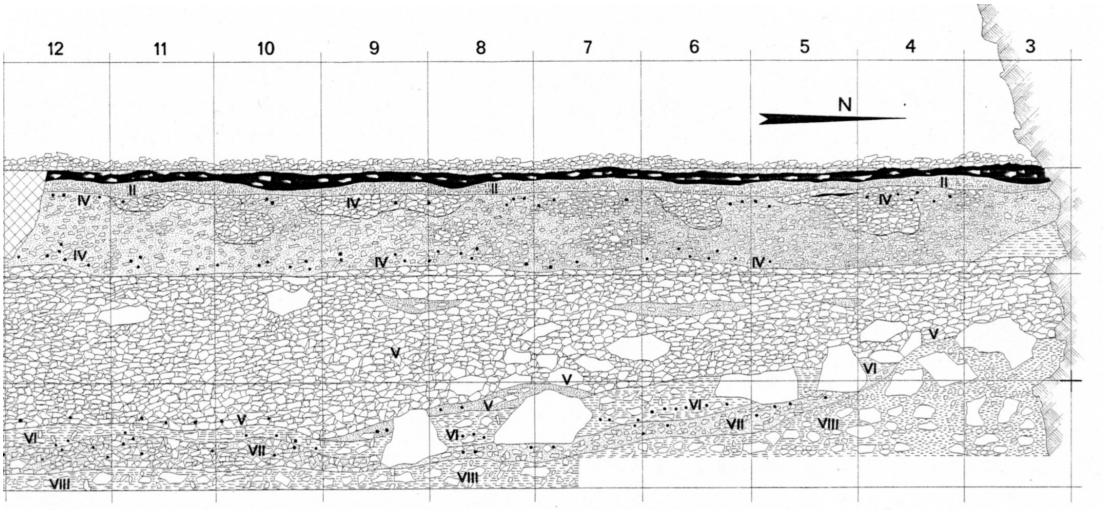

Figure 3.7: Longitudinal cross-section of the stratigraphy at Brillenhöhle. See text for explanation. Taken from Riek (1973).

Material examined Nineteen *Arvicola* M_1s were photographed from Layer IV. All molars were present within mandibles and were slightly stained but in very good condition. Enamel triangles were well defined and enamel layers clearly visible. No detailed information on the stratigraphic context of the fossil material could be found by this author but the sedimentological variability of the breccias recorded from Layer IV (Riek, 1973) suggests that the *Arvicola* fossils may not represent a temporally discrete assemblage.

Specimens were identified as *Arvicola antiquus* (= *Arvicola terrestris*) in the Senckenberg Forschungsinstitut und Naturmuseum, Frankfurt and by Storch (1973). *A. antiquus* has been recognise as a distinct form of small, possibly fossorial, water vole present in Late Pleistocene mixed vole and lemming faunas from France and Germany (Storch, 1971, cited in Gromov and Polyakov, 1992, p. 348).

Palaeoenvironments The sequence is predominantly composed of cold-climate, freeze-thaw breccias. In Layer IV there is an increase in the proportions of fine-grained, loessic, sediments. The small mammal fauna from Layer IV has not been published, but other mammals include mammoth, reindeer, arctic hare, arctic fox, and horse (Riek, 1958). This evidence suggest that periods of cold-climate existed around the time of deposition of Layer IV but there is little other evidence published on the site that can inform on palaeoenvironments.

Stratigraphy and correlation A Lateglacial Interstadial age has been tentatively estimated for Layer IV. Layer V is a clast-supported, angular breccia,

indicative of cold-climate freeze-thaw process, while Layer IV is a rough, loose, matrix-supported, angular breccia (Riek, 1958; Figure 3.7). No information on the fauna from Layer IV is available, but the increase in finer-grained sedimentation, and occurrence of *Arvicola* here suggests climatic amelioration with respect to the stratum below. A greater concentration of large angular clasts can be found at the top of Layer IV, which is then overlain by an organic-rich, fine-grained 'cave earth'. Bearing mind that Layer VII has a minimum age of 25 ^{14}C k yr BP (Table 3.11), and that the site is only 40 km away from the maximum extent of the Alpine ice-sheet during the Last Glacial Maximum (Velichko *et al.*, 2004), a speculative climatostratigraphic interpretation of this sequence could attribute Layer V to the Last Glacial Maximum, Layer IV to the Lateglacial Interstadial, and the uppermost strata to the Holocene. Riek (1973) followed this correlation, supported by archaeological evidence, and attributed Layer IV to the 'Older Younger Dryas' based on the presence of *Junges Madeleine* and *Harpun Madeleine* artefacts. In the absence of other evidence a tentative age-range spanning GI-1 will therefore be assumed for the *Arvicola* assemblage.

Table 3.11: Radiocarbon dates from Brillenhöle.

Layer	Lab no.	Material	^{14}C BP	cal BP
VII				
	B-492[a]	Charred bone	$> 25\,000$	
	KIA 19549[b]	Mammoth/rhino rib	$25\,870 \pm 230$	$30\,892 \pm 374$
	KIA 19549[b]	Mammoth/rhino rib	$27\,030 \pm 180/170$	$31\,800 \pm 152$
VIII				
	B-491[a]	Charred bone	$> 29\,000$	
XIV				
	KIA 19550[c]	?Reindeer antler	$30\,400 \pm 240/230$	$34\,537 \pm 211$
	KIA 19551[c]	?Reindeer antler	$32\,470 \pm 270/260$	$37\,018 \pm 753$

[a] Riek (1973) conventional date
[b] Conard and Moreau (2004) AMS date
[c] Bolus and Conard (2006) AMS date

3.5.3.3 Burgtonna South Black-earth

Location Near the village of Burgtonna, north-west of the city of Erfurt, Thüringia, Germany

Co-ordinates 51.06°N, 10.72°E

Age MIS 5d to MIS 5a

Archive Senckenberg Forschungsstation für Quartärpaläontologie, Weimar, Germany

Description Quarrying of 'travertine' deposits, extensively developed along the valley of the river Tonna, has led to the exposure of three fossiliferous Late Pleistocene sites. The area has been a focal point for geological research for four hundred years, but recent investigations have concentrated on the most southerly of two nearby quarries (Burgtonna South—BTS) at the eastern edge of the town of Burgtonna. The strata found at BTS encompass several phases of the Last Interglacial and Last Cold Stage, and provide a important record of palaeoenvironmental change through this period in south-central Germany (Heinrich and Jánossy, 1978; Meyrick and Maul, 2002).

Although generally referred to as travertines, the carbonate deposits are polygenetic: the product of precipitation around springs and cascades, and extensive freshwater lakes. These deposits can be up to 10 m thick but thin toward the edges of former lake basins, which developed upon Triassic clays and cold-climate gravels. The covering layers above the carbonate deposits have been found to contain a rich interglacial fossil assemblage, which has been intensively-studieds. An organic-rich, partially allocthonous *Schwarzerdekolluvium* (Black-earth or *Chernozem*) can be found overlying the carbonates locally, and both the carbonates and black-earth are overlain by loess (Meyrick and Maul, 2002).

Material examined The *Arvicola* fossils used in this study were found in the black-earth horizon. These specimens have been described as *Arvicola terrestris terrestris* (= *Arvicola terrestris*) based upon molar enamel possessing a *Microtus*-differentiation (Heinrich and Jánossy, 1978; Heinrich, 1982; Maul, 1994; Meyrick and Maul, 2002; Table 3.12).

Thirty-six M_1 teeth were photographed for this study. Molars were isolated and shared a similar preservational state: brown-grey discolouration, often with fractured posterior lobes. Tooth enamel does not appear to have suffered from erosion or corrosion and, due to the staining of dentine, enamel bands were prominent and well defined.

Table 3.12: Published SDQ values from the Burgtonna South black-earth horizon.

Author	SDQ			
	n	min	mean	max
Heinrich (1982)	40	76.34	99.651	116.95
Heinrich (1987)			98.44	

Palaeoenvironments In the 'travertines' at BTS the presence of woodland snails and temperate mammal species, such as elephant *Elephas antiquus*, demonstrate the existence of temperate interglacial conditions (Meyrick and Maul, 2002).

Black-earths—or *chernozems*—such as the one found at Burgtonna are considered to have formed in a relatively dry climate with warm springs and summers only capable of supporting grassland (Terhorst, 2000). The mammalian and molluscan assemblages support this palaeoenvironmental interpretation. In the small mammals no woodland taxa are found, but the fauna is composed exclusively of open-landscape fauna including common vole *Microtus arvalis* and narrow-skulled vole *Microtus gregalis*. The presence of species such as mole *Talpa europaea* shows that the climate was not excessively cold or dry (Heinrich and Jánossy, 1978; Meyrick and Maul, 2002).

The deposition of loess containing fossils of the steppe lemming *Lagurus lagurus* over the black-earth suggests that climate cooled and became wetter. Evidence of periglacial activity can be found in the form of ice-wedges penetrating from the loess horizon through the black-earth into the carbonates (Meyrick and Maul, 2002).

Stratigraphy and correlation Kahlke (1978) and Meyrick and Maul (2002) suggest that the travertines are Last Interglacial in age. Here, the occurrence of extinct porcupine *Hystrix* cf. *vinogradovi* and *Arvicola mosbachensis* are biostratigraphically significant, as are climatic indicators such as *E. antiquus* and Merck's rhinoceros *Stephanorhinus kirchbergensis* (Meyrick and Maul, 2002). How much of MIS 5e is represented in the carbonates is, however, still under debate (Meyrick and Maul, 2002).

The correlation of the carbonates with the Eemian (= MIS 5e) appears sound, and implies that the black-earth lying above was deposited during the early part of the Last Cold Stage (early Weichselian, MIS 5d–5a). This is supported by the climatic deterioration indicated by the deposition of loess and periglacial activity above the black-earth, which can be referred to the deepening climatic cooling of the Weichselian (Meyrick and Maul, 2002).

Arvicola SDQ values estimate an age of *c.* 80 k yr BP for the black-earth (Maul *et al.*, 1998b). However, to prevent circularity, this SDQ derived date cannot be used by this study to infer age and so, in the absence of other evidence, an age-range of MIS 5d–5a will be attributed to the *Arvicola* assemblage.

3.5.3.4 Fuchsloch im Krockstein

Location Near the village of Rübeland, Harz Mountains, Germany

Co-ordinates 51.75°N, 10.87°E

Age *c.* 13–11.3 k yr BP

Archive Museum für Naturkunde, Berlin, Germany

Description One of a number of caves in the Middle Devonian Massenkalk of the Harz Mountains, Fuchsloch im Krockstein is a small cave 20 m up a sheer cliff-face above the river Bode. A period of excavation began in July 1979 by A. Arnold and colleagues from the Museum für Naturkunde der Humboldt-Universität zu Berlin. Sediments consisted of alluvial sands, limestone breccias and calcium carbonate precipitates (Arnold *et al.*, 1982). Fossils were found almost exclusively as closely-packed masses of bone embedded within a *Sinterdecke* (stalagmite floor) at the top of the sedimentary sequence. A fossil assemblage of fish, amphibians, birds, and abundant mammals was discovered, all in an excellent preservation thanks to the encrusting sinter.

Material examined Twenty-six M_1 teeth were photographed, six molars were present within the mandible. Most molars were in a good state of preservation and had a superficially 'fresh' appearance, similar to skeletal material of modern water vole. On closer inspection the dentine of specimens has been partially dissolved, some enamel bands were eroded or had collapsed, and the enamel triangles of three M_1s were damaged, preventing full landmark configurations being taken for these specimens.

The fossil assemblage is thought to be an accumulation of owl-pellets, which Arnold *et al.* (1982) attributed to the eagle owl *Bubo bubo*. Water voles were identified as *Arvicola terrestris* by Arnold *et al.* (1982) and enamel thickness measurements (Heinrich, 1982; Table 3.13) reveal a *Microtus*-differentiation, characteristic of *A. terrestris* in western Europe.

Palaeoenvironments In the small mammals, modern-day Arctic genera such as the lemmings *Dicrostonyx* sp. and *Lemmus* sp. are present alongside open habitat/steppe species such as narrow-skulled vole *Microtus gregalis*, pika *Ochotona*

Table 3.13: Published SDQ values from Fuchsloch im Krockstein.

Author	SDQ			
	n	min	mean	max
Heinrich (1982)	40	72.20	89.076	102.926

pusilla, and hamster *Cricetus cricetus*. A range of species characteristic of more temperate environments today is also present such as *A. terrestris*, wood mouse *Apodemus sylvaticus*, mole *Talpa europaea*, shrew *Sorex* sp., and the barbastelle bat *Barbastella barbastellus*, which is a woodland species (Arnold *et al.*, 1982).

There are a number of possible explanations for the mixed palaeoenvironmental signal. Firstly, the fossil assemblage may be mixed. Arnold *et al.* (1982) rule out stratigraphic mixing and state that the fossil-rich sinter accumulated over a short-period of time. Time-averaging is certainly a problem to consider, however, especially in fossil assemblages accumulated during the later part of the Last Cold Stage. Many proxy records show short-term, high-amplitude climatic fluctuations during this period, and the rapid shifting response of species to this type of climate variation may have resulted in 'climatic time-averaging' (Roy *et al.*, 1996). Secondly, the assemblage may accurately represent the faunal community of the day. Either the whole community has no good analogue in the present, and therefore supplies palaeoenvironmental information that is difficult to interpret (Stewart, in press) or, because the region around Rübeland is topographically varied and allows a diverse range of habitats to exist in a relatively small geographical area, birds of prey may have accumulated prey from a range of local microhabitats.

Stratigraphy and correlation No attempt to radiometrically date the stalagmite floor has been made and therefore relative dating and biostratigraphy have up to now been used to date the fossil assemblage. Although many stalagmite floors across northern Europe were deposited in the early Holocene, the age of the *Sinterdecke* cannot be confidently correlated with similar structures in other caves. The nearby Rübeländ cave of Bielshöhle for example contains a cave loam with fauna dated to 16.5–18 ^{14}C k yr BP below a stalagmite floor (R. Lobst cited in Arnold *et al.*, 1982). However, other nearby caves contain multiple sinter horizons dating back to the Last Interglacial (Arnold *et al.*, 1982).

The cool climate nature of the fossil assemblage suggests a correlation with the middle or later part of the Last Cold Stage. The fauna is without any key stratigraphical indicator species but the assemblage bears a resemblance to the Gough's Cave MAZ in southwest England (Currant and Jacobi, 2001). *Ochotona*

and *Arvicola* were not included in this MAZ but Currant and Jacobi note that both of these taxa were recorded from Gough's Cave and, although not confirmed by direct dating from this site, were present in the Lateglacial Interstadial mammal fauna. Heinrich (1982) suggests a correlation of Fuchsloch im Krockstein with the *Hochglazial der Weichsel-Kaltzeit* ('height of the Weichselian glacial').

The *Arvicola* SDQ values (Table 3.13) led Arnold *et al.* (1982) to correlate the fossil fauna with that of Kematenhöhle in Bavaria, southern Germany, which has been radiocarbon dated to 31 459 ^{14}C BP (Koenigswald, 1978). According to these results the faunal assemblage dates from the 'Pleni-Weichselian' part of the Last Cold Stage. SDQ based dating is inadmissible as dating evidence in the present study but it is worth considering that the dating information it provides differs from that offered by the MAZ approach and the lithostratigraphy of the *Sinterdecke*.

To resolve the age of the fossil assemblage, samples of bone from some of the *Arvicola* specimens used in this study were sent for radiocarbon dating. The results of these analyses are given in Table 3.14. The dates clearly show that the *Arvicola* remains in fact originate from GS-1 to the earliest part of the Holocene. These dates will be used as a temporal range for the *Arvicola* OTU.

Table 3.14: Radiocarbon dating of *Arvicola* M_1s from Fuchsloch im Krockstein carried out for this study.

Lab no.	Material	^{14}C BP	cal BP
OxA-21111	*Arvicola* specimen 2907	$10\,035 \pm 50$	$11\,560 \pm 159$
OxA-21082	*Arvicola* specimen 2903	$11\,005 \pm 50$	$12\,916 \pm 102$
OxA-21118	*Arvicola* specimen 2902	$11\,110 \pm 50$	$12\,992 \pm 109$

3.5.3.5 Kartstein

Location Near the village of Dreimühlen, northern Eifel, Germany

Co-ordinates 50.54°N, 6.66°E

Age GI-1abc or Holocene 'Atlantic' phase

Archive Senckenberg Forschungsinstitut und Naturmuseum, Frankfurt, Germany

Description A rock-shelter in the low mountains of the northern Eifel region of Germany, developed within dolomite and travertine rocks. The site contains a mammalian, molluscan, and amphibian assemblage, alongside archaeology of the Ahrensburgian—or *Stielspitzengruppen*—culture (Street, 1998). There is evidence of intensive butchery of reindeer, which has led some workers to propose that Kartstein and a number of other contemporary northern European sites formed centres for the seasonal hunting of reindeer by humans (Baales, 1992). The site was excavated in 1977 by H. Löhr of the Rheinische Landesmuseum Bonn. The sedimentary sequence represents deposition from the Last Glacial Maximum to the early Holocene, and was divided into six lithological layers (Baales, 1992; Figure 3.8). Fossil and archaeological material was recovered from layers 1, 2 and 3.

Material examined Sixteen M_1s were photographed for this study. Generally preservation was good, but some posterior enamel bands were too eroded for measurement, and the the tips of salient angles were missing on three molars.

Details of the *Arvicola* fossils have not been published in any detail, and water vole is only mentioned as an uncommon member of the fossil assemblage in the faunal list given by Rabenstein (1996). Rabenstein lists the water vole as *Arvicola terrestris*. It is difficult to comment on the taphonomy of the assemblage as the context of the *Arvicola* cannot be identified from the literature (see below). However, stratigraphic mixing and climatic time-averaging (Roy *et al.*, 1996) in cave sediments from the later part of the Last Cold Stage is a potential problem.

Palaeoenvironments The fauna of Layer 2 is dominated by open landscape, arctic and steppic taxa, including reindeer *Rangifer tarandus*, pika *Ochotona pusilla*, collared lemming *Dicrostonyx torquatus*, Norway lemming *Lemmus lemmus*, and the ptarmigans *Lagopus lagopus* and *Lagopus mutus* (Rabenstein, 1996). Wood mouse *Apodemus* and water vole are present in the faunal list from the site, but are less common than the cold-climate species mentioned[1]. None of the liter-

[1]Exact proportions of the different components of the fauna are not given in Rabenstein (1996).

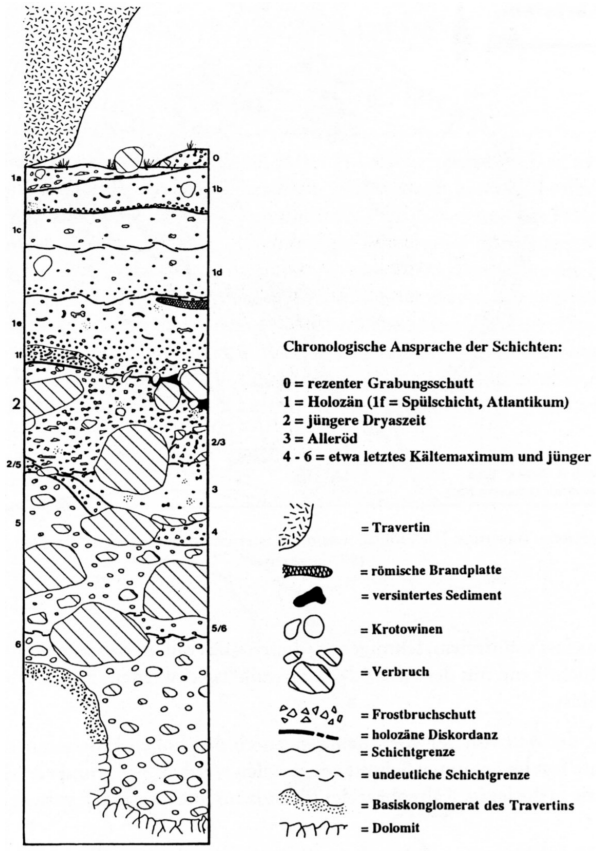

Figure 3.8: Summary stratigraphy of the Kartstein rock-shelter. Key to chronology: 0=recent spoil, 1=Holocene (1f=Atlantic phase), 2=Younger Dryas, 3=Allerød, 4–6=Lateglacial Maximum. Key to lithostratigraphy: Travertine, Roman hearth, sinter, burrows, fallen blocks, frost-shattered breccia, Holocene unconformity, layer boundary, indeterminate layer boundary, conglomerate, Dolomite. From Baales (1992).

ature seen refers to temperate species within discussions of the fauna of Layer 2, and it would appear that these taxa do not derive from this stratum (see below).

Stratigraphy and correlation Layer 1 was found to contain Mesolithic artefacts and fauna attributed to the 'Atlantic' phase of the Holocene at its base (Rabenstein, 1996). An unconformity separates Layer 1 from from the frost-shattered blocks and fine sands of Layer 2. Radiocarbon dating of butchered reindeer from Layer 2 give an age estimation of the Younger Dryas (= GS-1, Table 3.15); this supports the archaeological (Street, 1998), sedimentological, and palaeontological dating evidence. Layer 3 consists of a well-sorted loam, which, through its position below the cold-climate deposits of Layer 2, is considered to have been deposited during the Allerød (= GI-1abc).

Rabenstein (1996) specifically considers the fauna of Layer 2 but at no time mentions the presence of temperate species such as *Apodemus* sp. or *Arvicola* from this part of the stratigraphy. It would appear, then, that the *Arvicola* assemblage originates from either Layers 3 or 1, or both. This provides a maximum age of GI-1abc and a minimum age of the Holocene 'Atlantic' phase for the *Arvicola* assemblage.

Table 3.15: Radiocarbon dates from Kartstein Layer 2. These determinations were carried out at the Oxford radiocarbon accelerator unit without the ultrafiltration technique (Higham pers. comm., 2009). Data from Bronk Ramsey *et al.* (2002).

Lab no.	Material	^{14}C BP	cal BP
OxA-9031	*Rangifer tarandus* bone	$10\,220 \pm 75$	11490 ± 142
OxA-9032	*Lagopus lagopus* bone	$9\,995 \pm 65$	11938 ± 192

3.5.3.6 Tönchesberg II

Location River Nette, central Rhineland, Germany

Co-ordinates 50.37°N, 7.38°E

Age MIS 5e

Archive Universiteit Leiden, Leiden, the Netherlands

Description At Tönchesberg, in the eastern Eifel mountains of southwest Germany, loess deposits and humic-rich palaeosols from the late Middle and Late Pleistocene were found filling the crater of a volcanic debris-cone. Tönchesberg II—the second of two sections excavated in the late 1980s and early 1990s—constitutes a 15 m sequence of non-volcanogenic sediments containing pollen, molluscan, and vertebrate remains. The loess and soils were laterally variable across the basin and, in the centre, sediments had been redeposited within small lakes that formed within the crater (Kolfschoten and Roth, 1995). The sequence of deposition found at Tönchesberg II is echoed in a number of similar sites in the east Eifel region.

Material examined Twenty-three M_1s were photographed. From these, twenty-two molars provided full compliments of landmarks. M_1s were in a good condition but exhibited a variety of preservational colours: from virtually unstained to dark reddish-brown. This variation may indicate that specimens followed different taphonomic routes to fossilisation.

Specimens were derived from Layers 11–13: a humic-rich soil containing archaeology, located above a loess unit. The water vole was described by Kolfschoten and Roth (1995) who referred material to *Arvicola terrestris* through the presence of rootless molars, strongly developed cement, three enamel triangles, and a variable anterior lobe. Enamel thickness measurements (Table 3.16) show a *Mimomys*-differentiation for the *Arvicola* assemblage. Heinrich (1982) proposed that water vole with a *Mimomys*-differentiation be designated *Arvicola cantiana* (= *Arvicola mosbachensis*), but Kolfschoten (1988) argued that all rootless water vole should be referred to *A. terrestris*, as palaeontological species based on the SDQ are merely chronospecies rather than a biologically more realistic evolutionary lineage of populations through time.

Palaeoenvironments The Tönchesberg II crater hosted lake and marginal freshwater habitats within a temperate, mesic environment. A mosaic landscape of grassland and fragmentary woodland existed. Supporting evidence from the small mammal fauna includes the woodland taxa, wood mouse *Apodemus sylvaticus*

Table 3.16: Published SDQ values from Tönchesberg.

Author	SDQ			
	n	min	mean	max
Kolfschoten and Roth (1995)[a]	19	90	109	130

[a] Estimated from Kolfschoten and Roth, Figure 10

and bank vole *Clethrionomys glareolus*, and the grassland species, hamster *Cricetus cricetus* and short-tailed field vole *Microtus agrestis* (Kolfschoten and Roth, 1995). This interpretation is also supported by the molluscan assemblage (Kolfschoten and Roth, 1995).

Stratigraphy and correlation The volcanic debris-cone has been $^{40}Ar/^{39}Ar$ dated to 202 ± 14 k yr BP (Kolfschoten and Roth, 1995), indicating that the crater-fill sequence at Tönchesberg post-dates MIS 7. The loess unit lying immediately over the volcanic deposits is correlated with similar cold-climate sediments found at nearby sites, such as Plaidter Hummerich, that appear to date to the Saalian (possibly MIS 6). The palaeosol of Tönchesberg 11–13 occurs above this Saalian loess and beneath another loess that has been correlated with nearby deposits dated to MIS 5c–5b by TL dating (Kolfschoten and Roth, 1995). Tönchesberg 11–13, with its interglacial fauna, may therefore be assignable to the Eemian (= MIS 5e; Kolfschoten and Roth, 1995).

3.5.4 Holocene

3.5.4.1 Pisede bei Malchin

Location Near the town of Malchin, Mecklenburg-Vorpommern Region, Germany

Co-ordinates 53.74°N, 12.76°E

Age *c.* 3 k yr BP

Archive Museum für Naturkunde, Berlin, Germany

Description A former gravel pit near the town of Malchin was found to contain an extensive animal burrow system, excavated in moraine deposits of the *Gerswalder Staffel* stadial of the last Glacial. The infilling sediments were highly fossiliferous, and together with the accompanying sedimentological evidence, the site provides a valuable window on palaeoenvironmental development of the young morainic landscape of northern Europe from the Lateglacial through the Holocene. The complex of tunnels and chambers have been investigated in depth by a multidisciplinary team, primarily from the Humboldt-UniversitŁt, Berlin, during the period 1968–1971.

The stratigraphy of the burrow systems was morphologically complex (Heinrich, 1975b), and two sedimentologically distinct phases of burrowing were identified: an *oligochronic* group, formed over a single, short period of time; and a *polychronic* group, representing a longer period of working and reworking (Heinrich, 1975a). The strata were judged to become younger from the west to the east (Maul pers. comm., 2009), and excavations were structured in five strips along this path, numbered I in the west to V in the east. Strips IV and V were amalgamated together as IV&V.

Material examined Thirty-one M_1s were photographed from strip III, and thirty-six from strips IV&V. The majority of molars were in good condition with enamel layers well-defined and occlusal outlines complete, although a very few enamel triangles and posterior lobes were damaged. Most of the specimens were not discoloured and had a 'fresh' appearance, however, a minority of molars showed varying degrees of light-brown or reddish-brown staining.

The water vole specimens were identified as *Arvicola terrestris* (Heinrich and Maul, 1983a). Enamel thickness measurements from samples of *Arvicola* from throughout the Pisede sequence exhibit similar SDQ values (Table 3.5.4.1).

The taphonomy of the specimens is likely to have been complex. Most of the *Arvicola* are likely to have been the prey of the burrow-makers or burrow-

occupants such as badger *Meles meles* (Maul pers. comm., 2008). It was noted that strips IV&V had been reworked and so contained not only the youngest but also the oldest material in the site (Maul pers. comm., 2009).

Table 3.17: Published SDQ values from Pisede.

Context	SDQ			
	n	min	mean	max
Pisede ?stratum[a]	10	68.632	80.173	91.833
Pisede I[b]	27	78.7	89.7	112.5
Pisede II[b]	25	78.4	91.6	105.7
Pisede III[b]	24	75.0	91.8	117.4
Pisede IV&V[b]	38	70.4	90.9	108.6

[a] Heinrich (1982) [b] Heinrich and Maul (1983a)

Palaeoenvironments Heinrich and Maul (1983b) employed an ecological analysis of the rodent fauna to reconstruct palaeoenvironmental change at Pisede. Woodland species such as bank vole *Clethrionomys glareolus*, yellow-necked mouse *Apodemus flavicollis*, wood mouse *Apodemus sylvaticus*, and hazel dormouse *Muscardinus avellanarius* occur throughout, but a slight increase in the proportion of these taxa from Pisede III–I suggested an increase in wooded habitats over this period (Heinrich and Maul, 1983b). Open grassland was present, with common/short-tailed field vole *Microtus arvalis/agrestis* dominating the rodent fauna throughout. The occurrence of single specimens of Norway lemming *Lemmus lemmus* and ground squirrel *Spermophilus major* in Pisede IV&V appears to be the result of reworking and is not of palaeoenvironmental significance. The general impression given is of a temperate, mesic environment with a mosaic of woodland and meadow habitats.

Stratigraphy and correlation Radiocarbon dating carried out for this study on *Arvicola* specimens from Pisede indicate that the *Arvicola* assemblages from Pisede III and IV&V date from around 3 k yr BP (Table 3.18). These dates will be used to provide age-ranges for Pisede III and IV&V. These radiocarbon dates are in contrast with earlier understanding of the dating of these deposits that regarded them as originating from the early or middle Holocene (Heinrich and Maul, 1983a; Maul pers. comm., 2009).

Table 3.18: Radiocarbon and calibrated age estimations from Pisede. Data from the literature and from dating of *Arvicola* samples (with Specimen IDs) carried out for this study.

Context	Lab no.	Material	^{14}C BP	cal BP
I				
	GIN-461[a]	*Fagus sylvatica* wood	$1\,240 \pm 150$	$1\,146 \pm 139$
	BLN-994[a]	*Fagus sylvatica* wood	$1\,531 \pm 100$	$1\,445 \pm 92$
	BLN-993[a]	*Fagus sylvatica* wood	$1\,975 \pm 100$	$1\,943 \pm 121$
III				
	OxA-X-2332-14[b,c]	*Arvicola* mandible (2818)	$3\,048 \pm 26$	$3\,280 \pm 40$
IV&V				
	OxA-21080[b]	*Arvicola* mandible (2860)	$2\,546 \pm 26$	$2\,660 \pm 80$
	OxA-X-2335-54[b,c]	*Arvicola* mandible (2867)	$2\,921 \pm 30$	$3\,080 \pm 60$

[a] Heinrich and Jäger (1975)
[b] This study
[c] ORAU report carbon and nitrogen atomic ratios slightly outside the acceptance range. This means slight caution should be exercised regarding these dates.

3.6 Great Britain

3.6.1 Early Middle Pleistocene

3.6.1.1 Boxgrove

Location Near the villages of Halnaker and Boxgrove, West Sussex, England

Co-ordinates 50.86°N, 0.69°W

Age MIS 15 or MIS 13

Archive Natural History Museum, London, Great Britain

Description A sand and gravel quarry at the southern edge of the South Downs in West Sussex (Figure 3.9) was found to contain some of the most significant records of Pleistocene palaeontology and Palaeolithic archaeology in northwest Europe. The quarry was historically known as Amey's Eartham Pit but the site has now become familiar as Boxgrove after the nearby village and the Parish within which the Palaeolithic archaeology is found (Roberts and Parfitt, 1999). Two nearby quarries (Quarries 1 and 2) were the focus of excavations from 1983 to the present day (Roberts and Parfitt, 1999) and were found to share the same sedimentary sequence.[1]

Boxgrove is part of a laterally extensive raised beach complex, named the Goodwood-Slindon Raised Beach (extended by Roberts and Pope, 2009 as the Westbourne-Arundel Raised Beach). The site developed on a wave-cut platform during a period of high relative sea-level and was situated below Cretaceous Chalk cliffs at the edge of a marine embayment (Roberts and Parfitt, 1999; Roberts and Pope, 2009).

The Boxgrove deposits constitute a regressive sequence of marine and intertidal sands and silts, grouped together as the Slindon Formation (SF). Continued sea-level fall eventually led to subaerial exposure of the uppermost parts of the sequence and the sediments were reworked and redeposited as calcareous-rich silts in pools formed by freshwater from springs emanating from the nearby chalk cliffs. These freshwater deposits—specifically units 4b and 4c of the SF—have yielded a wide variety of floral and faunal remains, including a hominin assigned to *Homo heidelbergensis*, flint tools, butchered large mammals, and abundant small mammals (Roberts and Parfitt, 1999; Roberts and Pope, 2009). Above the SF lies the Eartham Formation (EF), a series of cold-climate silts, colluvium, breccias, and flints (Preece and Parfitt, 2000; Roberts and Pope, 2009).

[1] Save for the calcareous spring deposits of Unit 4d, which is missing from Quarry 2.

Material examined *Arvicola* from Boxgrove have been assigned to *Arvicola terrestris cantiana* (= *Arvicola mosbachensis*) on the basis of a lack of roots and SDQ measurements showing a *Mimomys*-differentiation (Parfitt, 1999). *Arvicola* molars were in excellent condition only displaying slight corrosion consistent with digestion by avian predators. A taphonomic study of Unit 4c suggests accumulation of remains on the land surface during a period of soil development (Parfitt, 1999). Digestive and diagenetic processes have given the *Arvicola* molars a translucent buff colour and have led to enamel layers becoming visually distinct from the dentine. This is likely to allow good levels of precision and accuracy of enamel thickness measurements to be obtained. In a small number of cases the posterior walls of posterior lobes were detached from a tooth or had been lost altogether, but this generally did not affect landmarking.

Twenty-seven M_1s were photographed from Unit 4b and thirty-three from the overlying Unit 4c. Samples came from the Slindon Soil Bed (specifically Unit 4b Quarry 1, Area GTP 30), and the overlying Unit 4c, from Quarry 2, Area GTP 17, (Figure 3.9). *Arvicola* fossils from units in both quarries were grouped together to form composite samples.

Palaeoenvironments Changes in lithology and palaeontology from the top of the SF and throughout the EF show that the fossiliferous Units 4b and 4c were deposited during a temperate but gradually cooling climate against a backdrop of falling sea-level. Boxgrove lay on a coastal plain where a mosaic of grassland and woodland habitats in Unit 4c—indicated by woodland species such as squirrel *Sciurus* sp. and hazel dormouse *Muscardinus avellanarius*, and grazing species such as rabbit *Oryctolagus* sp. and horse *Equus ferus*—gave way to a progressively more open landscape in Unit 4b, where steppic mammals such as Norway lemming *Lemmus lemmus* and narrow-skulled vole *Microtus gregalis* became more dominant (Parfitt, 1999; Preece and Parfitt, 2000).

Palaeogeographically, Boxgrove was protected in an embayment of a piece of coastline later to become the northern edge of the English Channel. To the east, the Weald-Artois chalk anticline formed a land connection between Britain and the rest of Europe (Roberts, 1999; Roberts and Pope, 2009). The exact location of the landbridge is not known but would not have been too far distant. This proximity, and shared geology, suggests that the environments that existed at Boxgrove are likely to have been continuous with much of what is now present day northern France and Belgium. The landbridge would likely have provided an easy and rapid colonisation route from Europe to the southern parts of peninsula Britain.

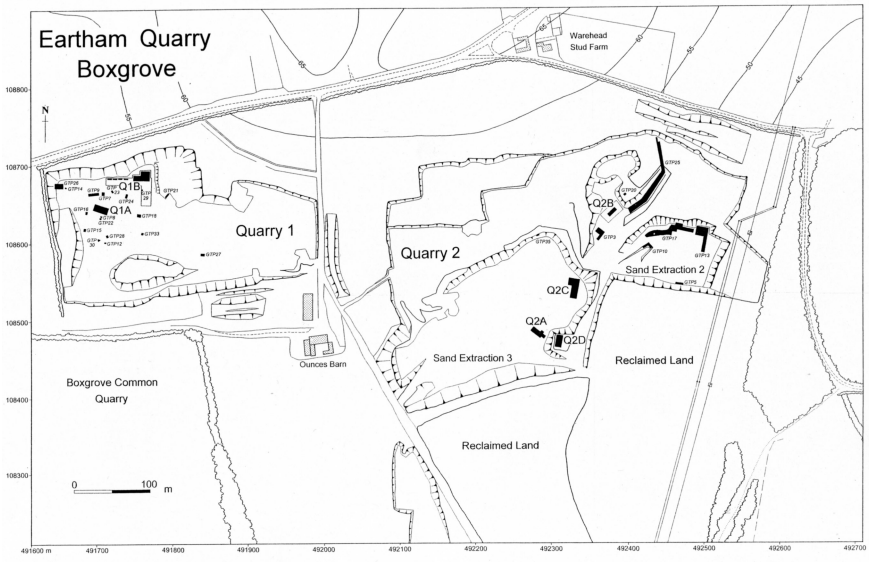

Figure 3.9: Plan of the Boxgrove site. Taken from Roberts and Parfitt (1999).

Stratigraphy and correlation Absolute dating methods and and coccolith biostratigraphy indicate an age of between MIS 6 and MIS 11 for Boxgrove (Roberts and Parfitt, 1999). However, a temperate period within the early Middle Pleistocene is now generally accepted as an age for the site based upon evidence from mammalian biostratigraphy. Seven fossil mammal species found are unknown after MIS 12: the shrew *Sorex* (*Drepanosorex*) *savini*, cave bear *Ursus deningeri*, rhinoceros *Stephanorhinus hundsheimensis*, the giant deer *Megaloceros dawkinsi* and *Megaloceros* cf. *verticornis*, and the vole *Pliomys episcopalis*. While the presence of *A. mosbachensis* establishes the site as being later than MIS 15 or MIS 16, which is the date of the *Mimomys–Arvicola* boundary established in central Europe (Koenigswald and Kolfschoten, 1996; Maul and Markova, 2007).

The occurrence of the narrow-skulled vole *Microtus gregalis* led Preece and Parfitt (2000) to suggest a correlation between Boxgrove and the early Middle Pleistocene Cromer IV Interglacial, which occurs immediately before deposits of the Elsterian (= MIS 12) Glaciation in The Netherlands (Zagwijn, 1992). Preece and Parfitt further suggest that Boxgrove post-dates Westbury Cave in Britain (Section 3.6.1.3) and Kärlich G in Germany due to the presence of the more 'primitive' narrow-skulled vole morphotype *Microtus gregaloides* at these sites. The transition between the *M. gregaloides–M. gregalis* morphotypes is, however, diachronous, and remains to be firmly established in central and western Europe (Maul and Markova, 2007).

A correlation with the Cromer IV Interglacial would imply that the periglacial deposits of the EF at Boxgrove were formed during the British MIS 12 (= Anglian) Glaciation, and that the SF is therefore a late MIS 13 deposit. The uncertainty

in the *M. gregaloides–M. gregalis* transition makes this correlation tentative, and the substantial amount of sub-stage variation observed in the global oxygen isotope record of the early Middle Pleistocene could accommodate the cold-climate deposits of the EF within MIS 13.

In summary, the main fossiliferous deposits at Boxgrove represent a warm period within the later part of the early Middle Pleistocene. Less confidence surrounds the position of Boxgrove within the early Middle Pleistocene, however, and so, given this uncertainty, an age of either MIS 15 or MIS 13 will be adopted for the *Arvicola* assemblage used in this study.

3.6.1.2 West Runton Freshwater Bed

Location Near the village of West Runton, Norfolk, England

Co-ordinates 52.94°N, 1.24°E

Age A temperate period between late MIS 19 and MIS 15

Archive Natural History Museum, London, Great Britain

Description The West Runton freshwater Bed (WRFB) is an interglacial deposit found exposed in the coastal cliffs of northern East Anglia. The site has been a focus of study since the late 19$^{\text{th}}$ century by such notable figures in Quaternary Science as C. Reid, A. C. Savin, M. A. C. Hinton, and R. West, and is the stratotype for the early Middle Pleistocene Cromerian Interglacial of northern Europe (West, 1980). The site comprises a lithologically complex freshwater deposit around 2 m thick, grossly formed from of a lower matrix-supported diamicton and an upper well-sorted silt, which fines upwards and contains lenses of sand, fossil molluscs, and vertebrate remains. Although the WRFB is black in colour throughout, the sediments actually contain little organic material, and the organic appearance is accentuated by strongly reducing conditions within the bed (Rose *et al.*, 2008). A rich molluscan and vertebrate assemblage has been recovered through years of study, but the site is probably most famous for the excavation during 1992–1995 of the nearly complete skeleton of a steppe mammoth *Mammuthus trogontherii*—the West Runton Elephant Project (WREP) excavation (Stuart, 2000)—which also saw the recovery of a substantial small mammal fauna (**?**).

The WRFB is thought to have been deposited in a body of standing water close to a fluvial channel. The diamicton is likely the result of a mass flow, probably from a collapsing bank, and the silts and sands derived from gradual infilling of the lake basin, which was punctuated by the periodic invasion of small channels (Rose *et al.*, 2008). The deposition of these sediments would have occurred

over a geologically short period of time: the diamicton potentially in a few minutes, the silts and sands perhaps over a few years or decades (Rose *et al.*, 2008). These recent findings contrast with earlier interpretations (e.g., West, 1980), which characterised the WRFB as representing a large part, or even the entirety, of an interglacial. Taphonomically this reinterpretation also contrasts with Hinton who, in describing *Mimomys* from the Cromerian of the north Norfolk coast, speculated that fossil material from the Freshwater bed includes '... the sweepings of a very large part of western and central Europe ...' (Hinton, 1926, p. 383).

Material examined Forty-seven M_1 molars were photographed, seven were within mandibles. Colouration varied from red-brown to dark-brown or black but most specimens were brown-grey. Many molars showed physical abrasion or corrosion of the occlusal surface, which is likely to compromise the precision and accuracy of landmarking and enamel thickness measurements. The abraded appearance has been attributed to corrosion by the stomach acids of birds of prey, which are thought to have been the major accumulators of small mammal remains (Stuart, 2000).

?, in their analysis of small mammal remains recovered during the WREP, identified the water vole as *Mimomys savini*. The characters cited in this attribution were the presence of roots in adult M_1s, a *Mimomys*-fold in some adult molars, enamel-islets in some juveniles, and enamel layers showing the *Mimomys*-differentiation (Table 3.19). Specimens were identified as *M. savini* and *Mimomys intermedius* in the Natural History Museum, London, collections but other species of *Mimomys* from the WRFB have been recognised in the literature (e.g., Hinton, 1926). These additional species are now understood to be the product of misinterpretation of ontogenetic variation as taxonomic differentiation (e.g., Kretzoi, 1965).

Table 3.19: Published SDQ measurements from West Runton.

Author	SDQ			
	n	min	mean	max
?	49	114.57	139.59	163.14

Palaeoenvironments Pollen sequences from different locations across the site show the dominance of mixed woodland; with oak, alder, and pine most significant but with herbs and shrubs present at lower levels in some samples (West, 1980; Rose *et al.*, 2008). The mammal fauna suggest the existence of some open

grassland habitats as well as woodland (Stuart, 1996). Browsing and grazing large mammals include steppe mammoth *M. trogontherii*, giant deer *Megaloceros* sp., and rhino *Stephanorhinus hundsheimensis*, while small mammals such as common hamster *Cricetus cricetus* and grey dwarf hamster *Cricetulus migratorius* are characteristic of steppe habitats today (Preece and Parfitt, 2000). Grassland voles such as the narrow-skulled vole ancestor *Microtus gregaloides* and common vole *Microtus arvalis* are found with obligate woodland species such as extinct squirrel *Sciurus whitei*. The presence of northern vole *Microtus oeconomus* and bank vole *Clethrionomys glareolus* show that mesic, well-vegetated environments were important, as were riparian habitats from the occurrence of beaver *Castor fiber*, desman *Desmana moschata* and the presumably semi-aquatic water vole *M. savini*. Well-vegetated streams and marshland are also indicated by the rich freshwater and terrestrial molluscan fauna (Preece and Parfitt, 2000).

Oxygen stable isotope studies (Rose *et al.*, 2008) and an absence of warm climate taxa suggest that climate was similar to that of the present-day. Additionally, there is little evidence of environmental change through the WRFB deposits. In summary, the WRFB was deposited in a moderately temperate floodplain alder carr/fenland landscape containing mixed woodland, some open grassland areas, and significant wetland environments.

Stratigraphy and correlation Some pollen studies have suggested that the WRFB accumulated over an extended period in the early temperate part of an interglacial (West, 1980). In contrast, reappraisal of the site by Rose *et al.* (2008) suggests that deposition occurred rapidly, with the vegetation changes observed a recolonisation response to a flood event. Thus, the WRFB is a discrete snapshot of a time when moderately temperate conditions prevailed.

The WRFB is normally magnetised, indicating the deposit post-dates the Brunhes-Matuyama magnetic reversal. An ESR date from tooth enamel gave an age of 460 ± 80 k yr BP (Rink *et al.*, 1996), but Stuart (2000) described a consensus estimated age for the WRFB of *c.* 600–700 k yr BP. The evolutionary development of the water vole is important in age estimation. Evidence from German and Dutch early Middle Pleistocene sites show that the loss of roots in water vole populations occurs around MIS 15 or MIS 16 in northwest Europe (Kolfschoten and Turner, 1996; Koenigswald and Heinrich, 1999; Maul and Markova, 2007), and correlation with the British Cromerian record has led to the suggestion that the *Mimomys-Arvicola* transition occurred in Britain at the same time (Preece and Parfitt, 2000, 2008).

In summary, there is sound evidence to indicate an age for the WRFB between the Brunhes-Matuyama magnetic reversal and MIS 15. Greater dating precision cannot be made with any confidence, therefore for the purposes of this study the

Mimomys assemblage will be regarded as dating from a temperate period between the later part of MIS 19 and MIS 15.

3.6.1.3 Westbury Cave

Location Near the village of Westbury-sub-Mendip, Somerset, England

Co-ordinates 51.25°N, 2.70°W

Age MIS 15 or MIS 13

Archive Natural History Museum, London, Great Britain

Description To the southwest of the Mendip Hills, near the village of Westbury-sub-Mendip, Somerset, a rich series of Early and Middle Pleistocene fossil faunas was exposed by quarrying activity in 1969. The site of Westbury Cave became a major focus of palaeontological and archaeological interest during the 1970s and 1980s through the work of Bishop (1974, 1982) and the Natural History Museum, London (Andrews *et al.*, 1999). The latter excavation in particular revealed a stratigraphically and climatically complex record. Further quarrying work resulted in the partial destruction of the site.

Westbury Cave comprised of two partly connected chambers in a cave system developed within Carboniferous limestone. The cave system is thought to have formed during the Early Quaternary (Stanton, 1999), and the earliest deposits recognised during excavation were water-lain clastics of the Siliceous Member (WCSM) at the base of the sequence (Andrews and Cook, 1999). Numerous fossiliferous units and sub-units of cave breccias accumulated above the WCSM and were grouped together as the Westbury Cave Calcareous Member (WCCM). Sediment accumulation ceased when the cave chambers became choked and partial roof collapse occurred (Andrews and Cook, 1999). *Arvicola* fossils were recovered from the WCCM and remaining discussion will be restricted to these deposits.

Early excavations at Westbury not only revealed abundant fossil material but also flint artefacts that were, at the time, the earliest evidence for human occupation of the British Isles (Bishop, 1975). Although Cook (1999) cast doubt on the archaeological origin of the flint finds most authors have accepted them as part of a Lower Palaeolithic industry (Schreve *et al.*, 1999), The later discovery of cut-marks on the metacarpal of a red deer *Cervus elaphus* provided clear evidence of human presence (Andrews and Ghaleb, 1999).

Table 3.20 gives a stratigraphic summary of the western side chamber. Excavations were first made at two restricted sites (W2 and W9) and the units identified were tracked laterally using lithology and sediment colour over a number of field seasons to a third site, W2/9 (Currant pers. comm. 2009). The side chamber

is thought to have undergone collapse at some point after the deposition of unit 15, producing a pronounced syncline across the exposure and pinching the lower parts of the sequence at its centre (Figure 3.10). The upper and central parts of the strata also suffered greatly from dissolution. Despite these events, clear stratification is evident across much of the sequence and strongly suggests that the original stratigraphy survived post-depositional alteration (Currant, 1999); a conclusion further supported by the distinct palaeoenvironmental signal provided by the faunal assemblages from each unit.

Table 3.20: Lithostratigraphy and palaeoclimatic changes in strata of the western exposure at Westbury Cave. Data taken from Currant (1999) and Preece and Parfitt (2000). Blacked-out layers contain *Arvicola* used in this study.

Layer	Lithology	Climate	Main climatic indicators
15/1&3	Lower breccia	Cool-arid	*Lemmus* sp., *Ochotona* sp.
14	Grey silty breccia	Cold-arid	*Cricetulus migratorius*, *Lemmus* sp., *Ochotona* sp.
13	Brown silty breccia	Cold-arid	*Cricetulus migratorius*
12	Dark brown breccia	Cool	
11	Pink breccia	Warm-mesic	Bats, soricids, *Talpa* sp., *Clethrionomys glareolus*
10	Yellow silty breccia	Cool	

Material examined *Arvicola* fossils were only found in the upper units of the WCCM, and of these only Units 11 and 14 contained sufficient specimens to constitute an adequate sample for primary morphometric analyses (16 and 38 M_1s respectively). Although some M_1s were found *in situ* in mandibles, the majority of *Arvicola* fossils were found as isolated teeth. Specimens were identified as *Arvicola terrestris cantiana* (= *Arvicola mosbachensis*) because of the absence of roots and enamel with a *Mimomys*-differentiation (Currant, 1999; Preece and Parfitt, 2000). Preservation of molars was generally good and enamel layers were clearly visible as pale grey bands.

Palaeoenvironments The units of the WCCM span a number of climatic episodes (Schreve *et al.*, 1999; Preece and Parfitt, 2000). Two temperate phases can be recognised in the strata of interest (Table 3.20) but an additional temperate-to-cold climatic shift occurs above unit 15/1, 15/3. Evidence from the small mammal

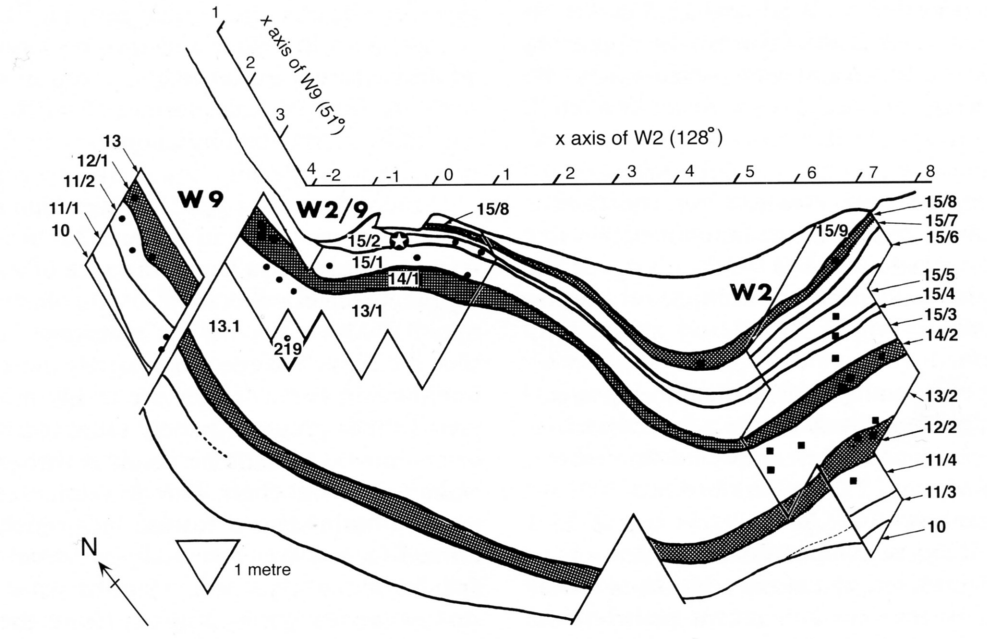

Figure 3.10: Stratigraphy of the side chamber at Westbury Cave. From Andrews and Cook (1999)

faunas of Units 11 and 14 record contrasting palaeoclimates. Unit 11 contains a faunal assemblage of abundant small mammals such as bats, glirids, and the voles *Clethrionomys glareolus* and *Microtus subterraneus*, indicating warm temperate conditions with deciduous woodland. In Unit 14 a number of species now characteristic of cold, open-landscape habitats are present such as Norway lemming *Lemmus lemmus*, pika *Ochotona*, and grey dwarf hamster *Cricetulus migratorius* (Currant, 1999; Preece and Parfitt, 2000). *Microtus gregaloides* occurs in abundance throughout the WC sequence, except for the deposits regarded as being most temperate; such as Unit 11, where this species is absent.

Palaeoenvironmental change is evident throughout the sequence but the fauna exhibit a general stability, which is not present in the fossil mammal record of late Middle and Late Pleistocene Britain (Schreve, 1997; Schreve *et al.*, 1999; Preece and Parfitt, 2000). This has been attributed to the absence of extreme climatic fluctuations across the sequence: for instance the presence of soricids and *Talpa* sp. throughout suggest the continued persistence of soils (Currant, 1999). This continuity in the fauna also suggests the maintenance of a land connection between the British Isles and continental Europe at a time prior to the formation of the straits of Dover (Schreve *et al.*, 1999; White and Schreve, 2000).

Stratigraphy and correlation The WCCM is richly fossiliferous, containing discrete faunal assemblages from a series of clearly lithologically distinct strata deposited over a considerable period during the early Middle Pleistocene (Currant,

1999). Mammalian biostratigraphy shows the WCCM to pre-date the Anglian (= MIS 12) Glaciation. The shrew *Sorex* (*Drepanosorex*) *savini*, rhinoceros *Dicerorhinus etruscus* (= *Stephanorhinus etruscus*), archaic cave bear *Ursus deningeri*, and bison *Bison schoetensacki* are all exclusively early Middle Pleistocene taxa (Currant, 1999), while the dog *Canis lycaonoides* is the only British occurrence of this species, and the large felids *Homotherium latidens* and *Panthera gombaszoegensis* are rare after MIS 12 (Preece and Parfitt, 2000).

The presence of *Arvicola* in the WCCM is highly significant. The earliest central European occurrence of *Arvicola* is at Kärlich G in Germany, which is dated to MIS 15 or MIS 16 and therefore appears to provide a maximum age for the WCCM fauna (Koenigswald and Kolfschoten, 1996; Preece and Parfitt, 2000). The co-occurrence of *Arvicola* and the primitive morphotype of the narrow-skulled vole *M. gregaloides* led Preece and Parfitt (2000) to further suggest that the WCCM correlates with the Cromer III Interglacial of the Dutch early Middle Pleistocene—possibly MIS 15. The presence of *M. gregaloides* also allowed Preece and Parfitt to consider the WCCM to be older than Boxgrove (Section 3.6.1.1) because the latter site contains *Microtus gregalis*, the descendant of *M. gregaloides*. The exact age of this transition is not well-established, however, and can only be placed within the early Middle Pleistocene (Maul and Markova, 2007). It is also interesting to reflect upon whether the palaeoclimatic complexity within the WCCM represents climatic change within one, or across two or more oxygen isotope stages.

In summary, strong support exists for an early Middle Pleistocene age for the WCCM, but there is a high level of uncertainty with more precise age estimates. An age within MIS 15 or MIS 13 will be adopted for the *Arvicola* assemblages.

3.6.2 Late Middle Pleistocene

3.6.2.1 Cudmore Grove

Location Mersea Island, Essex, England

Co-ordinates 51.79°N, 0.99°E

Age MIS 9

Archive Natural History Museum, London, Great Britain

Description Situated at the mouth of the river Thames at the eastern edge of Mersea Island, Essex, near Cudmore Grove Country Park. The Cudmore Grove 'Channel Site' is found on a stretch of rapidly eroding coastline and comprises a channel infilled with distal fluvial/estuarine facies sandwiched between terrace gravels (Figure 3.11). Within the channel-fill a thin but highly fossiliferous interglacial 'detrital mud'—Unit 3 of Roe *et al.* (2009)—has yielded pollen, vertebrates, molluscs, and beetles, and has been the focus of a major multidisciplinary research effort for a number of years (Bridgland, 1994; Roe, 1995; Schreve, 1997; Roe, 1999; Roe *et al.*, 2009). The sequence was the subject of extensive fieldwork during the 1980s and the *Arvicola* used in this study originate from this period of investigation.

Material examined Water voles were abundant in the Cudmore Grove deposits. Fifty-one M_1 teeth were photographed, all in excellent condition, being darkly stained but with enamel layers clearly distinguishable from dentine and occlusal outlines well defined. The specimens were identified as *Arvicola terrestris cantiana* (= *Arvicola mosbachensis*) based upon the lack of roots and *Mimomys*-differentiation of enamel (Roe *et al.*, 2009; Table 3.21). Three of the M_1s examined possessed a *Mimomys*-fold, which has been viewed as biostratigraphically significant (see below).

The taphonomy of fossils from the detrital mud is mixed. Fragile skeletal elements from herpetofauna and small mammals coexist alongside abundant well comminuted mollusc shells. Roe *et al.* (2009) described the generation of this unit through '... high-energy riverine or coastal processes that carried shell debris, insect remains, bones and other detritus into the site from the surrounding hinterland ...' (Roe *et al.*, 2009, p. 2366). The presence of superficial, ramifying canals on some *Arvicola* teeth, suggestive of the work of soil-dwelling saprophytic micro-organisms (Ruddy, 2005), provides supporting evidence for this taphonomic model. These trace fossils imply that *Arvicola* specimens had a taphonomic history resident in soils prior to the rapid event or series of events that led to the

deposition of Unit 2.

Table 3.21: Published SDQ values from Cudmore Grove.

Author	SDQ			
	n	min	mean	max
Roe *et al.* (2009)	48	105	133.36	147

Palaeoenvironments An estuarine marshland landscape is indicated from the lithology of the deposits and the abundance and ecology of key taxa such as the water vole and certain beetles. Bodies of slow flowing and still, permanent freshwater are indicated with well-vegetated margins of reed, sedge, grassy meadows, and stands of mixed-woodland nearby. The presence of brackish tolerant fauna may also indicate sheltered lagoonal areas (Holman *et al.*, 1990; Roe, 1999; R. Coope pers. comm., 2005; Roe *et al.*, 2009).

Fauna and flora from the channel-fill suggest an interglacial climate warmer than the present but not as warm as those that existed during the Last Interglacial in Britain (Roe *et al.*, 2009). The rich amphibian and reptile assemblage, including the tree frog *Hyla*, European pond terrapin *Emys orbicularis*, and the exotic snakes *Zamensis longissima* and *Natrix tessellata*/?*maura*, are thermophilous and the modern distribution of the snakes and some other herpetes is perhaps evidence of continentality of the climate (Gleed-Owen, 1999). This pattern is mirrored in the beetle fauna, which also indicates a warm, potentially continental palaeoclimate.

A palaeothermometer based upon oxygen isotopes from the tooth enamel of *Arvicola* from Cudmore Grove agrees with other palaeoclimatic proxies. This proxy suggests that summer temperatures were slightly warmer than the present-day—air temperatures between +20°C and +26°C—and climate may have been more continental and arid than the present (Ruddy, 2005).

Stratigraphy and correlation The Channel Site is clearly post-Anglian (= post-MIS 12) because of its southerly position in the Thames-Medway valley: a route adopted by the Thames following its diversion by the invasion of Anglian glacial ice through East Anglia (Clark *et al.*, 2004; Rose, 2008). Evidence from clast provenance analysis and terrace stratigraphy led Bridgland (1994) to conclude that the Cudmore Grove channel-fill sequence was part of a Thames-Medway river and to ascribe these deposits to the Hoxnian (MIS 11). Correlation was made with channel deposits of the nearby MIS 11 site at Clacton, however, the evidence for this correlation was not conclusive and more recent research suggests the Cud-

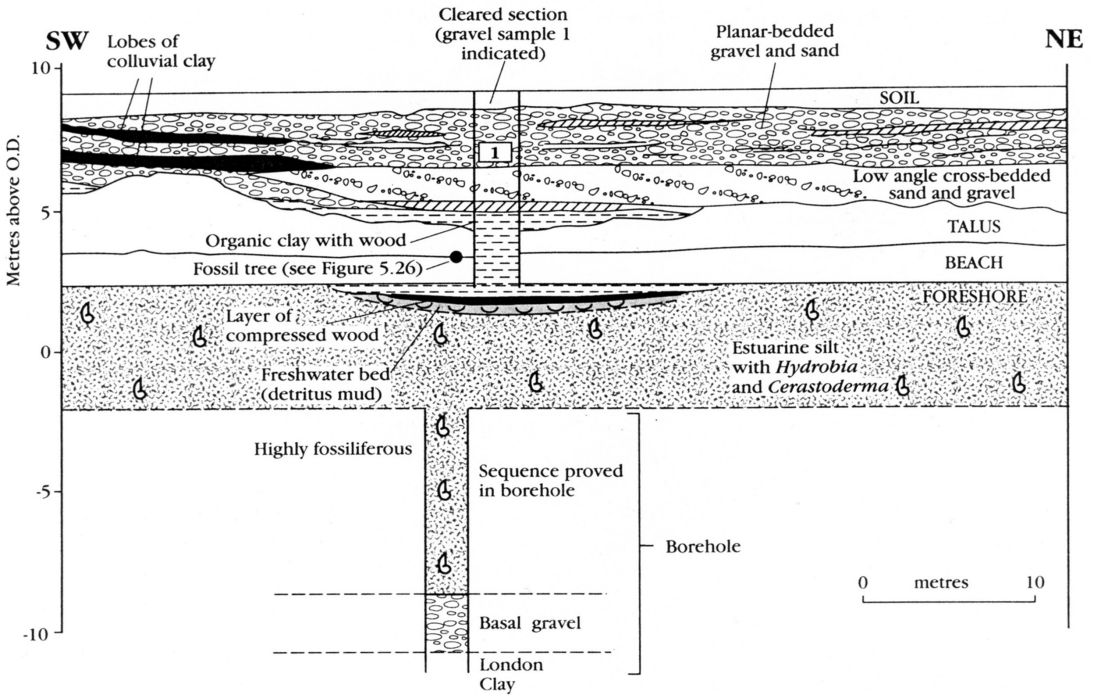

Figure 3.11: Stratigraphy of the Cudmore Grove Channel Site. Abundant *Arvicola* have been found in the fossiliferous Freshwater bed. This bed has also been referred to as 'detrital mud' by Roe (1995, 1999). From Bridgland (1994).

more Grove channel-fill was deposited during MIS 9 (Roe, 1995; Schreve, 2001; Roe *et al.*, 2009). A great deal of evidence points toward this attribution but is centred upon: 1) seemingly irreconcilable differences in height and timing of the onset of estuarine conditions between the Cudmore Grove deposits and nearby MIS 11 sites such as Clacton (Roe, 1995; Roe *et al.*, 2009), 2) biostratigraphic and palaeoenvironmental distinctiveness of the fauna of Cudmore Grove (Schreve, 2001), and 3) aminostratigraphic analysis of freshwater molluscs, which indicate an intermediate age between MIS 7 and MIS 11 deposits (Penkman *et al.*, 2007; Roe *et al.*, 2009). In view of this evidence, and the apparently temporally discrete nature of the fossil accumulation, an MIS 9 age will be assumed for the *Arvicola* assemblage.

3.6.3 Late Pleistocene and Holocene

3.6.3.1 Bridged Pot

Location Ebbor Gorge, Somerset, England

Co-ordinates 51.21°N, 2.67°W

Age Thermoclastic Gravel, GS-2 to *c.* 10 k yr BP; Inner Slope, MIS 1

Archive Natural History Museum, London, and Cambridge Museum of Archaeology & Ethnography, Cambridge, Great Britain

Description This is a small cave in Ebbor Gorge, Somerset, approximately 33 m above the valley floor, containing a debris cone formed beneath a dissolution hole approximately 3 m across. During the first excavation of the site by H. Balch (1926–1929) the 'top and inner slope' of the cone were removed (Price, 2003). Later, C. McBurney (in 1958) cut a trench through the remaining deposits and from a layer of 'thermoclastic gravel with sharp elements' (McBurney cited in Price, 2003) found a large quantity of small mammals (Price, 2003). McBurney speculated that the small mammal accumulation derived from pellets of the snowy owl.

Material examined The collections of the Natural History Museum, London, contained material originally from the excavations of the Inner Slope by Balch, donated to the museum by the daughter of J.W. Jackson of Buxton in the early 20th century. Sixteen M_1s were photographed from this collection which was labelled as deriving from the '6–7 foot level'. Molars were covered with red fine-grained sediment which was removed by brushing to reveal occlusal surfaces. Specimens were very lightly stained and the majority were in a good state of preservation. However, some showed damage to salient angles or the anterior lobe, and enamel layers of some specimens had collapsed or were irregularly worn. This damage allowed only thirteen M_1s to be fully landmarked and is likely to contribute to decreased precision and accuracy of enamel thickness measurements. Specimens were identified as *Arvicola terrestris* at the Natural History Museum, London but no studies of this material have, to this author's knowledge, been published.

Five M_1s came from McBurney's excavations of the thermoclastic gravel in the the L. Abbott collection held at the Cambridge Museum of Archaeology & Ethnography, Cambridge[1]. These specimens were in a similar but slightly better state of preservation overall than those of the Inner Slope described above. Price

[1]Viewed courtesy of John. R. Stewart.

(2003) listed these water vole as *A. terrestris* but again no more detailed studies have been made.

Palaeoenvironments A dry grassland environment on the plateau above the cave may be inferred from the dominant presence of narrow-skulled vole *Microtus gregalis* along with collared lemming *Dicrostonyx torquatus* and steppe pika *Ochotona pusilla* (Price, 2003). Water vole, northern vole *Microtus oeconomus*, and Norway lemming *Lemmus lemmus* are less frequent in the faunal assemblage (*A. terrestris* 5%). These taxa are more usually found in association with damp habitats and perhaps inhabited the gorge (Price, 2003).

Stratigraphy and correlation A single radiocarbon determination on a large mammal limb bone from McBurney's excavation of the 'thermoclastic gravel' indicated an early Holocene age (Table 3.22), but this single date cannot inform on how temporally discrete the fossil small mammal assemblage is. The uppermost parts of the 'thermoclastic gravel' contained pottery dating from the Bronze Age or Neolithic and small number of faunal elements—such as mole *Talpa europaea* and wood mouse *Apodemus sylvaticus*—were considered by Price (2003) to be of similar or younger age. A few specimens of rabbit *Oryctolagus cuniculus* have also been found, which demonstrates the potential for intrusion by more recent material, but the scarcity of material of obviously later provenance suggests that the majority of the 'thermoclastic gravel' does not include much material from the late Holocene.

O. pusilla and *D. torquatus* feature in the British Lateglacial small mammal fauna alongside *A. terrestris* (Currant and Jacobi, 2001; Section 3.6.3.3), which suggests that the fossil assemblage includes material from late MIS 2. Faced with a lack of detailed contextual confidence but with some dating evidence and perceived possible limits to the assemblage, the most conservative estimate for age estimation of the 'thermoclastic gravel' assemblage is between GS-2 and the early Holocene date given from radiocarbon dating.

The deposits excavated by Balch are described as being from the Inner Slope and top-most part of the sediment cone. No other information on this assemblage is available but stratigraphically one would expect the fossil material to post-date those of the thermoclastic gravel. The location of these deposits at the top of the sequence makes them more prone to sources of intrusion from Middle and late Holocene material than appears to be the case for the thermoclastic gravel. It is therefore possible that the Inner Slope assemblage may date from the early to late Holocene.

Table 3.22: Radiocarbon date from Bridged Pot 'thermoclastic gravel'. From Price (2003).

Lab no.	Material	^{14}C BP	cal BP
BM-2101R	Large mammal limb bone	9090 ± 350	10270 ± 480

3.6.3.2 Clacton Channel IV

Location Clacton-on-Sea, Essex, England

Co-ordinates 51.79°N, 1.16°E

Age MIS 5e

Archive Private collection of D. Bain, courtesy of Prof. Danielle Schreve

Description No published summary exists for this site. The material comes from sediments located below tide-level, recovered during piling work on the foreshore of the Lower Thames at Clacton-on-Sea, Essex. A complex of fluvial channels, the Clacton Channel Deposits, from a Thames-Medway river system have been identified in the area (Figure 3.12; Bridgland, 1994, p. 330–347). The position of the collection point of the water vole fossils (not shown) is within the region mapped as Channel IV (Schreve, pers. comm., 2009).

Material examined Twenty-two M_1s were photographed. Specimens were light-brown in colour and preservation was generally good and enamel layers were clearly defined, although the posterior lobes of two molars were missing.

The water vole material from Clacton Channel IV has not previously been studied. M_1s were unrooted and can be clearly identified as specimens of *Arvicola*.

Palaeoenvironments The lack of context for the water vole assemblage means that palaeoenvironments will not be considered.

Stratigraphy and correlation The channel complex at Clacton is part of a Thames–Medway river system that post-dates the diversion of the Thames by Anglian ice (Bridgland, 1994), indicating these fluvial deposits are later than MIS 12 in age. The sequence has been correlated with the British Hoxnian interglacial, generally recognised as corresponding to MIS 11. However, channel IV forms a separate feature to the main channel (Figure 3.12) and evidence provided by the vertebrate assemblage from Clacton Channel IV suggests a younger age for these sediments, perhaps with MIS 5e (Schreve, pers. comm., 2009).

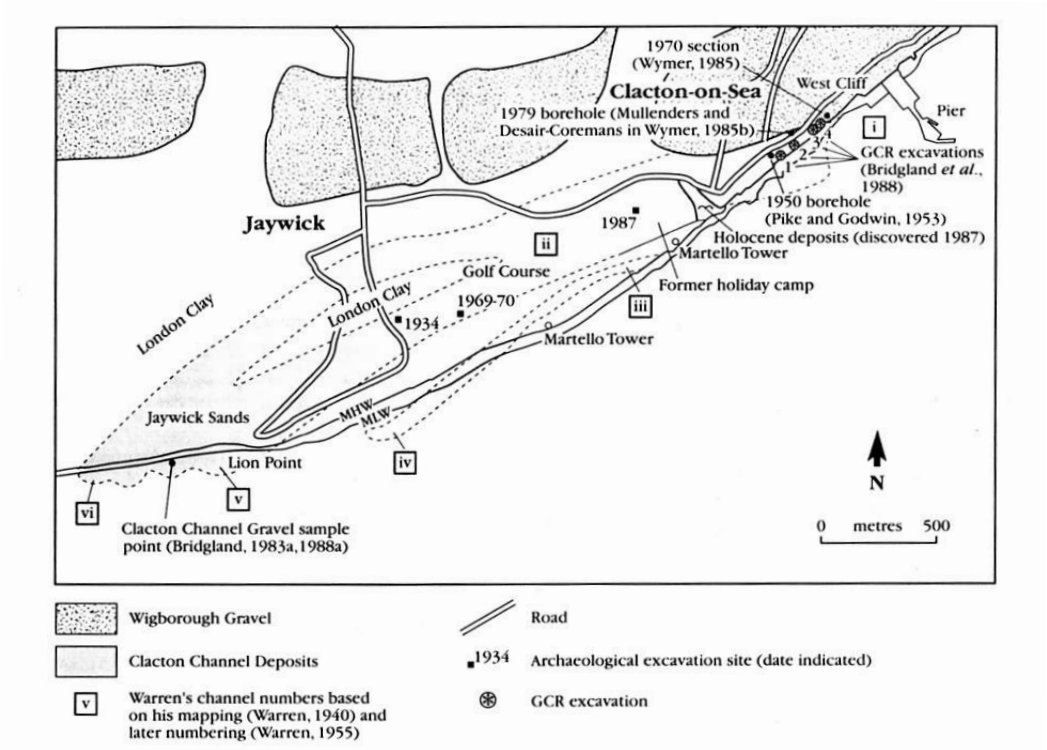

Figure 3.12: Overview map of the Clacton Channel Deposits. Taken from Bridgland (1994, p. 331).

3.6.3.3 Ightham Fissures

Location Near the village of Ightham, Kent, England

Co-ordinates 51.29°N, 0.3°W

Age GI-3 to Early MIS 1, *c.* 28–9.5 k yr BP

Archive Natural History Museum, London, Great Britain

Description Situated in the valley of the River Shode in Kent, the locality of Ightham Fissures is a group of open faults developed in Cretaceous limestone (locally known as 'ragstone'). It has been suggested that the fissures opened as a result of the development of the Shode Valley, which produced tensional stresses in the bedrock. The fissures have been extensively quarried for their pure sandy 'brickearth' infillings to the point where the majority no longer exist. In 1891 their fossiliferous potential was discovered and the rich vertebrate and mollusc assemblages found began to be studied. W. J. Lewis Abbott (from 1891 to 1897), Dr. F. Corner, and A. S. Kennard (from 1898 until 1910) collected here and their finds were later described by E. T. Newton and M. A. C. Hinton (Currant, 1977).

Fossils were found to have Lateglacial and early Holocene affinities. Unfortunately no contextual information was gathered during collection and this has

hindered research on the assemblages. No information even exists relating fossils to individual fissures, but despite this the presence of fossiliferous deposits spanning the last Termination in south-east England offers the potential to significantly increase understanding of palaeoenvironmental change and palaeobiogeography of fauna during this period.

Material examined The *Arvicola* material held at the Natural History Museum, London is from the Lewis Abbott collection and includes the type specimen of *Arvicola abbotti* (= *Arvicola terrestris*). The flattened skull and pro-odont incisors in *A. abbotti* have much in common with modern fossorial water vole *Arvicola scherman* (Hinton, 1910, 1926), and it has been proposed that *A. abbotti* forms part of a wider Late Pleistocene western European association of fossorial water voles that includes *Arvicola antiquus* (Storch, 1971, cited in Gromov and Polyakov, 1992, p. 348).

Seventeen M_1 teeth were photographed. All were found within mandibles and were in good enough condition to allow all landmarks to be positioned. The widths of enamel layers were difficult to determine in many instances because of erosion to the edges of enamel and the lack of colour contrast between enamel and dentine. This may lead to decreased accuracy and precision of enamel thickness measurements.

Palaeoenvironments The mammals obtained from the fissures are generally cold climate taxa such as collared lemming *Dicrostonyx torquatus*, Norway lemming *Lemmus lemmus*, pika *Ochotona pusilla*, and Arctic fox *Alopex lagopus*. However, species now regarded as temperate indicators such as *A. terrestris* are also present. The sedimentology of the fissure fillings range from cold-climate deposits with periglacial structures to temperate dark-earths (Currant, 1977). Both these sources of evidence reflect the mixture of fossil material accumulated over a long period of rapidly and widely fluctuating climate at the end of the Last Cold Stage.

Stratigraphy and correlation The mammal faunas of the fissures are characteristic of the Lateglacial Gough's Cave MAZ and, although not found at Gough's Cave itself (Currant and Jacobi, 2001), the occurrence of *O. pusilla* and *A. terrestris* are indicative of other British mammal faunas dated to the Lateglacial (Currant and Jacobi, 2001). Holocene fauna are also present, and Currant (1977) speculated that faunal remains probably continued accumulating until the late 19^{th} century.

Radiocarbon dating undertaken for this study on two *Arvicola* mandibles randomly chosen from the collections at the Natural History Museum, London has

revealed that the age of the *Arvicola* fossils ranges from at least GI-3 to the around 9 k yr BP (Table 3.23). Whether these specimens are part of a continual accumulation or derive from discrete periods cannot be ascertained but these dates allow morphological variation within an OTU to be explored in the context of a fossil assemblage containing specimens dating over at least twenty thousand years.

Table 3.23: Radiocarbon dates of *Arvicola* specimens from Ightham Fissures.

Lab no.	^{14}C BP	cal BP
OxA-21074	8650 ± 40	9610 ± 50
OxA-21075	23100 ± 170	27950 ± 140

3.6.3.4 Merlin's Cave

Location Near the village of Symonds Yat, Herefordshire, England

Co-ordinates 51.84°N, 2.65°W

Age early Holocene to Neolithic, *c.* 12–3 k yr BP

Archive Natural History Museum, London, Great Britain

Description Merlin's Cave is a cave formed in Carboniferous limestone of the Wye Valley, half a mile south of the village of Symonds Yat, Gwent, Wales. The first excavations were carried out by Dorothea Bate at the turn of the 19th century (Bate, 1901) who found a red cave-earth extremely rich in small mammal remains from the Lateglacial and early Holocene. Even though the cave was well hidden much of the cave-earth had been disturbed by '... miners looking for iron-ore ...' (Bate, 1901, p. 102) and a local inhabitant collecting artefacts for profit (Hewer, 1924). As a consequence, fossils from these sediments were found to be temporally mixed. A more homogeneous fossiliferous deposit was found in a calcareous cemented breccia adhering to the cave walls, but this was not excavated until the mid-1990s as part of the Wye Valley Project (Price, 2003). The cave was nameless at the time of Bate's excavations but was later dubbed Merlin's Cave by Hewer (1924) in acknowledgement of its proximity to King Arthur's Cave.

Material examined Two *Arvicola* specimens examined came from the first excavations by Bate[1], but the vast majority of the material viewed either derive from later workings by Hewer (1924) or M. A. C. Hinton's collection (Hinton, 1926,

[1]Specimen numbers 7765 and 7773. Referred to as *Microtus amphibius* in Bate (1901).

p. 417). It appears from the site reports of Bate and Hewer that all of these fossils were recovered from the cave-earth, which was considered to contain a fossil assemblage greatly mixed through earlier disturbance of the sediments. This conclusion has been supported by radiocarbon dating of *Arvicola* carried out for this study (see below). None of the material cemented to the cave walls excavated by the Wye Valley Project was examined.

One hundred and ten M_1 teeth were photographed, all were complete mandibles coated with reddish-buff sediment. The taphonomy of the fossil assemblage was considered by Price (2003) to be an owl pellet accumulation. Specimens showed some slight discolouration, likely as a result of staining from the cave-earth sediments, and darkening of dentine benefited enamel thickness measurements by raising colour contrast between the two tissues. Hinton (1926) assigned the water vole finds to *Arvicola abbotti* (= *Arvicola terrestris*) and remarked on the similarities with the modern fossorial water vole *Arvicola scherman*, the implication being that water vole from Merlin's Cave were fossorial. No other work has been published on the *Arvicola* from Merlin's Cave.

Palaeoenvironments Cold-climate and temperate species occur together in the fossil assemblage from the cave-earth and was the initial indicator of the temporally mixed nature of the fauna. For instance hazel dormouse *Muscardinus avellanarius* and wood mouse *Apodemus sylvaticus* appear alongside pika *Ochotona* and lemming (Hinton, 1924; Price, 2003). Considering the obvious heterogeneity of the fossil assemblage no attempt will be made at palaeoenvironmental interpretation.

Stratigraphy and correlation Radiocarbon dates have been obtained from small mammal specimens collected from the cemented breccia and on *Arvicola* from the cave-earth (Table 3.24). Dates from the breccia show a homogeneous assemblage originating from the earliest Holocene while the material from the cave-earth range from this period to the Neolithic, which confirms the conclusions of previous studies that the cave-earth fauna is temporally mixed. The *Arvicola* assemblage will be assumed to date between *c.* 12–3 k yr BP. Merlin's Cave provides an excellent opportunity to test the effects of temporal mixing on the pattern of morphological variation in a time-averaged fossil assemblage of known extent.

Table 3.24: Radiocarbon dates from Merlin's Cave.

Layer	Lab no.	Material	^{14}C BP	cal BP
Cave-earth[a]				
	OxA-21077	*Arvicola* mandible	$2\,797 \pm 27$	$2\,900 \pm 40$
	OxA-21076	*Arvicola* mandible	$10\,295 \pm 45$	$12\,130 \pm 120$
Breccia[b]				
	OxA-8072	Norway lemming	$9\,685 \pm 60$	$11\,030 \pm 150$
	OxA-8073	Pika	$9\,915 \pm 60$	$11\,390 \pm 120$
	OxA-8146	*Arvicola*	$10\,161 \pm 65$	$11\,820 \pm 150$
	OxA-8071	Arctic hare	$10\,270 \pm 65$	$12\,060 \pm 180$

[a] This study, [b] Price (2003).

3.6.3.5 Ossom's Eyrie

Location Manifold Valley, south Staffordshire, England

Co-ordinates 53.09°N, 1.85°W

Age Romano-British to Medieval, *c.* 1.7–1 k yr BP

Archive Manchester Museum, Manchester, Great Britain

Description Ossom's Eyrie is an approximately 4 m deep cave formed in Carboniferous limestone 30 m up the side of a steep gorge (Bramwell *et al.*, 1990). A high plateau of moorland and agricultural land surrounds the site and a number of similar caves occur in the region. The Peakland Archaeological Society excavated Ossom's Eyrie in the 1950s, finding a cave-earth and yellowish sandy clay around 60 cm deep. These deposits were highly fossiliferous with over ten thousand small mammal fossils recovered. The discovery of Romano-British pottery and other artefacts demonstrates that the site is a relatively recent accumulation. The occurrence of adult and juvenile golden eagle *Aquila chrysaetos* gave the site its name but other birds of prey, such as barn owl *Tyto alba*, were also present (Bramwell *et al.*, 1990).

Material examined Forty-nine M_1 teeth were photographed, all but one were found in mandibles. Specimens were slightly eroded and covered with fine-grained red sediment that required removal in order to examine occlusal surfaces clearly. Enamel layers were easily distinguishable as grey bands against discoloured dentine but were in many cases eroded, which hampered measurement of enamel thicknesses.

Specimens were identified as *Arvicola terrestris* by Bramwell *et al.* (1990) and, although occurring throughout the sequence, displayed a marked decrease in abundance after the time of occupation by golden eagle. Golden eagle is not thought to have been the main accumulator of *Arvicola*, rather the preservational characteristics of the assemblage indicate predation by barn owls (Bramwell *et al.*, 1990). No other work has been published on the *Arvicola* from Ossom's Eyrie.

Palaeoenvironments Two features of the palaeoenvironmental information presented by the site are of particular interest to this study. Firstly, the decline in numbers of water vole and similar declines, progressing to local extinctions, of other species such as hazel dormouse *Muscardinus avellanarius*[1], reflects human-mediated landscape change. A scrubby, open woodland, and moorland habitat was initially widespread in the region but was later replaced by greater amounts of grazed farmland (Bramwell *et al.*, 1990). Secondly, the abundance of remains of *A. terrestris* in an upland environment such as that surrounding Ossom's Eyrie is perhaps ecologically significant. Modern water voles in England are restricted to low-lying marshland areas, but their apparent historical presence in other habitats raise interesting questions as to whether *A. terrestris* has been effected by land-use changes or has changed habitat preferences over time, or whether the *Arvicola* found at Ossom's Eyrie is part of the same intraspecific lineage as that found in the rest of England and Wales today (Piertney *et al.*, 2005).

Stratigraphy and correlation The cave deposits represent accumulations of late Holocene age. A Late Roman occupation surface has been recognised (historically dated to approximately 1.7 k yr BP) near the base of the cave deposits with further fauna accumulated in conjunction with the likely existence of an eagle's nest. *Arvicola* numbers decline rapidly following the disappearance of the eagle's nest to finally make up less than 1% of the small mammal fauna in the highest levels of the cave deposits (Bramwell *et al.*, 1990). This decline is mirrored by other small mammal species and may be related to human-mediated landscape change. Bramwell *et al.* (1990) suggest that the eagle occupation is, at the very latest, medieval in age, based upon historic records of eagle presence in the central and northern England and the absence of rabbit *Oryctolagus* from the faunal assemblage, which was introduced to mainland Britain during Norman times (Rackham, 1986). Thus the earliest date for *Arvicola* can be placed at around 1.7 k yr BP, while the latest appears to be 1 k yr BP.

[1]Although it must be noted that *M. avellanarius* is rarely found in owl pellets (Yalden, 1999).

3.6.3.6 Tornewton Cave

Location Torbryan Valley, Devon, England

Co-ordinates 50.49°N, 3.68°W

Age MIS 5e to *c.* 27 k yr BP

Archive Natural History Museum, London, Great Britain

Description Tornewton Cave in south Devon is one of the most important sites for studies of the British Pleistocene, but interpretation is hampered by a fragmentary and complex excavation history. The cave is formed within Devonian limestone and consists of two near-vertical rifts—the larger referred to as the Main Chamber—and and a number of horizontal passages. J. L. Widger carried out the first excavations of the cave around 1877 to be followed in the 1930s by A. H. Ogilvie. Only posthumously published notes exist from Widger's workings, and no published or unpublished documentation remain from Ogilvie's (Sutcliffe and Zeuner, 1962; Currant, 1998). A full, published description did not emerge until after the excavations of Sutcliffe and Zeuner in the 1950s and 60s (Sutcliffe and Zeuner, 1962). The most recent investigations were by Currant (1990-1992) as part of the Torbryan Caves Research Project.

Both Widger and Ogilvie's excavations removed the uppermost parts of the sequence with Sutcliffe and Zeuner exploring the sediments before the main entrance and the deeper parts of the cave. The cave sediments (Figure 3.13) span the late Middle Pleistocene to the end of the Last Cold Stage, thought to be MIS 7 to MIS 2 (Currant, 1998; Gilmour *et al.*, 2007). Sutcliffe and Zeuner's stratigraphic scheme described climato-stratigraphic units in terms of significant faunal elements, but the stratigraphy is complicated by the occupation of the cave by bears and especially glutton *Gulo gulo*; the latter having apparently dug an extensive passage at the rear of the main chamber, which infilled to form the Glutton Stratum (Currant, 1998; Currant pers. comm., 2009; see below).

It seems that unidentified excavations also occurred during the period of Sutcliffe and Zeuner's explorations, and so overall a good deal of the fossil material recovered from Tornewton is without good stratigraphic control (Currant pers. comm.).

Material examined Nineteen M_1s were photographed. Only three molars were present within mandibles and all molars were in an excellent state of preservation, with only one M_1 unable to provide a full set of landmarks. Molars were unstained and had a 'fresh' appearance, and enamel layers were generally well-defined.

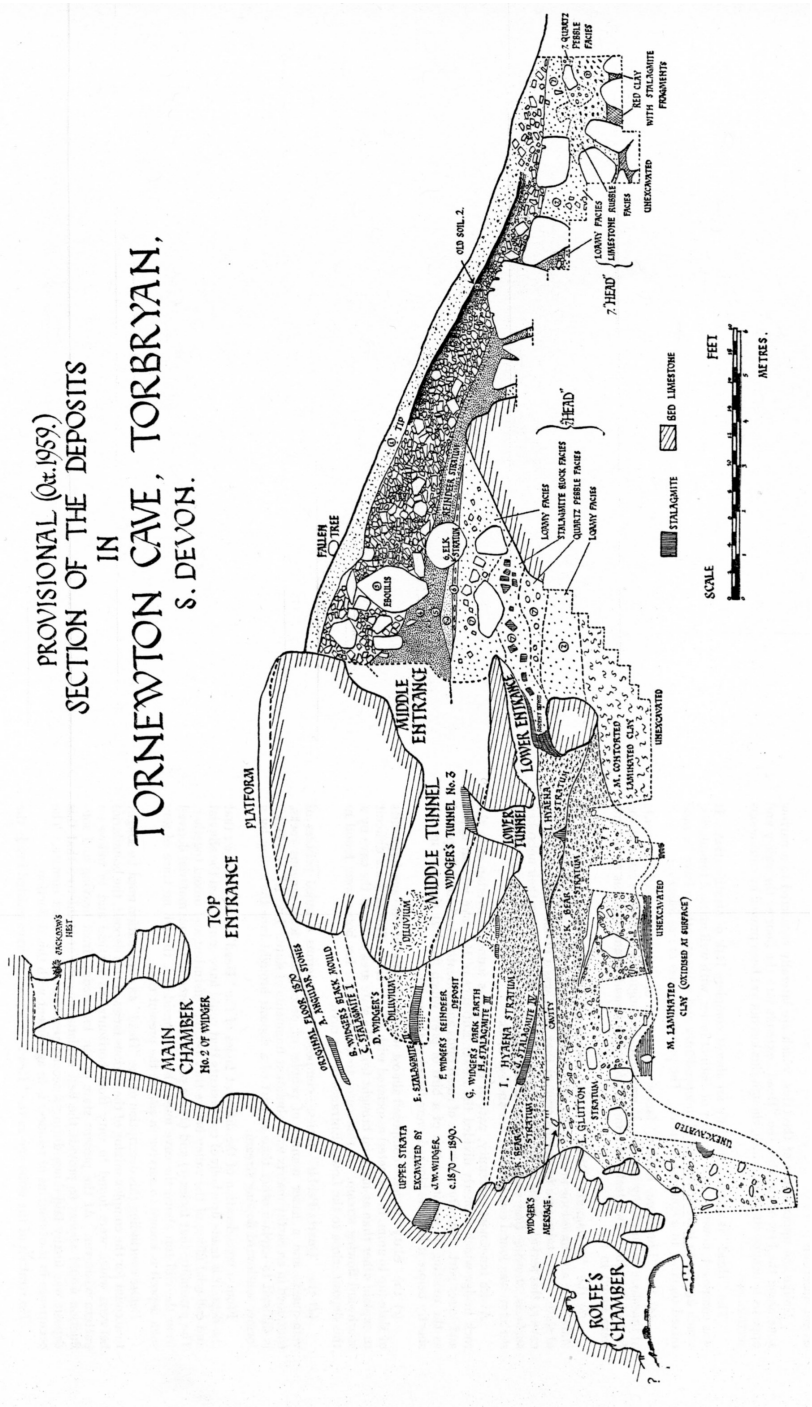

Figure 3.13: Sketch of the stratigraphy within Tornewton Cave. Taken from Sutcliffe and Zeuner (1962).

Specimens were labelled as deriving from the 'Main Chamber, base of Red Cave Earth. Equivalent to the Glutton Stratum'. 'Red Cave Earth' does not correspond with any published stratigraphy of the cave, but Sutcliffe and Kowalski (1976) list thirty-six *Arvicola* specimens from Sutcliffe and Zeuner's excavations of the Glutton Stratum.[1] *Arvicola* are also present in sediments thought to be correlated with the Hyaena Stratum (Currant, 1998). Currant (pers. comm.) has suggested that the 'Red Cave Earth' may be related to the 'rodent deposits' of Sutcliffe and Zeuner (1962), and appears to be the stratigraphic equivalent of the Bear or Hyaena strata (Figure 3.13). Although there is considerable uncertainty surrounding the provenance of the *Arvicola* material under consideration, the similar preservational state of the fossil *Arvicola* suggests a shared taphonomic history, and adds confidence in the integrity of the assemblage.

The *Arvicola* specimens examined were curated under the names *Arvicola terrestris* and *Arvicola cantiana-terrestris*. Koenigswald (1973) referred *Arvicola* from the Glutton Stratum to *A. cantiana-terrestris*; a morphological type with molar enamel layers of approximately equal thickness on trailing and leading edges. This form is intermediate between Middle Pleistocene and Late Pleistocene water voles, which possess *Mimomys*-differentiation and *Microtus*-differentiation respectively. No other *Arvicola* from the Tornewton Cave have been the subject of detailed study.

Palaeoenvironments The stratigraphic provenance of the *Arvicola* assemblage is uncertain but may originate from the Bear, Hyaena, or Glutton strata (see below). The Glutton Stratum contains an admixture of boreal and temperate taxa, and so will not be discussed further. The Hyaena Stratum has yielded a cool-temperate, mesic, generally open-landscape fossil assemblage including *A. terrestris*, northern vole *Microtus oeconomus*, bank vole *Clethrionomys glareolus*, field vole *Microtus agrestis*, and wood mouse *Apodemus sylvaticus* (Currant, 1998; Gilmour *et al.*, 2007). The cold climate assemblage of rodents from the Bear Stratum described by Sutcliffe and Kowalski (1976) in fact appear to originate from elsewhere in the cave (Currant, 1998). Recent excavations have shown that the Bear Stratum contains a warm interglacial fauna (Currant, 1998).

Table 3.25: Radiocarbon determination on the jaw of a glutton from the Glutton Stratum at Tornewton Cave. Data from Currant (1998).

Lab no.	Material	^{14}C BP	cal BP
OxA-4587	Glutton dentary	$22\,160 \pm 460$	$26\,684 \pm 785$

[1] Although the abundance in the Glutton Stratum may be attributed to greater sampling of this deposit (Sutcliffe and Kowalski, 1976).

Stratigraphy and correlation The labelling of the *Arvicola* examined for the present study suggests they are stratigraphically equivalent with the Glutton Stratum. Sutcliffe and Zeuner (1962) attributed the Glutton Stratum to the penultimate glacial due to the cold-climate fauna present and its stratigraphic position beneath the Hyaena Stratum, which they considered to be Last Interglacial in age based on the occurrence of *Hippopotamus*. However, a radiocarbon age estimate on a *G. gulo* dentary from the Glutton Stratum has shown that this layer is a later feature (Table 3.25). The Glutton Stratum is now considered to be the result of digging by glutton and other fauna, and contains a mixture of Devensian and earlier fossil material (Currant, 1998).

Currant (pers. comm., 2009) has suggested that the *Arvicola* studied in fact are stratigraphically closer to the Hyaena or Bear strata. The Last Interglacial age previously accepted for the Hyaena Stratum (Sutcliffe and Zeuner, 1962; Sutcliffe and Kowalski, 1976) has been called into question, firstly because the association of abundant *M. oeconomus* with *Hippopotamus* recorded at in the Hyaena Stratum is not characteristic of Last Interglacial faunas elsewhere in Britain, and secondly due to doubt over the stratigraphic provenance of the *Hippopotamus* finds (Currant, 1998; Gilmour *et al.*, 2007). Gilmour *et al.* (2007) constrain the age of the Hyaena Stratum within MIS 5 through U-Th dating of a speleothem from the cave, and specifically suggest a late MIS 5 age based on the mammalian faunal assemblage, which compares favourably with the Bacon Hole MAZ of Currant and Jacobi (2001). Currant (1998) also suggested MIS 5c as a possible correlation.

In the Bear Stratum—stratigraphically below the Hyaena Stratum—there is doubt over the context of some of the faunal remains excavated by Sutcliffe and Zeuner (Currant, 1998). More recent excavations have, however, confirmed the interglacial nature of the the Bear Stratum, and allowed an early MIS 5e age to be postulated for this deposit (Currant, 1998; Gilmour *et al.*, 2007).

In conclusion, the exact stratigraphic context of the *Arvicola* assemblage under study is not certain, but current understanding of the age of strata from which they may possibly originate suggests the assemblage may date from MIS 5e or earlier than *c.* 27 k yr BP (the age of the Glutton Stratum). An age range spanning MIS 5e to *c.* 27 k yr BP will be adopted for the *Arvicola* OTU.

3.6.3.7 Wigber Low

Location Near the village of Ashbourne, Derbyshire, England

Co-ordinates 53.06°N, 1.7°W

Age Bronze Age to Iron Age, 4–2.5 k yr BP

Archive Sheffield City Museum, Sheffield, England

Description A barrow mound located in the Peak District of northern England. Wigber Low was the subject of a rescue excavation between 1975 and 1976 by Sheffield University after treasure hunters began removing artefacts from the site. A complex of two cairns, 11 m by 14.4 m, was discovered, which contained a number of human burials dating from the Bronze Age and later. The remains of small mammals and the smaller bones of deer, sheep, horse, and cattle were found in a deposit referred to as the Old Ground Surface (OGS), which comprised soil and silt filling the spaces between blocks and boulders of the cairn (Collis, 1983).

Material examined Water vole was the species most commonly identified with over 5 500 individual bones (42% of the total fauna) found (Maltby, 1983). It is thought likely that the faunal remains derive from individuals that died naturally in or on the cairn and fell into inter-stone spaces after their bodies decayed. This process of accumulation ceased after the spaces between cairn boulders were filled by soil and silt (Maltby, 1983).

The apparent taphonomy of the fauna and the numbers of water vole found in an upland location led Maltby (1983) to suggest that the the *Arvicola* found at Wigber Low may have been a fossorial ecotype. The specimens were identified in the collection at Sheffield City Museum, Sheffield as *Arvicola terrestris* and all fifty-six M_1s photographed came from the OGS. Most samples were complete mandibles, slightly dirty with soil and silt but after light cleaning the occlusal surfaces and enamel bands were clearly visible.

Palaeoenvironments Although the number of faunal remains recovered from Wigber Low is high, the taxonomic list is fairly impoverished and provides little evidence that can be used to make detailed palaeonenvironmental inferences (Maltby, 1983). A major reason for this is likely to be taphonomic biases introduced by the structure and location of the barrow. *A. terrestris* dominates the fauna, with considerable numbers of short-tailed field vole *Microtus agrestis* and wood mouse *Apodemus sylvaticus* also present. Mole *Talpa europaea*, common shrew *Sorex araneus*, and stoat/weasel *Mustela* sp. were found in low numbers and the remaining mammals are domesticated large mammals.

Other records of Bronze Age and Iron Age (see below) environments from this region show that moorland and agriculture land were well established with wooded areas reducing rapidly (Rackham, 1986). This environmental picture does not agree well with the current habitat preferences of English *A. terrestris* and suggests that the water voles found at Wigber Low were perhaps fossorial in their ecology.

Stratigraphy and correlation The cairns are thought to date from the Early Bronze Age (Collis, 1983) and so the faunal assemblage found in the inter-block spaces must post-date this period. Maltby (1983) speculated that the small mammal remains date from a discrete period of time after the burials. The burrowing activity of rabbits was noted in parts of the mound but is not thought to have affected taphonomy of the fauna at the OGS. Roman finds which occurred in the upper parts of the cairn were not seen in the OGS and the original cairn construction, therefore it seems that the *Arvicola* specimens must be derived from between the Bronze Age to possibly the end of the Iron Age. A possible age-range of 4–2.5 k yr BP will be attributed to the *Arvicola* OTU, based on dates for the Bronze Age and Iron Age found in Fagan (1996).

3.7 Hungary

3.7.1 Early Middle Pleistocene

3.7.1.1 Fortuna utca 16–18/2 and Fortuna utca 25

Location	Várhegy, right bank of the Danube river, Budapest, Hungary
Co-ordinates	47.49°N, 19.04°E
Age	A warm temperate period between MIS 15 and MIS 11
Archive	Hungarian Institute of Geology, Budapest, and Hungarian Natural History Museum, Budapest, Hungary

Description These sites are two of many fossiliferous Pleistocene deposits from Várhegy (Castle Hill) in Budapest. Castle Hill is an elongate travertine plateau overlooking the river Danube upon which sits the Buda Castle and a residential district of Budapest dating back to medieval times. Mottl (1942) was the first to published details of fossil remains found in this area following construction work and continued building and development on Castle Hill has resulted in the emergence of new fossil localities throughout the 20th century. Fortuna utca 16–18/2 and 25 refer to house numbers on Fortuna Street, located at the northern end of the hill. Excavations in the cellars beneath these properties led to the discovery of fossil remains (Kordos, 2003).

The Danube in this region of Hungary flows along a fault line, and uplift to the west has led to the development of the Buda Hills, of which Castle Hill is a part. Castle Hill is formed around a Triassic limestone and Oligocene marl core, which has been overlain unconformably by a thick travertine sequence formed through thermal spring activity associated with local faulting throughout the Buda Hills (Krolopp *et al.*, 1976; Kordos, 2003; Ruszkiczay-Rudiger *et al.*, 2005; Figure 3.14). Cave systems subsequently formed at the base of the travertine later became filled with fluvial deposits containing Middle Pleistocene fossils. Later, surface karstification formed fissures, which became infilled with Late Pleistocene fossiliferous sediments. At least fourteen different sites have been studied from across Castle Hill, all of which have yielded fossil material. Castle Hill is also famous for its 'Buda Culture' artefacts: disputed pebble-tools from the fluvial sediments (Krolopp *et al.*, 1976; Kordos, 2003).

The remains from Fortuna utca 16–18/2 contain *Arvicola* and derive from the 'palaeosol'-like layer lying beneath the travertine (Figure 3.14 Layer 4). No detailed sedimentological description of the site was available but the 'palaeosol'-like layer is assumed to be descriptive of the lithology rather than a genetic inference.

Fortuna utca 25 also contains *Arvicola* but the fossils were found in calcareous silt and clay deposits (Figure 3.14 Layer 3) which Kordos (2003) refers to as laminated but Jánossy (1986) describes as cross-stratified.

Material examined

Fortuna utca 16–18/2 Twenty-three M_1 teeth were photographed, all from the Hungarian Institute of Geology, Budapest, Hungary. Six molars were still present within mandibles and all material was stained dark reddish-brown and dusted with fine calcareous sediment that was easily removed to expose the occlusal surface where necessary. Teeth were in good condition although one molar was too damaged to give a complete landmark configuration.

The water vole fossils were identified as *Arvicola cantiana* (= *Arvicola mosbachensis*) by Kordos (2003) and were registered under the same in the museum collections.

Fortuna utca 25 Six M_1 teeth were photographed, five from the Hungarian Natural History Museum, Budapest, and one from Hungarian Institute of Geology, Budapest, Hungary. Two molars were within mandibles and one molar could not give a full set of landmarks. In all other respects preservation was the same as for *Arvicola* from Fortuna utca 16–18/2.

The water vole fossils were listed as *A. mosbachensis* in the Hungarian Natural History Museum, Budapest, but as *A. cantiana* in the Hungarian Institute of Geology, Budapest. Jánossy (1986) and Kordos (2003) also assign the specimens to *A. cantiana*.

Palaeoenvironments The fossil fauna contains species mainly indicative of warm climates but with some suggestion of aridity or seasonality. Amphibians and reptiles, especially tortoises, are well represented (Jánossy, 1986). The horseshoe bat *Rhinolophus mehelyi*, today restricted to the Mediterranean, white-toothed shrew *Crocidura* sp. and house mouse *Mus musculus* are all typically warm climate species (Currant pers. comm.). Temperate woodland taxa such as edible dormouse *Glis* cf. *glis* and wood mouse *Apodemus sylvaticus* are present along with birch mouse *Sicista*, which is present in the Carpathians today in montane forests and alpine meadows. Riparian habitats are indicated by desman *Desmana* sp. and possibly *Arvicola*, which is expected given the close proximity of the Danube and many small tributaries. Single isolated teeth from each of the Fortuna utca sites are the only evidence of the presence of steppe lemming *Lagurus transiens*. This genus is today characteristic of steppe habitats and may provide tentative evidence that such conditions existed in the region of Castle Hill.

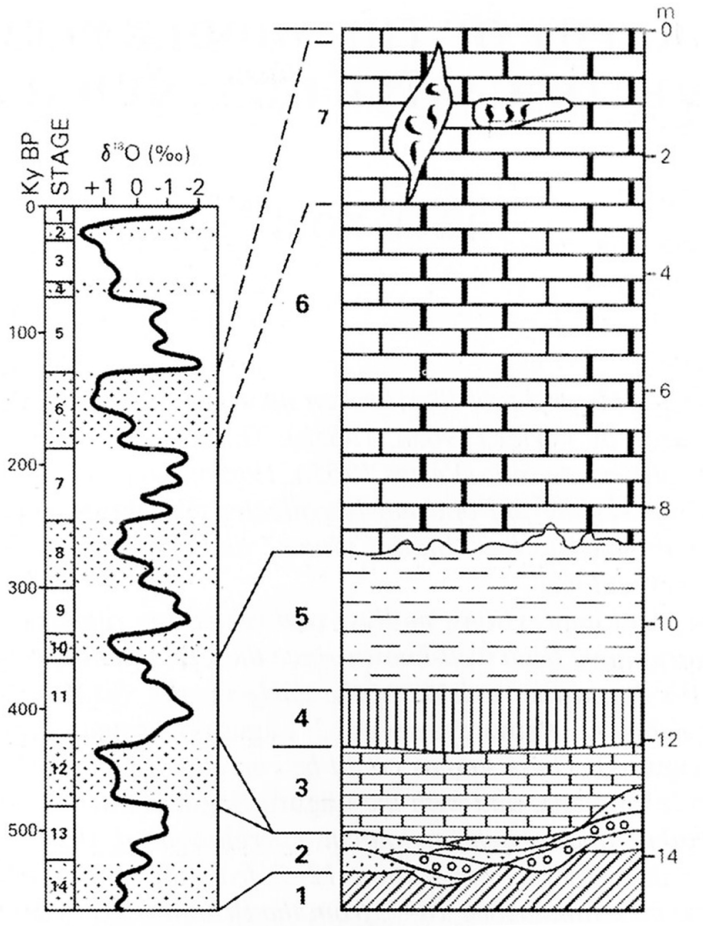

Figure 3.14: Generalised stratigraphy of the deposits at Castle Hill and their proposed correlation with the marine oxygen isotope stratigraphy. Strata: (1) palaeogenic [Oligocene] marl, (2) fluviatile gravel and sand, (3) laminated calcareous silt and clay, (4) 'palaeosol' horizon, (5) redeposited calcareous sandy sediment, (6) and (7) massive travertine. The freshwater limestone predates the fluvial deposits, which are infillings of a cave system developed at the base of the limestone. Taken from Kordos (2003).

Stratigraphy and correlation Palaeomagnetic and U-Th dating have shown that travertine deposition took place between the end of the Matuyama Chron (Korpás *et al*, 2003, referenced in Kordos, 2003) and 358 k yr BP (Hennig *et al*, 1983, referenced in Kordos, 2003). The cave systems therefore must have formed sometime between the Brunhes-Matuyama boundary and the first fluvial infillings. Biostratigraphically, Jánossy (1986) regarded all the cave infill deposits as being late Middle Pleistocene in age but Kordos (2003) concluded that the faunas were derived from both the early and late Middle Pleistocene. There is evidence of diachroneity in deposition because of subtle faunal differences between individual layers of some sites (Jánossy, 1986). This may been attributed to the complex structure of the cave system leading to a number of time-transgressive depositional episodes (Currant pers. comm.). Kordos (2003) assumes that this had a minimal effect on the biostratigraphic and ecological signal given by fossil assemblages from each layer.

Across Castle Hill *M. savini* is present in the basal sands and gravels, with *A. mosbachensis* found in the calcareous silts and clays of Layer 3 (e.g., Fortuna utca 25) and in Layer 4, which is a 'palaeosol'-like stratum above the silts and clays (e.g., Fortuna utca 16–18/2). At the site of Tácsics M. utca 23 both *A. mosbachensis* and *M. savini* occur together in Layers 3 and 4 (Kordos, 2003), which may indicate that these strata represent a transitional rooted–rootless water vole population. This pattern of co-occurrence is not seen in any other site on Castle Hill, and at Tácsics M. utca 23 the fossil assemblage is sparse and fragmentary[1]. Sediments deposited within karstified travertines are susceptible to temporal mixing as waters draining through the limestone pick up and redeposit material (Currant pers. comm.), and so it is possible that the water vole specimens at Tácsics M. utca 23 represent a temporally mixed thanatocoenosis (alluded to by Kordos, 2003). There is, however, no obvious juxtaposition of species, or of preservational states, which suggests broad temporal mixing in any of the sites of Castle Hill. It seems that firm conclusions as to the significance of the water vole assemblage from Tácsics M. utca 23 cannot be drawn at present. The chief reason that the biostratigraphy of the fluvial deposits is not clear is because the date of the last appearance of *Mimomys savini* in the Carpathian region is poorly constrained. The widely accepted last appearance of *M. savini* in Hungary is in the lower strata of the Tarkő rock-shelter in the northern Bükk Mountains, where it occurs in a cold-climate fauna alongside another index fossil *L. transiens* (Jánossy, 1986). The fauna at Tarkő form the Tarkőian faunal zone, whose base coincides with the '... upper part of the Middle Pleistocene [*sensu lato*] ...' (Jánossy, 1986, p. 179). The maximum age of the Tarkőian has been interpreted as any glacial from MIS 18 to MIS 12 (Kordos, 2003).

[1]Numbers of finds of *M. savini*: 10 M fragments, 1 M_1, 1 M^1, 1 M^2; of *A. mosbachensis*: 1 M^2

Kordos (2003) correlated Layers 3 and 4 with the Late Biharian (Jánossy, 1986) or Early Toringian (Fejfar and Heinrich, 1981) European faunal zones based upon the co-occurrence of *A. mosbachensis* with *L. transiens*. Furthermore, Kordos specifically estimated an MIS 11 (= Holsteinian) age for these strata. An age later than MIS 11 is not likely due to the presence of *Trogontherium*, but an earlier age for these strata is possible as *Arvicola* molars are not exclusively post MIS 12 indicators in central and western Europe. Kordos (2003), however, saw greater biogeographic affinities between the faunas of Castle Hill and eastern fossil assemblages containing *Lagurus* than with central and western Europe. In eastern Europe and the Russian Plain the current consensus is that *Arvicola* does not appear until after MIS 12 (= Oka glaciation) but in central Europe and Great Britain the loss of roots in water vole may have occurred by MIS 15 or MIS 16 (e.g., Maul and Markova, 2007). Jánossy (1986, p. 174) regards *A. mosbachensis* and *M. savini* as occurring together in the Hungarian early Middle Pleistocene but the position of the Carpathian region in this apparent east-west diachroneity of the *Mimomys–Arvicola* transition is not known. In summary, Layers 3 and 4 could date from a warm period from MIS 15 to MIS 11 and, not withstanding potential taphonomic mixing, the fauna of Layer 4 should be younger than Layer 3.

3.7.2 Late Middle Pleistocene

3.7.2.1 Hórvölgy

Location Western slope of Perpác Hill, Hór valley, Bükk Mountains, northern Hungary

Co-ordinates 48.08°N, 20.5°E

Age MIS 9 or MIS 7

Archive Hungarian Natural History Museum, Budapest, Hungary

Description The cave site of Hórvölgy (Hór Valley Cave) was first excavated in 1964 by D. Jánossy and Gy. Topál of the Hungarian Natural History Museum, Budapest, after reports in 1963 of fossil bones being discovered in a quarry. On visiting the locality the source of the fossil remains was found to be a cave uncovered and partially destroyed by quarrying activity. A rescue operation led to the removal of all the remaining sediment to be processed in the laboratory but the condition of the cave meant that no stratigraphic information could be ascertained. The sediment is reported to have been a 'greasy, brownish clay', 30 cm thick and 3 m^2 in area and was found to be relatively rich in vertebrate remains. A summary of the site and the fauna present can be found in Jánossy (1986).

Material examined Thirteen M_1 teeth were photographed for this study. Molars were isolated and generally in good condition, although two molars failed to provide complete configurations of landmarks. Fine-grained beige sediment lightly covered the molars and was easily removed by brushing to reveal the occlusal surface and prominent enamel bands. Enamel and dentine of all specimens were slightly darkened a reddish-orange colour.

The specimens were assigned to *Arvicola* sp. by Jánossy (1986). Jánossy notes that the *Arvicola* possessed '... triangles of thin enamel ...' which correspond to his *Arvicola* sp. III (Jánossy, 1986, p. 110; see Section 2.2.2.2). The length of the M_1 was found to be $3.4 - 4.1$mm ($n = 19$). No other work has been published on the *Arvicola* from Hórvölgy.

Palaeoenvironments Mole *Talpa* sp., wood mouse *Apodemus sylvaticus*, pika *Ochotona* cf. *pusilla*, and common vole *Microtus arvalis* dominate the small mammal assemblage and these taxa broadly summarise the palaeoenvironmental evidence offered by the entire faunal assemblage (Jánossy, 1986). A mix of woodland and open, perhaps steppe-like, grassland environments are indicated.

Stratigraphy and correlation Given the excavation history of the site, the only stratigraphic information that can be obtained is from the faunal assemblage. There is evidence that temporal mixing of the fossil fauna is fairly limited. This is based upon the occurrence of a single, large, morphotype of cave bear *Ursus spelaeus* and a uniform morphology of *Arvicola* (Jánossy, 1986). The shared preservational characteristics of the *Arvicola* fossils may also provide evidence of a temporally constrained accumulation.

Jánossy (1986) considered the fauna to be slightly older than but related to the Solymárian faunal stage. This zone occurs at the end of the Middle Pleistocene and corresponds to the 'Riss' glacial before the Last Interglacial (Jánossy, 1986). The presence of a large form of *Crocuta* cf. *spelaea* distinguishes Hórvölgy from the Last Interglacial Süttőian Hungarian faunal zone where small hyaena are characteristic. Correlation specifically with the end of the late Middle Pleistocene is based upon the presence of large common shrew *Sorex araneus*, medium-sized white-toothed shrew *Crocidura leucodon*, large *Talpa* sp., 'modern' steppe lemming *Lagurus lagurus*, dental characteristics of hamster *Cricetus cricetus*, and an abundance of common vole *Microtus arvalis*. The thin enamel of *Arvicola* (see above) is also used as stratigraphic evidence by Jánossy, although it is not clear whether absolute thickness or relative thickness between anterior and posterior enamel layers is being referred to. Kordos (1994) agreed with this correlation and positioned Hórvölgy in the Late Saalian as part of his proposed '*Lagurus lagurus* partial range zone'. This faunal zone was constrained by the presence of transi-

tional forms between *Arvicola cantianus* and *Arvicola terrestris*.

It would appear that the fauna of Hórvölgy can be dated with confidence to a warm period prior to the Last Interglacial. More specifically, a correlation with MIS 9 or MIS 7 would be consistent with the stratigraphic conclusions of Jánossy (1986) and Kordos (1994).

3.7.3 Late Pleistocene

3.7.3.1 Balla Cave

Location Near the village of Répáshuta, Bükk Mountains, northern Hungary

Co-ordinates 48.05°N, 20.53°E

Age *c.* 15 k yr BP

Archive Hungarian Institute of Geology, Budapest, Hungary

Description Part of the Balla cave complex, Balla Cave, also known as Répáshuta, was excavated between 1909 and 1913 by J. Hillebrand (Vértes, 1965). A moderately-sized small mammal fauna was recovered and the virtually complete skeleton of a human child was found along with a small number of Solutrean flint artefacts (Tillier *et al.*, 2009). According to Jánossy (1986) no contextual information was noted for any of the fossil material, save the human remains, and this has surely contributed to the lack of research on the fauna of Balla Cave.

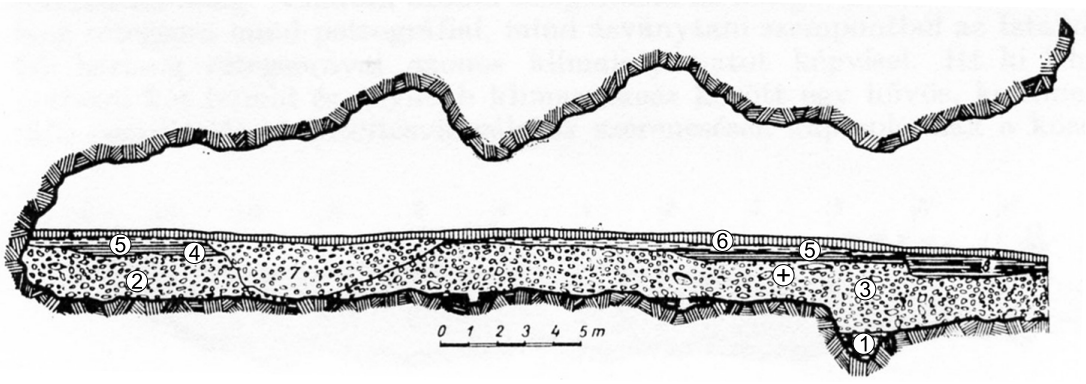

Figure 3.15: Longitudinal section of the stratigraphy at Balla Cave. Key: (+) Human remains, (1) red and yellow plastic clay, (2) greenish clay with limestone debris, (3) light yellow clay with limestone debris, (4) yellowish grey calcareous clay, (5) light-brown humus, (6) dark-brown humus. Modified from Vértes (1965).

Material examined Twelve M_1 teeth were photographed. All but three were within mandibles and the specimens were in good condition with only a slight covering of fine-grained cave sediment. Teeth were registered at the Hungarian Institute of Geology, Budapest, as *Arvicola minor* (= *Arvicola terrestris*) from Répáshuta but no contextual information was present. Vértes (1965) lists the water vole from Balla as *A. terrestris*. According to Jánossy (1986) it is likely that the fauna are mixed and consequently the fossil sample may not be a useful OTU to use to explore evolutionary relationships. However, if the period over which *Arvicola* accumulated was discrete post-excavation mixing would not render the fossil material unsuitable.

Palaeoenvironments The mixing of mammal fauna means that palaeoenvironmental evidence is likely to be misleading. Some taxa within the fauna are, nonetheless, suggestive of particular conditions. The presence of reindeer *Rangifer*, hamster *Cricetus*, and pika *Ochotona* indicate cold tundra-like climates, and while no clear temperate species were found, common shrew *Sorex araneus* and mole *Talpa europaea* show that moist habitats with soils and leaf litter must also have existed. *Arvicola* may or may not indicate widespread riparian environments depending upon the ecological type of water vole present.

Stratigraphy and correlation The material was registered at the Hungarian Institute of Geology, Budapest, as Magdalenian II in age. Jánossy (1986) supported this because some of the faunal elements allow at least part of the Répáshuta stratigraphy to be assigned to the 'Upper Würm' Pilisszántóian faunal phase—between 31–18 k yr BP.

The skeleton of the human child was discovered in a yellow clay layer (Layer 3) rich in microfauna (Hillebrand, 1911, referenced in Tillier *et al.*, 2009) 30 cm below the sediment surface. It was thought to be an example of an early *Homo sapiens* but direct radiocarbon dating has proven it to be Neolithic (Tillier *et al.*, 2009). Two radiocarbon dates were taken on samples of charcoal and bone by Vértes, which gave dates of $22\,300 \pm 180$ ^{14}C BP (GrN-4660) and $20\,000 \pm 190$ ^{14}C BP (GrN-4661) respectively. However, the charcoal was mixed with fragments of bone and sand, and no provenance was provided for the bone sample (Tillier *et al.*, 2009), making it difficult to usefully employ these dates. The lithic artefacts and the fauna also disagree with these dates and suggest an earlier age, although the potential for mixing in the fauna is apparent from the Neolithic age of the human skeleton.

Jánossy (1986) suspected the fauna to date to the Pilisszántóian faunal zone which approximates to GS-2 (see Section 3.7.3.5). An *Arvicola* mandible submitted by this study for radiocarbon dating gave an age of $14\,940 \pm 120$ cal BP (Table

3.26). This date is instructive in providing a younger minimum age for the fauna than other previous age estimations, and is the only good quality radiocarbon date for the fauna from the site. A single radiocarbon date cannot constrain the age of the entire *Arvicola* assemblage, but the seeming unreliability of other radiocarbon determinations and uncertainty involved in attempting to restrict the water vole fauna to a climatic period (e.g., GS-1), makes the use of a single date with a number of caveats arguably the most appropriate dating option. Thus, in the absence of other good dating evidence, an age of *c.* 15 k yr BP will be applied to the *Arvicola* OTU, whilst recognising that this date probably underestimates the age-range of the fossil assemblage.

Table 3.26: Radiocarbon date made for this study of an *Arvicola* mandible from Balla Cave.

Lab no.	Material	^{14}C BP	cal BP
OxA-21112	*Arvicola* mandible	12515 ± 60	14940 ± 120

3.7.3.2 Horváti-lik

Location Uppony Gorge, near the village of Uppony, Bükk Mountains, northern Hungary

Co-ordinates 48.21°N, 20.44°E

Age MIS 5d to MIS 5a

Archive Hungarian Institute of Geology, Budapest, Hungary

Description Horváti-lik (= Horváti hole) is a small cave 70 m above the valley floor in Uppony Gorge in north-eastern Hungary. The cave was excavated by L. Fűköh and L. Kordos in 1977–78 and over 4 m of Late Pleistocene and Holocene deposits were discovered. Twenty-five sedimentary layers were recognised. Layers 25–16 consisted of clays with limestone clasts that were generally devoid of fossils. The overlying strata were in contrast rich in vertebrate and molluscan remains (Figure 3.16). A summary of the stratigraphy of Horváti-lik and an analysis of the vertebrate fauna is given in Pazonyi and Kordos (2004).

Material examined The *Arvicola* M_1s from Horváti-lik used in this study came from Layers 8 ($n = 29$), 9a ($n = 35$), and 13 ($n = 22$). These strata are part of a series of deposits thought to have accumulated continually throughout MIS 5d (see below). No specific studies of the *Arvicola* from Horváti-lik have previously been

made. The specimens were registered as *Arvicola* sp. in the Hungarian Institute of Geology, Budapest, but were assigned to *Arvicola terrestris* by Pazonyi and Kordos (2004) and were explicitly excluded from *Arvicola cantiana-terrestris* without any supporting evidence. All molars were in good condition with clearly defined occlusal shape and enamel bands. Buff coloured clay and silt covered many of the teeth but was removed by brushing to expose the occlusal surface.

Palaeoenvironments The palaeoenvironmental evidence provided by the small mammal fauna from Layers 15–7 suggest a change from a temperate to a cool climate. This is indicated by a reduction in the abundance of woodland species such as bank vole *Clethrionomys glareolus* accompanied by an increase in abundance of narrow-skulled vole *Microtus gregalis*, Caucasian snow vole *Microtus nivalis*, steppe lemming *Lagurus lagurus*, and pika *Ochotona pusilla* (Pazonyi and Kordos, 2004). Shrew *Sorex* and mole *Talpa* were present throughout the sequence, however, as were herpetofauna and lesser numbers of woodland taxa such as wood mouse *Apodemus sylvaticus*. This evidence suggests that soils and moist wooded areas persisted in the region; perhaps aided by the local topography of deep, sheltered valleys. The occurrence of *Arvicola* may not necessarily indicate riparian habitats but their presence suggests that these environments may have occurred.

Stratigraphy and correlation Dating of the deposits has been attempted by Pazonyi and Kordos (2004) through climatostratigraphy based upon ecological preferences of the fauna and the recognition of 'MAZs'. Changes in faunal composition throughout the Horváti-lik sequence were compared with and matched against faunal records of other dated Late Pleistocene fossil assemblages of the Carpathian Basin, and climatic changes inferred from the ecological preferences of the fauna were 'wiggle-matched' to the oxygen isotope record. The sequence

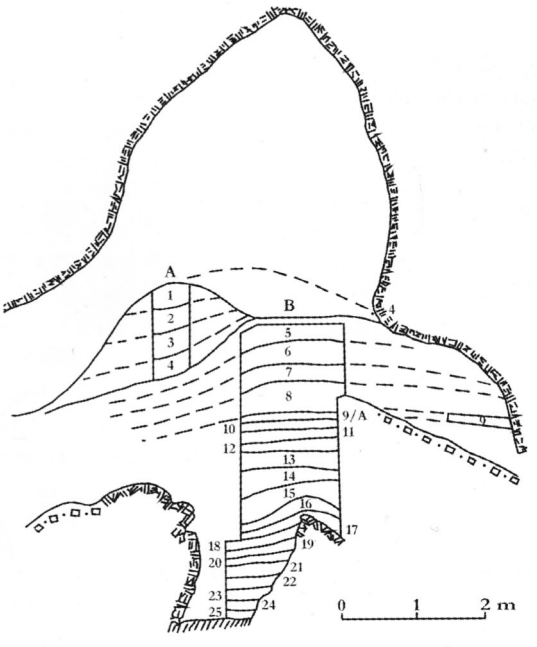

Figure 3.16: Diagrammatic cross-section of the deposits at Horváti-lik. Section A: Holocene deposits, section B: Pleistocene deposits. Taken from Pazonyi and Kordos (2004).

showed a transition from
temperate woodland in Layers 21–16 to cold-climate open steppe in Layers 15–7. The conclusion was that this sequence records the transition from the Eemian to the Last Cold Stage with Layers 15–7 representing continuous deposition through the early part of the Last Cold Stage: specifically MIS 5d. No other Hungarian faunas have hitherto been recognised as dating from just after the Last Interglacial and thus Horváti-lik would appear to occupy an extremely important stratigraphic position. In the regional stratigraphy, Layers 15–7 represent a faunal zone between the Süttőian (Last Interglacial) and the Varbóian (early Weichselian) faunal zones (Jánossy, 1986; Pazonyi and Kordos, 2004; cf. Section 3.7.3.3).

Without radiometric dating or the presence of biostratigraphically significant taxa to corroborate the age of the site suggested by Pazonyi and Kordos (2004) an MIS 5d age must be regarded with a degree of caution. This study will take a conservative approach and assign all the *Arvicola* OTUs from this site to an age-range from MIS 5d to MIS 5a, in line with age estimations the faunal zone approach of Jánossy.

3.7.3.3 Kálmán Lambrecht

Location Nagygallya Hill, 5 km southwest of the village of Varbó, Bükk Mountains, northern Hungary

Co-ordinates 48.12°N, 20.60°E

Age MIS 5d to MIS 5a

Archive Hungarian Natural History Museum, Budapest, Hungary

Description Kálmán Lambrecht cave is small hollow developed in the Triassic limestone of the Bükk Mountains in northern Hungary. The cave was excavated by L. Vértes and D. Jánossy in 1952 and 1960 where a Late Pleistocene sequence was found with two highly fossiliferous horizons containing a diverse assemblage of molluscs, small and large mammals, birds, and herpetofauna. The graphical summary depicted in Figure 3.17 approximately corresponds to the stratigraphy accompanying the faunal list given by Jánossy (1986) and summarised below:

Layers I–II Humus (= Layers 1–2)

Layer III Faunally sterile clay and limestone rubble (= Layer 3)

Layer IV Dark-grey clay with angular limestone clasts rich in faunal remains (= Layer 4)

Layer V Reddish-brown clay rich in faunal remains (= Layer 5)

Arvicola fossils dominate Layers IV and V but some fossil material was lost to a fire in the Hungarian Natural History Museum, Budapest, in 1956. Flint artefacts were recovered from Layer V and were described as 'pre-Mousterian' (Vértes referenced in Jánossy, 1986).

Material examined Twelve M_1 teeth were used in this study, all derived from sedimentary Layer IV (Jánossy, 1986). All molars were stained dark, reddish-brown and were covered in light-brown and grey, fine-grained sediment which was difficult to remove from some specimens. Enamel layers were well preserved and occlusal morphology was well-defined.

The shared preservational state of specimens suggests a shared taphonomy for the assemblage. The *Arvicola* were assigned to *Arvicola terrestris* (Jánossy, 1986) but no palaeontological analysis has been specifically directed toward the *Arvicola* fossils.

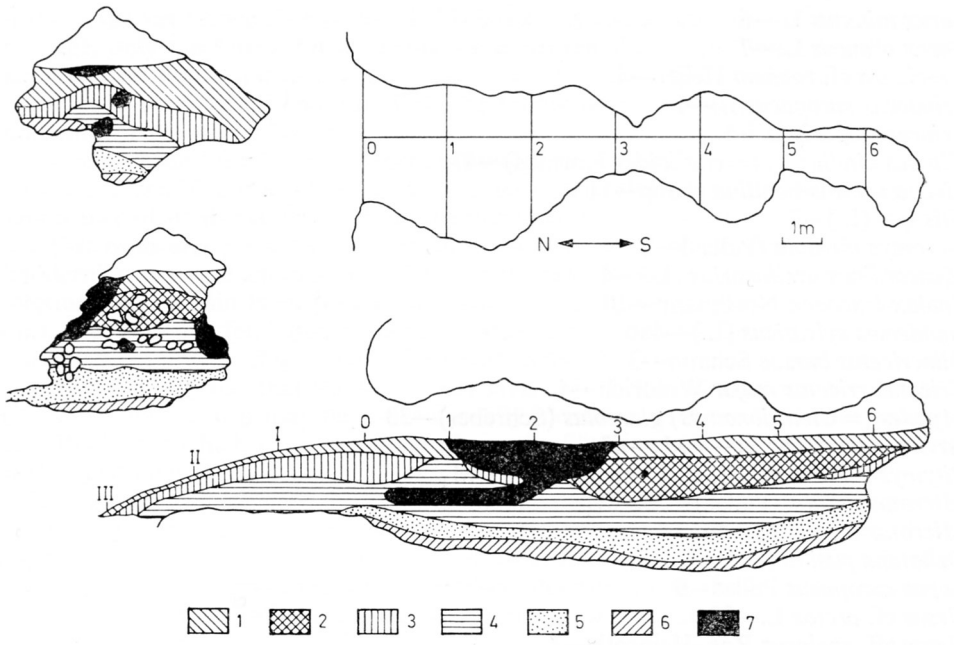

Figure 3.17: Plan, longitudinal and cross-sectional profiles of the strata of Kálmán Lambrecht cave. Key: (1) black humus, (2) brown humus, (3) yellow Pleistocene layer, (4) reddish, dark-brown layer, (5) reddish-black layer, (6) lower yellow layer, (7) badger digging. Taken from Jánossy (1986) after an original drawing by L. Vértes.

Palaeoenvironments A cooling climate trend can be observed throughout Layers V–III but overall the palaeoenvironmental data show the existence of a cool–temperate deciduous forest-steppe throughout the sequence (Jánossy, 1986). Pollen

records indicate the reduction in deciduous trees over this period but the occurrence of taxa such as edible dormouse *Glis glis*, wood mouse *Apodemus sylvaticus*, wild boar *Sus scrofa*, and badger *Meles meles* suggests that the presence of deciduous woodlands may be underestimated by over-representation of fir and pine pollen.

Although scarce, the occurrence of jerboa *Allactaga* and porcupine *Hystrix*, today found in the dry Asiatic steppe, was considered by Jánossy (1986) to posses some palaeoenvironmental and biogeographical significance. Together with common vole *Microtus arvalis* and hamster *Cricetus* sp. this suggests that arid-steppe habitats were in existence in the region. A cool climate is suggested by the presence of ptarmigan *Lagopus* sp., reindeer *Rangifer tarandus*, and arctic fox *Alopex lagopus*. The dominance of *Arvicola* in the small mammal assemblage could be used as evidence for riparian environments but its occurrence alongside arid-steppe indicators may provide evidence for a fossorial ecology for *Arvicola* at Kálmán Lambrecht.

Stratigraphy and correlation Layer V of Kálmán Lambrecht cave is the stratotype of the regional Varbóian faunal stage (Jánossy, 1986), but differs very little faunally from that of Layer IV. The distinctive faunal mix of late Middle Pleistocene and Late Pleistocene taxa, coupled with palaeoenvironmental evidence for a cooling and increasingly arid climate, was considered by Jánossy (1986) indicate that Layer IV dates from the early part of the Last Cold Stage. This study will conservatively assume an age range between MIS 5d and MIS 4 for the *Arvicola* OTU.

3.7.3.4 Peskö

Location Approximately 3 km southeast of the town of Szilvászárad, Bükk Mountains, northern Hungary

Co-ordinates 48.05°N, 20.43°E

Age 25–20 k yr BP

Archive Hungarian Institute of Geology, Budapest, Hungary

Description Peskö is a large cave, approximately 33 m long, 10 m wide, and with an entrance 14 m high, formed within Triassic limestone high on a bluff in the Bükk Mountains (Ehik, 1914; Vértes, 1965; Jánossy, 1986). The first excavations were carried out in 1912, initially by J. Hillebrand and later the same year by Gy. Ehik, M. Mottl, and O. Kadić, which yielded fossils and Aurignacian artefacts from a 'rodent-layer' and a 'green-yellow loam' (Ehik, 1914). In 1955 L. Vértes began a

new investigation aimed at clarifying the stratigraphy of the cave sediments. A rich fossil assemblage was found from two horizons, which he termed a 'brick-red' and a 'light-yellow cave loam' (Vértes, 1965; Jánossy, 1986; Figure 3.18). A small number of lithic artefacts classified as Aurignacian I were also recovered at this time from the lowest layer, Layer 1 (Vértes, 1965; Vogel and Waterbolk, 1972).

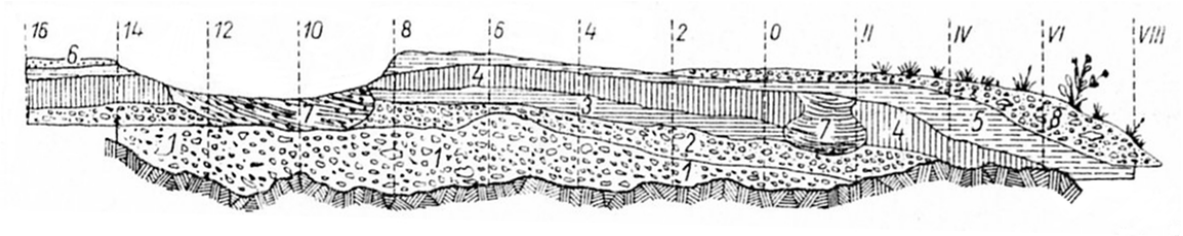

Figure 3.18: Longitudinal cross-section of the stratigraphy at Peskö. Key: (1) dark-brown layer, (2) green layer, (3) brick-red layer, (4) light-yellow cave loam, (5) black modern humus, (6) bat droppings, (7) prehistoric pit-fillings, (8) recent superficial deposits. Taken from Vértes (1965).

Material examined The water vole from Peskö was identified as *Arvicola terrestris amphibius* by Ehik (1914) and *Arvicola terrestris* by Vértes (1965). Heinrich (1982) analysed the enamel SDQ of specimens from this locality but no detailed investigation on the remains has been published.

Fourty-seven M_1 teeth from the 'brick-red' layer of Vértes were photographed. All the molars were present within mandibles and the fossils were coated with reddish, fine-grained sediment, which required removal by brushing in order to reveal the occlusal surface clearly. Molars were in good condition with the outlines of salient angles well defined and enamel layers clearly visible as bands of translucent grey contrasting against red-orange stained dentine.

Other *Arvicola* fossils from both the 'brick-red' and 'light-yellow cave loam' layers were curated separately as a mixture of material. An attempt was made to determine the stratigraphic origin of these specimens from the colour of the matrix adhering to the fossils. It was possible to allocate fifteen M_1s to each layer but in some instances it was difficult to assign specimens with certainty as the colour of the adhering sediment was not clearly red or yellow. This may reflect a continuum of colours present in the original deposits or be caused by post-excavation diagenesis. Whatever the cause, a degree of caution should be applied to the groups obtained from these mixed specimens, and consequently this fossil material will be analysed as two OTUs separate from the material labelled solely as from the 'brick-red' stratum.

Palaeoenvironments The faunal remains suggest a partially wooded steppe environment. The 'brick-red' layer contains a greater abundance of remains than

the 'light-yellow cave loam' layer but the relative abundances of individual taxa in both layers is similar (Vértes, 1965). Pika *Ochotona* sp. dominate the faunal assemblage, with nearly 1 500 finds in the 'brick-red' layer. *Arvicola*, common vole *Microtus arvalis*, short-tailed field vole *Microtus agrestis*, and northern vole *Microtus ratticeps* (= *oeconomus*) were also highly abundant and shrew *Sorex* sp., mole *Talpa* sp., collared lemming *Dicrostonyx torquatus*, bank vole *Clethrionomys glareolus*, and hamster *Cricetus* sp. were notable occurrences. The occurrence of steppe vole *Lagurus lagurus*, ptarmigan *Lagopus mutus*, reindeer *Rangifer*, woolly rhinoceros *Coelodonta antiquitatis*, glutton *Gulo gulo*, and arctic fox *Alopex lagopus* allows favourable comparison with the fauna and palaeoenvironments of Pilisszántó (see Section 3.7.3.5).

Stratigraphy and correlation Radiocarbon dating of Aurignacian bone artefacts from Layer 1 gave an age of 35 200 ± 670 ^{14}C BP (GrN-4950; Vogel and Waterbolk, 1972). Aurignacian archaeology has also been found at the nearby site of Istállóskő which has been recently dated to 28–33 ^{14}C k yr BP (Adams and Ringer, 2004). These dates are slightly younger than, but generally consistent with, the age of the Aurignacian artefacts at Peskö, and provide a maximum age for the *Arvicola* fossils.

Jánossy (1986) regarded the fauna of the 'brick-red' and 'light-yellow cave loam' layers as closely comparable to Pilisszántó (Section 3.7.3.5). The declining presence of cave bear *Ursus spelaeus* and the occurrence of *Dicrostonyx* sp. in particular were considered significant. Jánossy (1986) estimated the age of the 'brick-red' and 'light-yellow cave loam' layers as approximately 20–25 k yr BP. With the knowledge that the fauna is not older than the Aurignacian, but in the absence of other radiometric dating, the estimated age provided by biostratigraphy of 20–25 k yr BP will be applied to the *Arvicola* OTU.

3.7.3.5 Pilisszántó

Location Pilis Hill, 10 km northeast of Budapest

Co-ordinates 47.65°N, 19.16°E

Age *c.* 17 k yr BP

Archive Hungarian Institute of Geology, Budapest, Hungary

Description Pilisszántó is a rock-shelter developed within the Upper Triassic limestone of northern Hungary. O. Kadić excavated a test-pit in 1912 but the first systematic investigations were carried out by T. Kormos and K. Lambrecht in 1914. In 1951 D. Jánossy revisited the site to check Kormos's stratigraphy

but unfortunately all records of this investigation were destroyed by a fire at the Hungarian Natural History Museum, Budapest, in 1956. Kormos and Lambrecht identified seven Late Pleistocene layers which they grouped into an Upper, Middle, and Lower Diluvium apparently based upon the colour of the sediment (Jánossy, 1986; Figure 3.19). Fossil remains were recorded according to this 'Diluvium' stratigraphy but in a review of the site, Vértes (1965) commented that the lithology of individual layers was sufficiently different to have warranted distinguishing them faunally as well.

The faunal remains from Pilisszántó are diverse and abundant, with the avifauna being equally as well represented as large and small mammals. In terms of species richness the site is the most important in the Hungarian Late Pleistocene and forms the type locality for the Pilisszántóian faunal zone (Kretzoi, 1953, referenced in Jánossy, 1986; see below). It is therefore a pity that the limitations of the original excavation and later events hinder detailed stratigraphic interpretation of the fossil material. There is ample evidence for human occupation at the site with abundant butchered reindeer present in the fossil fauna (Vértes, 1965).

Material examined Forty-four M_1 teeth were used in this study. All were generally in good condition, although some erosion to the posterior walls of enamel triangles had occurred. A fine dusting of light-brown sediment coated all the molars and was easily brushed aside to reveal clean occlusal surfaces. Fossils were assigned to *Arvicola terrestris* (Vértes, 1965; Jánossy, 1986) and no detailed study of the *Arvicola* from Pilisszántó has been made, although Heinrich (1982) analysed the enamel SDQ.

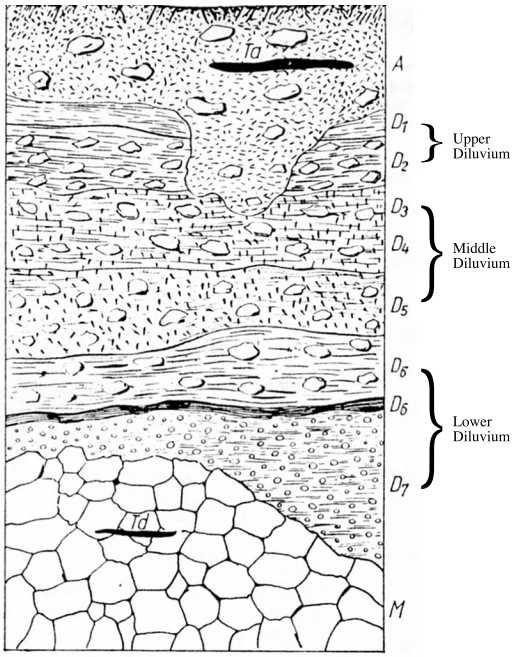

Figure 3.19: Summary of the stratigraphy at Pilisszántó established by Kormos and Lambrecht. Modified from Vértes (1965).

None of the *Arvicola* material registered at the Hungarian Institute of Geology, Budapest had contextual information. It is therefore not possible to determine from where in the stratigraphy established by Kormos and Lambrecht the fossils examined derive. The faunal list for the site (Vértes, 1965; Jánossy, 1986) show *Arvicola* as abundant in the Upper and Lower Diluvium but virtually absent from the Middle Diluvium

(376, 151, and 10 skeletal elements respectively). It seems likely then that the *Arvicola* fossils originated from either Upper or Lower Diluvium or from both of these strata. The inability to constrain the origins of *Arvicola* within the stratigraphy could undermine the concept of them as a discrete population in time. However, the sediments at Pilisszántó may not represent as broad a temporal span as Vértes (1965), for example, envisaged (see Stratigraphy and correlation below).

Palaeoenvironments Reindeer *Rangifer tarandus* dominates the large mammal fauna throughout the sequence. Pika *Ochotona pusilla* is also highly abundant, as are grouse *Lagopus lagopus* and ptarmigan *Lagopus mutus*, and alongside glutton *Gulo gulo*, collared lemming *Dicrostonyx torquatus*, arctic fox *Vulpes* (= *Alopex*) *lagopus*, woolly rhino *Coelodonta antiquitatis*, and mammoth *Mammuthus primigenius* indicates a cool tundra environment. Mole *Talpa europaea*, beaver *Castor fiber*, desman *Desmana* as well as *A. terrestris* were found in significant numbers in the Upper and Lower Diluvium. This suggests that soils, aquatic habitats, and wooded areas also existed in the region. The fauna here is similar to the assemblage found at Peskö (Section 3.7.3.4).

Stratigraphy and correlation Vértes (1965) proposed that the Upper Diluvium corresponded to the end of the Last Glacial Maximum and Lateglacial Interstadial, the Middle Diluvium to the Last Glacial Maximum, and the Lower Diluvium to the period prior to the Last Glacial Maximum based on faunal changes between these strata. A revised analysis of the faunal list of Vértes (1965) shows that the Upper and Lower Diluvial layers are very similar in their composition. The Middle Dilluvium contains a much sparser fauna than the Upper or Lower Diluvia, which could signify climatic deterioration. However, the Middle Dilluvium shares many of the same taxa as the overlying and underlying sediments, and the relative abundances of species in the Middle Diluvium are comparable. Faunal difference in the stratigraphy could therefore be accommodated by taphonomic rather than environmental differences.

Pilisszántó forms the type site for the Pilisszántóian faunal zone in Hungary (Kretzoi, 1953, referenced in Jánossy, 1986). According to Jánossy (1986) this substage covers the Lateglacial and is characterised by the dominance of reindeer *Rangifer tarandus* and pika *Ochotona pusilla*, with the eventual disappearance of 'northern faunal elements' and the appearance of 'animal assemblages of the contemporary temperate forests' (Jánossy, 1986, p. 149). Jánossy attributes the Pilisszántóian to *c.* 18–25 k yr BP, approximately equivalent to GS-2. A single *Arvicola* mandible submitted for this project for radiocarbon dating to ORAU has given an age of $13\,475 \pm 65$ ^{14}C BP (Table 3.27), which partially supports the date inferred by the faunal zone. A single radiocarbon date cannot constrain the age of

the entire *Arvicola* assemblage, but the absence of other evidence and uncertainty involved in attempting to restrict the water vole fauna to a climatic period (e.g., GS-2), makes the use of a single date with a number of caveats arguably the most appropriate dating option. Thus, in the absence of other good dating evidence, an age of $16\,740 \pm 80$ cal BP will be applied to the *Arvicola* OTU, whilst recognising that this date probably underestimates the age-range of the fossil assemblage.

Table 3.27: Radiocarbon date made for this study of an *Arvicola* mandible from Pilisszántó.

Lab no.	Material	^{14}C BP	cal BP
OxA-21119	*Arvicola* mandible	13475 ± 65	16740 ± 80

3.8 Italy

3.8.1 Late Pleistocene

3.8.1.1 Grotta del Broion, Sala Grande

Location Berici Hills, around 5 km south of the city of Vicenza, Veneto Region, Italy

Co-ordinates 45.46°N, 11.59°E

Age Layers R1–N, 116–45 k yr BP; Layer I, *c.* 45 k yr BP

Archive Dipartimento di Biologia ed Evoluzione, UniversitĹ di Ferrara, Ferrara, Italy

Description Grotta del Broion is a cave system formed within Oligocene limestone of the Berici Hills in northern Italy. The area is in the fore-Alpine region, and was around 40 km from the maximum extent of Alpine ice during the Last Glacial (Ehlers and Gibbard, 2004). The location of the site is biogeographically intermediate between western and southeastern Europe, with faunal exchanges and connections occurring through the Alps and the Po Plain (Sala and Marchetti, 2006). Initial exploration of Grotta del Broion was carried out in 1951 by P. Leonard and A. Da Schio of the Institute of Geology of the University of Ferrara. Excavations continued for seventeen years and resulted in numerous publications over this period (Sala, 1980).

In a large chamber (the Sala Grande), just within the cave entrance, a long sedimentary sequence was found, consisting of basal pre-Quaternary fluvial deposits, overlain by an approximately 8 m thick series of Last Cold Stage clays, sands, and breccias, divided into thirty layers and sub-layers (Figure 3.20). A stalagmite layer lines the walls of the Sala Grande, separating the two sedimentary packages. The Last Cold Stage deposits were found to contain large and small mammal remains, and Mousterian archaeology (Sala, 1980).

Material examined *Arvicola* were present throughout the sequence, and were abundant enough in five layers to provide samples for use in this study (see Table 3.28). All molars were stained a light-brown colour, but the preservational condition of specimens within strata was variable. The occlusal surfaces of many molars were damaged, which reduced both the number of M_1s giving full landmark configurations and the likely accuracy and precision of enamel thickness measurements. Additionally, some molars possessed calcareous concretions, also affecting the mea-

surement of morphometric variables. The juxtaposition of different preservational states may be evidence of taphonomic mixing.

All specimens were identified as *Arvicola terrestris* in the Dipartimento di Biologia ed Evoluzione, UniversitĹ di Ferrara, Ferrara, Italy, and to the knowledge of the author no specific study of the *Arvicola* from the Grotta del Broion, Sala Grande has been published. Given the upland location of the site it is interesting to speculate whether the ecology of the *Arvicola* was semi-aquatic or fossorial.

Palaeoenvironments Cold-climate breccias are prominent in the sedimentary sequence of the Sala Grande, and underline the proximity of the Grotta del Broion to the Alpine mountain range. The altitude and Alpine affinities of the site are also reflected in the large and small mammal fauna. Alpine ibex *Capra ibex*, Alpine chamois *Rupicapra rupicapra*, European snow vole *Chionomys nivalis*, and Alpine marmot *Marmota marmota* are all found at intervals (Sala, 1980). These taxa are distinctively montane in their habitat preferences today (e.g., Aulagnier *et al.*, 2008). Cool but temperate conditions evidently existed for extended periods between layers Q–E. But between layers N–I mesic, forested environments were present as indicated by the presences of the woodland species wood mouse *Apodemus sylvaticus*, shrew *Sorex araneus*, and bank vole *Clethrionomys glareolus*. Open meadow environments were also present at the time layers N–I were deposited, as indicated by the presence of short-tailed field vole *Microtus agrestis*, and possibly *A. terrestris*.

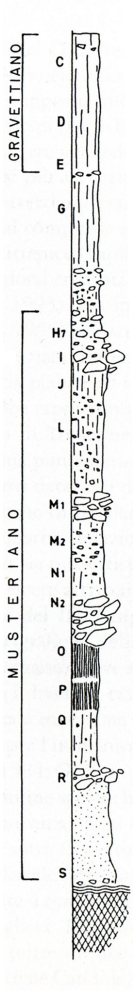

Figure 3.20: Generalised stratigraphy of Grotta del Broion, Sala Grande, showing major stratigraphic divisions and associated archaeology in the approximately 8 m deep sequence. See text for explanation. Modified from Broglio and Improta (1995).

Stratigraphy and correlation Radiocarbon dating of layers D and E (Table 3.28), together with Gravettian archaeology found in these strata (Figure 3.20), set a minimum age of the beginning of MIS 2 for layer I. The radiocarbon date from

layer I, being from a charcoal sample, may be viewed as problematic (Bowman, 1990), but agrees with the overlying radiocarbon determinations, and furthermore is derived from strata containing Mousterian archaeology. It will assumed that this radiocarbon date is accurate and will be applied as a date for the *Arvicola* assemblage from layer I.

The strata below layer I were considered to chronicle the Würm Glacial (= Last Cold Stage) by Sala (1980), with the stalagmite layer presumably representing deposition during the Last Interglacial. No absolute dating information is available for this part of the sequence, but Mousterian archaeology is found throughout, and the palaeoenvironmental fluctuations evident are strongly suggestive of the early and middle part of the Last Cold Stage (Sala, 1980). Strictly then, the remaining strata containing *Arvicola* (layers R, Q5, Q4, and N) can only be assumed to span a period from MIS 5d to the maximum age of layer I. However, significant deposition, and by inference a significant span of time, occurred between layer N and layer I. In the absence of any other evidence differentiating these strata an age-range from MIS 5d to the early part of MIS 3 will be adopted for layers R, Q5, Q4, and N.

Table 3.28: Numbers of *Arvicola* M_1 teeth photographed ($n_{Arvicola}$) from strata of Grotta del Broion, Sala Grande, together with radiocarbon dates available from the sequence.

		Radiocarbon dating			
$n_{Arvicola}$	Layer	Lab no.	Material	^{14}C BP	cal BP
	D	UtC-2694[a]	bone indet.	24 700 ± 400	29 503 ± 622
	E	UtC-2693[a]	bone indet.	25 250 ± 280	30 140 ± 325
11	I	GrN-4638[b]	charcoal	40 600 ± 1 200	44 276 ± 1099
		GrN-4637[b]	charcoal	46 400 ± 1 500	49 991 ± 2 507
36	N				
27	Q4				
34	Q5				
42	R1				

[a] Broglio and Improta (1995)
[b] Vogel and Waterbolk (1967)

3.9 Poland

3.9.1 Early Middle Pleistocene

3.9.1.1 Kozi Grzbiet

Location Kozi Grzbiet Hill, Holy Cross Mountains, south-central Poland

Co-ordinates 50.85°N, 20.35°E

Age A warm period between MIS 17 and MIS 13

Archive Institute of Systematics and Evolution of Animals, Polish Academy of Sciences, Krakow, Poland

Description An infilled cave in the karstic Devonian limestone landscape of south-central Poland. The site of Kozi Grzbiet was excavated in the 1970s following the discovery of fossiliferous deposits during quarrying (Głazek *et al.*, 1976). An Middle Pleistocene sedimentary sequence in the cave was divided into five lithological units (Figure 3.21) but only the 'cave loams' of Unit 2, near the top of the sequence, were found to contain fossils. Climatic warming occurs throughout Unit 2 while across the whole sequence a cold-temperate-cold transition is evident (Głazek *et al.*, 1976).

Material examined Fossil water voles were attributed to *Mimomys savini* by Nadachowski (1985) who further identified five M_1 morphotypes and morphotype variants named "*milleri*", "*majori*", and "*savini*"; corresponding to species descriptions given by Hinton (1926). All material was held at Institute of Systematics and Evolution of Animals, Polish Academy of Sciences, Krakow, Poland where fossils were labelled 2a, 2b, 2a+b, and 2c in reference to the sub-units of Unit 2 (see below). Forty-nine M_1 teeth were photographed in total. All were in an excellent state of preservation with clean enamel, sharp edges to salient and re-entrant angles, and well-defined enamel bands.

Palaeoenvironments There is a decreasing occurrence of the arvicolids *Dicrostonyx simplicior*, *Lemmus* sp., and *Microtus* ex gr. *arvalis* up Unit 2. At the same time in Units 2b and 2a species such as the extinct beaver *Trogontherium cuvieri*, bank vole *Clethrionomys glareolus*, and dormouse *Glis* cf. *sackdillingensis* become more frequent. This suggests that cool open grassland habitats gave way to moister climates with an increasing fraction of wooded areas through Units 2c, 2b, and 2a (Głazek *et al.*, 1976; Maul and Parfitt, 2010). Snails and the her-

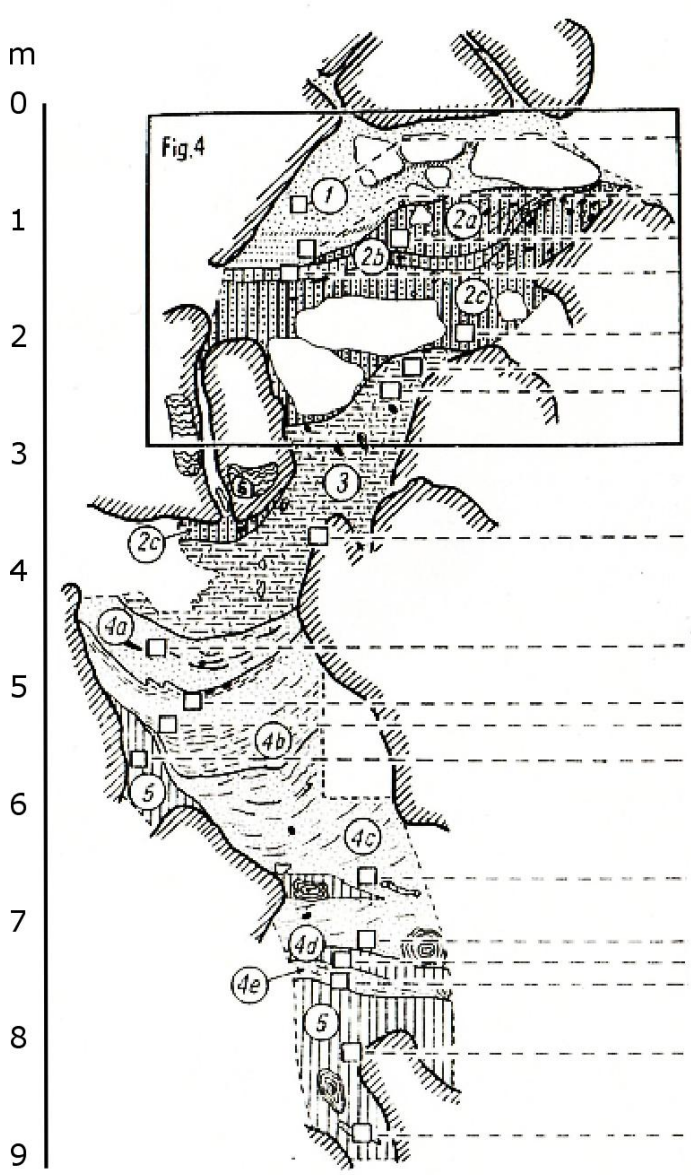

Figure 3.21: Sedimentary sequence at Kozi Grzbiet. Sedimentary units described as follows: (1) fine yellow sands with limestone blocks and flowstone debris, (2) sandy fossiliferous loams and flowstones, (3) brecciated cherry-red clay, (4) cherry-red clayey-sands, (5) brownish-yellow clays with carbonate concretions and limestone debris. Modified from Głazek *et al.* (1976).

petofauna support the interpretation of developing warm and mesic temperate conditions (Głazek *et al.*, 1976).

Stratigraphy and correlation Unit 2 at Kozi Grzbiet is normally magnetised and is considered to originate from above the Brunhes-Matuyama boundary. The change from cool-temperate to warm-temperate conditions indicated by the fauna of Unit 2 suggest that this layer was deposited during the early to middle part of an interglacial (Maul and Parfitt, 2010), and this discounts the latter part of MIS 19, which overlaps with the start of the Brunhes magnetic chron. Fluoro-chloro-apatite and collagen dating give an age for this layer as 630–560 k yr BP (Głazek *et al.*, 1976); although these are not considered reliable (Nadachowski pers. comm., 2008). The occurrence of *M. savini* and *Pliomys episcopalis* and the composition of the small mammal assemblage (see Nadachowski, 1990, for a full faunal list), which is similar to that at West Runton (Section 3.6.1.2), suggest that the deposits date from a period around the same time as the West Runton Freshwater Bed in the early Middle Pleistocene (Maul and Parfitt, 2010). In summary, Unit 2 can be dated to the early part of an warm period later than the Brunhes-Matuyama boundary but earlier than the widespread appearance of *Arvicola* in Europe.

The first appearance of *Arvicola* is recognised as diachronous: from MIS 15/16 in central Europe to MIS 12/13 in eastern Europe and Russia (Kolfschoten and Turner, 1996; Koenigswald and Heinrich, 1999; Maul and Markova, 2007), but the age of this transition in Poland is not known. Therefore the best statement that can be made on the age of Unit 2 is that it represents an warm period between MIS 17 and MIS 13.

3.9.1.2 Biśnik Cave

Location 2 km south-west of the village Smoleń, Małpolska Province, southern Poland

Co-ordinates 50.42°N, 19.67°E

Age MIS 8 to early MIS 4

Archive University of Wrocław, Wrocław, Poland

Description Biśnik Cave is located in the karstified Upper Jurassic limestone of the Krakow-Częstochowa uplands. The cave is formed from three chambers that were excavated from 1992 to 1999 under the supervision of K. Cyrek. A 7 m thick sequence of clays, loams, and limestone rubble was found which spanned the late Middle Pleistocene to the Holocene and produced a fossil vertebrate fauna and flint tools of the Micoquian and Mousterian cultures (Cyrek *et al.*, In Press).

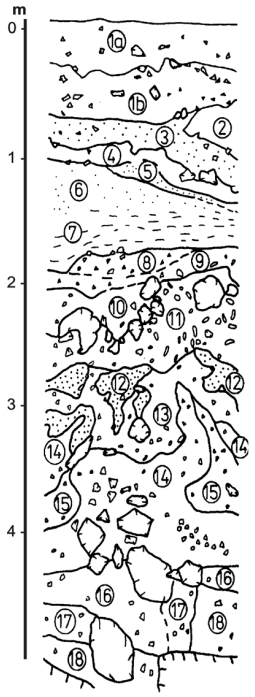

Figure 3.22: Generalised stratigraphy of Biśnik Cave. *Arvicola* for this study derive from layers 8, 8/9, 12–13, 15, 16, and 18. Modified from Mirosław-Grabowska (2002).

Material examined *Arvicola* were present but not common throughout the sequence and for the purposes of this study sufficient numbers of M_1s were only found from the layers shown in Table 3.29. Fifteen molars from layers 12 and 13 were considered together as a single assemblage. In all parts of the sequence specimens exhibited a variety of preservational states, ranging from very well-preserved, clean, unstained molars to darkly coloured, eroded teeth with sediment tightly adhered. No discussion of the taphonomy of the site has been made in the literature but the juxtaposition of such widely differing preservational states does raise concerns over the stratigraphic integrity of each fossil assemblage.

No specific discussion of the water vole assemblage has at this time been published. Cyrek *et al.* (In Press) identified water vole from Layer 18 as *Arvicola amphibious* (sic) whereas Mirosław-Grabowska (2002) listed the water vole as *Arvicola terrestris*. It is not known how taxonomically significant these assignments

are because the correlation of some parts of the stratigraphy containing *Arvicola* with the late Middle Pleistocene (see below) would otherwise indicate the presence of chronological species such as *Arvicola cantiana* or *Arvicola mosbachensis*.

Palaeoenvironments Cyrek *et al.* (In Press) performed ecological group analysis on the small mammals which showed relative changes in steppe, tundra, woodland, wetland, and generalist taxa. Sedimentological data were also used in palaeoenvironmental analysis. For the sake of brevity the evolution of climate and habitat throughout the sequence will not be discussed here in detail, but the main palaeoenvironmental conclusions of Cyrek *et al.* (In Press) are outlined in Table 3.29.

Although broad palaeoclimatic inferences are shown in Table 3.29 a considerable level of ecological diversity is maintained throughout, such as the presence of dormouse *Glis glis* in Layer 18. This may reflect the varied topography in the region of the cave providing opportunities for different habitats to persist, non-analogue communities, or stratigraphic mixing.

Stratigraphy and correlation A large number of U-Th and TL dates have been taken across the Biśnik Cave sequence, but the U-Th age estimates have less precision and accuracy than the evidence from other dating methods. Heavy mineral, lithological, faunal, archaeological, and TL dates indicate that Layers 18 to 8 span the late Middle Pleistocene to the early Late Pleistocene (Cyrek *et al.*, In Press; Table 3.29). The MIS correlations given by Cyrek *et al.* (In Press) will be applied to the *Arvicola* assemblages.

Table 3.29: Stratigraphic and palaeoenvironmental summary of the strata of interest at Biśnik Cave. Absolute dates in k yr BP. $n_{Arvicola}$ = numbers of *Arvicola* M_1 teeth photographed. Data from Mirosław-Grabowska (2002) and Cyrek *et al.* (In Press).

Layer	$n_{Arvicola}$	Climate	Habitat	U-Th	TL	Regional stratigraphy	MIS
8	9	Cold-moist	Steppe-tundra	106–270		Lower Plenivistulian	Early 4
9		Cold-moist	Steppe-tundra	11–30	81–127	Early Vistulian	5a
12	6	Warm-mesic	Steppe, Wood	31–66	122–142	Early Vistulian	5d
13		Warm-mesic	Wood	63–143	101–151	Eemian	5e
15	7	Warm-wet	Wood	216–930	160–230	Lubawa Interglacial	7
16	10	Cold-arid	Steppe-tundra				8
18	8	Cold-arid	Steppe-tundra	116–346	229–280	Odra Glacial	8

3.9.2 Late Pleistocene

3.9.2.1 Komarowa Cave

Location Puchacz Hill, Sokole Mountains, southern Poland

Co-ordinates 50.76°N, 19.22°E

Age 44–29 k yr BP

Archive Institute of Systematics and Evolution of Animals, Polish Academy of Sciences, Krakow, Poland

Description Komarowa Cave is a small cave, approximately 20 m long, situated about 100 km north of Krakow in the Sokole Mountains of southern Poland. The first chamber and the terrace in front of the cave entrance were excavated between 1998 and 2002. From two nearby trenches excavated in the cave chamber, thirteen lithologically defined layers and sub-layers were recognised. The whole sequence of clays, sands and limestone breccias is considered to span the Last Cold Stage and the Holocene to the modern era (Wojtal, 2007). The geology, archaeology and large mammals are detailed in Wojtal (2007) but the small mammals and other fauna are yet to be published.

A great many fossil large mammal bones were found. Most of the bones show signs of gnawing and are etched by stomach acids. This, together with the high proportion of deciduous hyaena *Crocuta crocuta* teeth present, suggests that the cave was a hyaena den for long periods. The cave was also used periodically by bears but only a small number of Palaeolithic flint tools were found.

Fossil material *Arvicola* were found in Layer D in sufficient quantities for use by this study. Eighteen M_1s were photographed but damage to the occlusal surface of three molars meant only fifteen could provide full configurations of landmarks. Molars were coloured a light reddish-brown and were coated with a dusting of fine, pale-grey silt and clay, which had to be removed to expose the occlusal surface. Enamel layers were generally clearly visible but in some specimens had become chipped or had completely collapsed.

Palaeoenvironments In general the sediments and fauna of the cave and terrace at Komarowa indicate a cool climate. It has been suggested that Layer D was deposited during a warmer period based on the lack of angular clasts within its sediments (Wojtal, 2007). To the knowledge of this author no publications have been made on the small mammal fauna but the large mammals of Layer D overall suggest a cool climate. The large mammal assemblage is dominated by hyaena *C. crocuta* and other carnivores such as cave bear *Ursus spelaeus*, cave lion *Panthera*

spelaea, red fox *Vulpes vulpes*, and badger *Meles meles* (Wojtal, 2007). Amongst the herbivores, reindeer *Rangifer tarandus* is most common along with red deer *Cervus elaphus* and giant deer *Megaloceros giganteus*, bovid *Bison/Bos*, and horse *Equus* sp. Many of these species are generalists but the presence of *R. tarandus* is a key indicator of cold environments. Information on the small mammal fauna, if it were available, would no doubt provide a more detailed palaeoenviromental picture. However, the presence of *Arvicola* in itself is suggestive of the existence of at least cool-temperate conditions for some period of time during the deposition of Layer D.

Stratigraphy and correlation The lack of angular breccia in Layer D led Wojtal (2007) to suggest that climates were warmer during deposition here than elsewhere in the sequence, and went on to correlate Layer D with the Polish Inter-pleni-Vistulian interstadial. Archaeological finds from Layer D indicate a Middle Palaeolithic age, and flint tools from Layer B have been ascribed to the Late Magdalenian. Radiocarbon dating of large mammal remains from Layer D indicate an MIS 3 age. Although these determinations are spread over seven thousand radiocarbon years, there are no age-reversals within or above and below Layer D (Table 3.30). The dates obtained from large mammals may not provide a good indication of the age of the *Arvicola* assemblage but in the absence of any other dating evidence the limits provided by the calibrated dates from layers E and C (Table 3.30) will be applied to the *Arvicola* OTU, giving an age-range of *c.* 44–29 k yr BP.

Table 3.30: Radiocarbon dates from Layer D, the origin of *Arvicola* material used in this study, and adjacent layers at Komarowa Cave. Data from Wojtal (2007).

Layer	Lab no.	Material	^{14}C BP	cal BP
Layer C				
	Poz-339	bear skull	24 550 ± 220	29 361 ± 508
Layer D				
	GdA-94	bear skull	28 500 ± 500	33 000 ± 550
	Poz-313	bone indet.	31 100 ± 400	35 110 ± 390
	Gd-13097	bone indet.	31 400 ± ?	
	Gd-15029	deer antler	35 500 ± ?	
Layer E				
	Poz-323	bone indet.	39 900 ± 1 200	43 792 ± 964

3.10 Romania

3.10.1 Early Middle Pleistocene

3.10.1.1 Rotbav-Dealul Ţiganilor

Location Approximately 2 km west of the town of Rotbav, Brasov Region, Romania

Co-ordinates 45.83°N, 25.51°E

Age MIS 15 to MIS 13

Archive Institute of Speleology "Emil Racovitza", Bucharest, Romania

Description Rotbav-Dealul Ţiganilor (RDT) is situated in a subsiding basin—the Baraolt Basin—within the Brasov geological depression of central Romania. The site contains a Middle Pleistocene fluvio-lacustrine sequence of coal, sand, and clay (Rădulescu and Samson, 1985), and occupies a particularly interesting geographical position in the bend of the Carpathian mountain chain: an interface between present-day eastern and Carpathian zoogeographic zones in some taxa (e.g., Kotlik *et al.*, 2006).

The deposits of RDT were discovered in a sand quarry. Ferruginous sands and gravels form the lowest strata of the sequence and yielded remains of large mammals. Above these deposits occurs a dark-grey, silty clay with olive-grey silty lenses at the base—named level 2 or Clay A—from which large mammals and a diverse small mammal fauna were recovered. A fossiliferous, light-olive clay—Clay B—overlies Clay A, and tops the succession (Rădulescu and Samson, 1985).

Material examined Thirty-two M_1 teeth were photographed, but only twenty-six molars were able to provide full landmark configurations due to breakage to posterior lobes and enamel prisms. Other than this damage, the occlusal surfaces of molars were in very good condition. Dentine of molars was stained a light-brown colour and contrasted well with darker enamel layers.

The specimens were identified as *Arvicola cantianus mosbachensis* (= *Arvicola mosbachensis*) by Rădulescu and Samson (1985) and Petculescu (2003). No discussion of this identification was provided by these authors but appears to have been based upon the lack of roots and high SDQ values for the *Arvicola* assemblage. Enamel thickness measurements by Petculescu (2003) gave a mean SDQ = 126.13[1].

[1] Petculescu (2003) provided no other descriptive statistics.

Palaeoenvironments The whole sequence records a series of climatic fluctuations (Rădulescu and Samson, 1985). A periglacial patterned ground was found on the olive-grey silts at the base of Clay A, and this horizon also contained steppic small mammal taxa such as steppe lemming *Lagurus* cf. *transiens* and the 'giant' hamster *Cricetus praeglacialis*. In the main body of Clay A a cool-temperate, mesic assemblage was found, including the mole *Talpa europaea*, common shrew *Sorex araneus*, and extinct shrew *Drepanosorex* cf. *austriucus* (Rădulescu and Samson, 1985). The occurrence of wood mouse *Apodemus sylvaticus* and beaver *Castor fiber* indicate the existence of broadleaved and coniferous woodland, but open landscapes were evidently also present from the occurrence of common/short-tailed field vole *Microtus arvalis/agrestis*, blind mole rat *Spalax* sp., and hare *Lepus* cf. *europaeus*, although this latter species occurs in various habitats in the present-day (Smith and Johnston, 2008). Freshwater habitats were also important with the occurrence of *C. fiber*, desman *Desmana* cf. *mosbachensis*, and *A. mosbachensis* (assuming a semi-aquatic ecology for the water vole).

At the top of Clay A a climatic deterioration is indicated through the presence of northern vole *Microtus* cf. *oeconomus* and reindeer *Rangifer tarandus* (Rădulescu and Samson, 1985).

Stratigraphy and correlation Biostratigraphic evidence suggests that the RDT Clay A is of early Middle Pleistocene age. The co-occurrence of *A. mosbachensis*, the archaic vole *Pliomys episcopalis*, and C. *praeglacialis* is the main evidence supporting this conclusion (Rădulescu and Samson, 1985; Koenigswald and Heinrich, 1999; Maul and Parfitt, 2010).

The presence of *Arvicola* in Clay A has been considered biostratigrphically significant (Petculescu, 2003). The current understanding of the origins of *Arvicola* in Europe suggests a diachronous *Mimomys–Arvicola* transition across Europe, with an MIS 15 or 16 age in central Europe (Koenigswald and Kolfschoten, 1996; Maul and Markova, 2007) and an MIS 13 or MIS 12 age in eastern Europe and Russia (e.g., Maul and Markova, 2007). The age of this transition in Romania has not been established, but there is some evidence to suggest that morphological changes in southeast Europe lag those of western and central Europe (e.g., Heinrich, 1982).

The base of the RDT sequence shows the existence of periglacial conditions but, although the RDT Clay A appears to date from a cool-temperate period, these deposits do not contain evidence for the cold climates one would expect for major glacials such as MIS 16 or MIS 12, and therefore MIS 15 or MIS 13 will be assumed as the maximum age of the site. The excursion associated with MIS 14 in the global oxygen isotope record does not suggest that this stage was a major, global, cold event. Furthermore, the Carpathian mountains offer the

potential for the persistence of temperate species during cold stages (e.g., Kotlik *et al.*, 2006), and so an MIS 14 age may be possible for the RDT Clay A. At the same time, it is recognised that the sub-stage climatic variability present in the global oxygen isotope record of the early Middle Pleistocene could account for climatic fluctuations such as those recorded in the RDT (Candy, 2009; Tzedakis *et al.*, 2009).

Petculescu (2003) used the SDQ of *Arvicola* from RDT to suggest a more specific correlation with the Dutch Cromer IV Interglacial—correlated by some authors with MIS 13 (e.g., Maul and Markova, 2007). Dating evidence from enamel thickness measurements is not admissible to the present study in order to avoid circularity, but—as has been stated above—this correlation is also tentative as the behaviour of the SDQ in southeast of Europe, and it's relationship with values derived from central Europe, is not well established.

In view of the evidence available a possible MIS 15 to MIS 13 age-range will be adopted for the RDT Clay A.

3.11 Russia

3.11.1 Early Middle Pleistocene

3.11.1.1 Ilovayski Kordon

Location On the river Ilovay, 4.5 km west of the village of Staroye Khobotovo, Tambov Region, Russia

Co-ordinates 53.06°N, 40.32°E

Age MIS 15 or MIS 13

Archive Moscow Institute of Palaeontology, Moscow, Russia

Description A series of exposures along the river Ilovay were discovered by Yu. Iossifova in 1961 whilst undertaking geological mapping. They were not investigated in detail until 1981 when a multidisciplinary research team recorded early Middle Pleistocene deposits and recovered a rich assemblage of small mammals, molluscs, and palaeobotanical evidence from a number of outcrops and cut sections (Krasnenkov *et al.*, 1981; Iossifova and Krasnenkov, 1994). Outcrops 8 and 10 provided the clearest stratigraphy of all the exposures along the river and in the grey-loam of Layer 4 abundant fossils were found (Figure 3.23).

Material examined The small mammal assemblage is dominated by *Mimomys intermedius* (= *Mimomys savini*), with over half the one-thousand two-hundred or so specimens found in Layer 4 of water vole (Agadjanian, 1981). Due to time constraints a randomly chosen subsample of twenty-eight M_1 teeth were were chosen to be photographed; the only selection criterion being a good state of preservation. All teeth were isolated save for one M_1 still within the mandible. Most specimens were stained dark-brown, but five were coloured a much lighter brown, which may indicate a differential taphonomy for the whole *Arvicola* assemblage. Stronger evidence for reworking comes from the presence of Early Pleistocene plant macrofossils in Layer 4 (Iossifova and Krasnenkov, 1994), and so it appears appropriate to assess the morphological variability of *Arvicola* M_1s in terms of potential taphonomic mixing prior to other morphometric analyses.

The specimens were archived as *M. intermedius* at the Moscow Institute of Palaeontology, Moscow, and were identified as the same species by Agadjanian (1981). Roots are well-developed in ontogenetically advanced individuals, but the development of a *Mimomys*-fold was restricted to the youngest members of the assemblage.

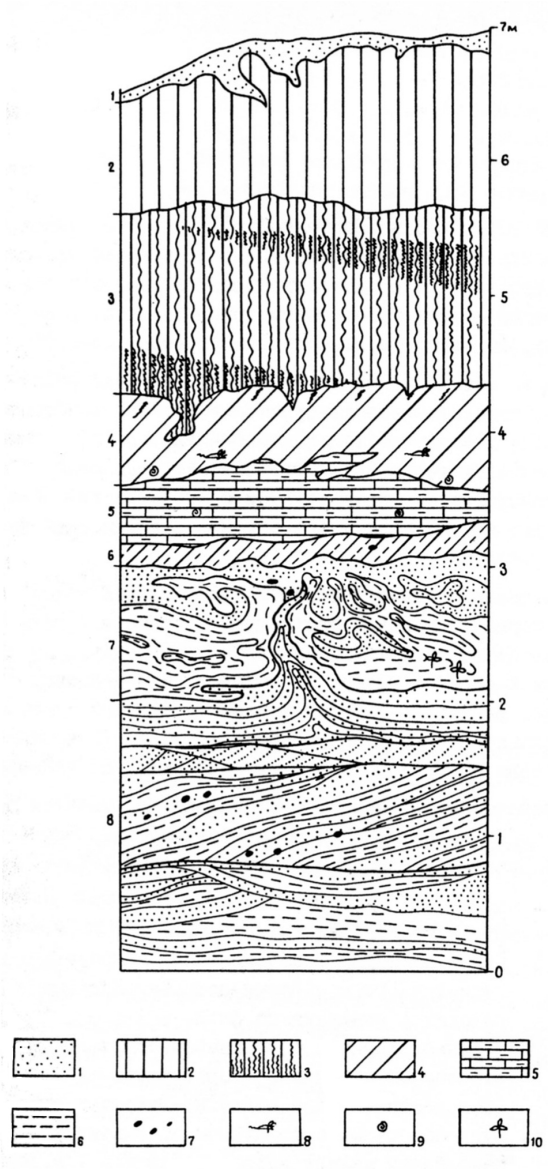

Figure 3.23: Statigraphy of Outcrop 10 at Ilovayski Kordon. Key: (1) Fine-grained sands, (2) Whitish loess, (3) Dark loam, (4) Grey loam with mollusc shells and small mammal remains, (5) Non-lamintated clay-rich fresh-water marl with some mollusc shells and small mammal remains, (6) Brown loam with gravel and pebbles, (7) Intensely cryoturbated blue clay with sand, (8) Cross-bedded grey loam and sand. Modified from Krasnenkov *et al.* (1981).

Palaeoenvironments The palaeoenvironmental evidence indicates cool-temperate conditions with wooded steppe. In Layer 4 the tree pollen is dominated by birch and pine, but oak, elm, and hazel were also present. *Artemisia* is abundant in the non-arboreal spectrum. The small mammal assemblage contains the woodland indicators wood mouse *Apodemus sylvaticus*, species of dormouse *Glis* sp., and bank vole *Clethrionomys glareolus*; the latter being particularly abundant. Shrew *Sorex* sp. and mole *Talpa* sp. were well-represented, suggesting moist conditions with soils and leaf litter. Open landscape species such as pika *Ochotona* sp., hamster *Cricetus* sp., and various *Microtus* species were found in reduced numbers. Wetland and riparian environments were evidently very important locally as indicated by the depositional environment and the occurrence of semi-aquatic small mammals such as desman *Desmana* sp. (Agadjanian, 1981). The abundance of *M. savini* in this fluvio-lacustrine setting supports a semi-aquatic, rather than fossorial, ecology for the water vole population.

Stratigraphy and correlation The fossil fauna indicates a cool-temperate period evidently post-dating a major cold event, as Layers 4, 5, and 6 unconformably overlie the intensely cryoturbated clays and sands of Layer 7 (Krasnenkov *et al.*, 1981). Furthermore, Layer 4 was traceable along the length of the river, where 300 m downstream it was found to overlie a diamicton attributed to the Donian Glaciation (Iossifova and Krasnenkov, 1994). This stratigraphic evidence shows that the fauna must post-date MIS 16. Furthermore, the cool-temperate conditions indicated by the palaeobotanical evidence are suggestive of the early phases of an interglacial (Iossifova and Krasnenkov, 1994).

Agadjanian (in Iossifova and Krasnenkov, 1994) correlated the faunal assemblage to the early Middle Pleistocene Muchkapian 'Interglacial' because of the presence of *M. intermedius*, steppe lemming *Lagurus* cf. *transiens*, and archaic vole *Pliomys episcopalis*. *M. savini* is considered not to occur in Russia after the Oka (= Elsterian, = MIS 12) Glaciation, but may have disappeared at this time or even slightly before (Maul and Markova, 2007). It is not possible to biostratigraphically differentiate between MIS 15, MIS 13, or their sub-stages within the Muchkapian (Maul and Markova, 2007), but Agadjanian noted that the occurrence of more 'ancient' taxa suggested an early Muchkapian age. The relevant species leading to this conclusion were not specified, and from the faunal list published in Agadjanian (1981) no 'archaic' forms are obvious, but the presence of well-developed roots in adult *M. intermedius* is one trait characteristic of older water vole populations. The occurrence of fossil seeds with Pliocene or Early Pleistocene affinities in Layers 4 and 5 (Iossifova and Krasnenkov, 1994) shows that some reworking has taken place that may account for the presence of more 'ancient' faunal elements. Sedimentalogically, a correlation with the early Muchkapian seems frag-

ile, although the stratigraphic relationship between the fossiliferous layers and the diamicton attributed to the Donian Glaciation opposes this. In conclusion, the best dating precision that can be achieved is either MIS 15 or MIS 13.

3.11.1.2 Korotoyak-4

Location Confluence of Don and Tikhaya Sosna rivers, village of Korotoyak, Voronezh Region, Russia

Co-ordinates 50.95°N, 39.09°E

Age MIS 15–MIS 13

Archive Moscow Institute of Palaeontology, Moscow, Russia

Description Near the village of Korotoyak, Pliocene and Pleistocene strata are exposed in river channels. These exposures have been investigated since their discovery in 1960, and have proven particularly important in the study of regional Middle Pleistocene stratigraphy. The sedimentary sequence here consists of a thin diamicton overlain by alluvial deposits containing freshwater molluscs and a relatively rich small mammal assemblage of early Middle Pleistocene affinities (Iossifova and Krasnenkov, 1994). The alluvium is a 3 m thick, generally poorly sorted coarse sand and gravel. Locally, clearly defined cross-stratified layers were highly fossiliferous; containing mollusc and small mammal remains (Iossifova and Krasnenkov, 1994).

Material examined Specimens were identified as *Mimomys intermedius* (= *Mimomys savini*) at the Moscow Institute of Palaeontology, Moscow, and in Iossifova and Krasnenkov (1994). No specific publication has been made on water vole from Korotoyak-4 but observations made by this author support the taxonomic identification made: molars were rooted, of small size, showed a *Mimomys*-differentiation of enamel, and one specimen displayed a *Mimomys*-fold.

Twenty-seven M_1 teeth were photographed. All specimens were stained a rich red-brown colour and molars were generally in good condition with enamel layers clearly visible and occlusal morphology well-defined. Five molars were *in situ* in mandibles but their angular processes were broken, and the fractured edges of breaks appeared rounded and worn. Some evidence of chipping and rounding of the enamel edges and other extremities of molars was also visible. The eroded appearance of specimens is most likely attributable to predator damage and digestive erosion by raptors (Andrews, 1990), rather than hydrodynamic abrasion which usually requires fluvial transport over considerable distances (Behrensmeyer, 1993). The degree of fluvial transport involved in the accumulation of the fossil

assemblage does require some consideration, however, in order to assess spatial and temporal limits of the assemblage.

Sedimentological descriptions of the alluvium report beds of fragmentary and well-preserved shells and small mammal remains within poorly sorted sands and gravels (Iossifova and Krasnenkov, 1994). This suggests deposition in an active channel (Tucker, 1991). During excavation, fossils were recovered by washing, but no details are given in the literature of how much sediment was processed, or from where in the alluvial unit samples were taken (Iossifova and Krasnenkov, 1994). Thus, the potential for mixing of fossil material through differential taphonomy and excavation approach is evident. Examination of the faunal list shows no major temporal juxtapositions in taxa, but there is an evident taphonomic bias in that *M. savini* and *Microtus* spp. dominate the fossil assemblage, while other taxa are generally present in single figures and are identified to a low taxonomic level (Iossifova and Krasnenkov, 1994). A taphonomic bias toward aquatic or semi-aquatic taxa may be expected given the depositional setting, and this context also lends support for a semi-aquatic ecology for the water vole population.

Although no obvious evidence exists of temporal mixing in the fossil assemblage such mixing has been documented in similar sedimentary contexts (Roy *et al.*, 1996; Popova, 2004). Prior to wider morphometric analyses the morphological homogeneity of the water vole assemblage will be assessed in an attempt to independently evaluate spatial and temporal mixing.

Palaeoenvironments The molluscan and small mammal fauna are predominantly suggestive of cool-climate, open-steppe and wetland habitats. The list of small mammal species given by Iossifova and Krasnenkov (1994) is dominated by *M. savini*. This is likely to reflect some taphonomic bias, but nevertheless demonstrates the importance of wetland environments in the region. Freshwater habitats are also suggested by the presence of Middendorff's vole *Microtus middendorffi*, today found in waterlogged tundra in northern Russia and Siberia (Corbet, 1978), *Microtus oeconomus*, which prefers moist areas dense in vegetation, and the riparian *Desmana* sp. The existence of open grasslands and steppe is suggested by the occurrence of common vole *Microtus arvalis*, ground squirrel *Citellus*, hamster *Cricetus*, zokor *Myospalax*, and a number of lagurids. The existence of some woodland in the region is indicated by the occurrence of bank vole *Clethrionomys glareolus*.

Cool climates are suggested by the steppic fauna and *M. oeconomus*, which in the Middle Pleistocene appears to have inhabited cooler climates (Currant pers. comm.). In the molluscan fauna, the single terrestrial species present (*Succinea oblonga*) is also indicative of cool climates (Iossifova and Krasnenkov, 1994, p. 142). Tortoise scutes found in the alluvium may be an indication of continental-

ity in the climate; although the possibility exists that tortoise remains may have been reworked.

Stratigraphy and correlation The fauna were recovered from sediments overlying the Don Till, making the alluvial deposits post-date MIS 16. The presence of *Mimomys* and absence of *Arvicola* permit an attribution to the late Tiraspolian faunal zone. This correlates with the Russian, early Middle Pleistocene, Muchkapian Interglacial (Velichko and Faustova, 1986; Iossifova and Krasnenkov, 1994; Velichko *et al.*, 2004). An early Middle Pleistocene age is also indicated by the presence of the vole *Pitymys gregaloides* (= *Microtus gregaloides*) and the mollusc *Valvata naticina*, which are found at a number of late Cromerian western European localities (Koenigswald and Kolfschoten, 1996; Preece and Parfitt, 2000). The occurrence of steppe lemming *Lagurus transiens* ($n = 1$) and the 'archaic' lagurid morphotype *Prolagurus pannonicus* ($n = 2$) suggests an age near to the Donian (Maul and Markova, 2007), although the rarity of these taxa possibly indicates these finds are the result of reworking.

There appears to be strong support for the water vole assemblage to date to the later part of the early Middle Pleistocene. Some faunal evidence points to deposition during the earlier part of the early Middle Pleistocene, but taphonomic problems mean that this is not conclusive. The evidence for a cool, steppic environment does not provide specific climatostratigraphic information; indeed the lack of evidence for warm temperate conditions means that the fauna may potentially have derived from MIS 14 or any of the stadials within MIS 15 and MIS 13 that are observed in the global oxygen isotope record. For the purposes of this study the *M. savini* assemblage will be assigned a possible age from MIS 15 to MIS 13.

3.11.1.3 Kuznetskova

Location Near the village of Kuznetsovka, 2 km east of the village of Srebnyaya Yagura, left slope of the Podgornyi Buerak gully, Kalachskaya Upland, Tambov Region, Russia

Co-ordinates 51.87°N, 42.20°E

Age MIS 15 or 13

Archive Moscow Institute of Palaeontology, Moscow, Russia

Description Kuznetsovka was discovered in 1979 by Yu. Iossifova during field mapping and consists of a 16 m thick exposure of Pleistocene sediments in a gully cut by a tributary of the river Don (Iossifova and Krasnenkov, 1994; Agadjanian and Kondrashov, 2007). At the base of the sequence is the fourth terrace of the river Don, this is overlain by the Donian Till and a series of alluvial, loess and palaeosol deposits (Figure 3.24). An organic-rich clay in the lower part of Bed 3 yielded an abundance of large and small mammals, reptiles, amphibians, and lesser numbers of molluscs. This fossiliferous horizon pinches out further up the gully and is considered to represent a lacustrine facies deposited in a warm environment, marginal to the influence of a main river channel.

Material examined Over half the nearly one thousand mammal specimens found were of *Mimomys intermedius*. This availability of such a considerable number of fossils provided an excellent opportunity to amass a large dataset to explore morphological variation. One hundred and one M_1 teeth were photographed. All were in good to fair condition, stained light brown in colour, enamel layers were in general easily resolvable as translucent light-grey bands set against brown dentine. A small number of molars were stained a much darker rich reddish-brown, which may suggests that these specimens have followed a different taphonomic route to the majority of the fossils recovered or may be caused by differential diagenesis *in situ*. The fossil assemblage includes many fragile elements such as egg shells and delicate herpetofaunal remains; suggesting deposition in a low energy environment which offers little opportunity for faunal mixing (Iossifova and Krasnenkov, 1994).

Specimens were identified as *M. intermedius* (= *Mimomys savini*) in the Moscow Institute of Palaeontology, Moscow, and by Agadjanian and Kondrashov (2007), and show a suite of typical *Mimomys* characters. Molars are relatively large, molar enamel shows the *Mimomys*-differentiation, and roots are present but are only well-developed in ontogenetically-advanced specimens. The M_1 shows little or no development of the *Mimomys*-fold, interprismatic cement is present from

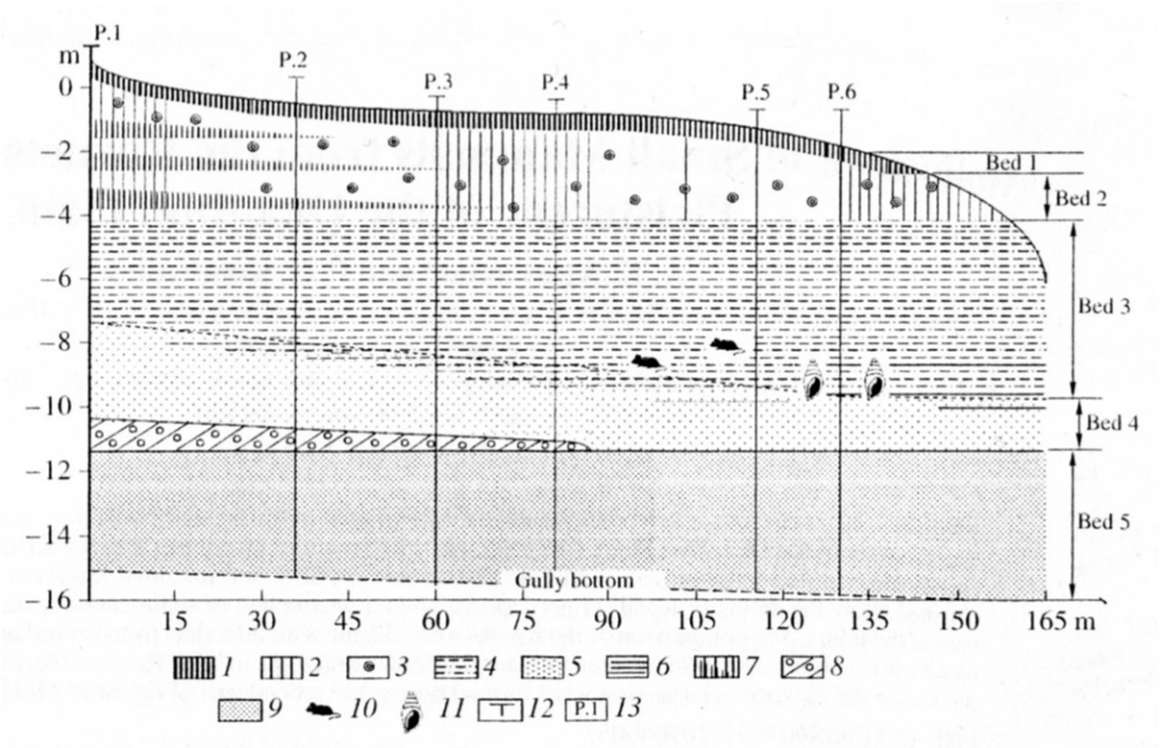

Figure 3.24: Generalised stratigraphy at Kuznetsovka. Key: (1) Modern soil, (2) loess-like loam, (3) carbonate concretions, (4) sandy loam, (5) gray fine-grained sand, (6) clayey interbeds, (7) paleosols, (8) Donian moraine, (9) gray-brown fine-grained sand (fourth terrace of the Don), (10) small mammals and other vertebrates, (11) mollusc shells, (12) trenches (13) trench numbers. Taken from Agadjanian and Kondrashov (2007).

early in development, and enamel islets are present only in the initial stages of tooth wear (Agadjanian and Kondrashov, 2007).

Palaeoenvironments The general palaeonenvironmental picture is of a warm, humid climate supporting a mosaic of broad-leaved woodland, steppe, and marginal habitats. Warm-climate taxa such as tortoises and lizards, are numerous, and the birch mouse *Sicista* is a recognised temperate species (Currant pers. comm.). Mesic conditions are suggested from the molluscan and amphibian fauna. Woodland taxa such as bank vole *Clethrionomys glareolus* and wood mouse *Apodemus sylvaticus* are common, and steppic species such as hamster *Cricetus* sp., ground squirrel *Spermophilus* sp., and steppe lemming *Lagurus transiens* show the presence of open landscapes. The occurrence of desman *Desmana* sp., the dominance of water vole and the sedimentary evidence shows that riparian and marginal habitats were also present (Iossifova and Krasnenkov, 1994).

Stratigraphy and correlation The biostratigraphic and lithostratigraphic evidence indicates that fossil assemblage from Kuznestovka originates from the second half of the early Middle Pleistocene (Iossifova and Krasnenkov, 1994; Agadjanian and Kondrashov, 2007). They lie above the fourth, and highest, terrace of the Don river and a diamicton deposit attributed to the Donian Glaciation. Therefore a post-MIS 16 age must be given to the fauna. The occurrence of abundant *M. savini* and *Terricola arvaloides*, *L. transiens*, and *Desmana* cf. *moschata* allows a correlation with the latter part of the Tiraspolian faunal zone (Iossifova and Krasnenkov, 1994; Agadjanian and Kondrashov, 2007). Tiraspolian faunas are pre-MIS 12 in age, therefore a correlation of Kuznetsovka with warm periods of or within MIS 15 or MIS 13 is possible. Root development in *M. savini* is ontogenetically very late and the appearance of morphologically advanced forms of *L. transiens* would perhaps support a cautious association with MIS 13, but for the purposes of this study an estimated age of MIS 15 or MIS 13 will be assumed.

3.11.2 Late Middle Pleistocene

3.11.2.1 Donskaya Negatchevka

Location Northwest of Donskaya Negatchevka village, Lipetsk Region, Russia

Co-ordinates 52.06°N, 39.00°E

Age MIS 11

Archive Moscow Institute of Palaeontology, Moscow, Russia

Description M. N. Grischenko noted an exposure of clay, rich in molluscs, in the vicinity of the village of Donskaya Negatchevka in 1976. It was not until 1986, when the geology of the area was explored in more detail by R. V. Krasnenkov and N. E. Kazantseva, that the importance of the deposits was recognised and a rich fossil fauna of small mammals, amphibians, and molluscs was recovered (Iossifova and Krasnenkov, 1994). The exposure lies in a gully, and consists of an approximately 14 m high sequence of loams, sands, and a poorly sorted diamicton. The fossiliferous stratum of interest occurs near the top of the section in a narrow (15 cm) calcareous clay-sand horizon: Bed 9 in Iossifova and Krasnenkov (1994). This horizon lies unconformably over a massively-bedded clay containing plant roots, and conformably underlies a 2 m thick unit of mollusc-rich clays capped by brown loams riddled with mole burrows (Iossifova and Krasnenkov, 1994).

Material examined Nineteen water vole M_1 teeth were photographed. Molars were high-crowned and rootless, although the base of one molar could not be examined as it was present within a mandible. Two molars exhibited a *Mimomys*-fold and superficially enamel layers showed a '*Mimomys*' or '*cantiana–terrestris*' differentiation. Specimens were identified as *Arvicola mosbachensis* in the Moscow Institute of Palaeontology, Moscow, and in Iossifova and Krasnenkov (1994) but to the knowledge of this author no investigation has been published on the water vole from Donskaya Negatchevka.

Palaeoenvironments *Arvicola* and *Microtus* sp. dominate the small mammal assemblage, and bank vole *Clethrionomys glareolus* is also well-represented (Iossifova and Krasnenkov, 1994). This suggests a local prevalence of marsh or riparian habitats, assuming a semi-aquatic ecology for *Arvicola*, with mesic grassland and coniferous and deciduous woodland, also supported by the amphibian fauna. The diversity of the vertebrates and the abundance of Insectivora are indicative of interglacial faunas (Iossifova and Krasnenkov, 1994).

Stratigraphy and correlation The presence of Scandinavian rocks in the basal alluvium is thought to reflect the erosion of the Donian till (Iossifova and Krasnenkov, 1994), but the fossiliferous clay is thought to be late Middle Pleistocene age. Donskaya Negatchevka has been declared the neostratotype of the Likhvinian (= Holsteinian = MIS 11) since the original stratotype at Strelitsa was destroyed by quarrying (Iossifova and Krasnenkov, 1994). This correlation has been based on the presence of *A. mosbachensis* and steppe lemming *Lagurus transiens* (Iossifova and Krasnenkov, 1994; Maul and Markova, 2007)—although only a single specimen of *L. transiens* was found. In the absence of other evidence a tentative MIS 11 date will be assigned to the *Arvicola* assemblage.

3.11.2.2 Rybnaya Sloboda

Location	Confluence of the Kama and Volga rivers, Tatarstan Region, Russia
Co-ordinates	55.60°N, 49.40°E
Age	MIS 11
Archive	Moscow Institute of Geography, Russian Academy of Sciences, Moscow, Russia

Description Rybnaya Sloboda is a fluvial site in northeastern Russia. No details on the sedimentology or excavation history of the site were available to this author at the time of writing. Markova (2006) regarded the composition of the fauna from Rybnaya Sloboda as unusual. She attributed this to the geographic position of the site, which is the most north-easterly of all Middle Pleistocene sites on the East European Plain.

Material examined Twenty-three M_1s were photographed. One molar was preserved within a mandible and most specimens were in excellent condition, although damage to the posterior lobes of four molars prevented full landmark configurations from being taken from these M_1s. Specimens were stained a rich red-brown colour and enamel layers were well-defined.

The water vole material was attributed to *Arvicola cantianus* (= *Arvicola mosbachensis*) by Markova (2006) and enamel thickness measurements indicate the fossil assemblage shows a *Mimomys*-differentiation. The present author notes that molars are small but high-crowned and no roots of *Mimomys*-folds were present.

The lack of information on the depositional context of the fossil fauna prevents any comment on the taphonomy of the *Arvicola* assemblage. However, the dark brown colouration of molars is likely to indicate residence within organic-rich

sediments, and the shared similarity in preservational characteristics gives some confidence in the temporal integrity of the assemblage.

Table 3.31: Published SDQ values from Rybnaya Slobada.

Author	SDQ			
	n	min	mean	max
Markova (2006)	23	112	124	160

Palaeoenvironments The small mammal fauna include bank vole *Clethrionomys glareolus*, steppe lemming *Lagurus transiens*, northern vole *Microtus oeconomus*, short-tailed field vole *Microtus agrestis*, common vole *Microtus* ex gr. *arvalis*, and grey red-backed vole *Clethrionomys rufocanus*, as well as *A. mosbachensis*. No clearly cold-climate taxa are present and the fauna generally indicates interglacial conditions (Markova, 2006), although *C. rufocanus* is today a boreal species. Markova (2006) referred Rybnaya Sloboda to the 'forest-steppe zone'.

Stratigraphy and correlation Rybnaya Sloboda has been correlated with the Russian Likhvinian interglacial (= Holsteinian = MIS 11). This is based on the faunal assemblage which contains *A. mosbachensis*, *L. transiens*, and a high abundance of *M. oeconomus* and *M. agrestis*, and compares favourably with the late Middle Pleistocene Singilian MAZ (Markova, 1998, 2006, 2007). Markova (2006) notes that the type section of the Singilian contains few small mammals and no *A. mosbachensis*.

In the absence of other dating evidence a tentative MIS 11 age will be applied to the *Arvicola* assemblage.

3.11.2.3 Vladimirovka

Location On the left bank of the Don river, approximately 30 km southeast of the town of Liski, Voronezh Region, Russia

Co-ordinates 51.93°N, 42.58°E

Age MIS 11

Archive Moscow Institute of Palaeontology, Moscow, Russia

Description Exposures of Middle Pleistocene sediments were found near the village of Vladimirovka in 1960 by Yu. Iossifova during geological mapping. Two horizons rich in small mammals, separated by a thin clay, were located within the humic-rich alluvium of Layer 4: Vladimirovka 1 at 3.0–3.6 m and Vladimirovka 2 at 3.95–4.33 m depth (Agadjanian and Erbajeva, 1983; Figure 3.25). The sequence constituted some of the earliest known records of fossiliferous deposits overlying what has been identified as the Donian Till (Iossifova and Krasnenkov, 1994).

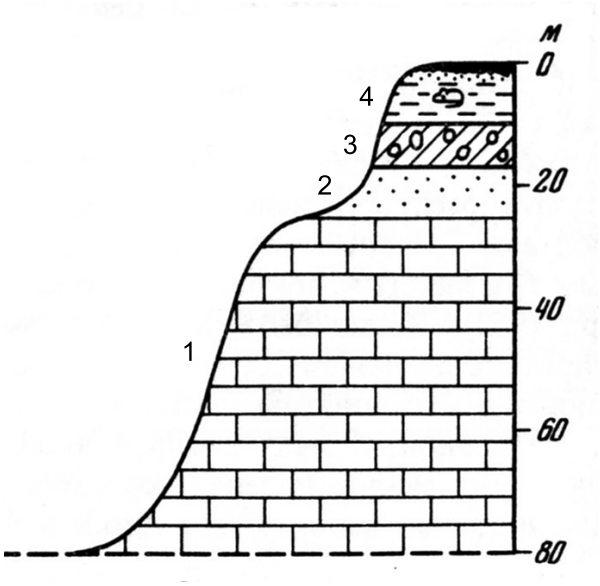

Figure 3.25: Summary stratigraphy of Vladimirovka. Key: (1) limestone, (2) sands, (3) moraine loam, (4) sandy floodplain loams with vertebrate fossil remains. Adapted from Agadjanian and Erbajeva (1983).

Material examined Water vole fossils were found in great numbers in both Vladimirovka 1 and 2 but in Valdimirovka 1 only three specimens were in good enough condition to allow a full compliment of landmarks to be taken, and therefore emphasis will be placed on the thirty-three specimens photographed from

Valdimirovka 2. The *Arvicola* from this horizon were stained very dark-brown or black. Generally enamel layers were clearly visible as pale grey-brown bands contrasted against the dark-brown dentine. Enamel triangles were well-defined.

Agadjanian (1983) noted that M_1 teeth were smaller than *Arvicola terrestris* and possessed enamel with a *Mimomys*-differentiation. Additionally, around 20 % of the M_1s examined in Agadjanian (1983) possessed a *Mimomys*-fold ($n = 68$). This was mostly a feature of juvenile specimens but was also present in a small number of adults. In view of these 'primitive' characteristics specimens were assigned to *Arvicola mosbachensis* (Agadjanian, 1983).

The fossiliferous alluvium consists of a sandy-loam, which suggests a low energy depositional environment. The faunas from Vladimirovka 1 differ from Vladimirovka 2 in that the former are taxonomically more diverse and contain freshwater molluscs and tortoise scutes. These dissimilarities could be attributed to taphonomic causes but Iossifova and Krasnenkov (1994) suggested that they signify ecological differences. Reworking of material is a potential problem in any fluvial system (e.g., Popova, 2004), but in the case of Vladimirovka the absence of taxa of starkly contrasting age, together with the sedimentary evidence, suggests that temporal mixing of the faunal assemblage is not a major concern. However, special attention will be paid to morphological variation within the fossil assemblage prior to further analyses.

Palaeoenvironments Faunal lists for both Vladimirovka horizons can be found in Agadjanian (1977, 1983), Agadjanian and Erbajeva (1983), and Iossifova and Krasnenkov (1994). The majority of the species from Vladimirovka 1 and 2 are open-landscape, steppic taxa such as ground squirrel *Citellus* sp., hamster *Cricetus* sp., and steppe lemming *Lagurus* sp. (although *Lagurus* is absent from Vladimirovka 2). Woodland species such as wood mouse *Apodemus sylvaticus* and bank vole *Clethrionomys glareolus* are sparsely represented. Tortoise scutes were found in Vladimirovka 1 but no such finds were made in Vladimirovka 2. This may indicate that climate was warmer in the latter stages of deposition of Layer 4 or taphonomic factors may be at play.

Arvicola is the second most abundant taxon in Vladimirovka 1 after *Lagurus*, and is the most numerous in Vladimirovka 2. This abundance of water vole and the presence of northern vole *Microtus oeconomus*, generally to be found in mesic well-vegetated environments today, agrees well with the floodplain/lacustrine depositional setting inferred from the sedimentology of Layer 4, and lends weight to the assumption that *Arvicola* from this site possessed a semi-aquatic ecology.

Stratigraphy and correlation The fossil assemblage lies above a diamicton recognised as the Donian Till. Vladimirovka is well within the limits of the Do-

nian Glaciation (= MIS 16) therefore this identification appears sound (Velichko *et al.*, 2004) and consequently the fossil assemblage must post-date MIS 16. Biostratigraphic evidence points more specifically to the late Middle Pleistocene. The combined occurrence of the steppe lemming morphotypes *Lagurus transiens* and *Lagurus lagurus* appears in fossil faunas of this age in central and eastern Europe (Maul and Markova, 2007), while *Eolagurus luteus* is found in Likhvinian (= Holsteinian) sites in eastern Europe such as Gunki (Maul and Markova, 2007; Section 3.14.1.2). *Lagurus* sp. are not present in Vladimirovka 2, however. Current consensus holds that no rooted water voles are found in sites of the Russian Plain after the Oka (= Elsterian = MIS 12) Glaciation (e.g., Maul and Markova, 2007). The presence of a suite of 'primitive' characteristics in the *Arvicola* assemblage, such as the *Mimomys*-fold, high SDQ values, and small size, has led a number of authors to infer that this population lies near the *Mimomys–Arvicola* transition in the Likhvinian (Agadjanian, 1977, 1983; Agadjanian and Erbajeva, 1983; Iossifova and Krasnenkov, 1994). In view of this combined evidence a tentative Likhvinian (= MIS 11) age will be assumed for the fauna of Vladimirovka 2. This implies a large hiatus between deposition of the diamicton attributed to the Donian glaciation and the fossiliferous sands of Layer 4.

3.11.3 Holocene

3.11.3.1 Bolshoi Tigany

Location 2 km south of the village of Bolshoi Tigany, bank of the river Tiganka, southeast of the Kama-Volga river confluence, Tartarstan Region, Russia

Co-ordinates 55.14°N, 50.15°E

Age *c.* 10.3–9.2 k yr BP

Archive Moscow Institute of Palaeontology, Moscow, Russia

Description The site of Bolshoi Tigany has yet to be published, and all the sedimentological and palaeontological information presented here has been obtained through personal communication with A. K. Agadjanian. The site is an exposure on the banks of the river Tiganka, near the village of Bolshoi Tigany. The Tiganka here cuts into a young alluvial terrace, which is extensively expressed across the floodplain of the Kama and Volga rivers. A bipartite sedimentary sequence was found: a lower, cold-climate alluvium; and an upper, organic alluvium that is rich in molluscan and small mammal remains, especially at the base of this layer.

Material examined Thirty-one M_1 teeth were photographed. Teeth were stained dark brown and the physical condition of molars was fair to good. Most enamel was easily resolvable as grey translucent bands against dark red-brown dentine and enamel triangles were clearly defined. Specimens were identified as *Arvicola terrestris* at the Moscow Institute of Palaeontology, Moscow, based upon large size and low SDQ values (unpublished data).

Fluvial sediments of the Middle Volga region may be susceptible to reworking as river systems within the catchment have been repeatedly recharged by large volumes of meltwater from melting ice-sheets to the north (Sidorchuk *et al.*, 2009). It is therefore possible that the assemblage of *Arvicola* fossils consists of a mixture of material. Agadjanian (pers. comm.) has suggested that the good state of preservation of delicate elements, such as shrew mandibles and egg shells, and the lack of obviously allochthonous material indicates that the fossil assemblage is temporally and spatially homogenous.

The material was assigned to *A. terrestris* by Agadjanian (pers. comm.) on the basis of SDQ measurements, although molars were generally smaller than those of recent *A. terrestris* from the area.

Palaeoenvironments The faunal assemblage is dominated by *Arvicola*, which although likely to represent some level of taphonomic bias, together with the presence of northern vole *Microtus oeconomus* shows the prominence of wetland environments at least locally. Bank vole *Clethrionomys glareolus*, which prefers mesic environments in densely vegetated habitats and woodlands, is common, but more obligate woodland taxa such as wood mouse *Apodemus sylvaticus* are rare. Steppic and grassland species are well-represented, and include *Microtus* spp., steppe lemming *Lagurus lagurus*, northern mole vole *Ellobius talpinus*, hamster *Cricetus cricetus*, ground squirrel *Spermophilus major*, and steppe polecat *Mustela eversmanii*. The overall palaeoenvironmental picture provided by the small mammal fauna is of an open steppe landscape with significant wetland habitats but little woodland. Climate appears to have been cool and moist.

Stratigraphy and correlation A radiocarbon date from a bulk sample of 'peat' has given an age of 9 000 ^{14}C BP for the fossil assemblage (Agadjanian, unpublished data). No information on the chemistry of the radiocarbon determination, or errors associated with the date, were available at the time of writing, and thus the accuracy and precision of this estimate cannot be judged. The fluvial terrace is recognised as a 'young' aggradation, which does not contradict the radiocarbon determination, and the small mammal fauna appears generically Late Quaternary (Maul and Markova, 2007).

The palaeoenvironmental evidence indicates the existence of a cool climate

with well-developed steppe and marshland habitats. Palynological data from other localities indicate that such conditions existed in the vicinity of Bolshoi Tigany in the 'Preboreal' or 'Boreal' climatic phases of the Holocene (Khotinskiy, 1984). Radiocarbon determinations help constrain these periods to between *c.* 10.3 and 9.2 k yr BP (Khotinskiy, 1984) and this age-range will be assumed for the *Arvicola* assemblage.

3.12 Slovak Republic

3.12.1 Late Pleistocene

3.12.1.1 Dzeravá skala Cave

Location Southeast of the village of Plavecký Mikuláš, Bratislava Region, western Slovak Republic

Co-ordinates 48.5°N, 17.32°E

Age *c.* 30–26 k yr BP

Archive Hungarian Institute of Geology, Budapest, Hungary

Description Dzeravá skala Cave is situated in the western part of the Lesser Carpathian Mountains of the Slovak Republic at 450 m a.s.l in a valley 37 m above a small stream. The site is now an open chamber, 18 m wide, 22 m deep, with a roof and mouth around 10 m high. A 2–3 m thick sequence of partially cryoturbated, sometimes discontinuous, medium to fine-grained sands, soils and loess spanning the Middle Weichselian to the Holocene are contained within (Figure 3.26). The first investigations were carried out by Jenö Hillebrand in 1912–1913 who dug a longitudinal trench from which were recovered a Late Pleistocene vertebrate assemblage and Magdalenian and Proto-Solutrean artefacts (Hillebrand, 1914; Figure 3.26a). Hillebrand called the cave Pálffy-bárlang (Pálffy's Cave) but later F. Prošek referred to the site as Dzeravá skala and it is this name by which the site is now commonly known in the literature (Kaminská *et al.*, 2005). Prošek excavated a trench in the northern part of the cave, parallel to that of Hillebrand, for a single season in 1950 and the few publications that arose from this work demonstrated the importance of Dzeravá skala to Upper Palaeolithic research. Other excavations by professional and amateur archaeologists have taken place but have been restricted to the Holocene sediments and, as no *Arvicola* have been found in these strata, need not concern this study.

In 2002–2003 part of the remaining Pleistocene sediments in the area of Prošek's trench were the subject of a detailed investigation, which included a radiometric

dating programme (Kaminská *et al.*, 2005; Figure 3.26b). This research aimed to resolve issues with the identification and provenance of archaeological material from Hillebrand and Prošek's excavations, and to examine the timing of the Middle–Upper Palaeolithic transition.

In the following discussion reference will be made to the stratigraphic schemes of both Hillebrand (1914) and Kaminská *et al.* (2005), which possess a partially overlapping nomenclature. To avoid confusion stratigraphic divisions will be suffixed with the author's name; e.g., Layer 4 Hillebrand or Layer 4 Kaminská *et al.*.

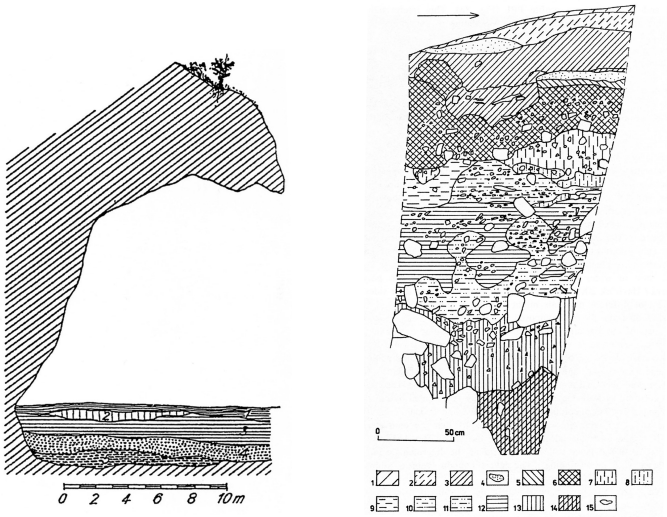

(a) (b)

Figure 3.26: Profiles of the Dzeravá skala Cave sequence: (a) taken from Hillebrand (1914), (b) taken from Kaminská *et al.* (2005).

Material examined Thirty-four M_1 teeth were photographed for this study. All molars were in good condition, many teeth still residing within the mandible. Salient angles were well defined and only four molars suffered from single broken enamel walls (ImageIDs 2518, 2520, 2526, and 2537). A light coating of fine-grained, beige sediment was easily cleaned from occlusal surfaces and dentine had been stained light-brown which enabled the edges of enamel layers to be easily determined.

The specimens were identified as *Arvicola terrestris amphibius* (= *Arvicola terrestris*) by Gy. Éhik (Kaminská *et al.*, 2005, p. 9) but no information on their stratigraphic context was present at the Hungarian Institute of Geology, Budapest. The taphonomy of these specimens is considered in detail below.

Palaeoenvironments The floral and faunal evidence portrays a Late Pleistocene steppe/tundra environment with cool and cold-climatic fluctuations occurring throughout the sequence. In the Aurignacian layers cold-climate mammals

such as reindeer *Rangifer tarandus*, arctic fox *Alopex lagopus*, and steppe lemming *Lagurus lagurus* occurred with spruce, pine, and fir. In the Gravettian layers a more humid steppe environment is indicated with a variety of herbaceous vegetation and trees such as dwarf beech, alder, willow, pine, larch, and spruce (Hajnalová and Hajnalová, 2005). The small mammals show a mixed community of open habitat species, such as European snow vole *Chionomys nivalis* and ground squirrel *Spermophilus citelloides*, and taxa linked to mesic, well-vegetated areas, such as *A. terrestris*, northern vole *Microtus oeconomus*, and short-tailed field vole *Microtus agrestis*. Norway and collared lemmings, *Lemmus lemmus* and *Dicrostonyx torquatus*, today inhabitants of arctic and subalpine environments (Horáček, 2005), are present in increasing numbers, while *L. lagurus* is virtually absent.

Of note here is the fact that *C. glareolus* and common shrew *Sorex araneus* occur throughout the sequence. This indicates the continuous presence of woodland and demonstrates the persistence of these taxa and their associated habitats in central Europe during the later part of the Weichselian.

Stratigraphy and correlation The *Arvicola* specimens examined came from Hillebrand's 1912–1913 excavation and were only registered as 'Pálffy-bárlang' in the Hungarian Institute of Geology, Budapest without any information on their stratigraphic context. Kaminská *et al.* (2005) report that Hillebrand recovered frequent *Arvicola* from Layers 3 and 4 Hillebrand but a description of the material or the exact numbers of specimens found is not given. The 2002–2003 excavations also found *Arvicola* to occur most frequently in two distinct horizons: Layers 4 and 9 Kaminská *et al.* (Horáček, 2005). It therefore seems apparent that there are two separate concentrations of *Arvicola* in the sedimentary sequence: one around Layer 4 and another in Layer 9 Kaminská *et al.*, which appear to correspond to Layer 3 and Layer 4 Hillebrand respectively (Kaminská *et al.*, 2005).

Layers 4 and 9 Kaminská *et al.* are distinguished by their association with Gravettian and Aurignacian archaeology respectively. Radiocarbon dating of pieces of long bone that displayed no sign of human modification has shown that these layers represent relatively short, coherent periods of accumulation, and that a dating gap of greater than 8 k ^{14}C BP (6 k cal BP) exists between them (Davies and Hedges, 2005; Table 3.32). In an attempt to resolve the stratigraphic origins of the *Arvicola* fossils, Specimen 1619 was radiocarbon dated and gave an age of 22 410 ± 150 ^{14}C BP (OxA-21081; Table 3.32), showing that this specimen originated from the upper, Gravettian part of the sequence. OxA-21081 is slightly younger than other dates obtained, which may be an indication that the small mammal component of the fossil assemblage possessed a different taphonomic history to the large mammal fauna that has been radiocarbon dated thus far. It may

be, for instance, that the pieces of long bone dated, although showing no signs of human modification, were the product of hunting activities. If human occupation was short-lived, the existing radiocarbon dates would give a biased perspective of the accumulation history of the sequence.

A single radiocarbon date cannot adequately characterise the age-range of the whole *Arvicola* assemblage, but dating of Gravettian and Aurignacian layers show these to be distinct in time, making it seem unlikely that the fossil *Arvicola* derived from both these layers. Inadequate excavation procedures could have led to the fauna being mixed but the literature shows that fauna and archaeology were analysed stratigraphically and therefore collection appears to have respected the context of specimens found. Less is known about the post-excavation care and curation of the fossils. Although the fossils have been resident in the Hungarian Institute of Geology, Budapest since Hillebrand's day, it is possible that through re-labelling or some other action, previously separate samples became mixed.

Climatostratigraphy suggests that the Aurignacian layers represent a 'cold-oscillation' in the Weichselian, and that the Gravettian strata show a more humid period just before the onset of the Last Glacial Maximum (Hajnalová and Hajnalová, 2005; Horáček, 2005). There is some disagreement with the radiocarbon dates of Layer 9 Kaminská *et al.* and the proposed climatic correlation. The fauna and flora present in the upper layers and the periglacial sedimentary structures developed in them do show that a marked cooling occurred after the Gravettian layers (Kaminská *et al.*, 2005).

From the evidence available, this study will consider that the *Arvicola* examined originated from the Gravettian strata, which were deposited in the later part of MIS 3. The possibility of post-excavation mixing of different fossil assemblages does exist; and this possibility will be noted and explored in later GM analyses. The palaeoenvironmental evidence, together with radiometric dates around 30–26 k cal BP, support an age just prior to the Last Glacial Maximum. This radiocarbon date obtained for the *Arvicola* will therefore be applied to the *Arvicola* assemblage.

Table 3.32: Radiocarbon dates from Dzeravá skala Cave. Values arranged in stratigraphic order then by date with reference to the stratigraphy of Kaminská *et al.* (2005) and the typology of archaeology found within each stratum. All determinations are AMS dates save for Wk-14865 where the method is uncertain. *Arvicola* Specimen 1619 dated for this study, other data from Davies and Hedges (2005).

Layer	Typology	Lab no.	Material	^{14}C BP	cal BP
?		OxA-21081	*Arvicola* specimen 1619	22 410 ± 150	27 050 ± 527
3	Gravettian	GrA-22756	bone indet.	25 050 ± 540	29 888 ± 621
4	Gravettian	GrA-22758	bone indet.	24 800 ± 130	29 837 ± 312
4b	Gravettian	GrA-22759[a]	bone indet.	31 770 ± 320	35 721 ± 523
5	Gravettian	OxA-13861	bone indet.	24 760 ± 130	29 809 ± 320
9					
	Aurignacian	Wk-16829	bone indet.	33 333 ± 820	38 394 ± 1 667
	Aurignacian	Beta-173341	bone indet.	34 100 ± 320	39 608 ± 916
	Aurignacian	OxA-13860	bone indet.	35 100 ± 400	40 089 ± 885
9/5a	Aurignacian	Wk-14865	bone indet.	37 370 ± 2 060	41 507 ± 2 026

[a] This date appears to be an outlier (Davies and Hedges, 2005) perhaps due to contamination as only OxA samples were carried out using the ultrafiltration technique of Bronk Ramsey *et al.* (2004).

3.13 Slovenia

3.13.1 Late Pleistocene

3.13.1.1 Divje babe I

Location Cerkno, Slovenia

Co-ordinates 46.11°N, 13.91°E

Age MIS 3

Archive National Museum of Slovenia, Ljubljana, Slovenia

Description The Divje babe I site is a long, wide cave formed within dolomite and located in the pre-Alpine region of north-west Slovenia. A thick (12 m) sequence of sediments was found which are thought to have accumulated throughout the early and middle parts of the Last Cold Stage (Turk *et al.*, 2007; Turk, 2007a). Fossil mammals were found throughout the sequence along with remains of *Homo neanderthalensis* and archaeology that included a 'Neanderthal flute'.

The cave was systematically but intermittently excavated between 1978 and 1999. Sedimentary layers were generally sub-horizontal and were divided into

upper (A - layers 2–6), middle (B - layers 7–15), and lower (C - layers 16–23) facies. Individual layers were determined on the basis of colour, and facies were distinguished lithologically; reflecting deposition mediated by broad-scale climatic phases with smaller-scale climatic variation evident within facies (Turk, 2007a,b). The sequence at Divje babe I has been proposed as the stratotype for the Middle Würm in Slovenia (Turk, 2007a).

Material examined Seven M_1s from Facies A were photographed. Four of these molars were still within mandibles and all the material was very well preserved, showing little staining or signs of erosion. Although cryoturbation has mixed Holocene remains into the upper parts of Facies A, the similarity in preservational state of the material examined for this study suggests that these specimens are of similar provenance.

Toškan and Kryštufek (2007) identified the water vole as *Arvicola terrestris* based upon qualitative assessment of the SDQ and morphotype analysis of the M_1 and M^3. M_1s and M^3s from Facies A were not as large as those from Facies B–C, which date to the later part of MIS 5 (Turk, 2007a). This trend in declining size through the Last Cold Stage has been observed in other sequences in southeast Europe (e.g., Mauch Lenardić, 2005), and Toškan and Kryštufek (2007) speculated whether this change reflected colonisation by different intraspecific lineages: i.e., *Arvicola amphibius* or *Arvicola scherman*.

Palaeoenvironments From Facies C and B the small mammal fauna and pollen shows a moderately warm, dry, open grassland with coniferous woodland developing into a moister, cooler, coniferous woodland dominated environment. A marked an increase in species diversity in Facies A indicates climatic warming and the presence of a mosaic of mixed woodland, meadows, and rocky areas similar to the present-day landscape of the region; indeed quantitative analysis of the small mammal assemblage from layers 2–5 shows an almost identical composition to the recent fauna (Toškan and Kryštufek, 2007).

Stratigraphy and correlation Turk (2007a) developed a chronology for Divje babe I based on a combination of absolute dating methods (radiocarbon dating of bone and ESR on tooth enamel) and climatostratigraphy (from pollen and faunal analysis). Using these data it was concluded that Facies B and C span a period from MIS 5d to *c.* 50 k yr BP and that Facies A was deposited *c.* 50–35 k yr BP. This study will take a conservative approach and employ an age-estimate of MIS 3 for the *Arvicola* assemblage.

3.14 Ukraine

3.14.1 Late Middle Pleistocene

3.14.1.1 Chigirin

Location Near the town of Chigirin, Cherkasy Region, Ukraine

Co-ordinates 49.08°N, 32.67°E

Age MIS 11

Archive Moscow Institute of Geography, Russian Academy of Sciences, Moscow, Russia

Description Chigirin, in the Middle Dnieper region of Ukraine, is a late Middle Pleistocene fluvial aggradation located on the left bank of the river Sokindrovki, a tributary of the river Tyasmina. The site was discovered in 1970 in a brick-pit excavated to exploit thick loess deposits which lie on river terraces, and was researched by A. I. Shevchenko and A. K. Markova (Markova, 1982). Small mammal remains were found in cross-bedded sands at the base of the sequence studied (Figure 3.27).

Material examined Forty-four M_1 teeth were photographed. Teeth were small, high-crowned, unrooted, and four molars showed a *Mimomys*-fold. Only thirty-one specimens were able to provide a full set of landmarks but, aside from damage to the posterior lobes and enamel triangles of some teeth, the general state of preservation was good.

Over half the small mammals found were from *Arvicola*, which given the depositional setting suggests that the water vole possessed a semi-aquatic ecology. The similar preservational state of specimens suggests a shared taphonomy for the assemblage and small mammal remains were discretely distributed within the cross-bedded sands, which may suggest concentration of fossils in a channel-lag deposit (Behrensmeyer, 1993). No obvious signs of temporal mixing, such as the juxtaposition of geologically young and old taxa, within the fossil remains can be discerned, and so it could be assumed that the assemblage is temporally discrete. Popova (2004), however, has shown that modern channel deposits of the Dnieper contain a mixture of modern, earlier Holocene, and Late Pleistocene remains.

Specimens were identified as *Arvicola mosbachensis* on the basis of the absence of roots (Markova, 1982). SDQ values for the assemblage show a *Mimomys*-differentiation (Table 3.33).

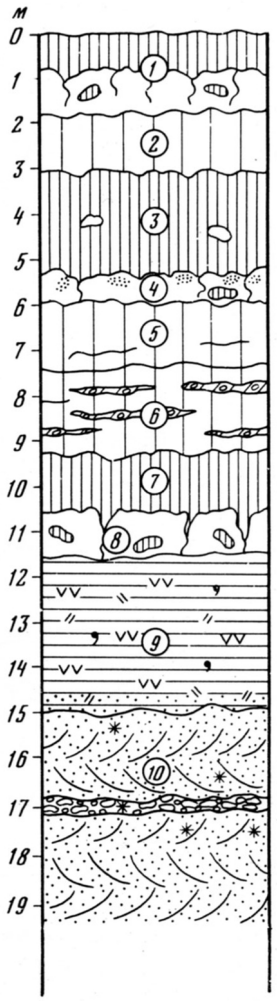

Figure 3.27: Generalised stratigraphy of Chigirin. Significant layers: (6) moraine; (9) loam with fossil molluscs; (10) thick, cross-bedded sands with small mammal remains. Taken from Markova (1982).

Palaeoenvironments The small mammal remains are dominated by water voles, reflecting the local importance of riparian habitats assuming a semi-aquatic ecology for *Arvicola*. Steppic elements such as steppe lemming *Lagurus transiens* and pika *Ochotona* sp. are present but the occurrence of blind mole rat *Spalax* sp. shows the development of soils, and bank vole *Clethrionomys glareolus* the presence of rich vegetation and woodlands in a temperate environment.

Stratigraphy and correlation The sequence at Chigirin lies under a diamicton identified as the late Middle Pleistocene Dnieper till, and is part of the fourth terrace of the Dnieper river (Markova, 1982, 2006). The small mammal composition allowed Markova (2006) to assign the assemblage to the Gunkovian small mammal zone, correlated with the Oka (= MIS 12) Glacial and Likhvinian (= MIS 11) Interglacial (Markova, 1990). The interglacial nature of the sediments and the fauna, and the presence of *A. mosbachensis*, led Markova (2006) to suggest a Likhvinian age for Chigirin and so, in the absence of other dating evidence, an MIS 11 age will be tentatively assigned to the *Arvicola* assemblage.

Table 3.33: Published SDQ values from Chigirin.

Author	SDQ			
	n	min	mean	max
Markova (1982)	62	101.67	129	166.67

3.14.1.2 Gunki II

Location Psel river near the villages of Gunki and Lamane, Ukraine

Co-ordinates 49.27°N, 33.6°E

Age MIS 11

Archive National Museum of Nature of the Academy of Sciences of Ukraine, Kiev, Ukraine, and Moscow Institute of Geography, Russian Academy of Sciences, Moscow, Russia

Description The site consists of richly fossiliferous Middle Pleistocene deposits found in cliffs about the Psel river, an eastern tributary of the the Dnieper river. The sedimentary sequence consists of channel, lacustrine, and gyttja deposits overlain by two thick loess and palaeosol layers and a till from the Dnieperian Glaciation (Markova, 2006; Figure 3.28). The site was first described by D. K. Bilenko in 1941 who found large mammal bones such as *Ursus spelaeus* and freshwater molluscs. From 1970–1971 a detailed investigation of the stratigraphy and palaeontology of the site was undertaken, which recovered a rich small mammal fauna dominated by rodents. Three fossiliferous horizons were discovered in Layers 16, 14, and 13, named Gunki I, II, and III respectively (Markova, 1982). The greatest abundance of molluscan and small mammal remains were found in the dark-brown gyttja and loam sediments of Gunki II, and it is from this horizon that the *Arvicola* fossils used in this study were taken. Gunki II was deposited in a low-energy marsh or lake setting with periodic fluvial inundation indicated by the presence of sand lenses within the clay Markova (1982, 1990).

Material examined Water vole were well-represented in the small mammal assemblage and nineteen M_1 teeth were used in this study. Thirteen molars were held at the Moscow Institute of Geography, Russian Academy of Sciences, Moscow, Russia, where they were registered as *Arvicola cantianus* (= *Arvicola mosbachensis*). Six were held at the National Museum of Nature of the Academy of Sciences of Ukraine, Kiev, Ukraine, and identified as *Arvicola* sp. In the literature the *Arvicola* from Gunki II have been assigned to *Arvicola mosbachensis* (Markova, 1982; Rekovets, 1994), *A. cantianus* (Markova, 2007), and *Arvicola cantiana* (Markova, 1990).

Molars were stained dark-brown or black, as reflects the dark-coloured sediments from which they were recovered. The low-energy depositional setting of Gunki II and low faunal diversity suggest that little allochthonous material is present in the taphocoenosis (Markova, 1990). The main agent for taphonomic mixing would presumably have been locally roosting predatory birds, which acted

as vectors for fossil accumulation. Fossil preservation, being generally very good, is consistent with these ideas: enamel layers are sharp and easily visible, and salient angles well-defined. Some molars do, however, suffer from missing parts of posterior lobes or eroded anterior lobes and this damage may be attributable to excavation damage of fragile specimens (see Section 3.6.1.1) and corrosion from partial digestion by predatory birds.

The near-channel lake or marsh setting envisaged for Gunki II bears many similarities with West Runton, England (Section 3.6.1.2). Here, dark-coloured clays and silts rich in molluscs and small mammals were deposited rapidly in a alder carr environment, with occasional influxes of sand through flooding from a nearby channel (Rose *et al.*, 2008). Gunki II appears an analogous environment and the fossils and sediments could also therefore represent a particularly temporally discrete accumulation.

Morphometric measurements carried out by Rekovets (1994) and Markova (2000) are shown in Table 3.34. There is a pronounced difference between the values obtained by these two authors. Such a large difference is difficult to explain through differences in measurement method alone. The low mean SDQ of Rekovets (1994) may reflect sampling error if the number of M_1s used to calculate this value was low (although n is not known). Alternatively, the fossils used by Rekovets and Markova may not be derived from the same part of the stratigraphy. M_1s are small compared to modern samples and the SDQ of Rekovets (1994) places the *Arvicola* population in the late Middle Pleistocene according to the central European enamel thickness trajectory of Maul *et al.* (1998b).

Table 3.34: Published SDQ values and M_1 lengths of *Arvicola* from Gunki II.

Author	SDQ				Length M_1			
	n	min	mean	max	n	min	mean	max
Rekovets, 1994			106		18	3.15	3.67	4.1
Markova, 2000	12	120.48	132	303.03	18	3.2	3.38	3.45

Palaeoenvironments The rodent fauna is dominated by *Lagurus* sp. and *Microtus* spp., which suggest open-grassland, steppe, and open-woodland environments. *A. mosbachensis* is also well represented and is likely to have been semi-aquatic given the riparian/wetland depositional environment. Gunki II has been stratigraphically linked with the Likhvinian interglacial (see below) and pollen records from elsewhere sugegst that during this interglacial Gunki was located in an area of mixed and broadleaved forest and forest-steppe (Markova, 2006).

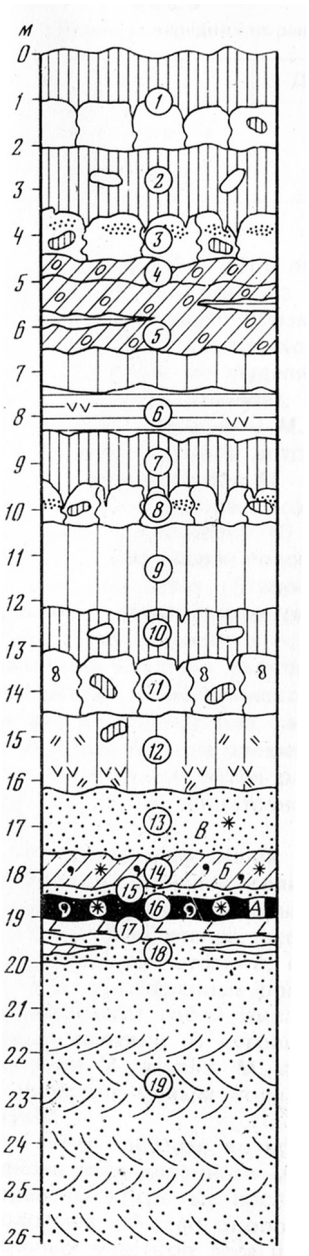

Figure 3.28: Summary of the sedimentary sequence at Gunki. See text for explanation. Taken from Markova (1982).

Stratigraphy and correlation A Middle Pleistocene age for the fossiliferous deposits is clear as the sequence lies on the pre-Dnieper fourth terrace of the Psel river and the Dnieper till can be found near the top of the section (Velichko *et al.*, 2004; Markova, 2006; Figure 3.28 Layers 4–5). More specifically, the fossiliferous layers are thought to date to the Likhvinian (= MIS 11) Interglacial. Two sources of evidence support this conclusion:

a) *Climatostratigraphy* Two palaeosols that occur between the fossiliferous deposits and the Dnieper till have been identified as the Kamenka and Romny palaeosols. These are warm-climate deposits widely recognised across the East European Plain to post-date the Likhvinian and pre-date the Dnieper (Markova, 1990, 2006).

b) *Biostratigraphy* An early Likhvinian pollen spectrum has been identified and the molluscan assemblage correlates with the Likhvinian Palaeo-Euxinian Black Sea transgression (Markova, 1990, 2006). The small mammal assemblage is strongly regarded as being characteristic of the Likhvinian. In particular, the presence of *A. mosbachensis* and an advanced form of the steppe lemming *Lagurus transiens* are important temporal markers. These taxa are found after the Oka Glaciation (= Elsterian = MIS 12) in Russia and the East European Plain, but do not persist into the Late Pleistocene. Furthermore, the absence of *Mimomys* is regarded as significant as a marker for a post-MIS 12 deposit (Markova, 1982, 1990, 2006; Rekovets, 1994; Maul and Markova, 2007).

The composition of the small mammal fauna at Gunki led Markova (1990) to recognise a Gunkovian MAZ. The Gunkovian emphasises differences between the pre-Oka Tiraspolian and subsequent small mammal faunas that were not illustrated by the existing post-Oka Singilian MAZ. The Singilian is ostensibly a large mammal zone because of the paucity of small mammal remains found at its type-site near the town of Raigorod on the Volga river (Markova, 1990). The small number of *Arvicola* specimens recovered from Raigorod could only be identified to generic level (Markova, 1990) and no *Lagurus* was found. So the differences between the Singilian and Gunkovian may be taphonomic or temporal, but within current understanding the Singilian and Gunkovian are effectively stratigraphically synchronous (Markova, 2007; Rekovets *et al.*, 2007).

In terms of oxygen isotope stratigraphy, the Likhvinian is considered equivalent to the Holsteinian of western Europe; itself widely assumed to be MIS 11. Therefore an MIS 11 age, perhaps early MIS 11 if considering palynological evidence (Markova, 2006), can be placed on the *Arvicola* assemblage material from Gunki II (Markova, 2007).

3.14.1.3 Medzhybozh-2

Location Left Bank of the Yuzhny Bug river, southwest of the town of Medzhybozh, Khmelnytskyi Province, western Ukraine

Co-ordinates 49.43°N, 27.42°E

Age MIS 11

Archive National Museum of Nature of the Academy of Sciences of Ukraine, Kiev, Ukraine

Description The geology and palaeontology of alluvial deposits of the Yuzhny Bug river have been studied since the beginning of the 20th century. Exposures in river cliffs to the east of the town of Medzhybozh were found by the geologist Laskarev to contain vertebrate and molluscan remains, and an Acheulian stone tool was discovered in the 1990s by Pyasetsky (Rekovets *et al.*, 2007). New excavations commenced at the beginning of the 21st century, opening an exposure at the site of Pyasetzky's find (Medzhybozh-1), at the site of Laskarev's investigations (Medzhybozh-2), and a new more complete section at Medzhybozh-3. Exposures were 8–17 m high and consisted of alluvial sediments, loess, and soils (Figure 3.29). Although not highly fossiliferous further finds of large and small mammals and molluscs were made. Additional Acheulian artefacts were also recovered and Rekovets *et al.* (2007) concluded that the archaeology dates from the Likhvinian (Holsteinian) warm-stage and is therefore the earliest evidence of *Homo* in the Ukraine.

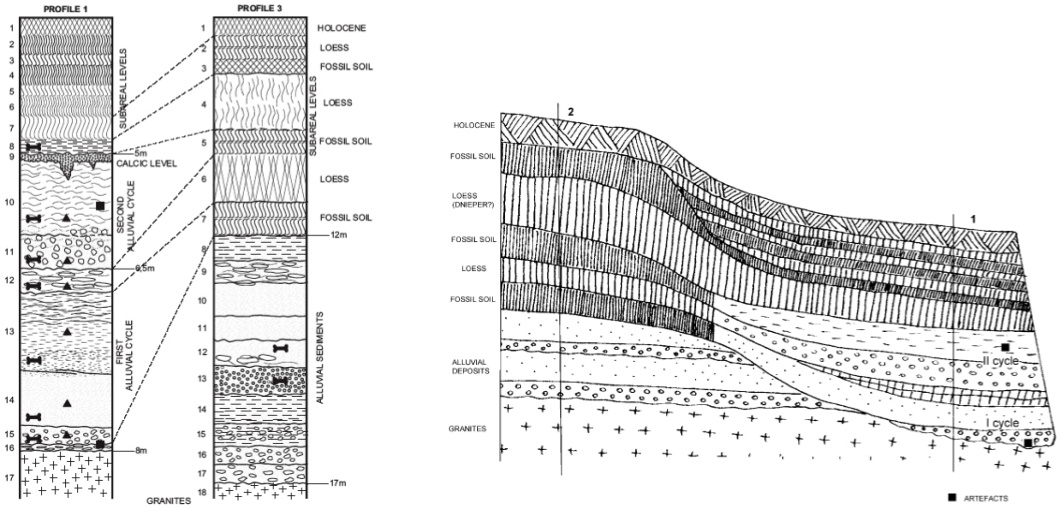

(a) (b)

Figure 3.29: (a) lithostratigraphy of, and proposed correlation between, Medzhybozh-1 and -3, (b) generalised combined section of the exposures at Medzhybozh-1 and -2. Taken from Rekovets *et al.* (2007).

Material examined Water vole dominated the limited small mammal fauna recovered from the basal sands of Medzhybozh-2 (Rekovets *et al.*, 2007) and twenty-two *Arvicola* M_1 teeth were examined from these deposits. Two *Mimomys* sp. teeth were also recorded from Medzhybozh-2 but were not examined. *Arvicola* also dominated the vertebrate finds in Medzhybozh-1 and -3 but this material was not available for study.

All molars were stained dark-brown or black, a feature commonly seen in fossils which have been exposed to highly organic sediments or have resided within soils. Despite the dark colouration of the teeth, enamel layers were easily discernible as a more transluscent material than the opaque dentine. Around one in ten teeth posses a *Mimomys*-fold, the anteroconid complex is rounded with little variation in shape, and the length and width of the M_1 is slightly less than later populations (Rekovets *et al.*, 2007). Measurements of enamel thickness showed enamel to possess a *Mimomys*-differentiation (Table 3.35). Rekovets and Nadachowski (1995) assigned the water vole fossils to *Arvicola cantianus* (= *Arvicola mosbachensis*) while Rekovets *et al.* (2007) used the name *A. mosbachensis*.

The occurrence of fossils within alluvial deposits raises the possibility that some molars may be reworked or at least that the fossil assemblage is aggregated over a long period of time. No detailed information about the context of the *Arvicola* finds from Medzhybozh-2 was available but the possibility of a mixed fossil assemblage is apparent as many bones from Cycle I were shattered, probably by fluvial action and some reworked fauna have been identified (see below). Cycle I does seem to be a higher energy deposit than the sands of Medzhybozh-2 (Rekovets *et al.*, 2007), however, and *Arvicola* molars examined showed few signs of erosion from fluvial transport. It may be that the fauna of the fossiliferous sands of Medzhybozh-2 are mixed in some way but because of the shared preservational appearance and similar morphology for the purposes of the analysis it will be assumed that the *Arvicola* assemblage is relatively homogenous.

Table 3.35: Published SDQ values from Medzhybozh-2.

Author	SDQ			
	n	min	mean	max
Rekovets and Nadachowski (1995)	29	91.66	118.7	150

Palaeoenvironments Mixing of fossils in the fluvial depositional setting may serve to produce a mixed palaeoenvironmental signal and the low representation of some taxa in fossil assemblages may also be problematic. However, the small

mammal and molluscan fauna from Medzhybozh-2 give a general indication of habitats in the floodplain of the Yuzhny Bug river. The occurrence of wood mouse *Apodemus sylvaticus* and bank vole *Clethrionomys glareolus* demonstrate the presence of woodland; beaver *Castor fiber*, *A. mosbachensis*, and freshwater molluscs indicate ponds and wetlands; and various *Microtus* spp. show that open grasslands and steppe also existed (Rekovets *et al.*, 2007). The alluvial cycles of Medzhybozh-1 also yielded pollen, with abundant pine and oak accompanied by lime, elm, and hazel pollen showing the existence of full interglacial conditions in the region. Pollen evidence further suggests environments cooling in Cycle II before deposition of the Dnieper Loess.

Stratigraphy and correlation Dating of the Medzhybozh exposures has relied upon relative dating, climatostratigraphy, and biostratigraphy. The basal sands and gravels of the Lower Alluvium of Medzhybozh-2 are located on third terrace of the Yuzhny Bug river, and Cycles I and II of Medzhybozh-1 and -3 all underlie the Dnieper Loess (Figure 3.29b). This means that all the fossiliferous deposits pre-date the Dnieper Glaciation (Gozhik, 1969, referenced in Rekovets *et al.*, 2007). By counting back loess and soil layers from the Dnieper Loess Rekovets *et al.* (2007) produced the preliminary stratigraphy shown in Table 3.36. This scheme correlates each warm and cold-climate sediment package with widely recognised deposits from the eastern European plain. Gerasimenko (2004, in Rekovets *et al.*, 2007) goes further by suggesting correlations between the Romny Soil and Schöningen II, Germany: with the Kamen (= Zavadov = Sanzhar) Soil of the East European Plain being the equivalent of the Reinsdorf warm period in Germany.

Rekovets *et al.* (2007) make no attempt to correlate with global oxygen isotope stratigraphy. While it is generally accepted that the Dnieper Glaciation dates from the second part of the Middle Pleistocene (Matoshko, 2004) it has been correlated with MIS 6 (Markova, 2007), MIS 8 (Matoshko *et al.*, 2004), and both MIS 6 and MIS 8 (Lindner *et al.*, 2004). Absolute dating of Dnieper Till is regarded as unreliable (Matoshko, 2004) but on biostratigraphic grounds MIS 6 is the favoured age for the Dnieper Glacial (Markova, 2007) and therefore on this basis the soil beneath the Dnieper Loess would be MIS 7, the Kamen Soil MIS 9, and the Lower Alluvium MIS 11.

In terms of biostratigraphy, the *Arvicola* of Medzhybozh-2 are assigned to the top of the Ozernoe phase of the Singilian 'faunal complex' (Rekovets and Nadachowski, 1995) or the early Singilian by Rekovets *et al.* (2007),[1] and Rekovets *et al.* (2007) further speculated that Medzhybozh may pre-date the other Ukrainian sites of Chigirin and Gunki (Sections 3.14.1.1 and 3.14.1.2 respectively). The Singilian

[1]This biochronological zone is, according to Markova (2007), restricted to large mammals; the age-equivalent small mammal assemblage zone being the Gunkovian.

Table 3.36: Proposed chronostratigraphy for the Medzhybozh sequence. See text for discussion. Modified from Rekovets *et al.* (2007).

Medzhybozh		SDQ	Regional deposits	Regional stratigraphy	Inferred MIS
2/3	1				
	Loess	-	Dnieper	Dnieper Glacial	6
	Cycle II	-	Romny Soil	-	7
		107	Orchik Loess	-	8
	Cycle I	116.8	Kamen Soil	Kamenka Interglacial	9
Lower alluvium		-	Borisogleb Loess	-	10
		118.7	Inzhava Soil	Likhvin Interglacial	11

encompasses the Likhvinian warm-stage of Russia, and is considered a correlative of the Holsteinian of Europe and of MIS 11. A single tooth of *Trogontherium cuvieri* has been recorded from Cycle II but is thought to be reworked from earlier deposits (Rekovets *et al.*, 2009).

Accepting that the loess at Medzhybozh represents the Dnieper Glaciation, the stratigraphic conclusions described rely on the assumption that each 'alluvial cycle' corresponds to a glacial-interglacial period. This is problematic as not all glacials result in the formation of a terrace or a fluvial aggradation (Matoshko *et al.*, 2004). The Yuzhny Bug is not a major river, such as the Dniester to the west, which possesses a well-recognised terrace staircase (Bridgland and Westaway, 2008). Additionally, the Yuzhny Bug flows over both the western edge of the Proterozoic Ukrainian Shield and the geologically more recent sediments of the Carpathian Foreland. The tempo of crustal uplift differs between these two regions and means that well-defined river terraces may not be formed because of mixed aggradation and downcutting (Bridgland and Westaway, 2008). Alluviation, and loess accumulation may then be the result of a complex interplay between tectonics, climate, deposition and erosion. Furthermore, soil formation may also operate at a sub-stage level, as occurred during the Russian Muchkapian interglacial (Velichko *et al.*, 2004), leading to deposition decoupled from the 100 k yr glacial-interglacial cyclicity.

In summary, the fossiliferous deposits are pre-Dnieper in age but problems exist with climatostratigraphic counting back of sediment packages. An MIS 11 age will be applied the the *Arvicola* OTU but will be treated with caution.

3.14.2 Late Pleistocene

3.14.2.1 Novonekrasovka

Location Near the village of Novonekrasovka, southwest of lake Yalpug, Odessa Region, Ukraine

Co-ordinates 45.38°N, 28.70°E

Age MIS 5e

Archive Moscow Institute of Geography, Russian Academy of Sciences, Moscow, Russia

Description In the delta of the lower Danube, alluvial and marine sediments interdigitate to form a thick Late Neogene sequence. At Novonekrasovka in the southwest of Ukraine, two units of lagoonal sediments on the second terrace of the Danube were both found to contain an abundant brackish and freshwater molluscan fauna with a small mammal assemblage, dominated by *Arvicola* (Mihailescu and Markova, 1992, p. 50; Dodonov *et al.*, 2000; Markova, 2000). Both brackish deposits occur above gravels, and are overlain by a 1.5 m lacustrine silt and 8 m of loess containing two palaeosols (Dodonov *et al.*, 2000).

Material examined Seventeen M_1s from the upper lagoonal sequence (ULS) were photographed; twelve molars were in good enough condition to give full configurations of landmarks. Seven M_1s from the lower lagoonal sequence (LLS) were also photographed but only three gave full landmark configurations. All specimens were stained a rich brown colour but those from the LLS were darker than molars from the ULS. Similarity in the preservation of each assemblage suggests a shared taphonomy, and may indicate a low level of temporal mixing in each group.

Markova (2000) identified the water vole as *Arvicola* ex gr. *terrestris*, and measured enamel thicknesses in both assemblages (Table 3.37). The abundance of water vole in this fluvial depositional environment strongly suggests a semi-aquatic ecology for *Arvicola*.

Palaeoenvironments Markova (2000) presents a faunal list consisting overwhelmingly of *A.* ex gr. *terrestris*, but with rare finds of *Microtus arvalis* and *Microtus* sp. This taxonomically biased assemblage likely reflects a local predominance of freshwater habitats. This is further supported by the molluscan fauna, which is rich and highly diverse in brackish and freshwater species (Dodonov *et al.*, 2000). Amongst the freshwater molluscs are the thermophiles *Corbicula fluminalis* and *Melanopsis praerosa*, which now have their northern-most distribution some

Table 3.37: Published SDQ values from Novonekrasovka. Data from Markova (2000).

Strata	SDQ			
	n	min	mean	max
Novonekrasovka upper	18	60	87	140
Novonekrasovka lower	14	59.9	92	110

500 km to the south in southern Bulgaria (Dodonov *et al.*, 2000). The overall palaeoenvironmental picture is one of a marginal marsh or estuarine landscape with a warm, temperate climate.

Stratigraphy and correlation The upper soil contains ice-wedge pseudomorphs and may be identified as the Bryansk soil, a widely recognised palaeosol in the region, dated elsewhere to 25–25 ^{14}C k yr BP (Dodonov *et al.*, 2000), and by inference the lower soil may be recognised as the Mezin palaeosol, another regional palaeosol that occurs below the Bryansk soil, and is correlated with the Last Interglacial Tesakov *et al.* (2007).

The lagoonal sequences are both attributed to the Mikulino interglacial (= MIS 5e), as these marginal facies appear to represent the Karangatian transgression of the Black Sea. This transgression comprises two 'cycles' and is correlated through liman deposits found in near-shore cores from the Black Sea with deposits in the lower parts of the Danube, Dniester, and Dnieper rivers (Dodonov *et al.*, 2000; Tesakov *et al.*, 2007). An MIS 5e age will applied to the *Arvicola* assemblages from this site.

Chapter 4

General Methodology

In Section 2.2 a case was made for using the occlusal morphology of the water vole M_1 as a structure with which to investigate phylogeny. This study will employ the toolkit of techniques provided by traditional and Geometric Morphometrics (GMM) to quantitatively analyse occlusal shape of the M_1. GMM represents a shift away from the use of linear measurements, areas, volumes, ratios, counts, and angles in morphological studies, that together can be referred to as 'traditional' morphometrics (Marcus, 1990). Rather, GMM uses Cartesian coordinates to capture information on shape. Coordinate data posses a number of more desirable mathematical properties than traditional data, and allow greater versatility in the visualisation of results. Furthermore, GMM allows morphological data from the M_1 to be applied to the investigation of biological processes, such as evolution, in novel ways.

The dominant methods previously used in the analysis of water vole evolution have, however, been of the traditional type, and have been outlined in Section 2.2. Of these traditional approaches the measurement of enamel thickness is prominent, and this method will also be used by this study to allow comparison both with results based on GMM and the existing literature.

This chapter outlines the general analytical approach taken by this study, the types of data to be used, data capture techniques, analytical methods, and considerations of likely sources of error, which includes some discussion and development of analytical approaches to the investigation of taphonomic effects (Section 4.4). In later chapters the methodological approaches taken to the study of allometry (Chapter 5) and phylogeny (Chapter 6) are outlined. Virtually all analyses are conducted within the open source R environment for statistical computing (R Development Core Team, 2008) using available packages and bespoke scripts written by the author with occasional contributions from the R community. Full citations relating to R and other computer programmes will be made where necessary.

4.1 Geometric morphometrics

The growth in the application of GMM methods since the 1980s has been described as a 'revolution' in the analysis of morphology (Rohlf and Marcus, 1993; Adams *et al.*, 2004). The foundation for this revolution was an explicit mathematical definition of shape as the geometric information that remains when location, scale and rotational effects are filtered from an object (Kendall, 1977). Many authors built upon this work to produce the modern 'morphometric synthesis' (Bookstein, 1996), which now comprises a variety of flavours of GMM—and statistical methods accompanying them—that offer differing advantages and disadvantages. There is no need to explore the milestones of the synthesis here, nor to catalogue the varieties of GMM that exist. Many comprehensive reviews have been published on the subject (e.g., Rohlf and Marcus, 1993; Zelditch *et al.*, 2004; Polly, 2008b; Lawing and Polly, 2010), and only one technique, Generalised Procrustes analysis (GPA) of two-dimensional landmarks (Rohlf, 1990), will be employed by this study (Section 4.1.2).

4.1.1 Comparison with traditional morphometrics

Traditional morphometric methods are not 'wrong' but do not offer the power and versatility that GMM such as GPA can (Rohlf and Marcus, 1993). Outputs from GPA hold a number of appealing properties (listed below), which suggest that the application of GPA to shape analysis of the M_1 is likely to be beneficial. Such benefits include:

Size independence In traditional morphometrics all measurements contain information about shape and size together. Correcting for the influence of size has often involved the use of ratios of distances (such as the A/L ratio of Van der Meulen, 1973) but ratios have questionable statistical properties (Atchley *et al.*, 1976; Atchley and Anderson, 1978; but see Corruccini, 1977 and Albrecht, 1978 for disagreements). Other descriptive statistics also behave unusually when confronted with variation in size (Polly, 1998). GPA removes size[1] as a separate variable—Centroid Size (CS)—that can be examined independently to shape variables.

Homologous Linear distances such as 'maximum length of a tooth' tend not to be defined between homologous points, risking reduced measurement accuracy, and making comparison between these distances difficult (MacLeod, 2002; Adams *et al.*, 2004). The landmark configurations of GMM are homologous

[1] Actually size is suppressed to an insignificant level (Dryden and Mardia, 1998).

and are likely to characterise shape more accurately, meaning shape variables hold greater statistical power (Adams *et al.*, 2004).

Information rich Many linear measurements are needed to capture the same amount of information as that contained in coordinate data (Monteiro *et al.*, 2002). For instance in Figure 4.1a, 66 inter-landmark distances are required to describe all between-landmark relationships. Many of these linear measurements travel along similar paths, duplicating information on morphology. The linear relationships between landmarks in Figure 4.1a are implicit when registered in a coordinate system, as are other possible traditional measures such as angles.

Flexible Outputs of traditional morphometrics are limited to descriptive statistics and abstract plots that make patterns or trends in morphological change difficult to visualise. In GPA the geometric relationships between landmarks are preserved, allowing shape models to be built and used for visualisation or further modelling (e.g., Figure 5.7; Chapter 6).

4.1.2 Generalised Procrustes analysis

GPA has become a common standard in GMM, with a solid theoretical basis and mature statistical framework (Dryden and Mardia, 1998; Adams *et al.*, 2004). In GMM Cartesian coordinates are taken at landmarks located at well-definable points on the objects under study (e.g., Figure 4.1b): giving k landmarks, in m dimensions (in this case two-dimensions), for n objects. GPA is a set of mathematical procedures that superimpose landmark configurations from different shapes together, eliminating non-shape variation mathematically to produce sets of 'shape variables'. Removing non-shape related variation involves superimposing shapes (Generalised Procrustes Superimposition, GPS) by translating configurations so they share a common origin, scaling configurations to unit size, and iteratively rotating configurations to minimise squared differences between corresponding landmarks (Rohlf and Slice, 1990). Following this process, a meanshape for each group of configuration can be calculated.

After GPA each shape exists mathematically as a single point on the surface of a curved, non-Euclidean shape space (Kendall's shape space) which is a multidimensional hypersphere (Dryden and Mardia, 1998). Distances between points on this surface are measures of shape difference between configurations. This is known as Procrustes distances (D_p), calculated as the square root of the summed squared differences between two landmark configurations. D_p has become a core metric of shape difference in GMM studies (Zelditch *et al.*, 2004). The nature of Kendall's shape space means that Euclidean statistical tests cannot be used

unless the data are projected into a tangent space, or the non-Euclidean space is observed to be closely similar to the tangent space. A further effect of GPA is that the dimensionality of the data is reduced to $2k - 4$ through the translation, rotation, and re-scaling process (Zelditch *et al.*, 2004). This loss of dimensions requires the application of a suite of specially tailored statistical methods, or referral to computer-based resampling approaches such as jack-knifing or bootstrapping, for statistical testing. Such approaches will be adopted and described as necessary.

Although some authors have applied other GMM techniques to shape analysis of water vole M_1s (e.g., outline analysis, Escudé *et al.*, 2008b), landmark based GPA has not been applied. This study is, then, a novel exploration. All GPA is carried out in the R environment for statistical computing (R Development Core Team, 2008) using the *shapes* package (Dryden, 2007). Where possible, results were cross-checked with the MorphoJ geometric morphometrics package (Klingenberg, 2008).

4.1.3 Landmarks

4.1.3.1 Location

The location and selection of landmark points that describe occlusal shape is a fundamental stage in the analytical process, the aim being to capture shape information in as complete, as accurate, and in as repeatable a manner possible. This requires the location of landmarks at easily and repeatably locatable parts of the morphology, in a pattern that adequately represents the morphology of the M_1 (Zelditch *et al.*, 2004). The occlusal outline of the M_1 does not offer much choice for landmark positions that fit these criteria, the most obvious sites for landmarks are the twelve points of maximum curvature (Type 2 landmarks of Bookstein, 1991) at the tips and troughs of enamel prisms (Figure 4.1b), and these landmarks will be used throughout the remainder of the study.

Early in the study the use of landmarks placed around the outline of the M_1 (semi-landmarks or Type 3 landmarks of Bookstein, 1991) was experimented with. Marcolini (2006) and Escudé *et al.* (2008b) used this approach but the present author found a number of practical reasons that favoured the adoption of Type 2 landmarks for quantitative description of M_1s. Firstly, many M_1 outlines are often incomplete due to breakage or wear—especially at the ACC and PL, and by the collapse of trailing edges of enamel prisms in Recent and Pleistocene material—or greater development of enamel-free areas (points of attachment of periodontal ligaments mostly visible at the edges of the posterior lobe and the distal part of the ACC). Unless the outline is estimated for these teeth (likely to introduce error), the whole tooth has to be disregarded from analyses if a semilandmark, outline approach is adopted. This would seriously affect sample

size for many fossil and modern assemblages. Secondly, PCA of semi-landmark shapes displayed biologically impossible shapes at the extremes of PC axes, where opposing reentrant angles crossed over one-another. Thirdly, Type 2 landmarks allow inter-landmark distances to be calculated *post hoc* through simple geometry. This cannot be done with outline landmarks that 'slide' around the periphery of the tooth.

The landmark positions chosen are in the main the same as those positions used by earlier authors as anchor points for measurements (Section 2.2), enabling cross-comparison between studies to be possible. The inclusion of other landmarks, for instance within BRA3, was considered, however, the outline of the M_1 is complicated by the presence of the *Mimomys*-fold in some specimens (Section 2.2). It is not possible for a landmark based approach to cope with such evolutionarily and ontogenetically ephemeral features because geometric homology breaks down. Essentially, landmarks cannot be assigned to features such as folds or islands that are present in some teeth yet not present in others. Instead of morphometrically describing features such as the *Mimomys*-fold or enamel islands, the presence and degree of development of these features was noted as discrete characters during data collection to be referred to later if required.

4.1.3.2 Homology

Escudé *et al.* (2008b) assert that two-dimensional landmarks are not appropriate descriptors of the M_1s occlusal outline because 'geometric morphometry requires a precise determination of homologous landmarks, which are relatively difficult to define and sometimes uncertain on vole molars' (Escudé *et al.*, 2008b, p. 2). This statement represents a misunderstanding of the nature of landmarks. MacLeod (2002, p. 129) describes landmarks as '... relocatable reference whose purpose is to locate the approximate relative positions of gross structural elements...'. Individual points, although geometrically homologous, are not biologically homologous, rather it is the whole configuration that describes an object's shape and is biologically homologous (MacLeod, 2002). Landmark based GPA can therefore legitimately be applied to the water vole M_1.

4.2 Data acquisition

The geographic and temporal scope of the project, and the need to adequately describe biological variation in populations, requires a dataset of many hundreds, if not thousands, of M_1 molars. The assessment of this amount of material can only realistically be achieved through digital photography of specimens. Such an approach enables quick and efficient access to museum collections, allows for

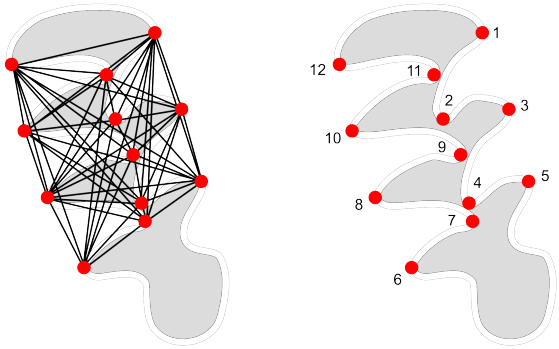

(a) (b)

Figure 4.1: (a) M_1 landmark configuration used in this study, (b) comparison with linear measurement method showing all possible inter-landmark distances required to capture morphological information equivalent to that of landmarks.

flexibility in the analytical approach taken, and builds a referenceable record of the original data for alternative or validatory work. Furthermore, the properties of digital images may be manipulated to improve sharpness and contrast between morphological features.

There are dangers in relying on data collected from photographs. Access time to some museum collections was limited, meaning replicate photographs of all specimens could not be taken. If a photograph was found for some reason to poorly show morphology in a specimen, it was impossible to obtain a replacement image. An attempt to employ an attentive approach to photography using a uniform equipment set-up appears to have made the occurrence of inadequate images rare.

The following section examines the approach taken to image capture and the gathering of raw data for morphological analyses. Copies of images, landmark coordinates, and enamel thicknesses measured can be found in Appendix C, along with data derived from them introduced later in the thesis.

4.2.1 Photography

The equipment used for image capture has a fundamental impact on the scope and analytical approach of the study. The mix of equipment used to photograph specimens (Figure 4.2) was chosen to be an inexpensive, transportable, and quick to assemble set-up, but importantly it permitted consistently detailed, high-magnification photographs to be taken in the wide variety of museum and

university environments encountered during data collection.[1] All images used in this study possess the same magnification, resolution, and background and, as far as could be accommodated, images share similar illumination. This approach was taken in an attempt to reduce error introduced through variable image quality and, because all images have the same properties, to enable a consistent methodology to be applied to measurement and landmarking throughout the entire dataset.

4.2.1.1 Photographic equipment and methodology

The camera set-up (Figure 4.2) consisted of a Canon EOS 350D digital SLR camera[2] fitted with a Sigma 105 mm f/2.8 EX DG macro lens[3] and a 68 mm set of Kenko extension tubes[4]. The camera was secured for desktop shooting using a Benbo 'Mini-trekker' tripod[5], and was positioned above the specimen with vertical shooting guaranteed through the use of a hot-shoe spirit-level. A flash-gun was used to provide additional illumination to background lighting in order to ensure consistent lighting between images[6]. Specimens were positioned in blue plasticine—to give colour contrast with the colour of the tooth—on a laboratory jack beneath the camera. The height of the jack was adjusted to bring the occlusal surface into focus beneath the camera, whose lens was adjusted to the minimum working distance. This procedure meant that the magnification of the camera remained constant between photographs. Specimens were oriented whilst looking through the camera viewfinder and, once positioned appropriately, tethered shooting from a laptop was used to trigger photography, thereby eliminating camera shake and allowing images to be downloaded and reviewed immediately. Photographs appearing poorly focussed or badly lit were retaken with adjustments to the aperture and shutter speed as appropriate.

The following discussion outlines a number of quantitative and qualitative characteristics shared by all the images used in the study, as well as photographic methodology.

[1] This involved extensive testing and thanks must be given to Harry Taylor at the Natural History Museum, London for advice and equipment loans.

[2] `http://www.canon.co.uk/for_home/product_finder/cameras/digital_slr/eos_350d/index.asp?specs=1` (last accessed 16th March 2010)

[3] `http://www.sigmaphoto.com/shop/105mm-f28-ex-dg-macro-sigma` (last accessed 16th March 2010)

[4] `http://www.kenkoglobal.com/` (last accessed 16th March 2010)

[5] `http://www.patersonphotographic.com/` (last accessed 16th March 2010)

[6] Using a Vivitar 283 flash gun, `http://www.vivitar.com/` (last accessed 16th March 2010)

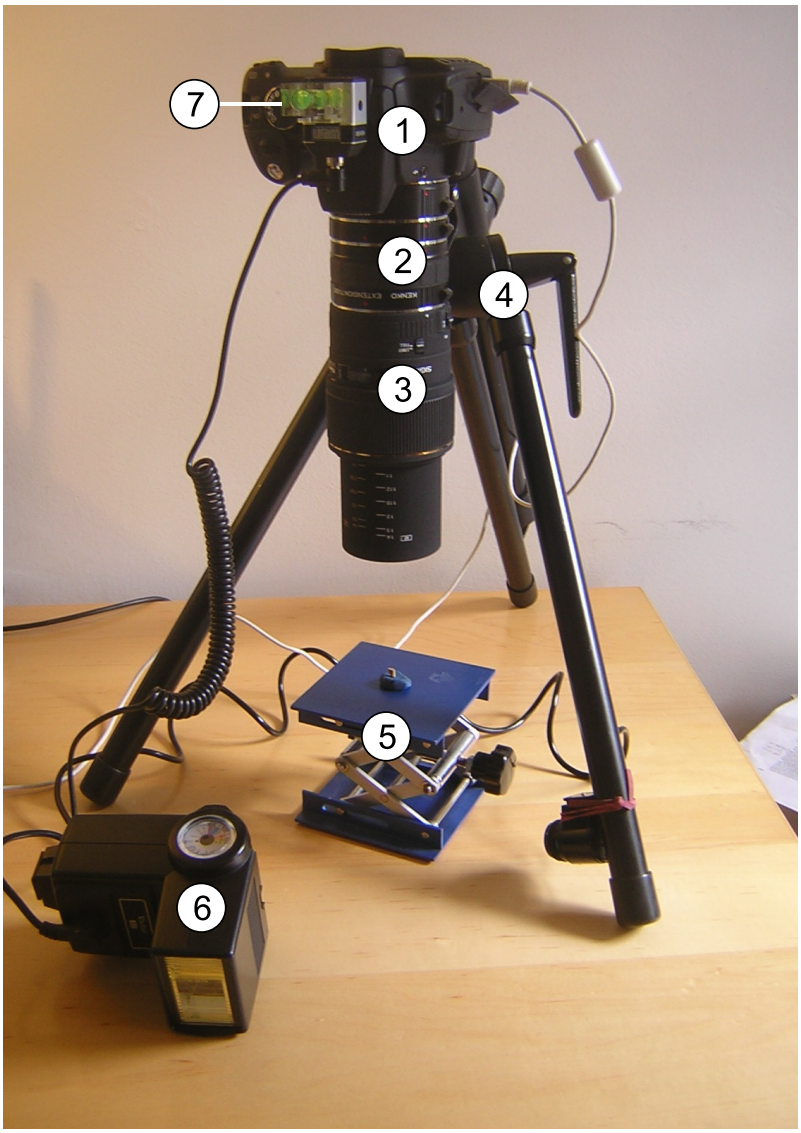

Figure 4.2: Photographic setup used in this study. (1) Canon EOS 350D digital SLR camera, (2) Kenko extension tubes, (3) Sigma 105 mm f/2.8 EX DG macro lens, (4) Benbo 'Mini-trekker' tripod, (5) Laboratory jack and mounted specimen, (6) Vivitar 283 flash gun, (7) Hot-shoe spirit-level.

4.2.1.2 Image magnification and scale

The magnification, or reproduction ratio R, of images was determined by using the following relationship:

$$R = \frac{\text{image size}}{\text{object size}} \tag{4.1}$$

The size of the image is specified by the size of the sensor of the camera, this is 22.2 mm high by 14.8 mm wide. The object size (size of the field of view captured in each image) was determined by taking a number of separate photographs of a Mitutoyo Digimatic CD-6″CSX Caliper set to 1 mm at the same working distance as other tooth images. These images were then viewed on-screen at 100% magnification and the width of the 1 mm scale measured using Screen Calipers 3.2[1], an on-screen measuring instrument. From these Screen Caliper measurements the width and height captured by the whole image was calculated as 10.8 mm wide and 7.2 mm high. Incorporating these dimensions into Equation 4.1 shows the lens and extension tube combination to give a magnification of ×2. This empirical method of quantifying magnification was chosen because of the complexities of using optical theory to accurately calculate magnification using a digital camera with a 35 mm camera lens, and the unknown degree of error in the published focal lengths of commercial lenses (H. Taylor pers. comm., 2009).

4.2.1.3 Image resolution

Photographs were taken at the highest pixel count possible for the equipment, 3456 × 2304 (approximately 8 million) pixels, and were recorded in RAW+JPEG format, which preserves the original level of photographic detail. This strategy attempted to reduce pixelation error (the inability to locate features, such as landmark positions, within an image due to 'blockiness' of that image, see Section 4.3) as much as possible. With an image width of 10.8 mm, this theoretically allows a resolution of just over 3 µm per image pixel (3.125 µm to four significant figures). This figure does not indicate the level of measurement precision obtainable, which is discussed in Section 4.3.

Distortion of images due to optical aberration in the lens is not considered an issue as data on the lenses used show only a 0.25% pincushion distortion (increasing magnification with distance from the centre of the image) across the full width of the frame[2]. This level of distortion is well below the limits of measurement precision (Sections 4.3.2 and 4.3.3) and in addition all tooth images were taken

[1] `http://www.iconico.com`, last accessed 15th July 2010

[2] `http://www.sigmauser.eu/content/view/79/47/` (last accessed 5th June 2007)

with the tooth in the centre of frame where pincushion distortion is virtually nil. The use of the same equipment set-up throughout the project means that any optical distortion effects present will be consistent features of all photographs and therefore should not effect results overall.

4.2.1.4 Depth of field

Depth of field (DOF—ratio of aperture diameter to focal length) is the distance around the focal plane where the image is acceptably sharp. The orientation of M_1s was such that the occlusal surface of the tooth was presented at an angle to the focal plane (Section 4.2.5). Therefore the DOF needs to be wide enough to accommodate the lower and upper parts of this angled occlusal surface. The DOF used was in the order of 2 mm (H. Taylor, pers. comm., 2008), which in the vast majority of instances allowed the whole of the occlusal surface to be well defined. In some specimens with very steep occlusal surfaces the DOF was increased by increasing the f-number on the camera, although this did also effect image quality by reducing image brightness.

4.2.1.5 Lighting

A flash gun was used to achieve consistent lighting of specimens. Camera settings were adjusted to prevent the need for a strong flash, which caused glare from reflections off the often shiny surface molars. White card was also positioned behind each specimen, opposite the flash, to improve diffusion of light from the flash across the whole of the specimen. The lens was set to $f/14$ as a compromise between focal depth and image brightness.

4.2.1.6 Camera orientation

Vertical orientation of the camera was maintained by the use of a photographic spirit-level attached to the hot-shoe of the camera body.

4.2.2 Specimen choice

The selection of specimens to include in an analysis is frequently beyond the control of the investigator, but in most cases some degree of specimen selection needs to be exercised; either because there are large numbers of specimens available and for logistic reasons a subset is required (e.g., Section 3.5.1.2) or because some specimens are damaged or are otherwise inappropriate for analysis.

All specimens were selected so as to possess as complete, as clear, and as well-defined an occlusal surface as possible. Completeness allows comparability of the greatest amount of morphological information between groups, and clarity of the

occlusal surface maximises accuracy and precision in the location of landmarks and the measurement of enamel thicknesses. This means that damaged or eroded specimens were not considered. Furthermore, M_1s from ontogenetically very young individuals were not included in analyses. Very young molars can be found in some collections of modern material but are rare in fossil assemblages. The individuals may be too young to be predated or, if predated, M_1s prove too fragile to withstand digestion. Young specimens may be difficult to landmark if the occlusal surface has eroded insufficiently, and likewise enamel thickness measurements may not be possible (e.g., Figure 2.4 a). These teeth also display extreme morphologies, which would distort the mean shape estimates for an assemblage from GPA. If encountered, only ontogenetically young M_1s with fully developed occlusal surfaces were included in analyses. Further discussion of the relationship between tooth morphology and ontogeny can be found in Section 2.2.3 and Chapter 5.

4.2.3 Landmarking

Images of left M_1s were flipped to make all images appear as right-hand teeth. Landmarks were placed using the graphics package Freehand version 11.0[1] then coordinates collected with a Java[2] script written by the author. Contrast, brightness, and colour balance of images was altered where necessary in order to improve the clarity of morphology. Landmarks were not placed if their location could not be discerned (e.g., if the tip of an enamel prism had been broken). Coordinates were stored in a MySQL database[3], allowing easy retrieval and manipulation. All configurations were checked for landmarking errors. Incorrect assignment of landmark number and misplacement of landmarks were identified by checking for outliers in landmark configurations.

4.2.4 Enamel thickness measurement

Enamel measurement followed (Heinrich, 1982; Figure 2.2b) with enamel thicknesses taken on leading and trailing enamel layers at the midpoints between the tips and troughs of all five prisms, and the midpoint between the extremeties of the PL. Only a single measurement was taken of the enamel layer Pp following Kolfschoten (1990). Many studies have employed two measurements of the posterior wall of the PL but a test dataset of 68 M_1s showed thicknesses at buccal and lingual ends of this enamel layer to be virtually identical (results not shown).

Measurements were carried out on-screen with images at 100% magnification using Screen Calipers, but because on-screen distances differ from real-wrold dis-

[1] `http://www.adobe.com/products/freehand/`, last accessed 26th July 2010
[2] `http://www.java.com/en/`, last accessed 26th July 2010
[3] `http://www.mysql.com/`, last accessed 26th July 2010

tances depicted in each photograph on-screen measurements required calibration. This was done using Screen Calipers by using a photograph containing a digital caliper set to 1 mm, as in Section 4.2.1.2. This 1 mm distance was measured on-screen multiple times using Screen Calipers, and the average on-screen distance obtained showed there to be 340 screen-pixels per millimetre on the photograph (2.94 µm per screen-pixel). This was used to convert on-screen to real-world measurements. The limit of photographic resolution is 3.125 µm (Section 4.2.1.3) and this is the mimimum size of structure that each photograph is able to discern. However, when viewing photographs on-screen, individual pixels within each photograph are not discernible at low to medium magnifications. Therefore, although the edge of an enamel layer cannot be theoretically identified to within ≈3 µm, it should be possible to estimate the limits of such structures within image pixels by considering the whole image and interpolating between adjacent pixels. Screen Calipers were consequently configured to measure below a level of ≈3 µm. The precision and accuracy obtained using this approach are discussed in Section 4.3.3.

As with landmarking, image properties were altered where necessary in order to aid the location of enamel edges. Measurements were stored in a MySQL database in an attempt to reduce retrieval and data manipulation error.

4.2.5 Specimen orientation

The appropriate orientation of specimens for photography is an important consideration. Although the occlusal surface of the M_1 is approximately a flat, 2-D one, the angle at which it develops relative to the direction of growth of the tooth can vary substantially (e.g., Figure 4.4). This is because the plane of the occlusal surface is determined by the angle at which the M_1 wears against opposing upper molars (Section 2.2.1). Empirically, the outline of an M_1 appears longer when the occlusal surface is viewed perpendicular to the line-of-sight—'occlusal view'—rather than when viewed down the growth axis of the tooth—'axial view'—(Figures 4.3c and d respectively), and so questions arise regarding the most appropriate direction from which to view specimens for measurement of occlusal shape and enamel thickness.

The reason this is a matter for concern is because M_1 shape is the model system being used to investigate evolution (Section 2.2). This system is a proxy for the suite of genes that determine M_1 shape and any influences on tooth shape outside this system may disrupt phylogenetic signals present within it. The angle of the occlusal surface is one such potentially disrupting influence. Occlusal angle is determined by factors such as the development of the mandible and jaw musculature and the angle at which the M_1 crown exits the mandible; factors that are not only outside the genetic complex of tooth shape but which are governed by

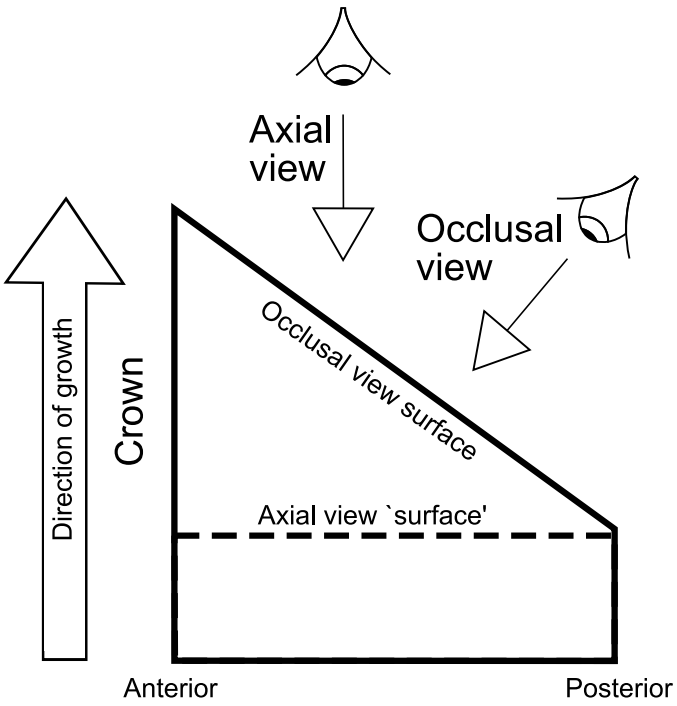

(a)

(b) (c) (d)

Figure 4.3: Orientation of the M_1. (a) Cartoon showing differences between occlusal and axial views. (b) Occlusal-lingual view of a right M_1 showing the angle of the occlusal surface in relation to the growth axis of the tooth (Specimen 3747, Museum ref - NHML 1936.11.16.61). (c) and (d) occlusal and axial views of Specimen 3745, Museum ref - NHML 1936.11.16.20. Scale=2mm.

an interaction between other genetic as well as ecophenotypic factors. In short, occlusal angle is the product of a range of ingredients that would appear largely separate from the complex of genes that determine the shape of the crown.

Previous studies are not explicit in stating the differences between occlusal and axial views or indeed which view is employed. Methodological descriptions generally refer to measurements of the occlusal surface, however, Röttger (1987, p. 99) figures a sketch of an M_1 with measurements taken parallel to prisms (corresponding to axial view), Kolfschoten (1988, p. 116) shows the tooth row of *Arvicola* mandibles with occlusal surfaces perpendicular to the line of sight, and Bermudez de Castro *et al.* (1999, p. 31) clearly figure an M_1 in the process of being digitally measured in occlusal orientation. In order to investigate how M_1 orientation affects morphometric variables a selection of specimens were photographed in both occlusal and axial views (Figure 4.3a), and morphometric measurements compared. The results are discussed below.

4.2.5.1 Achieving occlusal and axial orientations

Axial orientation was achieved by lining the mesial face of the molar with a vertical marker on the photographic stage. Then, while looking through the camera viewfinder, aligning the molar so that the sides of the crown were vertical.[1] Occlusal orientation was found by mounting a horizontal rule on the photographic stage and aligning the occlusal surface with this by eye.

Figure 4.4: Buccal view of an *Arvicola* M_1 showing extreme angle of the occlusive surface with respect to the axis of growth. Scale=2mm. (Specimen 3024, Museum ref - UNW Socha 202).

[1]Note that vertical shooting was ensured by the use of a hot-shoe mounted spirit-level (Section 4.2.1)

4.2.5.2 Orientation and enamel thickness

Do differences exist between enamel thickness measurements made from tooth images taken in either view? Assuming there is a straight plane of wear across the tooth, SDQ values should be the same in both axial and occlusal orientations as the ratio of axial enamel widths will be the same as the ratio of occlusal enamel widths. This assumption was investigated by taking repeated enamel thickness measurements (see Section 4.2.4) on five specimens from Recent populations of *Arvicola* in both views. Comparing SDQ values between orientations shows that SDQs from an occlusal view are generally higher than those in axial view (Figure 4.5). A Model I ANOVA of SDQ values grouped by view indicates that these differences are significant (p=0.05). This is contrary to expectation and could either be caused by trailing edges in occlusal view giving wider measurements than those in axial view or leading edges in occlusal view giving narrower measurements than those in axial view. This was investigated using using the same dataset described above, finding the ratio between the mean enamel thickness of each enamel layer (i.e., L1a, L1p, L2a, L2p, ...) measured in axial view and the complementary measurement in occlusal view (e.g., axial view thickness of L1a/occlusal view thickness of L1a, and so on). Ratios of 1 would indicate that enamel measurements in both orientations are the same, ratios of less than 1 would indicate that of enamel measured in axial view is thinner than that in occlusal view. Boxplots of all of these view ratios[1] grouped by enamel layer edge (Figure 4.6.) show that for leading edges, although very similar, ratios are generally lower in axial rather than occlusal orientations. Furthermore for trailing edges, axial view measurements are consistently lower than the same measurements made in occlusal view. This means that measurement differences in the trailing edge are driving the differences in SDQ between axial and occlusal view.

Observations suggest that these differences are most likely a product of the collapse of thin trailing edge enamel. In many Late Pleistocene and Recent *Arvicola* from central and western Europe the enamel of the trailing edge becomes very thin and weak, often breaking under the stresses of mastication to form a U-shaped trough bucco-lingually (Koenigswald, 1980), while the leading enamel edge remains intact. Fracturing may lead to the development of a cross-section in the trailing enamel that is steeper than that of the leading edge; indeed such breakage is thought to be a functional adaptation of the tooth, enabling molar edges to self-sharpen (Koenigswald, 1977). When viewed in an occlusal orientation this would lead to an exaggeration of the width of the trailing edge with respect to the leading edge. These ideas have not been tested by this study but certainly merit further attention given the importance of the measurement of enamel thickness in

[1]The specimen from Cerignola was omitted as SDQs from both views were very similar.

evolutionary and biostratigraphic research of water voles.

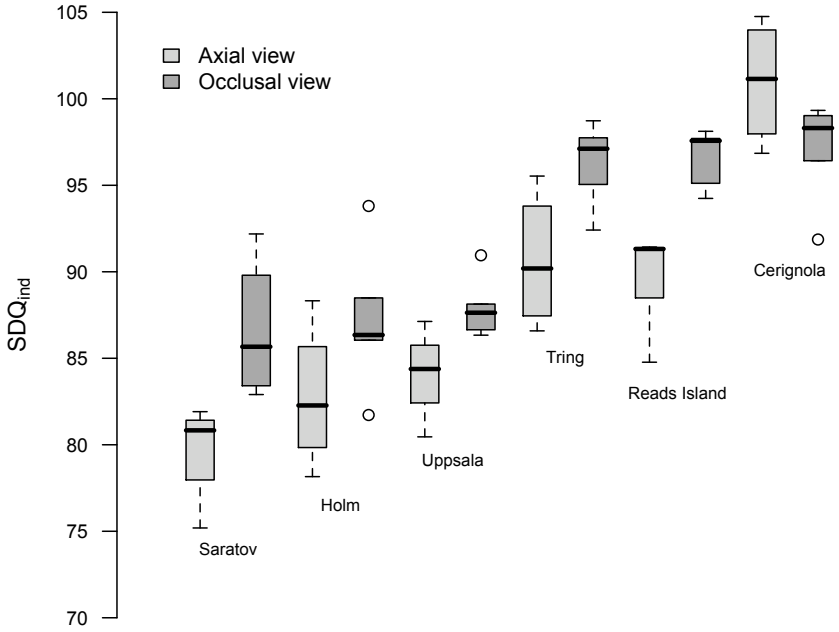

Figure 4.5: Boxplots showing n repeated SDQ values of the same specimens from a selection of Recent populations of *Arvicola* when photographed in axial and occlusal orientations. Cerignola (Specimen 510, Museum ref - NHML 16.7.8.1), $n = 5$; Holm (Specimen 521, Museum ref - NHML 8.8.9.24), $n = 5$; Reads Island (Specimen 462, Museum ref - NHML 60.2118), $n = 5$; Saratov (Specimen 502, Museum ref - NHML 28.4.4.36), $n = 4$; Tring (Specimen 423, Museum ref - NHML 24.12.2.1), $n = 5$; Uppsala (Specimen 514, Museum ref - NHML 0.5.15.1), $n = 4$.

4.2.5.3 Orientation and tooth shape

The effects of orientation on occlusal shape was investigated with a sample of 315 M_1s from a range of Recent and fossil assemblages. Molars were photographed in both axial and occlusal view, landmarked, and together included in a GPA. Shape differences were first assessed with a PCA of shape variables (Figure 4.7). Shapes from both views on the same specimen were found to occur in similar areas of shape space (highlighted by specimens 622 and 3747 in Figure 4.7), meaning similar shapes and patterns of shape change are present in both orientations. Occlusal view shapes are consistently offset to the lower end of PC1 and the upper end of PC2 with respect to axial view shapes. Thin-plate splines (Bookstein, 1991) of shape change (Figure 4.7), which show distortions with respect to the mean shape of a group, show these trends in shape change to be from relatively wider (bottom-right) to relatively longer (top-left) shapes. This is the sort of shape

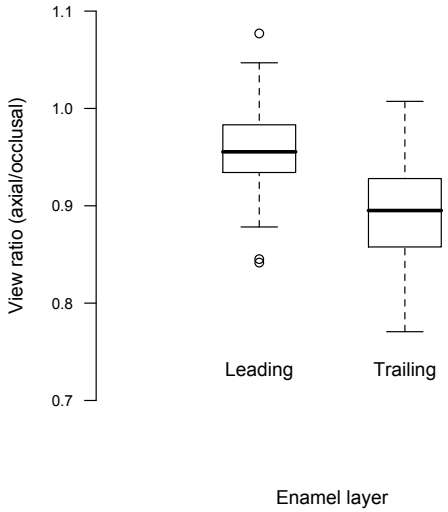

Figure 4.6: Boxplots showing between-orientation ratios of enamel thickness grouped by enamel edge. See Section 4.2.5.2 for further details.

change expected when moving from axial to occlusal view (Figure 4.3). Despite the similarity between specimens in different orientations, shape differences between views appear to become more exaggerated toward the top-left of Figure 4.7. Specimens in this area of the plot are fossil forms such as those from Westbury Cave (Section 3.6.1.3) and suggests that shape differences caused by the development of occlusal angles are greater in these groups than in other water vole groups.

In a second exploration of the relationship between axial and occlusal shapes the D_p—the metric of shape difference—of shapes from different views of the same specimens were plotted against one another (Figure 4.8). The similarities between different views seen in Figure 4.7 are reflected in the good correspondence between specimen views.

The effects of orientation on landmarking error was also investigated and this is detailed in Section 4.3.2. Together, landmarking and orientation error was found to be double that in axial view (9.86%) compared to occlusal view (4.06%).

4.2.6 Discussion

Similarities between shapes from different orientations suggest that inconsistencies in specimen orientation do not have a drastically damaging effect on relative shape relationships (Figures 4.7 and 4.8). However, shape variation does become biased toward longer shapes in occlusal orientations and the amount of shape variation present is around 7% greater in occlusal than axial views[1]. High morphological variation is not necessarily disadvantageous in a character used for evolutionary

[1]Sum of variances across all PC axes were 0.00367 versus 0.00392 respectively.

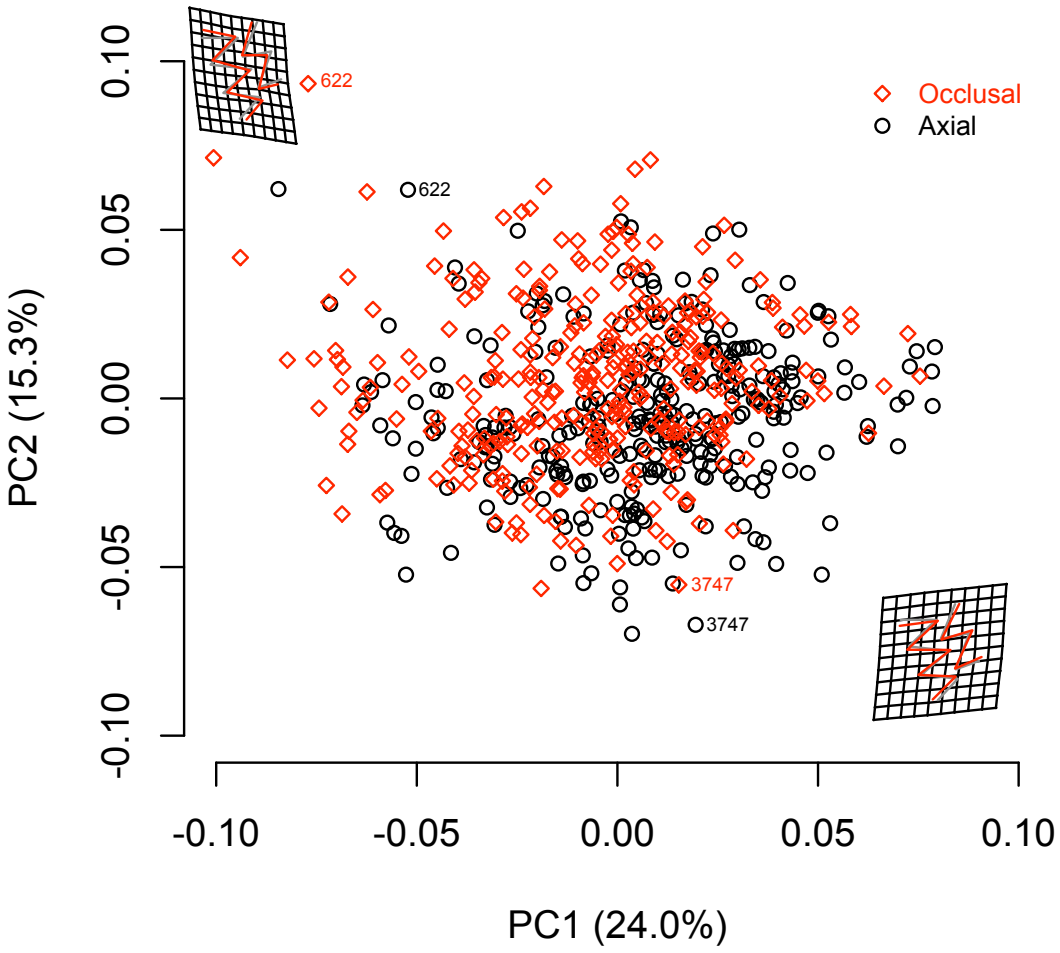

Figure 4.7: Plot of the first two principal component axes from a PCA of 315 occlusally and axially oriented M_1s. Inset thin-plate splines of shape change show the mean shape in grey and shape in that location of the PC plot in red. Wire-frames in thin-plate splines drawn with the anterior of the M_1 pointing bottom-right. Specimens highlighted: Specimen 622, Westbury 14, Museum ref - NHML M37679; Specimen 3747, Carsbreck Pond, Museum ref - NHML 1936.11.16.61.

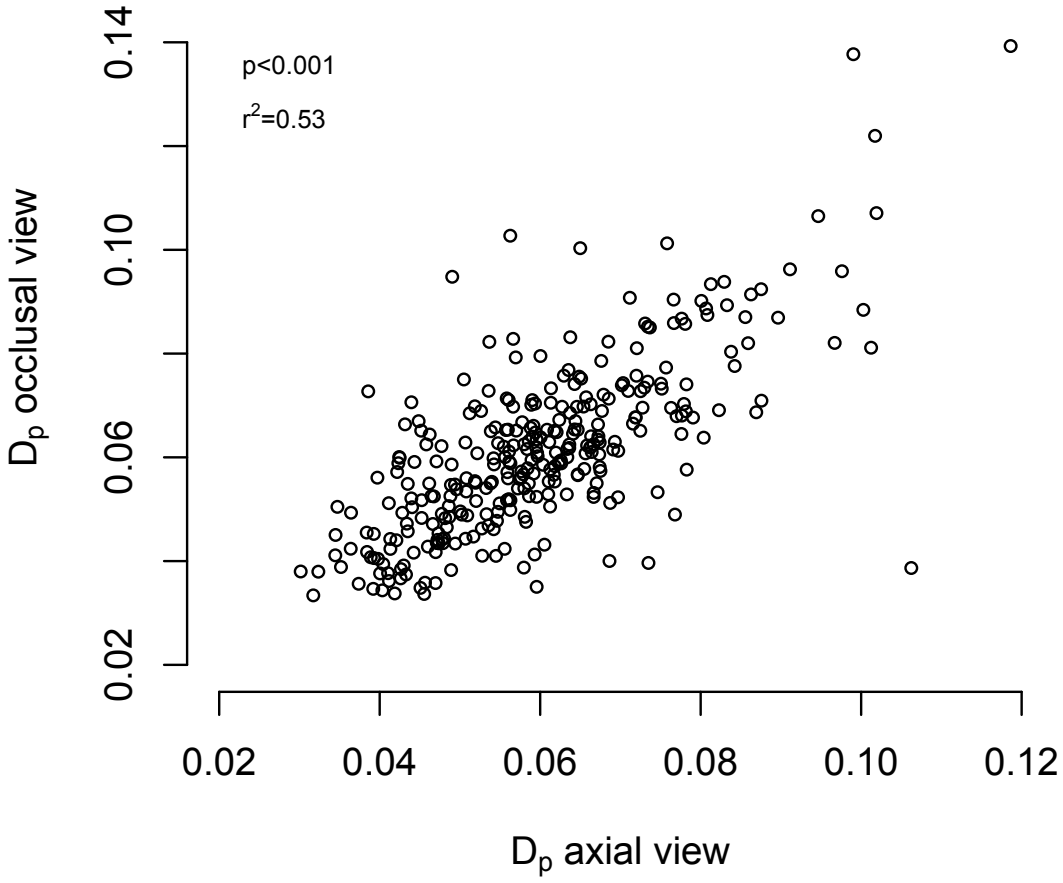

Figure 4.8: Plot of D_p distances from the same specimens viewed in axial and occlusal orientation.

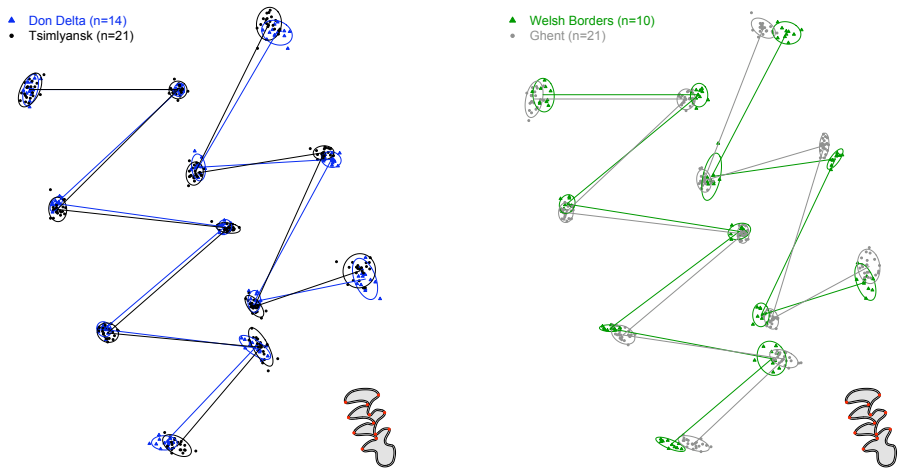

(a) (b)

Figure 4.9: GPS of landmark configurations of two pairs of modern populations from southern Russia (a) and northwest Europe (b). Scatterplots with 95% confidence ellipses and meanshapes, shown with joinlines, convey shape differences. Between population shape variation accounts for 49.5% of the total shape variance between the groups in (a), and 78.3% between the groups in (b).

studies, indeed some of the additional shape variation present in occlusally oriented specimens may be phylogenetically significant. However, the source of such additional variation is likely not to be from the shape of the tooth itself but from other factors (see above).

Axial view shapes seem more vulnerable to increased variation due to landmarking error (Section 4.3.2). This will diminish the ability to discriminate between groups but because variation due to error should be normally distributed around landmark points this should not introduce bias into results. A visual inspection of shape variation between groups—such as in Figure 4.9 for the Recent geographically close groups of Don Delta and Tsimlyansk in southern Russia, and phylogenetically close groups from the Welsh Borders and Ghent—suggests that while some closely related groups are resolvable, high levels of within-group variation may serve to interfere with the ability to identify between-group differences (e.g., Figure 4.9a).

In terms of enamel thickness measurements, evidence suggests true enamel thickness is overestimated in specimens viewed occlusally with increasingly narrow trailing edges. Whether this effect also occurs in specimens with narrow leading edges was not investigated in this study but the presence of such a bias in low-SDQ specimens is good reason to support an axial orientation for specimens.

In summary, the evidence suggests that axial orientation of specimens provides

a more appropriate representation of M_1 morphology than that given in occlusal orientation. Enamel thickness measurements of trailing edges appear to be overestimated in occlusal view as trailing edges become thinner, overall variation in M_1 shape is greater across specimens photographed in occlusal rather than axial view, and differences in shapes obtained from these two orientations become greater the greater the occlusal angle of the tooth. The theoretical basis for the use of the M_1 is therefore strengthened by using an axial orientation. It appears though that patterns of shape difference are generally preserved between shapes from different views, and this gives some confidence that shapes are not fundamentally affected by orientation of specimens. There may be problems comparing results obtained from axially oriented teeth with those in the literature and this issue will be explored in Section 5.6). Any conflicts may be instructive, however, in highlighting methodological differences rather than real patterns in the data.

4.3 Measurement error

The precision and accuracy obtainable in taking measurements and placing landmarks from digital photographs sets a lower limit to the discriminatory power of morphometric analyses. Sources of error may originate from variations in lighting, orientation of specimens, the resolution of the image, and human error in the measurement or landmarking process itself. The levels of error discussed below derive from a combination of all these sources. These errors are distinct from compositional features and biases of the assemblage that are controlled by other factors such as taphonomy (considered separately in Section 4.4).

4.3.1 Quantifying error

The contribution made by error to the measurement of morphometric variation was assessed by taking multiple photographs of specimens, taking multiple measurements and landmark configurations from these photographs, and also by taking multiple measurements from objects of known length. Model I ANOVA was used to partition variance in measurements and landmarks into between- and within-specimen/object components, allowing the percent measurement error (%ME) to be calculated following Bailey and Byrnes (1990):

$$\%\mathrm{ME} = 100.\frac{s^2_{\mathrm{within}}}{(s^2_{\mathrm{within}} + s^2_{\mathrm{between}})} \tag{4.2}$$

where s^2_{within} is the sum of squares within groups calculated as

$$s^2_{\text{within}} = \text{MS}_{\text{within}}, \tag{4.3}$$

where $\text{MS}_{\text{within}}$ is the mean squares within groups, and s^2_{between} is the sum of squares between groups calculated as

$$s^2_{\text{between}} = \frac{\text{MS}_{\text{between}} - \text{MS}_{\text{within}}}{m}, \tag{4.4}$$

where $\text{MS}_{\text{between}}$ is the mean squares between groups and m is the number of repeated measurements. Mean squares were taken from an ANOVA in R.

4.3.2 Landmarking

Error in landmarking was investigated in three ways. Firstly, an assessment of error differences between landmark configurations of specimens in occlusal and axial orientation was performed. Single specimens from four Recent sites[1] were photographed four times in both orientations. M_1s were positioned, photographed, removed, repositioned, and re-photographed non-consecutively. Images were landmarked, those landmarks analysed by GPA, and Procrustes distances (D_p) were used as variables in Equation 4.2. %ME in occlusal and axial views was found to be 4.06% and 9.86% respectively.

Secondly, twenty-two Recent and fossil specimens from nineteen assemblages from across the whole dataset[2] were photographed five times each in axial view in the manner described above, landmarked, and the Procrustes distances from GPA of all configurations were grouped by specimen and used with Equation 4.2. The %ME of samples taken across the whole dataset was found to be 11.7%, which is similar to the 9.86% axial view %ME found above and the same level of error as that found in other morphometric studies (e.g., Polly, 2001, who found %ME of 10–15%).

Thirdly, the effect this level of error has on the measurement of shape variation was explored by comparing differences in shape (%DIFF) between closely related modern populations through a one-way ANOVA (Equation 4.5) following Polly

[1]Drumso, Saratov, Tring, and Uppsala.

[2]Bolshoi Tiganye, Boxgrove, Brillenhöle, Chigirin, Cudmore Grove, Drumso, Dzeravá skala Cave, Frankfurt am Main, Fuchsloch im Krockstein, Kozi Grzbiet-2, Kálmán Lambrecht/IV, Leninsky, Mosbach, Novonekrasovka, Peskö brick red, Pilisszántó, Saratov, Tring, Uppsala.

(2001):

$$\%\text{DIFF} = 100.\frac{s^2_{between}}{(s^2_{within} + s^2_{between})} \tag{4.5}$$

Shape differences between samples from the nearby Recent localities of the Don Delta and Tsimlyansk in southern Russia were compared, and were found to differ by 49.5%. A second comparison between phylogenetically close populations from the Welsh Borders and Ghent were found to differ by 78.3%. Both of these between-group differences are greater than the approximately 10% level of landmarking error found above. This suggests that error on its own does not serve to obscure differences between groups. These comparisons may also be inspected visually (Figure 4.9), which shows the presence of sufficient between-group variation to allow groups to be resolved.

4.3.3 Enamel thickness

4.3.3.1 Measurement error

The precision and accuracy of the on-screen measurement method was investigated by considering the technical error relating to the measurement process itself. Twenty-five rectangles of widths between 10 to 60 screen-pixels were randomly generating (using ImageMagick[1] and and R). These objects approximately corresponded to the thickness variation (measured in screen-pixels) observed in digital images of enamel layers (Section 4.2.4 for details of the measurement process). Rectangle widths were then measured repeatedly, but non-consecutively, five times using Screen Calipers but without prior knowledge of their true size (see Appendix C for rectangle images and measurement data). Precision was calculated as half the mean range of all within-rectangle measurements; this was found to be 1.78 µm. This suggests that sub-micron measurement is not possible but precisions of better than 10 µm can be achieved, and so all enamel thickness measurements were rounded to the nearest micron. The amount of precisional error associated with rectangle measurements was also evaluated using Equation 4.2 and was found to be 0.12%.

Accuracy was estimated by finding the means of differences between the true widths of rectangles and their corresponding set of Screen Caliper measurements. This showed that screen measurements overestimated true widths by a mean of 3.20 µm across the whole dataset. Such a bias is likely to derive from uncertainty

[1] `http://www.imagemagick.org/script/index.php`, last accessed 10^{th} August 2010.

as to the position of the margin of Screen Caliper jaws and suggests that on-screen enamel thickness measurements should be reduced by 3.20 µm to improve accuracy.

Enamel thicknesses measured on-screen were also 'sense checked' for accuracy by comparing screen-based measurements made on M_1s from Biśnik Cave, Poland, with a group of microscope-based measurements taken on the same molars by another researcher[1]. The results of these two methods were found to be in accord, although the microscope-based measurements were larger than on-screen measurements. This can be attributed to the bias in Screen Caliper measurements described above and differences in the orientation of the M_1 adopted in the two different datasets (Section 4.2.5).

The absolute precision and accuracy of this measurement method is best thought of as a minimum set of values describing sources of error present in enamel thickness measurements. Although the rectangles generated are similar to enamel layers in their width on-screen they differ in that their boundaries are sharply defined to pixel edges. The edges of enamel layers are likely to be less easily definable than in rectangles because of natural irregularities in the boundaries of enamel walls, as well as variations of clarity of photographs (Section 4.2.1). A further source of measurement error comes from variation in the positioning and orientation of the M_1, and this is discussed in the following section.

4.3.3.2 Specimen orientation and measurement error

The contribution made by variations in photographic and measurement method to the total amount of error present was quantified by taking four repeated photographs of single specimens from five Recent sites: Cerignola, Holm, Reads Island, Saratov, and Tring. These sites were judged to constitute a representative subsample of morphological variation available at an early stage of the project, although the number of specimens used here do not meet the recommendations of Bailey and Byrnes (1990) for the thorough assessment of measurement error. Specimens were positioned, photographed, removed, repositioned, and re-photographed non-consecutively. Both axial and occlusal views were used (Section 4.2.5) in order to assess the effect of the type of specimen orientation on measurement error. Absolute enamel thicknesses were used in an assessment of error using Equation 4.2.

The relative amount of measurement error across diffferent enamel layers (Table 4.1) was found to range from 11–77% for axial orientation, and 13–45% for occlusal orientation. The two large %ME values for B2p and B3p in axial orientation appear to be outliers when compared with %ME values obtained for other

[1]Kindly provided by Mr. Paweł Socha of the University of Wrocław, Poland.

enamel layers. This is a result of higher within-specimen variation, with respect to between-specimen variation, than that found in other enamel layers; although the %ME for L4p in occlusal orientation is also greater than other occlusal %ME values. An examination of the raw data for B2p and B3p in axial view (see enamel thickness tables in Appendix C) shows there to be a small number of relatively high and low measurements within-specimens from Saratov and Tring, whilst between-specimen thicknesses from all sites is generally constant for these enamel layers. These distinctly different measurements appear to be erroneous because they were made on poorer quality photographs of M_1s whose B2p and B3p walls had collapsed (e.g., cf. ImageIDs 518 and 4185 in Appendix C). Because of these likely measurement errors the %ME values from B2p and B3p must be viewed with caution. The remaining %ME values are broadly comparable, both between enamel layers and between orientations, with around one fifth to a third of variation in enamel thickness accountable by measurement error.

Table 4.1: %ME in enamel thickness measurements from a sample of Recent specimens. Specimens described in Section 4.3.3.

View	B1a	B2a	B3a	L1a	L2a	L3a	L4a	Pp	B2p	B3p
Axial	35	32	30	17	28	20	37	36	63	77
Occlusal	31	20	39	13	30	32	16	37	21	26

cont.

View	L2p	L3p	L4p
Axial	28	11	39
Occlusal	23	27	45

4.3.4 Discussion

For landmarks, %ME in both orientations is within the range found in other morphometric studies. Greater levels of %ME are associated with axial orientation of specimens, which indicates that the process positioning specimens for axial view photography is less repeatable than that used for occlusal view. This elevated amount of relative error does not appear to be sufficient to obscure shape differences between populations, however.

For enamel thickness measurement, the on-screen measurement method allows a precision on the order of microns to be attained, which is comparable to the level of precision attained by other researchers using microscope based methods. The proportion that the measurement process itself theoretically contributes to total measurement error is an order of magnitude (0.12%) less than that estimated

from repeated measurements of photographs of enamel layers (≈20–33%). This indicates that it is variation in the orientation of the specimen and the quality of the photograph that are the major components of enamel thickness measurement error. There is no evidence that differences in the orientation of the M_1 (axial or occlusal) result in different levels of %ME and, as no further repeated measurements were taken on identical copies of photographs, the relative contributions made by these factors to total error cannot be calculated. However, empirically it appears that the quality of the photograph is most significant as, in some cases, it can be very difficult to accurately locate the edge of an enamel band or repeatedly measure enamel in the same location along the enamel layer (see Figure 2.2b). In terms of the latter issue, the definition of the location of landmark points is in many ways less subjective than that for enamel layer measurements (Zelditch *et al.*, 2004). In terms of the former issue, this is a particular problem where there is a lack of colour or textural difference between dentine and enamel such as in many Recent specimens that have a uniformly bleached-white appearance. The accuracy of enamel layer measurements can also be complicated by colour differences within the enamel—a likely reflection of internal microstructural patterns (Koenigswald, 1977)—that obscure the junction between enamel and dentine. Such contrast problems may be wholly or partly addressed by adjusting the colour balance of images to accentuate any colour differences between enamel and dentine. Despite these image modifications there still remain some specimens whose photograph confounds attempts to make secure measurements. In cases where it seems obvious that a photograph does not provide a sufficiently clear image for enamel measurements the specimen will be discounted from analyses.

It is clear from this investigation of measurement error that the measurement of enamel thickness is associated with much higher levels of error than those found in M_1 landmark data. A further issue to consider is that the measurements presented in this thesis are likely in some way to be specific to this study. Other workers with different measuring techniques and equipment may obtain different absolute measurements as well as better or worse levels of measurement error (S. Parfitt pers. comm., 2008). Even the time of day when measurements are taken can have an effect (A. Tesakov pers. comm., 2008). Such issues will be examined further in Section 5.6.

4.4 Sample structure

In this section an attempt is made to explore the influences on the composition of a sample of specimens. Factors such as sexual dimorphism and taphonomic mixing may structure morphological variation in a way that interferes with attempts to recover phylogenetic patterns. This could be because the morphologies present in a sample poorly represent the real evolutionary status of the assemblage, within-sample variation may be inflated and hinder accurate estimation of average morphology, or the array of morphologies may depart from a normal distribution and so undermine the assumptions of statistical tests. Thought of in this way these issues become sources of error. There are numerous factors potentially affecting sample variation, some are quantifiable while others may only be qualitatively estimated. For convenience they may be thought of as those that are natural in origin—either biological or taphonomic—and those related to collection, curation, and study of specimens.

4.4.1 Controls on sample structure

4.4.1.1 Population factors

An initial control on sample structure is the morphological variation within a living population at any one instant in time and space. Arvicolids undergo large fluctuations in population size on a decadal or sub-decadal scale that lead to apparently stochastic changes in genotypic and phenotypic variation at population minima (Gromov and Polyakov, 1992; Evsikov *et al.*, 1997; Giraudoux *et al.*, 1997; Weber *et al.*, 2002; Telfer *et al.*, 2003). Conceivably, modern specimens collected over a single season during a population crash may exhibit different morphologies to specimens collected when the population is at maximum size. Likewise for fossil material a rapid depositional event may capture population variation that is unrepresentative of the long term average. A fossil assemblage accumulated over a number of years, however, may have the advantage of eliminating morphological differences related to demographic change through the averaging of these fluctuations over time. The extent of morphological changes resulting from demographic cyclicity has not been quantified but is at most confined within the range of morphological variation present at maximum population size, and so are likely to be difficult to detect from morphology alone. Furthermore, even if such morphological differences were significant, the much lower numbers of individuals present during a population crash make it less likely that these morphologies would find their way into a fossil assemblage. So, fluctuations in morphology with population size would appear to be more of a potential problem for modern material than for fossil assemblages. If present at all, they are likely to be difficult to detect.

In fossil assemblages a major control on sample structure comes from predator-prey interactions. The vast majority of mortality in arvicolids is from predation of juveniles. Kazantseva and Tesakov (1998) place juvenile mortality at 22–92% in modern arvicolids and estimate that 70–80% of specimens in fossil assemblages were from 1–4 month olds (Kazantseva and Tesakov, 1998) while Woodroffe (2000) estimates *c.* 65% of modern British water vole mortality to be in juveniles. The age structure of a fossil assemblage may have important implications for the estimation of summary morphologies that are at comparable ontogenetic stages between populations (Kazantseva and Tesakov, 1998; Cardini and Elton, 2007; Maul and Parfitt, 2010). Young water voles leave the nest at around 22 days old (Corbet and Harris, 1991) and so are potential victims of predation from this point. The subject of ontogeny and allometry, and numerical methods to account for its presence, is dealt with in detail in Chapter 5.

Environmental conditions may only permit occupation of an area by water voles for a brief period of time, for instance during the decadal-scale climatic ameliorations of the Last Cold Stage. Such ephemeral colonisations were proposed by Roy *et al.* (1996) as an explanation for the occurrence of non-analogue communities, but testing for these brief events is difficult because absolute dating techniques have insufficient resolution prior to the reach of ^{14}C dating to the Last Glacial and Holocene (Jacobi and Higham, 2009).

4.4.1.2 Taphonomic factors

Post-mortem processes of decay and deposition govern resolution and completeness of the fossil record. The key issue with respect to this study is determining temporal resolution; the expectation being that the more discrete an assemblage is, the better the group of specimens within will reflect phylogenetic patterns (Bush *et al.*, 2002; Hunt, 2004). Initially, because the main source of mortality is predation (see above), specimens are subjected to some degree of digestive decay. Birds of prey are the major predator group of voles and lemmings (Kowalski, 2001) and depending on the species of raptor and the robustness of parts of the skeleton many bones and some teeth can be dissolved or substantially damaged by digestive acids (Andrews, 1990), for instance small juvenile molars may be entirely destroyed through digestion. Raptors also act as vectors for the transport and accumulation of specimens through the regurgitation of pellets in tree roosts and caves (Andrews, 1990; Stuart, 2000); this means water vole remains are for the most part autochthonous or parautochthonous assemblages (Behrensmeyer and Hook, 1992).

Following death, the depositional setting influences how discrete the assemblage is and the preservational quality of the material within. The more discrete

an assemblage, the more likely it is to resemble a contemporary sample of specimens. Some depositional events such as mass flow deposits (e.g., West Runton, Section 3.6.1.2, Rose *et al.*, 2008) are extremely brief and may last seconds to hours, however, the specimens entering such a deposit are unlikely to originate from as brief a period (Behrensmeyer and Hook, 1992), rather they may have already experienced perhaps decades or more of residence time in an intermediate deposit such as a superficial soil (e.g., Cudmore Grove, Section 3.6.2.1; Ruddy, 2005). Post-depositional mixing is a major problem for some types of deposit. In high-energy fluvial settings small mammal remains may be readily transported and reworked (Behrensmeyer, 1993), resulting in greatly time-averaged assemblages such as that studied by Popova (2004) who found *Arvicola* from the Last Interglacial to the Holocene in modern fluvial gravels from the Dnieper River, Ukraine. The stratigraphy of cave deposits may also contain time-averaged layers that result from instability or remobilisation of sediments (e.g., Tornewton Cave, Section 3.6.3.6, Currant, 1998). Remains may, however, become protected from disturbance and mixing through obrution (Fürsich, 1993; e.g., Biedensteg, Section 3.5.3.1, Jacobshagen, 1963) or cementation (e.g., Section Fuchsloch-im-Krockstein, 3.5.3.4, Arnold *et al.*, 1982).

The effects of the processes of biostratinomy can be understood through inspection of fossil specimens, sedimentological interpretation of the depositional environment, and absolute dating of specimens. These issues have been discussed on a site specific basis in Chapter 3 but are also explored numerically in Section 4.4.2.2.

4.4.1.3 Collection and study factors

The remaining series of potential controls on sample structure are those relating to collection and curation of remains. For Recent specimens the trapping technique, location, and timing of collection are important factors that may introduce size, age, and sex related biases. Section 5.2 presents tentative evidence that suggests age-structure does differ between groups of specimens in Recent *Arvicola*. The details of trapping are not known for most samples but are likely to have ranged from opportunistic shooting (D. Harrison pers. comm., 2007) to live trapping (various museum records). Where the information is present, collection periods for modern samples span less than a decade and are mostly restricted to the early half of the 20^{th} century.

For fossil material, excavation methods and protocols are paramount in allowing the original structure of a fossil assemblage to be preserved. Some fossil sites have been victim to disturbance by human digging before receiving the attentions of a professional excavation team (e.g., Merlin's Cave, Section 3.6.3.4,

Bate, 1901). Most excavations of the late 19th century and early 20th century were not concerned by small mammal remains and only with the introduction of wet sieving and more rigorous recording methods (e.g., J. W. Jackson, Currant pers. comm., 2009; Hibbard, 1948; Jánossy, 1986) did small mammal palaeontology begin to accrue well provenanced fossil material. Even after excavation, the original stratigraphic relationships of fossil material may be disrupted through poor conservation of specimens (e.g., Ightham Fissures, Section 3.6.3.3, Currant, 1977).

Disturbance of the original stratigraphy caused by excavation or conservation is in effect a form of reworking and may lead to time-averaging of the assemblage. Its occurrence may be explicitly mentioned in the literature, if pre-excavation disturbance was noticed (e.g., Bate, 1901), or hypothesised if excavation methodology seems lacking or if specimens appear to have diverse preservational characteristics, possibly reflecting a multiple provenance of material.

A final series of post-excavation modifications that can be made to the data is the choice and grouping of specimens by the researcher. As outlined in Section 4.2.2 specimens were chosen to be as morphologically complete as possible. This may bias the dataset towards larger, more robust teeth, but a conscious effort was made by the author to sample smaller teeth where they were present and in good enough condition. Furthermore, numerical treatment of the data may correct for ontogenetic variability introduced by the selection of differently sized, and therefore aged, specimens within groups (Chapter 5). Grouping together small samples can be employed as a strategy to obtain a sample of adequate size for analysis (e.g., Caumul and Polly, 2005). This was done in some circumstances for modern material only where specimens were found to be phylogenetically closely related based on the phylogeographic analysis of Piertney *et al.* (2005), and so is not considered likely to adversely inflate within-sample variation.

4.4.2 Observations on sample structure

Having appreciated some of the controls on sample structure, there follows a numerical exploration of some of these issues using the M_1 morphological data obtained for this study.

4.4.2.1 Sexual dimorphism

Other than body size differences between males and females from some populations, no sexual dimorphism has been reported in *Arvicola* (Reichstein, 1982b). Nonetheless, the data from this study were tested for sexual dimorphism using a sample of Recent specimens where the sex of individuals was known. Discontinuities in M_1 size and shape across OTUs were tested for using Model I ANOVA

using sex and OTU as factors to determine the interaction between locality and sex as well as the relationship between morphology and sex.

Size For the body size–sex relationship Centroid Size, a recognised proxy for body size (Section 5.2; Martin, 1993), showed no differences between males and females in size across OTUs and no relationship in size–sex differences between OTUs, but differences between OTUs are significant (Table 4.2).

Table 4.2: Reported results of ANOVA table exploring sexual dimorphism in body size in *Arvicola*. Number of OTUs (N) = 45. Number of specimens (n) = 414.

	Df	Sum Sq	Mean Sq	F value	Pr(>F)
Sex	1	148.41	148.41	0.01	0.9182
OTU	44	8613965.38	195771.94	13.93	0.0000
Sex:OTU	28	352845.29	12601.62	0.90	0.6205
Residuals	340	4778800.91	14055.30		

Shape For the body size–shape relationship D_p was used as a metric of shape. No differences between sex in shape were indicated across OTUs and no relationship in size–shape differences existed between OTUs, but differences between OTUs are significant (Table 4.3).

Table 4.3: Reported results of ANOVA table exploring sexual dimorphism in tooth shape in *Arvicola*. Number of OTUs (N) = 45. Number of specimens (n) = 414.

	Df	Sum Sq	Mean Sq	F value	Pr(>F)
Sex	1	0.00	0.00	0.47	0.4912
OTU	44	0.02	0.00	1.71	0.0046
Sex:OTU	28	0.01	0.00	0.80	0.7571
Residuals	340	0.09	0.00		

4.4.2.2 Sample size

Exploration The effects of sample size on the estimation of morphology from an OTU was investigated in two ways. Firstly, a scatterplot of sample size against shape variation in modern and fossil OTUs was used to explore the relationship between shape variation, sample size, and assemblage type (Figure 4.10). Shape variance was used as a metric of the amount of morphological difference within

OTUs resulting from the factors discussed above (Section 4.4.1). Variance was measured as the summed variance of all principal components of shape variables[1]. Figure 4.10 shows that there is a wider range of variance values with small sample sizes than with large samples, and that this applies to both fossil and modern groups. Modern samples generally possess lower shape variance than fossil assemblages, but there appears to be some structure within the variance of different modern groups.

A more detailed inspection of Figure 4.10 was made through examination of outliers. Initially the groups labelled in Figure 4.10 were inspected for landmarking errors, but the data were found to accurately represent original M_1 morphology. In the fossil samples a number of different taphonomic contexts are represented, these may be instructive of the influence of depositional setting on taphonomic mixing and are considered further in Section 4.4.2.3. In the Recent material none of the uppermost group of four OTUs (with variance around 0.0035) appeared to share common characteristics that explain their higher morphological variance. The sample from Huesca possesses a very small sample size and this may be a possible cause of low shape variation (see below). Huesca is also an Iberian sample and the endemism of taxa in this area of Europe could also be a possible explanation for low morphological variance (Centeno-Cuadros *et al.*, 2009).

Downsampling The appearance of a general pattern of greater range in morphological variance at lower sample sizes led to an second assessment of the effects of sample size on variance and other descriptive statistics through a rarefaction, or downsampling, experiment in the manner of Cardini and Elton (2007). Large samples of M_1s were obtained from three assemblages: Kuznetsovka (Section 3.11.1.3), Merlin's Cave (Section 3.6.3.4), and Mosbach 2 (Section 3.5.1.2). Firstly, one thousand random samples of M_1s were bootstrapped with replacement from each of these assemblages at sample sizes (n) ranging from 2 to n_{max}. Shape variance and mean D_p were measured for each bootstrap sample within groups and their dispersal assessed (Figure 4.11). Secondly, Centroid Size and SDQ values were bootstrapped in same manner as just described but this time just for the Mosbach 2 data, and the variance, mean and median calculated for each bootstrap (Figure 4.12). Both experiments show that small sample sizes provide poor estimates of descriptive statistics such as morphological variance. Only at sample sizes approximately greater than ten do estimates begin to stabilise around the value obtained from the maximum sample size. Figure 4.11 further shows that

[1]Other measures of total shape variation exist, such as the root mean square of the Procrustes distance (RMS D_p; Dryden and Mardia, 1998; Zelditch *et al.*, 2004) but these are, to all intents and purposes, mathematically the same as the summed variance of PCs (Polly pers. comm., 2009). To test this, RMS D_p was also calculated as a measure of shape variation and was found to produce almost identical results to those shown in Figure 4.10 (results not shown).

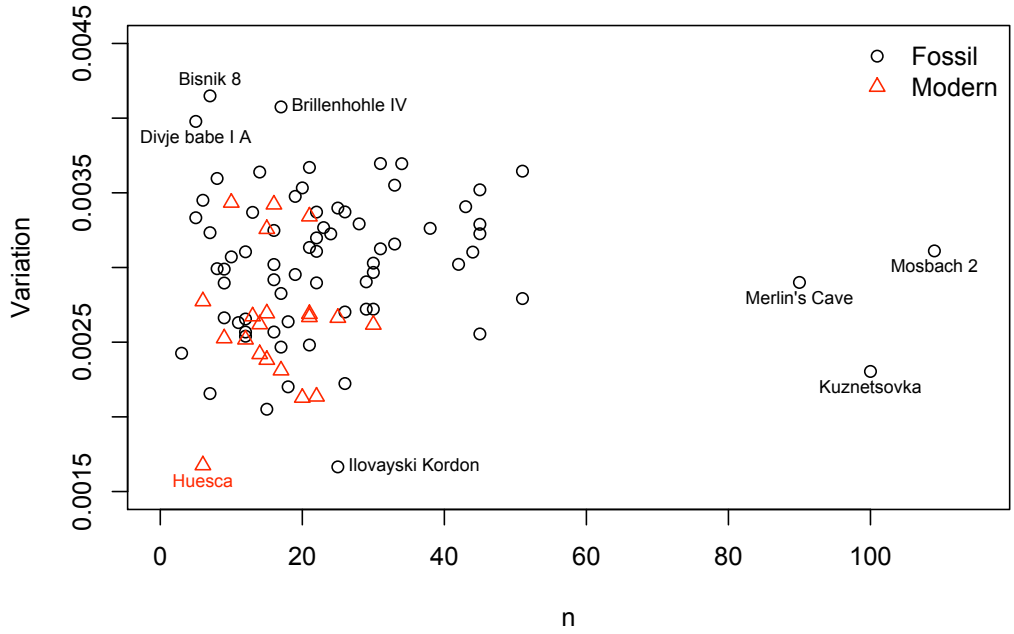

Figure 4.10: Scatterplot of total shape variation in modern and fossil groups of different sample size. See text for discussion.

the structure of the bootstrapped shape variance data are skewed toward lower variance and mean D_p at small sample sizes across all assemblages, a result also reported by Cardini and Elton (2007). In summary these data indicate that sample sizes of at least ten or more are required to provide accurate estimates of taphonomic population statistics. This is similar to sample sizes recommended by Polly (2004) and Cardini and Elton (2007).

4.4.2.3 Assemblage type

Differences in variance between modern and fossil OTUs and between fossil assemblages of different depositional types (Figure 4.10) were investigated. The purpose was to assess whether systematic differences exist in the amount of variation shown by fossil assemblages derived from difference depositional environments and between fossil and modern samples. Fossil assemblages were divided into the broad categories of cave, fluvial, lacustrine, and other type deposits. Boxplots were made of shape variance from OTUs within each category (Figure 4.13) and ANOVA tests were made between groups (Table 4.4[1]). Significant differences were found between modern and fossil OTUs but no differences in shape variance between different depositional groups were supported. Fluvial assemblages had the largest range of shape variance, which may reflect the grouping together of high-energy and low-energy fluvial settings. Low-energy deposits are widely recognised

[1]Barlett's (Sokal and Rohlf, 1995, p 397) and Levene's (Polly pers. comm., 2010) tests for equality of variances found no heteroscedasticity between groups.

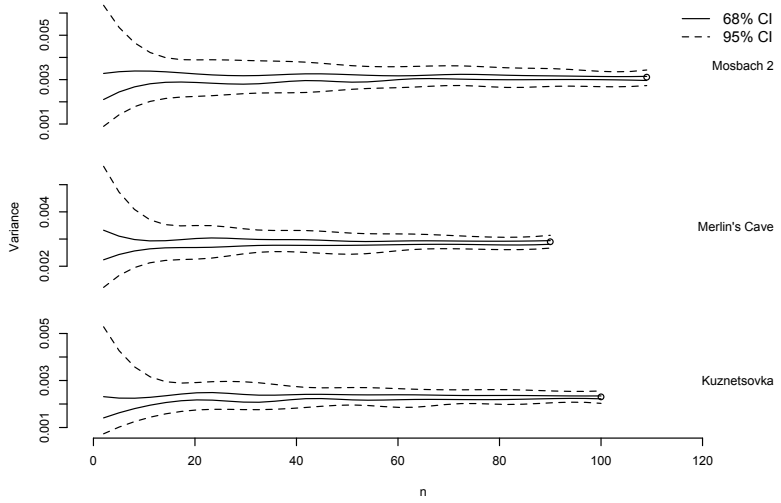

(a) Downsampled variance

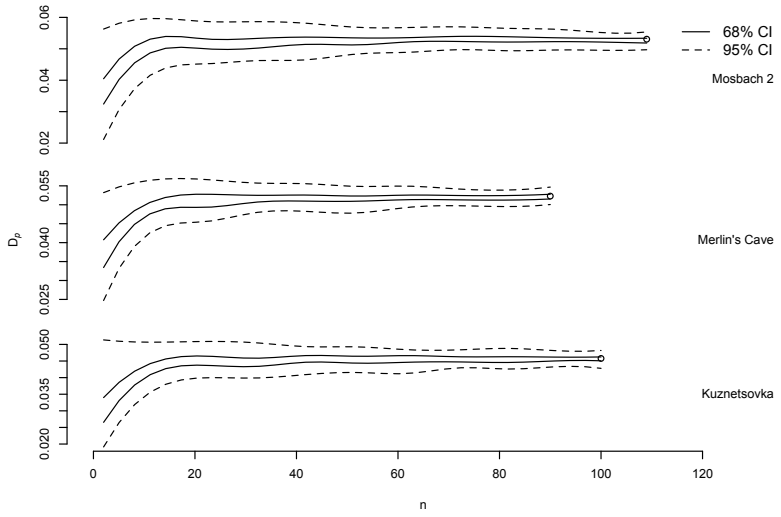

(b) Downsampled D_p

Figure 4.11: Downsampling experiment to show behaviour of M_1 shape variation and D_p with varying sample in three fossil assemblages with large sample size n. Variation is measured as before: the sum of the variance of principal components. 68% and 95% confidence interval estimates from 1000 bootstrapped replicates shown, calculated from the 2.5, 32, 68, and 97.5 percentiles, along with original sample statistics at maximum n. See text for further details and discussion

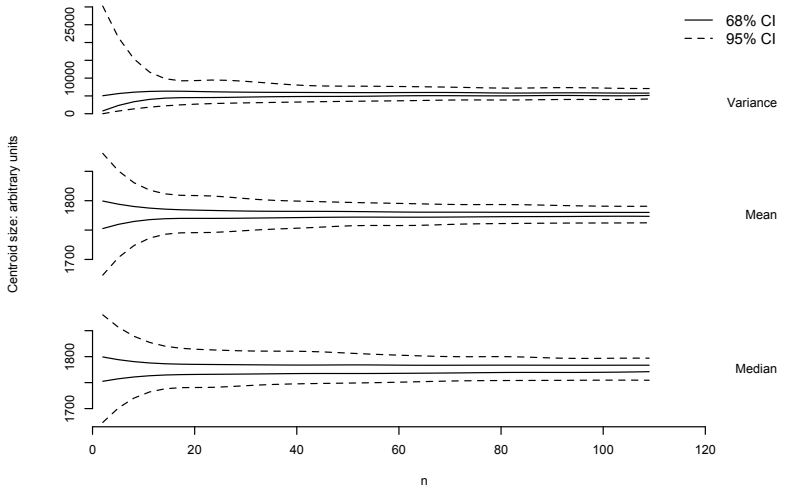

(a) Downsampled centroid size

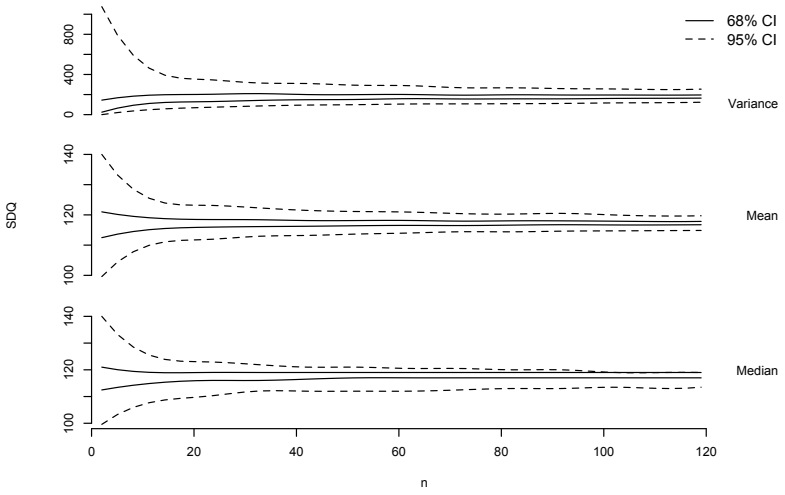

(b) Downsampled SDQ

Figure 4.12: Downsampling experiment to show behaviour of descriptive statistics of M_1 Centroid size and SDQ measurements from Mosbach 2. 68% and 95% confidence interval estimates from 1000 bootstrapped replicates shown, calculated from the 2.5, 32, 68, and 97.5 percentiles. See text for further details and discussion

as less prone to taphonomic mixing and containing better preserved material than high-energy deposits. Cave assemblages possess consistently greater levels of morphological variation than modern samples, and perhaps surprisingly lacustrine sites—low energy environments normally considered to be relatively undisturbed settings—also contain assemblages with high variation.

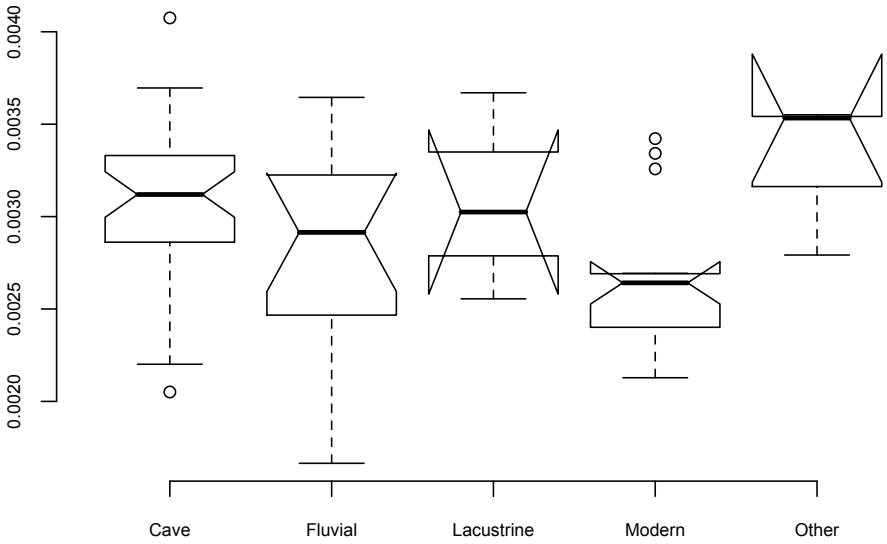

Figure 4.13: Boxplots comparing differences in shape variance between assemblages from different depositional settings. Sample size $n > 10$.

Table 4.4: ANOVA results from comparison of shape variance in different assemblage types.

Assemblage comparison	F-value	p-value
Fossil–Modern	8.4525	<0.01
Between fossil	1.3298	>0.05

Chapter 5

Ontogenetic effects

> Apparently, that is so far as my observation goes, voles of this genus [*Arvicola*] are animals which never stop growing and never grow old ... persistent growth of the cheek teeth appears to be accompanied by persistent growth of the skeleton; in the oldest individuals examined among the enormous amount of fossil and recent material at my disposal, not only are the molars in vigorous growth, but the epiphyses of the limb-bones are stil unfused with their shafts.

Hinton cited in Ellerman, 1940, p. 630

> The whole process of the postnidal ontogenetical development of the M_1 in Recent *Arvicola terrestris* can be seen as a repetition of the phylogenetical development of the species *Arvicola* in Central Europe.

Kratochvíl, 1980, p. 222

5.1 Introduction

Ontogenetic change in the phenotype through life-history is a subject that has attracted much, often controversial, attention in palaeontological studies because of the tantalising relationship between development and phylogeny ('heterochrony': e.g., Gould, 1977; Alberch *et al.*, 1979; Klingenberg, 1998). Evolutionary studies of arvicolids, including the water vole, are no exception here, and ideas about the pace and relative timing of the development of the molar dentition have been integral to the study of the phylogenetic history of the group (Koenigswald, 1982b, 1993; Kratochvíl, 1980; Chaline and Laurin, 1986; Viriot *et al.*, 1993; Neraudeau *et al.*, 1995) and in providing theoretical support for the biostratigraphic use of arvicolid molars (e.g., Heinrich, 1987; Preece and Parfitt, 2008). In terms of the

present study, the possible role played by heterochrony in the evolution of the water vole is not of primary concern to this study. However, as Hinton's comments (above) vividly illustrate, the role played by developmental processes throughout the life-history of water voles appears to be significant, and suggests that their influence on, and contribution to, population-level morphological variation should be investigated.

A consideration of the amount of morphological variation that ontogenetic changes contribute to variation in a sample of specimens is an important precursor to further analyses. For instance, if morphological differences between groups are just age-related differences then incorrect conclusions will be made about phylogenetic similarities between groups. This has certainly historically influenced taxonomic understanding of the water vole, where ontogenetic variation became confused with between-group variation (Hinton, 1926; cf. Kretzoi, 1965). Comparisons between populations should then be made with individuals at equivalent stages of development. Heinrich (1982) noted this issue, and pointed out that enamel thicknesses could only be used for comparisons between different populations in time if the effect of tooth size can be corrected for.

Many studies attempt to address the problem of ontogenetic equality by discarding juvenile specimens from their analyses entirely (e.g., Lister, 1992; Maul *et al.*, 1998a; Caumul and Polly, 2005). This strategy reduces ontogenetic variation in *Arvicola* because the major developmental changes to the M_1 occur very early on in life (Figure 2.3 and 2.4) but the persistence of obviously juvenile features in the adults of *Mimomys* and some *Arvicola*—e.g., the *Mimomys*-fold—(Miller, 1912; Hinton, 1926) show that morphological changes in water vole M_1s are not restricted to one period of ontogeny, nor limited by the age of sexual maturity (Ellerman, 1940; Koenigswald, 1982b). To account for these extended ontogenetic features some authors categorise specimens by their stage of ontogenetic development, using root development and crown height as an alternative measure of ontogenetic stage to occlusal morphology (e.g., Maul and Parfitt, 2010), and then employing age-specific morphology as data for biostratigraphy or phylogenetic reconstruction. The use of crown height and root development as measures of developmental stage may be questioned, however, because they themselves change through evolutionary history (Neraudeau *et al.*, 1995), and so cannot be thought of as accurate ontogenetic markers. Furthermore, for *Arvicola*, the lack of clearly age-dependent traits such as the root, and the subtlety of age-related changes to occlusal shape that may be inseparable from within-adult level variation, make the assessment of age structure difficult. Generally, only in large assemblages of specimens, where a range of tooth sizes and ontogenetically related morphologies are represented, can estimates of ontogenetic allometry begin to be made with some confidence (e.g., Maul and Parfitt, 2010).

Given that ontogeny influences morphology, it would be informative to develop an appreciation of how much of an issue ontogenetic change is in the accurate characterisation of M_1 morphology in fossil and Recent assemblages. This chapter quantitatively explores the way in which ontogeny effects M_1 shape and enamel thickness. The potential effects of ontogenetic variation on phylogenetic reconstruction are assessed in Chapter 6.

5.2 M_1 size: a proxy for ontogenetic age

To investigate ontogenetic effects it is necessary to have some measure of the age of each specimen under study. Martin (1993) noted a strong correlation between M_1 length and body mass for rodents, and this relationship was confirmed in *Arvicola sapidus* and *Arvicola terrestris monticola* (= *Arvicola terrestris*) by Cubo *et al.* (2006). Within groups, body mass is also a function of ontogenetic age, and so M_1 size was tested as a proxy for ontogenetic age in this study by using a sample of 427 specimens of Recent *Arvicola* that were age classified by the present author using the scheme of Hinton (1926).

Hinton's scheme consists of six age divisions (1, a few days or weeks old to 6, oldest adults) based upon proportional development of features of the cranium and mandible and sutures between cranial bones in *A. terrestris* from England. Classifications work well for those forms of *A. terrestris* that share the large, highly angular and rugose adult skull morphology of the English water vole but in other forms such as *Arvicola scherman*, ontogenetic changes in skull shape are less pronounced, and these differences may introduce uncertainty in the ageing of many specimens from continental Europe. Furthermore, imposing a categorical scheme onto the continuous process of growth may be inappropriate in that the amount of morphological change or time-span occurring between successive classes may not be equal, and this could impede mathematical investigation (Zelditch *et al.*, 2004).

Despite these potentially confounding factors, an ANOVA of tooth Centroid Size described by age-class and individual geographical group confirms a highly significant relationship between tooth size and age of the individual (Table 5.1). Group membership also has a highly significant effect on Centroid Size and the interaction between group and age-class is also significant at the 95% level, suggesting differences in age-structure of specimens between groups. These results indicate that M_1 size can be used as a proxy for ontogenetic age within groups of water voles.

Having established a means of estimating the relative ontogenetic position of M_1s within groups, the question of how morphology within groups varies with tooth size will now be explored.

Table 5.1: Reported results of ANOVA table exploring the relationship between age-class and Centroid Size in Recent populations of *Arvicola*.

Source of variation	Df	Sum Sq	Mean Sq	F value	Pr(>F)
Age-class	5	5677892.82	1135578.56	174.58	0.0000
Group	94	5152872.19	54817.79	8.43	0.0000
Age-class:Group	85	802790.33	9444.59	1.45	0.0148

5.3 Ontogenetic change in shape

The morphological changes that occur in the M_1 have been reviewed in Section 2.2.3. In this section the relationship between M_1 shape and tooth Centroid Size are investigated quantitatively. The amount of shape variation explainable by size is compared with total shape variation among molars, and the direction of shape–size change (ontogenetic trajectory) is also examined.

5.3.1 Relationships with size

5.3.1.1 Methods

Size-shape relationships were investigated in the following way. Principal component analyses (PCA) of Procrustes coordinates—relative warp analysis of Bookstein (1991) and Rohlf (1993)—were performed within groups and multivariate regressions were then carried out between tooth Centroid Size and the scores from each principal component (PC) axis using the linear regression equation

$$y = c + bx + e \tag{5.1}$$

where y is a vector of dependent variables (shape variables), c is a vector of constants equivalent to the intercept of bivariate regression, b is a vector of regression coefficients, x is a vector of independent variables (Centroid Size), and e is an error term. This use of PC scores as shape variables produces the same results as direct multivariate regression of shape variables on size (e.g., Frost *et al.*, 2003; Mitteroecker *et al.*, 2005; Cardini and Elton, 2007) but was computationally convenient in that it allowed immediate assessment of the amount of shape variance explained by size (e.g., Figure 5.6). Previous studies (e.g., Frost *et al.*, 2003; Mitteroecker *et al.*, 2005; Cardini and Elton, 2007) have employed the natural logarithm of size. In this study, data were found to be approximately normally distributed and did not show heteroscedasticity (results not shown), and experi-

mentation showed that log transforming Centroid Size had negligible effect on the regression results. Log transformations may also introduce bias into age estimations (Smith, 1993) and therefore it was felt that there was no good reason to use log Centroid Size in shape–size regressions.

Following the statistical framework for shape data proposed by Goodall (1991), the significance of shape–size regressions (P_{Goodall}) and the proportion of shape variation explained by tooth size within each sample (%var_{size}) were found from the amount of shape variation explained in each regression model compared with the total shape variation found within each sample. A permutation test was also used as a second test of regression significance, which simulates the null hypothesis of complete independence between size and shape (Good, 2000). For this permutation test, sizes and scores were randomly reassigned and regressed, and the sum of squared regression coefficients ($\sum b^2_{perm}$) compared with those derived from the original regression ($\sum b^2_{orig}$). This was repeated 1000 times and the proportion of permuted regressions where $\sum b^2_{perm}$ equals or exceeds $\sum b^2_{orig}$ determines the P-value (P_{perm}).

Only samples with $n \geq 10$ were used in an attempt to suppress sample size related variability in descriptive statistics (Section 4.4.2.2), leading to a dataset of 15 Recent samples and 63 fossil assemblages. The range of Procrustes distances (range D_p) within groups was also calculated and is shown alongside the regression diagnostics discussed above as a guide to relative amounts of total shape variation between groups. Regressions and significance tests were carried out in R with the Goodall's F-test based upon the scripts provided by Claude (2008) and the permutation test built by this author. One in ten R-based regressions were cross-checked in MorphoJ (Klingenberg, 2008) and were found to agree.

5.3.1.2 Results

Tables 5.2 and 5.3, and Figure 5.1 show results from shape–size regressions in Recent and fossil groups. In both sets of regressions there is good agreement between P_{perm} and P_{Goodall}, although the permutation test appears to be the more conservative of the two. Many groups show significant shape–size relationships. In Recent groups 10 and 11 of the 15 samples show significant shape–size regressions in P_{perm} and P_{Goodall} respectively. In the 63 fossil groups, 23 and 29 samples show significant shape–size regressions in P_{perm} and P_{Goodall} respectively. Where regressions were significant, size explained between 9.2% (Leninsky) and 29.4% (Novomirgorod) of total shape variation within Recent groups and between 2.5% (Mosbach 2) and 27.7% (Ightham Fissures) in fossil groups. Mean and median %var_{size} for Recent and fossil groups is 13.58/11.7% and 8.0/6.3% respectively.

Inspection of scatterplots of these data (Figure 5.1) suggest that no relationship

exists between range of shapes in a sample (range D_p) and $\%var_{size}$ in either Recent and fossil groups. This is confirmed by poorly supported regressions between $\%var_{size}$ and Range D_p (P=0.186 and P=0.453 respectively), and by reference to D_p values of apparently juvenile individuals that show no correspondence to extremes of D_p within groups. No significant relationship was found between sample size and $\%var_{size}$ for Recent groups (P=0.096) but a significant correlation was found between sample size and $\%var_{size}$ for fossil groups (P <0.05). This appears to be driven by three groups with large n (Merlin's Cave, Kuznetzovka, and Mosbach 2; Figure 5.1 B, Table 5.3). Although tooth size can account for up to nearly a third of total shape variation in all groups, size related shape variation explains less than 25% of total shape variation in 95% of all groups (Figure 5.1). Overall, $\%var_{size}$ is more variable and often greater in smaller samples, and the range of $\%var_{size}$ in Recent and fossil groups are similar in groups of similar size.

Examination of fossil groups suggests that shape–size relationships require more than ontogenetic allometry to explain the patterns of variation. In groups where the largest amount of shape variation is explained by tooth size, both population-level and other factors appear to be in operation. The Ightham Fissures group exhibits the greatest amount of shape variation explained by size of all fossil groups but no M_1s from this group are qualitatively identifiable as juveniles. The shape–size relationship in Ightham may be subtle, and therefore concealed from qualitative observations. Alternatively, the observed relationship reflects shape–size contrasts between different populations in time and space caused by excavation or post-excavation mixing of fossils (Section 3.6.3.3). In Marie-Jeanne Cave 4, some juvenile molars are present (e.g., SpecimenID 3630), and so the 23.7% of shape variation explained by size may be consistent with an allometric explanation, although this assemblage also has some taphonomic issues (Section 3.2.1.1). Pisede III (Section 3.5.4.1) appears to be a good candidate for a fossil group where allometric changes are prominent. This assemblage seems relatively unaffected by taphonomic mixing and contains some distinctively juvenile molars alongside adult molars—including one very young specimen (SpecimenID 2830), which explains the very large range of Procrustes distances within the assemblage.

5.3.2 Ontogenetic trajectories

Understanding whether age has the same effect on morphology between populations is important because it informs the approach needed to correct for the effects of ontogenetic age. In other words, can a single shape–size trajectory through shape space explain all ontogenetic shape changes, or do individual groups follow their own shape–size paths. The manner in which molar shape changes with age is investigated below.

5.3.2.1 Methods

Similarity between the trajectories of shape–size change through shape space was tested using a permutation test proposed by Mitteroecker *et al.* (2005). Shape–size regressions were performed within groups and the sum of the squared residuals (SSR_{orig}) from all regressions was calculated. Then the affiliation of specimens to groups were randomly reassigned, the within-group regressions recomputed, and the sum of squared residuals (SSR_{boot}) obtained. This last step was performed 10 000 times. If groups share a common ontogenetic trajectory then SSR_{orig} should be smaller than the distribution of values in SSR_{boot}. Identical trajectories can be rejected as a hypothesis when $(C + 1)/(N - 1) \leq \alpha$, where C is the number of instances where SSR_{orig} is less than values from SSR_{boot}, N is the number of permutations made (in this case 10 000), and α is significance level (in this case 0.05).

Samples from the Recent localities of Novomirgorod, Frankfurt am Main, and Prokhladny possess the strongest evidence for the ontogenetic allometry observed in all the Recent groups (Section 5.3.1.2) and so it was decided to use only these groups to test whether groups share common trajectories. The permutation test was performed using PC scores from PCA of Procrustes superimposed shape variables and was scripted in R by the author.

5.3.2.2 Results

The permutation test outlined above showed that ontogenetic trajectories were not shared between the groups Frankfurt am Main, Novomirgorod , and Prokhladny (P=0.000). This was explored further by visualising the ontogenetic trajectories of two of these groups—Novomirgorod and Frankfurt am Main—through a plot of scores from the first three PC axes with the size of the plotting symbols reflecting Centroid Size (Figure 5.2). Both groups in Figure 5.2 show that the main trends in shape–size change are associated with PC1, but the direction of size change across all three PC axes appears to be different in the two groups. A single, large specimen from Frankfurt can be seen to be an outlier on PCs 2 and 3, however, which acts to draw the two trajectories apart. This confirms the results of the permutation test.

In summary, it appears as though the relationship between shape and size in the Recent groups examined cannot be explained simply through a single shape–size relationship.

Table 5.2: Strength of correlation between shape and size in Recent groups with $n \geq 10$. Range D_p shows the range of D_p found within groups. P-values from a permutation test (P_{perm}) and Goodall's F-test ($P_{Goodall}$) presented alongside % variation explained by shape–size regressions (%var_{size}). Table ordered by %var_{size}.

Group	n	Range D_p	P_{perm}	$P_{Goodall}$	%var_{size}
Novomirgorod	13	0.0436	=0.000	=0.000	29.4
Frankfurt am Main	15	0.0703	=0.000	=0.000	28.5
Prokhladny	20	0.0394	<0.001	=0.000	20
Central Scotland	14	0.0587	<0.05	<0.001	16.5
Kama-Volga	17	0.0358	<0.01	=0.000	14.7
Moscow	25	0.0592	=0.000	=0.000	14.5
Linares de Riofrio	14	0.0376	0.079	<0.05	12.2
Welsh Borders	20	0.0510	<0.05	<0.001	11.7
Don Delta	14	0.0458	0.187	0.096	10.9
Leninsky	30	0.0757	<0.01	=0.000	9.2
Ghent	21	0.0398	0.12	0.052	7.7
Tsimlyansk	21	0.0708	0.206	0.156	6.5
Cheshskaya Guba	21	0.0479	0.281	0.259	5.9
Aggeel	15	0.0393	0.755	0.832	5.1
Kabardino-Balkariya	22	0.0366	0.765	0.85	3.3

Table 5.3: Strength of correlation between shape and size in fossil groups with $n \geq 10$. Range D_p shows the range of D_p found within groups. P-values from a permutation test (P_{perm}) and Goodall's F-test ($P_{Goodall}$) presented alongside % variation explained by shape–size regressions ($\%var_{size}$). Table ordered by $\%var_{size}$.

Group	n	Range D_p	P_{perm}	$P_{Goodall}$	$\%var_{size}$
Ightham Fissures	13	0.0591	<0.001	=0.000	27.7
Marie-Jeanne Cave 4	10	0.0291	<0.05	<0.001	23.7
Pisede III	20	0.1083	<0.01	=0.000	16.4
Kartstein	12	0.0309	<0.05	<0.05	15.6
Burgtonna South Black-earth	16	0.0731	<0.05	<0.001	15
Tönchesberg II 11-13	21	0.0481	<0.01	=0.000	14.5
Ossom's Eyrie Cave	44	0.0541	=0.000	=0.000	14.3
Novonekrasovka upper	12	0.039	0.095	<0.05	14.3
Clacton Channel IV	21	0.0457	<0.01	=0.000	13.1
Bolshoi Tiganye	30	0.0527	=0.000	=0.000	12.4
Fortuna utca 16-18/2	22	0.0515	<0.05	=0.000	11.8
Ilovayski Kordon	25	0.0317	<0.01	=0.000	11.6
Trou du Frontal	11	0.046	0.364	0.366	10.8
Cudmore Grove	51	0.0804	=0.000	=0.000	10.4
Brillenhohle IV	17	0.0653	0.109	<0.05	10.1
Régourdou 3	12	0.0231	0.371	0.37	9.8
Gunki II	16	0.0391	0.139	0.078	9.7
Pisede IV&V	33	0.0772	<0.01	=0.000	9.7
Westbury 11	16	0.0863	0.17	0.105	9.3
Régourdou 5	21	0.0613	0.056	<0.01	9.3
Marie-Jeanne Cave 2	16	0.062	0.188	0.109	9.2
Bridged Pot inner slope	13	0.0298	0.434	0.422	8.6
Komarowa D	16	0.0451	0.297	0.26	7.8
Marie-Jeanne Cave 6	16	0.0285	0.285	0.269	7.8
Abzac	19	0.0518	0.182	0.11	7.7
Poeymaü BS	18	0.0376	0.24	0.165	7.6
Merlin's Cave	90	0.0558	=0.000	=0.000	7.4
West Runton Freshwater Bed	45	0.0654	<0.01	=0.000	7
Wigber Low 26	51	0.0591	<0.001	=0.000	6.5
Korotoyak-4	26	0.0521	0.1	<0.05	6.5
Grotta del Broion, Sala Grande Q4	22	0.0484	0.189	0.117	6.5
Grotta del Broion, Sala Grande N	29	0.0394	0.065	<0.05	6.3
Kozi Grzbiet 2	42	0.1512	<0.05	=0.000	6.2
Grotta del Broion, Sala Grande R1	38	0.058	<0.05	<0.001	6.1
Régourdou 7	26	0.0319	0.1	0.061	6.1
Fuchsloch im Krockstein	23	0.066	0.191	0.148	6
Boxgrove 4c	22	0.0851	0.266	0.19	6
Medzhybozh-2	22	0.0633	0.228	0.202	5.9
Peskö "brick red" strata	45	0.0787	<0.01	=0.000	5.8
Westbury 14	31	0.0632	0.063	<0.05	5.8
Vindija G	43	0.0671	<0.05	=0.000	5.8
Kalman Lambrecht IV	12	0.057	0.831	0.921	5.5
Bisnik 12-13	14	0.069	0.7	0.842	5.4
Courbet	45	0.0692	<0.05	<0.001	5.3
Rybnaya Sloboda	19	0.0763	0.446	0.513	5.3
Kuznetsovka	100	0.0861	=0.000	=0.000	4.9
Tornewton Cave Red Cave Earth	18	0.0572	0.561	0.716	4.8
Donskaya Negatchevka	17	0.0267	0.633	0.764	4.8
Chigirin	31	0.047	0.185	0.124	4.6
Horváti-lik 13	22	0.0554	0.487	0.536	4.5

Continued on next page

Table 5.3 continued from previous page

Group	n	Range D_p	P_{perm}	$P_{Goodall}$	$\%var_{size}$
Vladimirovka 2	30	0.0585	0.207	0.158	4.5
Horváti-lik 8	29	0.0506	0.256	0.26	4.2
Horváti-lik 9a	33	0.0854	0.196	0.159	4.1
Rotbav-Dealul Ţiganilor Clay-A	26	0.0849	0.547	0.606	3.6
Pilisszántó	43	0.0669	0.136	0.075	3.5
Dzeravá skala Cave	34	0.0573	0.325	0.333	3.4
Schöningen 13-II-4	29	0.0412	0.461	0.566	3.3
Grotta del Broion, Sala Grande Q5	28	0.0598	0.53	0.634	3.2
Miesenheim I	24	0.0788	0.709	0.818	3.1
Vindija E-F	25	0.06	0.7	0.802	3.1
Boxgrove 4b	21	0.031	0.88	0.949	2.8
Hundsheim	45	0.0724	0.299	0.291	2.6
Mosbach 2	109	0.0768	<0.01	=0.000	2.5

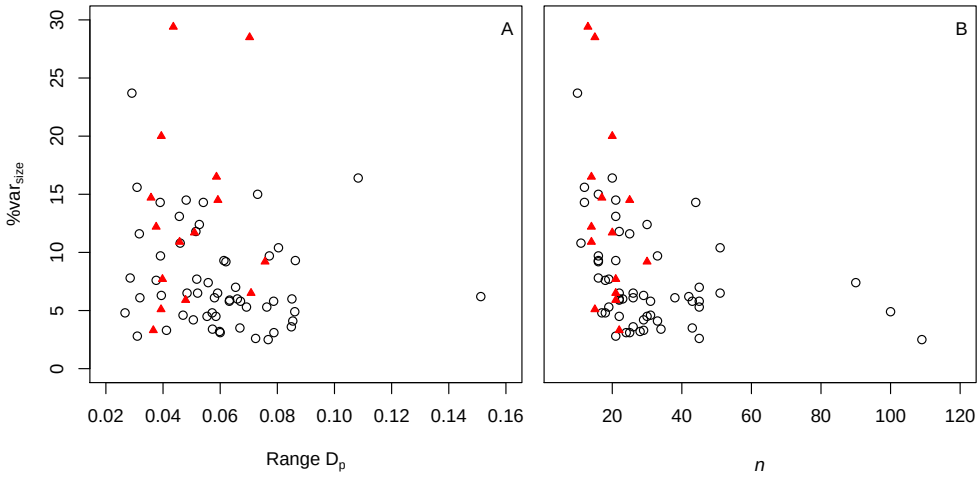

Figure 5.1: Scatterplots of $\%var_{size}$ with range D_p (A) and sample size n (B) from shape–size regressions of Recent (red triangles) and fossil (circles) groups.

5.4 Ontogenetic change in enamel thickness

Kratochvíl (1980) showed that in populations of Recent water voles from central Europe all enamel layers thicken during development. Furthermore, that leading edge enamel thickens more rapidly than trailing edge enamel, leading to juvenile animals possessing a *Mimomys*-differentiation and adults a *Microtus*-differentiation. This section examines the relationship between enamel thickness and tooth Centroid Size in the data obtained by this thesis. A sample of 212 Recent specimens from 15 localities[1] are used, which allow comparisons to be made with the findings of Kratochvíl (1980).

[1]Aggeel, Central Scotland, Cheshskaya Guba, Don Delta, Frankfurt am Main, Ghent,

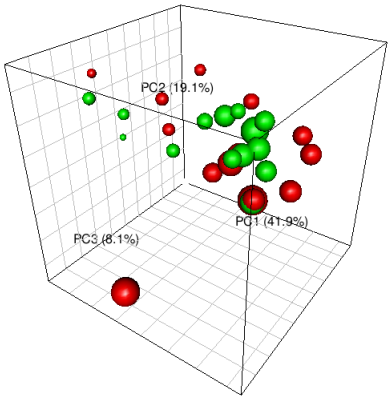

Figure 5.2: Change in molar shape with age. 3D plot of scores from the first three PC axes from a PCA of shape variables from Novomirgorod (green spheres) and Frankfurt am Main (red spheres). Sphere size corresponds to molar Centroid Size.

5.4.1 Relationships with size

Initial exploration of the whole dataset was carried out through pairwise plots of enamel thickness, SDQ, and Centroid Size (Figures 5.3 and 5.4). These suggest strong and positive enamel thickness–size relationships exist, as well as positive but less strong relationships between SDQ and Centroid Size. Furthermore, relationships between thickness and size of anterior enamel layers (Figure 5.3) superficially seem less strong than for posterior enamel layers (Figure 5.4). A trend appears to exist between SDQ and both enamel thickness and Centroid Size but these relationships do not seem to be simple.

Linear regressions were then carried out between enamel thicknesses from each enamel layer and Centroid Size within groups. Two of the regression diagnostics—significance, P, and coefficient of determination, R^2—are reported in Tables 5.4 and 5.5, and within-group enamel thickness–size relationships are plotted in Figures B.1–B.12 in the Appendix. In Recent groups only Leninsky and Novomirgorod were found to show significant enamel thickness–size relationships at the $P = 0.05$ level across all enamel layers (Table 5.4). R^2 values for these two groups show that size explains 20–55% of variation in enamel layer thickness within Leninsky, and 61–83% of variation in enamel layer thickness within Novomirgorod. In other groups the amount of enamel thickness explained by size varies greatly, for example between 0% (L3a and L4a) and 70% (L1a) in Aggeel (Figure B.1b) or 0% (B1a and L2a) and 15% (L3p) in Cheshskaya Guba.

Kabardino-Balkariya, Kama-Volga, Leninsky, Linares de Riofrio, Moscow, Novomirgorod, Prokhladny, Tsimlyansk, and Welsh Borders.

Additional within-group enamel–size regression statistics, including fossil groups, are reported in Appendix Tables B.2, B.3, B.4, and B.5. These data show that up to 95.1% of enamel thickness can be explained by size in Recent groups (Frankfurt am Main), and 88.2% in fossil groups (Kartstein).

5.4.2 Ontogenetic trajectories

Plots of enamel thickness and Centroid Size within groups show that enamel thickness in trailing and leading edges increases with molar size (Figures B.1–B.12 in the Appendix). This confirms the findings of Kratochvíl (1980). The trajectory of increase in thickness does not appear to be the same between groups, however. In the Recent groups Frankfurt am Main (Figure B.3e) and Novomirgorod (Figure B.8d) regressions predict leading edge enamel thickening at a faster rate than trailing edges, but rates of thicknening are different between these two groups. In Aggeel (Figure B.1b) no consistent between-triangle enamel–size relationships are indicated. Tests for difference between trajectories in Recent groups (Table 5.6; Warton *et al.*, 2006) suggest that enamel–size relationships between groups are not shared. Ontogenetic trajectories of eight of the thirteen enamel layers differ significantly between groups, and most other enamel layers approach significant difference at the 0.05 level (Table 5.6). This may not be considered surprising in view of the regressions shown in Novomirgorod and Aggeel, which demonstrate that the directions of ontogenetic trajectories are variable in groups where there is poor representation of individuals from across the whole ontogeny. The sample from Novomirgorod possesses a relatively large sample size (n=13) and comprises a range of molar sizes that result in similar regression trajectories between enamel triangles. Frankfurt am Main is a smaller sample (n=5) but trajectories are comparable with those of Novomirgorod due to the wide range of tooth sizes found within the group. Aggeel has a small sample size (n=5) and because tooth sizes within this sample are similar, there is little enamel thickness variation, and so attempts to fit regression models do not produce consistent results. Similar evidence for variable ontogenetic trajectories can also be found in shape–size relationships for differences in ontogenetic trajectories between groups, apparently for the same reasons (Section 5.3.2.2).

Only enamel thickness changes in Recent groups have been considered up to now. In fossil groups the general pattern of enamel thickness increasing with molar size remains. However, the relative trajectories of leading and trailing edge thickening differ between many fossil assemblages and Recent samples. Figure B.12b shows enamel thickness–size regressions for the early Middle Pleistocene West Runton Freshwater bed assemblage. Here trailing edge enamel thickens more rapidly than leading edge enamel, in contrast to the trajectories of Recent

groups.

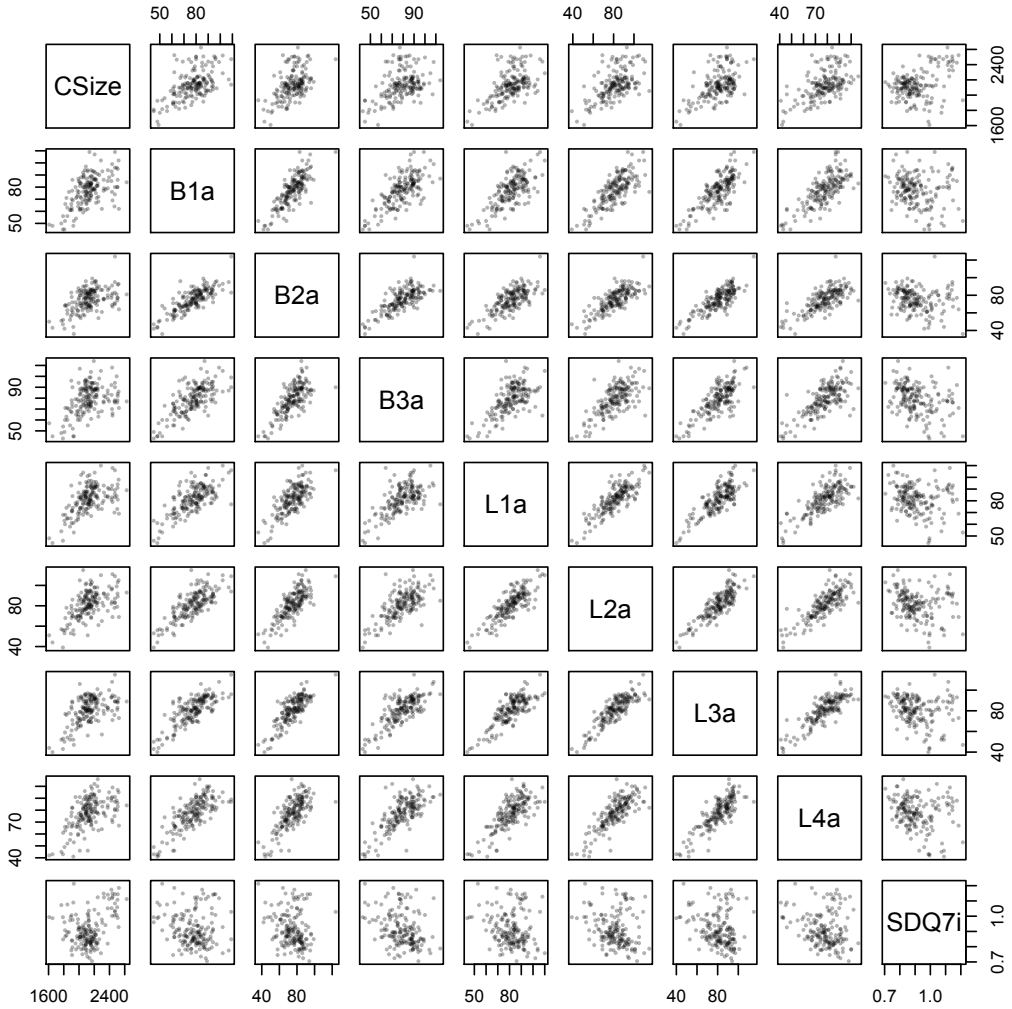

Figure 5.3: Matrix of pairwise plots of anterior enamel thickness in µm (refer to Figure 2.2b for enamel layer nomenclature), SDQ (SDQ7), and Centroid Size (CSize) in Recent specimens.

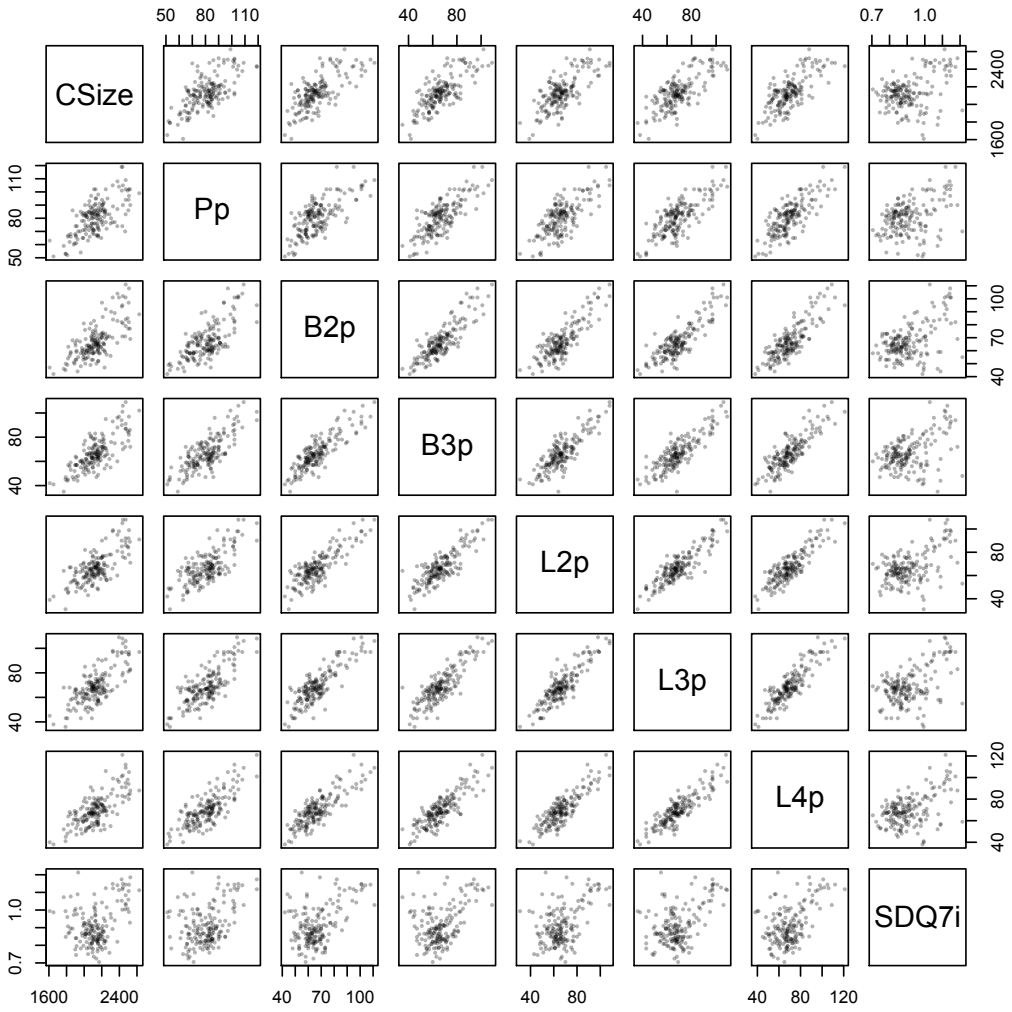

Figure 5.4: Matrix of pairwise plots of posterior enamel thickness in µm (refer to Figure 2.2b for enamel layer nomenclature), SDQ (SDQ7), and Centroid Size (CSize) in Recent specimens.

Table 5.4: Significance values of linear regressions of enamel thickness and Centroid Size within Recent groups. Group sample size given alongside group name. *P*-values marked by * denote significance at the 0.05 level.

	B1a	B2a	B3a	L1a	L2a	L3a	L4a	Pp	B2p	B3p	L2p	L3p	L4p
Aggeel (n=5)	0.697	0.877	0.425	0.076	0.595	0.994	0.988	0.396	0.655	0.736	0.784	0.431	0.133
Central Scotland (n=13)	0.021*	0.062	0.020*	0.002*	0.091	0.019*	0.009*	0.000*	0.023*	0.003*	0.037*	0.140	0.000*
Cheshskaya Guba (n=19)	0.766	0.505	0.136	0.456	0.857	0.718	0.257	0.238	0.119	0.446	0.545	0.095	0.590
Don Delta (n=7)	0.830	0.925	0.919	0.645	0.765	0.513	0.328	0.487	0.360	0.830	0.829	0.312	0.379
Frankfurt am Main (n=5)	0.147	0.255	0.055	0.028*	0.099	0.053	0.092	0.005*	0.580	0.945	0.755	0.492	0.812
Ghent (n=18)	0.806	0.941	0.845	0.370	0.768	0.980	0.048*	0.340	0.021*	0.899	0.293	0.936	0.329
Kabardino-Balkariya (n=19)	0.460	0.251	0.329	0.029*	0.698	0.812	0.724	0.709	0.627	0.698	0.987	0.479	0.264
Kama-Volga (n=13)	0.002*	0.002*	0.169	0.023*	0.033*	0.085	0.016*	0.135	0.048*	0.010*	0.011*	0.021*	0.042*
Leninsky (n=20)	0.002*	0.006*	0.002*	0.001*	0.001*	0.000*	0.008*	0.047*	0.007*	0.000*	0.000*	0.001*	0.002*
Linares de Riofrio (n=7)	0.913	0.597	0.948	0.477	0.055	0.016*	0.260	0.106	0.239	0.733	0.048*	0.192	0.040*
Moscow (n=21)	0.246	0.678	0.898	0.220	0.148	0.202	0.363	0.013*	0.571	0.021*	0.077	0.166	0.202
Novomirgorod (n=13)	0.000*	0.000*	0.001*	0.001*	0.001*	0.000*	0.000*	0.001*	0.000*	0.000*	0.019*	0.012*	0.008*
Prokhladny (n=15)	0.146	0.409	0.726	0.766	0.788	0.489	0.263	0.625	0.682	0.085	0.750	0.187	0.721
Tsimlyansk (n=15)	0.113	0.098	0.170	0.225	0.466	0.278	0.116	0.937	0.014*	0.430	0.578	0.037*	0.240
Welsh Borders (n=22)	0.067	0.062	0.311	0.214	0.831	0.173	0.022*	0.743	0.005*	0.007*	0.013*	0.299	0.016*

Table 5.5: R^2 values of linear regressions of enamel thickness and Centroid Size within Recent groups. Group sample size given alongside group name.

	B1a	B2a	B3a	L1a	L2a	L3a	L4a	Pp	B2p	B3p	L2p	L3p	L4p
Aggeel (n=5)	0.058	0.009	0.221	0.704	0.105	0.000	0.000	0.245	0.075	0.044	0.029	0.215	0.584
Central Scotland (n=13)	0.398	0.281	0.403	0.607	0.237	0.408	0.479	0.744	0.386	0.574	0.339	0.187	0.805
Cheshskaya Guba (n=19)	0.005	0.027	0.126	0.033	0.002	0.008	0.075	0.081	0.137	0.035	0.022	0.155	0.017
Don Delta (n=7)	0.010	0.002	0.002	0.046	0.020	0.090	0.190	0.101	0.169	0.010	0.010	0.202	0.157
Frankfurt am Main (n=5)	0.558	0.396	0.758	0.844	0.650	0.763	0.666	0.951	0.113	0.002	0.038	0.169	0.022
Ghent (n=18)	0.004	0.000	0.002	0.051	0.006	0.000	0.223	0.057	0.291	0.001	0.069	0.000	0.059
Kabardino-Balkariya (n=19)	0.033	0.077	0.056	0.251	0.009	0.003	0.007	0.008	0.014	0.009	0.000	0.030	0.073
Kama-Volga (n=13)	0.598	0.601	0.165	0.389	0.350	0.245	0.424	0.191	0.309	0.463	0.460	0.397	0.325
Leninsky (n=20)	0.420	0.351	0.407	0.454	0.438	0.543	0.332	0.202	0.341	0.545	0.556	0.465	0.425
Linares de Riofrio (n=7)	0.003	0.060	0.001	0.106	0.553	0.720	0.244	0.437	0.263	0.025	0.575	0.313	0.602
Moscow (n=21)	0.070	0.009	0.001	0.078	0.107	0.084	0.044	0.285	0.017	0.249	0.156	0.099	0.084
Novomirgorod (n=13)	0.705	0.703	0.681	0.678	0.652	0.832	0.757	0.621	0.804	0.762	0.405	0.448	0.485
Prokhladny (n=15)	0.155	0.053	0.010	0.007	0.006	0.038	0.095	0.019	0.013	0.211	0.008	0.130	0.010
Tsimlyansk (n=15)	0.182	0.196	0.140	0.111	0.042	0.090	0.179	0.001	0.384	0.049	0.024	0.295	0.104
Welsh Borders (n=22)	0.158	0.164	0.051	0.076	0.002	0.091	0.234	0.006	0.330	0.307	0.273	0.054	0.257

Table 5.6: Results of tests for similarity of regression trajectory between enamel thickness and Centroid Size in Recent groups

	B1a	B2a	B3a	L1a	L2a	L3a	L4a	Pp	B2p	B3p	L2p	L3p	L4p
P-value	0.01	0.03	0.25	0.00	0.02	0.00	0.00	0.00	0.00	0.01	0.00	0.21	0.00

5.5 Correcting for ontogeny

Unlike other sources of morphological variation in M_1s, such as time-averaging in fossil assemblages, ontogenetic effects can be quantified through the regression of morphological variables with tooth size (Sections 5.3 and 5.4). This allows the possibility of removing morphological variation related to ontogeny and therefore perhaps improving the phylogenetic information contained within morphological data in the process. Burnaby (1966) proposed a 'correction' for the effects of allometry that projects individuals along a morphology–size regression into a space orthogonal to the trajectory of allometry. The method, as originally conceived, produces growth-invariant variables by applying the same allometric trajectory across many groups. The evidence presented in Sections 5.3.2 and 5.4.2, however, suggests that ontogenetic trajectories are not shared between, or cannot be sufficiently well resolved in, water vole groups. This would make Burnaby's approach invalid, but a modification of the method may allow ontogenetic variation to be removed within groups. This involves using within-group regressions to project morphometric variables to the maximum specimen size within each group by adding the residuals to the estimate at maximum size. In this way a population of individuals with 'adult' morphological characters can be modelled (Figure 5.5). This section outlines the steps that can be used to model the ontogenetic component of shape variation from a sample of specimens.

5.5.1 Modelling adult shape

The effects of size were removed from M_1 shape data by regressing scores on Centroid Size as in Section 5.3.1, taking the estimated fitted score from each PC axis at maximum Centroid Size and adding these to the residuals to give estimated scores for each specimen at maximum size. Each PC score represents an M_1 shape in shape space that can be modelled as a shape in real space. It is therefore possible to use estimated scores at maximum tooth size to create models of shapes that represent an adult population. Shape models are constructed by multiplying each estimated score by its corresponding eigenvectors, summing the results across all PCs, and finally adding the mean-shape for the OTU (Rohlf, 1993; Polly, 2008a). This procedure can be formalised as

$$\hat{X} = PU^T \tag{5.2}$$

where $\hat{X}$ is the modelled shape, P is the position being modelled, and U^T is the transpose of the eigenvectors.

An example of the whole approach is can be seen for the Recent Frankfurt am

Main group. In Figure 5.5, PC1 scores are regressed against Centroid Size and a series of modelled scores at maximum size are estimated. Figure 5.6 develops the modelling process into more dimensions of shape space by showing shapes projected to maximum Centroid Size across the first three PC axes. Over 40% of shape variation is explained by PC1 and it is along this axis that the greatest size changes occur. Finally, Figure 5.7 shows how the original Procrustes superimposed coordinates relate to whole shapes modelled to 'adults' of maximum Centroid Size using Equation 5.2.

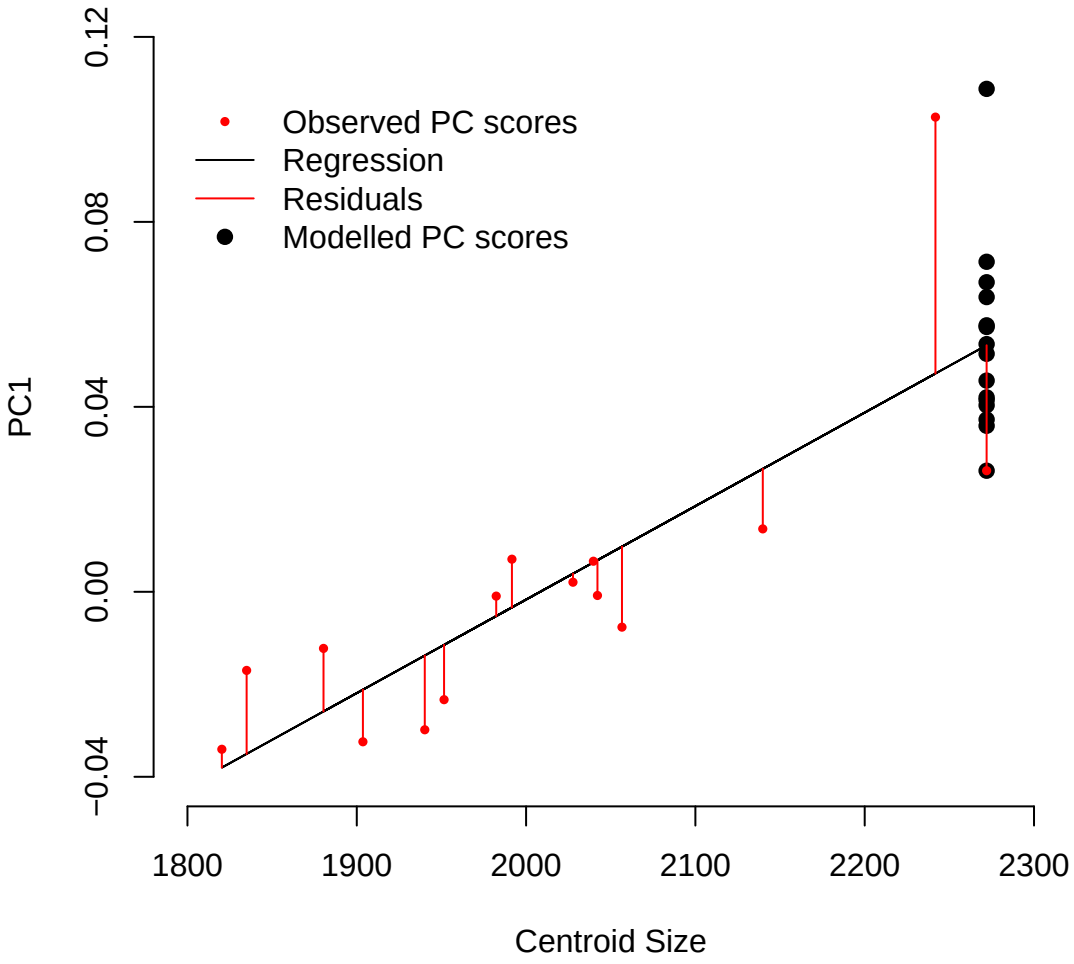

Figure 5.5: Modelling shape to create an adult population from an ontogenetic range of individuals. Here, scores along PC1 are regressed against Centroid Size and the residuals are added to the score estimated at maximum Centroid Size to give a series of scores for all individuals modelled to maximum Centroid Size. Data from Frankfurt am Main.

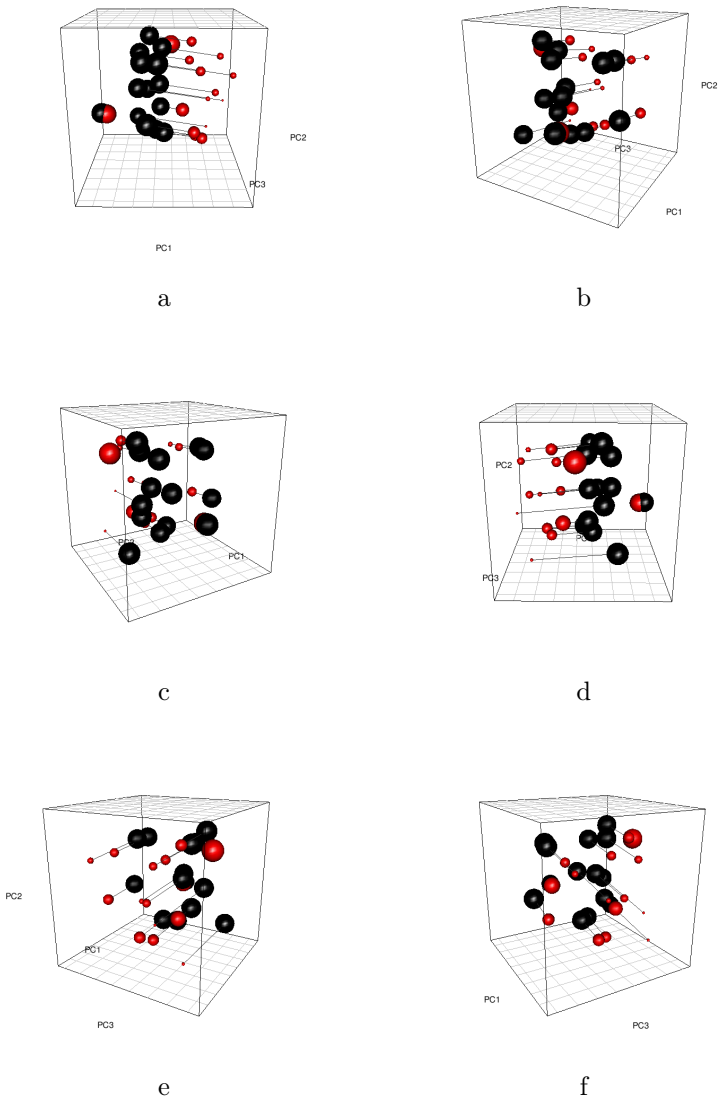

Figure 5.6: Ontogenetic shape change in a sample of Recent *Arvicola* from Frankfurt am Main, Germany. Plots of the first three principal components of morphospace shown in six views (a–f) rotated anti-clockwise about the north pole of the plot. Red spheres represent observed shapes while black spheres show shapes of specimens when modelled to 'adult' size, with the path of projection shown by lines connecting spheres. Radius of spheres proportional to Centroid Size. PCs 1, 2,and 3 account for 41.5%, 15%, and 9.7% of total shape variation respectively.

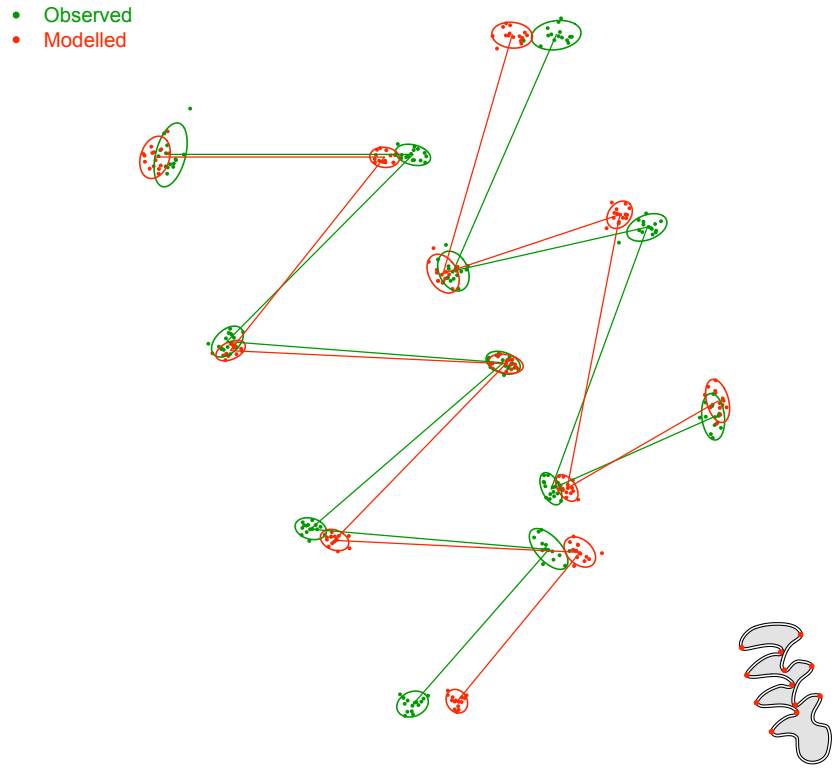

Figure 5.7: Comparison of observed shape variation and shape variation modelled at maximum Centroid Size in *Arvicola* from Frankfurt am Main, Germany. 95% confidence intervals and wireframes of meanshapes shown.

5.5.2 Modelling adult enamel thickness

The enamel thickness ratio (SDQ) is a derived value describing the relationships between two traits, and not a morphological trait in itself. Furthermore, Figures 5.3 and 5.4 indicate that enamel thickness–size relationships are stronger than the strength of correlation between SDQ and size. It is therefore more appropriate to carry out any modelling exercise on enamel thickness rather than the SDQ. Modelling can be accomplished in the same manner as for shape variables, namely the thickness of each enamel layer is regressed with Centroid Size within groups and the residuals added to the thickness estimate at maximum Centroid Size. Graphical examples of this method applied to all fossil and modern groups can be found in Figures B.1–B.12 in the Appendix. For the majority of groups enamel thickness increases with molar size but the slopes of enamel thickness–size regressions differ between groups, as discussed in Section 5.4.2.

Comparisons of unmodified and size-corrected enamel thicknesses are shown in Figure 5.8, and enamel thickness and SDQs in Figure 5.9. These plots show good correspondence between both datasets, with size-corrected enamel thickness explaining between 63% and 77% of the variation in unmodified enamel thickness. A small number of size corrections give thinner modelled enamel than that from the original enamel layers (points plotting below the 1:1 regression slope, which can be seen traced by the break in the density of plotted points). However, there is a systematic bias towards higher size corrected values, showing that size-correction overwhelmingly results in thickening of modelled enamel.

In terms of the effect that size-correction has on the SDQ (Figure 5.9 bottom right panel), the two datasets are strongly comparable in that almost all the variation in size-corrected SDQs can be explained by original SDQ values. There appears to be a tendency, however, for SDQs based on size-corrected enamel thickness to have lower values than those calculated from unmodified enamel thickness, although this is not a strong effect. The stratigraphic implications of changes in SDQ values that result from size-correction will be considered in Chapter 7.

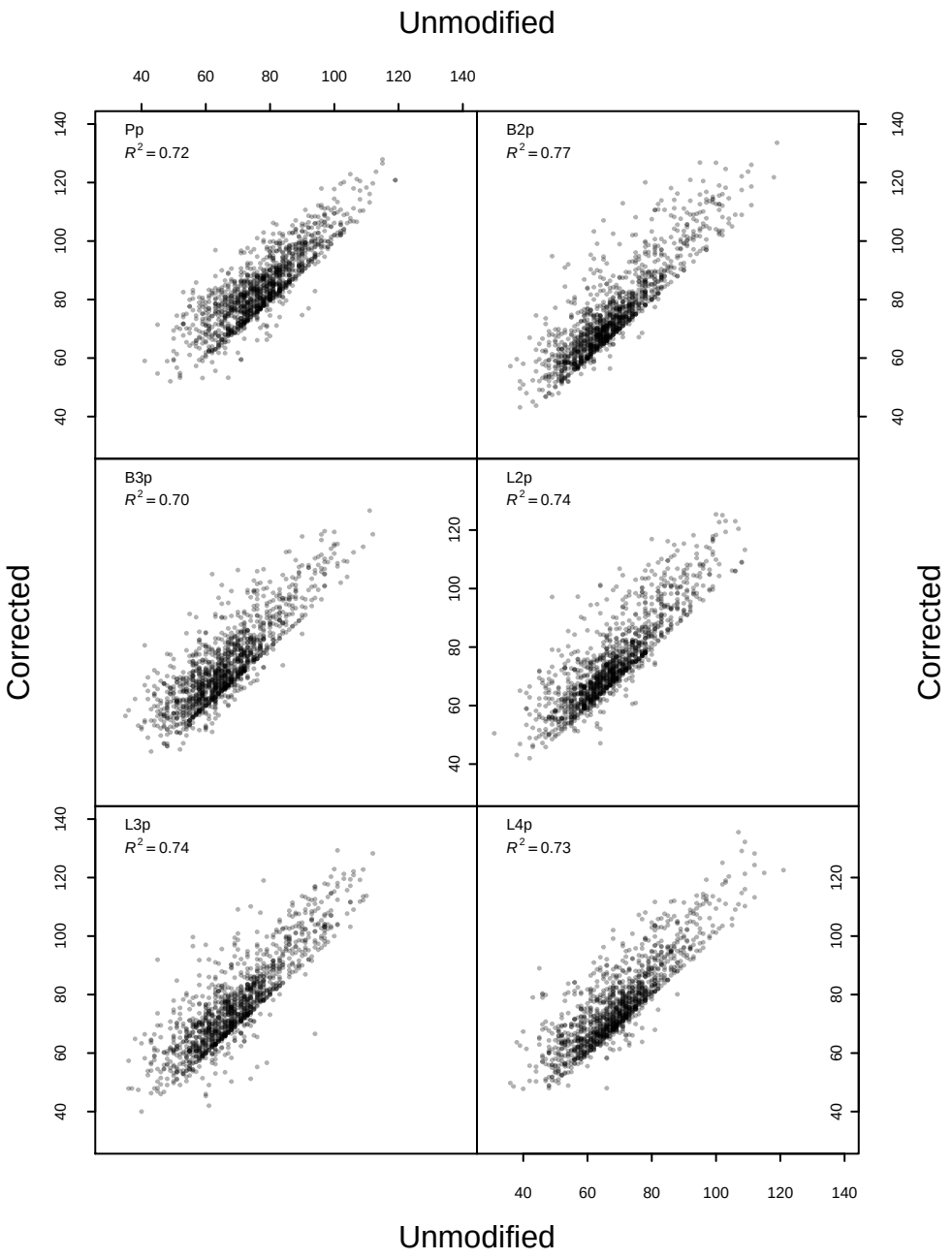

Figure 5.8: Comparison of unmodified and size-corrected enamel thickness in trailing enamel layers across the whole dataset.

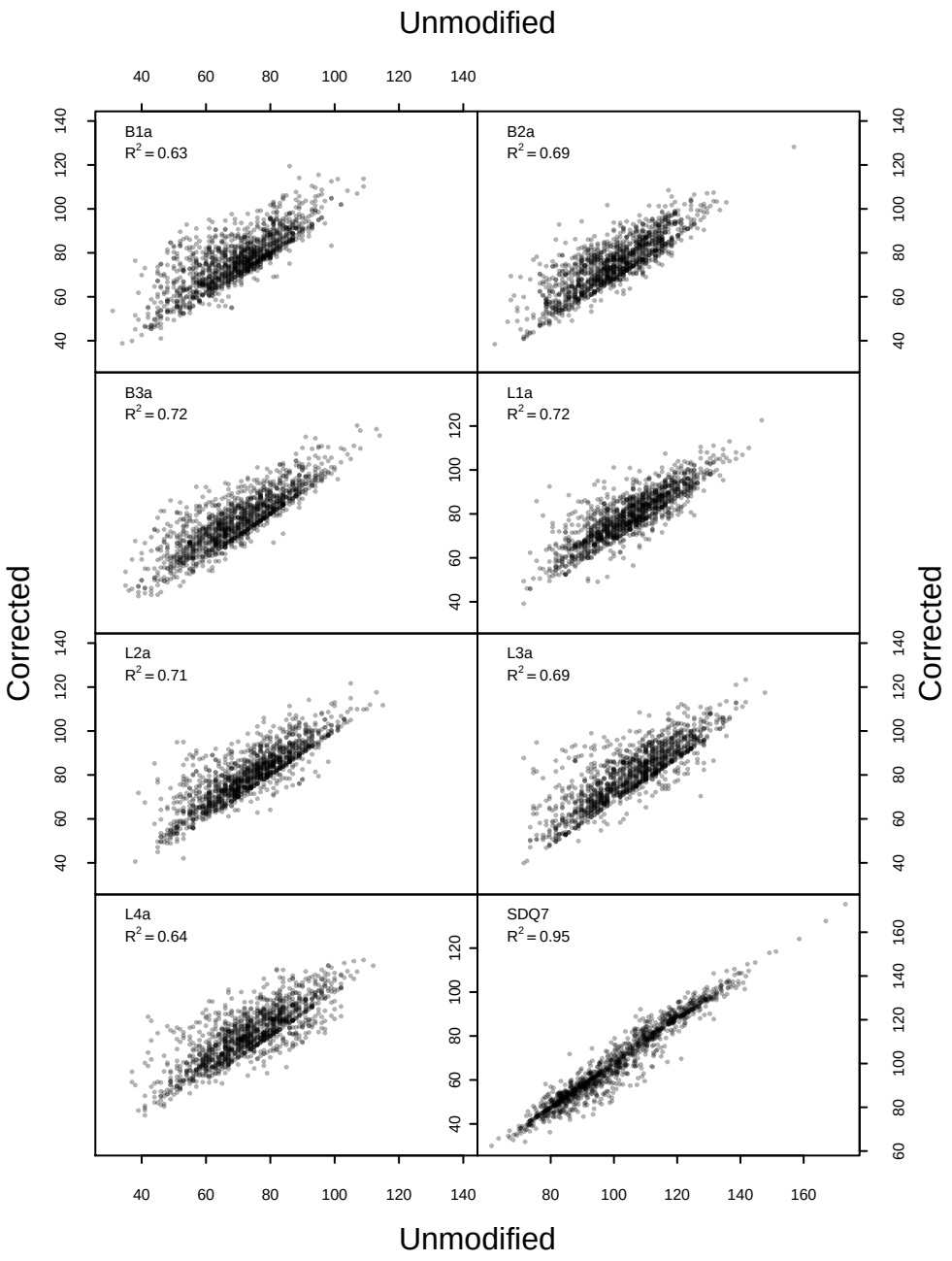

Figure 5.9: Comparison of unmodified and size-corrected enamel thickness in leading enamel layers across the whole dataset and in SDQ7.

5.6 Enamel measurement approach

This chapter has explored the relationship between morphology and size of the M_1. Up to 30% of shape variation can be explained by tooth size (Tables 5.2 and 5.3) and up to 95% of enamel thickness variation can be explained by tooth size (Tables B.4 and B.5). Whether the removal of this source of morphological variation produces data that can be used to improve biostratigraphy will be considered in Chapters 6 and 7, but at the very least the analyses presented above show that applying an ontogenetic correction to morphological data will produce values that are different to unmodified data.

Shape variables have no inherent only relative value, while enamel thicknesses and the SDQ are scalar quantities that can be independently derived. These latter, measured variables have been used for many years and the methodology behind them is simple. Modifying enamel thicknesses, and therefore also the SDQ, by removing ontogenetic variation introduces an additional methodological step, the details of which and the differences with unmodified measurements may not be fully appreciated by some workers at first glance. In addition, this thesis has taken a slightly different approach to enamel thickness measurement than previous studies (Section 4.2.5), namely measurement with the tooth orientated vertically (axial orientation) rather than with the occlusal surface perpendicular to the measurer (occlusal orientation). With these methodological differences in mind, and acknowledging the importance of the SDQ in biostratigraphy, it is appropriate to compare SDQ values produced by the various approaches outlined.

In order to prevent possible confusion between the methodologies of previous studies and this thesis the term SDQ will be reserved as a general shorthand for enamel thickness ratio or for enamel thickness ratios derived using enamel thickness measurements taken in the more traditional occlusal orientation. The term SDQAU will be introduced to refer purely to enamel thickness ratios derived from axial orientation thickness measurements that are unmodified in terms of ontogenetic effects. Whilst the term SDQAC will be used to describe enamel thickness ratios based upon axially measured enamel thicknesseses that have been modelled in the manner of Section 5.4 in order to remove the effects of ontogeny.

5.6.1 Published SDQs and this thesis

Seventeen of the fossil assemblages assessed by this study also have published SDQ values. This enables a comparison to be made between SDQ values derived using pre-existing methodology and the measurement methodology and size-correction approach developed in Section 4.2.5 and Chapter 5 respectively. Figures 5.10 and 5.11 depict the stratigraphic pattern of mean SDQAU and SDQAC ($SDQAU_p$

and $SDQAC_p$ denoting population level statistics) alongside published mean SDQ (SDQ_p) values, with the data upon which these plots are based found in Table 5.7. Both plots show the same trend of decreasing SDQ over time and that SDQ_p values are in general larger than both $SDQAU_p$ and $SDQAC_p$ values. This latter trend is in accord with the comparison between occlusal and axial view measurements carried out in Section 4.2.5.2. The assemblage of Novonekrasovka contradicts the general pattern of higher SDQ_p values, with $SDQAU_p$ and $SDQAC_p$ being 8.1 and 14.6 units greater than SDQ_p respectively. The SDQ_p estimate provided by Rekovets (1994) for Gunki is also lower than SDQs from this thesis (2.9 and 11.6 units lower than $SDQAU_p$ and $SDQAC_p$ respectively).

SDQAU and $SDQAC_p$ values are more similar to SDQ_p in the geologically youngest assemblages but differences appear to increase in assemblages of increasing geological age. For the Late Pleistocene and Holocene assemblages of Burgtonna South, Fuchsloch im Krockstein, and Pisede SDQ_ps are about the same or up to approximately 3 SDQ units greater than $SDQAU_p$ values. For the same assemblages SDQ_ps are about 3 to 4 units greater than $SDQAC_p$. In the MIS 5e assemblage of Tönchesberg differences between SDQ_p and $SDQAU_p$/$SDQAC_p$ are greater than those for younger assemblages, $SDQAU_p$ being 12.8 units greater and $SDQAC_p$ 18.9 units greater.

The late Middle Pleistocene assemblages display a maximum difference of 23.1 units (for Gun(a)), and a minimum difference of 12.9 units (for Medzhybozh, discounting Gun(b)) between SDQ_p and $SDQAU_p$, and a maximum difference of 26.1 units (for Chigirin) and minimum difference of 14.4 units (for Gun(a), again discounting Gun(b)) between SDQ_p and $SDQAC_p$. The corrected and unmodified SDQs for Cudmore Grove are both around 18 units less than the SDQ_p of Roe *et al.* (2009). Gunki is the only assemblage whose $SDQAC_p$ is greater than $SDQAU_p$.

As with other assemblages (save Novonekrasovka and the SDQ_p of Rekovets (1994) from Gunki) the early Middle Pleistocene groups possess SDQ_p values greater than those estimated by this thesis. The largest difference between SDQ_p and $SDQAU_p$ is 33.1 for the SDQ_p of Kolfschoten (1988) from Miesenheim I, whilst the least difference is 6.43 for Rotbav-Dealul Ţiganilor. $SDQAC_p$s are generally fairly similar to $SDQAU_p$ values with slight increases or decreases of only a few units in this ratio. The West Runton Freshwater bed assemblage shows the largest shift towards SDQ_p through the size-corrected, with a 19.59 unit difference between $SDQAU_p$ and SDQ_p being reduced to 13.69 for $SDQAC_p$.

5.6.2 Discussion

The comparison between SDQs derived from varying methodologies provides a number of conclusions. Firstly, the photographic methodology used by this thesis, which orients the tooth axially, almost always results in lower SDQs than those derived from occlusally orientated measurements. Two exceptions to this are the SDQ_ps provided by Markova (2000) for Novonekrasovka upper and by Rekovets (1994) for Gunki II. This may indicate that an error exists in the measurement of enamel used to derive either SDQ_p or SDQAU/SDQAC or, given the magnitude of the differences involved, that different fossil material was examined by this thesis than that used by the publications cited. This certainly may be the case for Gunki II because an alternative SDQ_p for this assemblage given by Markova (2000) is markedly different to that from Rekovets (1994). These differences in SDQ may have biostratigraphic implications (Section 7.3). An alternative possibility is that the $SDQAC_p$ of Gunki II represents a more realistic estimate of adult SDQ within an assemblage than the $SDQAC_p$ values of other East European Plain groups of similar age. An examination of the enamel thickness–size regressions for Chigirin, Donskaya Negatchevka, Medzhybozh, Rybnaya Sloboda, and Vladimirovka (Section B) shows that size corrections for these assemblages are based on poorly defined regressions that are often oriented in an inconsistent and biologically dubious manner. But, because little enamel thickness variation is explained by size in these groups, $SDQAC_p$ values are not much different to $SDQAU_p$ ones.

Figure 5.10: (Following page) Comparative stratigraphic patterns of mean enamel thickness ratios from published sources (SDQ_p) and those derived by this study that have not received a size-correction ($SDQAU_p$). Refer to Table 5.7 for data. **BSB**-Burgtonna South Black-earth (n=40, Heinrich, 1982); **Chg**-Chigirin (n=62, Markova, 2000); **CGr**-Cudmore Grove 'Detrital mud' (n=48, Roe *et al.*, 2009); **FiK**-Fuchsloch im Krockstein (n=40, Heinrich, 1982); **Gun(a)**-Gunki II (n=12, Markova, 2000); **Gun(b)**-Gunki II (n=46, Rekovets, 1994); **Hun**-Hundsheim (n=17, Heinrich, 1987); **Mdz**-Medzhybozh-2 (n=29, Rekovets *et al.*, 2007); **Mhm(a)**-Miesenheim I C-H (n=9, Maul *et al.*, 2000); **Mhm(b)**-Miesenheim I C-H (n=29, Kolfschoten, 1988); **Msb**-Mosbach 2 (n=45, Maul *et al.*, 2000); **Nvk**-Novonekrasovka upper (n=18, Markova, 2000); **PIII**-Pisede III (n=24, Heinrich and Maul, 1983a); **PIVV**-Pisede IV&V (n=38, Heinrich and Maul, 1983a); **RDT**-Rotbav-Dealul Ţiganilor Clay-A (n=32, Petculescu, 2003); **RSb**-Rybnaya Sloboda (n=23, Markova, 2006); **Sch**-Schöningen 13-II-4 (n=NA, Kolfschoten, 1993a); **Ton**-Tönchesberg II B (n=19, Kolfschoten and Roth, 1995); **WRF**-West Runton Freshwater Bed (n=49, Maul and Parfitt, 2010).

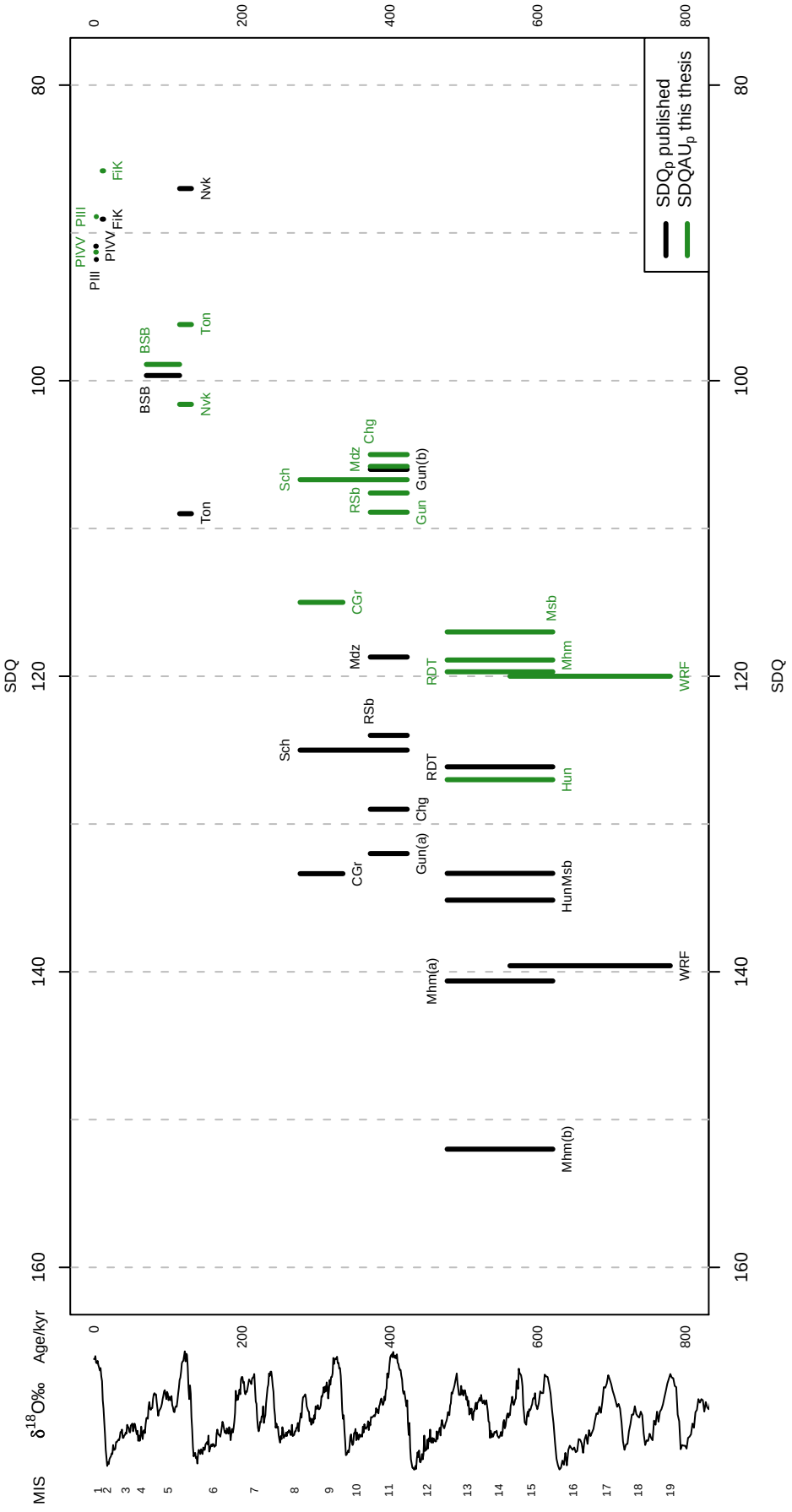
SDQ
SDQ
MIS
δ18O‰
Age/kyr
SDQp published
SDQAUp this thesis
PIII
PIVV
FIK
Nvk
Ton
BSB
Sch
RSb
Mdz
Chg
Gun
Gun(b)
CGr
Msb
Mhm
RDT
WRF
Hun
Gun(a)
HunMsb
Mhm(a)
Mhm(b)

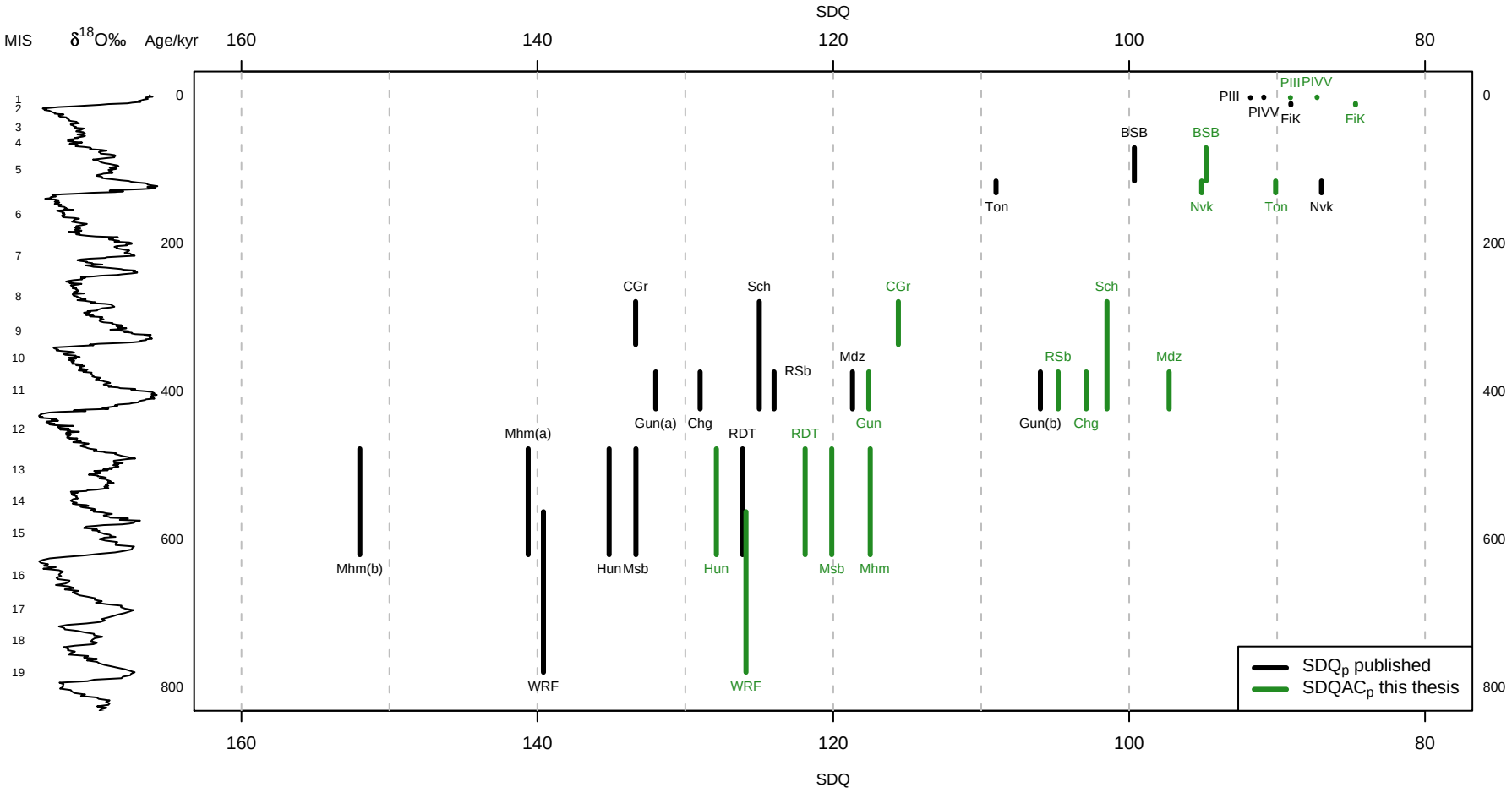

Figure 5.11: Comparative stratigraphic patterns of mean enamel thickness ratios from published sources (SDQ_p) and those derived by this study that have received a size-correction ($SDQAC_p$). Refer to Table 5.7 for data and Table 5.7 or Figure 5.10 for assemblage labels.

Table 5.7: Enamel thickness ratios from published sources compared with those derived from this study. Minimum ($x_{\min}$), mean ($\bar{x}$), maximum ($x_{\max}$), standard deviation (σ), and, where published, the standard error of the mean ($\sigma_{\bar{x}}$) of SDQ values. PlotID refers to plot labels in Figures 5.10 and 5.11.

		Published SDQ_p						$SDQAU_p$				$SDQAC_p$				
PlotID	Assemblage	$x_{\min}$	$\bar{x}$	$x_{\max}$	$\sigma_{\bar{x}}$	n	Source	$x_{\min}$	$\bar{x}$	$x_{\max}$	σ	$x_{\min}$	$\bar{x}$	$x_{\max}$	σ	n
BSB	Burgtonna South Black-earth	76.34	99.651	116.95	1.46	40	Heinrich, 1982	83.0	98.9	115.7	9.0	81.6	94.8	102.6	6.7	9
Chg	Chigirin	101.67	129	166.67		62	Markova, 2000	89.3	105.0	117.2	8.1	88.2	102.9	111.8	7.5	9
CGr	Cudmore Grove 'Detrital mud'	105	133.36	147		48	Roe *et al.*, 2009	99.0	115.0	132.2	8.8	101.8	115.6	131.5	8.1	29
FiK	Fuchsloch im Krockstein	72.20	89.076	102.926	1.01	40	Heinrich, 1982	69.9	85.8	102.7	9.1	70.4	84.7	98.5	7.9	13
Gun(a)	Gunki II	120.48	132	303.03		12	Markova, 2000	92.4	108.9	129.6	11.9	100.8	117.6	133.1	9.9	9
Gun(b)			106			46	Rekovets, 1994									
Hun	Hundsheim	102	135.15	152		17	Heinrich, 1987[a]	108.9	127.0	145.3	7.6	108.9	127.9	145.1	7.2	31
Mdz	Medzhybozh-2	91.66	118.7	150		29	Rekovets *et al.*, 2007	94.9	105.8	114.5	7.4	89.8	97.3	107.0	5.2	9
Mhm(a)	Miesenheim I C-H	123.32	140.62	155.26	3.38	9	Maul *et al.*, 2000	98.5	118.9	136.3	10.5	99.5	117.5	133.9	9.3	23
Mhm(b)		126	152.03	180		29	Kolfschoten, 1988									
Msb	Mosbach 2	117.60	133.34	159.27	1.72	45	Maul *et al.*, 2000	90.8	117.0	171.2	14.5	95.4	120.1	168.6	12.9	75
Nvk	Novonekrasovka upper	60	87	140		18	Markova, 2000	93.54	101.23	116.94	8.19	89.57	95.33	100.71	4.34	6
PIII	Pisede III	75.00	91.80	117.40	2.04	24	Heinrich and Maul, 1983a	74.4	88.9	101.7	7.0	75.6	89.1	100.7	6.4	13
PIVV	Pisede IV&V	70.40	90.90	108.60	1.30	38	Heinrich and Maul, 1983a	78.1	91.3	108.5	8.2	76.7	87.3	100.2	6.2	25
RDT	Rotbav-Dealul Ţiganilor Clay-A		126.13			32	Petculescu, 2003	104.7	119.7	139.0	9.0	109.1	121.9	138.4	7.7	26
RSb	Rybnaya Sloboda	112	124	160		23	Markova, 2006[b]	93.9	107.6	128.8	12.0	90.4	104.8	127.8	12.9	6
Sch	Schöningen 13-II-4	120	125	130		?	Kolfschoten, 1993a[c]	88.5	106.7	132.1	9.2	86.6	101.5	124.1	8.1	26
Ton	Tönchesberg II B	90	109	130		19	Kolfschoten and Roth, 1995[d]	84.6	96.2	110.1	8.3	81.4	90.1	99.0	5.5	15
WRF	West Runton Freshwater Bed	114.57	139.59	163.14		49	Maul and Parfitt, 2010	106.5	120.0	142.1	10.3	110.4	125.9	143.6	8.3	35

[a] Estimated from Figure 1 of Heinrich (1987).
[b] Estimated from Figure 2 of Markova (2006).
[c] Only minimum and maximum given. Mean assumed from these values.
[d] Estimated from Figure 10 of Kolfschoten and Roth (1995).

Secondly, in general size correction leads to a decrease in SDQ in late Middle Pleistocene, Late Pleistocene and Holocene assemblages, and very little change in early Middle Pleistocene assemblages. The reason for this appears to be the relative relationships between enamel thickness–size regression slopes for different assemblages at different points in time (Figures B.1–B.12 in the Appendix). In late Middle Pleistocene, Late Pleistocene and Holocene groups the slopes of leading edge enamel thickness–size regressions are steeper than those for trailing edge enamel. Furthermore, the regression slopes of Holocene groups appear to be more similar to one another than in late Middle Pleistocene and Late Pleistocene assemblages. Size correction of enamel thicknesses based on these regressions result in lower or similar SDQ_ps. In the late early Middle Pleistocene assemblages enamel thickness–size regression slopes are generally similar for both enamel edges or the trailing edge slope is slightly steeper than the leading edge slope. This produces size corrected SDQs that are similar or slightly greater than $SDQAU_p$ values. Finally the assemblage of West Runton Freshwater bed shows quite steeply diverging trailing and leading enamel thickness–size regression slopes (Figure B.12b), which give a larger $SDQAC_p$ value. These changing enamel thickness–size relationships must relate to changes in the timing of the development of the structure of the M_1 through the evolution of the genus.

These observations make it clear that the enamel thickness measurements made by this thesis are different to those present in the literature. But is it possible to convert between the different datasets that appear to separated by different methodologies? Figure 5.12 shows the extent to which both $SDQAU_p$ and $SDQAC_p$ are correlated. The SDQ_p–$SDQAU_p$ relationship is highly significant and SDQ_p explains 73% of the variation in $SDQAU_p$. The SDQ_p–$SDQAC_p$ relationship is also highly significant but SDQ_p explains less of the variation, 64%, in $SDQAC_p$ than SDQ_p explains $SDQAU_p$. The nature of the relationship between SDQ_p and other enamel thickness ratios also differ. The slopes of the two regression lines indicate that, despite being qualitatively different, $SDQAC_p$ values change in a manner more similar to SDQ_p than $SDQAU_p$, the latter of which is more divergent from SDQ_p than $SDQAU_p$. The between SDQ regressions in Figure 5.12 replicate the relationships seen in Figures 5.10 and 5.11 in that both $SDQAU_p$ and $SDQAC_p$ become progressively more different from SDQ_p over time. These biases are caused by the differences in perceived thickness of enamel layers between the different orientations (Section 4.2.5.2). It is possible to convert between SDQ_p and the varieties of SDQ introduced in this thesis by applying the linear equations given in 5.11. However, appreciable amounts of variation in the SDQs derived by this thesis (between 27% and 36% for $SDQAU_p$ and $SDQAC_p$ respectively) cannot be explained by published SDQs. Such unexplained variation could be attributable to measurement error between researchers or possible

compositional differences between the fossil material examined from each assemblage. For $SDQAC_p$ values an additional source of error could be the potential introduction of inaccurately modelled adult morphologies if enamel thickness–size regressions are biologically implausible. This may be because of inadequate sampling of a population or mixing of a number of populations together through any of the mechanisms described in Section 4.4.

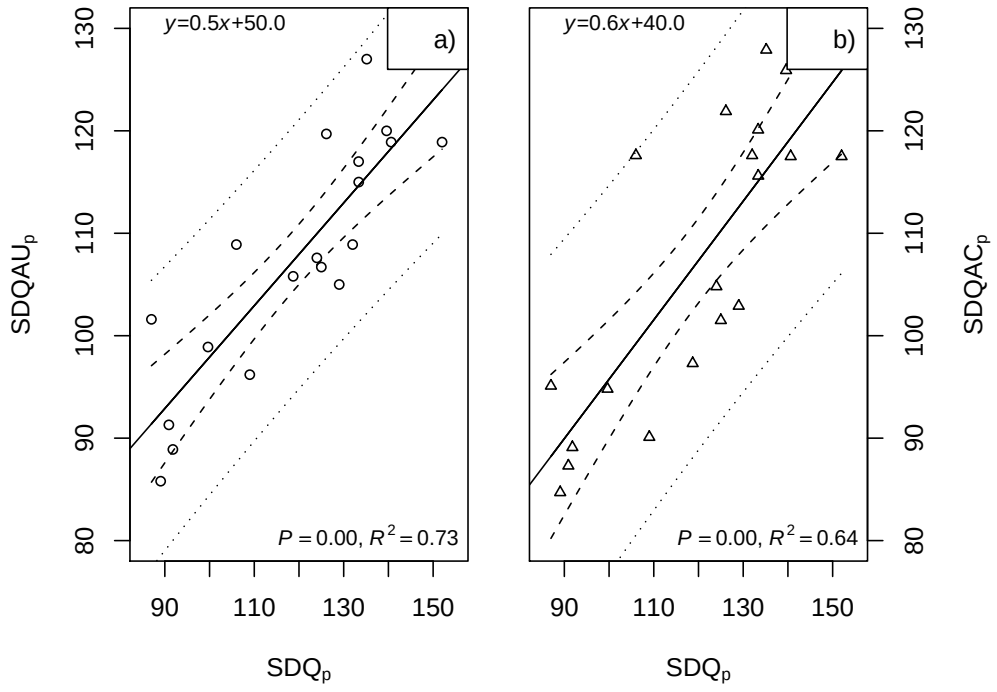

Figure 5.12: Plots comparing published mean SDQ (SDQ_p) with a) $SDQAU_p$, unmodified enamel thicknesses made from axially orientated M_1s, and b) $SDQAC_p$, size corrected enamel thicknesses made from axially orientated M_1s. Significance of regression (P), coefficient of determination (R^2), and equation of regression slope given. Dashed and dotted and lines show 95% confidence limits on the regression and the data respectively. Data taken from Table 5.7.

5.7 Discussion and conclusions

Ontogenetic variation Exploration of the relationships between molar shape, enamel thickness and molar size shows that morphology and tooth size, and therefore morphology and ontogenetic age, are linked. The estimation of these relationships is best where groups include representatives from throughout ontogenetic development. This can be seen from regressions and plots of shape and enamel thickness with size (Tables 5.2, 5.4, and 5.5; Figures 5.2 and Figures B.1–B.12 in the Appendix). An inspection of the original photographs of specimens from Recent groups confirms these patterns. Specimens from Novomirgorod contain three distinctly juvenile M_1s (SpecimenIDs 3307, 3313, and 3315), possessing characteristically reduced and convoluted ACCs, straight-sided faces to enamel prisms, and low Centroid Sizes. Similarly, in the Frankfurt am Main group, one specimen (SpecimenID 3044) appears to be a juvenile, albeit not as distinctive a young molar as those from Novomirgorod. In contrast, M_1s from Kabardino-Balkariya and Aggeel—where only 3.3 and 5.1% of total shape variation is explained by size—all appear superficially very similar in occlusal shape.

The lack of correspondence between the range of shapes seen within both fossil and Recent groups and the amount of shape variation explained by tooth size (Figure 5.1) suggests that the extremes of molar shape within a group do not wholly reflect the end points of ontogenetic trajectories of shape. Well-defined enamel thickness–size trajectories, however, are associated with large amounts of enamel thickness variation explained by size. Continuing the example of the case of Novomirgorod, which apparently contains a good representative ontogenetic sample, 29.4% of shape variation is explained by size (Table 5.2), while up to 83% of enamel thickness variation is explained by size (Table 5.5).

Correcting for ontogenetic variation Quantification of ontogenetic variation allows this source of morphological variability to be removed from analyses with potentially beneficial effects for phylogenetic reconstruction (Chapter 6). As described above, the examination of ontogenetic change described throughout this chapter has uncovered not only the strong association of morphology with ontogenetic age but the difficulty in characterising that change where examples of individuals from throughout ontogeny are not present. This presents a problem for any attempt to correct for the effects of age because it is difficult to estimate with confidence the appropriate ontogenetic correction to apply to groups. Should a single ontogenetic trajectory, found in a group with a wide range of age categories present (such as Novomirgorod), be applied across all groups, or should each group receive a unique correction described by the data within each group?

The use of a single correction across Recent groups may be correct and pooling

several Recent groups, to build a dataset with better representation of individuals from throughout ontogeny, could be a legitimate way of determining this single ontogenetic allometry more accurately. However, growth history has been cited as a major player in arvicolid evolution (Martin, 1993), and it is possible that separate populations of Recent *Arvicola*, subject to distinctive environmental conditions, perhaps with separate phylogenetic histories for hundreds of thousands of years (e.g., Tougard *et al.*, 2008; Brace, 2010) possess distinct molar shape allometries. In other words, groups may genuinely possess separate trajectories and such between-population differences in age structure were also noted at the beginning of the chapter when M_1 size was being tested as a proxy for ontogenetic age (Section 5.2). It is difficult, however, to separate potentially genuine developmental differences from sampling error without more thorough ontogenetic sampling from a wider number of Recent groups, and so a correction based upon a single trajectory could inaccurately model adult shape or enamel thickness. The application of a single allometric trajectory for enamel across all groups, Recent and fossil, can be quickly dismissed when the enamel thickness–size relationships from all groups are considered (Figures B.1–B.12 in the Appendix). It is evident that enamel thickness–size trajectories from geologically older assemblages such as West Runton Freshwater bed are radically different from the Recent groups examined. Such changes in allometry are at the heart of the enamel thickness differences that exist between fossil and Recent populations and the allometries may in themselves be of interest within the context of evolutionary-development studies. For this study, however, the fact that these differences in the rate of enamel development exist is sufficient to demonstrate that if size corrections are to be applied to enamel layer thickness they should be done within groups, rather than collectively across groups.

Where size range within groups is small, and morphology–size trajectories are not found to be significant, estimations of ontogenetic trajectories become more variable (Section 5.4.2). While they become more variable, these regressions generally also describe smaller amounts of within-group variation, even where sample sizes are greater than 10 (Section 4.4.2.2): e.g., in Cheshskaya Guba (n=19), Kabardino-Balkariya (n=19), and Tsimlyansk (n=15), where less than 10% of total shape variation and generally less than 10% of enamel thickness variation is described by size (Tables 5.2 and B.4). Furthermore, groups where morphology–size relationships are poorly defined appear to possess, for the most part, large specimens that are indicative of ontogenetically advanced individuals (e.g., Aggeel Figure B.1b). Thus, any regression-based correction, when applied to these more poorly defined groups, is likely to have limited effect on the overall description of adult morphology compared with groups that contain a mixture of juveniles and adults.

Given that some correction for ontogeny seems appropriate, and that there are no independent criteria that inform on the best corrective method, a correction based upon each within-group morphology–size regression would seem to be a valid approach to removing the effects of ontogenetic age on molar morphology. Such an approach is not without riskes, however, and may result in the removal of phylogenetically or biostratigraphically important information. For instance one potentially spurious effect of size corrections for shape data is to project some landmarks beyond the range of original maximum-sized shape (Figure 5.7), potentially resulting in shapes that may be unrepresentative of the real morphologies present in the real population. Another is that enamel thickness–size regressions may be poorly defined and result in the estimation of 'incorrect' adult shapes and enamel morphologies. It is also clear that the enamel thickness ratios $SDQAU_p$ and $SDQAC_p$ of this thesis cannot be used as biometric or stratigraphic variables alongside published SDQ because they are methodologically distinct. Although all these flavours of SDQ appear to present the same general pattern there are important differences, however, there may be additional benefit to be gained from the calculation of $SDQAU_p$ and $SDQAC_p$ values, as well as by examining the enamel thickness–size relationships of leading and trailing edges. Knowledge of onogenetic trajectories within groups and the juxtaposition of estimated adult enamel morphologies could provide an additional means of stratigraphically resolving fossil assemblages. The phylogenetic and stratigraphic information contained within M_1 morphology will be investigated in further detail in the following chapters.

Chapter 6

Morphology and phylogeny

Chapter 5 illustrates that M_1 morphology in both Recent and fossil groups includes a component of variation that is related to ontogeny. The question for evolutionary studies is whether this type of variation in morphology has the potential to affect evolutionary models constructed using molar morphology. This chapter attempts to address this question using molar shapes determined through Geometric Morphometrics, which provide a rich supply of continuous quantitative characters that can be used in systematics (e.g., Felsenstein, 2002; Caumul and Polly, 2005).

6.1 Introduction

Morphology has been used to infer phylogeny since the earliest ideas on the relatedness and shared ancestry of species were formulated (e.g., Darwin, 1859), but the use of morphometric data to reveal phylogeny has not been widely adopted (MacLeod, 2002). The main reason for this has been the conceptual and practical difficulties involved in transforming 'morphometric variables' such as the length of a limb, into apparently nominal and discrete 'systematic characters' such as eye colour that can be used in parsimony analysis (Farris *et al.*, 1970 cited in MacLeod, 2002). Some authors view the use of the continuous quantitative variables produced by morphometrics as invalid in systematics because these variables do not represent homologous 'characters' and gaps cannot be objectively identified in the data (e.g., Pimentel and Riggins, 1987). Others consider these variables admissible but only after they have been coded into discrete states through a variety of methods (e.g., Thiele, 1993; Zelditch *et al.*, 1995, 2000; Swiderski *et al.*, 2002). Both of these perspectives have been critiscised as misunderstanding the nature of quantitative data and the relationship between continuous and nominal variables (MacLeod, 2002). Advocates of this latter viewpoint argue that morphometric variables can be used, without the need to transform them into discrete variables,

by employing statistical methods (e.g., Felsenstein, 2002; MacLeod, 2002), and this will be the position adopted in this chapter. There is unquestionably a phylogenetic signal in morpological data (e.g., Gingerich, 1993). The main problematic issues surrounding the use of morphology to understand phylogeny relate to tempo and mode of change, the temporal scale of the characters under study, and the effect of homoplasy on the ability to detect relationships (e.g., Polly, 2001).

The aim of the chapter is to assess the effect that removing molar shape variation explainable by molar size has on phylogenetic inference. Two shape datasets are used, one of 'adults' modelled in the manner outlined in Section 5.5.1, the other of the original shapes observed from specimens. Phylogenetic hypotheses constructed from these data are then compared with a modern and historical mitochondrial DNA (mtDNA) 'reference' phylogeny, and the degree of congruence between molecular and shape data is examined. The expectation is that correcting for the effects of ontogeny in molar shape will improve congruence between the two datasets. Results will have consequent implications for how morphology can be used in empirical biostratigraphic models.

6.2 Methods

The ability of morphology to reconstruct phylogeny was tested by comparing molar shapes with a dataset of mtDNA sequences obtained from water vole specimens from a number of fossil and Recent groups. Extraction and sequencing was performed by Selina Brace (School of Biological Sciences, Royal Holloway, University of London; Brace, 2010), using samples whose M_1s were also photographed for use in this study. A 645 base-pair section of the mitochondrial control region was obtained[1] and sequences were aligned in `ClustalX`.[2] In many cases the same specimen was photographed, sequenced, and ^{14}C dated, in order to provide the greatest possible certainty on age and phylogenetic affiliation. Two intraspecific lineages, perhaps with a most recent common ancestor during the Last Interglacial (Brace, pers. comm., 2010), are present in the mtDNA data of (Figure 6.1b; Brace, 2010), and this pattern was also recovered in a more limited modern mtDNA study of British water vole by Piertney *et al.* (2005). These lineages are broadly associated with western and eastern Europe (although there is geographic overlap between the two) and from here on are informally referred to as 'Western' and 'Eastern' lineages.

For the purposes of phylogenetic analysis, each Recent group and fossil assemblage was treated as a discrete Operational Taxonomic Unit (OTU). Eleven

[1] In Marie-Jeanne Cave 4 and Fuchsloch im Krockstein (eastern lineage) only 575 base pairs were obtained but were still included in the analysis.

[2] `http://www.clustal.org/`. Last accessed 10$^{\text{th}}$ August 2010.

fossil and Recent groups[1] where $n \geq 10$ and with complimentary, near-complete, mtDNA sequences were used to assess similarity between molecular and morphological datasets. Molecular data were compared with two molar shape datasets: M_1 shapes modelled to maximum size ('size corrected' shapes; Section 5.5.1) and the original, unmodified, M_1 shape variables.

6.2.1 Shape and mtDNA divergence

The degree of association between mtDNA and shape was examined by comparing pairwise distances between OTUs. Between-OTU distances for unmodified and size-corrected M_1 shapes were found by Procrustes superimposition of M_1s within-OTUs to estimate a consensus or meanshape for the OTU, these meanshapes were themselves then superimposed to allow Procrustes distances between group means to be calculated (Caumul and Polly, 2005). Procrustes distances were then used to calculate Euclidean distances between OTU meanshapes. For the mtDNA data, % sequence divergence was found by calculating Kimura 2-paramter (K2P) distances (Kimura, 1980).

Distance data were then used to examine the strength of agreement between shape and molecular data in two ways. Firstly, a bivariate plot of shape distances and molecular distances with respect to the Welsh Borders OTU was made, and the distances regressed. As Caumul and Polly (2005) point out, this approach allows strength of association between datasets to be easily interpreted visually but only some of the pairwise comparisons are used—i.e., only between Welsh Borders and other OTUs. A second approach was to employ a Mantel test (Sokal and Rohlf, 1995; Polly, 2001) to estimate the association between pairwise distance matrices. Both molecular and shape datasets were log transformed to linearise them and 50 000 random permutations were used to determine a P-value for the probability of correlation between distances (Polly, 2001). Distance matrices, regressions, and Mantel tests were all computed in R.

6.2.2 Phylogeny

Phylogenetic congruence was examined by reconstructing phylogenetic trees from shape data and comparing these with the phylogeny derived from mtDNA. Molecular phylogeny was then estimated using a maximum likelihood (ML) method (Felsenstein, 1981a) with *Microtus agrestis* as an outgroup and boostrap support included. Molecular phylogeny was estimated in R using the package ape.

M_1 shape trees were estimated using the following method of Caumul and Polly (2005):

[1] Bridged Pot inner slope, Dzeravá skala Cave, Fuchsloch im Krockstein, Novomirgorod, Ormozu, Ossom's Eyrie Cave, Pilisszántó, Pisede III, Pisede IV&V, Welsh Borders, Wigber Low 26.

1. Meanshapes are estimated for each OTU
2. A PCA is carried out on OTU meanshapes
3. PC scores for each meanshape (estimated in 2) are used as continuous characters to build a ML tree

ML trees were estimated using the restricted maximum likelihood algorithm of Felsenstein (1981b) as implemented in PHYLIP (Felsenstein, 2008). PC scores are suitable for use as quantitative characters in ML estimation as they are continuously distributed, uncorrelated, and are standardised to a mean of 0 and a variance equal to the amount of variance explained by each principal component. Support was found for molar shape trees by randomly sampling with replacement n specimens from each OTU (i.e., the same number of individuals from each OTU), performing steps 1–3 above, and then evaluating each boostrapped tree for branches shared with the original estimated tree (Caumul and Polly, 2005). Bootstraps were repeated 1000 times[1]. Trees were rooted using a subsample of $n \geq 10$ specimens from Mosbach 2 (Section 3.5.1.2). *Arvicola* from this Middle Pleistocene assemblage pre-date the age of the other Recent and fossil groups used by at least 500 k yr, and are therefore likely to exhibit 'primtive' morphologies against which the molar shapes of other groups can be compared.

6.3 Results and discussion

6.3.1 Shape and mtDNA divergence

Pairwise distance matrices of mtDNA and the two molar shape datasets are shown in Table B.1. On first inspection, a bivariate scatterplot of mtDNA and shape distances between Welsh Borders and other OTUs (Figure 6.1a) suggests that a weakly negative relationship exists between K2P distances and unmodified shape data. No significant association is supported between these data, however, ($P = 0.78$). Size-corrected shapes show a significant ($P < 0.05$), positive association with mtDNA divergence, with 41% of molar shape variance explained by K2P distance. Mantel tests between shape and mtDNA distance matrices show a similar pattern to the bivariate comparison. For unmodified shape and K2P distances the association is insignificant ($P = 0.565$), the relationship between size-corrected shape and K2P distances approaches significance at the 0.05 level ($P = 0.068$).

Although not perfect, there appears to be much better agreement between mtDNA divergence and size-corrected molar shape than with uncorrected shape

[1]I am grateful to Dr. Christoph Helb of the Ludwig-Maximilians-Universität München, Germany, for assistance scripting this procedure in R.

data. Size-corrected molar shape divergence appears to reflect both genetic divergence and geographic separation (Figure 6.1a). British groups from the Holocene (Ossom's Eyrie Cave, Welsh Borders, Wigber Low 26) are clustered near the origin with the Late Holocene German site of Pisede and the Recent sample Ormozu from Slovenia. The Recent sample from Novomirgorod, Ukraine, and the Late Pleistocene OTU from Pilisszántó, Hungary, are more distant and the three OTUs of Bridged Pot inner slope (Britain), Dzeravá skala Cave (Slovak Republic), and Fuchsloch im Krockstein (Germany) are all fossil OTUs from the Western mtDNA lineage. Although there is agreement between the two datasets, the association between mtDNA and shape divergence appears to become weaker for taxa more distant from the Welsh Borders OTU.

6.3.2 Phylogenetic relationships

The mtDNA ML phylogeny in Figure 6.1b shows a Western lineage that includes Bridged Pot inner slope, Dzeravá skala Cave, and Fuchsloch im Krockstein; and an Eastern lineage of Novomirgorod, Ormozu, Ossom's Eyrie Cave, Pilisszántó, Pisede III, Pisede IV&V, Welsh Borders, and Wigber Low 26. ML trees based on molar shapes without (Figure 6.1c) and with size-correction (Figure 6.1d) are topologically different to the molecular tree but share some general similarities. The Mosbach 2 OTU consistently appears as separate from other groups but this receives better bootstrap support in the size-corrected tree. In the unmodified shape tree, internal branch support is variable throughout, but in the size-corrected data branch support improves in dichotomies higher up the tree. In both molar shape trees OTUs from the Western lineage appear higher in the topology, although they are not grouped together. The pairing of Ossom's Eyrie Cave and Wigber Low 26 is well-supported in the size-corrected shape tree and is present but less well defined in the unmodified shape tree.

No specific agreement occurs between either of the shape trees and the mtDNA tree. The Eastern lineage forms a monophyletic group in the mtDNA tree but the largest such grouping in shape trees appears in the size-corrected tree containing Novomirgorod, Pisede III, and Welsh Borders. One persistent feature of both shape trees is the strong, erroneous, pairing of the Eastern lineage OTU of Ormozu with the Western lineage OTUs Fuchsloch im Krockstein and Bridged Pot inner slope—in unmodified and size-corrected shape trees respectively. This cannot be due to effects of the size correction as it is present in both shape datasets and is otherwise difficult to explain given the mtDNA data.

There is little to distinguish one shape tree as better than the other at reconstructing phylogeny but the size-corrected tree offers better support for Mosbach 2 as separate from other OTUs and for some sister-group pairings of Eastern lin-

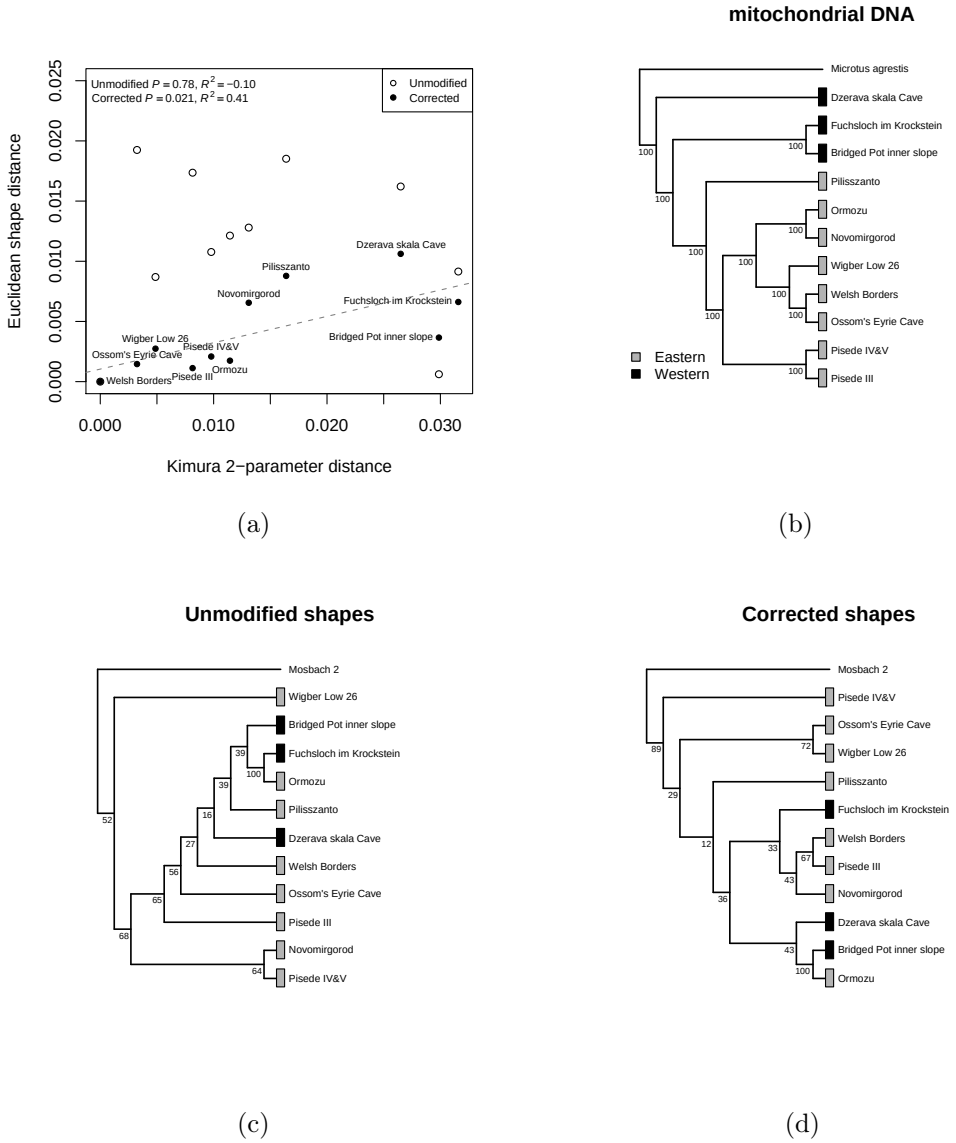

(a) (b)

(c) (d)

Figure 6.1: Phylogenetic relationships based on mtDNA and M_1 shape. (a) Relationship between genetic divergence (% sequence divergence, Kimura 2-parameter distance) and Euclidean shape distance from unmodified shapes and shapes corrected to adult size in eleven fossil and Recent groups. Distances shown relative to the Recent Welsh Borders OTU. Linear regression P-values for both relationships given and regression line drawn for model with corrected M_1 shapes. (b)–(d) Maximum-likelihood trees based on mtDNA, unmodified M_1 shapes, and M_1 shapes corrected to adult size. Branch tip colours show lineage affiliations determined from mtDNA phylogeny and percentage values from 1000 bootstrap replicates shown at tree nodes. Branch lengths not shown to aid clarity.

eage OTUs. An examination of the first two axes from a PCA of shape variables from both shape datasets suggests that separation between mtDNA lineages is less clear in unmodified shapes (Figure 6.2a) compared with size-corrected shape data (Figure 6.2b). These differences are small, however, and are restricted in Figure 6.2 to the first two axes of PC space. One reason for the lack of strong, consistent phylogenetic signal in shape data may be that shape differences between OTUs are much less than shape differences within OTUs. This is shown in Figure 6.3 where it can be seen that the variance in both unmodified and size-corrected shapes is less between OTUs that within OTUs. Such a distribution of shape variance potentially obscures any between-OTU differences that exist and therefore any phylogenetic pattern contained. Given that only 41% of shape morphology can be attributed to mtDNA divergence (Section 6.3.1) the low level of between-OTU variance appears likely to affect adversely the ability to distinguish phylogenetic relationships from molar shape.

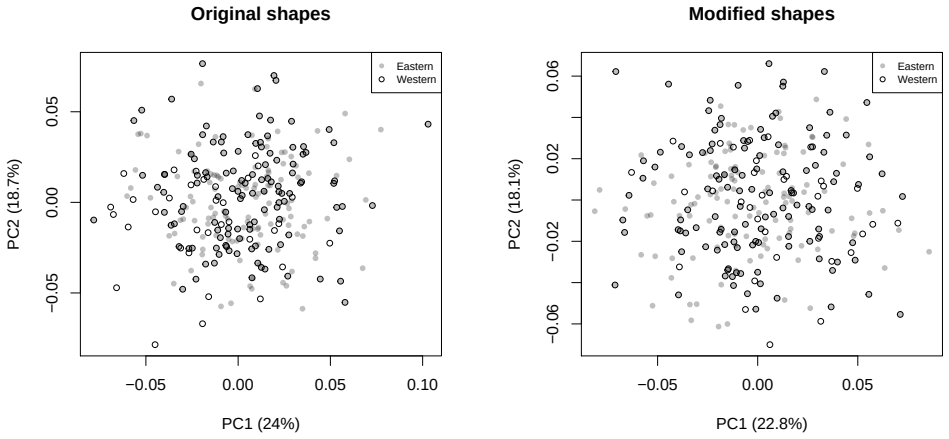

(a) (b)

Figure 6.2: Shape differences between 'Eastern' and 'Western' water vole lineages. Scatterplots show the first two PC axes from PCAs of shape variables. Each point is a specimen from OTUs corresponding to mtDNA groups in Figure 6.1b. Plot characters show membership of mtDNA 'lineage'. (a) shows shape differences between lineages using unmodified shapes. (b) shows shape differences between shapes after correction for shape–size effects.

6.4 Conclusions

Size-corrected molar shape divergence appears to reflect time since common ancestry, something that original, unmodified shapes do not. The correspondence between size-corrected molar shape and mtDNA divergence does contain uncertainty, however, with less than half of molar shape divergence explained by mtDNA

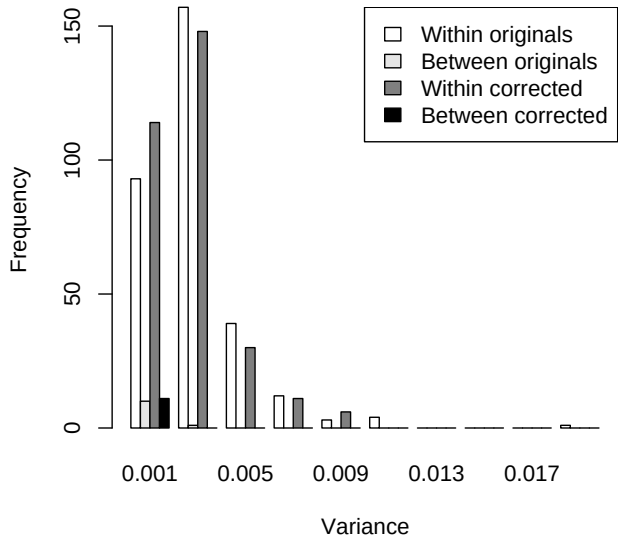

Figure 6.3: Within- and between-group shape variances in original and size corrected molars from the OTUs used earlier in phylogenetic comparison.

divergence and the correlation between the two datasets is close to significance. It may also be that this relationship becomes weaker with increasing phylogenetic distance. Size-corrected molar shape is marginally better at reconstructing mtDNA phylogeny than unmodified shapes but only partially recovers phylogenetic patterns. This may be due in part to within-OTU shape variance obscuring between-OTU shape differences as well as aspects of molar shape that cannot be explained by phylogenetic divergence.

Chapter 7

Spatial and temporal patterns in morphology

7.1 Introduction and approach

Chapter 5 presents evidence that ontogeny has an appreciable influence on molar morphology and Chapter 6 further suggests that the removal of morphological variation explainable by ontogeny improves the phylogenetic information present within morphology. This chapter pursues these ideas further by using enamel thickness ratio (SDQ) and M_1 shape to investigate patterns of morphological change in time and space. Both unmodified and size-corrected (Section 5.4) morphological data will be employed in order to assess which appear most appropriate for use in evolutionary and biostratigraphic studies. The enamel thickness data presented in this study represent a new dataset that is not directly comparable with previously published SDQ values (Section 5.6). Where previous SDQ data are available they will be referred to in the discussion of temporal and spatial patterns and related to pre-existing biostratigraphic or biogeographic ideas. The nomenclature introduced in Section 5.6 to distinguish between unmodified, size-corrected and published SDQs will used throughout ($SDQAU_p$, axially oriented, unmodified SDQ of a population; $SDQAC_p$, axially oriented, size-corrected SDQ_p of a population; and SDQA, axially oriented SDQ).

The following exploration looks at seventy-one water vole from the early Middle Pleistocene to the Recent, analysed in a series of chronostratigraphic plots. The same assemblages are present in both enamel thickness and shape datasets, with 1 328 and 2 015 M_1s being used in the enamel thickness and shape datasets respectively. To increase the size of each dataset, assemblages with five or more specimens are included in enamel thickness analysis and eight or more specimens are included in shape analysis. The possible problems of small sample sizes (Section 4.4.2.2) will, however, be borne in mind during discussion. The mean, min-

imum, maximum, and 1 standard deviation (1σ) of SDQs from each assemblage are used in enamel thickness plots. It is assumed that the mean SDQ or shape is a good representative average morphology. Minimum and maximum SDQ is shown where possible where it does not affect the visual clarity and descriptive simplicity of the plot. Regression statistics for enamel thickness and Centroid Size are reported directly in Tables B.2, B.3, B.4, and B.5, and SDQs are reported in Tables B.6 (unmodified) and B.7 (size-corrected). These data can also be found in Appendix C, along with unmodified and size-corrected enamel thicknesses.

The SDQ is the pre-eminent metric in water vole biostratigraphy, it being easily obtained and intuitive to understand and interpret. Tooth shape on the other hand is harder to apply to practical biostratigraphy because the metric of shape difference—the Procrustes distance (D_p)—is a measure of relative distance to other shapes. In the following exploration, tooth shape will be measured with respect to the Recent Welsh Borders assemblage (in the manner of Section 6.2). This group was chosen because the overall aim of this study is to attempt to relate British stratigraphy with that of continental Europe, and using shape distance has the advantage of taking into account whole shape differences. One disadvantage of using relative distances is that each shape distance plotted is dependent on its relationship with the Welsh Borders OTU. Another disadvantage is that groups that occur together in the same area of the plot are not necessarily the same shape, unless shape differences approach zero. The Procrustes distance for each shape will be found in the same way as in Chapter 6: namely by finding the mean shape for each group, carrying out a GPA using these mean shapes, and using D_p from this analysis to calculate pairwise Euclidean distances between each group relative to the Welsh Borders shape. Only OTUs that had matching SDQ datasets were used. Size-corrected shapes were assessed in the investigation of morphological change over MIS 3–MIS 1 (Section 7.2) because these were found to offer a better dataset of phylogenetic relationships than unmodified shapes over this period (Chapter 6). In assessing assemblages dating between MIS 19 and MIS 3 both size-corrected (Figure 7.12) and unmodified (Figure 7.13) shape differences were employed. This was to understand the effects of allometric corrections on the relationships between OTUs for which no molecular data were available. The use of OTUs that are different and additional to those in Section 6.2 mean that the patterns found in this previous analysis will not be exactly replicated. The matrix of Euclidean distances between group mean shapes can be found in Section C of the Appendix.

Assemblages are grouped into seven geographic zones—defined in the maps accompanying the chapter—in an attempt to represent areas that have been implicated as biogeographically significant as regions of endemism or refugia, or areas where immigration events or hybrid zones exist: the Caucasus, Central Europe, Eastern Europe, Great Britain, Italy, Southeast Europe, and Southwest Europe

(e.g., Bilton *et al.*, 1998; Taberlet *et al.*, 1998; Hewitt, 1999; Jaarola and Searle, 2002; Zima, 2004). Further to this geographic division the data will be considered in two chronological sections: MIS 19–MIS 3 and MIS 3–Recent. Discussion will overlap chronologies, however, in an attempt to stitch together longer-term patterns and trends. The period from MIS 3 to the Recent will be considered first as this interval contains Recent groups and a number of fossil and extant populations whose phylogenetic relationships are known through mtDNA analysis. The structure and patterns shown by these groups can then be used as comparative data with which earlier populations can be contrasted.

7.2 MIS 3–Recent

7.2.1 Setting

This interval encompasses events that have most recently shaped the fauna, flora, and terrain of Europe. It includes a sustained period of cool and cold climate, the Last Cold Stage, during which steppe-tundra environments existed over much of northern and western Europe, and extensive ice sheets and ice-masses developed across the continent, reaching their maximum extent around 20 k yr BP (Figure 7.1). The temperate conditions of the present Holocene interglacial developed in a climatically complex manner around 14–10 k yr BP (e.g., Steffensen *et al.*, 2008) and a marine transgression that accompanied climatic warming isolated the British Isles from continental Europe during the Early Holocene, possibly around 8000 ^{14}C BP (Shennan and Horton, 2002). This period sees the extinction of the majority of the remaining members of the mammalian megafauna (e.g., Stuart *et al.*, 2004) and the Neanderthals (e.g., Stewart, 2007), and the appearance and spread of anatomically modern humans in Europe (e.g., Mellars, 2004). During the Last Cold Stage obligate temperate species were not present in northern and western Europe but were restricted to southerly refugia (e.g., Hewitt, 1999), and perhaps to cryptic northern refugia (Stewart and Lister, 2001). During the mid and late Holocene the spread of agriculture and the growth of human populations has led to major landscape changes across virtually the whole of Europe and western Asia.

A key feature of the analysis of *Arvicola* molar morphology over this interval is the availability of a mtDNA phylogeny (Section 6.2). This very recent work, from an as yet unpublished Ph.D thesis by Selina Brace (School of Biological Sciences, Royal Holloway, University of London; Brace, 2010), includes modern and ancient DNA (aDNA) sequences from the same specimens or assemblages examined in this morphological study. Where known, the lineage affiliation of an assemblage is indicated in the SDQA plots of Figures 7.4 and 7.5, and the Euclidean distance

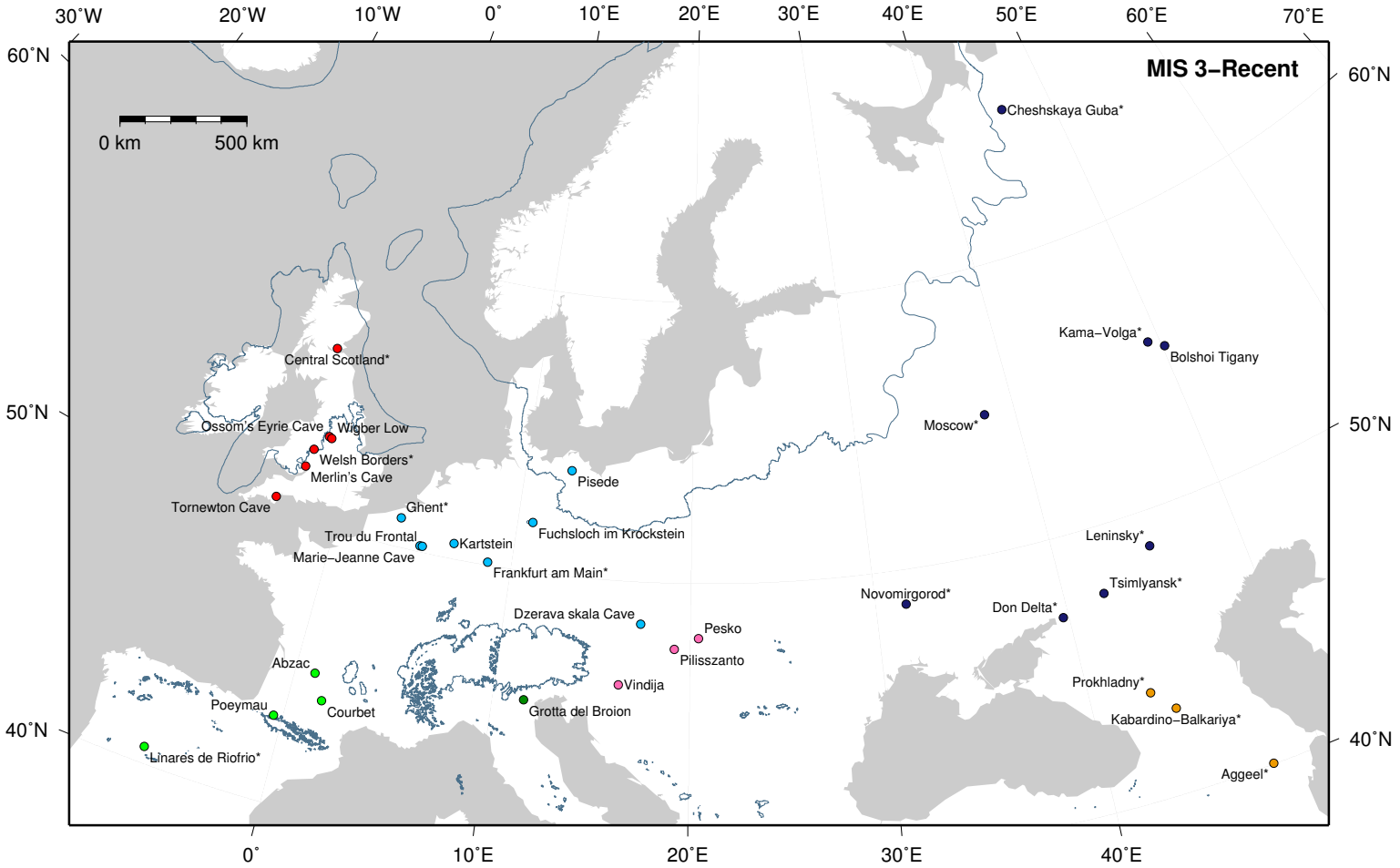

Figure 7.1: Map showing localities dating between MIS 3 and the Recent. Recent groups marked by an *. Colour coding of localities refers to geographic zones outlined in Section 7.1. Blue-grey line shows estimated maximum extent of Last Glacial Maximum ice (Ehlers and Gibbard, 2004).

plots of Figure 7.8. Geographic groupings are shown in the SDQ plots of Figures 7.2, and 7.3, and in the Euclidean distance plot of Figure 7.7. Figure 7.1 shows the locations of fossil localities referred to in the following discussion.

7.2.2 Morphological patterns

7.2.2.1 Iberia and the Caucasus

Recent groups display a greater range in SDQAs than fossil ones, but this is a result of the inclusion of two groups of *Arvicola terrestris* from the Caucasus region—Aggeel ($SDQAU_p$=108.0, $SDQAC_p$=113.5) and Prokhladny ($SDQAU_p$=111.9, $SDQAC_p$=112.9)—and a single group of *Arvicola sapidus* from Spain (Linares de Riofrio, $SDQAU_p$=100.3, $SDQAC_p$=101.8). The remaining Caucasus group of Kabardino-Balkariya has a much lower SDQA value than the other Caucasus populations and is nested with a number of Russian populations from the Eastern Europe zone. The specimens from Kabardino-Balkariya are all of a very similar size meaning that enamel thickness–size regressions have little effect on modelled enamel thickness (Figure B.5f), and so unmodified and size-corrected SDQA values are very similar: $SDQAU_p$=84.8 and $SDQAC_p$=84.7. *Arvicola* populations from Iberia and the Caucasus have previously been recognised as possessing much

Figure 7.2: (Following page) Unmodified SDQ ($SDQAU_p$) values in assemblages dating from MIS 3 to the Recent. Plot shows $SDQAU_p$ mean (point) and range (horizontal whiskers; $SDQAU_p$ range omitted in Recent populations for clarity), along with the possible age of each assemblage (vertical whisker heights; see Chapter 3). Assemblages colour-coded by geographic zone (see Section 7.1) and labelled as follows (* denotes Recent material): **Abz** - Abzac (n=17); **Agl** - Aggeel* (n=5); **BTg** - Bolshoi Tiganye (n=10); **CSc** - Central Scotland* (n=13); **ChG** - Cheshskaya Guba* (n=19); **Crb** - Courbet (n=29); **DDt** - Don Delta* (n=7); **DSC** - Dzeravá skala Cave (n=24); **FaM** - Frankfurt am Main* (n=5); **FiK** - Fuchsloch im Krockstein (n=13); **Ghe** - Ghent* (n=18); **GBN** - Grotta del Broion, Sala Grande N (n=10); **GBQ4** - Grotta del Broion, Sala Grande Q4 (n=8); **GBQ5** - Grotta del Broion, Sala Grande Q5 (n=11); **GBR1** - Grotta del Broion, Sala Grande R1 (n=16); **KBa** - Kabardino-Balkariya* (n=19); **KVg** - Kama-Volga* (n=13); **Kar** - Kartstein (n=7); **Len** - Leninsky* (n=20); **LdR** - Linares de Riofrio* (n=7); **MJ2** - Marie-Jeanne Cave 2 (n=11); **MJ4** - Marie-Jeanne Cave 4 (n=9); **MJ6** - Marie-Jeanne Cave 6 (n=7); **Mer** - Merlin's Cave (n=64); **Mcw** - Moscow* (n=21); **Nvm** - Novomirgorod* (n=13); **OEy** - Ossom's Eyrie Cave (n=37); **Psk** - Peskö "brick red" strata (n=26); **Pil** - Pilisszántó (n=10); **PIII** - Pisede III (n=13); **PIVV** - Pisede IV&V (n=25); **Poe** - Poeymaü BS (n=15); **Prk** - Prokhladny* (n=15); **Tor** - Tornewton Cave Red Cave Earth (n=10); **TdF** - Trou du Frontal (n=9); **Tsm** - Tsimlyansk* (n=15); **VnE** - Vindija E-F (n=15); **VnG** - Vindija G (n=20); **WBd** - Welsh Borders* (n=22); **WLw** - Wigber Low 26 (n=49).

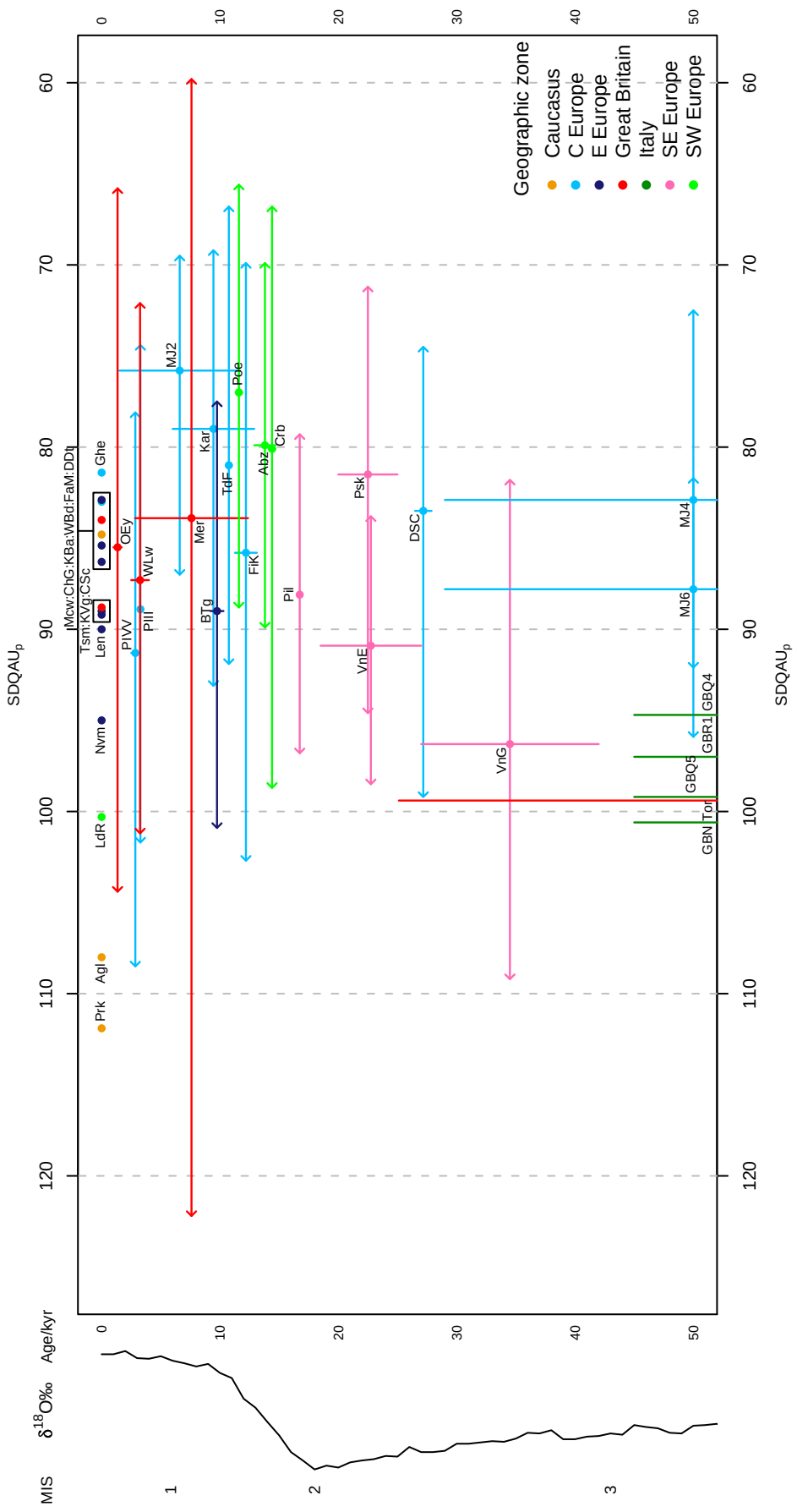
MIS
δ18O‰
Age/kyr
SDQAUp
SDQAUp
Geographic zone
Caucasus
C Europe
E Europe
Great Britain
Italy
SE Europe
SW Europe
Prk
Agl
LdR
Nvm
Len
Tsm:KVg:CSc
IMcw:ChG:KBa:WBd:FaM:DDt
Ghe
OEy
PIVV
PIII
WLw
MJ2
Mer
BTg
Kar
TdF
FiK
Pde
Abz
Crb
Pil
Psk
VnE
DSC
VnG
MJ4
MJ6
GBQ5
GBR1
GBQ4
GBN
Tor

higher SDQs than other water vole populations (Section 2.3.1; Kratochvíl, 1981; Röttger, 1987), and the generally high SDQA values shared by Aggeel, Prokhladny, and Linares de Riofrio may betray a more recent common ancestry between them with respect to other populations. The SDQA of Kabardino-Balkariya perhaps suggests that this group is phylogenetically more distinct from the water voles from the nearby locality of Prokhladny. These patterns of SDQA are interesting given the presence of the Caucasus mountains between Aggeel and Prokhladny, which would otherwise seem to be a sizeable biogeographic barrier. A deep sister-group relationship between Linares de Riofrio and the Caucasus groups of Aggeel and Prokhladny may be conceivable, as *A. sapidus* is estimated to have speciated from *A. terrestris* earlier in the Pleistocene (Taberlet *et al.*, 1998) and the early origins of *Arvicola* are thought to lie in the Early Quaternary migration of populations from Asia into western Europe (Lister, 2004). This would require, however, a long period of evolutionary stasis, or that parallel evolution had occurred, in order to maintain similarities in SDQA between these groups up to the present day. No palaeontological data were available from Iberia or the Caucasus to reveal relative differences in SDQ between these groups in the past, but the lack of correspondence between either $SDQAC_p$ or $SDQAU_p$ values from Linares de Riofrio and three fossil populations from southwest France (Abzac, Courbet, and Poeymaü) would appear to suggest that the water vole from this latter region are not *A. sapidus*. It is interesting to contrast this conclusion with the mtDNA evidence of Taberlet *et al.* (1998), which shows that both *A. sapidus* and *A. terrestris* are found in close proximity in southwest France today.

Shape differences between Caucasus and Iberian groups tell a different story to that given by SDQA (Figures 7.6 and 7.7). There is a substantial shape difference in both DAU_p and DAC_p between Aggeel and the populations from Kabardino-Balkariya, Prokhladny, and Linares de Riofrio. Indeed Aggeel is the group that is most distinct in terms of shape across the whole dataset, fossil and Recent. This difference may be caused by the Aggeel groups being isolated for a long period of time, to the south of the Caucasus mountain range, from other *Arvicola* populations, and possibly also evolving under different set of selective pressures to those populations to the north of the Caucasus. A further possibility is that the specimens from this locality have been misidentified as *Arvicola*, and certainly the anterior lobe of M_1s from Aggeel (e.g., ImageID 3610) are atypical of M_1s from other *Arvicola* populations. The shape data for Kabardino-Balkariya and Prokhladny show these groups to fall within the morphological range of other European *A. terrestris* assemblages, as does the *A. sapidus* material from Linares de Riofrio. The lack of morphological distinctiveness of the Linares de Riofrio *A. sapidus*, despite the supposed long history of this water vole as a separate species from *A. terrestris*, may be due to stochastic convergence, which is more

likely to occur between distantly related groups than recently separated populations (Gingerich, 1993). Alternatively, similarities in tooth shape could be maintained through stasis, constraining adult M_1 outlines to a narrow range of possibilities that are limited by the opitimum performance of the M_1 in processing vegetation.

7.2.2.2 Historical intraspecific relationships and SDQA

At the gross level both SDQA datasets show a decrease in enamel thickness ratios from MIS 3 to the middle Holocene, followed by a increase in SDQA in the late Holocene and Recent (Figures 7.2–7.8). Such a pattern can either be attributed to an evolutionary cause or to the immigration of populations possessing different phenotypes, but the availability of mtDNA evidence for intraspecific lineages offers the possibility of resolving between these two models.

Sudden changes in morphology over time have been previously noted in the fossil record of Holocene water voles from central Europe. Heinrich (1982) commented on enamel thickness differences between water voles from the northern European lowlands and earlier fossils from the Last Cold Stage. While Storch (cited in Gromov and Polyakov, 1992, p. 348) recognised *Arvicola antiquus* as a group of Late Pleistocene fossorial water voles present in 'mixed and lemming faunas' that existed in England and continental western Europe (France and the area of the former West Germany). It was suggested that *A. antiquus* eventually disappeared with the regrowth of forests in the Holocene (Storch *ibid*). Such observations are consistent with the mtDNA evidence presented here and by Brace (2010), which show shifts in the spatial distribution of intraspecific lineages over the Lateglacial and Holocene. Although the dataset is geographically and temporally patchy, these molecular data indicate that Eastern lineage water voles shifted their distribution from the east and southeast of Europe northwestwards across central and western Europe, replacing Western lineage *Arvicola* that previously had occupied these areas.

The earliest Western lineage assemblages recorded in continental Europe are from Marie-Jeanne Cave 4 and Dzeravá skala Cave (27 050±527 cal BP). Although this is not a comprehensive geographic sample, these occurrences appear to indicate that the Western lineage was present across a wide part of central Europe, at least during the later part of the Last Cold Stage. It also may be the case, given that that Eastern lineage groups are not found at all in the far west and southwest of Europe, that the Western lineage was present in France and possibly parts of Spain during this period. The first record of the Western lineage in Britain comes from Gully Cave (Ebbor Gorge, Somerset, England), a site currently being investigated by Prof. Danielle Schreve (Department of Geog-

raphy, Royal Holloway, University of London), where an *Arvicola* mandible has been dated at 14 791±302 cal BP (OxA-20249). Western lineage *Arvicola* have also been found in the British 'Lateglacial' site of Bridged Pot (Brace, 2010) but this lineage may also be present in other Lateglacial sites such as Ightham Fissures, where *Arvicola* have been dated at 27 950±140 cal BP (Section 3.6.3.3). Unfortunately fossil *Arvicola* from Ightham Fissures have not yielded aDNA. The Eastern lineage is first recorded in continental Europe at Pilisszántó in Hungary (16 740±80 cal BP), and later is found at two sites that also contain Western lineage assemblages, with the Eastern always found to be younger than the Western lineage. At Fuchsloch im Krockstein (Section 3.5.3.4) a single *Arvicola* specimen from the Western lineage yielded a date of 12 992±109 cal BP, while another single *Arvicola* specimen from the Eastern lineage dated to 11 560±159 cal BP. At Merlin's Cave (Section 3.6.3.4) a single *Arvicola* mandible from the Western lineage was dated to 12 130±120 cal BP and another mandible, found to be from the Eastern lineage, was dated to 2 900±40 cal BP. An earlier record of the Eastern lineage in Britain may be at Wigber Low 26, which has an age of 4–2.5 k yr BP (Section 3.6.3.7). Brace (2010) also shows that at the locality of Trou Al'Wesse, in the Ardennes region of southeast Belgium, Western lineage *Arvicola* are found at around 20 k yr BP, while Eastern lineage *Arvicola* are present in sediments dating to the Holocene. In Great Britain this lineage replacement has culminated today in the restriction of Western lineage water voles to Scotland (Piertney *et al.*, 2005), a pattern replicated in other British small mammals that has led to a modern 'Celtic fringe' in this component of the Recent fauna (Searle *et al.*, 2009). Elsewhere in Europe, Western lineage populations can be found today in Belgium, southwest France, and Switzerland (Piertney *et al.*, 2005; Brace, 2010). The suture between the two lineages in continental Europe at present appears to run through Belgium and roughly along the border between France and Germany to the Alps (Taberlet *et al.*, 1998).

Eastern and Western mtDNA lineages are potentially separable in terms of SDQA (Figures 7.4 and 7.5), with the chrono-stratigraphic plots suggesting that Western lineage groups possess lower SDQAs than Eastern lineage groups. A cluster of Late Pleistocene and early Holocene assemblages from the Central and Southwest European zones share similarly low SDQAs (SDQA $\lesssim 80$: Abzac, Courbet, Karstein, Marie-Jeanne Cave 2, Poeymaü, and Trou du Frontal). The Marie-Jeanne Cave 2 assemblage is part of the Western mtDNA lineage and it is interesting to speculate whether the other low SDQA *Arvicola* are also Western lineage populations. The localities of Abzac, Courbet, and Poeymaü fall within the modern distributional range of *A. sapidus* (Reichstein, 1982d). It seems unlikely, however, that the *Arvicola* from the these three assemblages are *A. sapidus* as their SDQs are much lower (Linares de Riofrio SDQA ≈ 100; Röttger, 1987)

and body size much smaller (see Centroid Size in Figures B.1–B.12; Röttger, 1987) than in *A. sapidus* today. Although *A. sapidus*, an obligate semi-aquatic species today, could possibly have inhabited the landscape surrounding Abzac, Courbet, and Poeymaü as the palaeoenvironmental data for these sites suggests a mosaic of upland and riparian habitats were present Chapter 3, and Centeno-Cuadros *et al.* (2009) estimate that the colonisation of France by *A. sapidus* from Iberia occured around 100–35 k yr BP. In its modern distribution, the Western lineage can be found in France, central Europe, and parts of northern Spain (Taberlet *et al.*, 1998; Brace, 2010), and there is no indication from the aDNA dataset that Eastern lineage populations occurred further west than Belgium or Switzerland (Brace, 2010). This may be because of a lack of molecular evidence from this western part of Europe during the Last Cold Stage and Holocene. The most parsimonious hypothesis is that the water vole from Abzac, Courbet, and Poeymaü all belong to the Western lineage of *A. terrestris* (although see Section 7.2.2.4 for the perspective of molar shape). The water voles from Karstein and Trou du Frontal may also be Western lineage populations but it is difficult to estimate their intraspecific affiliation independent of morphology. This is because of uncertainty in locating the western-most edge of the Eastern lineage relative to Karstein and Trou du Frontal during the Lateglacial and early Holocene. This appears to be the period when Eastern lineage *Arvicola* are rapidly shifting their distribution through the west and northwest of Europe. The Eastern lineage was present at Fuchsloch im Krockstein, several hundred miles to the northeast of Kartstein, by around 11.5 k yr BP, while the earliest record of the Eastern lineage in Belgium is at some point during the Holocene (Brace, 2010). At present Kartstein and Trou du Frontal are approximately located at the suture between Western and Eastern lineages, but the location of this edge may have been further west in the past and may also have been geographically diffuse. So, although the low SDQA values of *Arvicola* from Kartstein and Trou du Frontal would seem to associate them with populations from the nearby assemblage of Marie-Jeanne Cave 2, and other probable Western lineage groups from the Lateglacial and early Holocene, the proximity of Kartstein and Trou du Frontal to the shifting edge of the join between two lineages means that a firm link cannot be made.

A pattern of Late Pleistocene SDQA decrease and Holocene SDQA increase may occur within the Eastern lineage, but this is difficult to ascertain because two of the possible Lateglacial assemblages where Eastern lineage aDNA sequences have been recovered (Fuchsloch im Krockstein and Merlin's Cave) contain a mixture of both Eastern and Western lineage populations. Unfortunately it so happens that the specimens that could be dated, sequenced, and morphometrically analysed did not coincide for these two assemblages, and so it is not possible to comment on the possible relationship between SDQA and genetic lineage. But

perhaps more detailed analysis of M_1 morphology (SDQA and shape data) could resolve any differences between morphological groups that may be present within these assemblages. There may be evidence of an increase in SDQ from the early Holocene to the Recent from the $SDQAC_p$ differences between Bolshoi Tiganye and Recent Russian and Ukrainian populations, which despite not all bearing sequences are highly likely to be Eastern lineage groups (Brace, 2010). This is only visible in $SDQAC_p$ and not $SDQAU_p$, however.

The Southeast European zone assemblages from Peskö and Vindija may belong to the Eastern lineage because these groups are south of the Carpathian and eastern Alpine mountain ranges, as is Pilisszántoó and other Recent populations from Romania and Slovenia that are confirmed as from the Eastern lineage (Brace, 2010). This type of intraspecific pattern has also been observed in *Clethrionomys glareolus* (Deffontaine *et al.*, 2005) and is consistent with research that implicates the Carpathian region as a glacial refugium for temperate species (e.g., Provan and Bennett, 2008). Differences appear to exist in $SDQAC_p$ between the assemblages of Peskö, Pilisszántó, and Vindija, and those of similar age that are affiliated with the Western lineage (Marie-Jeanne and Dzerava skala Cave). These differences are evident for Peskö where the $SDQAC_p$ (86.4) is relatively much higher than $SDQAU_p$ (81.5) compared wtih the other OTUs. Peskö also appears to have more in common in terms of shape distance with Western lineage water voles than with Eastern lineage OTUs (Section 7.2.2.4). Pilisszántó, on the other hand, seems superficially to be a good representative of an Eastern lineage group in terms of SDQA and shape.

An inspection of the enamel thickness–tooth size regressions for both Peskö (Figure B.9a) and Pilisszántó (Figure B.9b) show that the structure of the population in terms of allometric relationships is not as expected for an instantaneous population. Some regressions are negative, which appear to be driven by a small number of large-sized M_1s with thin leading-edge enamel, and small-sized molars with thick leading-edge enamel. Re-examination of digital photographs and the measurements made from them these patterns appear to be accurate. Some of the *Arvicola* material from the Peskö 'brick red' stratum were curated as mixed with other sedimentary layers (Section 3.7.3.4) and it could be that the inaccurate size-correction given to Peskö is a consequence of it being a mixed fossil assemblage. At Pilisszántó, the excavation history of the site suggests that there is a high probability the fossil *Arvicola* assemblage is temporally mixed (Section 3.7.3.5), yet both SDQA values from this assemblage are similar ($SDQAU_p$=88.1, $SDQAC_p$=85.8; Figure B.9b). Mixing in these assemblages may lead to further complications because lineage diversity has been observed within the Carpathian region (Kotlik *et al.*, 2006), meaning that it is possible both Eastern and Western lineages are represented Peskö and/or Pilisszántó, as is the case at Fuchsloch im

Krockstein and Merlin's Cave.

The Italian assemblages from Grotta del Broion, Sala Grande and the British Tornewton Cave assemblage, have similar SDQA values that are higher than those from other groups, which is to be expected from the oldest assemblages in this part of the discussion. The assemblage from Vindija G, which is estimated to be younger than any from Grotta del Broion, has $SDQAU_p$ values that are similar to and $SDQAC_p$ values that are slightly lower than those from Grotta del Broion. Recent water voles from the Italian peninsula have been recognised as genetically distinct from other populations in Europe (Taberlet *et al.*, 1998; Brace, 2010) but the similarity in SDQA between Grotta del Broion and Vindija G may betray a phylogenetic relationship. Connections between the fauna of northeastern Italy and the western Balkan peninsula are recognisable throughout the Quaternary, and are geographically easy to develop during glacial periods because sea-level fall at these times exposes the northern Adriatic as dry land (Sala and Marchetti, 2006). If the *Arvicola* from these areas were phylogenetically connected during the Last Cold Stage then Vindija G, and also perhaps Vindija E, could be populations of an Italian lineage. Alternatively, some or all of the *Arvicola* from Grotta del Broion could be Eastern lineage water voles, and this latter scenario may be most likely as it mirrors faunal movements observed in other groups during the Middle and Late Pleistocene (Sala and Marchetti, 2006). It is interesting that Grotta del Broion, Sala Grande, layer N, the stratigraphically highest deposit analysed, shows higher SDQA values than layers R1, Q4, or Q5. Paunescu *et al.* (2004) found that Late Pleistocene populations of *Arvicola* from France have lower SDQs than those from southern Italy. It could be that the *Arvicola* assemblage from layer N is derived from a southern Italian population. Layers N–I at Grotta del Broion show evidence of warmer climates with than occur earlier in the stratigraphy, and this climatic change may relate to any immigration of *Arvicola* that might have occurred. The relationships between the *Arvicola* from Grotta del Broion and assemblages from earlier in the Late Pleistocene are discussed in Section 7.3.2.3.

In summary, there do appear to be difference in SDQA values between Western and Eastern lineages of *A. terrestris*, as well as between *A. terrestris*, *A. sapidus*, and some populations from the Caucasus.

7.2.2.3 Environmental factors and SDQA

An alternative, or additional, explanation for differences in SDQA between assemblages, and possibly between lineages, could be as phenotypic or even adaptive responses to environmental change. Where changes in vegetation brought about by environmental changes could prompt responses in dental morphology. It has been suggested that, during periods of cold climate, levels of tooth wear could be

elevated because of the development of tougher vegetation (Massey *et al.*, 2007) or increased amounts of inorganic sediment ingested incidentally (Kolfschoten, pers. comm., 2005). The modifications to enamel that environmental changes may drive could include the development of thicker enamel, especially leading edge enamel (Rensberger, 1973), and increased rates of tooth growth (Schour and Medak, 1951). Populations from all the European zones established above could potentially be effected in this manner. If there were such ecophenotypic effects at play then it would be expected that fluctuations in SDQA would mirror fluctuations in climate (inferable from the MIS record and palaeoenvironmental analyses such as those in Chapter 3).

The SDQA plots do offer some support for such ecophenotypic interactions. The cluster of low SDQA assemblages mentioned above (Abzac, Courbet, Karstein, Marie-Jeanne Cave 2, Poeymaü, and Trou du Frontal) could all potentially date from the Lateglacial, and palaeonenvironmental evidence from a number of these sites suggests cool-climate, open landscapes were present during accumulation of some of the fossil assemblages (e.g., Abzac, Section 3.4.1.1; Kartstein, Section 3.5.3.5; and Poeymaü, Section 3.4.1.3). In Marie-Jeanne Cave, however, Layer 2 contains evidence of temperate woodland environments (Section 3.2.1.1), which would seem to be inconsistent with a correlation between open, steppic environments and low SDQA. The age of Marie-Jeanne Cave Layer 2 is, however, not well understood and the palaeoenvironmental indicators may not temporally match the *Arvicola* assemblage (Section 3.2.1.1). In the Holocene a reversal of the previous trend in decreasing SDQA over time occurs that appears to be found at least within the Western lineage (from Marie-Jeanne Cave 2: $SDQAU_p$=75.8 and $SDQAC_p$=74.6, to Central Scotland: $SDQAU_p$=88.8 and $SDQAC_p$=87.7). A link between the increase in the SDQA of Central Scotland and a specific environmental effect is possible. As stated above, the palaeonvironments at Marie-Jeanne Cave Layer 2 appear to be temperate woodland (Section 3.2.1.1). Conversely Recent Scottish populations inhabit a cool-temperate environment and are, in many instances, animals of upland areas and in some cases fossorial[1] (Jefferies, 2003b).

A Holocene reversal in SDQA is not apparent in the Eastern lineage, despite assemblages from this intraspecific group have been found in a variety of environments such as temperate, mesic habitats (Pisede, Section 3.5.4.1 and Recent Welsh Borders), upland moor environments (Wigber Low, Section 3.6.3.7 and Ossom's Eyrie, Section 3.6.3.5), and cool-climate tundra or steppe (Pilisszántó, Section 3.7.3.5).

If Peskö and Pilisszántó were to be considered as representative of Western

[1]Although not in the central Scottish region today, at the time the specimens viewed for this thesis were collected a fossorial form of the water vole may have been present in Britain (Jefferies, 2003b).

and Eastern lineages respectively these stratigraphically similar OTUs provide an example of differences in SDQA between lineages that have similar palaeonenvironmental indicators. Although there are taphonomic and curatorial problems with these sites (Section 7.2.2.2), meaning palaeoenvironmental and morphometric data may be of low resolution.

7.2.2.4 Historical intraspecific relationships and shape

There is a general pattern of increased shape difference with increased age difference between Welsh Borders and other OTUs (Figures 7.7 and 7.8). This mirrors the pattern seen in Figure 6.1a, which shows that over 40% of size-corrected shape differences can be explained by mtDNA divergence. However, it must be remembered that, by virtue of clock-like base-pair substitution in the mitochondrial genome, mtDNA divergence is a proxy for time since common ancestry (Polly, 2001). Figures 7.7 and 7.8 therefore show time since common ancestry of various populations at difference points in time. Of the OTUs whose lineage is known (Figure 7.8), Eastern lineage OTUs show an approximately linear shape difference–age relationship, which conforms to expectations drawn from Chapter 6. Molecular data from Piertney *et al.* (2005) and Brace (2010) show that Recent Eastern lineage populations occur across the East European Plain and Scandinavia, and therefore it seems reasonable to assume that Recent groups from these areas, as well as the early Holocene Bolshoi Tiganye assemblage, are also Eastern lineage populations. These groups display a range of Euclidean distance values, rather than a cluster of OTUs of low shape difference, which likely reflects aspects of time since common ancestry, within the Eastern lineage, with the Welsh Borders population.

The pattern of occurrence of Western lineage OTUs shown in Figure 7.8 is different to that shown by Eastern lineage groups. These OTUs are similar shape distances from Welsh Borders, regardless of their age. This may reflect the difference between the Welsh Borders OTU and the Western lineage as a function of the last common ancestor of both lineages (Polly pers. comm., 2011).

The position of OTUs without a mtDNA sequence may offer some clue as to their intraspecific relationships. However, these distributions are interplays between time since common ancestry and evolutionary tempo and mode, as well as being prone to possible errors introduced through sampling, landmarking and size-correction. Some assemblages, such as Bolshoi Tiganye—mentioned above—and Kartstein appear to show shape differences that are compatible with SDQA evidence and biogeographic understanding (Section 7.2.2.2). Others, such as Abzac and Poeymaü (good candiidates as Western lineage groups from SDQA data), and Peskö (a possible Eastern lineage group in terms of $SDQAC_p$), seem to have relative shape distances that are at odds with possible evidence for lineage affiliation

provided by SDQA. In the case of Peskö at least an inaccurate size correction may contribute to the shape difference observed in this OTU, but also this assemblage may include individuals from the Western lineage (Section 7.2.2.2). Abzac and Poeymaü on the other hand are clearly closer in terms of shape to the Eastern lineage OTU of Pilisszántó and the probable Eastern OTU of Bolshoi Tiganye, rather than the Western OTUs that Abzac and Poeymaü otherwise seem to group with from their geographic location and low SDQA. Vindija E is an OTU that appears to belong to the Eastern lineage from shape and SDQA data but Vindija G shows a shape difference that perhaps has more in common with Western lineage groups. It is not inconceivable, given the interconnections observed between the fauna of southern France, northern Italy, and the western Balkans (Sala and Marchetti, 2006) that an Eastern lineage group could disperse from the Balkans to southwest France at some point after the age of *Arvicola* at Vindija G. However, there is no evidence for the persistence of this Eastern lineage in the Southwest Europe zone in modern times, with only Western lineage *A. terrestris* and *A. sapidus* present in this region today (Centeno-Cuadros *et al.*, 2009; Brace, 2010). Such a phylogeographic pattern is also not supported by SDQA, which suggest lower SDQAs in Western lineage groups—including Vindija G and E—compared with Eastern lineage groups (Section 7.2.2.2), although ecophenotypic effects could be at play here (Section 7.2.2.3).

The assemblages of Fuchsloch im Krockstein and Merlin's Cave contain fossil *Arvicola* from both lineages. The shape differences these OTUs display are in some respects intermediate between lineages and may reflect the mixture of M_1 shapes from both lineages. The assemblages from Grotta del Broion may, as outlined above (Section 7.2.2.2), be part of an entirely different lineage to the Eastern or Western lineages. The possible connection between these Italian groups and the Western lineage, suggested by SDQA values, does not appear to be reflected in shape data. Instead M_1 shape distances indicates a potential similarity with the Western lineage or supports the association of Grotta del Broion assemblages with an independent lineage. The OTUs from the oldest assemblages in this discussion, Grotta del Broion and Tornewton Cave, become increasingly prone to the influence of evolutionary tempo and mode on molar shape. Specifically, the risk of homoplasy between molar shapes generated stochastically through random walks through evolutionary space. This risk becomes greater the larger the intervals of time separating OTUs (Gingerich, 1993).

7.2.2.5 Biostratigraphic implications

There is a general reduction in SDQA values across all assemblages over time. Differences exist, however, in the relative trajectories of this trend between geo-

graphic regions, which may reflect morphological differences between intraspecific lineages (Section 7.2.2.2) and/or ecophenotypic responses (Section 7.2.2.3). Higher SDQAs are recorded in assemblages in the Southeast European zone relative to assemblages of similar age in the Central and Southwest European zones up until the early Holocene. A similar pattern was noted by Heinrich (1982) and indicates that age-estimations of fossil assemblages from these areas based on SDQA need to be placed in a regional context. But is this SDQA variation best described as a morphological cline or as a sharply discontinuous difference between lineages or environments? The data presented here are not capable of resolving this one way or another, mainly because of stratigraphic and geographic gaps in the dataset, and Recent enamel thickness data presented by Röttger (1987) from across Europe are also open to interpretation. Morphologies of other Pleistocene rodents suggest that a cline is the most appropriate model to adopt (e.g., Martin, 1993), but such studies also require an understanding of subspecific phylogeography and historial biogeography in order to provide an accurate explanation of patterns. If SDQA variation is discontinuous then the boundaries between 'states' of enamel thickness are all important. Yet, as the aDNA data show, the intraspecific phylogeography of *Arvicola* is dynamic across the Lateglacial and Holocene, which has the potential to confound biostratigraphic interpretations.

Although uncertainties exist surrounding the detailed pattern of SDQA variation, after taking evidence for the immigration of Eastern lineage populations into account, the temporal patterns of SDQA appear to agree in general with the age-estimations given to assemblages. The age-estimation for Marie-Jeanne Cave 4 is broad but may be refinable. The SDQA values for all Marie-Jeanne Cave assemblages are in stratigraphic order and, assuming Marie-Jeanne Cave 6 is also a Western lineage group and that the trend in SDQ change over time is approximatey linear, the SDQA of Marie-Jeanne Cave 4 fits best with an age for this assemblage at the younger limit of its estimated age-range. The fact that mtDNA was preserved in the fossils from Marie-Jeanne Cave 4 also suggests that this assemblage is at the younger limit of the age estimation given in Section 3.2.1.1, and may even be as young as MIS 2 given the low SDQA of this assemblage. Water vole has been recorded from Belgium at around 20 k yr BP (from Trou Al'Wesse; Brace, 2010), from southeast England at 27 950±140 cal BP (from Ightham Fissures; Section 3.6.3.3) and from other British sites that equate with the Lateglacial Gough's Cave mammal assemblage zone Currant and Jacobi (2001). So the presence of water vole, which would otherwise be considered a temperate species from its ecology in western Europe today, at Marie-Jeanne Cave 4 during the cold climate of MIS 2 is not problematic. Although *Arvicola* have been recorded in Great Britain during the Lateglacial, a possible Lateglacial age for Tornewton Cave Red Cave Earth appears unlikely given the relatively high SDQA in comparison with

those of other groups at this time.

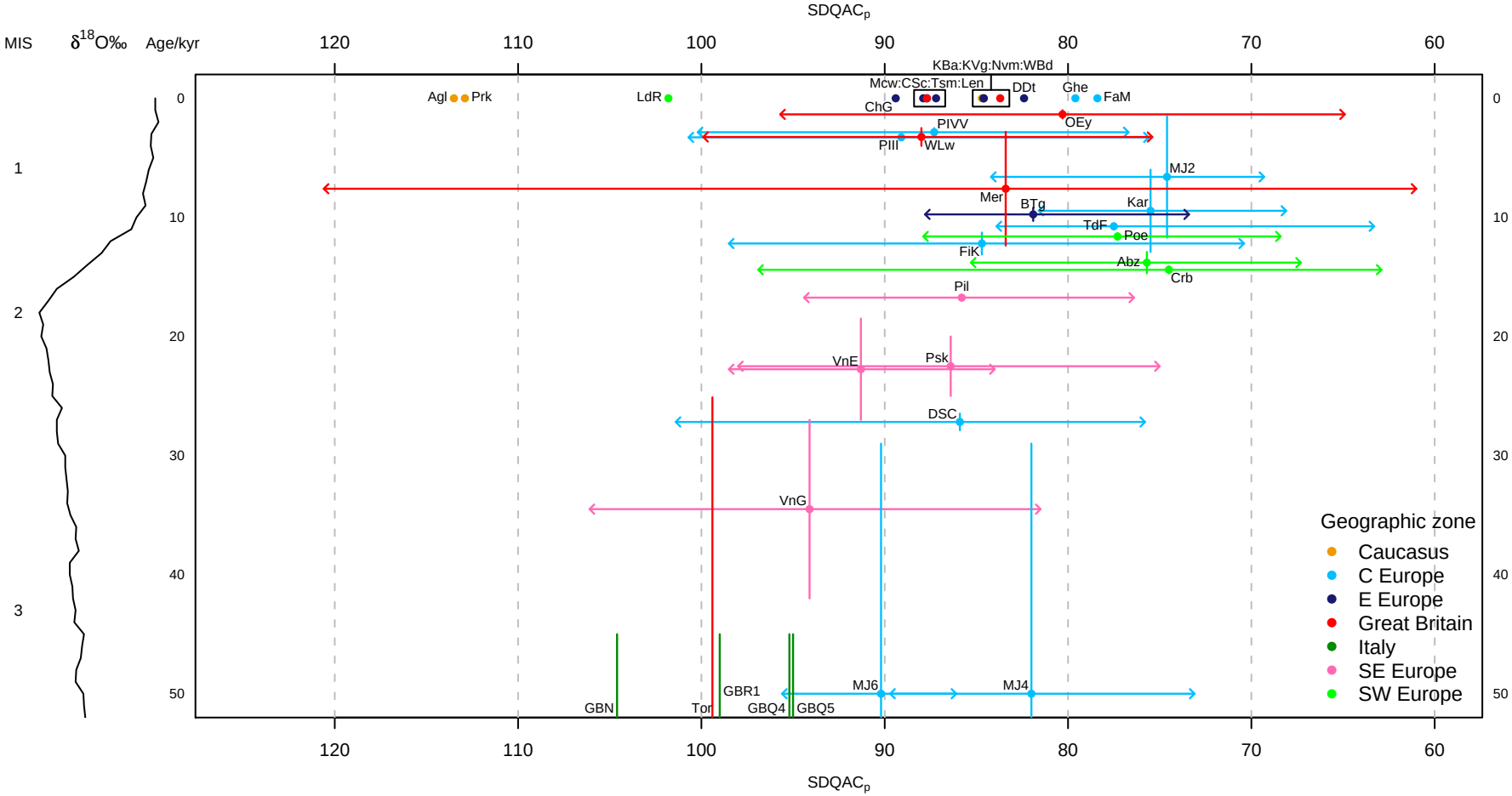

Figure 7.3: Size-corrected SDQ (SDQAC$_p$) values in assemblages dating from MIS 3 to the Recent. Plot shows SDQAC$_p$ mean (point) and range (horizontal whiskers; SDQAC$_p$ range omitted in Recent populations for clarity), along with the possible age of each assemblage (vertical whisker heights; see Chapter 3). Assemblage labels and other plotting features as for Figure 7.2.

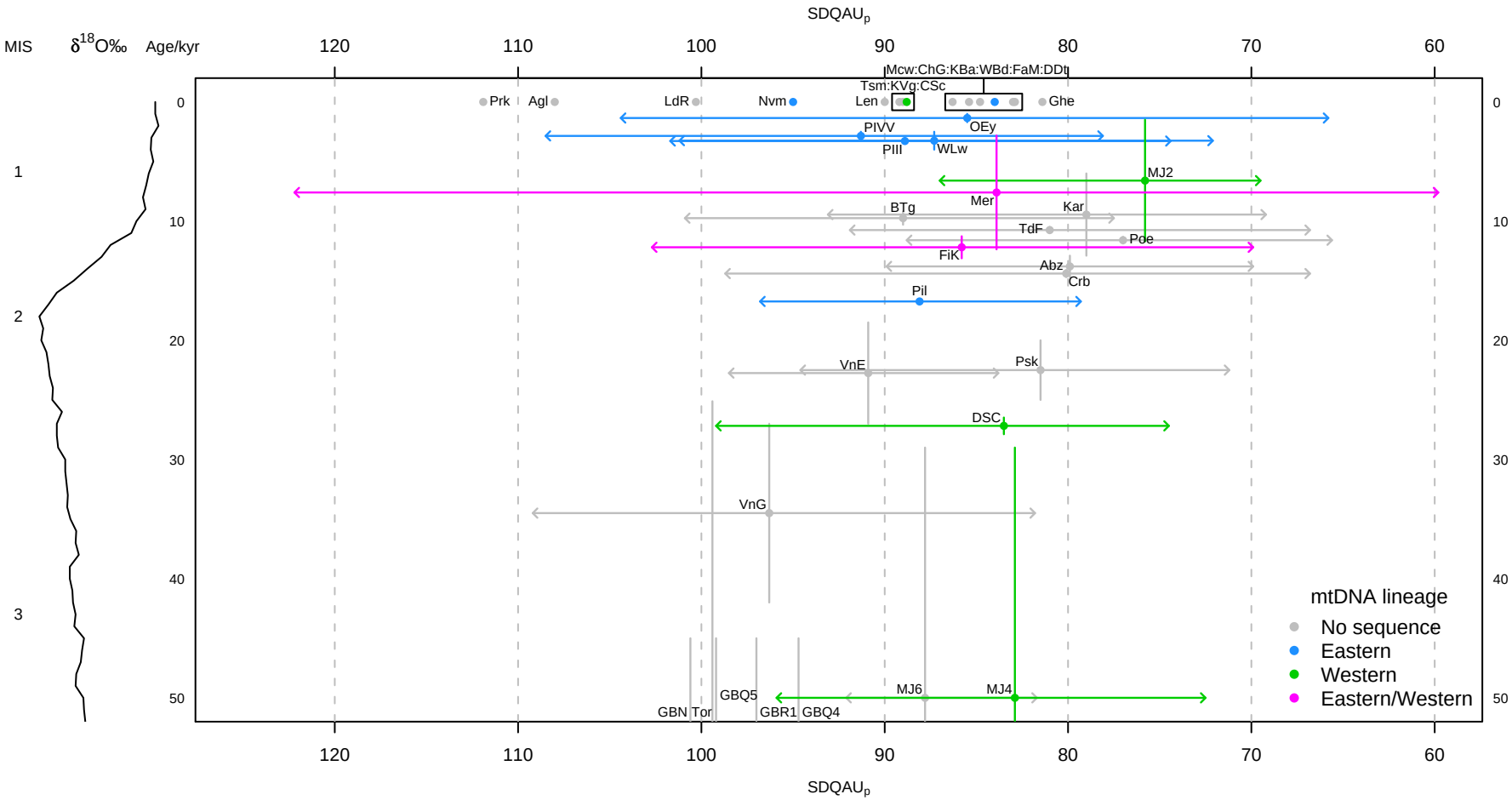

Figure 7.4: Unmodified SDQ (SDQAU$_p$) values in assemblages dating from MIS 3 to the Recent with mtDNA lineages highlighted where known (Brace, 2010). Assemblage labels as for Figure 7.2. Other plotting features as for Figure 7.2.

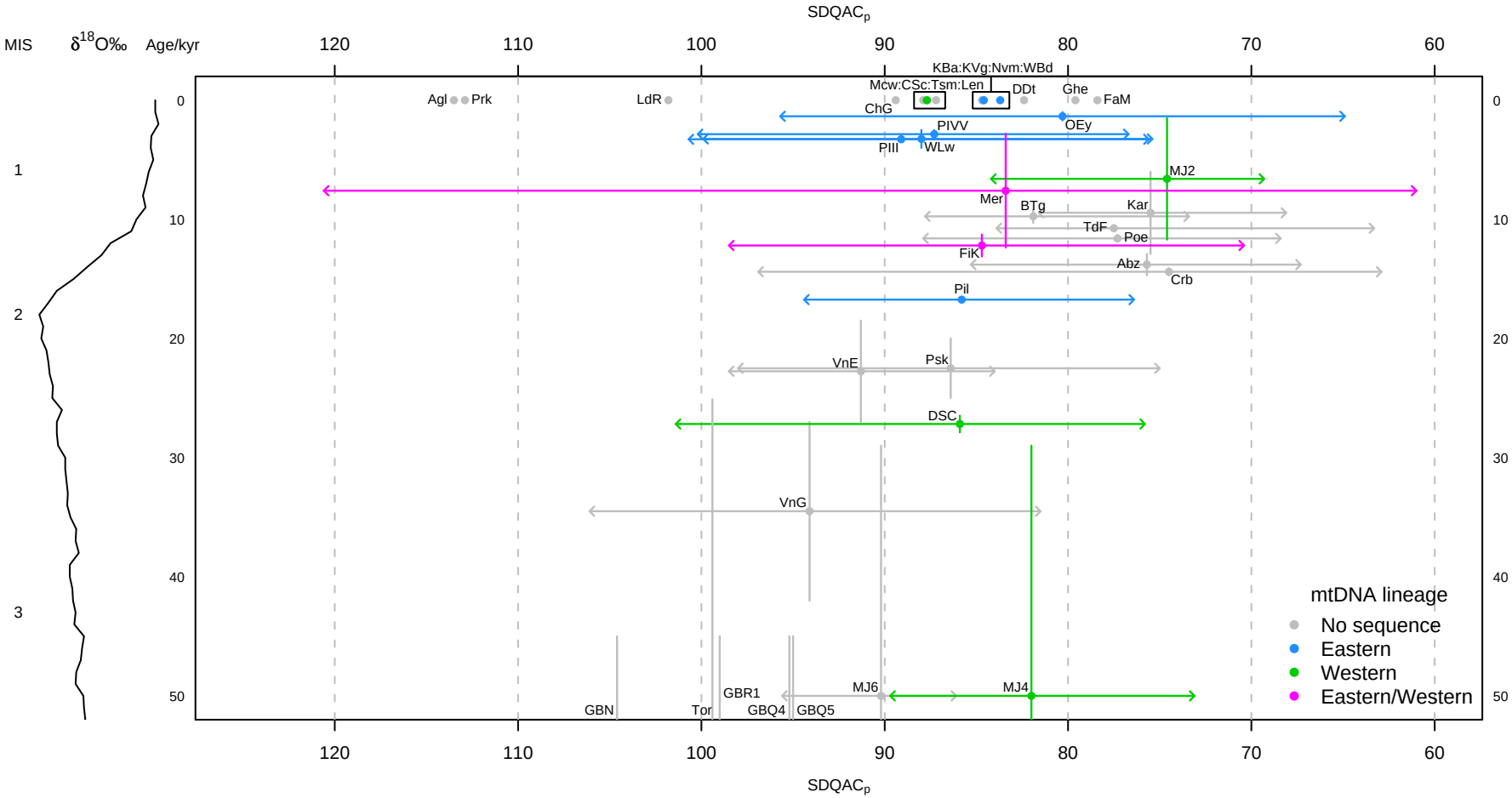

Figure 7.5: Size-corrected SDQ (SDQAC$_p$) values in assemblages dating from MIS 3 to the Recent with mtDNA lineages highlighted where known (Brace, 2010). Assemblage labels as for Figure 7.2. Other plotting features as for Figure 7.2.

Figure 7.6: (Following page) Euclidean distances between unmodified M_1 shapes from assemblages dating from MIS 3 to the Recent. Distances taken with respect to the Recent Welsh Borders OTU. Assemblages colour-coded by geographic zone (see Section 7.1), vertical whiskers show possible age of each assemblage (see Chapter 3), assemblages labelled as follows (* denotes Recent material): **Abz** - Abzac (n=19); **Agl** - Aggeel* (n=15); **BTg** - Bolshoi Tiganye (n=30); **CSc** - Central Scotland* (n=14); **ChG** - Cheshskaya Guba* (n=21); **Crb** - Courbet (n=45); **DDt** - Don Delta* (n=14); **DSC** - Dzeravá skala Cave (n=34); **FaM** - Frankfurt am Main* (n=15); **FiK** - Fuchsloch im Krockstein (n=23); **Ghe** - Ghent* (n=21); **GBN** - Grotta del Broion, Sala Grande N (n=29); **GBQ4** - Grotta del Broion, Sala Grande Q4 (n=22); **GBQ5** - Grotta del Broion, Sala Grande Q5 (n=28); **GBR1** - Grotta del Broion, Sala Grande R1 (n=38); **KBa** - Kabardino-Balkariya* (n=22); **KVg** - Kama-Volga* (n=17); **Kar** - Kartstein (n=12); **Len** - Leninsky* (n=30); **LdR** - Linares de Riofrio* (n=14); **MJ2** - Marie-Jeanne Cave 2 (n=16); **MJ4** - Marie-Jeanne Cave 4 (n=10); **MJ6** - Marie-Jeanne Cave 6 (n=16); **Mer** - Merlin's Cave (n=90); **Mcw** - Moscow* (n=25); **Nvm** - Novomirgorod* (n=13); **OEy** - Ossom's Eyrie Cave (n=44); **Psk** - Peskö "brick red" strata (n=45); **Pil** - Pilisszántó (n=43); **PIII** - Pisede III (n=20); **PIVV** - Pisede IV&V (n=33); **Poe** - Poeymaü BS (n=18); **Prk** - Prokhladny* (n=20); **Tor** - Tornewton Cave Red Cave Earth (n=18); **TdF** - Trou du Frontal (n=11); **Tsm** - Tsimlyansk* (n=21); **VnE** - Vindija E-F (n=25); **VnG** - Vindija G (n=43); **WBd** - Welsh Borders* (n=20); **WLw** - Wigber Low 26 (n=51).

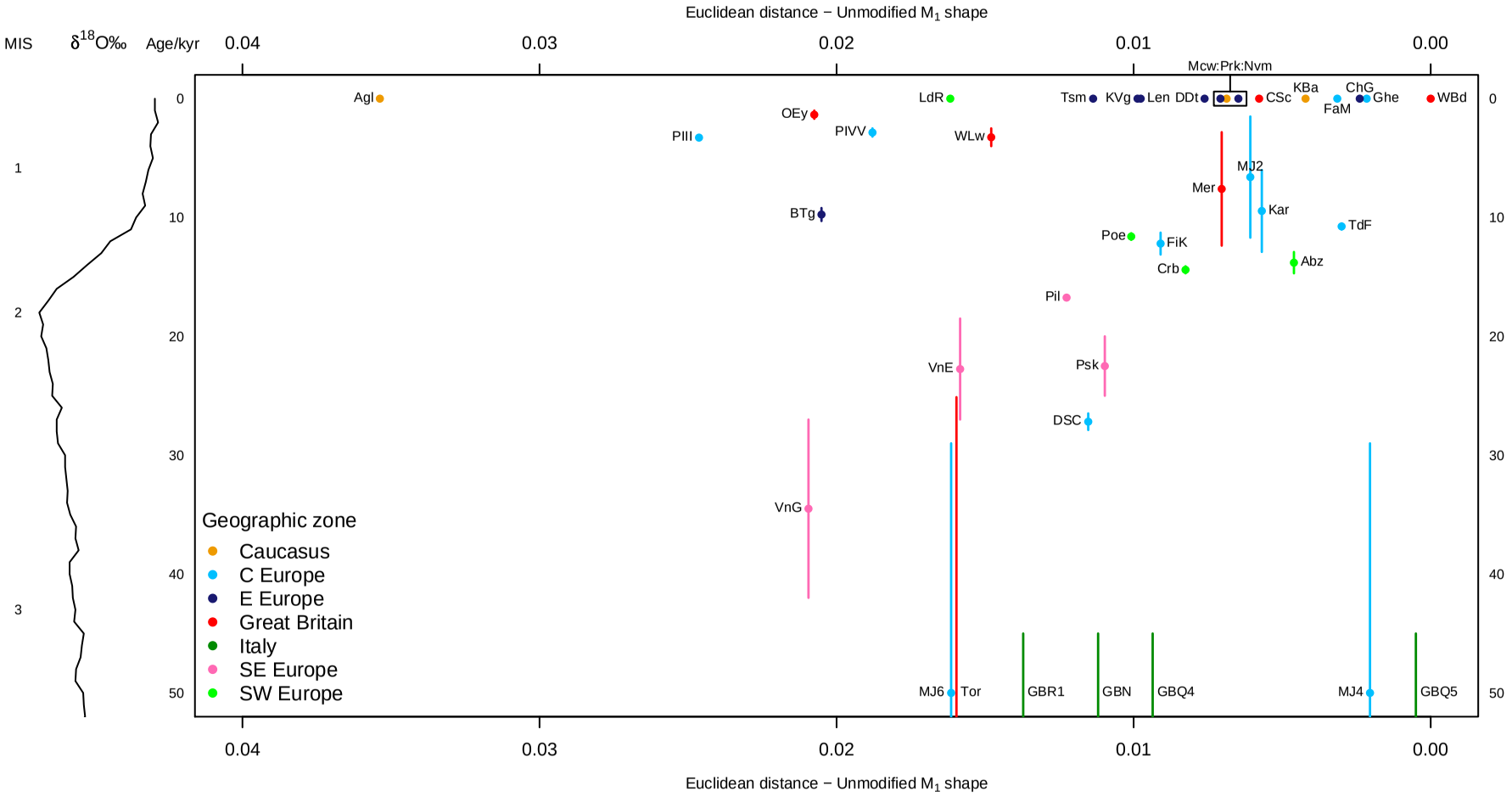
Euclidean distance − Unmodified M1 shape
MIS
δ18O‰
Age/kyr
0.04
0.03
0.02
0.01
0.00
Mcw:Prk:Nvm
Agl
LdR
Tsm
KVg
Len
DDt
CSc
KBa
ChG
FaM
Ghe
WBd
OEy
PIII
PIVV
WLw
MJ2
Mer
Kar
BTg
TdF
Poe
FiK
Crb
Abz
Pil
VnE
Psk
DSC
VnG
MJ6
Tor
GBR1
GBN
GBQ4
MJ4
GBQ5
Geographic zone
Caucasus
C Europe
E Europe
Great Britain
Italy
SE Europe
SW Europe

Figure 7.7: Euclidean distances between size-corrected M_1 shapes from assemblages dating from MIS 3 to the Recent. Distances taken with respect to the Recent Welsh Borders OTU. Assemblages colour-coded by geographic zone (see Section 7.1), vertical whiskers show possible age of each assemblage (see Chapter 3), assemblages labelled as follows (* denotes Recent material): **Abz** - Abzac (n=19); **Agl** - Aggeel* (n=15); **BTg** - Bolshoi Tiganye (n=30); **CSc** - Central Scotland* (n=14); **ChG** - Cheshskaya Guba* (n=21); **Crb** - Courbet (n=45); **DDt** - Don Delta* (n=14); **DSC** - Dzeravá skala Cave (n=34); **FaM** - Frankfurt am Main* (n=15); **FiK** - Fuchsloch im Krockstein (n=23); **Ghe** - Ghent* (n=21); **GBN** - Grotta del Broion, Sala Grande N (n=29); **GBQ4** - Grotta del Broion, Sala Grande Q4 (n=22); **GBQ5** - Grotta del Broion, Sala Grande Q5 (n=28); **GBR1** - Grotta del Broion, Sala Grande R1 (n=38); **KBa** - Kabardino-Balkariya* (n=22); **KVg** - Kama-Volga* (n=17); **Kar** - Kartstein (n=12); **Len** - Leninsky* (n=30); **LdR** - Linares de Riofrio* (n=14); **MJ2** - Marie-Jeanne Cave 2 (n=16); **MJ4** - Marie-Jeanne Cave 4 (n=10); **MJ6** - Marie-Jeanne Cave 6 (n=16); **Mer** - Merlin's Cave (n=90); **Mcw** - Moscow* (n=25); **Nvm** - Novomirgorod* (n=13); **OEy** - Ossom's Eyrie Cave (n=44); **Psk** - Peskö "brick red" strata (n=45); **Pil** - Pilisszántó (n=43); **PIII** - Pisede III (n=20); **PIVV** - Pisede IV&V (n=33); **Poe** - Poeymaü BS (n=18); **Prk** - Prokhladny* (n=20); **Tor** - Tornewton Cave Red Cave Earth (n=18); **TdF** - Trou du Frontal (n=11); **Tsm** - Tsimlyansk* (n=21); **VnE** - Vindija E-F (n=25); **VnG** - Vindija G (n=43); **WBd** - Welsh Borders* (n=20); **WLw** - Wigber Low 26 (n=51).

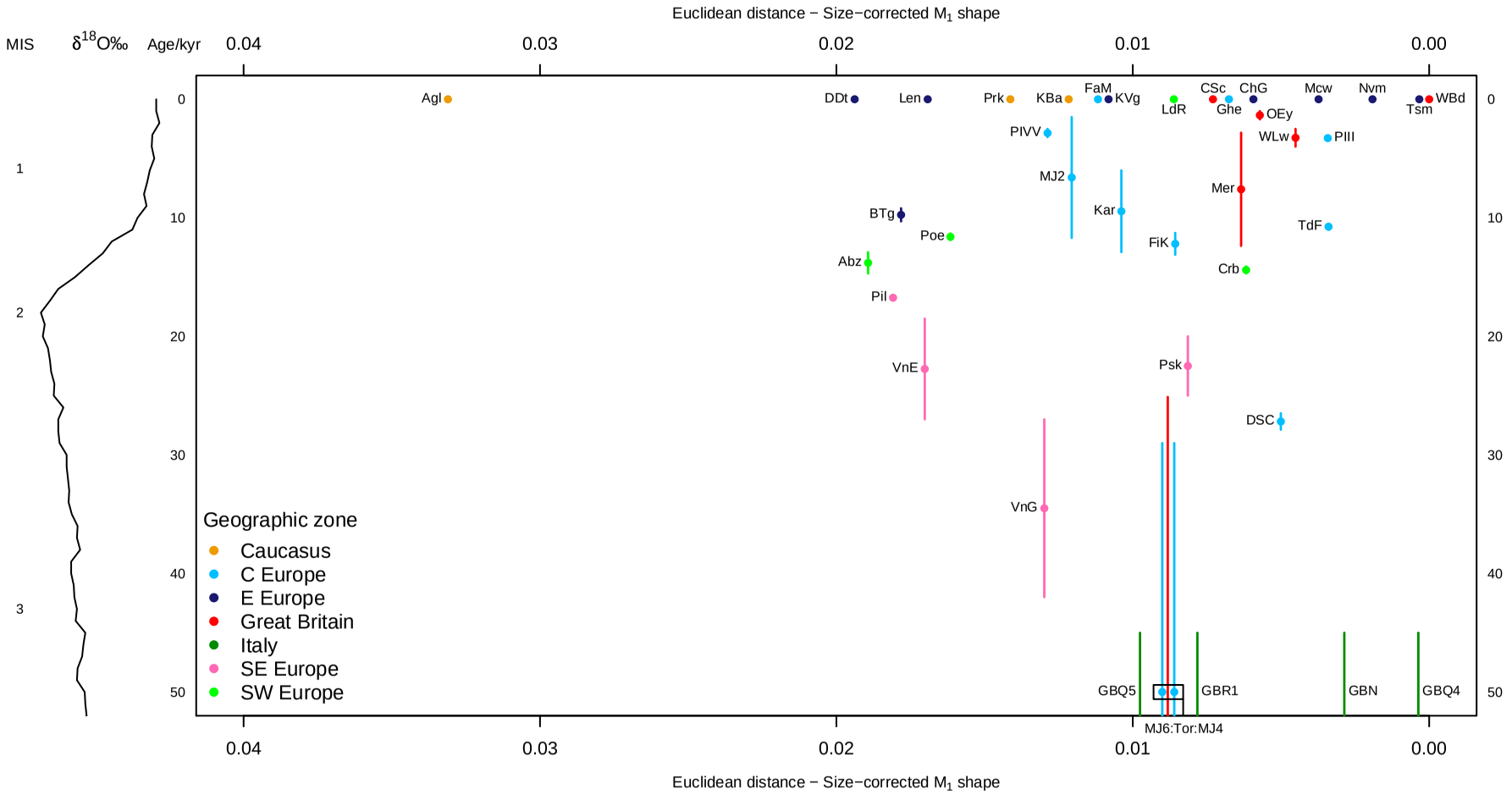
Euclidean distance − Size−corrected M1 shape
MIS
δ18O‰
Age/kyr
0.04
0.03
0.02
0.01
0.00
0
10
20
30
40
50
1
2
3
Agl
DDt
Len
Prk
KBa
FaM
KVg
LdR
CSc
Ghe
ChG
OEy
Mcw
Nvm
Tsm
WBd
PIVV
WLw
PIII
MJ2
Mer
BTg
Kar
TdF
Poe
FiK
Abz
Crb
Pil
VnE
Psk
DSC
VnG
GBQ5
GBR1
GBN
GBQ4
MJ6:Tor:MJ4
Geographic zone
Caucasus
C Europe
E Europe
Great Britain
Italy
SE Europe
SW Europe

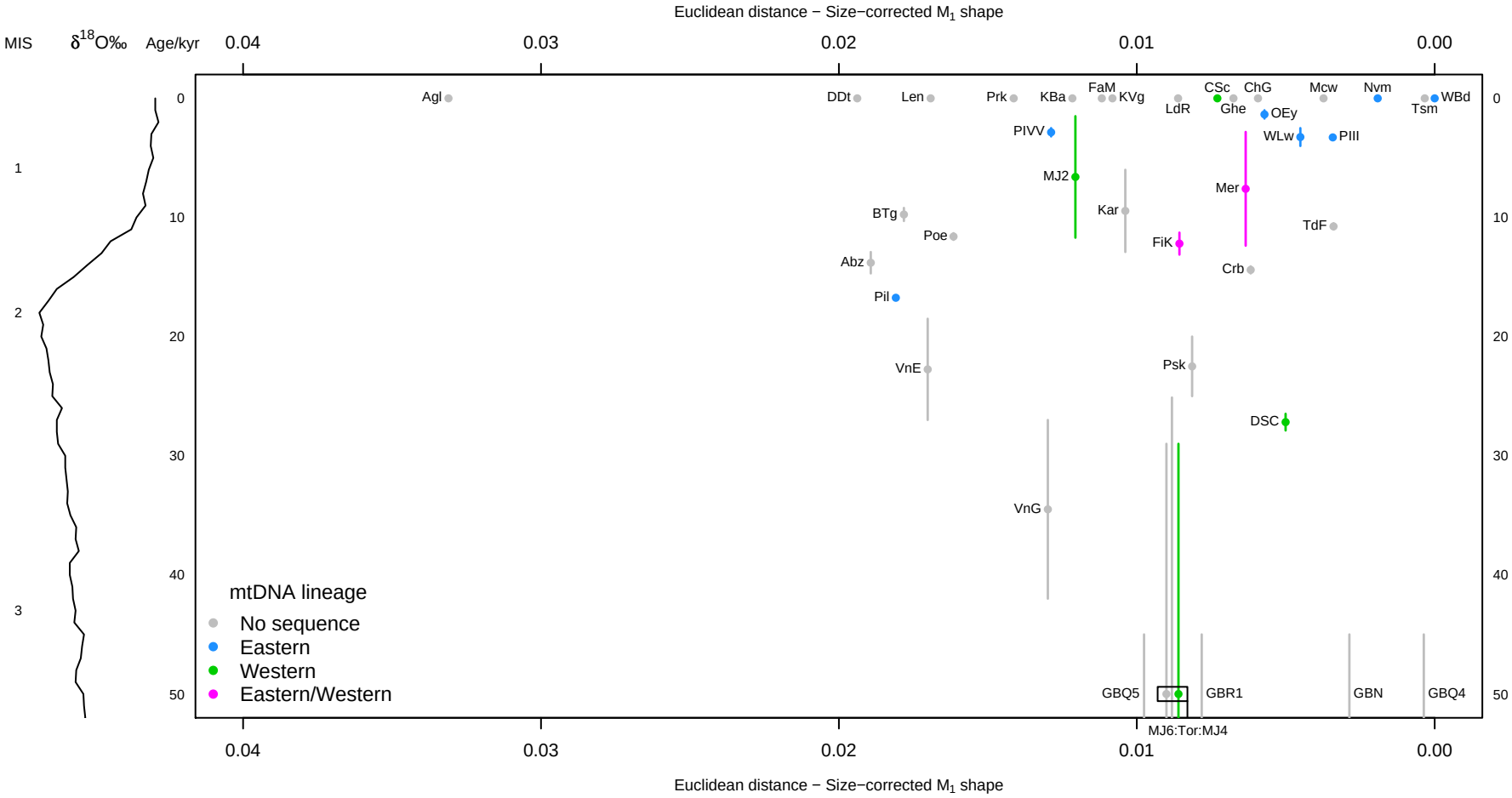

Figure 7.8: Euclidean distances between size-corrected M_1 shapes from assemblages dating from MIS 3 to the Recent with mtDNA lineages highlighted where known (Brace, 2010). Distances taken with respect to the Recent Welsh Borders OTU. Assemblage labels and other plotting features as for Figure 7.7.

7.3 MIS 19–MIS 3

7.3.1 Setting

The period from MIS 19 to MIS 3 is one that includes a considerable amount of climatic variation, visible in global marine oxygen isotope records and terrestrial archives. Several major glacial events over this interval have left extensive geomorphological imprints across Europe (Figure 7.9). The 'Saalian' glaciation (= Dnieperian of Russia) has been linked both with MIS 8 and MIS 6 (Eissmann, 2002) and at its estimated maximum extent reached across much of Germany, Poland and in a lobe penetrating the Dnieper basin in the Ukraine (Ehlers and Gibbard, 2004). The Elsterian glaciation of western Europe (= Anglian in Great Britain or Oka in Russia) is associated with MIS 12, and appears to have had a considerable effect on the palaeogeography of northwest Europe, through the diversion of major river systems such as the Thames in Great Britain (Bridgland, 1994; Rose, 2008), and is also implicated in the formation of the English Channel (Gupta *et al.*, 2007). The 'Donian' glaciation, which penetrated deeply into the drainage basin of the Russian Don river system (Figure 7.9), is commonly correlated with the large negative excursion in the global marine oxygen isotope record at MIS 16. This glaciation is likely to have also covered large areas of western Europe, perhaps including Great Britain (Hamblin *et al.*, 2000; Rose, 2008).

Four interglacials are present in the marine oxygen isotope record between MIS 12 and MIS 3 but the identification of specific interglacials in the terrestrial record over this period is problematic, and the presence of sub-stage variation (e.g., the pronounced drop in δ^{18}O‰ within MIS 7) further complicates stratigraphic interpretation. The transformation of Britain from a permanent peninsula at the western edge of Europe to an ephemeral island with the opening of the English Channel appears to have had lasting consequences for the type and mix of temperate flora and fauna of the British Isles during interglacial periods post-MIS 12 (White and Schreve, 2000; Schreve, 2001).

Palaeogeographic and palaeoclimatic contrasts can be made between the period from MIS 19 and MIS 12 (the early Middle Pleistocene), and the late Middle Pleistocene and Late Pleistocene. Before the Elsterian glaciation Great Britain was still connected to mainland Europe through a land-bridge between southeastern England and France, and the southern part of the North Sea and the eastern end of the present English Channel were shallow-marine embayments (Gibbard, 1988). The global marine isotope record suggests that interglacials older than 430 k yr BP were cooler and less climatically variable than those that followed (Tzedakis *et al.*, 2009). However, terrestrial records indicate, in contrast, that periods of extreme warmth and cold existed during the early Middle Pleistocene (Candy, 2009).

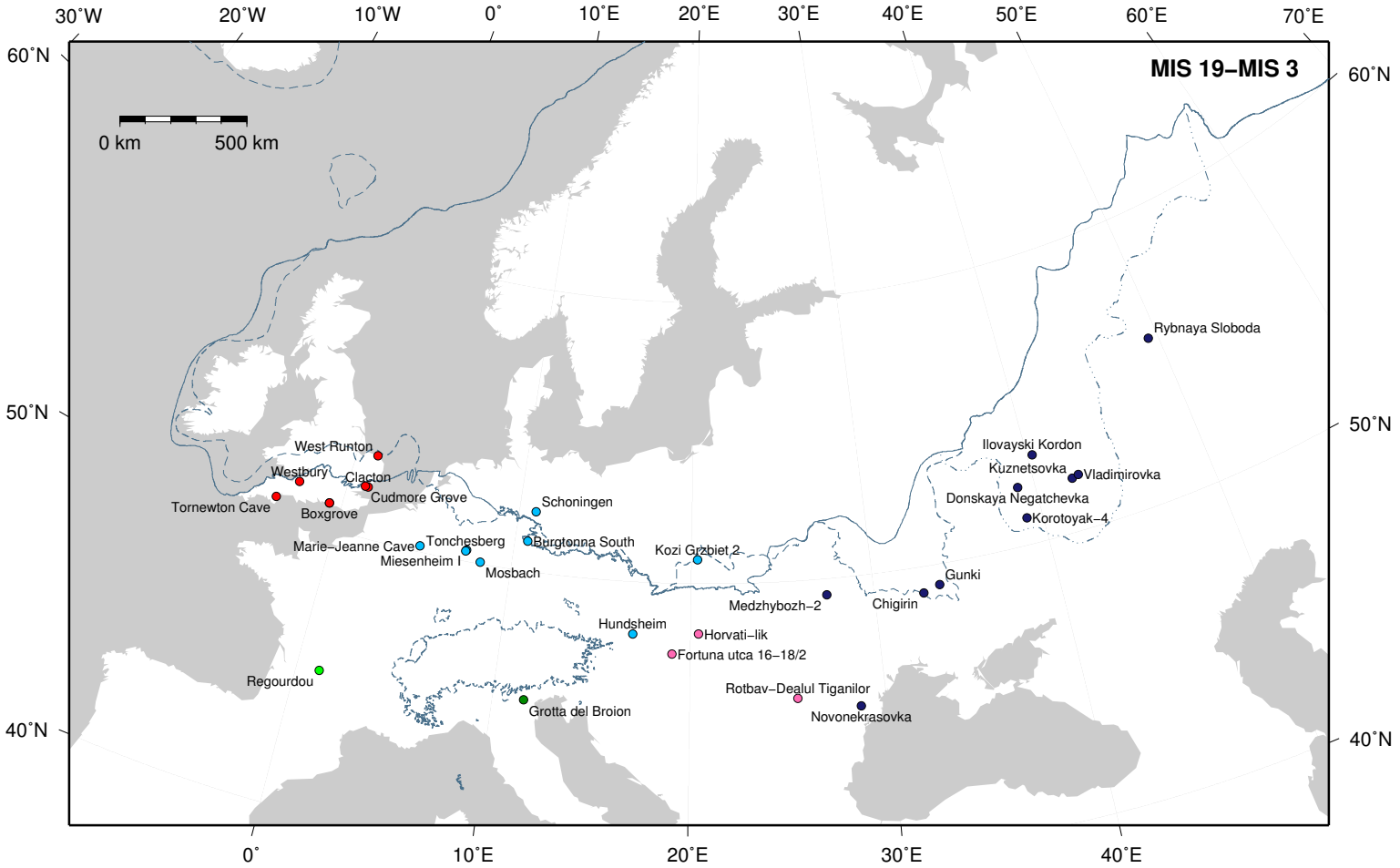

Figure 7.9: Map showing localities with assemblages estimated as dating between MIS 19 and MIS 3. Colour coding of localities refers to geographic zones outlined in Section 7.1. Blue-grey lines show estimated maximum extents of 'Saalian' ice (solid line), 'Elsterian' ice (dashed line), and 'Donian' ice (dashed and dotted line) (Ehlers and Gibbard, 2004).

The evolution of the water vole M_1 over this period is notable for the complete loss of roots in all populations after MIS 12, an increase in molar size, gradual reduction in enamel SDQ through time, and the development of an east-west morphocline where assemblages in the east tend to have lower SDQs than groups in the west of the same age (Maul and Markova, 2007). Observed trends in the evolution of the water vole during the early Middle Pleistocene involve the loss of roots, growth in molar size, and gradual reduction in SDQ. The loss of roots is diachronous across Europe, the earliest *Arvicola* populations being found in Germany (Section 3.5.1.1) while it seems that *Arvicola* do not appear in eastern Europe until after MIS 12, although there is some evidence to the contrary (Maul and Markova, 2007; Preece and Parfitt, 2008).

Figure 7.9 shows the locations of fossil localities referred to in the following discussion. Figures 7.10 and 7.11 variation over time in $SDQAU_p$ and $SDQAC_p$ values respectively. Euclidean distance plots of size-corrected and unmodified M_1 shapes from OTUs with respect to the Recent Welsh Borders OTU are show in Figures 7.12 and 7.13. The lack of assemblages attributed to MIS 9 and 7 is notable and may represent a genuine gap in the fossil record or a tendency to conflate assemblages within a well-recognised stratigraphic framework, frequently those based on pollen biostratigraphy.

7.3.2 Morphological patterns

7.3.2.1 Early Middle Pleistocene

The SDQA values of the *Arvicola* from Fortuna utca suggest that a warm period in the very late early Middle Pleistocene or MIS 11 is the most appropriate correlation for this assemblage ($SDQAU_p$=112.7, $SDQAC_p$=118.1). The relatively low SDQA values do not suggest that Fortuna utca is as old as other early Middle Pleistocene *Arvicola* assemblages such as Mosbach 2 or Hundsheim. At Rotbav-Dealul Ţiganilor, the correlation with MIS 15 or 13 is not challenged by SDQA data ($SDQAU_p$=119.7, $SDQAC_p$=121.9) but the possibility of a MIS 15 age is also not ruled out. The allometric relationships between enamel thickness and tooth size appear to be very consistent between enamel triangles (Figure B.10c) and suggest that the $SDQAC_p$ value for this assemblage is a good representation of adult the adult value. It is interesting to observe similarities between the $SDQAC_p$ from Rotbav and those of Kuznetsovka and Korotoyak 4 from the Eastern European zone. Kuznetsovka and Korotoyak 4 have been correlated with the later part of the early Middle Pleistocene (Sections 3.11.1.3 and 3.11.1.2 respectively), which supports the conclusion of Petculescu (2003) that the *Arvicola* assemblage from Rotbav can be attributed to MIS 13, and by implication the cold event record in sediments below Clay A are either MIS 14 or a sub-stage with MIS 13 (Section

3.10.1.1).

The $SDQAC_p$ from West Runton shows this group to be older than assemblages with rootless water vole apart from Hundsheim. The $SDQAU_p$ of West Runton is, however, almost identical with Boxgrove 4c (120.0 and 120.1 respectively). There appears to be a good representation of specimens from throughout ontogeny (Figure B.12b) but steep allometric corrections produce size-corrected enamel layers much thicker than those observed. This may or may not be problematic in terms of 'over-correcting' the SDQ for the assemblage but certainly there the enamel thickness–size relationships observed for West Runton make some size correction appropriate. The $SDQAC_p$ of West Runton makes a correlation with MIS 19 unlikely and, although a MIS 15 could still be envisaged from the SDQAs of later assemblages, an MIS 17 age is the best fit for the West Runton data. Kozi Grzbiet has the highest SDQA values of all the early Middle Pleistocene assemblages under consideration ($SDQAU_p$=128.5, $SDQAC_p$=131.9), which is consistent with ideas that Kozi Grzbiet is older than West Runton (e.g., Maul and Parfitt, 2010). At Hundsheim the very high SDQA would appear to suggest that this assemblage is older than any of the other early Middle Pleistocene assemblages where *Arvicola* has been found. Furthermore, SDQA values from Hundsheim are greater than the $SDQAC_p$ of *Mimomys savini* from West Runton. This does not necessarily imply, however, that Hundsheim is older than West Runton. It is evident that the loss of roots in water voles occurs in a diachronous manner (e.g., Maul and Markova, 2007; Section 3) and the data presented in this thesis shows instances where *M. savini* possibly post-date *Arvicola* assemblages that have a lower SDQA (e.g., Ilovayksi Kordon in Figure 7.10). These contrasts have been most prominent between assemblages from the west of Europe and the east of Europe and Russia. A central piece of evidence supporting a MIS 15 or 13 age for Hundsheim is the absence of roots from the water vole found here (Section 3.1.1.1). But if enamel thickness is considered a good indicator of relative geological age, and given the high SDQA at Hundsheim, it is possible that roots were lost by water voles ancestral to the Hundsheim population earlier than is recognised elsewhere in Europe (Koenigswald and Kolfschoten, 1996; Maul and Markova, 2007). Alternatively, the assemblage from Hundsheim could represent a morphologically distinct intraspecific group, perhaps with close relations to Kozi Grzbiet, that possessed much higher enamel thickness values than water voles elsewhere. Some support for this idea comes from Rekovets and Nadachowski (1995), who argued that *Mimomys* from southeastern Europe belonged to a distinct lineage. Such ideas are speculative and require comparative measurements and analyses to be made from a series of nearby sites to attempt to resolve these relative relationships. For instance from the nearby 'transitional' *Arvicola* assemblages found at Voigstedt, Germany, or Přezletice, Czech Republic (Koenigswald and Kolfschoten, 1996).

In Russia the assemblages of Kuznetzovka, Korotoyak-4 and Ilovayski Kordon have the same relative relationships in both SDQA metrics. Kuznetzovka has been favourably correlated with MIS 13 because of the warm and humid palaeoenvironmental indicators present, fauna corresponding with the late Tiraspolian faunal zone, and the late development of water vole roots (Section 3.11.1.3). Korotoyak-4 is another assemblage correlated with the late Tiraspolian faunal zone but may be older than this based on palaeoenvironmental data (Section 3.11.1.2). Ilovayski Kordon is correlated with the early part of the Muchkapian warm stage (Agadjanian in Iossifova and Krasnenkov, 1994; Section 3.11.1.1) but the SDQA for this group is lower than Kuznetzovka or Korotoyak-4. The general stratigraphic evidence suggesting Kuznetzovka and Korotoyak-4 are younger than the nearby site of Ilovayski Kordon is at odds with the lower SDQA of the water vole assemblage from Ilovayski Kordon. A possible explanation for the differences in SDQA between these three sites is natural variation, and the limits of precision and accuracy in measuring SDQA, across the region. The enamel thickness ratio variation observed between Kuznetzovka. Korotoyak-4 and Ilovayski Kordon is 6 units for $SDQAU_p$ and 3.1 for $SDQAC_p$. The range of SDQA values of Recent *Arvicola* from a comparable part of Russia was found to be 3.4 for $SDQAU_p$ and 5.5 for $SDQAC_p$ (between Don Delta and Moscow; Section 7.2). So, the empirical evidence from Recent populations from the Russian Plain suggests it is possible for SDQA differences between Kuznetzovka, Korotoyak-4 and Ilovayski Kordon to be accommodated within natural variation across a single interglacial. It may then be beyond the limits of the SDQ to stratigraphically resolve between these three Eastern European assemblages. Another possible explanation is that the water vole from Ilovayski Kordon is morphologically distinct intraspecific group. There is no mtDNA evidence available for the presence of different *Arvicola* lineages in this part of Russia today. However, Eastern European and Ural lineages are present in Recent *Clethrionomys glareolus* (Deffontaine *et al.*, 2005), and SDQA and M_1 shape data presented in Section 7.2.2.1 hint at major differences between some populations from the Caucasus and Russia. If lineage diversity were a factor in the SDQA differences observed in these MIS 15 or 13 assemblages from Russia, the stimulus for distributional shifts in lineages could be found in the stage and sub-stage level complexity seen in the marine oxygen isotope record. The cold periods recorded at MIS 14 and within MIS 15 and MIS 13 do not appear to be as extreme as the earlier MIS 16 (correlated with the Don glaciation) and later MIS 12 (correlated with the Oka glaciation) global events. But their terrestrial effects are difficult to understand because they are difficult to identify in terrestrial archives. At Aveley in Great Britain, deposits that have been attributed to MIS 7 are thought to record a sub-stage level climatic fluctuation in this interglacial that resulted in dramatic faunal changes (Schreve, 2001). It would seem

highly likely, then, that sub-stage variability elsewhere in the Pleistocene caused similar changes elsewhere in Europe, including distributional shifts in populations of small mammals across the Russian Plain.

Considering the assemblages from Great Britain. At Boxgrove, the $SDQAU_p$ from Unit 4b is lower than and that from 4c, however, the opposite is the case with $SDQAC_p$ values (Boxgrove 4b $SDQAU_p$=117.0, $SDQAC_p$=122.7; Boxgrove 4c $SDQAU_p$=120.1, $SDQAC_p$=118.4). The allometric corrections applied to Boxgrove 4b and 4c (Figure B.1d and B.1e) are complex because most M_1s are of similar size, which suggests that size-corrections should be treated with some caution. At Westbury, both units 11 and 14 have almost identical values within the different SDQA metrics (Westbury 11 $SDQAU_p$=121.9, $SDQAC_p$=117.8, Westbury 14 $SDQAU_p$=122.4, $SDQAC_p$=118.1). This uniformity in SDQA is interesting given evidence of a transition from temperate conditions in Unit 11 to cold, open habitats in Unit 14 of the Westbury sequence (Section 3.6.1.3). Shape differences are also quite pronounced between these two stratigraphic layers (Figure 7.12). Boxgrove 4c has SDQAs almost identical to those from Westbury 11 and 14, but Westbury has been considered to be an older site than Boxgrove based on a number of lines of evidence; including the presence of *Microtus gregalis* at Boxgrove (Section 3.6.1.1) rather than its supposed ancestor *Microtus gregaloides*, which occurs at Westbury (Section 3.6.1.3). The last occurrence of *Microtus gregaloides* in central Europe is at Hundsheim, thought to be no older than 'Cromerian Interglacial III or IV' (MIS 15 or 13: Maul and Markova, 2007; Section 3.1.1.1). But the transition between *Microtus gregaloides* and *Microtus gregalis* occurs in the Muchkapian in Russia (Maul and Markova, 2007) and is regarded by some workers as difficult to determine generally (Currant, pers. comm., 2009). Superficially, the $SDQAU_p$ data would suggest that Units 11 and 14 at Westbury and Boxgrove 4c are of a similar age, and that Boxgrove 4b is either of an earlier age (from mean $SDQAC_p$ value) or contains an *Arvicola* assemblage of a different morphological type. It is difficult to imagine how the climatic complexity evident in the Westbury sequence can be accommodated within Boxgrove 4c: a relatively narrow soil horizon within a rapid regressional sequence (Roberts and Pope, 2009). Thus, the only other explanations for these differences is either sampling error or the presence of a morphologically distinct population at Westbury that colonised the Boxgrove area during the time of deposition of Boxgrove 4c, replacing a different morphotype that was found at Boxgrove 4b. The lack of any correspondence between environment and morphology at Westbury make it appear unlikely that the seemingly more minor environmental changes between Boxgrove 4b and 4c should result in distributional shifts in water vole lineages. However, the relative geographic locations of Westbury and Boxgrove may be pertinent here: the former an upland area at the western edge of a peninsula of Europe, the latter a

lowland site more intimately connected to the continent. Perhaps the water vole at Westbury was of a lineage akin to the 'Celtic fringe' of small mammals present in the British Isles today (Searle *et al.*, 2009), that may have been restricted to upland habitats. It is conceivable that during cold periods, when open landscapes expanded, such populations may have also expanded into the east of Britain. This range-shift may only be observable at present at Boxgrove, during the climatic deterioration towards MIS 12, because no fossil assemblage has yet been discovered in a region equivalent to Boxgrove but contemporary to Westbury that records the type of stage or sub-MIS stage level climatic events recorded at Westbury. Such an interpretation is not inconsistent with the evidence from Late Pleistocene to Recent *Arvicola* described in Section 7.2.2 that show apparently climate related distributional shifts in intraspecific lineages. Furthermore, the $SDQAU_p$ values from nearby continental sites such as Miesenheim I and Mosbach 2 are closer to Boxgrove 4b than they are to Boxgrove 4c. The $SDQAC_p$ of Mosbach 2 is also close to Boxgrove 4b and the size-correction applied to Miesenheim I may, in fact, be erroneous (see below).

The assemblage at Mosbach 2 (Section 3.5.1.2) consists of a large sample that produces clear allometries in enamel thickness–size relationships (Figure B.8b). The SDQAs for Mosbach 2 are fairly similar but size-corrected SDQA values are slightly higher than unmodified ones ($SDQAU_p$=117.0, $SDQAC_p$=120.1). At Miesenheim I $SDQAU_p$ and $SDQAC_p$ values are almost identical ($SDQAU_p$=118.9, $SDQAC_p$=117.5). While Miesenheim I consists of a large sample size, allometries on three triangles appear developmentally incorrect and inconsistent across the M_1 (T1, T4, and T5; Figure B.8a). This suggests the size-correction at Miesenheim should be treated with caution. The data suggest that Miesenheim I is older than Mosbach 2 in terms of $SDQAC_p$ but younger in terms of $SDQAU_p$. But, given the likely erroneous $SDQAC_p$ value for Miesenheim I, and the strong evidence correlating Miesenheim I with a post-Cromer III warm period via volcanogenic deposits at Kärlich (Kolfschoten and Turner, 1996; Section 3.5.1.1), the case for an older age for Miesenheim I appears weak. The relative stratigraphic relationships between Mosbach 2 and Miesenheim I, and British MIS 15–13 sites are difficult to understand in terms of SDQA. Mosbach 2 and Miesenheim I are closer in their SDQA with Boxgrove 4b than with Westbury 11 and 14 and Boxgrove 4c. The similarity between Boxgrove 4b and Miesenheim I is consistent with current stratigraphic opinion (e.g., Maul and Parfitt, 2010), but Mosbach 2 is thought to be of a similar age to Westbury and older than Boxgrove 4b. The discussion above postulated that intraspecific morphotypes may be a cause of these complex relationships, as has been explored in Section 7.2.2.2. A further interesting observation of SDQA values from these assemblages is that there appears to be less variation across northwest Europe at this time than across an equivalent region later in the Pleis-

tocene. SDQA variation in British and German water vole assemblages dated to MIS 15 or 13 was found to be 5.4 for $SDQAU_p$ (Westbury 14 $SDQAU_p$=122.4, Boxgrove 4b $SDQAU_p$=117.0) and 5.2 for $SDQAC_p$ (Boxgrove 4b $SDQAC_p$=122.7, Miesenheim I $SDQAC_p$=117.5). This compares with SDQA variation across the two most recent interglacials, MIS 5e and the Holocene, where the range of $SDQAU_p$ is 27.2 (Clacton Channel IV $SDQAU_p$=103.0, Marie-Jeanne Cave 2 $SDQAU_p$=75.8) and of $SDQAC_p$ is 27.3 (Clacton Channel IV $SDQAC_p$=101.9, Marie-Jeanne Cave 2 $SDQAC_p$=74.6). This lack of contrast in SDQA between populations in northwest Europe during the later part of the early Middle Pleistocene may inhibit the ability to resolve between them stratigraphically, or distinguish between intraspecific groups that might have existed, because of greater within-group variation compared with between-group variation. Possible reasons for this contrast in morphological variance will be discussed in Section 8.

Figure 7.10: (Following page) Unmodified SDQ ($SDQAU_p$) values in assemblages estimated to date between MIS 19 and MIS 3. Plot shows $SDQAU_p$ mean (point; $SDQAU_p$ range omitted for clarity) along with the possible age of each assemblage (vertical whisker heights; see Chapter 3). Assemblages colour-coded by geographic zone (see Section 7.1) and labelled as follows: **B4b** - Boxgrove 4b (n=16); **B4c** - Boxgrove 4c (n=17); **BSB** - Burgtonna South Black-earth (n=9); **Chg** - Chigirin (n=9); **CCIV** - Clacton Channel IV (n=19); **CGr** - Cudmore Grove (n=29); **DNg** - Donskaya Negatchevka (n=12); **FUt** - Fortuna utca 16-18/2 (n=17); **GBN** - Grotta del Broion, Sala Grande N (n=10); **GBQ4** - Grotta del Broion, Sala Grande Q4 (n=8); **GBQ5** - Grotta del Broion, Sala Grande Q5 (n=11); **GBR1** - Grotta del Broion, Sala Grande R1 (n=16); **Gun** - Gunki II (n=9); **Ho8** - Horváti-lik 8 (n=19); **Ho9a** - Horváti-lik 9a (n=21); **Ho13** - Horváti-lik 13 (n=8); **Hun** - Hundsheim (n=31); **IKo** - Ilovayski Kordon (n=11); **Kor** - Korotoyak-4 (n=20); **KGr** - Kozi Grzbiet 2 (n=32); **Kuz** - Kuznetsovka (n=89); **MJ4** - Marie-Jeanne Cave 4 (n=9); **MJ6** - Marie-Jeanne Cave 6 (n=7); **Mdz** - Medzhybozh-2 (n=9); **Mhm** - Miesenheim I (n=23); **Msb** - Mosbach 2 (n=75); **Nvk** - Novonekrasovka upper (n=6); **Rg5** - Régourdou 5 (n=8); **Rg7** - Régourdou 7 (n=16); **RDT** - Rotbav-Dealul Ţiganilor Clay-A (n=26); **RSb** - Rybnaya Sloboda (n=6); **Sch** - Schöningen 13-II-4 (n=26); **Ton** - Tönchesberg II 11-13 (n=15); **Tor** - Tornewton Cave Red Cave Earth (n=10); **Vld** - Vladimirovka 2 (n=16); **WRF** - West Runton Freshwater Bed (n=35); **W11** - Westbury 11 (n=12); **W14** - Westbury 14 (n=10)

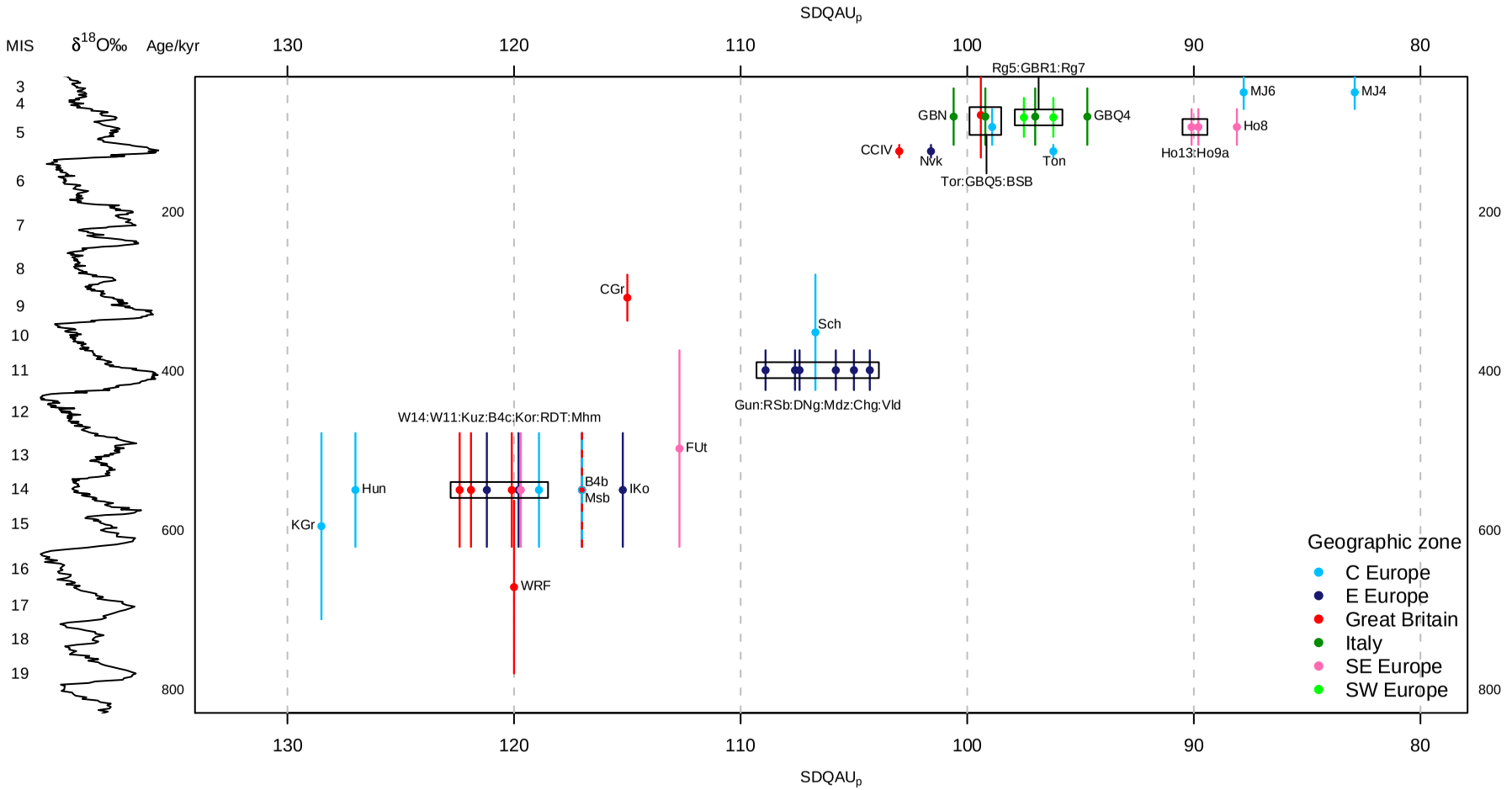
SDQAU$_p$
MIS
δ^{18}O‰
Age/kyr
130
120
110
100
90
80
3
4
5
6
7
8
9
10
11
12
13
14
15
16
17
18
19
200
400
600
800
Rg5:GBR1:Rg7
GBN
GBQ4
MJ6
MJ4
Ho8
CCIV
Nvk
Ton
Tor:GBQ5:BSB
Ho13:Ho9a
CGr
Sch
Gun:RSb:DNg:Mdz:Chg:Vld
W14:W11:Kuz:B4c:Kor:RDT:Mhm
FUt
Hun
KGr
B4b
Msb
IKo
WRF
Geographic zone
C Europe
E Europe
Great Britain
Italy
SE Europe
SW Europe

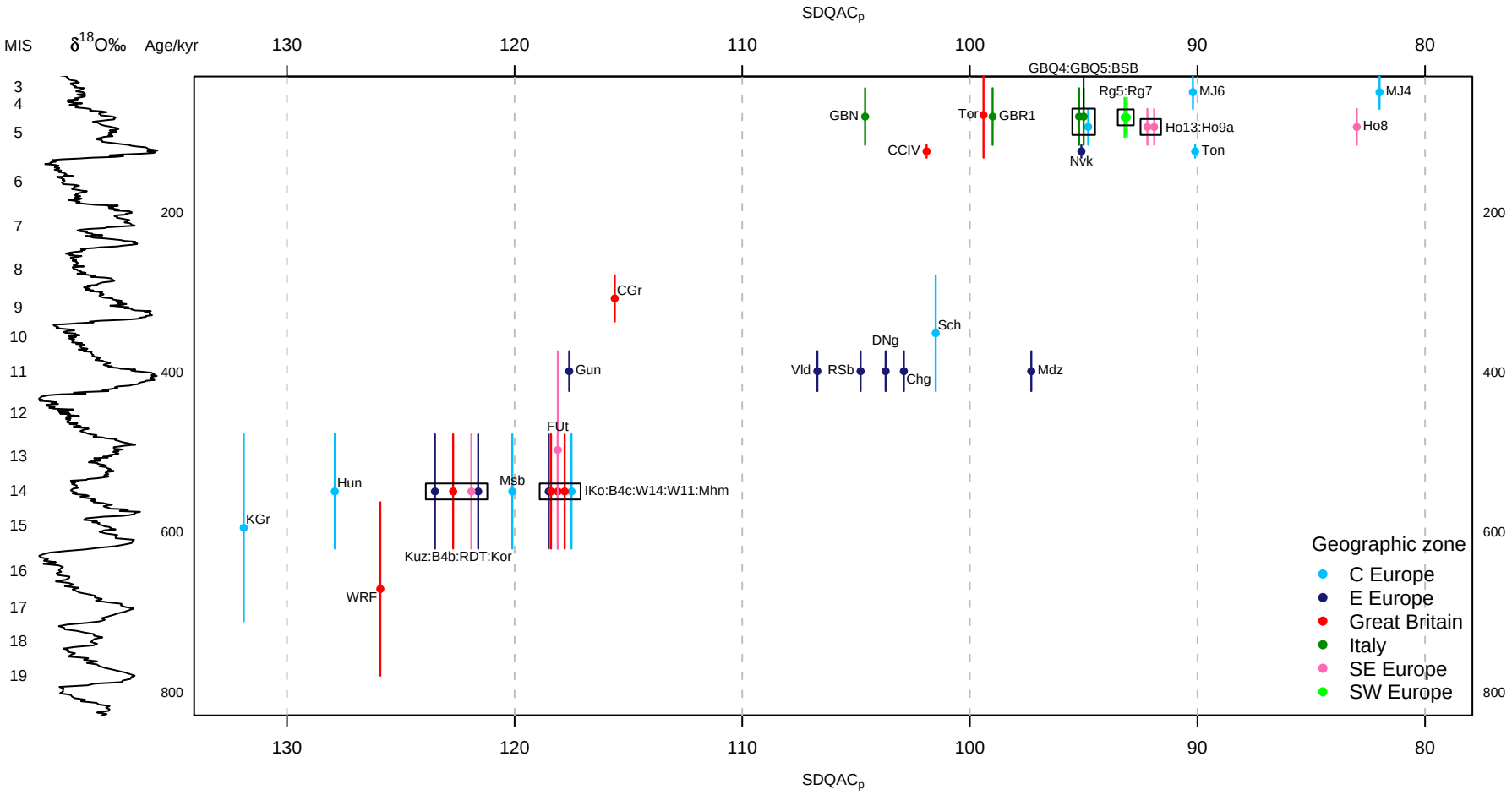

Figure 7.11: Size-corrected SDQ (SDQAC$_p$) values in assemblages estimated to date between MIS 19 and MIS 3. Plot shows SDQAC$_p$ mean (point; SDQAC$_p$ range omitted for clarity) along with the possible age of each assemblage (vertical whisker heights; see Chapter 3). Assemblage labels and other plotting features as for Figure 7.10.

7.3.2.2 Late Middle Pleistocene

The majority of assemblages analysed from the late Middle Pleistocene period are estimated to date from MIS 11 and furthermore are nearly all from Eastern Europe. These Eastern European zone groups have very similar mean $SDQAU_p$s (104.3–108.9) but show a much broader range of $SDQAC_p$ values (97.3–117.6). The size-corrections applied to the assemblages of Gunki II and Medzhybozh 2 are the main reason for this increased range of SDQA values. These two groups also appear to be markedly different in terms of mean size-corrected M_1 shape from other MIS 11 Eastern European zone assemblages (Figure 7.12) .

In the case of Gunki II ($SDQAU_p$=108.9, $SDQAC_p$=117.6), high $SDQAC_p$ values appear at odds with the $SDQAC_p$s of other late Middle Pleistocene assemblages because it seems to correspond better with size-corrected SDQAs from early Middle Pleistocene groups such as Miesenheim I and Westbury 11 (Figure 7.11). The size-correction applied to enamel measurements from Gunki II is partially significant and conforms to the general expectation of the ontogenetic development of enamel (Figure B.4f). But the increase in enamel thickness in these regressions is very rapid and is driven by a small number of small molars with very thin enamel. The fossil material examined from this assemblage derived from two separate archival collections whose history was not fully known (Section 3.14.1.2). It could be that this separately curated material is stratigraphically different, and

---

Figure 7.12: Euclidean distances between size-corrected M_1 shapes from assemblages dating from MIS 19 to MIS 3. Distances taken with respect to the Recent Welsh Borders OTU. Assemblages labelled as follows: **B4b** - Boxgrove 4b (n=21); **B4c** - Boxgrove 4c (n=22); **BSB** - Burgtonna South Black-earth (n=16); **Chg** - Chigirin (n=31); **CCIV** - Clacton Channel IV (n=21); **CGr** - Cudmore Grove (n=51); **DNg** - Donskaya Negatchevka (n=17); **FUt** - Fortuna utca 16-18/2 (n=22); **GBN** - Grotta del Broion, Sala Grande N (n=29); **GBQ4** - Grotta del Broion, Sala Grande Q4 (n=22); **GBQ5** - Grotta del Broion, Sala Grande Q5 (n=28); **GBR1** - Grotta del Broion, Sala Grande R1 (n=38); **Gun** - Gunki II (n=16); **Ho13** - Horváti-lik 13 (n=22); **Ho8** - Horváti-lik 8 (n=29); **Ho9a** - Horváti-lik 9a (n=33); **Hun** - Hundsheim (n=45); **IKo** - Ilovayski Kordon (n=25); **Kor** - Korotoyak-4 (n=26); **KGr** - Kozi Grzbiet 2 (n=42); **Kuz** - Kuznetsovka (n=100); **MJ4** - Marie-Jeanne Cave 4 (n=10); **MJ6** - Marie-Jeanne Cave 6 (n=16); **Mdz** - Medzhybozh-2 (n=22); **Mhm** - Miesenheim I (n=24); **Msb** - Mosbach 2 (n=109); **Nvk** - Novonekrasovka upper (n=12); **Rg5** - Régourdou 5 (n=21); **Rg7** - Régourdou 7 (n=26); **RDT** - Rotbav-Dealul Ţiganilor Clay-A (n=26); **RSb** - Rybnaya Sloboda (n=19); **Sch** - Schöningen 13-II-4 (n=29); **Ton** - Tönchesberg II 11-13 (n=21); **Tor** - Tornewton Cave Red Cave Earth (n=18); **Vld** - Vladimirovka 2 (n=30); **WRF** - West Runton Freshwater Bed (n=45); **W11** - Westbury 11 (n=16); **W14** - Westbury 14 (n=31). Other plotting features as for Figure 7.6.

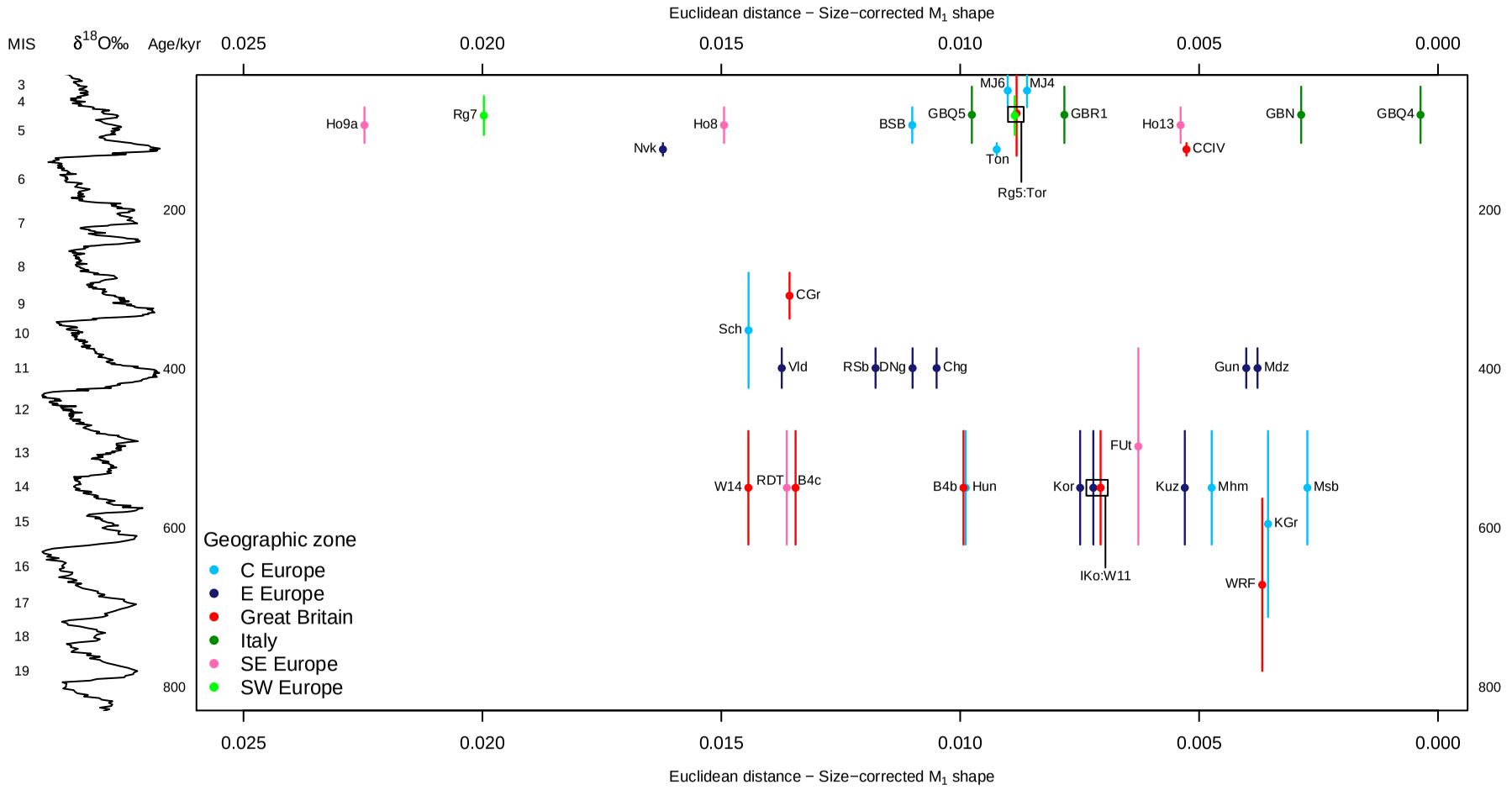
Euclidean distance − Size−corrected M1 shape
MIS
δ18O‰
Age/kyr
0.025
0.020
0.015
0.010
0.005
0.000
3
4
5
6
7
8
9
10
11
12
13
14
15
16
17
18
19
200
400
600
800
Ho9a
Rg7
Nvk
Ho8
BSB
GBQ5
MJ6
MJ4
GBR1
Ton
Rg5:Tor
Ho13
CCIV
GBN
GBQ4
CGr
Sch
Vld
RSb
DNg
Chg
Gun
Mdz
FUt
W14
RDT
B4c
B4b
Hun
Kor
Kuz
Mhm
Msb
KGr
IKo:W11
WRF
Geographic zone
C Europe
E Europe
Great Britain
Italy
SE Europe
SW Europe

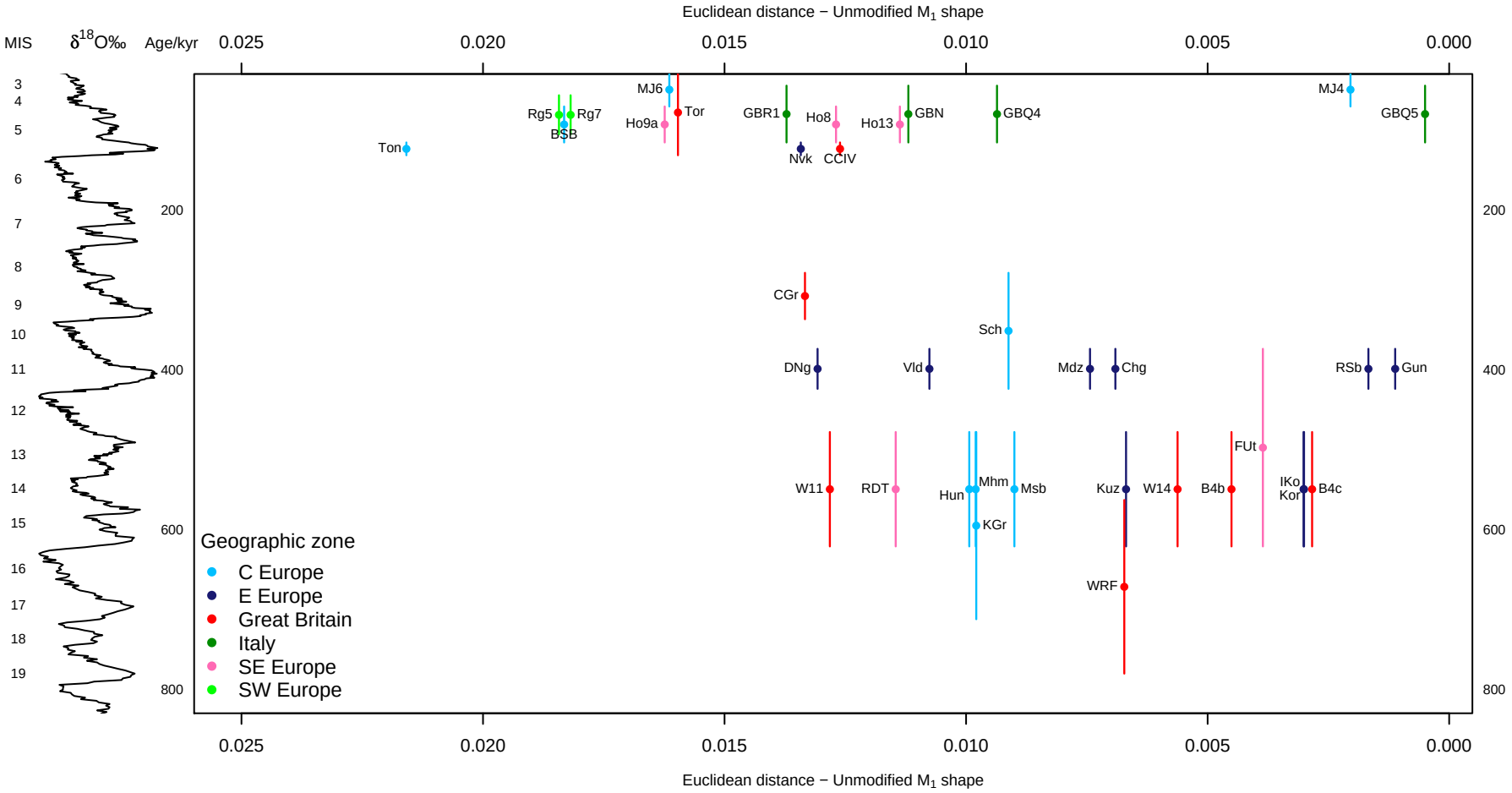

Figure 7.13: Euclidean distances between size-corrected M_1 shapes from assemblages dating from MIS 19 to MIS 3. Distances taken with respect to the Recent Welsh Borders OTU. Assemblage labels and other plotting features as for Figure 7.6.

the fact that published SDQ values for Gunki II by Rekovets (1994) and Markova (2000) are very different (Figures 5.10 and 5.11 and Table 5.7) adds support to this idea. In any event, it appears as though the allometric correction applied to Gunki II is potentially misleading. The $SDQAU_p$ from Gunki II is close to the $SDQAU_p$s and $SDQAC_p$s of many other supposed MIS 11 assemblages from the Eastern European zone. Additionally, Gunki itself forms the type site for the late Middle Pleistocene Gunkovian MAZ (Markova, 1990; Section 3.14.1.2), therefore an early Middle Pleistocene age for Gunki II would be a controversial proposition, not least because the presence of rootless water vole is a general indicator of post-MIS 12 deposits in the Russian Plain (Maul and Markova, 2007, cf. Preece and Parfitt, 2008). In summary, the SDQA data from Gunki II do not challenge the existing opinion on its age.

For Chigirin, Donskaya Negatchevka, Rybnaya Sloboda, and Vladimirovka 2 the differences between $SDQAU_p$ and $SDQAC_p$ values are fairly small, and all four of these assemblages remain closely grouped in terms of both SDQA metrics, in terms of mean size-corrected shape difference, but not in unmodified shape distance. The enamel thickness–size regressions of these assemblages appear biologically sound, aside from those for Rybnaya Sloboda (Figure B.10d), which are negative probably because the sample size for this assemblage is very low (n=6). This probably also explains the large discrepancy between size-corrected and unmodified shape distances for this assemblage. Despite appearing erroneous, the difference between the $SDQAU_p$ (107.6) and $SDQAC_p$ (104.8) of Rybnaya Sloboda is quite low. A general post-MIS 12 age is strongly supported by the SDQA values from Chigirin, Donskaya Negatchevka, Rybnaya Sloboda, and Vladimirovka 2 because they are lower than SDQAs from any of the Eastern European zone assemblages that have been attributed to the early Middle Pleistocene (Section 7.3.2.1). All these deposits fall within the Gunkovian small mammal zone (Markova, 1990), with *Arvicola mosbachensis* and steppe lemming *Lagurus transiens* stratigraphically significant components of these faunas that have led to the correlation of these deposits with the Likhvinian Interglacial (=MIS 11). Chigirin, Donskaya Negatchevka, and Rybnaya Sloboda all include indicators of an interglacial 'forest-steppe' environment (Sections 3.14.1.1, 3.11.2.1, and 3.11.2.2 respectively). In Vladimirovka 2, there is evidence of an open-landscape, steppic environment preceding a warm period, recorded in the overlying stratum of Vladimirovka 1 from where tortoise scutes have been recovered (Section 3.11.2.3). The M_1s of *A. mosbachensis* recovered from Vladimirovka 2 possess relatively high percentages of the *Mimomys*-fold and are small-sized (Agadjanian, 1977; Agadjanian, 1983; Agadjanian and Erbajeva, 1983; Iossifova and Krasnenkov, 1994; Section 3.11.2.3). These 'primitive' characters have led to suggestions that Vladimirovka 2 contains a population of water voles near the *Mimomys–Arvicola* transition in Russia (Sec-

tion 3.11.2.3). The $SDQAC_p$ from Vladimirovka 2 is higher, but the $SDQAU_p$ is lower, relative to other possible MIS 11 Eastern European zone groups (excluding Gunki II, which appears erroneous), and so appears unable to inform on relative relationships between these late Middle Pleistocene groups. One stratigraphic interpretation of the primitive *A. mosbachensis* characters observed in Vladimirovka 2 could be that this assemblage dates to the earliest part of MIS 11. The evidence for more temperate conditions in Vladimirovka 1 could imply that this unit is correlated with the main part of MIS 11. However, at Vladimirovka 1 both steppe lemming morphotypes, *L. transiens* and *Lagurus lagurus*, are present, which are only regarded as co-occurring after MIS 11 (Maul and Markova, 2007). This would imply that a significant hiatus is present between Vladimirovka 2 and 1. It is a pity that so few M_1s from Vladimirovka 1 were in a good enough condition for morphometric analysis (Section 3.11.2.3) as this material may date to a post-MIS 11 warm period, perhaps the Kamenka warm event, and would be important in tracking the development of enamel thickness in Russia through the late Middle Pleistocene. It is difficult to stratigraphically differentiate between Chigirin, Donskaya Negatchevka, and Rybnaya Sloboda from their faunal assemblages, palaeoenvironmental indicators and the SDQA values presented here. The $SDQAU_p$ and $SDQAC_p$ values from these assemblages are very close to one another and firm judgements over relative relationships would be foolhardy considering the substantial overlap in the range and standard deviation of SDQAs obtained (Tables B.6 and B.7). There is nothing to suggest from SDQA data that these assemblages are younger than MIS 11 and, within the current biostratigraphic framework of Russia and eastern Europe, the occurrence of *L. transiens* within the fossil fauna is decisive in correlating these sites with the Likhvinian Interglacial.

The SDQA of Medzhybozh 2 is consistent with the estimated early Middle Pleistocene age for this assemblage. A large negative shift occurs from unmodified to size-corrected SDQA ($SDQAU_p$=105.8, $SDQAC_p$=97.3), which would otherwise suggest the fossil assemblage dates from much later in the early Middle Pleistocene than MIS 11. The enamel thickness–size regressions in Figure B.7e are generally insignificant and poorly defined (especially in T4), which suggests that the $SDQAC_p$ value found should be treated with caution. The mean size-corrected shape difference of Medzhybozh (Figure 7.12) is also very different from the other Easter European zone groups of Chigirin, Donskaya Negatchevka, Rybnaya Sloboda, and Vladimirovka 2. Unmodified shape difference is close to that of the geographically neaby assemblage from Chigirin (Figure 7.13). Although reworking was cited as perhaps being a risk from the sedimentology of the deposit (Section 3.14.1.3) there are no M_1s with distinctively different morphologies or sizes present in Figure B.7e. The sample size from Medzhybozh-2 is quite low

($n = 9$) and molars are fairly similar in size, so the inaccurate regressions appear to be the product of low morphological and size contrast within the sample. It may be that the $SDQAU_p$ value is the most appropriate measure of enamel thickness ratio for Medzhybozh-2, meaning that enamel thickness measurements are more similar to those from the other late Middle Pleistocene groups from the Eastern European zone.

Across a large area of the whole of central Russia, and through to the Don and Dnieper basins, variation in SDQA values in late Middle Pleistocene assemblages is somewhat lower than the SDQA variation found in Holocene groups from a similar region. In the late Middle Pleistocene, the range in $SDQAU_p$ is 4.6 (Gunki II $SDQAU_p$=108.9 to Vladimirovka 2 $SDQAU_p$=104.3) and in $SDQAC_p$ is 3.8 (Vladimirovka 2 $SDQAC_p$=106.7 to Chigirin $SDQAC_p$=102.9, discounting Gunki II and Medzhybozh because of possible problems with size-corrections). In Holocene groups from a similar geographic area the range in$SDQAU_p$ is 8.7 (Novomirgorod $SDQAU_p$=95.0 to Moscow $SDQAU_p$=86.3, although a large amount of enamel thickness variation is explainable by size at Novomirgorod) and in $SDQAC_p$ is 6 (Moscow $SDQAC_p$=87.9 to Bolshoi Tiganye $SDQAC_p$=81.9). If the sample of water vole material obtained is regarded as an accurate representation of variation across the entire distributional range. This evidence indicates that it is possible to accommodate the SDQA variation found in the late Middle Pleistocene in Russia and the Ukraine within one interglacial. Although not directly supporting a correlation of Eastern European zone fossil assemblages with MIS 11, this at least suggests that such a correlation is possible. Reduced SDQA variation in comparison with Holocene populations has also been seen in Section 7.3.2.1 and it is interesting to speculate on the possible causes of such different patterns (see Chapter 8).

The assemblage from Schöningen shows SDQA values that are the same, or slightly lower than, SDQA values from Eastern European zone assemblages attributed to MIS 11 ($SDQAU_p$=106.7, $SDQAC_p$=101.5). The allometric correction applied to enamel thickness appears to be well-supported (Figure B.10e) and suggests a correlation of Schöningen with with MIS 9 is more appropriate than with MIS 11. An MIS 9 correlation is in agreement with a U-Th date of *c.* 320 k yr BP from travertine at the base of the Schöningen II channel (Section 3.5.2.1). Furthermore, it implies a correlation between the Reinsdorf interglacial (Section 3.5.2.1) and the Kamen Soil of the Russian Plain (Gerasimenko, 2004, in Rekovets *et al.*, 2007). Published SDQ data for Schöningen II are similar to SDQ values from Holsteinian (=MIS 11) sites in central Europe such as Bilzingsleben (Kolfschoten, 1993a). Unfortunately no other late Middle Pleistocene assemblages from Central Europe form part of the dataset presented is the present discussion, which would allow comparison between groups based on the methodology used by this thesis.

SDQA values and size-corrected and unmodified shape differences from the British late Middle Pleistocene site of Cudmore Grove are virtually identical ($SDQAU_p$=115.0, $SDQAC_p$=115.6). Examination of the enamel thickness–size relationships for the assemblage (Figure B.2f) show that regressions near significance and are generally consistent in their trajectories, although the allometries in triangle T2 is biologically implausible. Much evidence points to an MIS 9 age for Cudmore Grove (Roe *et al.*, 2009; Section 3.6.2.1), including published SDQ data (SDQ_p=133.36 Roe *et al.*, 2009), which are lower than SDQ values from British MIS 11 assemblages (Roe *et al.*, 2009). In terms of the present data, an MIS 11 age appears to give a better 'by-eye' linear fit between pre-MIS 12 and MIS 5e British groups (Figures 7.10 and 7.11). But, because there is little data of comparable age with which to understand possible geographic and temporal variation, the security of this correlation can only be regarded as weak given the other stratigraphic evidence available. If an MIS 9 age is assumed for Cudmore Grove then this suggests British sites had more primitive SDQA values than expected. Furthermore, if Schöningen is also regarded as an MIS 9 assemblage then the range of SDQA between Great Britain and Germany at this time was around 10–15 units, which compares favourably with SDQA variation observed in the Holocene. In the Holocene much of the SDQA variation across northwest Europe may be attributable to the presence of different intraspecific lineages (Section 7.2.2.2). The maximum difference between Eastern and Western lineages in the Holocene in terms of $SDQAU_p$ is 15.5 (Pisede IV&V $SDQAU_p$=91.3 to Marie-Jeanne Cave 2 $SDQAU_p$=75.8) and in terms of $SDQAC_p$ is 14.5 (Pisede III $SDQAC_p$=89.1 to Marie-Jeanne Cave 2 $SDQAC_p$=74.6).

7.3.2.3 MIS 5e–MIS 3

In assemblages attributed to the Last Interglacial and the earlier part of the Last Cold Stage some geographic patterning appears to be present. The Central and Southeast European zone assemblages tend to possess loweest SDQA values, northern Italy and Great Britain show the highest SDQAs, while the two Southwest and East European Zone assemblages are generally intermediate in their SDQA.

At Clacton Channel IV, SDQA ($SDQAU_p$=103.0, $SDQAC_p$=101.9) values from the *Arvicola* assemblage are the highest of all the groups thought to date to the Late Pleistocene (save for the $SDQAC_p$ of Grotta del Broion, Sala Grande, N). This appears consistent with evidence from the whole vertebrate assemblage that this deposit dates from MIS 5e (Section 3.6.3.2). With respect to SDQA variation across the whole of the Middle and Late Pleistocene Clacton Channel IV could potentially be MIS 7 in age. The $SDQAU_p$ values of British assemblages from the Middle Pleistocene appear to be higher than those of other contemporary groups

across Europe, and this also appears to be the case for the $SDQAC_p$ from Cudmore Grove. An MIS 5e correlation for Clacton Channel IV would suggest that a similar pattern of European geographic variation in SDQA was present in the Late Pleistocene.

The assemblage from Tornewton Cave Red Cave Earth shows identical size-corrected and unmodified SDQA values ($SDQAU_p$=99.4, $SDQAC_p$=99.4). The curation of the *Arvicola* material suggested that the Red Cave Earth corresponded to deposits of the Glutton Stratum. But the security of this has been called into question owing to problems with the excavation and the recording of stratigraphy at in the cave. Currant (1998) suggested that the Hyaena (late MIS 5, possibly MIS 5c) or Bear (early MIS 5e) stratum would be a more appropriate association for the *Arvicola* assemblage (Section 3.6.3.6). The SDQA results presented here are lower than those obtained from Clacton Channel IV and, if Clacton is considered a Last Interglacial deposit, suggest that the Red Cave Earth assemblage is younger than MIS 5e. If this age estimate is correct, and the *Arvicola* assemblage does originate from the Bear stratum, then the early Last Interglacial age postulated for this unit (Currant, 1998) would appear incorrect. A correlation with the Bacon Hole mammal assemblage zone may be a more suitable fit in terms of enamel thickness data.

Data from Recent populations of *Arvicola* also raise the possibility that the SDQA differences observed between Clacton and Tornewton assemblages can be explainable as variation within a single lineage in an interglacial. For instance, in the late Holocene in Great Britain the range of $SDQAU_p$ is 3.3 (Wigber Low 26 $SDQAU_p$=87.3 to Welsh Borders $SDQAU_p$=84.0) and in $SDQAC_p$ is 8.3 (Wigber Low 26 $SDQAC_p$=88.0 to Ossom's Eyrie $SDQAC_p$=80.3). In these terms the 3.6 unit difference in $SDQAU_p$ and 2.5 unit difference in $SDQAC_p$ are concievably insignificant from a stratigraphic perspective.

The sole Eastern European site for the Late Pleistocene, Novonekrasovka upper, shows SDQA values of $SDQAU_p$=101.6 and $SDQAC_p$=95.1. Enamel thickness allometries for this assemblage are variable (Figure B.8e; especially T4 and T5), and size-corrected M_1 shape is also different from the mean shapes of other assemblages (Figure 7.12). Although there is evidently some correspondance between enamel layer thickness and M_1 size, a low sample size (n=6) probably inhibits consistent regressions from being consistently found in the assemblage. On balance the SDQA from Novonekrasovka upper appears close to that from Clacton Channel IV. A Last Interglacial age for this assemblage has been estimated through correlation with the Karangatian transgression of the Black Sea (Section 3.14.2.1), but the probable inaccuracies in deriving $SDQAC_p$ values complicate interpretation. In the Holocene, similar SDQA values existed in British and Eastern European zone groups from the same intraspecific lineage (e.g., $SDQAC_p$ of

Novomirgorod and Welsh Borders, Section 7.2.2.2). If we accept the correlations of Novonekrasovka upper and Clacton Channel IV with the Last Interglacial, then the enamel thickness data from these assemblages may demonstrate that similar intraspecific relationships existed between these geographic regions in the early part of the MIS 5 as do today.

In the assemblages from Grotta del Broion, Sala Grande the $SDQAU_p$ values range from 100.6 (layer N) to 94.7 (layer Q4) and $SDQAC_p$ range from 104.6 (layer N) to 95.0 (layer Q5). $SDQAC_p$ values for layers Q4 and Q5 are virtually identical (95.2 and 95.0 respectively). Only low resolution dating information is available for the strata from Grotta del Broion (Section 3.8.1.1), and although these assemblages show relatively high SDQA values, considerations of intraspecific-level morphological variation are important in the stratigraphic interpretation of SDQA data. Allometries of enamel thickness are identifiable but their regressions are not well defined (Figures B.4b–B.4e), and in particularly those applied to the *Arvicola* from layer N appear partly erroneous. The assemblage from layer N has a higher $SDQAU_p$ value than assemblages from earlier strata, which is interesting in terms of the general pattern of a reduction in SDQA over time. Maul *et al.* (1998a) showed that *Arvicola* from the Late Pleistocene of southern Italy displayed consistently higher SDQs than contemporaneous populations in northern Italy and central Europe, and so it may be that *Arvicola* from layer N represent a population of southern Italian water voles. Southern Italian populations were estimated to have SDQs around 115–110 SDQ units during MIS 5–4, with other groups possessing SDQs around 15 units lower (Maul *et al.*, 1998a). Using the equation in Figure 5.12a to transform the $SDQAU_p$ value from layer N to SDQ units gives an SDQ=101.2. This is lower than observed and predicted SDQs from southern Italy, but error in the conversion between the different SDQ metrics may interfere with the accuracy of this converted value. Immigration events are linked to environmental changes (e.g., Hewitt, 1999) and, from the dating estimations of *Arvicola* assemblages from Grotta del Broion, a link with a climatic change in the early part of the Last Cold Stage would be implicated as causal. It is likely that a climatic warming would be required to stimulate an immigration of *Arvicola* from southern to northern Italy, and palaeoenvironmental evidence shows that a change from cool-temperate to warm, mesic habitats occurred from layer Q to layer N (Section 3.8.1.1). Given the general correlation between the Grotta del Broion, Sala Grande sequence and the early and middle part of the Last Cold Stage, a date for a this warming, and any potential immigration event, could be MIS 5c or MIS 5a. In summary, although an immigration event is possible cause, the increase in SDQA from layer Q4 to N does not appear to be of a magnitiude that would be expected if southern Italian populations were the source population for such an immigration. There is concern over the accuracy of the $SDQAC_p$ value

from layer N, and the $SDQAU_p$ differences between layer N and earlier *Arvicola* assemblages could be explainable by sampling variation alone.

The descending SDQA values from the two Belgian assemblages Marie-Jeanne Cave 6 ($SDQAU_p$=87.8, $SDQAC_p$=90.2) and Marie-Jeanne Cave 4 ($SDQAU_p$=82.9, $SDQAC_p$=82.0), agree with the stratigaphic order of these deposits. The enamel thickness–size regressions for Marie Jeanne Cave 6 are poorly defined (Figure B.7d) and so the $SDQAC_p$ value calculated for this assemblage must be viewed with caution. The size-corrected shape differences of Marie-Jeanne Cave 4 and 6 are very similar, however, and perhaps suggest that these two assemblages contain related populations. The two assemblages show much lower SDQAs than most other groups thought to be of Late Pleistocene age in Figures 7.10 and 7.11, and after comparison with Lateglacial and Holocene populations from the Central Europe zone, are correlated more appropriately with MIS 3 (Section 7.2.2.2).

At Burgtonna South Black-earth ($SDQAU_p$=98.9, $SDQAC_p$=94.8), despite a relatively small sample size (n=9) the good range of M_1 sizes, enamel thickness–size regressions appear to have consistent trajectories and are significant or are near significance (Figure B.1f). There is a high level of confidence in the stratigraphy of the travetines below the Black-earth as an MIS 5e deposit from biostratigraphic evidence. The relationship between the Black-earth and the travertine below would seem to strongly imply an MIS 5d age for the Black-earth (Section 3.5.3.3).

The assemblage at Tönchesberg II ($SDQAU_p$=96.2, $SDQAC_p$=90.1) shows very strong and consistent allometries in enamel thickness (Figure B.10f). This gives confidence in the size-corrected SDQA as a good representation of adult morphology. The humic-rich soil at Tönchesberg II has been correlated with the Last Interglacial (Section 3.5.3.6) but the $SDQAC_p$ value from the *Arvicola* assemblage is much lower than SDQAs from Clacton Channel IV in Great Britain and Novonekrasovka upper from the Ukraine that may date to MIS 5e. A published mean SDQ of 109 for the assemblage at Tönchesberg II (Kolfschoten and Roth, 1995) can be converted to a size-corrected SDQ of 105.4 (using the equation in Figure 5.12b). This calculated value is much higher than the actual $SDQAC_p$ obtained and either suggests different fossil material was measured by Kolfschoten and Roth (1995) than by this study, or the conversion between SDQ metrics is inaccurate. Data from the present study suggest that either *Arvicola* populations with lower SDQAs than most other western European groups were present at Tönchesberg II, that this deposit is younger than the current age estimation suggests, or that differences can be explained by within-species variation. It has been notes that in Germany, assemblages of *Arvicola* from the Saalian are observed to display lower SDQ values than in the Eemian (Kolfschoten, 1992). This

was interpreted as the result of the immigration of more primitive (higher SDQ) *Arvicola* populations from the east or southeast of Europe, replacing Saalian water voles possessing lower SDQs. The immigration appears coincident with the climatic warming that occurred from the Saalian to the Last Interglacial. The palaeoenvironmental data from Tönchesberg II record a mosaic of open and woodland habitats without any clear indicators of the warm-termperate conditions that may be expected from a Last Interglacial deposit (Section 3.5.3.6). Could it be that the *Arvicola* from Tönchesberg II are part of the low SDQ Saalian population? Differences in SDQ between Saalian and Eemian *Arvicola* populations are around 20 SDQ units (Kolfschoten, 1992). Furthermore, dfferences between Tönchesberg II and the nearby, but stratigraphically younger, assemblage from Burgtonna South Black-earth (difference in $SDQAU_p$=2.7 and $SDQAC_p$=4.7) are less than the SDQA difference observed between Fuchsloch im Krockstein and Kartstein (difference in $SDQAU_p$=6.8 and $SDQAC_p$=9.2; Section 7.2), which are early Holocene groups in Germany that appear to be from different intraspecific lineages (Section 7.2). The presence of other intraspecific groups is speculative and the existing stratigraphic interpretation of Tönchesberg II appears difficult to challenge based on SDQA data alone. Therefore the stratigraphic relationship between Tönchesberg II and Burgtonna South Black-earth appears unaffected by SDQA data.

The *Arvicola* assemblages from Régourdou 5 and 7 have very similar SDQA values (Régourdou 5 $SDQAU_p$=97.5 and $SDQAC_p$=93.2; Régourdou 7 $SDQAU_p$=96.2 and $SDQAC_p$=93.1). Regressions for both assemblages are generally consistent but T4 in Régourdou 7 appears erroneous (Figure B.10b). The close agreement in SDQA between both Régourdou 5 and 7 suggest that these layers are temporally close, and the stratigraphic description from Régourdou does indicate that these layers are intimately related, if not genetically identical (Section 3.4.1.4). In terms of shape, however, there appears to be a large mean size-corrected shape difference between these two assemblages (Figure 7.12) which is difficult to reconcile with SDQA data. The The $SDQAU_p$ of the layers are nested within $SDQAU_p$s of strata at Grotta del Broion, while $SDQAC_p$ values are slightly lower than from Grotta del Broion. Both Régourdou 5 and 7 have lower SDQAs than those from Burgtonna South Black-earth, which appears to be a fairly securely dated assemblage from the early part of the Last Cold Stage. Unmodified shape differences from Régourdou and Burgtonna South Black-earth are very similar, however. Lower SDQAs than Burgtonna South Black-earth suggest that Régourdou may be younger than Section refsite:Regourdou:strat. Stratigraphic (Section 3.4.1.4) and palaeoenvironmental evidence from Régourdou suggests that layers 5 and 7 were deposited in a temperate, wooded phase of the early or middle part of the Last Cold Stage, while later strata record climatic cooling during this

period (Section 3.4.1.4). This implies layers 7–5 correlate with MIS 5c or MIS 5a, which is ostensibly consistent with the SDQA data. A complicating factor may be whether the *Arvicola* from Southwest Europe were morphologically distinct from water voles elsewhere, especially the Central European zone. If these groups were distinct in their enamel thickness and shape, as Eastern and Western mtDNA lineages from the Lateglacial and Holocene appear to be, then SDQA differences between assemblages that are in the order of a few units (e.g., between Régourdou, Tönchesberg, and earlier strata from Grotta del Broion) may interfere with stratigraphic inferences. One conclusion that can be drawn is that the assemblages from Régourdou do not appear to represent *Arvicola sapidus* as the enamel thickness ratios from Recent *A. sapidus* are far higher and M_1s much larger than those recovered from Régourdou.

At Horváti-lik, assemblages have good sample sizes but show highly variable enamel thickness–size regressions (Figures B.5a–B.5c). In the case of Horvati-lik 13 this appears to be because M_1s are of a similar size, but for the other two assemblages there are a number of large M_1s with particularly low enamel thickness measurements, and these contradictory allometries suggest that $SDQAU_p$ values are likely to be more accurate than size-corrected ones. Further evidence for the insecurity of correcting morphology with size can be found from the wide range of shape differences found between the assemblages (Figure 7.12). $SDQAU_p$ values are very similar to one another (Horváti-lik 8 $SDQAU_p$=88.1, Horváti-lik 9a $SDQAU_p$=89.8, Horváti-lik 13 $SDQAU_p$=90.1), which suggests that the assemblages are closely associated. The low $SDQAU_p$ values obtained are much less than those from other assemblages dated to the early part of the Last Cold Stage, which either implies that the Horváti-lik assemblages are younger than other groups or that the Hungarian *Arvicola* are different morphotypes. The Carpathians have been recognised as a faunally separate region (e.g., Deffontaine *et al.*, 2005; Stewart *et al.*, 2010) and so the *Arvicola* from Horváti-lik may represent a morphologically distinct group inhabiting the Bükk Mountains of northern Hungary around MIS 5d. However, biogeographic links between any such group and later populations are not clear, given knowledge of the morphologies of later *Arvicola* assemblages from this region (i.e., Peskö and Pilisszántó; secn 7.2.2.2). This southeastern area of Europe has been implcated as the source region for 'primitive' populations immigrating into northwestern Europe during interglacials (see Section 7.2.2.2 and the discussion of the Saalian–Eemian SDQ fluctuation above). If the Horváti-lik population were part of such a source population it would perhaps be expected that higher SDQA values would be obtained than those observed. Dating of the sequence has only been attempted through climatostratigraphy, which generally attributes layers 15–7 to the early part of the Last Cold Stage (Section 3.7.3.2). Given that intraspecific variation seems unlikely, the most par-

simonious explanation for the the low $SDQAU_p$ values obtained from Horváti-lik would be that these assemblages are younger than MIS 5c. Palaeoenvironmental evidence suggests that a transition from a wooded, temperate to cool climate occurs through layers 15 to 7 (Section 3.7.3.2), which would imply a correlation with MIS 5a to the beginning of MIS 4 through referral to the global isotope stratigraphy.

Chapter 8

Discussion

8.1 Methodology

This thesis has focussed on the study of morphological variation in samples of M_1 teeth in Pleistocene and Holocene water voles. It has attempted to understand the relative contributions made by a range of factors that influence the total amount of variation seen within samples, and by so doing, enable the variation in morphology that is related to phylogeny to be more clearly defined. The starting point for breaking down variation into its component parts is with the collection of morphological data itself. This study has asserted that landmarks and enamel thicknesses measured from molars oriented with the plane of the occlusal surface perpendicular to the line of sight ('occlusal view') do not solely describe molar morphology because the occlusal surface is developed at an angle determined by masticatory wear. This plane reflects aspects of the development of the mandible and jaw musculature, themselves a product of genetic complexes and phenotypic variability that are unrelated to molar morphology. If one's aim is to investigate the molar, such additional influences should, if possible, be removed. Therefore the measurement of morphometric variables in a true cross-sectional plane of the molar ('axial view') appears to be biologically more appropriate. A disadvantage of measurement in axial orientation was an increase in measurement error compared with occlusal orientation. However, elevated levels of error do not appear to mask differences between groups and the trade-off between reduced precision but a potential increase in phylogenetic accuracy was considered worthwhile. The angle of the occlusal plane may, of course, contain phylogenetically useful information but this should be considered separately from true molar shape. Such an investigation was outside the bounds of this thesis but may be of benefit to evolutionary studies, as well as having interesting ecological and functional aspects.

Morphometric variables may be used to examine the contribution to total variation made by non-biological factors such as those derived from taphonomic effects.

The idea is that fossil groups that show departures in total within-group variance from that observed in modern samples may indicate increased time-averaging or lineage-mixing in assemblages. Elevated levels of variation are found in some assemblages from cave deposits but systematic differences were not found between assemblages from different depositional settings. It is unclear how powerful this approach is at highlighting taphonomic mixing because there is also considerable variability in the patterns of within-group variance in Recent samples. What is needed is a concept as to what constitutes a 'good' sample, and this is likely to be study-dependent. For instance in this thesis ideas surrounding allometric change and the removal of ontogenetic variation are highly important, and these are best explored where a good ontogenetic range of samples is present. The benefit of examining and comparing variation within groups is certainly a useful undertaking, however, in that it gives the researcher an awareness of potentially problematic groups. The influence of sample size on the perception of variation and other descriptive statistics such as the mean was also examined and was found to be considerable. Estimates of descriptive statistics become highly inaccurate where $n \lessapprox 10$.

The sources of non-biological variation discussed above can only be qualitatively assessed and cannot be removed as there is no expectation of how each of these sources of variation modifies the original sample structure. One aspect of sample structure that can be accounted for is the component relating to ontogenetic variation. This approach is only possible thanks to the availability of a geometric morphometric definition of molar size that is independent of molar shape. Linear regressions of morphology on size show that up to 95.1% of variation in enamel thickness and between 9.2 and 29.4% of shape variation can be explained by ontogenetic age in Recent groups, and up to 88.2% of enamel thickness variation and between 2.5 and 27.7% of shape variation can be explained by ontogenetic age in fossil groups. By using linear regression to project morphometric variables (molar shape or enamel thicknesses) to their estimated values at maximum size, the variation explained by molar size can be removed. This produces 'adult' populations that consequently allow for more meaningful comparisons between groups because all groups are at the same point in ontogenetic development.

8.2 Phylogeny, biogeography, and ecology

The availability of a mtDNA dataset as a compliment to morphological data for some of the groups examined by this thesis is significant, since it has provided a reference set of relationships against which phylogenetic information and phylogenetic hypotheses can be compared and tested. Size-corrected molar shapes describe phylogenetic distances more accurately than original shape variables, and

can be thought of as analogous to mtDNA in that molar shape changes regularly with time, leading to the concept of 'morphological clock' (Polly, 2001). Phylogenies based on both size-corrected and unmodified data are similar in structure. The topology of the trees based on M_1 shape is interesting, however, in that they place the eastern mtDNA lineage as ancestral rather than the western mtDNA lineage, as is the case in the mtDNA phylogeny. The former arrangement, based on morphology, is intuitively easier to understand given the current deeper phylogeographic understanding that water voles originated from eastern Europe or Siberia cricetid groups (Chaline *et al.*, 1999). These patterns perhaps indicate that molar morphology captures different aspects of evolutionary history, over different timescales, compared to those recounted by mtDNA.

Molecular data (Piertney *et al.*, 2005; Brace, 2010) show that two intraspecific lineages, Eastern and Western lineages, were present in central, western, and northwestern Europe from MIS 3 to the Recent. At present the Eastern lineage occupies the whole of the Balkan peninsula, the East European Plain, and the Baltic and Scandinavian regions. The western lineage is found in France and parts of the Alpine region. In Great Britain both lineages are present but an interesting pattern has developed where the Eastern lineage is found in England and Wales but the Western lineage is only found in Scotland, forming a 'Celtic fringe' (Piertney *et al.*, 2005; Searle *et al.*, 2009; Brace, 2010). The general location of the suture zone between the two lineages in continental Europe appears to run northwest–southeast through Belgium and central Europe to the Carpathian region. The data from aDNA show that the Western lineage at least occupied the western and southern parts of central Europe during MIS 3, with the earliest records found in Belgium at Marie-Jeanne Cave 4 (*c.* late MIS 3) and Trou Al'Wesse (*c.* 20 k yr BP), and in the Slovak republic from Dzeravá skala Cave (*c.* 30–26 k yr BP). The earliest record of the Eastern lineage is dated to *c.* 17 k yr BP from Pilisszántó in the Carpathian region of northern Hungary. From these earliest known distributions it appears that the Eastern lineage came to progressively occupy areas further to the north and west. The progress of this immigration is recorded in the Lateglacial and early Holocene assemblages from Fuchsloch im Krockstein, Germany, and the Belgian site of Trou Al'Wesse, where Eastern lineage populations are found above Western ones. Both lineages are also found at the Holocene site of Merlin's Cave, Great Britain, and, although the stratigraphic relationship of these lineages are not known here, the expectation is that the Eastern occurs above the Western.

The combination of molecular and morphological data presented in this thesis has allowed morphology to be mapped onto mtDNA phylogeography, and suggests that faunal movements can be traced through the morphology of M_1 teeth. Although not categorical, there is evidence that differences exist in both size-corrected and unmodified SDQA data between Eastern and Western mtDNA lin-

eages. Eastern lineage populations appear to have consistently higher SDQA values than Western lineage groups (Section 7.2.2.2). However, there are no areas of the stratigraphy where contemporaneous assemblages from the two lineages are juxtaposed, which would allow direct comparison of enamel morphology at the same point in time to be made. A cluster of Lateglacial–early Holocene assemblages exist with low SDQAs, which includes the Western lineage assemblage from Marie-Jeanne Cave 2, and it could be assumed that the other assemblages with similarly low SDQAs are also affiliated to the Western lineage. For the Belgian assemblage of Trou du Frontal and the southwest French assemblages of Abzac, Courbet, and Poeymaü this appears likely given their geographic location (Brace, 2010). But the German assemblage of Kartstein, which also shows low SDQs, could potentially be an Eastern or Western group, since this site is located close to the suture zone between lineages. The affiliation of the *Arvicola* from the Last Glacial assemblage of Peskö is also unclear given the contrasting $SDQAU_p$ and $SDQAC_p$ values obtained.

An alternative explanation to phylogeny as the cause of differences in enamel thickness between groups are ecophenotypic effects. An examination of palaeoenvironmental data from fossil assemblages that also possess mtDNA sequences is inconclusive as to whether correlations exist between SDQA and environment within- or between-lineages. The Eastern lineage assemblage from Pilisszántó (Section 3.7.3.5) and the Western lineage assemblage from Dzeravá skala (Section 3.12.1.1) both show evidence for steppe/tundra conditions and have comparable SDQA values, although the temporal gap between these assemblages could mask SDQA differences. The Eastern lineage late Holocene assemblages from Pisede (Section 3.5.4.1), Wigber Low and Ossom's Eyrie (Section 3.6.3) record evidence of temperate woodlands, meadows and uplands, and the ecology of the Recent Welsh Borders group is a semi-aqautic population in an agricultural, floodplain environment. All these Eastern groups have similar SDQAs to Lateglacial *Arvicola* from Pilisszántó with its steppe/tundra environment. On the other hand, the two Western lineage groups from Marie-Jeanne Cave 2 and Central Scotland are very different in SDQA. At Marie-Jeanne Cave 2 there is evidence of temperate woodland environments while the ecology of the Central Scotland group was either semi-aquatic or fossorial in a cool-temperate environment (Jefferies, 2003a). Across populations that possess mtDNA sequences it appears that the relationship between environment and morphology is not clear, and generally intraspecific affiliation is a better explanation for the morphological patterns observed. Many fossil sites, particularly from the Last Cold Stage, contain evidence for a range of habitats (e.g., Abzac, France, Section 3.4.1.1, or Peskö, Hungary, Section 3.7.3.4), and this lack of palaeoenvironmental detail may interfere with our ability to interpret any ecophenotypic interactions that may be in operation. Environmental

factors such as altitude have been shown to influence molar morphology in Recent *Arvicola* (Kratochvíl, 1983a), but to rigorously test for the presence or strength of ecophenotypic effects an analysis of the ecology of populations which takes account of evolutionary correlations is required (Cunningham *et al.*, 1998). This would appear to be an important piece of further work.

Recent *Arvicola terrestris* are found to adopt either fossorial or semi-aquatic ecologies. Fossorial forms exist in central Europe, and mountainous regions such as the Alps, the Pyrenees, northern Spain and in Italy, with semi-aquatic forms predominating elsewhere (Reichstein, 1963; Ventura, 1991; Gromov and Polyakov, 1992). The phylogenetic significance of these ecotypes has often been debated by systematists and the molecular evidence suggests that these ecologies are indicative of intraspecific groups. For instance, the fossorial Italian form *Arvicola italicus* appears to be a well-defined clade, groups within the Western lineage are generally fossorial and appear to approximate to the named form *Arvicola scherman*, and the Eastern lineage encompasses more semi-aquatic forms that have generally been named *A. terrestris* and *Arvicola amphibius*. How rigid these ecological modes are is not clear, however. Western lineage populations in northern England and Scotland from the early 20$^{\text{th}}$ century are reported to have been fossorial but present-day Scottish *Arvicola* are semi-aquatic (Jefferies, 2003a). This suggests that an element of plasticity exists around any core intraspecific ecological types. Should ecotypes conform to intraspecific lineages, as the molecular data suggest, then the apparent morphological distinction in terms of SDQA that appears to exist between Eastern and Western lineages also indicates the palaeoecologies of fossil groups.

The identification of intraspecific groups of *Arvicola* in the fossil record and the mapping of their biogeography has often been attempted by researchers. Storch (1971, cited in Gromov and Polyakov, 1992, p. 348) recognised *Arvicola abbotti* and *Arvicola antiquus* as similar morphological forms, which led him to propose that these species were representatives of a group of fossorial water voles that inhabited England and continental western Europe in the Late Pleistocene (France and the area of the former West Germany) as part of 'mixed and lemming faunas'. This fossorial group disappeared from the region with the onset of reforestation in the Holocene. The fossorial character of this group noted by Storch could possibly be a consequence of local populations plastically occupying whatever habitat space is available, rather than a reflection of the existence of a phylogenetically determined ecological type. Especially when one considers that western and northwestern Europe at the time were largely covered by mixed open steppe/tundra type environments for much of the Last Glacial (Taberlet *et al.*, 1998). However, the new molecular evidence of intraspecific diversity in this region during the Last Glacial supports Storch's morphologically-based interpretations. The

scenario painted by Storch has striking parallels with the observations made from the data presented in this thesis: a central European and Great British group of Last Cold Stage water voles becoming replaced in parts by another group with different dental morphologies and probably a different ecology. Further in the geological past, Kolfschoten (1992) uncovered a fluctuation in the SDQ measurements of *Arvicola* populations from the late Saalian to the Eemian of northwest and central Europe. In this instance, late Saalian assemblages showed much lower SDQs than the Eemian assemblages that immediately post-dated them. It was postulated that this pattern reflected the replacement of populations in the north by a group from the south and/or east, which possessed a more primitive (higher) SDQ. Again, the pattern of morphological change recorded by Kolfschoten (1992) is very similar to that identified above in the Lateglacial–Holocene of this region of Europe. Namely, a gradual decrease in SDQ during glacial times, followed by a sudden increase in SDQ after the onset of interglacial warming, as a 'primitive' lineage from the east or southeast expands its range across central and northwest Europe. If these patterns of phylogeographic change are shared between the last two glacial–interglacial transitions, then this suggests at least some of the present-day patterns of faunal distribution have deeper origins than the shaping effects of the Last Cold Stage or Last Glacial alone. Preliminary estimates from molecular data suggest the Last Interglacial as the date of the most recent common ancestor of Eastern and Western lineages of *Arvicola* (Brace, pers. comm., 2010, although there is significant error related to this estimate), and evidence from other small mammals further point to earlier in the Late and Middle Pleistocene for the origins of modern intraspecific groups (e.g., Tougard *et al.*, 2008). But if modern faunal patterns do have their origins early in the Late Pleistocene or even late Middle Pleistocene, what were the conditions that led to the formation of the intraspecific water vole groups now present in northern and western Europe, and how were the distributional differences between groups maintained?

Most of the post-glacial range expansion of the Eastern lineage appears to involve the exploitation of new environments as climate warmed, e.g., the morainic landscapes of northern Germany at Pisede. But during the Last Glacial–Holocene the Eastern lineage appears to have partially replaced the Western lineage at Britain, northern Germany, and possibly southern central Europe, and at the Saalian–Eemian transition a similar replacement occurred in Germany. Why such partial replacements should occur, and what conditions determine the location of the suture zone between lineages is unclear. The detail of the shape and location of the interface between lineages, and the factors that influence its development and evolution must be the subject of conjecture. However, some of the broad issues can be discussed. The presence of between-lineage competition would not be likely if lineages were strictly differentiated by ecological preference (i.e., semi-

aquatic forms would not compete for resources with fossorial forms) but the fact that the Eastern lineage geographically replaces the Western at all suggests that either habitats preferred by Eastern lineage populations became unavailable or scarce, or some degree of competition did indeed occur. Many boundaries between intraspecific groups follow major geographical features such as mountain ranges or major rivers (Mayr, 1963), but the area of central Europe across which the Eastern populations expanded is a largely barrier-free, permeable landscape. This suggests that the maintenance of the join between groups is either related to detailed ecological factors such as soil type or altitude, which are as yet unknown, or difficulties overcoming lower fitness within hybrid zones (Barton and Hewitt, 1985).

One major discussion point relating to post-glacial recolonisation is the role played by refugia. Data from the last glacial–interglacial transition shows that the southern refugial paradigm (e.g., Hewitt, 1999) appears to be insufficient and too simplistic to apply to *Arvicola*. Movement of populations from the east/southeast appears important in the recolonisation of north and northwest Europe, but the northern refugial hypothesis (Stewart and Lister, 2001) is also supported, with populations of *Arvicola* recorded in northwest Europe during the Last Glacial period (Ightham Fissures, Great Britain, Section 3.6.3.3; and Trou Al'Wesse, Belgium, Brace, 2010). The empirical similarities between distributional change in *Arvicola* of north/northwest Europe across the last two glacial–interglacial transitions may also indicate that similar refugia operated in the Saalian as the Last Glacial.

An interesting feature of the dataset presented in this thesis is that greater geographical variation in SDQA appears to exist across the Late Pleistocene and Holocene in comparison with the early Middle Pleistocene. Unfortunately, spatial and temporal gaps mean that morphological variation across Europe in the late Middle Pleistocene is difficult to comment upon. Greater morphological similarity between early Middle Pleistocene assemblages could indicate less diversity at the intraspecific group-level than observed in the Late Pleistocene and Holocene, which would imply that some feature of the early Middle Pleistocene or late Middle Pleistocene provided a catalyst for the development of intraspecific groups. The classic model for speciation is based upon the genetic isolation of populations, usually by geographic factors, which then diverge through adaptation to local conditions or by stochastic mechanisms (allopatric speciation *sensu* Mayr, 1963). The global marine isotope record suggests that interglacials in the early Middle Pleistocene were cooler and less climatically variable than those that followed (Tzedakis *et al.*, 2009). This reduced climatic variability could mean that populations of *Arvicola* across Europe were less fractured by period shifts in environmental conditions than later in the Pleistocene. Furthermore, with respect to Great Britain, the

English Channel was not formed until MIS 12 (Gupta *et al.*, 2007), which would have allowed faunal links with mainland Europe to be maintained throughout interglacial periods in the early Middle Pleistocene, reducing the likelihood of endemism. Terrestrial records, however, indicate that periods of extreme warmth and cold existed during the early Middle Pleistocene (e.g., Westbury Cave, Section 3.6.1.3; Candy, 2009). Additionally, other forms of morphological variation have been noted across the range of water voles in the early Middle Pleistocene, most notably in the development of roots, which are lost first in western Europe around MIS 16/15 and later in Russia around MIS 12 (e.g., Maul and Markova, 2007). Such morphological clines may reflect the existence of genetic isolation between intraspecific groups. Alternatively this may be a graded adaptational response to local environmental conditions across a whole population, which can eventually result in genetic fragmentation of that population. This is because metapopulations at either end of a cline may be selectively pulled to environmental extremes at the limits of the whole population range, eventually leading to a break in gene-flow between them (sympatric speciation *sensu* Mayr, 1963). Comparing SDQA data from late Middle and Late Pleistocene assemblages in Britain (Cudmore Grove, Clacton Channel IV and Tornewton Cave) with contemporaneous assemblages in central and eastern Europe (including Tönchesberg II for instance) demonstrates these extremes existed, and had a persistant form, with British assemblages displaying consistently higher SDQAs than other groups. This may also reflect the fact that Britain's biogeographic relationship with Europe changed after the formation of the English Channel in MIS 12 (Gupta *et al.*, 2007). Following MIS 12 Britain's has switched between being an island during interglacials and a peninsula during glacials (White and Schreve, 2000). These geographic changes would also have provided periodic opportunities for the effects of allopatric speciation to manifest while British water voles were isolated from communicating with wider populations on the continent.

The main force driving evolutionary change in molar teeth has been assumed to be biomechanical adaptation of the grinding surface to improve efficiency of food processing (Rensberger, 1973; Koenigswald, 1982a). Such pressures derive either directly from the toughness of vegetation, usually from the silica (phytolith) content of grasses (Hunt *et al.*, 2008), or indirectly through incidental ingestion of sediment during feeding (Rensberger, 1973). Adaptation has not only occurred at the level of the gross structure of the molar—such as loss of roots, heightening of the crown, and enamel thickness changes—but has also led to modification of the crystal microstructure of enamel as a mechanism to prevent the propagation of stresses through the molar, and to allow enamel surfaces to 'self-sharpen' during mastication (Koenigswald, 1982a). Fossorial species may be considered particularly susceptible to the ingestion of sediments by virtue of their lifestyle.

It is also expected that during cold climatic phases substrates are less rich in organic material and contain a higher fraction of inorganic sediment because of less well-developed vegetational cover and increased weathering. Vegetation during these periods is also comprised of less succulent species such as sedges, and any adaptation to allow consumption of these tougher species would be advantageous. Adaptive pressures from diet, that reflect wider climatic changes, would be a credible mechanism directing evolution of the molar across the whole of the considerable geographic range of the water vole. The existence of these pressures would be capable of explaining the apparently directional evolution observed in so many of the morphological characters of the M_1, including the enamel thickness ratio. Furthermore, vegetational differences caused by regional climatic variation could easily be imagined to result in differential morphologies in local water vole groups, either as an ecophenotypic or adaptive response. An alternative proposed evolutionary mechanism, however, subordinates the role of vegetation and climate in favour of intraspecific competition. In this model, competition for resources, primarily between members of the same species, leads to selection for larger body size. The increased forces exerted during mastication, because of more powerful jaw musculature associated with larger body size, provide the selective pressure on the dentition to cope with increased wear (Martin, 1993). Body size in water voles (inferred from M_1 size) has increased markedly from the early Middle Pleistocene (Martin, 1993), and so this proposal may have traction. However, it is difficult to envisage how within-species differences could be generated without some role played by variation in vegetation composition or climate, at the very least in terms of limiting resources.

8.3 Biostratigraphy

The analysis of evolutionary history made in Chapter 7 recalls many of the same general patterns of SDQ change as those observed by previous studies, from the long-term decrease in SDQs over the Middle and Late Pleistocene and Holocene, to the regional differences observed in Recent groups and postulated immigration events in fossil groups. Absolute SDQA values, from both size-corrected and unmodified enamel thicknesses presented in this study, are generally lower than previously published SDQ values (SDQ_{pub}), a systematic difference resulting from the axial orientation of specimens. The relationship between published data and those presented here can be quantified through linear regression (Section 5.6). However, there is appreciable error in converting between the different metrics. Sources of error between SDQ_{pub} and SDQAU are sample composition and measuring error. Error in converting between SDQ_{pub} and SDQAC is greater because this also includes error from inconsistent or biologically inappropriate regressions

of enamel thickness and size. In some cases size correction of enamel thickness produces seemingly erroneous or inconsistent results. Examples of this include the large, positive size-corrections for Grotta del Broion, Sala Grande N and Peskö "red brick" strata. These 'problematic' corrections can be explained in terms of assemblage structure, where the range of ontogenetic stages is insufficient to accurately define an ontogenetic regression. Such sample structuring could, if it were considered appropriate, be used as evidence to remove assemblages from analyses and to assess them separately. Indeed, such issues may even be informative in highlighting interesting aspects of taphonomy. It would be possible to impose an ontogenetic trajectory, mapped from another group, on such assemblages, but care would have to be taken in selecting an appropriate foster group as ontogenetic trajectories appear to be highly variable between groups and to change over evolutionary history.

How do SDQA values from this study relate to values communicated in the literature? The earliest population of water voles examined with accompanying SDQ_ps is from the West Runton Freshwater bed. This study gives a corrected mean SDQ_c of 124.82 and an unmodified mean SDQ of 118.99. Maul and Parfitt (2010), in contrast, derive an SDQ of 139.59[1] ($n = 51$) for the same assemblage. Later in the early Middle Pleistocene, the assemblages examined by this study exhibit minimum mean SDQs no lower than at Miesenheim I (116.5) for size-corrected SDQs, and no lower than at Boxgrove 4b (115.93) for unmodified SDQs. This compares with published means of 152 ($n = 29$) and 140.62 ($n = 9$) for Miesenheim I (Kolfschoten, 1988 and Maul *et al.*, 2000 respectively) and a mean of 139.54 for Boxgrove ($n = 13$, Parfitt, pers. comm., 2009, although the unit specimens originated from was not specified). The water vole from the West Runton Freshwater bed is *Mimomys savini* and this deposit is thought likely to correlate with MIS 17 (Maul and Parfitt, 2010) and the assemblages from Boxgrove and Miesenheim I are of *Arvicola mosbachensis* and are considered to be from MIS 15 or MIS 13 deposits. Given these age estimates, the data from this study appear to be more consistent with the relative ages of these early Middle Pleistocene assemblages than the published data.

Later in the Pleistocene, the SDQ value of 100 is an important marker for many palaeontologists as the arbitrary boundary distinguishing the chronospecies *A. mosbachensis* and *Arvicola terrestris*. This transition occurs in a slightly different position in the stratigraphy presented in this thesis than in prior analyses. At Burgtonna South Black-earth, a size-corrected SDQ of 95.24 and an unmodified SDQ of 98.86 from this study are slightly lower than a mean SDQ of 99.65 ($n = 40$) reported by Heinrich (1982). Tracing this boundary further,

[1]Juvenile specimens were not removed for the derivation of this value (Maul, pers. comm., 2010).

size-corrected SDQs from this study suggest that the *A. mosbachensis–A. terrestris* transition runs along a stratigraphically disparate group of assemblages: where SDQ $\lesssim 100$, at Grotta del Broion, Sala Grande R1, Tornewton Cave Red Cave Earth, and Medzhybozh-2; and where SDQ $\gtrsim 100$, at Clacton Channel IV, Schöningen 13-II-4, Chigirin, and Donskaya Negatchevka. The east-west trend in this transition zone—i.e., eastern assemblages appear to have lower SDQs than central and western groups of the same age—has also been noted in previous studies, and is considered to have occurred fairly rapidly from the Last Interglacial to the later stages of MIS 5 (Maul and Markova, 2007). The data produced by this thesis suggest this boundary to have a similar Last Interglacial age in the west of Europe (as is currently recognised) but to have greater temporal depth in the east, perhaps even extending to MIS 11 in the Ukraine and Russia (assuming the dating of the eastern MIS 11 assemblages is accurate). This observation implies that the geographic cline across Europe is steeper than currently acknowledged, and that regional-level patterning in the morphology of the water vole M_1 may be even more of a problem to long distance correlation using the SDQ than previously considered *in terms of the methodology employed by this thesis*.

The existence of spatial variation in morphology has been a major source of concern for biostratigraphers whose aim has been to correlate between palaeontological sites. Although the existence of morphological variation across the range of fossil populations is often recognised as a potential issue, the exact nature of spatial differences is difficult to clarify. Do differences manifest themselves as abrupt boundaries between morphotypes or as gradual clines across the landscape? Enamel thickness data from Late Pleistocene and Holocene populations in north/northwestern Europe show at least two sudden shifts in SDQ that occur in concert with glacial–interglacial climatic changes (Section 8.2). These patterns of SDQ change appear to demonstrate the replacement of one intraspecific group by another, and suggests that intraspecific boundaries, at this period in central Europe, were abrupt. However, in the regions west or east of the suture between these intraspecific groups, greater morphological similarity exists, meaning that greater confidence can be applied to biostratigraphic hypotheses. The identification of biostratigraphically 'secure' areas, where potentially confusing immigration events are less likley to occur, is important for successful correlations through water vole biostratigraphy. However, without access to a detailed sequence of water vole assemblages from a region (as with Kolfschoten, 1992), these areas are difficult to identify unless independent evidence for faunal immigrations is present, such as from molecular data or from compositional changes in other members of the fauna. There appears to be strong evidence for morphologically and phylogenetically distinctive populations in central and southern Italy (Masini *et al.*, 2003; Paunescu *et al.*, 2004; Taberlet *et al.*, 1998; Brace, 2010). However, in northern Italy, faunal

connections with southern France, the Balkan peninsula via the Po Plain and, during glacials, the Adriatic (Sala and Marchetti, 2006), as well as possibly with southern Italy (Section 7.3.2.3) mean that this area must be carefully considered before using *Arvicola* morphology stratigraphically. In western southwestern Europe, fossil assemblages from the Late Pleistocene and early Holocene suggest that enamel morphology evolves in a stable manner (Section 7.3.2.3), although data are unavailable from before the Late Pleistocene. In Great Britain during the early Middle Pleistocene SDQA values are very similar, which suggests that the SDQA from water voles is not the most appropriate biostratigraphic tool to employ at this time. In late Middle and Late Pleistocene, although the data are patchy, British assemblages from interglacials appear to possess higher SDQAs than elsewhere in Europe. For instance at Cudmore Grove $SDQAC_p$=115.6, which suggests an MIS 11 correlation, despite abundant alternative stratigraphic evidence for an MIS 9 age for this site. This apparent systematic difference should be taken into consideration when attempting correlations using water vole enamel between British sites and other sites in continental Europe. The Carpathian mountains appear to have been a region occupied by at least more than one intraspecific group (Dzeravá skala, Pilisszántó, and possibly Peskö) and so should be used with caution in correlations. The Balkans are an area of endemism today and in the past (Rekovets and Nadachowski, 1995; Griffiths *et al.*, 2004), but data from this thesis cannot properly test this in water vole. The east of Europe and the Russian Plain appear to be important source regions for water vole populations immigrating into western Europe, at least during interglacials in the Late Pleistocene. But morphological variation within this region is difficult to interpret other than in terms of the general pattern of reduced SDQ over time. In the late Middle Pleistocene assemblages attributed to MIS 11 (Chigirin, Donskaya Negatchevka, Gunki II, Medzhybozh, Rybnaya Sloboda, and Vladimirovka 2) the variation in SDQA is lower than that observed in this region in the Holocene, which may suggest that this region can act as a good basis for correlation with central Europe at this time.

The real test of a biostratigraphically useful model of evolution is the ability to make predictions about the value or state of a morphological character though time. One approach to constructing such a model for quantitative characters such as the SDQ could be to take character values from two assemblages of known age and calculate a linear rate of evolution between them. This is inappropriate, however. A constant rate of evolution is an assumption that only holds for taxa that are under strong, continuous, directional selection or under stasis (Roopnarine, 2003).[1] For many evolutionary sequences, evolution is best described through a

[1]Although, if evolution is static then the character is biostratigraphically useless as the rate of evolutionary change is zero!

Brownian motion or random walk model[1] (Raup, 1977), or some variant of this (Hunt, 2006). Characters evolving by a random walk change as a function of the square root of time (Gingerich, 1993; Polly, 2002), which means that with time, t, along an evolutionary sequence, differences between characters at t_0 and t_i are likely to be greater than differences between characters at t_0 and t_{i+1}. In other words, closely related groups are likely to show proportionally larger differences from one another than more distantly related groups, a concept analogous to molecular clocks (Polly, 2002). This, perhaps counter-intuitive, occurrence means that the calculation of a rate of change for an evolutionary sequence is dependent on the length of the interval over which the rate is calculated (Gingerich, 1993). It also means that a limit exists to the temporal range over which a quantitative character is useful in biostratigraphy because homoplasy erases differences over time. Theoretical discussions such as this may seem academic given the clear empirical trend in the SDQ—and other measures of morphology—through time. Also, other groups of Pleistocene rodents show similar evolutionary trends in molar dentition to those observed in water voles that appear linked to broader selection pressures on life-history traits, which suggests a common driver for selection exists across groups during this period (Martin, 1993). However, intraspecific variation—touched on above—complicates the issue and raises the possibility that evolutionary tempo and mode vary geographically and temporally (Benton and Emerson, 2007).

Some authors suggest that the water vole is only biostratigraphically useful within a zonal system (e.g., Escudé *et al.*, 2008b) and it is certainly true that differentiating between fossil assemblages on shorter timescales (e.g., between interglacials) appears difficult using the SDQ as it is presently understood. However, changes in the morphology of the water vole M_1 are empirically obvious over longer timescales (e.g., Heinrich, 1982; Maul *et al.*, 1998b) and the evidence presented in this thesis shows, as other studies have shown, that morphological data incontrovertibly reflect phylogeny, and therefore time since common ancestry. Fluctuations and contrasts in morphology between fossil populations of water voles in space and time (Kolfschoten, 1992; Maul *et al.*, 1998b; Paunescu *et al.*, 2004) remain difficult to explain in terms of anything other than intraspecific variation and, as phylogenies based upon ancient DNA are now routinely revealing, within-species lineage or 'deme'-level diversity appears to be the norm in Late Pleistocene mammals. The biostratigraphic appreciation and 'usefulness' of the water vole can only be advanced by continually framing questions concerning its evolution within a quantitative concept of evolution. The real issues surrounding the study of morphological evolution in water voles—and other small mammals—relate to the resolution that morphological characters can offer the palaeontologist

[1]Evolution is not truly stochastic here but likely mimics fluctuating selection.

who aspires to understand evolution at the edge of speciation.

Chapter 9

Conclusions and further work

A number of conclusions may be drawn from the research presented in this thesis. An examination of the gross structure of the M_1 molar of the water vole suggests that morphometric measurements of the occlusal surface should be made with the tooth in axial, rather than occlusal orientation. Enamel thickness ratios (SDQs) from measurements made by these two methods are systematically different. The term SDQA is introduced to describe enamel thickness ratios based on measurements from axially oriented molars. This highlights the contrast between the two measurement approaches and makes differences with previously published values, which likely employed an occlusal orientation, explicit.

Overall, patterns of change over time in water vole enamel thickness were found by this study to be similar to those previously recognised, confirming that the SDQ describes an apparently directional evolutionary trend. The SDQA shows differences with previously published SDQ values that can be accounted for computationally, but significant error may be present in attempting to convert between different metrics. This causes concern for between-study comparisons. The source of differences between SDQA and published data not only stem from the different tooth orientations employed, but also include comparability of samples, and methodologies of individual workers. Some researchers have voiced concerns over worker-specific measurement technique (e.g., Parfitt pers. comm., 2008) and so it would be of benefit to the whole community if clear, concise expositions of measurement technique, along with explorations of measurement error, are presented alongside results in order to allow better cross-comparison between studies and to encourage a move towards a uniform approach.

The type of sedimentary deposit within which fossil assemblages are found does not appear to bias the morphological structure of samples. This observation appears to deserve further research, however, in order to anticipate how time-averaging may affect the amount of variation found in small mammal assemblages (e.g., Hunt, 2004). Sample-size has a major effect on the accuracy of estimations of means and other descriptive statistics. Samples of no fewer than 10 individuals

should ideally be used but if they are, caution should be attached to results they provide.

Morphology of the M_1 is significantly related to ontogenetic age and the removal of this source of variation results in a strong correspondence between molar shape and mtDNA differences. This suggests that studies should either discard juvenile individuals before morphometric analyses or account statistically for the effect of ontogenetic age. Enamel thickness may also be ontogenetically corrected, and the new modelled thicknesses can be used to calculate size-corrected enamel thickness ratios (SDQAC) as distinct from unmodified enamel thickness ratios (SDQAU).

Conclusions may be drawn regarding stratigraphic and temporal patterns in SDQA. Relationships between stratigraphically or geographically close assemblages appear to be described more accurately when calculated from size-corrected rather than unmodified enamel thicknesses. Although by no means conclusive, this further suggests that size-corrected morphologies are better at describing phylogenetic relationships. Some assemblages receive 'erroneous' corrections because morphology–size regressions are poorly defined due to lack of ontogenetic variation in the assemblage. However, such occurrences may in themselves be of interest and may have taphonomic significance.

Both SDQA and shape data indicate that intraspecific lineages can be identified from morphology. Ecophenotypic responses were not discernible from the palaeoenvironmental data available but it is possible that distinct ecological modes relate to intraspecific groups. These perhaps correspond with the Recent fossorial *Arvicola scherman* and semi-aquatic *Arvicola terrestris* taxonomic groups. Some ecological plasticity observed within Recent lineages is present, however. In northwestern and central Europe a fluctuation in enamel thickness ratios observed during the last two glacial–interglacial transitions (the Last Glacial–Holocene and Saalian–Eemian transitions) suggests that similar phylogeographic events occurred. A reduction in SDQA during glacials followed by an increase in interglacials points to the replacement of a western intraspecific group by an eastern immigrant group. Competition between the two groups is likely to have been minimal, however. The eastern group appears to have exploited space and resources that became newly available with climatic warming, while the western group may have become restricted to habitats once common in cold periods but in retreat during warm stages (e.g., mountain zones). Recent material from Iberia (*Arvicola sapidus*) is morphologically distinct in terms of SDQA from *A. terrestris*, but populations from the Caucasus are also morphologically distinct in terms of SDQA and M_1 shape from populations elsewhere. These differences may have palaeontological significance in terms of a shared ancestry between Iberian and Caucasus groups.

In terms of SDQACs, assemblages that are thought to date between MIS 15 and MIS 13 possess a mean $SDQAC_p$ no lower than 119. There is a large difference in $SDQAC_p$ between assemblages immediately older and younger than MIS 12, although almost all assemblages examined that are thought to correlate with MIS 11 are from eastern Europe and geographic variation may thus play a part in these differences. The transition between the chronospecies *Arvicola mosbachensis* and *A. terrestris* (where SDQ=100) occurs in SDQAC early in MIS 5 in the west of Europe but may be as early as MIS 11 in eastern Europe.

In the majority of cases the age estimations attributed to assemblages (Chapter 3) have not been challenged by SDQA data. In Late Pleistocene and Holocene groups this is generally because the precision of SDQA data relative to the error of age-estimations is too great to effect those estimations. Furthermore, there may be uncertainty regarding how much SDQA values reflect intraspecific rather than temporal variation (e.g., Peskö, Section 7.2.2.2).

In the late Middle Pleistocene, intraspecific patterning is also a concern. This may be discernible in assemblages form the British sites of Cudmore Grove, Clacton Channel IV and Tornewton Cave, which possess much higher SDQAs than those from the rest of Europe. Caution should be exercised when attempting correlations using water vole enamel between British sites and those from continental Europe over this period. Two assemblages from Russia and the Ukraine attributed to MIS 11, Gunki II and Medzhybozh-2, may suffer from temporal mixing either pre- or post-excavation and their morphometric data should be re-examined. Other MIS 11 assemblages from the Russian Plain (Chigirin, Donskaya Negatchevka, Gunki II, Medzhybozh, Rybnaya Sloboda, and Vladimirovka 2) have low SDQA diversity, and may represent a single lineage. This region may also provide good opportunities for long-distance correlations with central Europe. Water voles from the assemblage of Schöningen may be related to populations farther east and this assemblage may be best correlated with MIS 9 based on size-corrected SDQA.

The relative order of *Arvicola* assemblages in the early Middle Pleistocene is difficult to decipher based upon SDQA alone. The steep cross-continental morphocline observed post-MIS 12 contrasts with seemingly more conservative enamel thickness morphologies during the early Middle Pleistocene. Notable assemblages such as Miesenheim I, Mosbach 2, Boxgrove and Westbury Cave show a range of SDQAs that could easily be accommodated within a single interglacial in the Late Pleistocene rather than potentially across a number of warm stages. These patterns may indicate that geographic or climatic conditions that led to later morphological diversity in water voles were not present during the early Middle Pleistocene.

The use of molecular data from modern and ancient DNA in tandem with

morphometric variables is confirmed as a powerful approach. Future investigations relating morphology to mtDNA phylogenies will be able to determine whether, and to what degree, morphology is able to resolve mtDNA lineages, thereby raising the novel prospect of a phylogeography for the Middle Pleistocene. A model-based approach should also be taken to assess tempo and mode of evolution in enamel thickness and other aspects of morphology such as occlusal shape (e.g., Polly, 2004; Hunt, 2006), in attempts to calculate evolutionary rates for water vole evolution that would undoubtedly have biostratigraphic significance. Likewise, model-based methods, with carefully-framed hypotheses that are falsifiable, should be able to test for the existence of immigration events.

This thesis has, hopefully, taken the study of small mammal evolution a little further forward. The author has attempted to explore the nature of the data upon which evolutionary and biostratigraphic ideas are based and it has been shown that it is possible to refine these data to provide greater accuracy in the estimation of evolutionary models. Perhaps even more importantly, however, is the gathering together of such a large, uniform, geographically broad and temporally deep dataset that may be used by other students and researchers to investigate some of the issues covered in this thesis and beyond. To facilitate research, it is therefore intended to make the raw data used in this thesis freely available through the internet. Some of the possible research directions relating to evolutionary studies have been touched upon above but many others can be explored. These data reflect spatial phenomena and so should appeal to geographical analysis within a GIS to test phylogeographic hypotheses (e.g., Stigall and Lieberman, 2006) and relate morphology to environmental data (Banks *et al.*, 2006; Kozak *et al.*, 2008; Lawing and Polly, 2010). The interactions between an almost ubiquitous member of the temperate and cool-temperate fauna of the recent geological past, the landscape, and climate are likely to be complex but are intriguing (Panteleyev, 2001). There are also interesting evolutionary-developmental questions surrounding water voles, given the obvious significance of ontogenetic change in the characters under study. Whatever the study, however, understanding variation at the geographic-, temporal-, and population-level remains at the heart of understanding the evolution of the water vole.

Bibliography

Adams, B., Ringer, A. (2004). New ^{14}C dates for the Hungarian early Upper Palaeolithic. *Current Anthropology*, 45(4), 541–551.

Adams, D., Rohlf, F., Slice, D. (2004). Geometric morphometrics: ten years of progress following the 'revolution'. *Italian Journal of Zoology*, 71(1), 5–16.

Agadjanian, A.K. (1977). Quartäre Kleinsäger aus der Russischen Ebene. *Quartär*, 27/28, 111–145.

Agadjanian, A.K. (1981). Early Pleistocene small mammal locality on the river Ilovay. In: *Novye donnye po stratigrafii verkhnego pliotsena i pleistotsena tsentral'nykh raionov Evropeiskoi chasti SSSR (New data on the stratigraphy and palaeogeography of the Upper Pliocene and Pleistocene of the central region of the European USSR)*, 32–51. INQUA.

Agadjanian, A.K. (1983). Eine altertümliche *Arvicola* (Rodentia, Mammalia) aus dem Mittelpeistozän der Russischen Ebene. *Schriftenreihe für Geologische Wissenschaften*, 19/20, 9–29.

Agadjanian, A.K., Erbajeva, M.Z. (1983). *Late Cenozoic rodents and Lagomorpha on the USSR territory*. Nauka Press, Moscow.

Agadjanian, A.K., Kondrashov, P.E. (2007). Mollusks and small mammals from the Kuznetsovka locality, Pleistocene of the Oka-Don Plain. *Paleontological Journal*, 41(4), 395–406.

Alberch, P., Gould, S.J., Oster, G.F., Wake, D.B. (1979). Size and shape in ontogeny and phylogeny. *Paleobiology*, 5, 296–317.

Albrecht, G.H. (1978). Some comments on the use of ratios. *Systematic Zoology*, 27(1), 67–71.

Andersen, K.K., Svensson, A., Johnsen, S.J., Rasmussen, S.O., Bigler, M., Röthlisberger, R., Ruth, U., Siggaard-Andersen, M.L., Peder Steffensen, J., Dahl-Jensen, D., Vinther, B.M., Clausen, H.B. (2006). The Greenland Ice Core Chronology 2005, 15-42 ka. Part 1: constructing the time scale. *Quaternary Science Reviews*, 25(23–24), 3246–3257.

Andres, W. (1971). Sedimentologische und morphoskopische Untersuchungen eines Fundprofiles aus den pleistozänen Mosbacher Sanden bei Wiesbaden-Bieberich. *Mainzer Naturwissenschaftliches Archiv*, 10, 101–112.

Andrews, P. (1990). *Owls, Caves and Fossils: predation, preservation and accumulation of small mammal bones in caves, with analysis of the Pleistocene cave faunas from Westbury-sub-Mendip, Somerset, UK.* British Museum (Natural History), London.

Andrews, P., Cook, J. (1999). Description of the sedimentary sequence in Westbury Cave. In: P. Andrews, J. Cook, A. Currant, C.B. Stringer (eds.), *Westbury Cave: The Natural History Museum Excavations 1976–1984*, 19–57. Western Academic & Specialist Press Limited, Bristol.

Andrews, P., Cook, J., Currant, A., Stringer, C.B. (eds.) (1999). *Westbury Cave: The Natural History Museum Excavations 1976-1984.* Western Academic & Specialist Press Limited, Bristol.

Andrews, P., Ghaleb, B. (1999). Taphonomy of the Westbury Cave bone assemblages. In: P. Andrews, J. Cook, A. Currant, C.B. Stringer (eds.), *Westbury Cave: The Natural History Museum Excavations 1976-1984*, 87–126. Western Academic & Specialist Press Limited, Bristol.

Arnold, A., Böhme, G., Fischer, K., Heinrich, W.D. (1982). Eine neue jungpleistozäne Wirbeltierfauna aus Rübeland (Harz) (Vorläufige Mitteilung). *Wissenschaftliche Zeitschrift der Humbolt-Universität zu Berlin*, 31, 169–175.

Atchley, W.R., Anderson, D. (1978). Ratios and the statistical analysis of biological data. *Systematic Zoology*, 27(1), 71–78.

Atchley, W.R., Gaskins, C.T., Anderson, D. (1976). Statistical properties of ratios. I. Empirical results. *Systematic Zoology*, 25(2), 137–148.

Aulagnier, S., Kranz, A., Lovari, S., Jdeidi, T., Masseti, M., Nader, I., de Smet, K., Cuzin, F. (2008). *Capra ibex.* In: *IUCN 2009. IUCN Red List of Threatened Species. Version 2009.1.* URL `http://www.iucnredlist.org/`. Accessed 18 February 2010.

Baales, M. (1992). Ubberreste von Hunden aus der Ahrensburger Kultur am Kartstein, Nordeifel. *Archäologisches Korrespondenzblatt*, 22(4), 461–471.

Bahlo, E., Malec, F. (1969). Insectivoren (Mammalia) uas den oberen Mosbacher Sanden (Mittelpleistozän bei Wiesbaden-Bieberich/Hessen). *Mainzer Naturwissenschaftliches Archiv*, 8, 56–76.

Bailey, R., Byrnes, J. (1990). A new, old method for assessing measurement error in both univariate and multivariate morphometric studies. *Systematic Zoology*, 39(2), 124–130.

Banks, W., d'Errico, F., Dibble, H., Krishtalka, L., West, D., Olszewski, D., Peterson, A., Anderson, D., Gillam, J., Montet-White, A., Crucifix, M., Marean, C., Sánchez-Goñi, M.F., Wohlfarth, B., Vanhaeran, M. (2006). Eco-cultural niche modeling: New tools for reconstructing the geography and ecology of past human populations. *PaleoAnthropology*, 4, 68–83.

Barnes, I., Shapiro, B., Lister, A., Kuznetsova, T., Sher, A., Guthrie, D., Thomas, M. (2007). Genetic structure and extinction of the woolly mammoth, *Mammuthus primigenius*. *Current Biology*, 17(12), 1072–1075.

Barton, N.H., Hewitt, G.M. (1985). Analysis of hybrid zones. *Annual Review of Ecology and Systematics*, 16, 113–148.

Bate, D.M.A. (1901). A short account of a bone cave in the Carboniferous limestone of the Wye Valley. *Geological Magazine*, 8(4), 101–106.

Behrensmeyer, A.K. (1993). Bones. In: D.E.G. Briggs, P.R. Crowther (eds.), *Palaeobiology: a synthesis*, 232–235. Blackwell, Oxford.

Behrensmeyer, A.K., Hook, R.W. (1992). Palaeoenvironmental Contexts and Taphonomic Modes. In: A.K. Behrensmeyer, J.D. Damuth, W.A. DiMichele, R. Potts, H.D. Sues, S.L. Wing (eds.), *Terrestrial Ecosystems Through Time*, 15–136. University of Chicago, Chicago.

Benton, M.J., Emerson, S.B. (2007). How did life become so diverse? The dynamics of diversification according to the fossil record and molecular phylogenetics. *Palaeontology*, 50(1), 23–40.

Bermudez de Castro, J.M., Arsuaga, J.L., Carbonell, E., Rodriguez, J. (eds.) (1999). *Atapuerca: Neustros Ancestores*. Fundacion del patrimonio historico de Castilla y Leon.

Bilton, D.T., Mirol, P.M., Mascheretti, S., Fredga, K., Zima, J., Searle, J.B. (1998). Mediterranean europe as an area of endemism for small mammals rather than a source for northwards postglacial colonization. *Proceddings of the Royal Society of London. Series B*, 265(1402), 1219–1226.

Bishop, M.J. (1974). A preliminary report on the Middle Pleistocene mammal bearing deposit of Westbury-sub-Mendip, Somerset. *Proceedings of the Speleological Society*, 13, 301–318.

Bishop, M.J. (1975). Earliest record of Man's presence in Britain. *Nature*, 253, 95–97.

Bishop, M.J. (1982). *The mammal fauna of the early Middle Pleistocene cavern infill site of Westbury-sub-Mendip, Somerset*. Special Papers in Palaeontology. The Palaeontological Association, London.

Bolus, M., Conard, N.J. (2006). Zur Zeitstellung von Geschoßspitzen aus organischen Materialen im späten Mittelpaläolithikum und Aurignacien. *Archäologisches Korrespondenzblatt*, 36, 1–15.

Bonifay, E. (1964). La grotte de Régourdou (Montignac, Dordogne). Stratigraphie et industrie lithique moustérienne. *L'Anthropologie*, 68, 49–64.

Bonifay, E., Vandermeersch, B., Couture, C., Panattoni, R. (2007). *Sepulture Neandertalienne du Régourdou*. Centre d'Etudes et de Recherches sur les Lacs Anciens Iacs et Tourbières Du Massif-Central.

Bookstein, F.L. (1996). Biometrics, biomathematics and the morphometric synthesis. *Bulletin of Mathematical Biology*, 58(2), 313–365.

Bookstein, F.L. (1991). *Morphometric Tools for Landmark data*. Cambridge University Press, Cambridge.

Bowman, S. (1990). *Radiocarbon Dating*. British Museum, London.

Boyce, C.C.K. (1991). Genus *Arvicola*. In: S. Harris (ed.), *The Handbook of British Mammals*. Blackwell Scientific Publications, Oxford.

Brace, S. (2010). *Investigating evolutionary processes using ancient and historical DNA of rodent species*. Ph.D. thesis, Royal Holloway, University of London.

Bramwell, D., Yalden, D.W., Yalden, P.E. (1990). Ossom's Eyrie Cave: an archaeological contribution to the recent history of vertebrates in Britain. *Zoological Journal of the Linnean Society*, 98, 1–25.

Bridgland, D.R. (1994). *Quaternary of the Thames*. Geological Conservation Review Series 7. Chapman & Hall, London.

Bridgland, D.R., Westaway, R. (2008). Climatically controlled river terrace staircases: A worldwide Quaternary phenomenon. *Geomorphology*, 98(3–4), 285–315.

Broglio, A., Improta, S. (1995). Nuovi dati di cronologia assoluta del Paleolitico Superiore e del Mesolitico del Veneto, del Trentino e Friuli. *Atti Dell'Istituto Veneto di Scienze, Lettere ed Arti*, CLIII, 1–45.

Bronk Ramsey, C., Higham, T.F.G., Bowles, A., Hedges, R.E.M. (2004). Improvements to the pretreatment of bone at Oxford. *Radiocarbon*, 46, 155–163.

Bronk Ramsey, C., Higham, T.F.G., Owen, D.C., Pike, A., Hedges, R.E.M. (2002). Radiocarbon dates from the Oxford AMS system: Archaeometry Datelist 31. *Archaeometry*, 44(3s), 1–149.

Buckland, W. (1823). *Reliquiae Diluvianiae*. London.

Burnaby, T. (1966). Growth-invariant discriminant functions and generalized distances. *Biometrics*, 22(1), 96–110.

Bush, A., Powell, M., Arnold, W., Bert, T., Daley, G. (2002). Time-averaging, evolution, and morphologic variation. *Paleobiology*, 28(1), 9.

Calvet, M. (2004). Quaternary Glaciation of the Pyrenees. In: J. Ehlers, P. Gibbard (eds.), *Quaternary Glaciations – Extent and Chronology*, 119–128. Elsevier.

Candy, I. (2009). Climates and landscapes of the earliest humans in Northern Europe: environments of Britain during the early Middle Pleistocene. In: S.P.E. Blockley, C.S. Lane, A. Oh, P. Ditchfield, A. Bogaard, P.G. Langdon, D.C. Schreve, D.S.G. Thomas, R.M. Bailey (eds.), *Quaternary abstracts: The human dimension in rapid environmental change*, Annual discussion meeting. Quaternary research Association, QRA, University of Oxford.

Cardini, A., Elton, S. (2007). Sample size and sampling error in geometric morphometric studies of size and shape. *Zoomorphology*, 126(2), 121–134.

Caumul, R., Polly, P.D. (2005). Phylogenetic and environmental components of morphological variation: Skull, mandible, and molar shape in marmots (*Marmota*, Rodentia). *Evolution*, 59(11), 2460–2472.

Centeno-Cuadros, A., Delibes, M., Godoy, J. (2009). Phylogeography of southern water vole (*Arvicola sapidus*): evidence for refugia within the Iberian glacial refugium? *Molecular Ecology*, 18(17), 3652–3667.

Chaline, J. (1972). *Les rongeurs du Pléistocène moyen et supéieur de France; Cahiers de paléontologie*. Centre national de la recherche scientifique, Paris.

Chaline, J. (1987). Arvicolid data (Arvicolidae, Rodentia) and evolutionary concepts. *Evolutionary Biology*, 21, 237–310.

Chaline, J., Laurin, B. (1986). Phyletic gradualism in a European Plio-Pleistocene *Mimomys* lineage (Arvicolidae, Rodentia). *Paleobiology*, 12(2), 203–216.

Chaline, J., Laurin, B., Brunet-Lecomte, P., Viriot, L. (1993). Morphological trends and rates of evolution in arvicolids (Arvicolidae, Rodentia): towards a punctuated equilibria model. *Quaternary International*, 19, 27–39.

Chaline, J., Brunet-Lecomte, P., Montuire, S., Viriot, L., Courant, F. (1999). Anatomy of the arvicoline radiation (Rodentia): palaeogeographical, palaeoecological history and evolutionary data. *Annales Zoologica Fennici*, 36, 239–267.

Chaline, J., Graf, J.D. (1988). Phylogeny of the Arvicolidae (Rodentia): Biochemical and paleontological evidence. *Journal of Mammalogy*, 69(1), 22–33.

Charles, R. (1998). The faunal assemblage from the Trou du Frontal, Furfooz. In: R. Makjanić (ed.), *Late Magdelanian Chronology and Faunal Exploitation in the North-Western Ardennes*, BAR International Series 737. Archaeopress, Oxford.

Clark, C., Gibbard, P., Rose, J. (2004). Pleistocene glacial limits in England, Scotland and Wales. In: J. Ehlers, P. Gibbard (eds.), *Quaternary Glaciations – Extent and Chronology*. Elsevier.

Claude, J. (2008). *Morphometrics with R*. Springer, New York.

Collis, J. (ed.) (1983). *Wigber Low, Derbyshire: a Bronze Age Anglian Burial Site in the White Peak*. Department of Prehistory and Archaeology, University of Sheffield.

Comte de Lacepède (1799). *Discours de l'ouverture et de clôture du cours d'Histoire Naturelle donné dans le Muséum National d'Histoire Naturelle : l'an VII de la République, et Tableaux méthodiques des Mammifères et des Oiseaux*. Paris, An VII, I edn.

Conard, N., Moreau, L. (2004). Current research on the Gravettian of the Swabian Jura. *Mitteilungen der Gesellschaft für Urgeschichte*, 13, 29–59.

Conroy, C., Cook, J. (1999). Mtdna evidence for repeated pulses of speciation within arvicoline and murid rodents. *Journal of Mammalian Evolution*, 6, 221–245.

Cook, J. (1999). Description and analysis of the flint finds from Westbury Cave. In: P. Andrews, J. Cook, A. Currant, C.B. Stringer (eds.), *Westbury Cave: The Natural History Museum Excavations 1976-1984*, 211–274. Western Academic & Specialist Press Limited, Bristol.

Cook, J., Welté, A.C. (1995). La Grotte du Courbet (Tarn): sa contribution dans l'histoire de l'homme fossile et de l'art paléolithique. *Bulletin de la Société Préhistorique Ariége-Pyrénées*, L, 85–96.

Corbet, G.B. (1978). *The Mammals of the Palaearctic Region: a taxonomic review*. British Museum (Natural History).

Corbet, G.B., Cummins, J., Hedges, S.R., Krzanows, W. (1970). Taxonomic status of British water voles, genus *Arvicola*. *Journal of Zoology*, 161, 301–316.

Corbet, G.B., Harris, S. (1991). *The handbook of British mammals*. Blackwell Scientific Publications, Oxford, 3 edn.

Corruccini, R.S. (1977). Correlation properties of morphometric ratios. *Systematic Zoology*, 26, 211–214.

Croizet, J.P., Jobert, A.C.G. (1828). *Reserches sur les ossements fossiles du Departement du Puy-de-Dome*. Paris.

Cubo, J., Ventura, J., Casinos, A. (2006). A heterochronic interpretation of the origin of digging adaptations in the northern water vole, *Arvicola terrestris* (Rodentia : Arvicolidae). *Biological Journal of the Linnean Society*, 87(3), 381–391.

Cuenca-Bescós, G., Agustí, J., Lira, J., Rubio, M.M., , Rofes, J. (In press). A new *Arvicola* species from the Early Pleistocene of Southern Europe. *Acta Palaeontologica Polonica*.

Cunningham, C.W., Omland, K.E., Oakley, T.H. (1998). Reconstructing ancestral character states: a critical reappraisal. *Trends in Ecology and Evolution*, 13, 361–366.

Currant, A.P. (1977). Ightham Fissures. *Newsletter of the Pengelly Cave Research Centre*, Symposium - Natural caves in south-east England(30), 13–15.

Currant, A.P. (1998). Tornewton Cave. In: S. Campbell, C.O. Hunt, J.D. Scourse, D.H. Keen (eds.), *Quaternary of South-West England*, 138–145. Chapman & Hall, London.

Currant, A.P. (1999). A brief review of the Westbury Cave small mammal faunas. In: P. Andrews, J. Cook, A. Currant, C.B. Stringer (eds.), *Westbury Cave: The Natural History Museum Excavations 1976-1984*, 127–138. Western Academic & Specialist Press Limited, Bristol.

Currant, A.P., Jacobi, R.M. (2001). A formal mammalian biostratigraphy for the Late Pleistocene of Britain. *Quaternary Science Reviews*, 20, 1707–1716.

Cuvier, G. (1824). *Reserches sur les ossements fossiles*. Paris.

Cyrek, K., Socha, P., Stefaniak, K., Madeyska, T., Miroslaw-Grabowska, J., Sudol, M., Czyzewski, L. (In Press). Palaeolithic of Biśnik Cave (Southern Poland) within the environmental background. *Quaternary International*, In Press, Corrected Proof.

Darwin, C. (1859). *On the origin of species by means of natural selection, or the preservation of favoured races in the struggles for life*. John Murray, London.

Davies, W., Hedges, R. (2005). Dating the Middle-to-Upper palaeolithic transition: a new chronometric framework. In: L. Kaminská, J. Kozłowski, J. Svoboda (eds.), *Pleistocene environments and archaeology of the Dzerava skala Cave, Lesser Carpathians, Slovakia*, 59–66. Polish Academy of Arts and Sciences, Kraków.

Deffontaine, V., Libois, R., Kotlik, P., Sommer, R., Nieberding, C., Paradis, E., Searle, J.B., Michaux, J.R. (2005). Beyond the mediterranean peninsulas: evidence of central european glacial refugia for a temperate forest mammal species, the bank vole (*Clethrionomys glareolus*). *Molecular Ecology*, 14(6), 1727–1739.

Dodonov, A., Tchepalyga, A., Mihailescu, C., Zhou, L., Markova, A., Trubikhin, V., Simakova, A., Konikov, E. (2000). Last-interglacial records from central asia to the northern black sea shoreline: stratigraphy and correlation. *Geologie en Mijnbouw*, 79(2/3), 303–312.

Dryden, I.L., Mardia, K.V. (1998). *Statistical Shape Analysis*. John Wiley & Sons, Chichester.

Dryden, I.L. (2007). *shapes: Statistical shape analysis*. URL `http://cran.r-project.org/web/packages/shapes/index.html`. Accessed 15 July 2010.

Ehik, G. (1914). A Borsod megyei Peskö-barlang pleistocaen faunaja (Die Pleistozane Fauna der Pesko-Hohle im Komitat Borsod). *Barlangkutatas*, 2(4), 191–199.

Ehlers, J., Gibbard, P. (eds.) (2004). *Quaternary Glaciations – Extent and Chronology*. Elsevier.

Eissmann, L. (2002). Quaternary geology of eastern Germany (Saxony, Saxon-Anhalt, South Brandenburg, Thuringia), type area of the Elsterian and Saalian stages in Europe. *Quaternary Science Reviews*, 21(11), 1275–1346.

Ellerman, J.R. (1940). *The Families and Genera of Living Rodents*, vol. II. Family Muridae. British Museum (Natural History), London.

Escudé, E., Montuire, S., Desclaux, E. (2008a). Variabilitié morphologique de l'espéce *Arvicola cantiana* (Arvicolinae, Rodentia) du Pléstocène moyen au Pléstocène supérieur de France et de Ligurie (Italie). *Quaternaire*, 19(1), 31–41.

Escudé, E., Montuire, S., Desclaux, E., Quere, J.P., Renvoise, E., Jeannet, M. (2008b). Reappraisal of 'chronospecies' and the use of *Arvicola* (Rodentia, Mammalia) for biochronology. *Journal of Archaeological Science*, In Press, Corrected Proof.

Evsikov, V.I., Nazarova, G.G., Potapov, M.A. (1997). Genetic-ecological monitoring of a cyclic population of water voles (*Arvicola terrestris* L.) in the south of Western Siberia. *Genetika*, 33(8), 1133–1143.

Fagan, B.M. (ed.) (1996). *The Oxford Companion to Archaeology*. Oxford University Press, Oxford.

Farris, J.S., Kluge, A., Eckhardt, M. (1970). A numerical approach to phylogenetic systematics. *Systematic Zoology*, 19, 172–189.

Fejfar, O. (1961). Review of Quaternary Vertebrata in Czechoslovakia. *Prace Instytut Geologiczny*, 34, 109–118.

Fejfar, O., Heinrich, W.D. (1981). Zur biostratigraphischen Untergliederung des kontinentalen Quartärs in Europa anhand von Arvicoliden (Rodentia, Mammalia). *Eclogae Geologicae Helvetiae*, 74(3), 997–1006.

Felsenstein, J. (1981a). Evolutionary trees from DNA sequences: a maximum likelihood approach. *Journal of Molecular Evolution*, 17, 368–376.

Felsenstein, J. (1981b). Evolutionary trees from gene frequencies and quantitative characters: finding maximum likelihood estimates. *Evolution*, 35, 1229–1242.

Felsenstein, J. (2002). Quantitative characters, phylogenies and morphometrics. In: N. MacLeod, P.L. Forey (eds.), *Morphology, Shape and Phylogeny*, 27–44. CRC Press, Boca Raton.

Felsenstein, J. (2008). *PHYLIP (Phylogeny Inference Package) version 3.68*. Distributed by the author. Department of Genome Sciences, University of Washington, Seattle.

Frank, C., Rabeder, G. (1997). Hundsheim. In: D. Döppes, G. Rabeder (eds.), *Pliozäne und Pleistozäne Faunen Österreichs*. Österreichischen Akademie der Wissenschaften, Vienna.

Frost, S., Marcus, L., Bookstein, F., Reddy, D., Delson, E. (2003). Cranial allometry, phylogeography, and systematics of large-bodied papionins (Primates: Cercopithecinae) inferred from geometric morphometric analysis of landmark data. *The Anatomical Record Part A: Discoveries in Molecular, Cellular, and Evolutionary Biology*, 275(2), 1048–1072.

Fürsich, F.T. (1993). Fossil concentrations and life and death assemblages. In: D.E.G. Briggs, P.R. Crowther (eds.), *Palaeobiology: a synthesis*, 235–239. Blackwell, Oxford.

Gautier, A., de Heinzelin, J. (eds.) (1980). *La Caverne Marie-Jeanne*. Mémoire N^o 177. Institut Royal des Sciences Naturelles de Belgique.

Gibbard, P.L. (1988). The history of the great northwest European rivers during the past three million years. *Philosophical Transactions of the Royal Society of London*, B318, 559–602.

Gilmour, M., Currant, A.P., Jacobi, R., Stringer, C. (2007). Recent TIMS dating results from British Late Pleistocene vertebrate faunal localities: context and interpretation. *Journal of Quaternary Science*, 22(8), 793–800.

Gingerich, P.D. (1993). Quantification and comparison of evolutionary rates. *American Journal of Science*, 293, 453–478.

Giraudoux, P., Delattre, P., Habert, M., Quere, J.P., Deblay, S., Defaut, R., Duhamel, R., Moissenet, M.F., Salvi, D., Truchetet, D. (1997). Population dynamics of fossorial water vole (*Arvicola terrestris scherman*): a land use and landscape perspective. *Agriculture Ecosystems & Environment*, 66(1), 47–60.

Głazek, J., Lindner, L., Wysoczański-Minkowicz, T. (1976). Interglacial Mindel I/Mindel II in fossil-bearing karst at Kozi Grzbiet in the Holy Cross Mts. *Acta Geologica Polonica*, 26(3), 377–393.

Gleed-Owen, C.P. (1999). The palaeoclimatic and biostratigraphic significance of herpetofaunal remains from the British Quaternary. In: P. Andrews, P. Banham (eds.), *Late Cenozoic Environments and Hominid Evolution: a Tribute to Bill Bishop*, 201–215. The Geological Society, London.

Gonzalez-Samperiz, P., Valero-Garces, B., Carrion, J., Pena-Monne, J., Garcia-Ruiz, J., Marti-Bono, C. (2005). Glacial and Lateglacial vegetation in northeastern Spain: New data and a review. *Quaternary International*, 140, 4–20.

Good, P. (2000). *Permutation tests: a practical guide to resampling methods for testing hypotheses*. Springer, New York.

Goodall, C.R. (1991). Procrustes methods in the statistical analysis of shape (with discussion). *Journal of the Royal Statistical Society, Series B*, 53, 285–339.

Gould, S.J. (1977). *Ontogeny and Phylogeny*. Harvard University Press, Cambridge, Massachusetts.

Gray, J.E. (1821). On the natural arrangement of Vertebrose Animals. *London Medical Repository*, 15, 229–239.

Green, R.E., Krause, J., Ptak, S.E., Briggs, A.W., Ronan, M.T., Simons, J.F., Du, L., Egholm, M., Rothberg, J.M., Paunović, M., Pääbo, S. (2006). Analysis of one million base pairs of Neanderthal DNA. *Nature*, 444, 330–336.

Griffiths, H.I., Kryštufek, B., Reed, J.M. (eds.) (2004). *Balkan biodiversity : pattern and process in the European hotspot*. Kluwer Academic, Dordrecht.

Gromov, I.M., Polyakov, I.Y. (1992). Voles (Microtinae).

Gupta, S., Collier, J.S., Palmer-Felgate, A., Potter, G. (2007). Catastrophic flooding origin of shelf valley systems in the English Channel. *Nature*, 448, 342–345.

Hajnalová, M., Hajnalová, E. (2005). The plant macro-remains: the environment and plant foods exploited by the hunter-gathers [*sic*]. In: L. Kaminská, J. Kozłowski, J. Svoboda (eds.), *Pleistocene environments and archaeology of the Dzerava skala Cave, Lesser Carpathians, Slovakia*, 91–135. Polish Academy of Arts and Sciences, Kraków.

Hamblin, R.J.O., Moorlock, B.S.P., Rose, J. (2000). A new glacial stratigraphy for Eastern England. *Quaternary Newsletter*, (92), 35–43.

Heim de Balsac, H., Guislain, R. (1955). Evolution et spéciation des campagnols du genre *Arvicola* en territoire Français. *Mammalia*, 19, 367–390.

Heinrich, W.D. (1975a). Lithologische Kennzeichnung der Tierbautensedimente von Pisede bei Malchin. *Wissenschaftliche Zeitschrift der Humboldt-Universität zu Berlin, Mathematisch-Naturwissenschaftliche Reihe*, 24(5), 677–687.

Heinrich, W.D. (1975b). Morpholographische und strukturelle Kennzeichnung des fossilen Tierbautensystems von Pisede bei Malchin. *Wissenschaftliche Zeitschrift der Humboldt-Universität zu Berlin, Mathematisch-Naturwissenschaftliche Reihe*, 24(5), 647–664.

Heinrich, W.D. (1978). Zur evolution und biometrischen erfassung eines evolutionstrends bei *Arvicola* (Rodentia, Mammalia) aus dem Pleistozän Thüringens. *Säugetierk. Inform.*, 2, 3–21.

Heinrich, W.D. (1982). Zur Evolution und Biostratigraphie von *Arvicola* (Rodentia, Mammalia) im Pleistozán Europas. *Zeitschrift für Geologische Wissenschaften*, 10, 683–735.

Heinrich, W.D. (1987). Neue Ergebnisse zur Evolution und Biostratigraphie von *Arvicola* (Rodentia, Mammalia) in Quartär Europas. *Zeitschrift fur Geologische Wissenschaften*, 15(3), 389–406.

Heinrich, W.D. (1990a). Review of fossil arvicolids (Mammalia, Rodentia) of the Pliocene and Quaternary in the German Democratic Republic. In: O. Fejfar, W.D. Heinrich (eds.), *International Symposium on Evolution, Phylogeny and Biostratigraphy of Arvicolids*, 183–200. Geological Survey, Praha.

Heinrich, W.D. (1990b). Some aspects of evolution and biostratigraphy of arvicola (Mammalia, Rodentia) in the central European Pleistocene. In: O. Fejfar, W.D. Heinrich (eds.), *International Symposium on Evolution, Phylogeny and Biostratigraphy of Arvicolids*, 165–180. Geological Survey, Praha.

Heinrich, W.D., Jäger, K. (1975). ^{14}C-Datierungen zur Chronologie des fossilen Tierbautensystems von Pisede bei Malchin. *Wissenschaftliche Zeitschrift der Humboldt-Universität zu Berlin, Mathematisch-Naturwissenschaftliche Reihe*, 24(5), 689–691.

Heinrich, W.D., Jánossy, D. (1978). Fossile Säugetierreste aus einer jungpleistozänen Deckschichtenfolge über dem interglazialen Travertin von Burgtonna in Thüringen. In: H.D. Kahlke (ed.), *Das Pleistozän von Burgtonna in Thüringen*, vol. 3, 231–254. Akademie Verlag, Berlin.

Heinrich, W.D., Maul, L.C. (1983a). Skelettreste von Nagetieren (Rodentia, Mammalia) aus dem fossilen Tierbautensystem von Pisede bei Malchin. Teil 1. Taxonomische und biometrische Kenneichnung des Fundgutes. *Wissenschaftliche Zeitschrift der Humboldt-Universität zu Berlin, Mathematisch-Naturwissenschaftliche Reihe*, 32(6), 729–743.

Heinrich, W.D., Maul, L.C. (1983b). Skelettreste von Nagetieren (Rodentia, Mammalia) aus dem fossilen Tierbautensystem von Pisede bei Malchin. Teil 2. Paläoökologische und faunengeschichtliche Auswertung des Fundgutes. *Wissenschaftliche Zeitschrift der Humboldt-Universität zu Berlin, Mathematisch-Naturwissenschaftliche Reihe*, 32(6), 745–752.

Heller, F. (1933). Die Wühlmäuse der Mosbacher Sande. *Notizblatt des Vereins für Erdkunde und der Hessischen Geologischen Landesanstalt*, 1931/1932, 108–116.

Heller, F. (1969). Eine Kleinsaügerfauna aus den Mittleren Mosbacher sander bei Beibrich, Weisbaden. *Mz. Naturwiss. Archiw.*, 8, 25–55.

Hérail, G., Hubschman, J., Jalut, G. (1986). Quaternary glaciation in the French Pyrenees. *Quaternary Science Reviews*, 5, 397–402.

Hewer, T.F. (1924). First report on excavations in the Wye Valley. *Proceedings of the Speleological Society*, 2, 147–153.

Hewitt, G.M. (1999). Post-glacial recolonization of European biota. *Biological Journal of the Linnean Society*, 68, 87–112.

Hibbard, C.W. (1948). Techniques for collecting microvertebrate fossils. *Bulletin of the Geological Society of America*, 59, 1330.

Higham, T.F.G., Bronk Ramsey, C., Karavanic, I., Smith, F., Trinkaus, E. (2006). Revised direct radiocarbon dating of the Vindija G(1) upper Paleolithic Neandertals. *Proceedings of the National Academy of Sciences of the United States of America*, 103(3), 553–557.

Hillebrand, E. (1914). Ergebnisse meiner Höhlenforschungen im Jahre 1913. *Barlangkutatás*, 2, 147–153.

Hillson, S. (1986). *Teeth*. Cambridge University Press, Cambridge.

Hinton, M.A.C. (1910). A preliminary account of the British voles and lemmings; with some remarks on the Pleistocene climate and geography. *Proceedings of the Geologists' Association*, 21, 489–507.

Hinton, M.A.C. (1911). The British fossil shrews. *Geological Magazine*, 5(8), 529–539.

Hinton, M.A.C. (1924). Preliminary note upon the mammalian remains from Merlin's Cave. *Proceedings of the Speleological Society*, 2, 156–158.

Hinton, M.A.C. (1926). *Monograph of the voles and lemmings (Microtinae) living and extinct*. British Museum (Natural History), London.

Hinton, M.A.C., White, G. (1902). Note on the occurrence of *Microtus intermedius* in the Pleistocene deposits of the Thames Valley . *Proceedings of the Geologists' Association*, 17, 414–415.

Hofreiter, M., Serre, D., Rohland, N., Rabeder, G., Nagel, D., Conard, N., Munzel, S., Pääbo, S. (2004). Lack of phylogeography in European mammals before the last glaciation. *Proceedings of the National Academy of Sciences*, 101(35), 12963–12968.

Holman, J.A., Stuart, A.J., Clayden, J.D. (1990). A Middle Pleistocene herpetofauna from Cudmore Grove, Essex, England, and its palaeogeographic and palaeoclimatic implications. *Journal of Vertebrate Palaeontology*, 10, 86–94.

Horáček, I. (2005). Small vertebrates in the Weichselian series: list of the samples and a brief summary. In: L. Kaminská, J. Kozłowski, J. Svoboda (eds.), *Pleistocene environments and archaeology of the Dzerava skala Cave, Lesser Carpathians, Slovakia*, 157–167. Polish Academy of Arts and Sciences, Kraków.

Hulbert, R.C. (1993). Taxonomic evolution in North American Neogene horses (subfamily Equinae): the rise an fall of an adaptive radiation. *Palaeobiology*, 19, 216–234.

Hunt, G. (2004). Phenotypic variation in fossil samples: modeling the consequences of time-averaging. *Paleobiology*, 30(3), 426–443.

Hunt, G. (2006). Fitting and comparing models of phyletic evolution: random walks and beyond. *Paleobiology*, 32(4), 578–601.

Hunt, J.W., Dean, A.P., Webster, R.E., Johnson, G.N., Ennos, A.R. (2008). A novel mechanism by which silica defends grasses against herbivory. *Annals of Botany*, 102(4), 653–656.

International Commission on Zoological Nomenclature (1999). *International Code of Zoological Nomenclature*. The International Trust for Zoological Nomenclature. URL http://www.nhm.ac.uk/hosted-sites/iczn/code/. Accessed 2 February 2011.

Iossifova, Y.I., Krasnenkov, R.V. (eds.) (1994). *The Lower-Middle Pleistocene of the Upper Don basin - Guidebook for Excursion*. The Committee of the Russian Federation on Geology and Subsurface Usage. Central Region's Geological Center State Enterprise "Geosynthes", Moscow.

Jaarola, M., Searle, J.B. (2002). Phylogeography of field voles (*Microtus agrestis*) in Eurasia inferred from mitochondrial DNA sequences. *Molecular Ecology*, 11(12), 2613–2621.

Jacobi, R.M., Higham, T.F.G. (2009). The early Lateglacial re-colonization of Britain: new radiocarbon evidence from Gough's Cave, southwest England. *Quaternary Science Reviews*, 28, 1895–1913.

Jacobshagen, E. (1963). Die Faunen und ihre Bindung an Klima und Umwelt. In: E. Jacobshagen, R. Huckriede, V. Jacobshagen (eds.), *Eine Faunenfolge aus dem jungpleistozänenn Löß bei Bad Wildungen*, vol. 44, 7–86.

Jalut, G., Marti, J.M., Fontugne, M., Delibrias, G., Vilaplana, J.M., Julia, R. (1992). Glacial to interglacial vegetation changes in the northern and southern Pyrénées: Deglaciation, vegetation cover and chronology. *Quaternary Science Reviews*, 11(4), 449–480.

Jánossy, D. (1986). *Pleistocene vertebrate faunas of Hungary*. Developments in Palaeontology and Stratigraphy 8. Elsevier Academic Press, Amsterdam.

Jefferies, D.J. (2003a). The aquatic and fossorial forms of the water vole, their history, evolution, morphology and ecology. In: D.J. Jefferies (ed.), *The water vole and mink survey of Britain 1996-1998 with a history of the long term changes in the status of both species and their causes*, 14–21. The Vincent Wildlife Trust, Ledbury, UK.

Jefferies, D.J. (2003b). The changes in the population of the water vole in Britain, its size and constitution since the last ice age. In: D.J. Jefferies (ed.), *The water vole and mink survey of Britain 1996-1998 with a history of the long term changes in the status of both species and their causes*, 14–21. The Vincent Wildlife Trust, Ledbury, UK.

Jernvall, J., Keranen, S.V.E., Thesleff, I. (2000). Evolutionary modification of development in mammalian teeth: Quantifying gene expression patterns and topography. *Proceedings of the National Academy of Sciences*, 97(26), 14444–14448.

Kaagan, L.M. (2000). *The horse in Late Pleistocene and Holocene Britain*. Ph.D. thesis, University College, London.

Kahlke, H.D. (1978). Das Pleistozän von Burgtonna in Thüringen.

Kaminská, L., Kozłowski, J., Svoboda, J. (eds.) (2005). *Pleistocene environments and archaeology of the Dzerava skala Cave, Lesser Carpathians, Slovakia*. Polish Academy of Arts and Sciences, Kraków.

Kaminská, L., Kozłowski, J., Svoboda, J. (2005). Sequence of the Palaeolithic occupations. In: L. Kaminská, J. Kozłowski, J. Svoboda (eds.), *Pleistocene environments and archaeology of the Dzerava skala Cave, Lesser Carpathians, Slovakia*, 7–58. Polish Academy of Arts and Sciences, Kraków.

Kazantseva, N.E., Tesakov, A.S. (1998). Evolution of Plio-Pleistocene voles with the special reference to demographic features of fossil assemblages. In: T.v. Kolfschoten, P.L. Gibbard (eds.), *The Dawn of the Quaternary - Proceedings of the SEQS-EuroMam symposium 1996*, TNO Nr60, 555–564. Mededelingen Nederlands Institut voor Toegepste Geowetenschappen TNO.

Kendall, D.G. (1977). The diffusion of shape. *Advances in Applied Probability*, 9, 428–430.

Khotinskiy, N.A. (1984). Holocene vegetation history. In: A.A. Velichko, H.E. Wright Jr, C.W. Barnosky (eds.), *Late Quaternary Environments of the Soviet Union*, 179–200. Longman, London.

Kimura, M. (1980). A simple method for estimating evolutionary rates of base substitutions through comparative studies of nucleotide sequences. *Journal of Molecular Evolution*, 16, 111–120.

Klingenberg, C.P. (1998). Heterochrony and allometry: the analysis of evolutionary change in ontogeny. *Biological Reviews*, 73(01), 79–123.

Klingenberg, C.P. (2008). *MorphoJ version 1.02d*. Faculty of Life Sciences, University of Manchester, Manchester, UK. URL http://www.flywings.org.uk/MorphoJ_page.htm. Accessed 08 August 2010.

Koenigswald, W.v. (1970). Mittelpleistozäne Kleinsäugerfauna aus der Spaltenfüllung Petersbuch bei Eichstätt. *Mitteilungen der Bayerischen Staatssammlung für Paläontologie und Historische Geologie*, 10, 407–432.

Koenigswald, W.v. (1973). Veränderungen in der Kleinsäugerfauna von Mitteleuropa zwischen Cromer und Eem (Pleistocän). *Eiszeitalter und Gegenwart*, 23-24, 159–167.

Koenigswald, W.v. (1977). *Mimomys* cf. *reidi* aus der villafranchischen Spaltenfüllung Schambach bei Treuchtlingen. *Mitt. bayer. Staatssamml. Paläont. Hist. Geol.*, 17, 197–212.

Koenigswald, W.v. (1978). Die Säugetierfauna des Mittel-Würms aus der Kemathenhöhle im Altmühltal (Bayern). *Mitteilungen Bayerischen Staatssammlung für Paläontologie und historische Geologie*, 18, 117–130.

Koenigswald, W.v. (1980). Schmelzstruktur und morphologie in den molaren der Arvicolidae (Rodentia). *Abhandlungen der Senckenbergischen Naturforschenden Gesellschaft*, 539, 1–129.

Koenigswald, W.v. (1982a). Enamel structure in molars of Arvicolidae (Rodentia) a key to functional morphology and phylogeny. In: B. Kurten (ed.), *Teeth: form, function and evolution*, 109–122. Columbia University Press, New York.

Koenigswald, W.v. (1982b). Zum Verstädnis der Morphologie der Wühlmausmolaren. *Zeitschrift für Geologische Wissenschaften*, 10(7), 951–962.

Koenigswald, W.v. (1985). Die Kleinsäugerfauna aus der Allactaga-Fauna von der Villa Seckendorff in Stuttgart-Bad Cannstatt aus dem Frühen letzen Glazial. *Stuttgarter Beiträge zur Naturkunde*, B 110, 1–40.

Koenigswald, W.v. (1993). Heterochronies in morphology and schmelzmuster of hypsodont molars in the Muroidea (Rodentia). *Quaternary International*, 19, 57–61.

Koenigswald, W.v., Heinrich, W.D. (1999). Mittelpleistozane saugetierfaunen aus mitteleuropa - der versuch einer biostratigraphischen zuordnung. *Kaupia*, 9(53-112).

Koenigswald, W.v., Kolfschoten, T.v. (1996). The *Mimomys-Arvicola* boundary and the enamel thickness quotient (SDQ) of *Arvicola* as stratigraphic markers in the Middle Pleistocene. In: A. Turner (ed.), *The early Middle Pleistocene in Europe*, 211–225. Balkema, Rotterdam.

Koenigswald, W.v., Tobien, H. (1987). Bemerkungen zur Altersstellung der pleistozänen Mosbach-Sande bei Wiesbaden. *Geologisches Jahrbuch Hessen*, 115, 227–237.

Kolfschoten, T.v. (1988). *The evolution of the mammal fauna of the Netherlands and the Middle Rhine area (Western Germany) during the late Middle Pleistocene*. Ph.D. thesis, University of Utrecht.

Kolfschoten, T.v. (1990). The evolution of the mammal fauna of the Netherlands and the Middle Rhine area (Western Germany) during the late Middle Pleistocene. *Mededelingen Rijks Geologische Dienst*, 43(3), 1–69.

Kolfschoten, T.v. (1992). Aspects of the migration of mammals to northwestern Europe during the Pleistocene, in particular the reimmigration of *Arvicola terrestris*. *Courier Forschungsinstitut Senckenberg*, 153, 213–220.

Kolfschoten, T.v. (1993a). Die Vertebraten des Interglazials von Schöningen 12 B. *Ethnographisch-archaologische Zeitschrift*, 34(4), 623–628.

Kolfschoten, T.v. (1993b). On the origin of the Middle Pleistocene larger voles. *Quaternary International*, 19, 47–50.

Kolfschoten, T.v., Roth, G. (1995). Die mittel- und spätpleistozänen Mollusken und Kleinsäuger von Schlackenkegeln der Osteifel. *Jahrbuch Römisch-Germanisches Zentralmuseum*, 40(27-74).

Kolfschoten, T.v., Turner, E. (1996). Early Middle Pleistocene mammalian faunas from Kärlich and Miesenheim I and their biostratigraphical implications. In: A. Turner (ed.), *The early Middle Pleistocene in Europe*, 227–253. Balkema, Rotterdam.

Kordos, L. (1994). Revised Biostratigraphy of the Early Man Site at Vértessölös, Hungary. *Courier Forschungsinstitut Senckenberg*, 171, 225–236.

Kordos, L. (2003). Stratigraphy of the Middle Pleistocene "Buda Culture" of Castle Hill, Budapest (Hungary). *Praehistoria*, 4-5, 9–32.

Kormos, T. (1937). Revision der Kleinsäger von Hundsheim. *Földtani Közlöni*, 67, 157–171.

Kotlik, P., Deffontaine, V., Mascheretti, S., Zima, J., Michaux, J.R., Searle, J.B. (2006). A northern glacial refugium for bank voles (*Clethrionomys glareolus*). *Proceedings of the National Academy of Sciences*, 103(40), 14860–14864.

Kowalski, K. (2001). *Pleistocene rodents of Europe.* Folia Quaternaria. Polska Akademia.

Kozak, K.H., Graham, C.H., Wiens, J.J. (2008). Integrating GIS-based environmental data into evolutionary biology. *Trends in Ecology & Evolution*, 23(3), 141–148.

Krasnenkov, R.V., Iossifova, Y.I., Shuleshkina, Y.A. (1981). A Lower Pleistocene reference section on the river Ilovay near the town of Michurinsk. In: *Novye donnye po stratigrafii verkhnego pliotsena i pleistotsena tsentral'nykh raionov Evropeiskoi chasti SSSR (New data on the stratigraphy and palaeogeography of the Upper Pliocene and Pleistocene of the central region of the European USSR)*, 14–31. INQUA.

Kratochvíl, J. (1980). The phylogeny and ontogeny in *Arvicola terrestris* (Rodentia, Arvicolidae). *Folia Zoologica*, 29(3), 209–224.

Kratochvíl, J. (1981). *Arvicola cantiana* vit-elle encore. *Folia Zoologica*, 30(4), 289–300.

Kratochvíl, J. (1983a). The effect of altitude on some taxonomical criteria of the Asian population group of *Arvicola terrestris*. *Acta Scientiarum Naturalium-Academiae Scientiarum Bohemoslovacae Brno.*, 24–40.

Kratochvíl, J. (1983b). Variability of some criteria in *Arvicola terrestris* (Arvicolidae, Rodentia). *Acta Scientiarum Naturalium, Academiae Scientarum Bohemoslovacae (Brno)*, 17, 1–40.

Kretzoi, M. (1965). Die Nager und Lagomorphen von Voigstedt in Thüringen und ihre chronologische Aussage. *Paläontologische Abhandlungen. Abteilung A - Paläozoologie*, 2, 585–661.

Kretzoi, M. (1969). Skizze einer Arvicoliden-Phylogenie-Stand 1969. *Vertebrata Hungarica*, 11(1-2), 155–193.

Kretzoi, M. (1990). History of research of fossil arvicolids. In: O. Fejfar, W.D. Heinrich (eds.), *International Symposium on Evolution, Phylogeny and Biostratigraphy of Arvicolids*, 305–309. Geological Survey, Praha.

Krolopp, E., Schweitzer, F., Scheuer, G., Denes, G., Kordos, L., Skoflek, I., Jánossy, D. (1976). Quaternary formations of Castle Hill in Buda. *Földtani Közlöni*, 106(3), 193–228.

Lawing, A.M., Polly, P.D. (2010). Geometric morphometrics: recent applications to the study of evolution and development. *Journal of Zoology*, 280(1), 1–7.

Lindner, L., Gozhik, P., Marciniak, B., Marks, L., Yelovicheva, Y. (2004). Main climatic changes in the quaternary of Poland, Belarus and Ukraine. *Geological Quarterly*, 48(2), 97–114.

Linnæus, C. (1758). *Systema Naturae*. Stockholm, 10 edn.

Linnæus, C. (1788). *Systema Naturae*. Stockholm, 13 edn.

Lisiecki, L.E., Raymo, M.E. (2005). Pliocene-Pleistocene stack of globally distributed benthic stable oxygen isotope records. URL http://doi.pangaea.de/10.1594/PANGAEA.704257. Accessed August 20, 2010.

Lister, A.M. (1992). Mammalian fossils and Quaternary biostratigraphy. *Quaternary Science Reviews*, 11(3), 329–344.

Lister, A.M. (2004). The impact of quaternary ice ages on mammalian evolution. *Proceedings of the Royal Society B: Biological Sciences*, 359, 221–241.

MacLeod, N. (2002). Phylogenetic signals and morphometric data. In: N. MacLeod, P.L. Forey (eds.), *Morphology, Shape and Phylogeny*, 100–138. CRC Press, Boca Raton.

Maltby, M. (1983). Animal bones. In: J. Collis (ed.), *Wigber Low, Derbyshire: a Bronze Age Anglian Burial Site in the White Peak*, chap. Environment and Subsistence, 47–51. Department of Prehistory and Archaeology, University of Sheffield.

Marcolini, F. (2006). Fourier Analysis Applied to *Mimomys* (Arvicolidae, Rodentia, Mammalia) First Lower Molars – Biochronological Implication. *Mathematical Geology*, 38(6), 667–678.

Marcus, L.F. (1990). Traditional morphometrics. In: F.J. Rohlf, F.L. Bookstein (eds.), *Proceedings of the Michigan Morphometrics Workshop*, Special publication no. 2, 77–122. University of Michigan Museum of Zoology, Ann Arbour, Michigan.

Markova, A.K. (1982). *Pleistocene rodents of the Russian Plain (their paleogeographic and stratigraphic implications).* Nauka, Moscow.

Markova, A.K. (1990). Pleistocene microtheria of the European part of the USSR. In: O. Fejfar, W.D. Heinrich (eds.), *International Symposium on Evolution, Phylogeny and Biostratigraphy of Arvicolids*, 313–338. Geological Survey, Praha.

Markova, A.K. (1998). Pleistocene rodents of the Central and Southern Russian Plain. In: J. Saunders, B. Styles, F. Baryshnikov Gennady (eds.), *Quaternary Paleozoology in the Northern Hemisphere*, vol. XXVI of *Illinois State Museum Scientific papers*, 119–143. Illinois State Museum.

Markova, A.K. (2000). The Mikulino (= Eemian) mammal faunas of the Russian Plain and Crimea. *Geologie en Mijnbouw*, 79(2-3), 293–301.

Markova, A.K. (2006). Likhvin Interglacial small mammal faunas of Eastern Europe. *Quaternary International*, 149(1), 67–79.

Markova, A.K. (2007). Pleistocene mammal faunas of Eastern Europe. *Quaternary International*, 160(1), 100–111.

Martin, R.A. (1987). Notes on the classifications and evolution of some North American fossil *Microtus* (Mammalia, Rodentia). *Journal of Vertebrate Palaeontology*, 7, 270–283.

Martin, R.A. (1993). Patterns of variation and speciation in Quaternary rodents. In: R.A. Martin, A.D. Barnosky (eds.), *Morphological change in Quaternary mammals of North America*, 227–391. Cambridge University Press.

Martin, Y., Gerlach, G., Schlotterer, C., Meyer, A. (2000). Molecular phylogeny of european muroid rodents based on complete cytochrome b sequences. *Molecular Phylogenetics and Evolution*, 16(1), 37–47.

Martinson, D.G., Pisias, N.G., Hays, J.D., Imbrie, J., Moore, T.C., Shackleton, N.J. (1987). Age dating and the orbital theory of the ice ages: Development of a high-resolution 0 to 300,000-year chronostratigraphy. *Quaternary Research*, 27(1), 1–29.

Masini, F., Maul, L., Abbazzi, L., Petruso, D. (2003). Inpedendent *Arvicola* lineages in Italy and Central Europe? In: M. Macholan, J. Bryja, J. Zima (eds.),

Fourth European Congress of Mammalogy—July 27–August 1, Brno, program and abstracts volume, 164.

Massey, F.P., Ennos, A.R., Hartley, S.E. (2007). Grasses and the resource availability hypothesis: the importance of silica-based defences. *Journal of Ecology*, 95(3), 414–424.

Matoshko, A. (2004). Pleistocene glaciations of the Ukraine. In: J. Ehlers, P. Gibbard (eds.), *Quaternary Glaciations – Extent and Chronology*, 431–439. Elsevier.

Matoshko, A., Gozhik, P., Danukalova, G. (2004). Key late Cenozoic fluvial archives of Eastern Europe: the Dniester, Dnieper, Don and Volga. *Proceedings of the Geologists Association*, 115, 141–173.

Matthey, R. (1955). Nouveaux documents sur les chromosomes des Muridae. Problèmes de cytologie comparée et de taxonomie chez les Microtinae. *Revue Suisse de Zoologie*, 62, 163–206.

Matthey, R. (1957). Cytologie comparée systématique et phylogenie des microtinae (rodentia-muridae). *Revue Suisse de Zoologie*, 64, 39.

Matthey, R. (1958). Les chromosomes des mammifères euthériens. Liste critique et essai sur l'évolution chromosomique. *Archiv der Julius Klaus-Stiftung fur Vererbungsforschung, Sozialanthropologie und Rassenhygiene*, 33, 253.

Mauch Lenardić, J. (2005). *Metrijska I Morfotipska Analiza Zuba Gornjopleistocenskih*. Ph.D. thesis, Sveučilište U Zagrebu, Zagreb.

Mauch Lenardić, J. (2007). Comparative metric analysis of Late Pleistocene *Microtus* ex gr. *arvalis/agrestis* (Arvicolidae, Rodentia, Mammalia) teeth from some Croatian localities. *Courier Forschungsinstitut Senckenberg*, 259, 149–154.

Maul, L.C. (1994). Erster Nachweis von *Hystrix* in der Pleisrozän-Fundstelle Burgtonna (Thüringen, Mitteldeutschland). *Säugetierkundliche Informationen*, 3(18), 673–682.

Maul, L.C., Markova, A.K. (2007). Similarity and regional differences in Quaternary arvicolid evolution in Central and Eastern Europe. *Quaternary International*, 160, 81–99.

Maul, L.C., Masini, F., Abbazzi, L., Turner, A. (1998a). Geochronometric application of evolutionary trends in the dentition of fossil arvicolidae. In: T.v. Kolfschoten, P.L. Gibbard (eds.), *The Dawn of the Quaternary - Proceedings of the SEQS-EuroMam symposium 1996*, no. 60 in TNO Nr, 565–572. Mededelingen Nederlands Institut voor Toegepste Geowetenschappen TNO.

Maul, L.C., Masini, F., Abbazzi, L., Turner, A. (1998b). The use of different morphometric data for absolute age calibration of some South- and Middle-European arvicolid populations. *Palaeontographica Italica*, 85, 111–151.

Maul, L.C., Parfitt, S.A. (2010). Micromammals from the 1995 Mammoth Excavation at West Runton, Norfolk, UK: Morphometric data, biostratigraphy and taxonomic reappraisal. *Quaternary International*, 228(1–2), 91–115.

Maul, L.C., Heinrich, W.D., Parfitt, S.A., Paunescu, A.C. (2007). Comment on the correlation between magnetostratigraphy and the evolution of *Microtus* (Arvicolidae, Rodentia, Mammalia) during the Early and early Middle Pleistocene. *Courier Forschungsinstitut Senckenberg*, 259, 243–263.

Maul, L.C., Rekovets, L.I., Heinrich, W.D., Keller, T., Storch, G. (2000). *Arvicola mosbachensis* (SCHMIDTGEN) of Mosbach 2: a basic sample for the early evolution of the genus and a reference for further biostratigraphical studies. *Senckenbergiana lethaea*, 80(1), 129–147.

Mayr, E. (1963). *Animal species and evolution*. Oxford University Press.

Mellars, P. (2004). Neanderthals and the modern human colonization of europe. *Nature*, 432, 461–465.

Meyrick, R.A., Maul, L.C. (2002). Stratigraphy and biostratigraphy of the Eemian deposits of Burgtonna. In: R.A. Meyrick, D.C. Schreve (eds.), *The Quaternary of Central Germany (Thuringia and surroundings) Field Guide*, 145–162. Quaternary Research Association.

Mihailescu, C., Markova, A.K. (1992). *Palaeogeographical type fauna of the Anthropogene of southern Moldova*. Shtiintsa, Kishinev.

Miller, G.S. (1896). Genera and Subgenera of Voles and Lemmings. *North American Fauna*, 12.

Miller, G.S. (1912). *Catalogue of the Mammals of western Europe (Europe exlusive of Russia)*. British Museum (Natural History).

Mirosław-Grabowska, J. (2002). Geological value of Biśnik Cave sediments (Cracow-Częstochowa Upland). *Acta Geologica Polonica*, 52(1), 97–110.

Mitteroecker, P., Gunz, P., Bookstein, F.L. (2005). Heterochrony and geometric morphometrics: a comparison of cranial growth in *Pan paniscus* and *Pan troglodytes*. *Evolution and Development*, 7(3), 244–258.

Mlíkovský, J. (2009). Middle Pleistocene birds of Hundsheim, Austria. *Journal of the National Museum (Prague)*, 177(7), 69–82.

Monteiro, L.R., Diniz-Filho, J.A.F., dos Reis, S.F., Araujo, E.D. (2002). Geometric estimates of heritability in biological shape. *Evolution*, 56(3), 563–572.

Montgomery, W.I. (1975). On the relationship between sub-fossil and recent British water voles. *Mammal Review*, 5, 23–29.

Mottl, M. (1942). Beiträge zur Sägetierfauna der ungarischen Alt- und Jungpleistozänen Flussterrassen. *Annales Instituti Regii Hungarici Geologici*, 36(2), 1–70.

Münster, G.v. (1833). *Verzeichnis der Versteinerungen etc.* Bayreuth.

Musser, G.G., Carleton, M.D. (1993). Family Muridae. In: D.E. Wilson, M. Reeder D-A (eds.), *Mammal species of the world: A taxonomic and geographic reference*, 501–535. Smithsonian Institution Press, London, 2nd edn.

Nadachowski, A. (1982). *Late Quaternary rodents of Poland with special reference to morphotype dentition analysis of voles.* Panstwowe Wydawnictwo Naukowe, Warsaw.

Nadachowski, A. (1985). Biharian voles Arvicolidae, Rodentia, Mammalia from Kozi Grzbiet (Central Poland). *Acta Zoologica Cracoviensia*, 29(2), 13–28.

Nadachowski, A. (1990). Lower Pleistocene rodents of Poland: faunal succession and biostratigraphy. *Quatärpälaontologie*, 8, 215–223.

Neraudeau, D., Viriot, L., Chaline, J., Laurin, B., Kolfschoten, T.v. (1995). Discontinuity in the Plio-Pleistocene Eurasian Water Vole Lineage. *Palaeontology*, 38, 77–85.

Nowak, R.M., Paradiso, J.L. (1983). *Walker's Mammals of the World*, vol. II. John Hopkins University Press, 4 edn.

Owen, R. (1846). *A History of British Fossil Mammals, and Birds.* London.

Paleoclimate Database of the Quaternary (2001). Übernahme des Datenbestandes der PKDB in das Informationssystem PANGAEA: Schlussbericht ; Laufzeit: 01.07.2000 bis 30.06.2001.

Panteleyev, P.A. (2001). *The water vole : mode of the species.* Nauka Press.

Parfitt, S.A. (1999). Mammalia. In: M.B. Roberts, S.A. Parfitt (eds.), *Boxgrove. A Middle Pleistocene hominid site at Eartham pit, Boxgrove, West Sussex*, vol. Archaeological Report 17, 197–290. English Heritage.

Paunescu, A.C., Maul, L.C., Masini, F. (2004). Comparison of evolutionary patterns of *Arvicola* in Germany, France and Italy. *18th International Senckenberg Conference in Weimar*.

Paunović, M., Jambrešić, G., Brajković, D., Malez, V., Mauch Lenardić, J. (1999). Last Glacial settlement of Croatia: catalogue of fossil sites dated to the OIS 2&3. *Acta Geologica*, 26(2), 27–70.

Pazonyi, P., Kordos, L. (2004). Late Eemian (Late Pleistocene) vertebrate fauna from the Horváti-lik (Uppony, NE Hungary). *Fragmenta Palaeontologica Hungarica*, 22, 107–117.

Penkman, K.E.H., Preece, R.C., Keen, D.H., Maddy, D., Schreve, D.C., Collins, M.J. (2007). Testing the aminostratigraphy of fluvial archives: the evidence from intra-crystalline proteins within freshwater shells. *Quaternary Science Reviews*, 26(22-24), 2958–2969.

Petculescu, A. (2003). New data on the evolution of *Arvicola* (Mammalia, Rodentia) from the karst of Romanian. *Theoretical and Applied Karstology*, 16, 99–103.

Peyrony, D. (1947). La Grotte d'Abzac, a Gorge d'Enfer. *Bulletin de la Société Historique et Archéologique du Périgord*, 74, 167–171.

Piertney, S., Stewart, W., Lambin, X., Telfer, S., Aars, J., Dallas, J. (2005). Phylogeographic structure and postglacial evolutionary history of water voles (*Arvicola terrestris*) in the United Kingdom. *Molecular Ecology*, 14(5), 1435–1444.

Pimentel, R.A., Riggins, R. (1987). The nature of cladistic data. *Cladistics*, 3, 201–209.

Polly, P.D. (1998). Variability in mammalian dentitions: size-related bias in the coefficient of variation. *Biological Journal of the Linnean Society*, 64, 83–99.

Polly, P.D. (2001). On morphological clocks and paleophylogeography: Towards a timescale for *Sorex* hybrid zones. *Genetica*, 112-113, 339–357.

Polly, P.D. (2002). Phylogenetic tests for difference in shape and the importance of divergence times: Eldrege's enigma explored. In: N. MacLeod, P.L. Forey (eds.), *Morphology, Shape and Phylogeny*, 220–246. CRC Press, Boca Raton.

Polly, P.D. (2003). Palaeophylogepgraphy of *Sorex araneus*: molar shape as a morphological marker for fossil shrews. *Mammalia*, 6(2), 233–243.

Polly, P.D. (2004). On the simulation of the evolution of morphological shape: multivariate shape under selection and drift. *Palaeontologia Electronica*, 7(2), 7–28.

Polly, P.D. (2008a). Adaptive zones and the inniped ankle: a 3D quantitative analysis of carnivoran tarsal evolution. In: E. Sargis, M. Dagosto (eds.), *Mammalian Evolutionary Morphology: A Tribute to Frederick S. Szalay*, 167–196. Springer, Dordrecht, The Netherlands.

Polly, P.D. (2008b). Developmental dynamics and G-matrices: Can morphometric spaces be used to model evolution and development? *Evolutionary Biology*, 35, 1–20.

Popova, L. (2004). The micromammal fauna of the Dnieper modern channel alluvium: taphonomic and biostratigraphic implications. *Quaternaire*, 15(1–2), 233–242.

Preece, R.C., Parfitt, S.A. (2000). The Cromer Forest-bed Formation: new thoughts on an old problem. In: S.G. Lewis, C.A. Whiteman, R.C. Preece (eds.), *The Quaternary of Norfolk & Suffolk Field Guide*, 1–28. Quaternary Research Association.

Preece, R.C., Parfitt, S.A. (2008). The Cromer Forest-bed Formation: some recent developments relating to early human occupation and lowland glaciation. In: I. Candy, J. Lee, A. Harrison (eds.), *The Quaternary of northern East Anglia: Field Guide*, 60–83. Quaternary Research Association.

Price, C.R. (2003). *Late Pleistocene and Early Holocene Small Mammals in South West Britain: Environmental and Taphonomic Implications, and their Role in Archaeological Research*. Ph.D. thesis, University of Wales College, Newport.

Provan, J., Bennett, K.D. (2008). Phylogeographic insights into cryptic glacial refugia. *Trends in Ecology & Evolution*, 23(10), 564–571.

R Development Core Team (2008). *R: A Language and Environment for Statistical Computing*. R Foundation for Statistical Computing, Vienna, Austria. URL http://www.R-project.org. Accessed 15 July 2010.

Rabeder, G. (1981). Die Arvicoliden (Rodentia, Mammalia) aus dem Pliozän und dem älteren Pleistozän von Niederösterreich. *Beiträge zur Paläontologie von Österreich*, 8, 1–373.

Rabeder, G. (1972). Die Insectoriven und Chiropteran (Mammalia) aus dem Altpleistozän von Hundsheim (NÖ.). *Annalen des Naturhistorischen Museums in Wien*, 76, 375–474.

Rabenstein, R. (1996). Die Kleinsäugerfauna des Kartsteins. Ein Beitrag zur Rekonstruktion spätpleistozäner Umweltverhältnisse der nördlichen Mittelgebirge. In: M. Baales (ed.), *Umwelt und Jagdökonomie der Ahrensburger Rentierjäger im Mittelgebirge*, vol. Monographien des Römisch-Germanischen Zentralmuseums 38, 137–150. Römisch-Germanischen Zentralmuseums, Mainz & Bonn.

Rackham, O. (1986). *The History of the English Countryside*. Phoenix Press.

Rasmussen, S., Andersen, K., Svensson, A., Steffensen, J., Vinther, B., Clausen, H., Siggaard-Andersen, M., Johnsen, S., Larsen, L., Dahl-Jensen, D., Röthlisberger, R., Fischer, H., Goto-Azuma, K., Hansson, M., Ruth, U. (2006). A new Greenland ice core chronology for the last glacial termination. *Journal of Geophysical Research*, 111, D06102.

Raup, D. (1977). Stochastic models in evolutionary paleontology. In: A. Hallam (ed.), *Patterns of evolution, as illustrated by the fossil record*, 59–78. Elsevier, Amsterdam.

Reichstein, v.H. (1963). Beitrag zur systematischen Gliederung des Genus *Arvicola* Lacépède 1799. *Zeitschrift fuer Zoologische Systematik und Evolutionsforschung*, 1, 155–204.

Reichstein, v.H. (1982a). *Arvicola sapidus* Miller, 1908—Südwesteuropaische Schermaus. In: J. Niethammer, F. Krapp (eds.), *Handbuch der Säugetiere Europas*, vol. 2, 211–216. Akademische Verlagsgesellschaft, Wiesbaden.

Reichstein, v.H. (1982b). *Arvicola terrestris* LINNÆUS, 1758. In: J. Niethammer, F. Krapp (eds.), *Handbuch der Säugetiere Europas*, vol. 2, 158–182. Akademische Verlagsgesellschaft, Wiesbaden.

Reichstein, v.H. (1982c). Familie *Arvicolidae* Gray, 1821 —Wühlmäuse. In: J. Niethammer, F. Krapp (eds.), *Handbuch der Säugetiere Europas*, vol. 2, 51–69. Akademische Verlagsgesellschaft, Wiesbaden.

Reichstein, v.H. (1982d). Gattung *Arvicola* Lacépède, 1799 —Schermäse. In: J. Niethammer, F. Krapp (eds.), *Handbuch der Säugetiere Europas*, vol. 2, 209. Akademische Verlagsgesellschaft, Wiesbaden.

Reille, M., Andrieu, V. (1995). The late Pleistocene and Holocene in the Lourdes Basin, Western Pyrénées, France: new pollen analytical and chronological data. *Vegetation History and Archaeobotany*, 4(1), 1–21.

Reimer, P., Baillie, M., Bard, E., Bayliss, A., Beck, J., Bertrand, C., Blackwell, P., Buck, C., Burr, G., Cutler, K., Damon, P., Edwards, R., Fairbanks, R.,

Friedrich, M., Guilderson, T., Hogg, A., Hughen, K., Kromer, B., McCormac, G., Manning, S., Ramsey, C., Reimer, R., Remmele, S., Southon, J., Stuiver, M., Talamo, S., Taylor, F., van der Plicht, J., Weyhenmeyer, C. (2004). Intcal04 terrestrial radiocarbon age calibration, 0-26 cal kyr bp. *Radiocarbon*, 46(3), 1029–1058.

Rekovets, L.I. (1994). *Small mammals of the Anthropogene of the southern part of East Europe*. Naukova Dumka, Kiev.

Rekovets, L.I., Chepalyga, A., Povodyrenko, V. (2007). Geology and mammalian fauna of the Middle Pleistocene site, Medzhybozh, Ukraine. *Quaternary International*, 160(1), 70–80.

Rekovets, L.I., Kopij, G., Nowakowski, D. (2009). Taxonomic diversity and spatio-temporal distribution of late Cenozoic beavers (Castoridae, Rodentia) of Ukraine. *Acta Zoologica Cracoviensia*, 52(1–2), 95–105.

Rekovets, L.I. (1990). Principle developmental stages of the water vole genus *Arvicola* (Rodentia, Mammalia) from the Eastern European Pleistocene. In: O. Fejfar, W.D. Heinrich (eds.), *International Symposium on Evolution, Phylogeny and Biostratigraphy of Arvicolids*, 125–132. Geological Survey, Praha.

Rekovets, L.I., Nadachowski, A. (1995). Pleistocene voles (Arvicolinae) of the Ukraine. *Paleontologia i Evolucio*, 28-29, 145–245.

Rensberger, S.M. (1973). An occlusion model for mastication and dental wear in herbivorous mammals. *Journal of Palaeontology*, 47(3), 515–528.

Repenning, C.A. (1968). Mandibular musculature and the origin of the subfamily Arvicolinae (Rodentia). *Acta Zoologica Cracoviensia*, 13, 29–72.

Repenning, C.A., Fejfar, O., Heinrich, W.D. (1990). Arvicolid rodent biochronology of the Northern Hemisphere. In: O. Fejfar, W.D. Heinrich (eds.), *International Symposium on the Evolution and Phylogenetic Biostratography of Arvicolids*, 385–418. Pfeil-Verlag, Prague.

Riek, G. (1958). Das Paläolithikum der Brillenhöle in achtal bei Blaubeuren (Schwäb, Jura). *Neue Ausgrabungen in Deutschland*, 6–22.

Riek, G. (1973). *Das Paläolithikum der Brillenhöhle bei Blaubeuren (Schwäbische Alb)*, vol. Teil I. Verlag Müller & Gräff, Stuttgart.

Rink, W.J., Schwarcz, H., Stuart, A.J., Lister, A.M., Marsegelia, E., Brennan, B.J. (1996). ESR dating of the type Cromerian Freshwater Bed at West Runton, U.K. *Quaternary Science Reviews*, 15, 727–738.

Roberts, M.B., Parfitt, S.A. (1999). *Boxgrove. A Middle Pleistocene hominid site at Eartham pit, Boxgrove, West Sussex*, vol. Archaeological Report 17. English Heritage.

Roberts, M.B. (1999). Geological summary. In: M.B. Roberts, S.A. Parfitt (eds.), *Boxgrove. A Middle Pleistocene hominid site at Eartham pit, Boxgrove, West Sussex*, vol. Archaeological Report 17, 149–155. English Heritage.

Roberts, M.B., Pope, M.I. (2009). The archaeological and sedimentary records from Boxgrove and Slindon. In: R.M. Briant, M.R. Bates, R.T. Hosfield, F.F. Wenban-Smith (eds.), *The Quaternary of the Solent Basin and West Sussex Raised Beaches: Field Guide*, 96–122. Quaternary Research Association.

Roe, H.M. (1995). The Cudmore Grove Channel site (TM 067144). In: D.R. Bridgland, P. Allen, B.A. Haggart (eds.), *The Quaternary of the lower reaches of the Thames: Field Guide*, 258–169. Quaternary Research Association.

Roe, H.M. (1999). Late Middle Pleistocene sea-level change in the southern North Sea: the record from eastern Essex, UK. *Quaternary International*, 55, 115–128.

Roe, H.M., Coope, G.R., Devoy, R.J.N., Harrison, C.J.O., Penkman, K.E.H., Preece, R.C., Schreve, D.C. (2009). Differentiation of MIS 9 and MIS 11 in the continental record: vegetational, faunal, aminostratigraphic and sea-level evidence from coastal sites in Essex, UK. *Quaternary Science Reviews*, 28(23-24), 2342–2373.

Rohlf, F.J. (1990). Rotational fit (Procrustes) methods. In: F.J. Rohlf, F.L. Bookstein (eds.), *Proceedings of the Michigan Morphometrics Workshop*, 227–236. University of Michigan Museum of Zoology.

Rohlf, F.J., Marcus, L.F. (1993). A revolution in morphometries. *Trends in Ecology and Evolution*, 8, 129–132.

Rohlf, F.J. (1993). Relative warp analysis and an example of its application to mosquito wings. In: L.F. Marcus, E. Bello, A. García-Valdecasas (eds.), *Contributions to morphometrics*, 131–159. Museo Nacional de Ciencias Naturales.

Rohlf, F.J., Slice, D.E. (1990). Extensions of the Procrustes method for the optimal superimposition of landmarks. *Systematic Zoology*, 39, 40–49.

Roopnarine, P.D. (2003). Analysis of rates of morphologic evolution. *Annual Review of Ecology, Evolution, and Systematics*, 34(1).

Rose, J. (2008). Palaeogeography of eastern England during the Early and Middle Pleistocene. In: I. Candy, J. Lee, A. Harrison (eds.), *The Quaternary of northern East Anglia: Field Guide*, 5–41. Quaternary Research Association.

Rose, J., Juby, C., Bullen, M., Davies, S., Branch, N., Gammage, I., Candy, I., Palmer, A. (2008). The stratigraphy, sedimentology, palaeoenvironments, palaeoclimate and duration of the early Middle Pleistocene sediments at West Runton, north Norfolk. In: I. Candy, J. Lee, A. Harrison (eds.), *The Quaternary of northern East Anglia: Field Guide*, 157–181. Quaternary Research Association.

Röttger, U. (1987). Schmelzbandbreiten and Molaren von Schermäusen (*Arvicola* Lacépéde, 1799). *Bonner Zoologische Beitraege*, 38, 95–105.

Roy, K., Valentine, J.W., Jablonski, D., Kidwell, S.M. (1996). Scales of climatic variability and time averaging in Pleistocene biotas: implications for ecology and evolution. *Trends in Ecology and Evolution*, 11(11), 458–463.

Rădulescu, C., Samson, P.M. (1977). *Arvicola* (Rodentia, Mammalia) dans le Pliéistocène moyen de Roumanie. *Travaux de l'institut de Spéologie"Emile Racovitza"*, 16, 151–162.

Rădulescu, C., Samson, P.M. (1993). Dental morphology of the *Mimomys/Arvicola* transition forms. *Theoretical and Applied Karstology*, 6, 199–206.

Rădulescu, C., Samson, P. (1985). Pliocene and Pleistocene mammalian biostratigraphy in southeastern Transylvania (Romania). *Travaux de l'institut de Spéologie "Emile Racovitza"*, 24, 85–95.

Ruddy, M. (2005). *Oxygen stable isotope analysis of water vole (*Arvicola*) incisor tooth enamel: a proxy record of terrestrial climate from MIS 9 Britain.* Master's thesis, Royal Holloway, University of London.

Ruszkiczay-Rudiger, Z., Dunai, T.J., Bada, G., Fodor, L., Horvath, E. (2005). Middle to late Pleistocene uplift rate of the Hungarian mountain range at the Danube Bend, (Pannonian Basin) using *in situ* produced He-3. *Tectonophysics*, 410(1-4), 173–187.

Sala, B. (1980). Interpretazione crono-bio-stratigrafica dei depositi Pleistocenici della Grotta Del Broion (Vicenza). *Geografia Fisica e Dinamica Quaternaria*, 3, 66–71.

Sala, B. (1983). La fauna del giacimento di Isernia La Pineta. In: *Estratto da Isernia La Pineta: un accampamento piú antico di 700 000 anni*, Soprintendenza Archeologica E Per I Beni Ambientali Architettonici Artistici E Storici Del Molise, 71–79. Calderini Editore, Bologna.

Sala, B., Marchetti, M. (2006). The Po Valley floodplain (Northern Italy): a transitional area between two zoogeographical areas during the Late Neogene and Quaternary. *Courier Forschungsinstitut Senckenberg*, 256, 321–328.

Schmidtgen, O. (1911). Über Reste von Wühlmausen aus dem Mosbacher Sand. *Notizblatt des Vereins fur Erkunde*, 4(32), 185–193.

Schour, I., Medak, H. (1951). Experimental increase in rate of eruption and growth of rat incisor by eliminating attrition. *Journal of Dental Research*, 30, 521.

Schreve, D.C. (1997). *Mammalian biostratigraphy of the later Middle Pleistocene in Britain*. Ph.D. thesis, University College London.

Schreve, D.C. (2001). Differentiation of the British late Middle Pleistocene interglacials: the evidence from mammalian biostratigraphy. *Quaternary Science Reviews*, 20, 1693–1705.

Schreve, D.C., Bridgland, D.R. (2002). Correlation of English and German Middle Pleistocene fluvial sequences based on mammalian biostratigraphy. *Geologie en Mijnbouw*, 81(3-4), 357–373.

Schreve, D.C., Currant, A.P., Stringer, C. (1999). Conclusion: correlation of the Westbury Cave deposits. In: P. Andrews, J. Cook, A. Currant, C.B. Stringer (eds.), *Westbury Cave: The Natural History Museum Excavations 1976-1984*, 275–284. Western Academic & Specialist Press Limited, Bristol.

Searle, J.B., Kotlík, P., Rambau, R.V., Marková, S., Herman, J.S., McDevitt, A.D. (2009). The celtic fringe of britain: insights from small mammal phylogeography. *Proceedings of the Royal Society B: Biological Sciences*, 1–8.

Shapiro, B., Drummond, A.J., Rambaut, A., Wilson, M.C., Matheus, P.E., Sher, A.V., Pybus, O.G., Gilbert, M.T.P., Barnes, I., Binladen, J., Willerslev, E., Hansen, A.J., Baryshnikov, G.F., Burns, J.A., Davydov, S., Driver, J.C., Froese, D.G., Harington, C.R., Keddie, G., Kosintsev, P., Kunz, M.L., Martin, L.D., Stephenson, R.O., Storer, J., Tedford, R., Zimov, S., Cooper, A. (2004). Rise and Fall of the Beringian Steppe Bison. *Science*, 306, 1561–1565.

Shennan, I., Horton, B. (2002). Holocene land- and sea-level changes in Great Britain. *Journal of Quaternary Science*, 17, 511–526.

Sidorchuk, A.Y., Panin, A.V., Borisova, O.K. (2009). Morphology of river channels and surface runoff in the Volga River basin (East European Plain) during the Late Glacial period. *Geomorphology*, 113(3-4), 137–157.

Simard, S. (1966). *Etude paléontologique des micromammiféres de la grotte de Regourdou (Montignac, Dordogne)*. Ph.D. thesis, Université de Paris, Paris.

Simpson, G.G. (1945). The principles of classification and a classification of the mammals. *Bulletin of the American Museum of Natural History*, 85, 1–350.

Smith, A.T., Johnston, C.H. (2008). *Lepus europaeus*. In: *IUCN 2009. IUCN Red List of Threatened Species. Version 2009.1.* URL `http://www.iucnredlist.org/`. Accessed 05 October 2009.

Smith, R.J. (1993). Logarithmic transformation bias in allometry. *American Journal of Physical Anthropology*, 90(215–228).

Sokal, R.R., Rohlf, F.J. (1995). *Biometry: The Principles and Practice of Statistics in Biological Research*. W. H. Freeman and Company, New York, 3rd edition edn.

Stanton, W. (1999). Early stages in the development of Westbury Cave. In: P. Andrews, J. Cook, A. Currant, C.B. Stringer (eds.), *Westbury Cave: The Natural History Museum Excavations 1976-1984*, 13–18. Western Academic & Specialist Press Limited, Bristol.

Steffensen, J.P., Andersen, K.K., Bigler, M., Clausen, H.B., Dahl-Jensen, D., Fischer, H., Goto-Azuma, K., Hansson, M., Johnsen, S.J., Jouzel, J., Masson-Delmotte, V., Popp, T., Rasmussen, S.O., Roethlisberger, R., Ruth, U., Stauffer, B., Siggaard-Andersen, M.L., Sveinbjornsdottir, A.E., Svensson, A., White, J.W.C. (2008). High-resolution Greenland Ice Core data show abrupt climate change happens in few years. *Science*, 321(5889), 680–684.

Stewart, J.R. (2007). Neanderthal extinction as part of the faunal change in Europe during Oxygen Isotope Stage 3. *Acta Zoologica Cracoviensia*, 50(1-2), 93–124.

Stewart, J.R. (2008). The progressive effect of the individualistic response of species to Quaternary climate change: an analysis of British mammalian faunas. *Quaternary Science Reviews*, 27(27-28), 2499–2508.

Stewart, J.R. (In press). The evolutionary consequence of the individualistic response to climate change. *Journal of Evolutionary Biology*.

Stewart, J.R., Lister, A.M. (2001). Cryptic northern refugia and the origins of the modern biota. *Trends in Ecology & Evolution*, 16(11), 608–613.

Stewart, J.R., Lister, A.M., Barnes, I., Dalén, L. (2010). Refugia revisited: individualistic responses of species in space and time. *Proceedings of the Royal Society B: Biological Sciences*, 277(1682), 661–671.

Stigall, A.L., Lieberman, B.S. (2006). Quantitative palaeobiogeography: GIS, phylogenetic biogeographical analysis, and conservation insights. *Journal of Biogeography*, 33(12), 2051–2060.

Storch, G. (1969). Über Kleinsäuger der Tundra und Steppe in jungeiszeitlichen Eulengewöllen aus dem nordhessischen Löß. *Natur und Museum: Bericht der Senckenbergischen Naturforschenden Gesellschaft*, 99(12), 541–551.

Storch, G. (1973). Jungpleistozäne Kleinsägerfunde (Mammalia: Insectivora, Chiroptera, Rodentia) aus der Brillenhöhle. In: G. Riek (ed.), *Das Paläolithikum der Brillenhöhle bei Blaubeuren (Schwäbische Alb)*, vol. Teil I, 106–123. Verlag Müller & Gräff, Stuttgart.

Street, M. (1998). The archaeology of the Pleistocene-Holocene transition in the northern Rhineland, Germany. *Quaternary International*, 49/50, 45–67.

Stuart, A.J. (1996). Vertebrate faunas from the early Middle Pleistocene of East Anglia. In: A. Turner (ed.), *The early Middle Pleistocene in Europe*, 9–24. Balkema, Rotterdam.

Stuart, A.J. (2000). The West Runton Freshwater Bed. In: S.G. Lewis, C.A. Whiteman, R.C. Preece (eds.), *The Quaternary of Norfolk & Suffolk Field Guide*, 67–72. Quaternary Research Association.

Stuart, A., Kosintsev, P., Higham, T., Lister, A. (2004). Pleistocene to Holocene extinction dynamics in giant deer and woolly mammoth. *Nature*, 431(7009), 684–689.

Sutcliffe, A.J., Kowalski, K. (1976). Pleistocene rodents of the British Pleistocene rodents of the British Isles. *Bulletin of the British Museum (Natural History), Geology Series*, 27, 31–147.

Sutcliffe, A.J., Zeuner, F. (1962). Excavations in the Torbryan Caves, Devonshire: I. Tornewton Cave. *Proceedings of the Devon Archaeological Exploration Society*, 5(5-6), 127–145.

Swiderski, D.L., Zelditch, M.L., Fink, W.L. (2002). Comparability, morphometrics and phylogenetic systematics. In: N. MacLeod, P.L. Forey (eds.), *Morphology, Shape and Phylogeny*, chap. Quantitative characters, phylogenies and morphometrics, 67–99. CRC Press, Boca Raton.

Taberlet, P., Fumagalli, L., Wust-Saucy, A.G., Cosson, J.F. (1998). Comparative phylogeography and postglacial colonization routes in Europe. *Molecular Ecology*, 7(4), 453–464.

Telfer, S., Dallas, J., Aars, J., Piertney, S., Stewart, W., Lambin, X. (2003). Demographic and genetic structure of fossorial water voles (*Arvicola terrestris*) on Scottish islands. *Journal of Zoology*, 259, 23–29.

Terhorst, B. (2000). The influence of Pleistocene landforms on soil-forming processes and soil distribution in a loess landscape of Baden–Württemberg (southwest Germany). *Catena*, 41(1-3), 165–179.

Tesakov, A.S., Dodonov, A.E., Titov, V.V., Trubikhin, V.M. (2007). Plio-Pleistocene geological record and small mammal faunas, eastern shore of the Azov Sea, Southern European Russia. *Quaternary International*, 160, 57–69.

Thaler, L. (1962). Campagnols primitifs de l'ancien et du nouveau monde. *Coll. int. CNRS*, 104, 387–398.

Thiele, K. (1993). The holy grail of the perfect character: The cladistic treatment of morphometric data. *Cladistics*, 9(3), 275–304.

Thieme, H. (1997). Lower Paleolithic throwing spears from Germany. *Nature*, 385, 807 –810.

Thieme, H. (ed.) (2007). *Die Schöningen Speere: Mensch und Jagd vor 400 000 Jahren*. Theiss Verlag, Stuttgart.

Tillier, A., Mester, Z., Bocherens, H., Henry-Gambier, D., Pap, I. (2009). Direct dating of the "Gravettian" Balla child's skeleton from Bükk Mountains (Hungary): unexpected results. *Journal of Human Evolution*, 56(2), 209–212.

Tougard, C., Renvoisé, E., Petitjean, A., Quéré, J.P. (2008). New insight into the colonization processes of common voles: Inferences from molecular and fossil evidence. *PLoS ONE*, 3(10), e3532–.

Toškan, B., Kryštufek, B. (2007). Small Terrestrial Mammals (Erinaceomorpha, Soricomorpha, Chiroptera, Rodentia) From Divje Babe I. In: I. Turk (ed.), *Divje babe I. Upper Pleistocene Palaeolithic site in Slovenia. Part I: Geology and Palaeontology*, no. 13 in Opera Instituti Archaeologici Sloveniae, 209–216. Založba ZRC, Ljubljana.

Tucker, M.E. (1991). *Sedimentary Petrology*. Blackwell, second edn.

Turk, I. (2007a). Chronology of the Divje babe I Site. In: I. Turk (ed.), *Divje babe I. Upper Pleistocene Palaeolithic site in Slovenia. Part I: Geology and Palaeontology*, no. 13 in Opera Instituti Archaeologici Sloveniae, 163–165. Založba ZRC, Ljubljana.

Turk, I. (2007b). Stratigraphy of the Divje babe I Site. In: I. Turk (ed.), *Divje babe I. Upper Pleistocene Palaeolithic site in Slovenia. Part I: Geology and Palaeontology*, no. 13 in Opera Instituti Archaeologici Sloveniae, 59–61. Založba ZRC, Ljubljana.

Turk, I., Skaberne, D., Orel, B., Turk, J., Kranjc, A., Slemenik-Perše, L., Meden, A. (2007). Sediments at the Divje babe I Site. In: I. Turk (ed.), *Divje babe I. Upper Pleistocene Palaeolithic site in Slovenia. Part I: Geology and Palaeontology*, no. 13 in Opera Instituti Archaeologici Sloveniae, 105–121. Založba ZRC, Ljubljana.

Tzedakis, P.C., Raynaud, D., McManus, J.F., Berger, A., Brovkin, V., Kiefer, T. (2009). Interglacial diversity. *Nature Geoscience*, 2, 751–755.

Urban, B. (2007). Quatäre vegetations- und Klimaentwicklung im Tagebau Schöningen. In: H. Thieme (ed.), *Die Schöningen Speere: Mensch und Jagd vor 400 000 Jahren*, 66–75. Theiss Verlag.

Van der Meulen, A.J. (1973). Middle Pleistocene smaller mammals from the Monte Peglia (Orvieto, Italy) with special reference to the phylogeny of *Microtus* (Arvicolidae, Rodentia). *Quaternaria*, 17, 144.

Velichko, A.A., Faustova, M.A. (1986). Glaciations in the East European region of the USSR. *Quaternary Science Reviews*, 5, 447–461.

Velichko, A.A., Faustova, M.A., Gribchenko, Y.N., Pisareva, V., Sudakova, N. (2004). Glaciations of the East European Plain - distribution and chronology. In: J. Ehlers, P. Gibbard (eds.), *Quaternary Glaciations – Extent and Chronology*, 337–354. Elsevier.

Ventura, J. (1991). Morphological characteristics of the molars of *Arvicola terrestris* (Rodentia, Arvicolidae) in its southwestern distribution area. *Zoologischer Anzeiger*, 226(1-2), 64–70.

Ventura, J., Gosalbez, J. (1989). Taxonomic review of *Arvicola terrestris* (Linnaeus, 1758) (Rodentia, Arvicolidae) in the Iberian Peninsula. *Bonner Zoologische Beiträge*, 40, 227–242.

Vermeersch, P., Boon, J. (2010). Radiocarbon Palaeolithic Database Europe v10. URL http://ees.kuleuven.be/geography/projects/14c-palaeolithic/. Accessed 2010-01-12.

Vértes, L. (1965). *Az őskőkor és az átmeneti kőkor emlékei Magyarországon*. Akadémiai Kiadó, Budapest.

Vialou, D. (2004). *La Préhistoire: Histoire et Dictionnaire*. Robert Laffont.

Viriot, L., Chaline, J., Schaaf, A., Boulangé, L. (1993). Ontogenetic change of *Ondatra zibethicus* (Arvicolinae, Rodentia) cheek teeth analysed by digital image processing. In: R.A. Martin, A.D. Barnosky (eds.), *Morphological change in Quaternary mammals of North America*, 373–391. Cambridge University Press.

Vogel, J., Waterbolk, H. (1967). Groningen radiocarbon dates VII. *Radiocarbon*, 9, 107–155.

Vogel, J., Waterbolk, H. (1972). Groningen radiocarbon dates X. *Radiocarbon*, 14(1), 6–110.

Vrba, E.S. (1993). Turnover-pulses, the red queen, and related topics. *American Journal of Science*, 293(A), 418–452.

Walker, M., Johnsen, S., Rasmussen, S.O., Popp, T., Steffensen, J.P., Gibbard, P., Hoek, W., Lowe, J., Andrews, J., Bjorck, S., Cwynar, L.C., Hughen, K., Kershaw, P., Kromer, B., Litt, T., Lowe, D.J., Nakagawa, T., Newnham, R., Schwander, J. (2009). Formal definition and dating of the GSSP (Global Stratotype Section and Point) for the base of the Holocene using the Greenland NGRIP ice core, and selected auxiliary records. *Journal of Quaternary Science*, 24(1), 3–17.

Warton, D., Wright, I., Falster, D., Westoby, M. (2006). Bivariate line-fitting methods for allometry. *Biological Reviews*, 81, 259–291.

Weber, J.M., Aubry, S., Ferrari, N., Fischer, C., Feller, N.L., Meia, J.S., Meyer, S. (2002). Population changes of different predators during a water vole cycle in a central European mountainous habitat. *Ecography*, 25(1), 95–101.

Weninger, B., Jöris, O., Danzeglocke, U. (2009). CalPal-2007. Cologne Radiocarbon Calibration & Palaeoclimate Research Package. URL `http://www.calpal.de/`. Accessed 2009-12-31.

West, R.G. (1980). *The Pre-glacial Pleistocene of the Norfolk and Suffolk Coasts*. Cambridge University Press, Cambridge.

White, M.J., Schreve, D.C. (2000). Island Britain - Peninsula Britain: Palaeogeography, Colonisation, and the Lower Palaeolithic Settlement of the Britiah Isles. *Proceedings of the Prehistoric Society*, 66, 1–28.

Wojtal, P. (2007). *Zooarchaeological studies of the Late Pleistocene sites in Poland*. Institute of Systematics and Evolution of Animals of the Polish Academy of Sciences.

Woodroffe, G.L. (2000). *The Water Vole*. The Mammal Society.

Yalden, D. (1999). *The History of British Mammals*. Poyser Natural History, London.

Zagwijn, W.H. (1992). The beginning of the Ice-Age in Europe and its major subdivisions. *Quaternary Science Reviews*, 11(5), 583–591.

Zazhigin, V.S. (1980). *Late Pliocene and Anthropogene rodents of the south of Western Siberia*. Nauka Press, Moscow.

Zejda, J., Zukal, J., Steiner, H.M. (1994). Variation in the shape pattern of molars in populations of the bank vole (*Clethrionomys glareolus* Schreb). *Folia Zoologica*, 43(2), 121–133.

Zelditch, M.L., Swiderski, D.L., Fink, W.L. (2000). Discovery of phylogenetic characters in morphometric data. In: J.J. Wiens (ed.), *Phylogenetic Analysis of Morphological Data*, 37–83. Smithsonian, London.

Zelditch, M.L., Fink, W.L., Swiderski, D.L. (1995). Morphometrics, homology, and phylogenetics: Quantified characters as synapomorphies. *Systematic Biology*, 44(2), 179–189.

Zelditch, M.L., Swiderski, D.L., Sheets, H.D., Fink, W.L. (2004). *Geometric Morphometrics for Biologists: A Primer*. Elsevier Academic Press, Amsterdam.

Zima, J. (2004). Karyotypic variation in mammals of the Balkan peninsula. In: H.I. Griffiths, B. Kryštufek, J.M. Reed (eds.), *Balkan biodiversity : pattern and process in the European hotspot*. Kluwer Academic, London.

Appendices

Appendix A

Collection information

Table A.1: Archives of water vole specimens used in this study.

Archive name	Code	City	Country	Specific thanks
Cambridge Museum of Archaeology & Ethnography	CMAE	Cambridge	England	
Dipartimento di Scienze Geologiche e Paleontologiche dell'Universita di Ferrara	UNIFE	Ferrara	Italy	Prof. Benedetto Sala
Harrison Zoological Museum	HAZM	Sevenoaks	England	Dr. Paul Bates and Dr. David Harrison
Hungarian Institute of Geology	HIGB	Budapest	Hungary	Dr. Lázló Kordos
Hungarian Natural History Museum	NHMH	Budapest	Hungary	Dr. Mihai Gasparic
Institute for Quaternary Paleontology and Geology	CRIQ	Zagreb	Croatia	Dr. Jadranka Mauch-Lenardić
Institute of Speleology "Emil Racovitza"	ISER	Bucharest	Romania	Mr. Alexandru Petculescu
Institute of Systematics and Evolution of Animals, Polish Academy of Sciences	ISEK	Krakow	Poland	Prof. Adam Nadachowski and Mr. Paweł Socha
Institut für Paläontologie der Universität Wien	IPUW	Vienna	Austria	Dr. Doris Nagel and Dr. Gernot Rabeder
Manchester University Museum	MUM	Manchester	England	Mr. David Gelsthorpe
Moscow Institute of Geography, Russian Academy of Sciences	MIGG	Moscow	Russia	Dr. Anastasia Markova
Moscow Institute of Palaeontology	MIPA	Moscow	Russia	Prof. Alexander Agandjanian, Dr. Valentina Rossina, and Dr. Natalia Serdyuk
Museé National de Préhistoire	LEMP	Les Eyzies-de-Tayac-Sireuil	France	Mr. Stéphane Madelaine
Museum für Naturkunde, Berlin	MFNB	Berlin	Germany	Prof. Wolf-Dieter Heinrich
National Museum of Nature of the Academy of Sciences of Ukraine	KIEV	Kiev	Ukraine	Prof. Leonid Rekovets
National Museum of Slovenia	SLOV	Ljubljana	Slovenia	Dr. Borut Toškan and Dr. Neva Trampuž Orel
Natural History Museum, London	NHML	London	England	Mr. Andrew Currant, Ms. Daphne Hills, Ms. Paula Jenkins, Ms. Louise Tomsett,
Rheinland-Pfalz Natural History Collection	MAIN	Mainz	Germany	Mr. Thomas Engel, Dr. Thomas Keller, and Dr. Herbert Lutz
Royal Belgian Institute of Natural Sciences	RBINS	Brussels	Belgium	Dr. Mietje Germonpré and Dr. Georges Lenglet
Senckenberg Forschungsstation für Quartärpaläontologie, Weimar	SFIW	Weimar	Germany	Prof. Lutz Maul
Senckenberg Forschungsinstitut und Naturmuseum, Frankfurt	SFIF	Frankfurt	Germany	Dr. Angelika Helfricht and Dr. Gerhard Storch
Sheffield City Museum	SCM	Sheffield	England	Ms. Gill Woolrich
Universiteit Leiden	LEID	Leiden	Netherlands	Prof. Thijs van Kolfschoten
University of Wrocław	UNW	Wrocław	Poland	Mr. Paweł Socha
Zoological Museum of Moscow State University	ZMMS	Moscow	Russia	Dr. Vladimir Lebedev

Appendix B

Results

Table B.1: Pairwise distance matrices of mtDNA distances (middle triangle), unmodified shape distances (upper triangle), and size-corrected shape distances (lower triangle),

	Bridged Pot inner slope	Dzeravá skala Cave	Fuchsloch im Krockstein	Novomirgorod	Ormozu	Ossom's Eyrie Cave	Pilisszántó	Pisede III	Pisede IV&V	Welsh Borders	Wigber Low 26	
Bridged Pot inner slope		0.01560	0.00853	0.01341	0.01152	0.01863	0.01790	0.01674	0.01016	0.00062	0.00808	
Dzeravá skala Cave	0.01142		0.00707	0.02901	0.00408	0.00303	0.00230	0.00115	0.00544	0.01621	0.00752	
Fuchsloch im Krockstein	0.00162	0.01307		0.02195	0.00299	0.01010	0.00937	0.00821	0.00162	0.00915	0.00045	
Novomirgorod	0.02987	0.02650	0.03158		0.02493	0.03205	0.03132	0.03016	0.02357	0.01280	0.02149	
Ormozu	0.03158	0.02820	0.03330	0.00814		0.00711	0.00638	0.00523	0.00136	0.01213	0.00344	
Ossom's Eyrie Cave	0.02987	0.02650	0.03158	0.00979	0.00814		0.00073	0.00189	0.00848	0.01925	0.01055	
Pilisszántó	0.03325	0.03330	0.03497	0.01974	0.01473	0.01307		0.00116	0.00775	0.01852	0.00982	
Pisede III	0.02477	0.02142	0.02646	0.00814	0.00650	0.00487	0.01473		0.00659	0.01736	0.00867	
Pisede IV&V	0.02646	0.02311	0.02816	0.00979	0.00814	0.00650	0.01640	0.00162		0.01077	0.00208	
Welsh Borders	0.02987	0.02650	0.03158	0.01309	0.01144	0.00324	0.01640	0.00814	0.00979		0.00870	
Wigber Low 26	0.02816	0.02480	0.02987	0.00814	0.00650	0.00162	0.01473	0.00324	0.00487	0.00487		
		0.00696	0.00296	0.01021	0.00192	0.00512	0.00512	0.00254	0.00157	0.00366	0.00092	Bridged Pot inner slope
			0.00400	0.01717	0.00888	0.01208	0.00183	0.00950	0.00853	0.01062	0.00788	Dzeravá skala Cave
				0.01317	0.00488	0.00808	0.00217	0.00549	0.00453	0.00662	0.00388	Fuchsloch im Krockstein
					0.00830	0.00509	0.01534	0.00768	0.00864	0.00655	0.00929	Novomirgorod
						0.00320	0.00704	0.00062	0.00035	0.00174	0.00100	Ormozu
							0.01025	0.00258	0.00355	0.00146	0.00420	Ossom's Eyrie Cave
								0.00766	0.00670	0.00879	0.00604	Pilisszántó
									0.00096	0.00112	0.00162	Pisede III
										0.00209	0.00065	Pisede IV&V
											0.00274	Welsh Borders

Table B.2: Significance values of linear regressions of enamel thickness and Centroid Size within fossil and Recent assemblages (assemblage names A to L) where $n \geq 5$. Group sample size given alongside group name. P-values marked by * denote significance at the 0.05 level.

	B1a	B2a	B3a	L1a	L2a	L3a	L4a	Pp	B2p	B3p	L2p	L3p	L4p
Abzac (n=17)	0.013*	0.008*	0.591	0.052	0.023*	0.090	0.005*	0.107	0.215	0.687	0.170	0.235	0.496
Aggeel (n=5)	0.697	0.877	0.425	0.076	0.595	0.994	0.988	0.396	0.655	0.736	0.784	0.431	0.133
Bolshoi Tiganye (n=10)	0.022*	0.002*	0.001*	0.002*	0.009*	0.014*	0.015*	0.061	0.008*	0.014*	0.002*	0.058	0.047*
Boxgrove 4b (n=16)	0.862	0.306	0.740	0.961	0.975	0.798	0.405	0.030*	0.287	0.064	0.179	0.869	0.637
Boxgrove 4c (n=17)	0.064	0.032*	0.018*	0.606	0.610	0.333	0.212	0.612	0.028*	0.007*	0.476	0.052	0.057
Burgtonna South Black-earth (n=9)	0.306	0.033*	0.060	0.758	0.371	0.116	0.148	0.470	0.063	0.242	0.212	0.210	0.104
Central Scotland (n=13)	0.021*	0.062	0.020*	0.002*	0.091	0.019*	0.009*	0.000*	0.023*	0.003*	0.037*	0.140	0.000*
Cheshskaya Guba (n=19)	0.766	0.505	0.136	0.456	0.857	0.718	0.257	0.238	0.119	0.446	0.545	0.095	0.590
Chigirin (n=9)	0.728	0.939	0.568	0.660	0.077	0.212	0.157	0.895	0.146	0.048*	0.927	0.842	0.788
Clacton Channel IV (n=19)	0.048*	0.001*	0.001*	0.009*	0.026*	0.016*	0.058	0.005*	0.008*	0.013*	0.003*	0.094	0.001*
Courbet (n=29)	0.003*	0.000*	0.001*	0.004*	0.003*	0.013*	0.001*	0.554	0.092	0.021*	0.654	0.779	0.225
Cudmore Grove (n=29)	0.128	0.143	0.141	0.111	0.144	0.193	0.048*	0.056	0.374	0.047*	0.238	0.167	0.121
Don Delta (n=7)	0.830	0.925	0.919	0.645	0.765	0.513	0.328	0.487	0.360	0.830	0.829	0.312	0.379
Donskaya Negatchevka (n=12)	0.666	0.723	0.957	0.125	0.550	0.609	0.448	0.728	0.732	0.405	0.452	0.878	0.853
Dzeravá skala Cave (n=24)	0.927	0.059	0.525	0.265	0.957	0.494	0.075	0.108	0.537	0.668	0.859	0.940	0.242
Fortuna utca 16-18/2 (n=17)	0.685	0.560	0.874	0.123	0.151	0.724	0.439	0.012*	0.076	0.273	0.188	0.121	0.131
Frankfurt am Main (n=5)	0.147	0.255	0.055	0.028*	0.099	0.053	0.092	0.005*	0.580	0.945	0.755	0.492	0.812
Fuchsloch im Krockstein (n=13)	0.156	0.021*	0.001*	0.023*	0.426	0.094	0.037*	0.062	0.161	0.083	0.351	0.212	0.087
Ghent (n=18)	0.806	0.941	0.845	0.370	0.768	0.980	0.048*	0.340	0.021*	0.899	0.293	0.936	0.329
Grotta del Broion, Sala Grande N (n=10)	0.190	0.622	0.601	0.109	0.417	0.644	0.893	0.160	0.299	0.145	0.482	0.036*	0.512
Grotta del Broion, Sala Grande Q4 (n=8)	0.388	0.996	0.743	0.444	0.209	0.789	0.465	0.788	0.706	0.903	0.368	0.258	0.367
Grotta del Broion, Sala Grande Q5 (n=11)	0.002*	0.101	0.495	0.003*	0.002*	0.015*	0.470	0.054	0.215	0.053	0.558	0.567	0.179
Grotta del Broion, Sala Grande R1 (n=16)	0.014*	0.002*	0.143	0.057	0.179	0.237	0.197	0.164	0.096	0.059	0.057	0.002*	0.033*
Gunki II (n=9)	0.176	0.037*	0.106	0.079	0.165	0.463	0.137	0.003*	0.050	0.007*	0.023*	0.003*	0.002*
Horváti-lik 13 (n=8)	0.248	0.865	0.240	0.700	0.524	0.964	0.218	0.593	0.027*	0.248	0.973	0.601	0.465
Horváti-lik 8 (n=19)	0.269	0.029*	0.268	0.018*	0.132	0.001*	0.549	0.685	0.181	0.223	0.747	0.104	0.717
Horváti-lik 9a (n=21)	0.445	0.412	0.412	0.165	0.355	0.814	0.174	0.864	0.327	0.880	0.183	0.149	0.757
Hundsheim (n=31)	0.274	0.672	0.253	0.008*	0.303	0.854	0.259	0.387	0.178	0.027*	0.112	0.013*	0.759
Ilovayski Kordon (n=11)	0.104	0.007*	0.003*	0.073	0.029*	0.091	0.031*	0.035*	0.058	0.014*	0.017*	0.004*	0.008*
Kabardino-Balkariya (n=19)	0.460	0.251	0.329	0.029*	0.698	0.812	0.724	0.709	0.627	0.698	0.987	0.479	0.264
Kama-Volga (n=13)	0.002*	0.002*	0.169	0.023*	0.033*	0.085	0.016*	0.135	0.048*	0.010*	0.011*	0.021*	0.042*
Kartstein (n=7)	0.014*	0.033*	0.196	0.107	0.002*	0.016*	0.004*	0.414	0.912	0.292	0.146	0.101	0.082
Korotoyak-4 (n=20)	0.556	0.379	0.489	0.083	0.808	0.646	0.261	0.318	0.238	0.317	0.217	0.129	0.298
Kozi Grzbiet 2 (n=32)	0.033*	0.023*	0.017*	0.349	0.177	0.054	0.102	0.028*	0.003*	0.013*	0.004*	0.002*	0.246
Kuznetsovka (n=89)	0.000*	0.000*	0.000*	0.000*	0.000*	0.000*	0.000*	0.000*	0.000*	0.000*	0.000*	0.000*	0.000*
Leninsky (n=20)	0.002*	0.006*	0.002*	0.001*	0.001*	0.000*	0.008*	0.047*	0.007*	0.000*	0.000*	0.001*	0.002*
Linares de Riofrio (n=7)	0.913	0.597	0.948	0.477	0.055	0.016*	0.260	0.106	0.239	0.733	0.048*	0.192	0.040*

Table B.3: Significance values of linear regressions of enamel thickness and Centroid Size within fossil and Recent assemblages (assemblage names M to W) where $n \geq 5$. Group sample size given alongside group name. P-values marked by * denote significance at the 0.05 level.

	B1a	B2a	B3a	L1a	L2a	L3a	L4a	Pp	B2p	B3p	L2p	L3p	L4p
Marie-Jeanne Cave 2 (n=11)	0.004*	0.133	0.063	0.003*	0.010*	0.050	0.069	0.098	0.120	0.027*	0.175	0.005*	0.045*
Marie-Jeanne Cave 4 (n=9)	0.204	0.091	0.082	0.041*	0.054	0.004*	0.169	0.104	0.456	0.055	0.002*	0.118	0.308
Marie-Jeanne Cave 6 (n=7)	0.307	0.863	0.745	0.852	0.424	0.497	0.356	0.170	0.753	0.240	0.551	0.466	0.351
Medzhybozh-2 (n=9)	0.767	0.538	0.185	0.686	0.014*	0.094	0.107	0.890	0.722	0.166	0.662	0.546	0.422
Merlin's Cave (n=64)	0.003*	0.000*	0.030*	0.067	0.024*	0.007*	0.017*	0.008*	0.054	0.001*	0.022*	0.075	0.008*
Miesenheim I (n=23)	0.004*	0.593	0.137	0.301	0.042*	0.383	0.144	0.117	0.250	0.106	0.331	0.073	0.002*
Mosbach 2 (n=75)	0.174	0.046*	0.034*	0.016*	0.050	0.076	0.011*	0.019*	0.012*	0.001*	0.002*	0.015*	0.005*
Moscow (n=21)	0.246	0.678	0.898	0.220	0.148	0.202	0.363	0.013*	0.571	0.021*	0.077	0.166	0.202
Novomirgorod (n=13)	0.000*	0.000*	0.001*	0.001*	0.001*	0.000*	0.000*	0.001*	0.000*	0.000*	0.019*	0.012*	0.008*
Novonekrasovka upper (n=6)	0.033*	0.031*	0.051	0.284	0.012*	0.092	0.077	0.012*	0.192	0.843	0.001*	0.193	0.032*
Ossom's Eyrie Cave (n=37)	0.000*	0.000*	0.000*	0.000*	0.000*	0.000*	0.000*	0.000*	0.003*	0.012*	0.000*	0.000*	0.000*
Peskö "brick red" strata (n=26)	0.617	0.584	0.931	0.221	0.050	0.049*	0.011*	0.913	0.567	0.952	0.697	0.588	0.595
Pilisszanto (n=10)	0.207	0.235	0.795	0.083	0.231	0.123	0.106	0.012*	0.967	0.743	0.720	0.021*	0.096
Pisede III (n=13)	0.104	0.553	0.194	0.546	0.261	0.418	0.432	0.015*	0.950	0.174	0.908	0.953	0.768
Pisede IV&V (n=25)	0.000*	0.000*	0.000*	0.002*	0.005*	0.000*	0.000*	0.003*	0.000*	0.000*	0.042*	0.000*	0.015*
Poeymaú BS (n=15)	0.008*	0.030*	0.001*	0.027*	0.059	0.015*	0.059	0.003*	0.005*	0.037*	0.050*	0.059	0.043*
Prokhladny (n=15)	0.146	0.409	0.726	0.766	0.788	0.489	0.263	0.625	0.682	0.085	0.750	0.187	0.721
Régourdou 5 (n=8)	0.563	0.419	0.141	0.116	0.363	0.067	0.225	0.727	0.986	0.656	0.318	0.664	0.315
Régourdou 7 (n=16)	0.280	0.085	0.820	0.032*	0.104	0.112	0.019*	0.069	0.914	0.181	0.017*	0.545	0.546
Rotbav-Dealul Ţiganilor Clay-A (n=26)	0.007*	0.080	0.006*	0.003*	0.020*	0.001*	0.001*	0.006*	0.000*	0.004*	0.001*	0.003*	0.000*
Rybnaya Sloboda (n=6)	0.605	0.278	0.426	0.015*	0.831	0.120	0.626	0.272	0.222	0.670	0.096	0.147	0.363
Schóningen 13-II-4 (n=26)	0.044*	0.094	0.009*	0.069	0.339	0.221	0.011*	0.770	0.266	0.174	0.158	0.596	0.064
Tónchesberg II 11-13 (n=15)	0.001*	0.004*	0.000*	0.004*	0.000*	0.001*	0.001*	0.103	0.001*	0.007*	0.002*	0.012*	0.026*
Tornewton Cave Red Cave Earth (n=10)	0.065	0.321	0.790	0.348	0.070	0.008*	0.086	0.193	0.103	0.243	0.328	0.167	0.795
Trou du Frontal (n=9)	0.734	0.107	0.176	0.163	0.409	0.002*	0.079	0.416	0.981	0.461	0.730	0.524	0.321
Tsimlyansk (n=15)	0.113	0.098	0.170	0.225	0.466	0.278	0.116	0.937	0.014*	0.430	0.578	0.037*	0.240
Vindija E-F (n=15)	0.053	0.265	0.162	0.266	0.364	0.277	0.705	0.621	0.177	0.150	0.227	0.063	0.064
Vindija G (n=20)	0.058	0.008*	0.000*	0.003*	0.026*	0.011*	0.001*	0.035*	0.016*	0.072	0.007*	0.127	0.591
Vladimirovka 2 (n=16)	0.168	0.042*	0.003*	0.334	0.052	0.250	0.252	0.002*	0.007*	0.005*	0.085	0.394	0.137
Welsh Borders (n=22)	0.067	0.062	0.311	0.214	0.831	0.173	0.022*	0.743	0.005*	0.007*	0.013*	0.299	0.016*
West Runton Freshwater Bed (n=35)	0.000*	0.000*	0.011*	0.001*	0.002*	0.005*	0.015*	0.004*	0.000*	0.000*	0.000*	0.000*	0.000*
Westbury 11 (n=12)	0.007*	0.003*	0.051	0.212	0.303	0.581	0.489	0.700	0.327	0.103	0.161	0.028*	0.475
Westbury 14 (n=10)	0.395	0.021*	0.261	0.119	0.066	0.351	0.093	0.279	0.235	0.111	0.070	0.403	0.314
Wigber Low 26 (n=49)	0.000*	0.000*	0.002*	0.017*	0.062	0.008*	0.006*	0.000*	0.051	0.000*	0.056	0.001*	0.000*

Table B.4: R^2 values of linear regressions of enamel thickness and Centroid Size within fossil and Recent assemblages (assemblage names A to L) where $n \geq 5$. Group sample size given alongside group name.

	B1a	B2a	B3a	L1a	L2a	L3a	L4a	Pp	B2p	B3p	L2p	L3p	L4p
Abzac (n=17)	0.345	0.379	0.020	0.229	0.298	0.180	0.426	0.164	0.100	0.011	0.122	0.093	0.031
Aggeel (n=5)	0.058	0.009	0.221	0.704	0.105	0.000	0.000	0.245	0.075	0.044	0.029	0.215	0.584
Bolshoi Tiganye (n=10)	0.499	0.719	0.748	0.714	0.592	0.553	0.540	0.373	0.609	0.552	0.705	0.380	0.407
Boxgrove 4b (n=16)	0.002	0.074	0.008	0.000	0.000	0.005	0.050	0.295	0.080	0.224	0.125	0.002	0.016
Boxgrove 4c (n=17)	0.210	0.271	0.320	0.018	0.018	0.062	0.102	0.018	0.282	0.394	0.034	0.229	0.221
Burgtonna South Black-earth (n=9)	0.148	0.499	0.419	0.014	0.116	0.315	0.275	0.077	0.411	0.189	0.212	0.214	0.332
Central Scotland (n=13)	0.398	0.281	0.403	0.607	0.237	0.408	0.479	0.744	0.386	0.574	0.339	0.187	0.805
Cheshskaya Guba (n=19)	0.005	0.027	0.126	0.033	0.002	0.008	0.075	0.081	0.137	0.035	0.022	0.155	0.017
Chigirin (n=9)	0.018	0.001	0.049	0.029	0.381	0.212	0.264	0.003	0.277	0.451	0.001	0.006	0.011
Clacton Channel IV (n=19)	0.211	0.480	0.483	0.339	0.260	0.295	0.196	0.382	0.349	0.310	0.410	0.156	0.498
Courbet (n=29)	0.275	0.477	0.364	0.271	0.284	0.206	0.360	0.013	0.101	0.183	0.008	0.003	0.054
Cudmore Grove (n=29)	0.084	0.078	0.079	0.091	0.077	0.062	0.137	0.129	0.029	0.138	0.051	0.069	0.087
Don Delta (n=7)	0.010	0.002	0.002	0.046	0.020	0.090	0.190	0.101	0.169	0.010	0.010	0.202	0.157
Donskaya Negatchevka (n=12)	0.019	0.013	0.000	0.219	0.037	0.027	0.059	0.013	0.012	0.070	0.058	0.002	0.004
Dzeravá skala Cave (n=24)	0.000	0.153	0.019	0.056	0.000	0.022	0.137	0.113	0.018	0.009	0.001	0.000	0.062
Fortuna utca 16-18/2 (n=17)	0.011	0.023	0.002	0.151	0.133	0.009	0.040	0.350	0.195	0.079	0.112	0.152	0.146
Frankfurt am Main (n=5)	0.558	0.396	0.758	0.844	0.650	0.763	0.666	0.951	0.113	0.002	0.038	0.169	0.022
Fuchsloch im Krockstein (n=13)	0.174	0.397	0.641	0.388	0.058	0.234	0.339	0.282	0.170	0.249	0.079	0.138	0.243
Ghent (n=18)	0.004	0.000	0.002	0.051	0.006	0.000	0.223	0.057	0.291	0.001	0.069	0.000	0.059
Grotta del Broion, Sala Grande N (n=10)	0.204	0.032	0.036	0.289	0.084	0.028	0.002	0.230	0.133	0.246	0.064	0.441	0.056
Grotta del Broion, Sala Grande Q4 (n=8)	0.126	0.000	0.019	0.101	0.248	0.013	0.092	0.013	0.025	0.003	0.136	0.207	0.137
Grotta del Broion, Sala Grande Q5 (n=11)	0.678	0.270	0.053	0.634	0.667	0.497	0.059	0.354	0.165	0.355	0.040	0.038	0.191
Grotta del Broion, Sala Grande R1 (n=16)	0.363	0.501	0.147	0.235	0.125	0.098	0.116	0.133	0.185	0.232	0.235	0.499	0.285
Gunki II (n=9)	0.245	0.486	0.329	0.376	0.256	0.079	0.287	0.749	0.443	0.671	0.545	0.729	0.779
Horváti-lik 13 (n=8)	0.215	0.005	0.221	0.026	0.071	0.000	0.239	0.051	0.584	0.214	0.000	0.048	0.092
Horváti-lik 8 (n=19)	0.071	0.252	0.072	0.289	0.128	0.494	0.022	0.010	0.103	0.086	0.006	0.148	0.008
Horváti-lik 9a (n=21)	0.031	0.036	0.036	0.099	0.045	0.003	0.095	0.002	0.051	0.001	0.091	0.107	0.005
Hundsheim (n=31)	0.041	0.006	0.045	0.219	0.037	0.001	0.044	0.026	0.062	0.157	0.085	0.194	0.003
Ilovayski Kordon (n=11)	0.266	0.567	0.640	0.314	0.426	0.285	0.422	0.407	0.345	0.505	0.484	0.615	0.557
Kabardino-Balkariya (n=19)	0.033	0.077	0.056	0.251	0.009	0.003	0.007	0.008	0.014	0.009	0.000	0.030	0.073
Kama-Volga (n=13)	0.598	0.601	0.165	0.389	0.350	0.245	0.424	0.191	0.309	0.463	0.460	0.397	0.325
Kartstein (n=7)	0.732	0.632	0.308	0.434	0.882	0.717	0.832	0.137	0.003	0.217	0.372	0.446	0.486
Korotoyak-4 (n=20)	0.020	0.043	0.027	0.157	0.003	0.012	0.070	0.055	0.077	0.056	0.083	0.123	0.060
Kozi Grzbiet 2 (n=32)	0.143	0.161	0.177	0.029	0.060	0.118	0.087	0.152	0.251	0.190	0.240	0.283	0.045
Kuznetsovka (n=89)	0.229	0.141	0.213	0.174	0.220	0.242	0.253	0.215	0.233	0.255	0.347	0.285	0.235
Leninsky (n=20)	0.420	0.351	0.407	0.454	0.438	0.543	0.332	0.202	0.341	0.545	0.556	0.465	0.425
Linares de Riofrio (n=7)	0.003	0.060	0.001	0.106	0.553	0.720	0.244	0.437	0.263	0.025	0.575	0.313	0.602

Table B.5: R^2 values of linear regressions of enamel thickness and Centroid Size within fossil and Recent assemblages (assemblage names M to W) where $n \geq 5$. Group sample size given alongside group name.

	B1a	B2a	B3a	L1a	L2a	L3a	L4a	Pp	B2p	B3p	L2p	L3p	L4p
Marie-Jeanne Cave 2 (n=11)	0.612	0.233	0.333	0.636	0.541	0.362	0.321	0.275	0.247	0.434	0.194	0.595	0.375
Marie-Jeanne Cave 4 (n=9)	0.219	0.355	0.370	0.472	0.434	0.717	0.252	0.332	0.082	0.431	0.774	0.312	0.147
Marie-Jeanne Cave 6 (n=7)	0.205	0.007	0.023	0.008	0.131	0.097	0.171	0.340	0.022	0.262	0.075	0.111	0.174
Medzhybozh-2 (n=9)	0.013	0.057	0.236	0.025	0.603	0.348	0.328	0.003	0.019	0.255	0.029	0.054	0.094
Merlin's Cave (n=64)	0.135	0.328	0.073	0.053	0.080	0.113	0.089	0.108	0.059	0.169	0.081	0.050	0.109
Miesenheim I (n=23)	0.328	0.014	0.102	0.051	0.183	0.036	0.099	0.113	0.063	0.120	0.045	0.145	0.368
Mosbach 2 (n=75)	0.025	0.053	0.060	0.077	0.051	0.042	0.085	0.073	0.083	0.145	0.127	0.079	0.105
Moscow (n=21)	0.070	0.009	0.001	0.078	0.107	0.084	0.044	0.285	0.017	0.249	0.156	0.099	0.084
Novomirgorod (n=13)	0.705	0.703	0.681	0.678	0.652	0.832	0.757	0.621	0.804	0.762	0.405	0.448	0.485
Novonekrasovka upper (n=6)	0.720	0.729	0.654	0.277	0.826	0.550	0.584	0.824	0.380	0.011	0.941	0.379	0.724
Ossom's Eyrie Cave (n=37)	0.594	0.415	0.391	0.333	0.506	0.648	0.551	0.336	0.231	0.168	0.538	0.337	0.328
Peskö "brick red" strata (n=26)	0.011	0.013	0.000	0.062	0.150	0.152	0.241	0.001	0.014	0.000	0.006	0.012	0.012
Pilisszanto (n=10)	0.191	0.171	0.009	0.329	0.174	0.271	0.294	0.566	0.000	0.014	0.017	0.505	0.308
Pisede III (n=13)	0.222	0.033	0.148	0.034	0.113	0.060	0.057	0.429	0.000	0.161	0.001	0.000	0.008
Pisede IV&V (n=25)	0.588	0.465	0.570	0.334	0.295	0.455	0.537	0.321	0.500	0.521	0.167	0.466	0.231
Poeymaü BS (n=15)	0.427	0.314	0.612	0.324	0.248	0.377	0.247	0.514	0.474	0.293	0.265	0.249	0.279
Prokhladny (n=15)	0.155	0.053	0.010	0.007	0.006	0.038	0.095	0.019	0.013	0.211	0.008	0.130	0.010
Régourdou 5 (n=8)	0.059	0.111	0.324	0.360	0.139	0.455	0.233	0.022	0.000	0.035	0.165	0.033	0.167
Régourdou 7 (n=16)	0.083	0.197	0.004	0.289	0.178	0.170	0.334	0.217	0.001	0.124	0.343	0.027	0.027
Rotbav-Dealul Ţiganilor Clay-A (n=26)	0.266	0.122	0.271	0.312	0.207	0.351	0.376	0.273	0.431	0.293	0.367	0.314	0.468
Rybnaya Sloboda (n=6)	0.073	0.283	0.164	0.808	0.013	0.493	0.065	0.288	0.343	0.050	0.541	0.447	0.208
Schöningen 13-II-4 (n=26)	0.159	0.112	0.254	0.131	0.038	0.062	0.242	0.004	0.051	0.076	0.081	0.012	0.136
Tönchesberg II 11-13 (n=15)	0.553	0.480	0.622	0.491	0.642	0.594	0.606	0.191	0.604	0.441	0.534	0.398	0.325
Tornewton Cave Red Cave Earth (n=10)	0.365	0.123	0.009	0.111	0.353	0.607	0.324	0.202	0.297	0.166	0.120	0.224	0.009
Trou du Frontal (n=9)	0.018	0.329	0.244	0.258	0.099	0.770	0.376	0.097	0.000	0.080	0.018	0.060	0.140
Tsimlyansk (n=15)	0.182	0.196	0.140	0.111	0.042	0.090	0.179	0.001	0.384	0.049	0.024	0.295	0.104
Vindija E-F (n=15)	0.258	0.095	0.145	0.094	0.064	0.090	0.011	0.019	0.135	0.153	0.110	0.241	0.239
Vindija G (n=20)	0.185	0.330	0.534	0.403	0.246	0.312	0.443	0.225	0.282	0.169	0.339	0.124	0.016
Vladimirovka 2 (n=16)	0.131	0.262	0.488	0.067	0.243	0.093	0.093	0.506	0.417	0.438	0.197	0.052	0.151
Welsh Borders (n=22)	0.158	0.164	0.051	0.076	0.002	0.091	0.234	0.006	0.330	0.307	0.273	0.054	0.257
West Runton Freshwater Bed (n=35)	0.434	0.427	0.180	0.289	0.265	0.213	0.165	0.226	0.531	0.449	0.456	0.319	0.361
Westbury 11 (n=12)	0.539	0.612	0.329	0.151	0.106	0.031	0.049	0.015	0.096	0.243	0.187	0.396	0.052
Westbury 14 (n=10)	0.092	0.505	0.154	0.275	0.361	0.109	0.312	0.144	0.171	0.286	0.353	0.089	0.126
Wigber Low 26 (n=49)	0.288	0.230	0.195	0.116	0.072	0.139	0.151	0.260	0.078	0.330	0.075	0.213	0.261

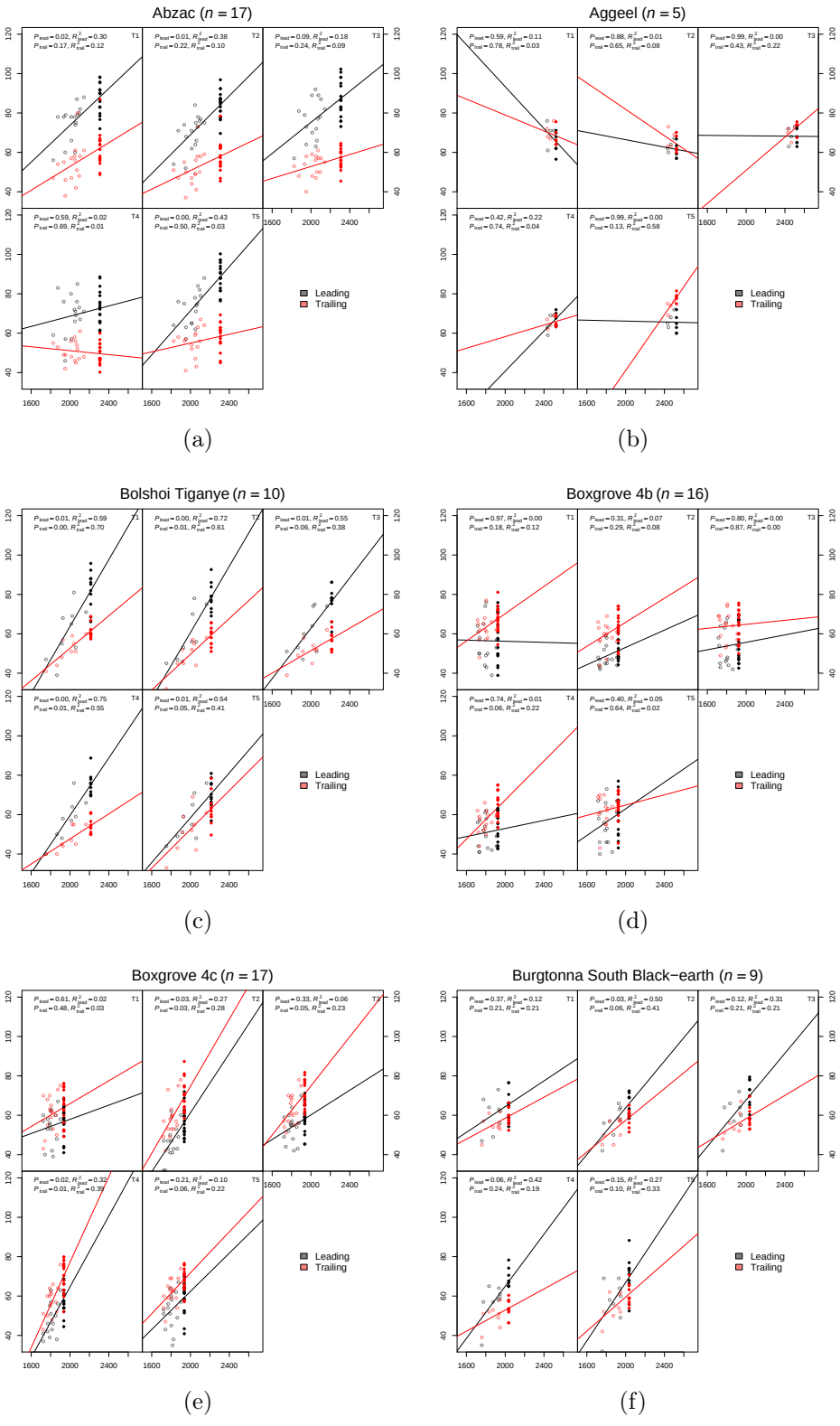

Figure B.1: Regression of enamel thickness (ordinate, µm) with Centroid Size (abscissa, arbitrary units) for the assemblages Abzac, Aggeel, Bolshoi Tiganye, Boxgrove 4b, Boxgrove 4c, and Burgtonna South Blackearth. Regressions shown for each of the five enamel triangles (T1–T5). Observed thickness plotted as circles, modelled adult thicknesses plotted as diamonds, regression diagnostics shown for each enamel triangle.

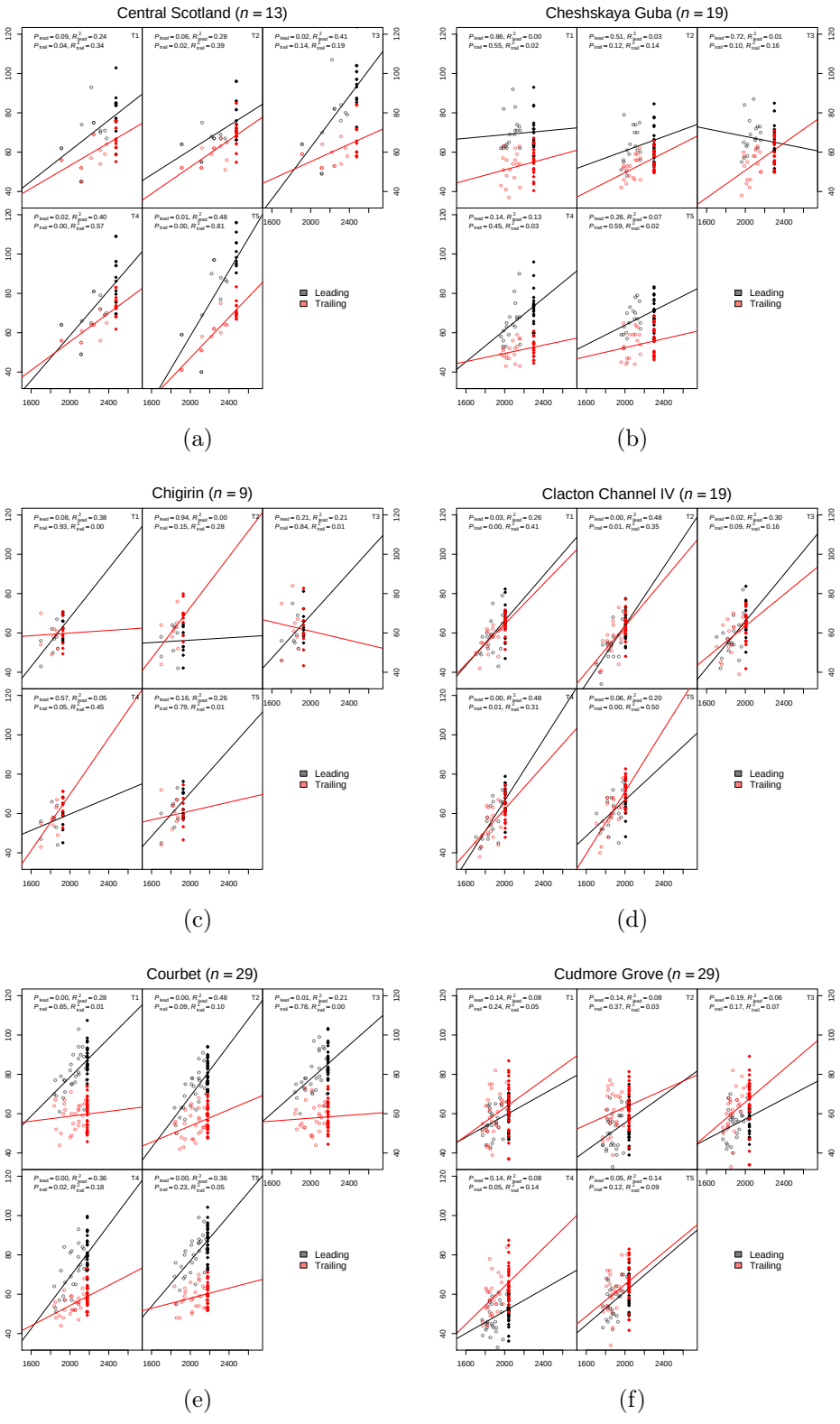

Figure B.2: Regression of enamel thickness (ordinate, µm) with Centroid Size (abscissa, arbitrary units) for the assemblages Central Scotland, Cheshskaya Guba, Chigirin, Clacton Channel IV, Courbet, and Cudmore Grove. Regressions shown for each of the five enamel triangles (T1–T5). Observed thickness plotted as circles, modelled adult thicknesses plotted as diamonds, regression diagnostics shown for each enamel triangle.

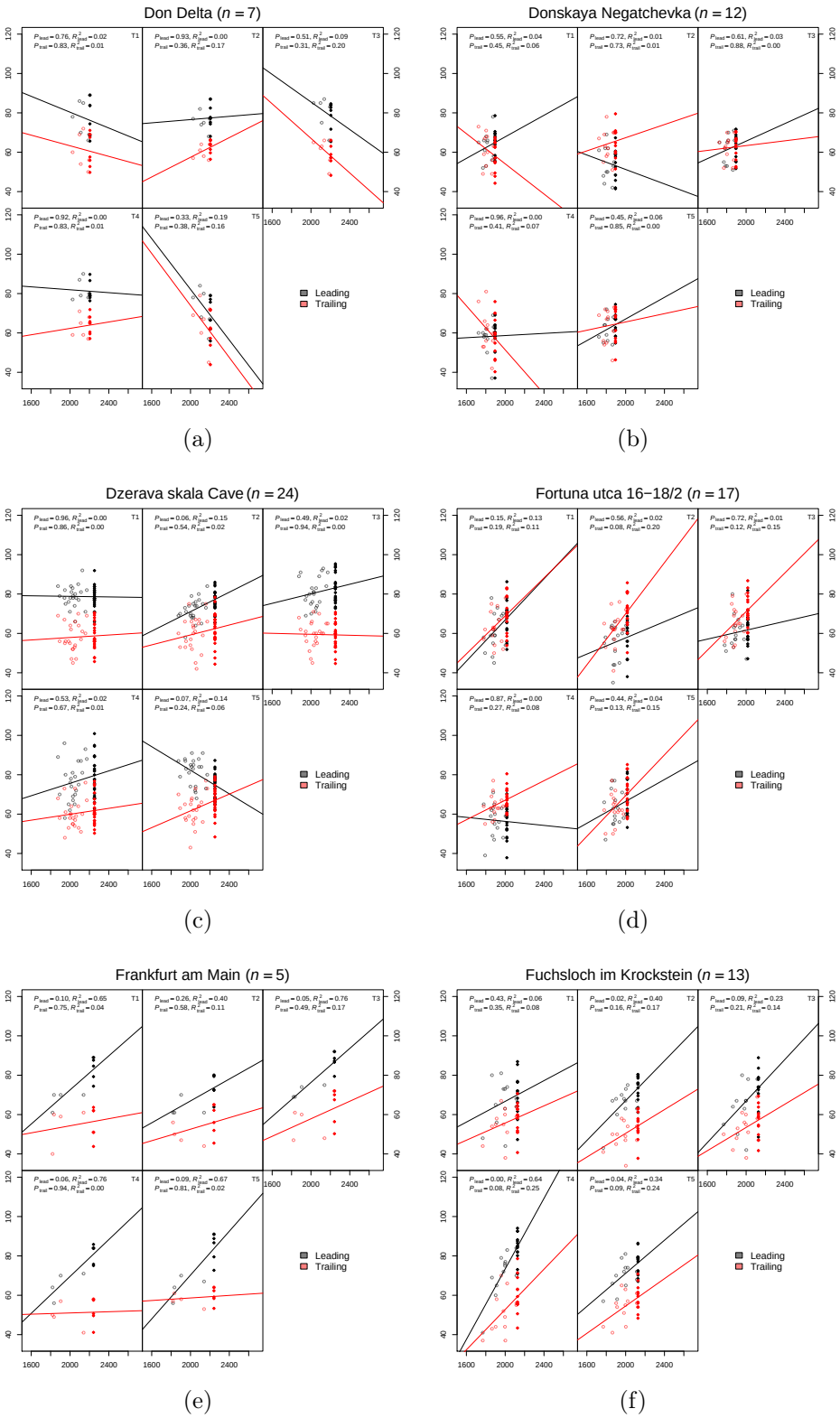

Figure B.3: Regression of enamel thickness (ordinate, µm) with Centroid Size (abscissa, arbitrary units) for the assemblages Don Delta, Donskaya Negatchevka, Dzeravá skala Cave, Fortuna utca 16-18/2, Frankfurt am Main, and Fuchsloch im Krockstein. Regressions shown for each of the five enamel triangles (T1–T5). Observed thickness plotted as circles, modelled adult thicknesses plotted as diamonds, regression diagnostics shown for each enamel triangle.

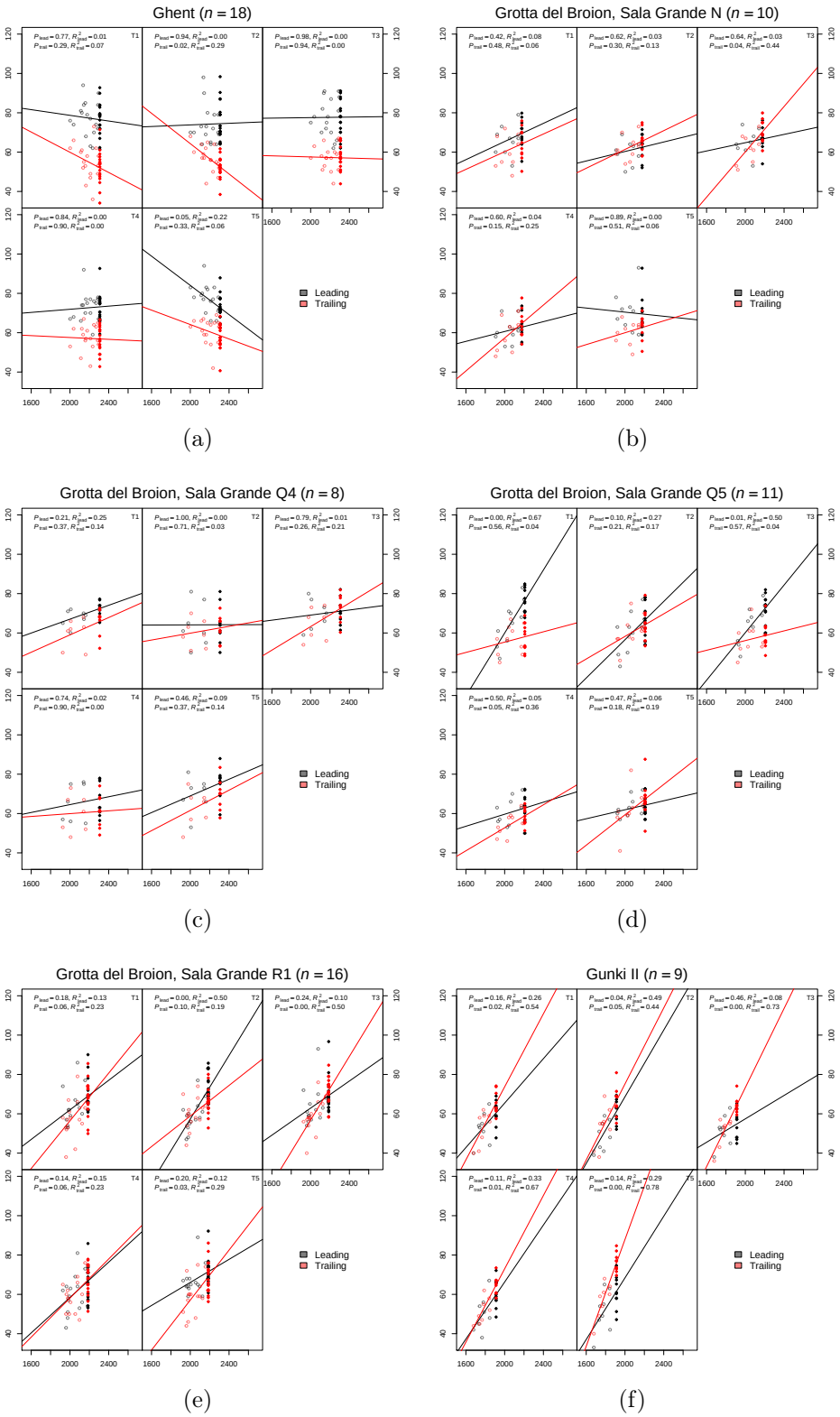

Figure B.4: Regression of enamel thickness (ordinate, µm) with Centroid Size (abscissa, arbitrary units) for the assemblages Ghent, Grotta del Broion Sala Grande N, Grotta del Broion Sala Grande Q4, Grotta del Broion Sala Grande Q5, Grotta del Broion Sala Grande R1, and Gunki II. Regressions shown for each of the five enamel triangles (T1–T5). Observed thickness plotted as circles, modelled adult thicknesses plotted as diamonds, regression diagnostics shown for each enamel triangle.

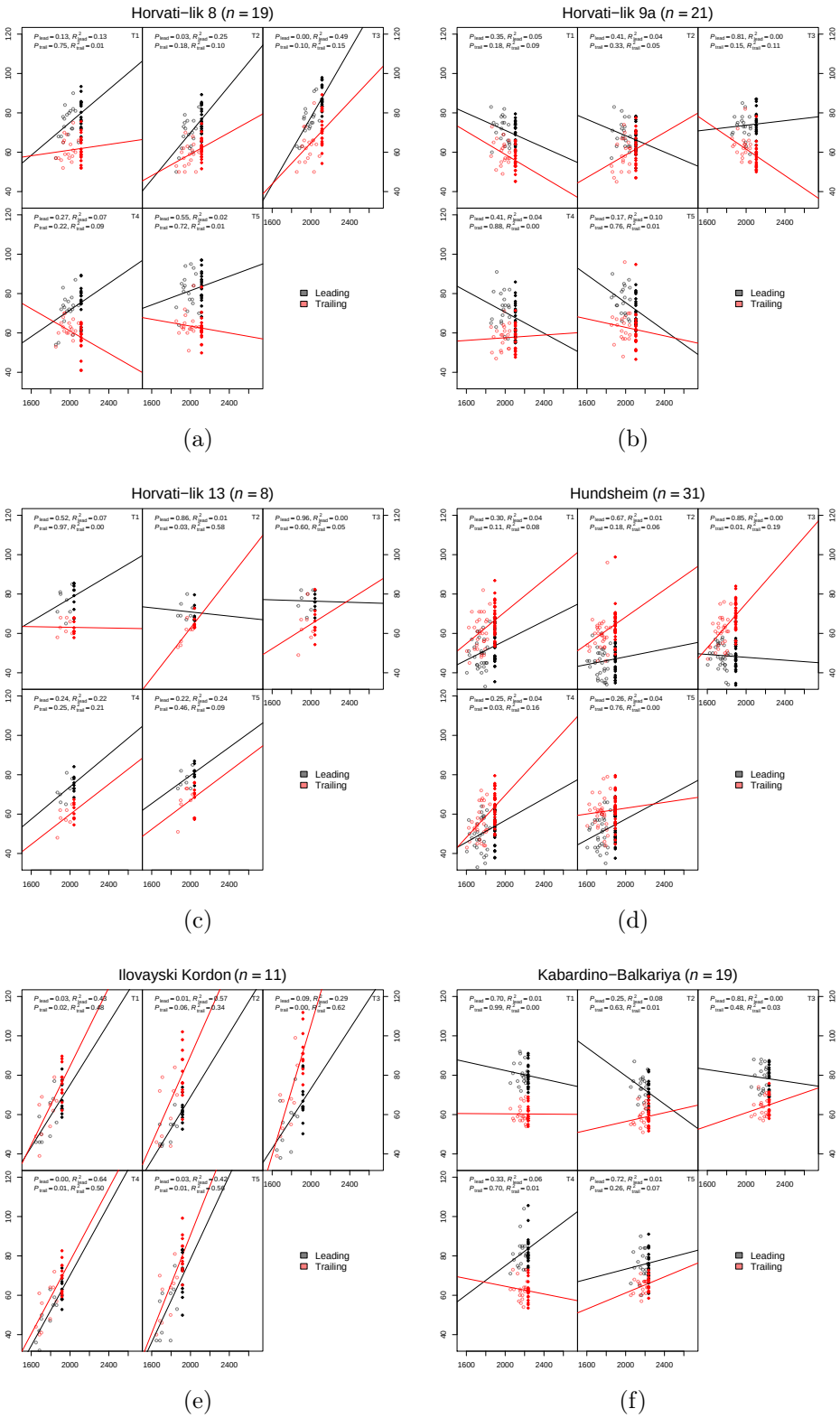

Figure B.5: Regression of enamel thickness (ordinate, µm) with Centroid Size (abscissa, arbitrary units) for the assemblages Horváti-lik 8, Horváti-lik 9a, Horváti-lik 13, Hundsheim, Ilovayski Kordon, and Kabardino-Balkariya. Regressions shown for each of the five enamel triangles (T1–T5). Observed thickness plotted as circles, modelled adult thicknesses plotted as diamonds, regression diagnostics shown for each enamel triangle.

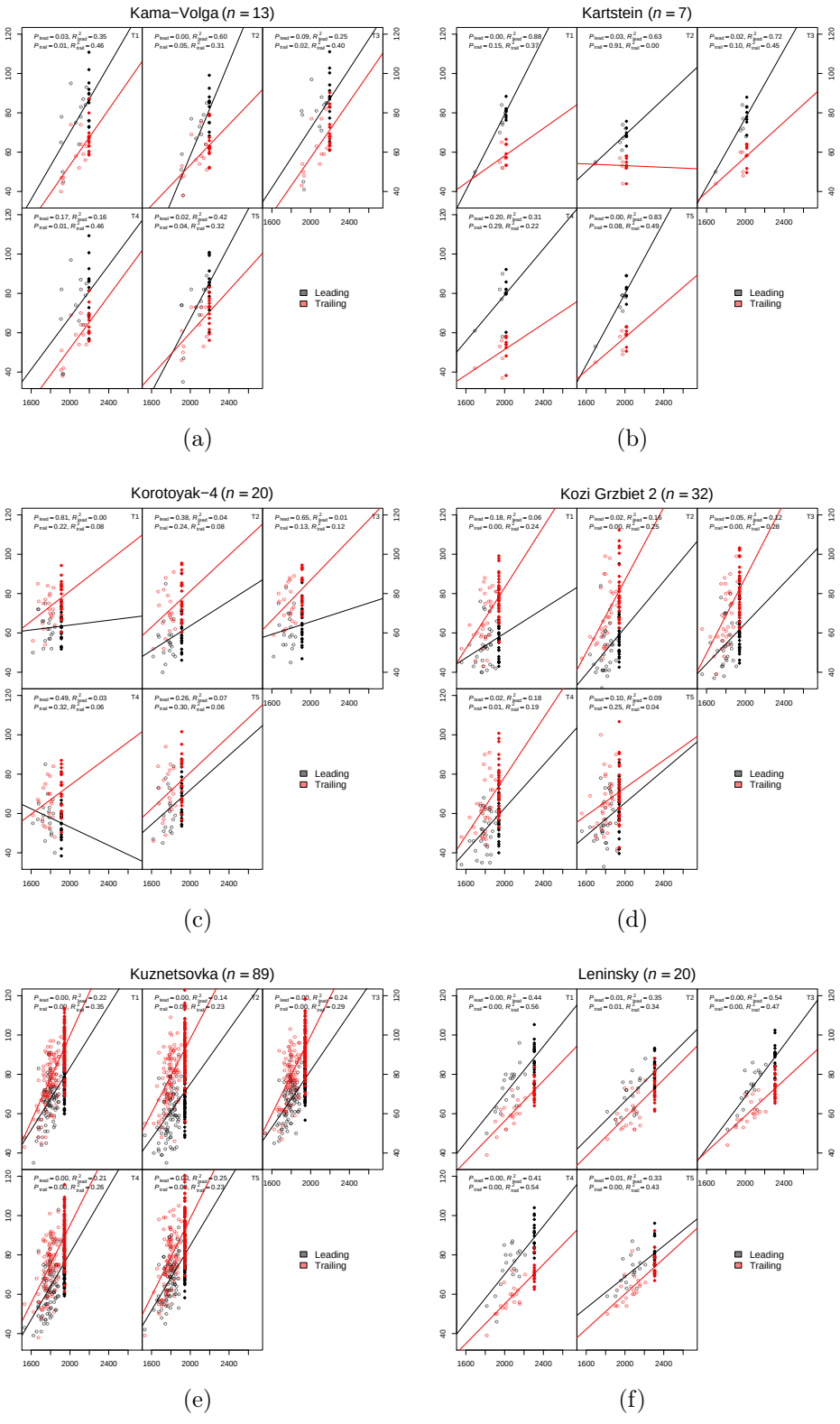

Figure B.6: Regression of enamel thickness (ordinate, µm) with Centroid Size (abscissa, arbitrary units) for the assemblages Kama-Volga, Kartstein, Korotoyak-4, Kozi Grzbiet 2, Kuznetsovka, and Leninsky. Regressions shown for each of the five enamel triangles (T1–T5). Observed thickness plotted as circles, modelled adult thicknesses plotted as diamonds, regression diagnostics shown for each enamel triangle.

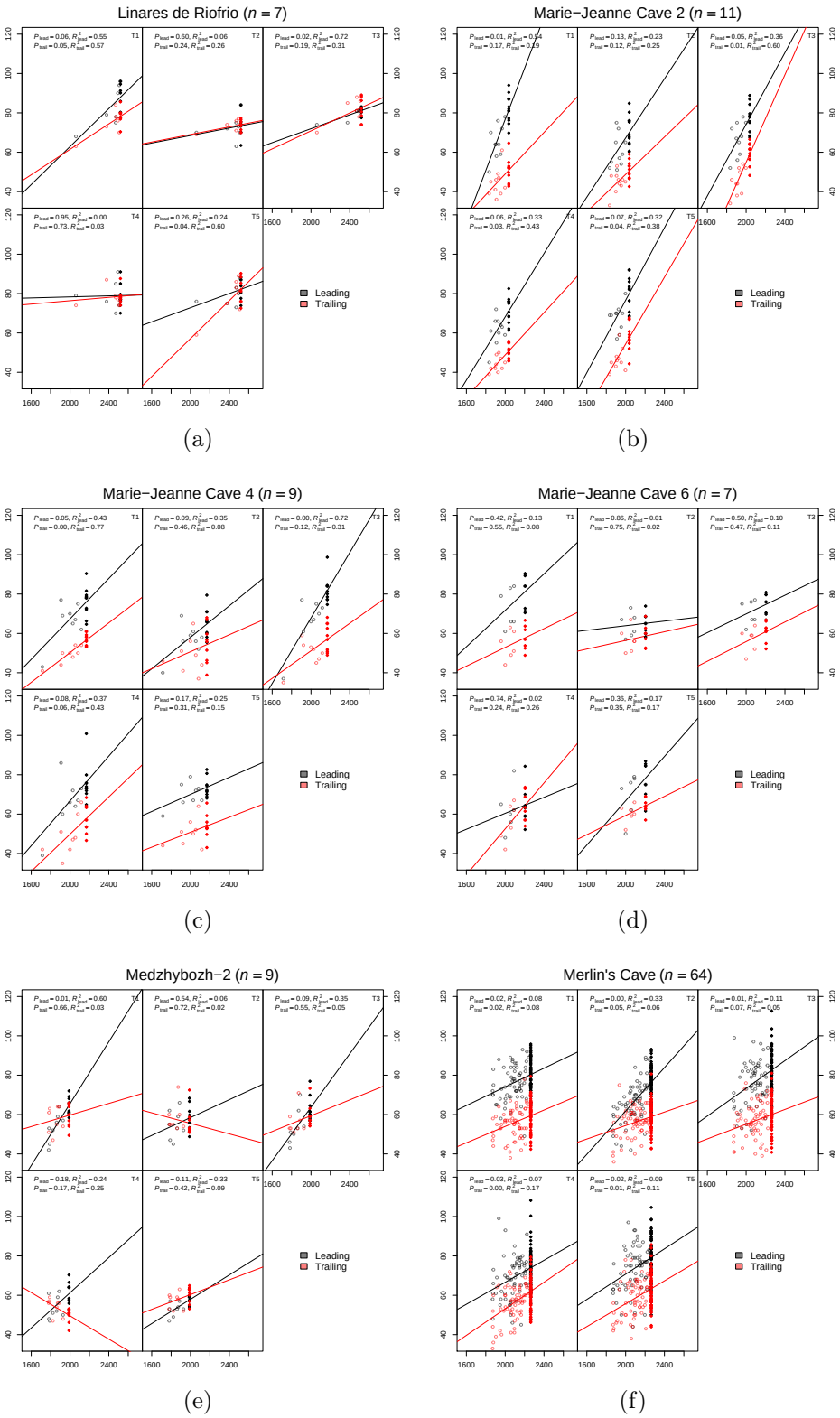

Figure B.7: Regression of enamel thickness (ordinate, µm) with Centroid Size (abscissa, arbitrary units) for the assemblages Linares de Riofrio, Marie-Jeanne Cave 2, Marie-Jeanne Cave 4, Marie-Jeanne Cave 6, Medzhybozh-2, and Merlin's Cave. Regressions shown for each of the five enamel triangles (T1–T5). Observed thickness plotted as circles, modelled adult thicknesses plotted as diamonds, regression diagnostics shown for each enamel triangle.

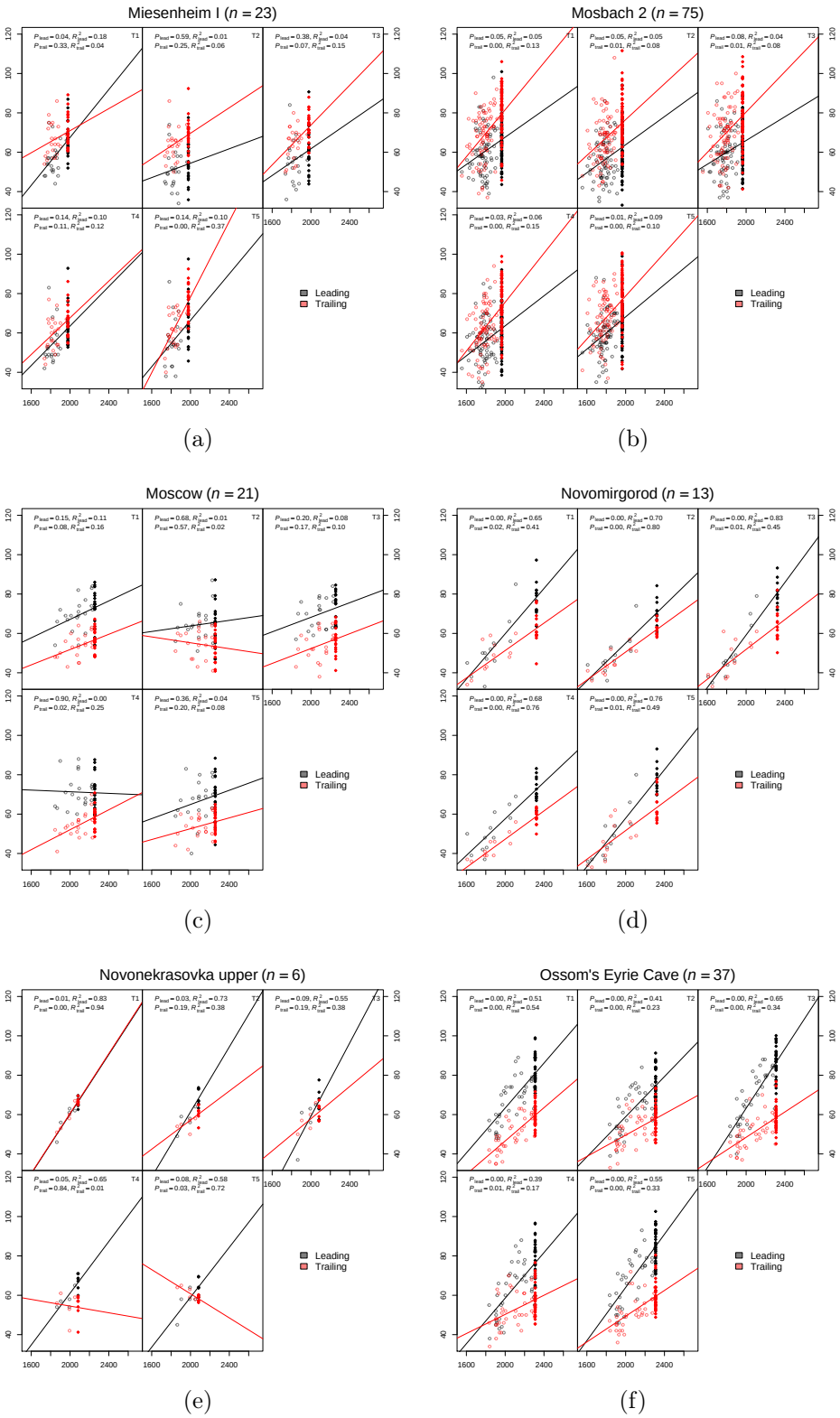

Figure B.8: Regression of enamel thickness (ordinate, µm) with Centroid Size (abscissa, arbitrary units) for the assemblages Miesenheim I, Mosbach 2, Moscow, Novomirgorod, Novonekrasovka upper, and Ossom's Eyrie Cave. Regressions shown for each of the five enamel triangles (T1–T5). Observed thickness plotted as circles, modelled adult thicknesses plotted as diamonds, regression diagnostics shown for each enamel triangle.

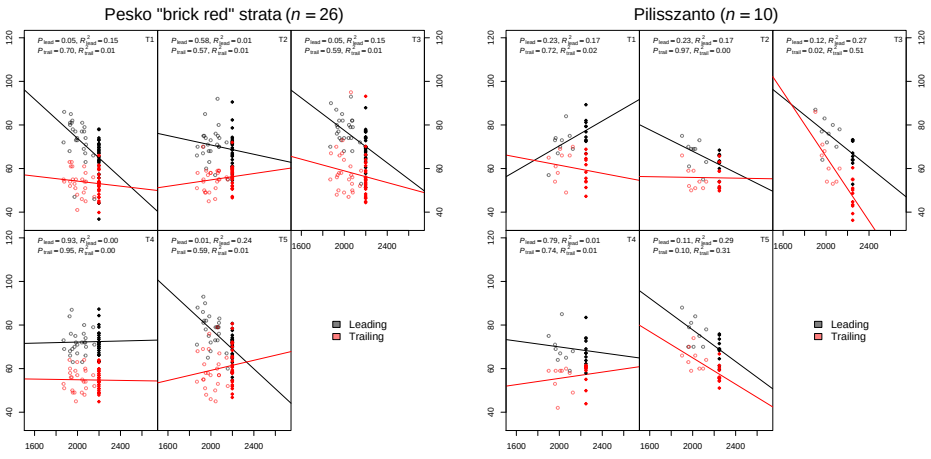

(a)

(b)

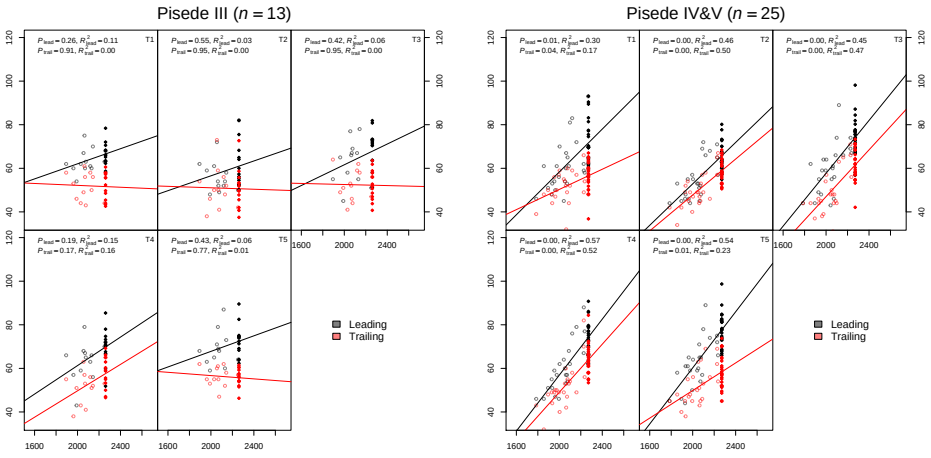

(c)

(d)

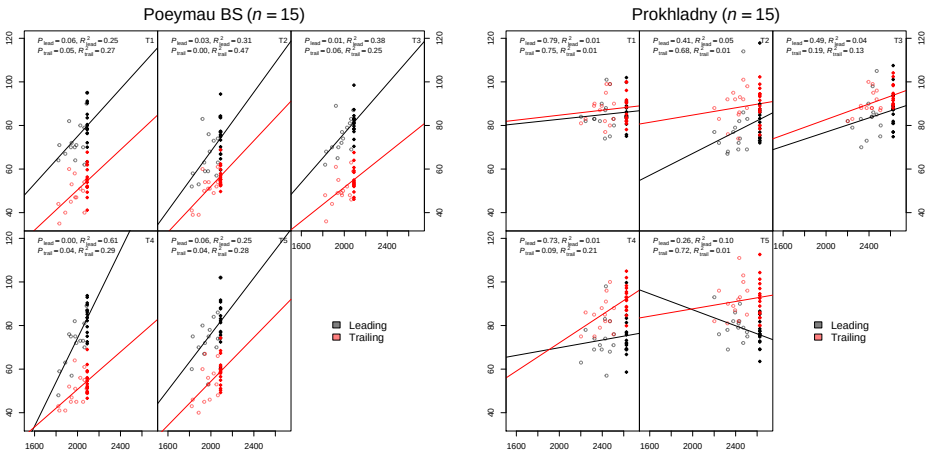

(e)

(f)

Figure B.9: Regression of enamel thickness (ordinate, µm) with Centroid Size (abscissa, arbitrary units) for the assemblages Peskö "brick red" strata, Pilisszántó, Pisede III,Pisede IV&V, Poeymaü BS, and Prokhladny. Regressions shown for each of the five enamel triangles (T1–T5). Observed thickness plotted as circles, modelled adult thicknesses plotted as diamonds, regression diagnostics shown for each enamel triangle.

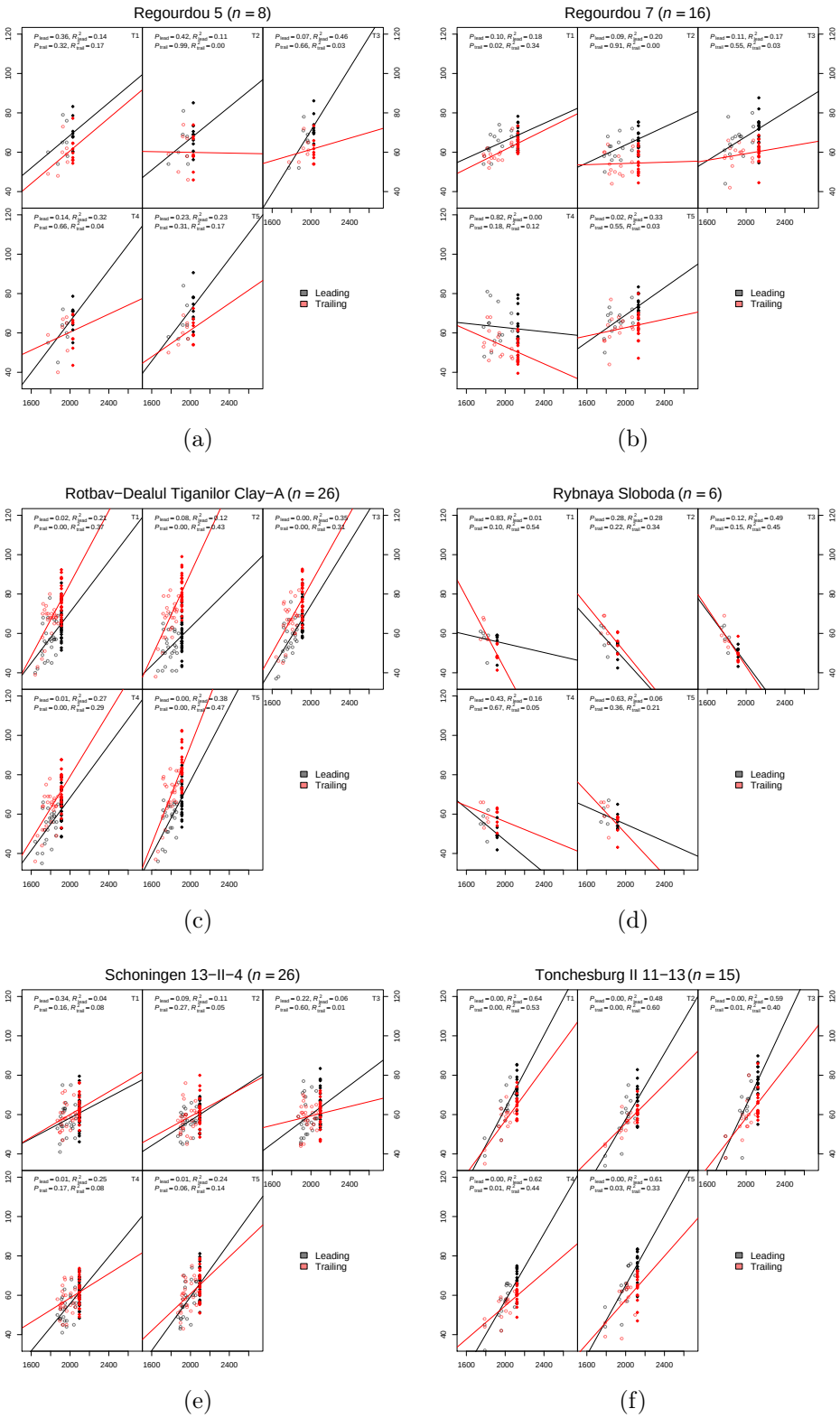

Figure B.10: Regression of enamel thickness (ordinate, µm) with Centroid Size (abscissa, arbitrary units) for the assemblages Régourdou 5, Régourdou 7, Rotbav-Dealul Ţiganilor Clay-A, Rybnaya Sloboda, Schöningen 13-II-4, Tönchesberg II 11-13. Regressions shown for each of the five enamel triangles (T1–T5). Observed thickness plotted as circles, modelled adult thicknesses plotted as diamonds, regression diagnostics shown for each enamel triangle.

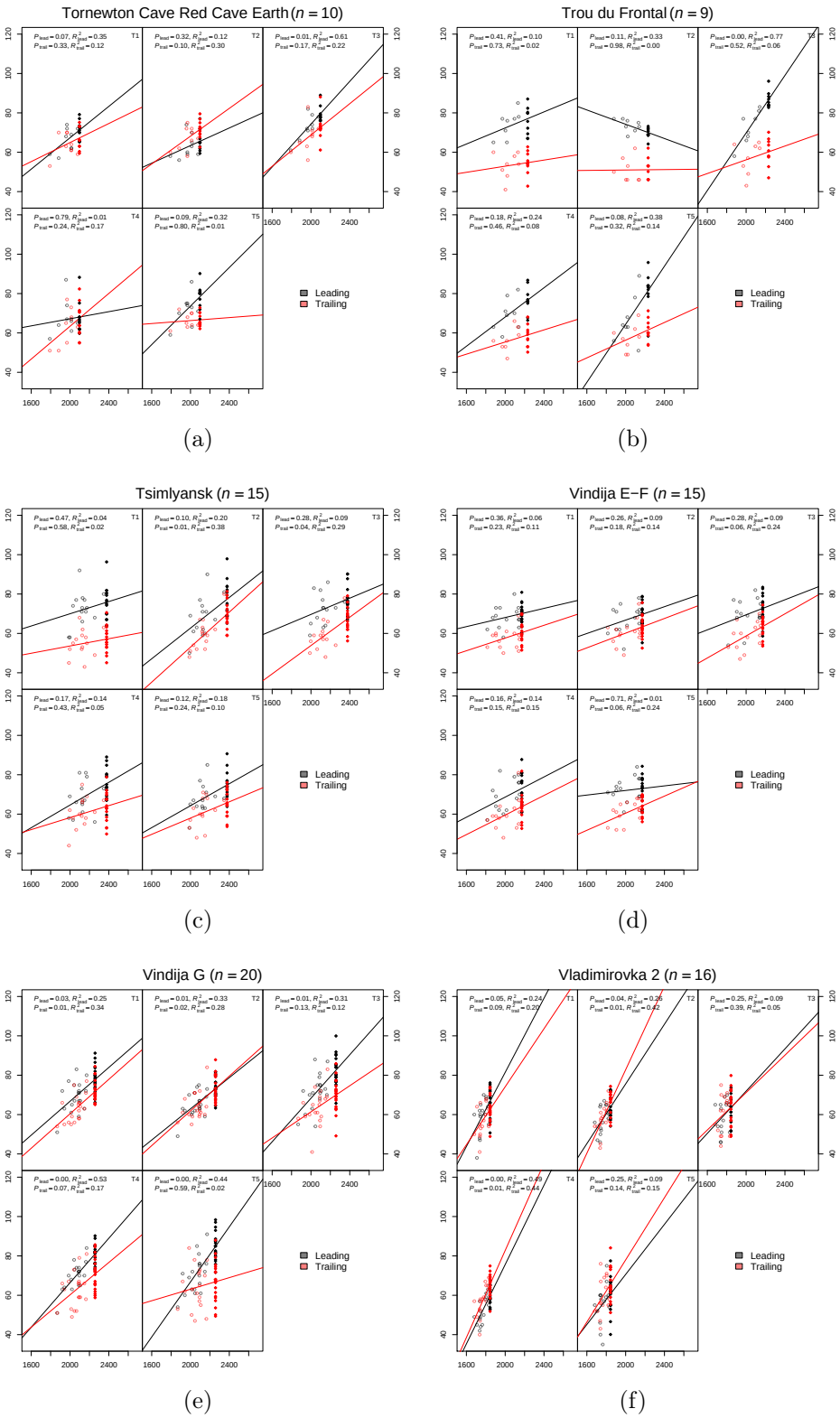

Figure B.11: Regression of enamel thickness (ordinate, µm) with Centroid Size (abscissa, arbitrary units) for the assemblages Tornewton Cave Red Cave Earth, Trou du Frontal, Tsimlyansk, Vindija E-F, Vindija G, Vladimirovka 2. Regressions shown for each of the five enamel triangles (T1–T5). Observed thickness plotted as circles, modelled adult thicknesses plotted as diamonds, regression diagnostics shown for each enamel triangle.

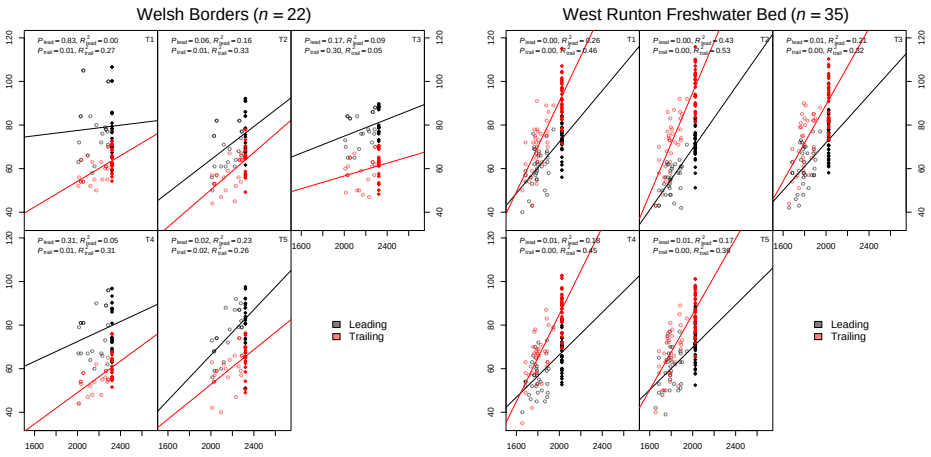

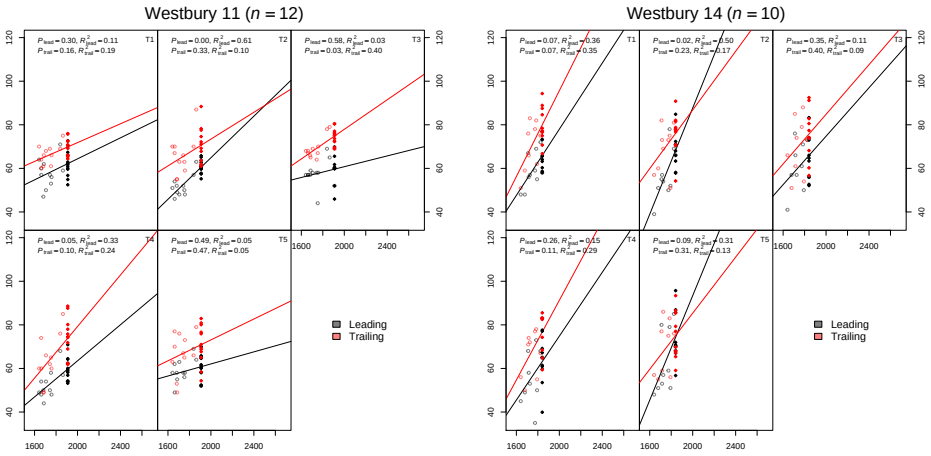

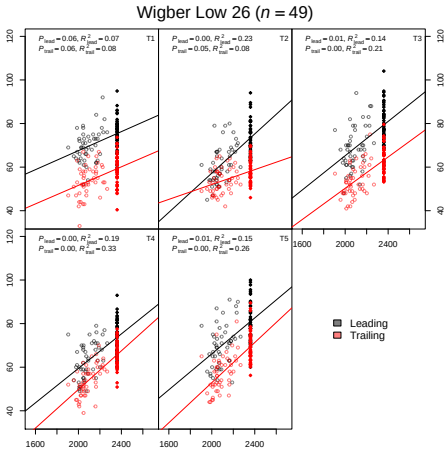

Figure B.12: Regression of enamel thickness (ordinate, µm) with Centroid Size (abscissa, arbitrary units) for the assemblages Welsh Borders, West Runton Freshwater Bed, Westbury 11, Westbury 14, Wigber Low 26. Regressions shown for each of the five enamel triangles (T1–T5). Observed thickness plotted as circles, modelled adult thicknesses plotted as diamonds, regression diagnostics shown for each enamel triangle.

Table B.6: Summary SDQ statistics from unmodified enamel thickness measurements ($SDQAU_p$).

Assemblage	x_{min}	$\bar{x}$	x_{max}	σ	n
Abzac	69.9	79.9	89.9	6.3	17
Aggeel	99.6	108.0	119.3	9.0	5
Bolshoi Tiganye	77.5	89.0	100.9	7.9	10
Boxgrove 4b	95.2	117.0	145.2	15.7	16
Boxgrove 4c	101.3	120.1	144.6	12.1	17
Burgtonna South Black-earth	83.0	98.9	115.7	9.0	9
Central Scotland	78.9	88.8	109.9	11.0	13
Cheshskaya Guba	74.1	85.4	98.0	7.3	19
Chigirin	89.3	105.0	117.2	8.1	9
Clacton Channel IV	91.3	103.0	119.0	7.5	19
Courbet	66.8	80.1	98.7	8.5	29
Cudmore Grove	99.0	115.0	132.2	8.8	29
Don Delta	76.6	82.9	85.2	3.0	7
Donskaya Negatchevka	89.6	107.4	116.7	7.4	12
Dzeravá skala Cave	74.5	83.5	99.2	4.8	24
Fortuna utca 16-18/2	101.8	112.7	135.4	8.3	17
Frankfurt am Main	77.4	83.0	86.7	3.7	5
Fuchsloch im Krockstein	69.9	85.8	102.7	9.1	13
Ghent	69.0	81.4	98.2	7.9	18
Grotta del Broion, Sala Grande N	92.8	100.6	109.7	5.8	10
Grotta del Broion, Sala Grande Q4	88.8	94.7	104.7	5.0	8
Grotta del Broion, Sala Grande Q5	80.6	99.2	107.2	7.5	11
Grotta del Broion, Sala Grande R1	86.1	97.0	108.4	7.4	16
Gunki II	92.4	108.9	129.6	11.9	9
Horváti-lik 8	76.9	88.1	96.7	5.1	19
Horváti-lik 9a	77.9	89.8	107.8	7.4	21
Horváti-lik 13	81.5	90.1	96.5	5.5	8
Hundsheim	108.9	127.0	145.3	7.6	31
Ilovayski Kordon	100.4	115.2	134.5	9.6	11
Kabardino-Balkariya	75.6	84.8	96.6	5.7	19
Kama-Volga	69.8	89.0	123.4	15.5	13
Kartstein	69.2	79.0	93.1	8.1	7
Korotoyak-4	107.2	119.8	130.3	5.7	20
Kozi Grzbiet 2	97.3	128.5	177.7	14.5	32
Kuznetsovka	97.4	121.2	144.4	10.5	89
Leninsky	80.1	90.0	101.8	6.5	20
Linares de Riofrio	92.2	100.3	109.3	6.4	7
Marie-Jeanne Cave 2	69.5	75.8	87.0	5.3	11
Marie-Jeanne Cave 4	72.5	82.9	95.9	7.2	9
Marie-Jeanne Cave 6	81.7	87.8	92.1	3.6	7
Medzhybozh-2	94.9	105.8	114.5	7.4	9
Merlin's Cave	59.8	83.9	122.2	9.9	64
Miesenheim I	98.5	118.9	136.3	10.5	23
Mosbach 2	90.8	117.0	171.2	14.5	75

Continued on next page

Table B.6 continued from previous page

Assemblage	$x_{\min}$	$\bar{x}$	$x_{\max}$	σ	n
Moscow	75.3	86.3	101.2	6.4	21
Novomirgorod	72.8	95.0	108.6	9.7	13
Novonekrasovka upper	93.5	101.6	118.7	8.8	6
Ossom's Eyrie Cave	65.8	85.5	104.4	9.0	37
Peskö "brick red" strata	71.2	81.5	94.6	6.3	26
Pilisszántó	79.3	88.1	96.8	5.7	10
Pisede III	74.4	88.9	101.7	7.0	13
Pisede IV&V	78.1	91.3	108.5	8.2	25
Poeymaú BS	65.6	77.0	88.8	7.3	15
Prokhladny	103.1	111.9	118.6	4.3	15
Régourdou 5	82.8	97.5	102.0	6.5	8
Régourdou 7	85.7	96.2	116.2	7.8	16
Rotbav-Dealul Ţiganilor Clay-A	104.7	119.7	139.0	9.0	26
Rybnaya Sloboda	93.9	107.6	128.8	12.0	6
Schöningen 13-II-4	88.5	106.7	132.1	9.2	26
Tönchesberg II 11-13	84.6	96.2	110.1	8.3	15
Tornewton Cave Red Cave Earth	91.7	99.4	110.2	5.5	10
Trou du Frontal	66.8	81.0	91.9	6.9	9
Tsimlyansk	80.0	89.2	103.8	7.2	15
Vindija E-F	83.8	90.9	98.5	4.6	15
Vindija G	81.8	96.3	109.2	6.9	20
Vladimirovka 2	88.5	104.3	119.5	7.0	16
Welsh Borders	74.9	84.0	104.2	7.4	22
West Runton Freshwater Bed	106.5	120.0	142.1	10.3	35
Westbury 11	112.5	121.9	130.6	6.1	12
Westbury 14	108.5	122.4	143.3	12.8	10
Wigber Low 26	72.1	87.3	101.2	5.8	49

Table B.7: Summary SDQ statistics from size-corrected enamel thickness measurements ($SDQAC_p$).

Assemblage	x_{min}	$\bar{x}$	x_{max}	σ	n
Abzac	67.3	75.7	85.3	5.0	17
Aggeel	105.9	113.5	125.2	8.3	5
Bolshoi Tiganye	73.4	81.9	87.8	4.7	10
Boxgrove 4b	100.5	122.7	148.4	15.6	16
Boxgrove 4c	101.6	118.4	140.1	10.6	17
Burgtonna South Black-earth	81.6	94.8	102.6	6.7	9
Central Scotland	79.4	87.7	102.9	8.5	13
Cheshskaya Guba	79.3	89.4	103.0	6.9	19
Chigirin	88.2	102.9	111.8	7.5	9
Clacton Channel IV	91.4	101.9	114.8	6.5	19
Courbet	62.9	74.5	96.9	6.6	29
Cudmore Grove	101.8	115.6	131.5	8.1	29
Don Delta	76.6	82.4	85.1	3.0	7
Donskaya Negatchevka	88.8	103.7	113.9	7.0	12
Dzeráva skala Cave	75.8	85.9	101.4	4.7	24
Fortuna utca 16-18/2	104.2	118.1	135.9	7.8	17
Frankfurt am Main	77.4	78.4	79.9	1.0	5
Fuchsloch im Krockstein	70.4	84.7	98.5	7.9	13
Ghent	66.7	79.6	97.4	7.8	18
Grotta del Broion, Sala Grande N	97.6	104.6	115.0	4.9	10
Grotta del Broion, Sala Grande Q4	89.3	95.2	104.9	4.8	8
Grotta del Broion, Sala Grande Q5	80.2	95.0	100.9	6.3	11
Grotta del Broion, Sala Grande R1	88.8	99.0	109.1	6.7	16
Gunki II	100.8	117.6	133.1	9.9	9
Horváti-lik 8	75.2	83.0	91.5	3.7	19
Horváti-lik 9a	78.7	91.9	109.7	7.6	21
Horváti-lik 13	85.6	92.2	98.5	5.1	8
Hundsheim	108.9	127.9	145.1	7.2	31
Ilovayski Kordon	104.8	118.5	134.5	8.2	11
Kabardino-Balkariya	75.5	84.7	96.4	5.7	19
Kama-Volga	69.7	84.6	102.6	10.6	13
Kartstein	68.1	75.5	81.6	5.0	7
Korotoyak-4	110.8	123.5	133.0	5.3	20
Kozi Grzbiet 2	100.8	131.9	177.1	13.3	32
Kuznetsovka	100.2	121.6	142.2	9.0	89
Leninsky	79.5	87.2	96.8	5.2	20
Linares de Riofrio	92.6	101.8	109.9	5.8	7
Marie-Jeanne Cave 2	69.3	74.6	84.2	4.4	11
Marie-Jeanne Cave 4	73.1	82.0	89.7	5.7	9
Marie-Jeanne Cave 6	86.1	90.2	95.6	3.3	7
Medzhybozh-2	89.8	97.3	107.0	5.2	9
Merlin's Cave	61.0	83.4	120.6	9.1	64
Miesenheim I	99.5	117.5	133.9	9.3	23
Mosbach 2	95.4	120.1	168.6	12.9	75

Continued on next page

Table B.7 continued from previous page

Assemblage	$x_{\min}$	$\bar{x}$	$x_{\max}$	σ	n
Moscow	77.0	87.9	101.2	6.2	21
Novomirgorod	71.7	84.6	93.1	5.9	13
Novonekrasovka upper	89.1	95.1	100.6	4.4	6
Ossom's Eyrie Cave	64.9	80.3	95.7	6.9	37
Peskö "brick red" strata	75.0	86.4	98.0	6.3	26
Pilisszántó	76.4	85.8	94.4	6.0	10
Pisede III	75.6	89.1	100.7	6.4	13
Pisede IV&V	76.7	87.3	100.2	6.2	25
Poeymaü BS	68.4	77.3	87.9	6.4	15
Prokhladny	103.8	112.9	119.3	4.2	15
Régourdou 5	82.8	93.2	99.2	5.6	8
Régourdou 7	82.6	93.1	107.9	6.7	16
Rotbav-Dealul Ţiganilor Clay-A	109.1	121.9	138.4	7.7	26
Rybnaya Sloboda	90.4	104.8	127.8	12.9	6
Schöningen 13-II-4	86.6	101.5	124.1	8.1	26
Tönchesberg II 11-13	81.4	90.1	99.0	5.5	15
Tornewton Cave Red Cave Earth	92.2	99.4	109.6	5.2	10
Trou du Frontal	63.3	77.5	83.9	6.0	9
Tsimlyansk	79.0	87.7	101.1	6.6	15
Vindija E-F	84.0	91.3	98.5	4.5	15
Vindija G	81.5	94.1	106.1	5.9	20
Vladimirovka 2	95.6	106.7	120.9	6.2	16
Welsh Borders	75.0	83.7	101.3	6.7	22
West Runton Freshwater Bed	110.4	125.9	143.6	8.3	35
Westbury 11	108.9	117.8	127.2	5.2	12
Westbury 14	106.6	118.1	135.2	10.8	10
Wigber Low 26	75.4	88.0	99.9	5.1	49

Appendix C

Illustrative material

On the accompanying DVD can be found images of M_1 teeth collected during the research presented in this thesis, alongside landmark coordinates, enamel thickness measurements, and derived data such as SDQ values. Please refer to the `ReadMe.txt` file on the DVD for further details regarding these datasets.